Les glutathion peroxydases et protéine disulfure isomérases de peuplier : potentialités du repliement thiorédoxine pour la catalyse des réactions redox

Benjamin Selles

UFR Sciences et Technologies
E.D. Ressources, Procédés, Produits et Environnement
Biologie Végétale et Forestière

IFR 110 Génomique, Ecophysiologie et Ecologie Fonctionnelle
Unité Mixe de Recherche INRA/UHP/1136
Interactions arbres-microorganismes

Thèse
présentée pour l'obtention du grade de

Docteur de l'Université Henri Poincaré, Nancy I
en Biologie Forestière

par ***Benjamin SELLES***

Les glutathion peroxydases et protéine disulfure isomérases de peuplier : potentialités du repliement thiorédoxine pour la catalyse des réactions redox

JURY:

Pierre LEROY, Professeur Faculté Sciences Pharmaceutiques et Biologiques Nancy
Jean-François COLLET, Professeur Université Catholique de Louvain — Rapporteur
Pascal REY, Ingénieur-Chercheur, CEA Cadarache — Rapporteur
Florence VIGNOLS, Chargée de Recherche CNRS Montpellier
Nicolas ROUHIER, Maître de Conférences Nancy I — Co-directeur de thèse
Jean-Pierre JACQUOT, Professeur Nancy I — Co-directeur de thèse

Résumé

La formation de ponts disulfure constitue une modification post-traductionnelle des protéines importante pour de nombreux processus physiologiques, jouant un rôle particulier dans le repliement, la catalyse et la régulation de leur activité. Ce travail concerne l'étude des relations structure-fonction d'oxydoréductases de peuplier appartenant à deux familles de la superfamille des thiorédoxines, les glutathion peroxydases (Gpxs) et les protéine disulfure isomérases (PDIs).
L'étude biochimique fine de la Gpx5 a permis de montrer que cette peroxydase réduit le peroxynitrite, propriété inconnue pour ce type de Gpx et de détailler plusieurs étapes du mécanisme catalytique (formation de l'acide sulfénique, changement structural entre formes réduites et oxydées, régénération par les Trxs). La dimérisation de la Gpx5 n'est pas requise pour son activité mais pourrait jouer un rôle dans la reconnaissance de certains substrats. Enfin, l'inactivation de la cystéine peroxydatique par suroxydation suggère que les Gpxs pourraient également avoir une fonction dans la signalisation en réponse aux peroxydes.
Concernant les PDIs, suite à une analyse phylogénétique détaillée amenant à proposer une nouvelle classification en 9 classes chez les organismes photosynthétiques, la caractérisation biochimique de plusieurs isoformes présentant des organisations modulaires distinctes et appartenant à trois classes de PDIs a été entreprise. Aucune activité enzymatique typique n'a été identifiée pour la PDI-A, alors que les PDI-L1a et -M possèdent à la fois une activité oxydase et réductase. Les deux modules *a* de la PDI-M catalysent des réactions spécifiques, de réduction ou d'oxydation.

Mots clés: Protéine disulfure isomérase, glutathion peroxydase, thiorédoxine, stress oxydant, oxydation, réduction.

Abstract

Protein activity and folding can be regulated by post-translational modifications that can impact on their physiological functions. One of these is the formation/reduction of disulfide bridges. The aim of the present work is to study the structure-function relationship of protein members of the thioredoxin superfamily, the protein disulfide isomerases (PDI) and the glutathione peroxidases (Gpx).
A precise biochemical study has allowed us to demonstrate that this enzyme is an efficient peroxynitrite scavenger, a new finding for this type of protein and allowed investigating several steps of the Gpx5 catalytic mechanism (i.e. sulfenic acid formation, structural changes between reduce dand oxidized forms, Trx-mediated recycling). We also demonstrate that the dimer form of Gpx5 is not absolutely required for peroxide reduction but probably involved in peroxide specificity. Finally, the capability of the peroxidatic cysteine to be overoxidized brings some new clues in favor of an additional signaling function for Gpx5.
Concerning PDIs, a detailed phylogenetic analysis of photosynthetic organisms allowed us to identify 9 classes of PDIs and to propose a new nomenclature that fits all these organisms. The biochemical characterization of isoforms of interest has allowed us to highlight some specificity of PDI-L1a and PDI-M in terms of reduction or oxidation reactions catalyzed. A detailed analysis of PDI-M isoform also indicates that the two Trx modules of this protein show differential oxidation or reduction capacities. We could not detect any activity for PDI-A isoforms, leaving us to wonder whether this enzyme is simply active or possesses highly specific protein partners.

Key words: Protein disulfide isomerase, glutathione peroxidase, thioredoxin, oxidative stress, oxidation, reduction.

ADN, Acide désoxyribonucléique

ADNc, ADN complémentaire

APX, Ascorbate peroxydase

ARN, Acide ribonucléique

ARNm, ARN messager

ATP, Adénosine tri-phosphate

CDSP32, pour "Chloroplastic drought-induced stress protein of 32 kDa"

Cys_C, Cytochrome C

DHA / MDHA, Déhydroascorbate / Monodéhydroascorbate

dNTP Désoxyribonucléotide triphosphate

Dsb, pour "Disulfide bond protein"

DTT, Dithiothréitol

EAO, Espèces activées de l'oxygène

ERAD, pour "Endoplasmic reticulum associated degradation"

ERO, pour "Endoplasmic reticulum oxidoreductase"

ERp, pour "Endoplasmic reticulum protein"

ERQC, pour "Endoplasmic reticulum quality control"

Erv/Alr, pour "Essential for respiration and viability/ Augmenter of liver regeneration"

FAD, Flavine adenine dinucléotide

FBPase, Fructose-1,6-bisphophatase

Fdx, Ferrédoxine

FF, pour "Fully folded"

FNR, Ferrédoxine-$NADP^+$ oxydoréductase

GADPH, Glycéraldéhyde-3-phosphate déshydrogénase

Gpx, Glutathion peroxydase

GR, Glutathion réductase NADPH-dépendante

Grx, Glutarédoxine

GSH / GSSG, Glutathion réduit et glutathion disulfure

GST, Glutathion transférase

kDa, Kilodalton

LU, pour "locally unfolded"

MDH-NADP, Malate déshydrogénase à NADP

MSR, Méthionine sulfoxyde réductase

mV, Millivolts

NADP(H) Nicotinamide adénine dinucléotide phosphate (réduite)

NRX, pour "Nucleoredoxin"

NTR, Thiorédoxine réductase NADPH-dépendante

PAGE, pour "Polyacrylamide gel electrophoresis"

PAPS réductase, 3'-phosphoadénosyl sulfate réductase

PBS, pour "Phosphate buffer saline"

PCR, pour "Polymerase chain reaction"

PDB, pour "Protein data bank"

PDI, Protéine disulfure isomérase

Prx, Peroxyrédoxine

PS, Photosystème

QSOX, pour "Quiescin sulfhydryl oxydase"

RNR, Ribonucléotide réductase

RuBisCO, Ribulose-1,5-bisphosphate carboxylase oxygénase

SDS, Sodium dodecyl sulfate

SOX, Sulfhydryle oxydase

TDX, pour « Tetratricopeptide domain-containing thioredoxin »

Trx, Thiorédoxine

Tpx, Peroxydase thiol dépendante

UPR, pour "Unfolded protein response"

Table des matières

Introduction 13

Synthèse bibliographique 16

I. Généralités 16

I.1. Modification de l'activité des protéines 16

I.2. Origine de la formation des ponts disulfure 16

I.3. Importance des ponts disulfure dans les protéines 18

I.4. Acteurs des échanges dithiol/disulfure 18

II. La superfamille des thiorédoxines 19

II.1. Un repliement tridimensionnel spécifique 19

II.2. Caractéristiques structurales 19

II.3. Caractéristiques oxydoréductrices 22

II.3.a. Le pKa de la cystéine catalytique 22

II.3.b. Le potentiel d'oxydoréduction du pont disulfure entre la Cys catalytique et la Cys de recyclage 23

II.3.c. Impact des structures primaire, secondaire et tertiaire sur les caractéristiques redox 24

II.4. Les réactions catalysées 25

III. Les systèmes réducteurs impliquant des protéines à repliement thiorédoxine, exemple du système thiorédoxine 27

III.1 Une famille multigénique 27

III.2 Sources de pouvoirs réducteurs 28

III.3 Partenaires, fonctions et systèmes de régulation au sein de la cellule 31

IV. Rôle des thiol-peroxydases, protéines à repliement thiorédoxine, dans la réponse au stress oxydant 34

IV.1. Définition d'un stress oxydant 34

IV.2. Les EAOs, nature et sites de production 35

IV.3. La détoxication des EAOs 37

IV.3.a. Les systèmes de détoxication non enzymatiques 37

IV.3.a.1. L'acide lipoïque et dihydrolipoïque 37

IV.3.a.2. Les caroténoïdes 38

IV.3.a.3. Les flavonoïdes 38

IV.3.a.4. Le glutathion 38

IV.3.a.5. Les vitamines C (acide ascorbique) et E (α-tocophérol et tocotriénols) 40

IV.3.b. Les systèmes de détoxication enzymatiques impliquant des protéines à repliement thiorédoxine.....40
IV.3.b.1. Diversité des thiol-peroxydases et localisation subcellulaire.....41
IV.3.b.2. Les mécanismes catalytiques des thiol-peroxydases une base commune et des modalités variées.....44
IV.3.b.1. Caractéristiques biochimiques et structurales des Tpxs.....45
IV.3.b.2. Rôles physiologiques des thiol-peroxydases, plus que de simples enzymes de détoxication? 48
V. Les systèmes d'introduction et d'isomérisation des ponts disulfure 50
V.1. Le repliement redox dépendant au sein du périplasme des bactéries, le système Dsb.....50
V.1.a. La voie d'introduction des ponts disulfure.....52
V.1.b. La voie d'isomérisation des ponts disulfure.....53
V.1.c. Le trajet des électrons, illustration d'un paradoxe thermodynamique.....54
V.1.d. Le système Dsb, conservation et variation chez les organismes procaryotiques.....55
V.1.e. Rôles physiologiques.....56
V.1.e.1. La maturation des cytochromes c.....56
V.1.e.2. Système Dsb et virulences bactériennes.....57
V.2. Le repliement des protéines redox-dépendant dans le réticulum endoplasmique des organismes eucaryotiques.....58
V.2.a. Les sulfhydryl oxydases et la formation des ponts disulfure.....59
V.2.a.1.Les protéines de type Erv/Alr.....60
V.2.a.2. Les protéines de type Qsox.....61
V.2.a.2.α. Organisation modulaire et trajet des électrons au sein de la protéine 62
V.2.a.2.β. Localisation subcellulaire et rôle physiologique des protéines Qsox.....65
V.2.a.3. Les protéines de type ERO.....66
V.2.a.3.α. Caractéristiques biochimiques et structurales des EROs..67
V.2.a.3.β. Régulation redox dépendante de l'activité des EROs.....70
V.2.a.4. Redéfinition du statut redox du RE.....71
V.2.a.5. Les sulfhydryl oxydases: sources de molécules oxydantes.....72

V.2.b. Les protéine disulfure isomérases, protéines responsables de la formation et de l'isomérisation des ponts disulfure.....73
V.2.b.1.Caractéristiques des PDIs chez les organismes photosynthétiques (Article 1. Comparative genomic study of protein disulfide isomerases from photosynthetic organisms).....74
V.2.b.2.Les PDIs : oxydoréductases « à tout faire ».....90
V.2.b.3. Implication des différents modules de la PDI dans les réactions redox.....91
V.2.c. Interaction des protéines responsables de la maturation au sein du RE.....92
V.3. Le repliement des protéines dans l'espace inter-membranaire des mitochondries.....95
V.3.a. L'adressage au sein de la matrice.....95
V.3.b. L'adressage au sein de l'IMS.....95
V.3.c. Le repliement redox dépendant des protéines de classe II est nécessaire à leur localisation dans l'IMS.....96
V.3.d. Les cibles du système Mia40-Erv1 et leurs rôles physiologiques.....97
VI. Problématiques et Objectifs.....103

Résultats.....107
I. Article 2: Catalytic mechanism and oxidative inactivation of the poplar thioredoxin-dependent glutathione peroxidase 5.....107

II. Article 3: Biochemical characterization of three poplar PDI isoforms with different domain organizations: emphasis on the oxidoreductase properties of PDI-M.....145

Discussion et perspectives.....175
I. Dissection des caractéristiques mécanistiques et biochimiques de la Gpx5 de peuplier.....176
I.1. La tétrade catalytique des Gpxs, plus qu'un modulateur du pKa de la Cys_P.....176
I.2. La dualité de fonction de la Cys_P.....177
I.2.a. Rôle de la Cys_P dans les modifications structurales.....177

I.2.b. L'état d'oxydation de la Cys_P, un indice en faveur d'une multiplicité de fonctions des Gpxs de plantes?.....179
I.3. Les modalités d'interaction entre la Gpx5 et la Trxh1.....182
I.4. Les rôles physiologiques des Gpxs dans la réponse au stress oxydant.....183
***II. Les PDIs chez les organismes photosynthétiques*.....185**
II.1. Analyse phylogénétique et classification.....185
II.2. Caractérisation biochimique de trois isoformes de PDIs de peuplier.....186
II.2.a. Propriétés des protéines sauvages vis-à-vis de tests classiques d'activité PDI.....187
II.2.b. Recherche des spécificités des deux modules Trx *a*° et *a* de la protéine PtPDI-M.....189
II.2.c. La versatilité des réactions catalysées in vitro par les PDIs, un aperçu de leur activité in planta?.....191

***Annexes*.....193**
***Références*.....261**
***Communications scientifiques et distinctions*.....289**

Introduction

L'uniformisation de la recherche scientifique a depuis de nombreuses années abouti à la sélection de certains organismes qualifiés « d'organismes modèles ». Ceux-ci sont sélectionnés suivant certains critères objectifs. Ainsi le peuplier a été choisi comme espèce modèle pour les organismes ligneux du fait de la taille de son génome (485 ±10 mégabases), de la relative rapidité de son cycle de croissance (environ 5 mètres par an), de la disponibilité de bases de données génomiques ainsi que d'outils de transformation génétique. De plus, par rapport aux espèces non pérennes, type *Arabidopsis thaliana*, l'étude du peuplier peut apporter des informations essentielles sur les processus de formation du bois, des variations phénotypiques saisonnières, ou lors d'interactions pathogènes ou mutualistes.

Le peuplier est le système biologique d'étude de l'unité « Interaction Arbres-Microorganismes » au sein de laquelle se sont déroulés mes travaux de thèse. Mon équipe d'accueil, « Réponse aux stress et régulation redox » a pour principal objectif la caractérisation « systématique » de protéines de peuplier impliquées dans des mécanismes d'oxydoréduction et appartenant à la grande famille des thiorédoxines (Trx). Ces protéines ubiquitaires présentes des procaryotes aux eucaryotes, sont généralement de petite taille (aux alentours de 15 kDa) et possèdent des caractéristiques structurales et/ou fonctionnelles communes. La principale caractéristique est la présence de résidus cystéine (Cys) généralement conservés. Ce résidu, constitué d'une chaîne latérale possédant un atome de soufre a la particularité de former dans certains cas des liaisons covalentes avec d'autres atomes (soufre ou oxygène notamment). Ainsi, grâce à cette propriété, des échanges d'électrons peuvent être réalisés par les protéines de la superfamille des Trx suivant des réactions de réduction/formation de ponts disulfure entre deux résidus Cys. La superfamille des Trx regroupe, de façon non exhaustive, les Trx, les glutarédoxines (Grx), les thiol -peroxydases (Tpx) et les protéine disulfure isomérases (PDI). Au cours de mon travail de thèse, je me suis particulièrement intéressé à deux processus nécessitant l'intervention de protéines de la superfamille des Trx chez le peuplier, la réduction des espèces réactives de l'oxygène (ROS), et la formation et l'isomérisation des ponts disulfure à travers la caractérisation biochimique de certaines membres de la famille des Tpx (les glutathion peroxydases ; Gpx) et des PDI.

Synthèse bibliographique

I. Généralités

I.1. Modification de l'activité des protéines

Parmi les processus mis en œuvre dans la réponse des plantes aux fluctuations environnementales figurent les modifications post-traductionnelles ayant pour but de changer et/ou de réguler la fonction des protéines. De nombreuses modifications post-traductionnelles des protéines ont été recensées dont notamment les *phosphorylations, glycosylations, acétylations, méthylations, sumoylations, isoprénylations, ubiquitinations, citrullinations, etc.…*. Certaines de ces modifications ont potentiellement un fort impact sur la structure tridimensionnelle des protéines, en particulier la formation/réduction de ponts disulfure. Nous allons approfondir les mécanismes responsables de ces modifications post-traductionnelles de type redox dans la suite de cette synthèse bibliographique.

I.2. Origine de la formation des ponts disulfure

Les ponts disulfure sont des liaisons covalentes entre deux atomes de soufre, résultant d'un processus oxydoréducteur impliquant des transferts d'électrons et de protons. Au niveau des protéines, les acides aminés responsables de la formation de telles liaisons sont les résidus cystéinyls (Cys). Ces acides aminés présentent sur leur chaîne latérale, un atome de soufre, qui à l'état réduit est sous forme de thiol (S-H) ou de thiolate (S^-) (Figure 1A). Cet atome de soufre est un élément déterminant dans les réactions d'oxydoréduction, au même titre que l'oxygène, le fer ou le cuivre, de par sa propension à subir des réactions de réduction et d'oxydation (Figure 1B). Il existe deux voies principales de formation des ponts disulfure :

→ Une voie de réponse à des molécules oxydantes qui peuvent oxyder l'atome de soufre sous différentes formes (Figure 2). L'une de ces formes oxydées, l'acide sulfénique (R-SOH), peut être directement attaqué par un autre atome de soufre sous forme thiolate ($R\text{-}S^-$, Figure 2), libé-

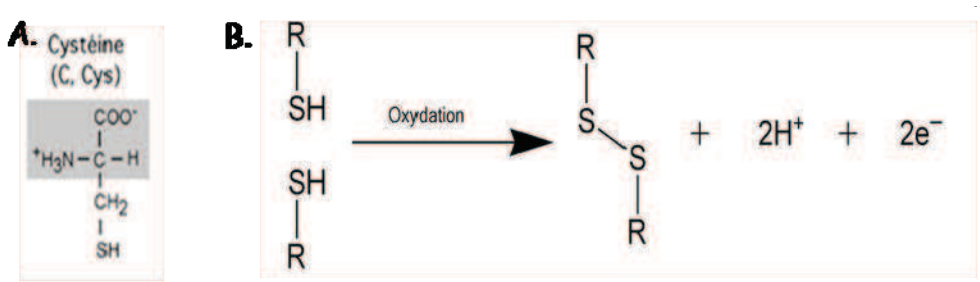

Figure 1. Le résidu cystéinyl

A. Formule chimique de l'acide aminé cystéine. B. Mécanisme schématique de la formation d'un pont disulfure entre deux résidus cystéines.

rant une molécule d'eau et formant une liaison covalente ou liaison cystine entre les deux résidus Cys via leurs atomes de soufre respectifs (Figure 2).

Figure 2. L'oxydation du résidu cystéinyl

Schéma récapitulatif de l'oxydation des résidus cystéine par des composés oxygénés (EAO) ou azotés (RNS). Les éléments XH_2 représentent des réducteurs chimiques ou biologiques tels que le DTT, le glutathion ou des protéines contenant des résidus cystéinyls (Poole *et al.* 2004).

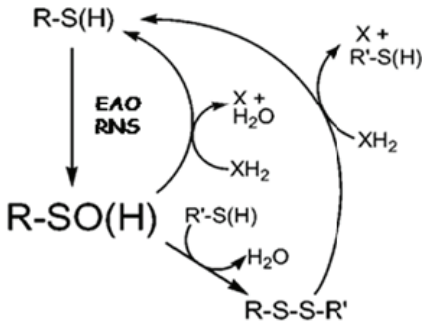

→ Une voie de formation par transfert direct consistant en un échange de pont disulfure s'effectuant entre une protéine donneuse d'électrons dont les cystéines sont sous la forme de thiols et une protéine acceptrice dont les résidus cystéinyls sont sous la forme cystine (Figure 3). Ce phénomène est appelé « échange dithiol/disulfure ».

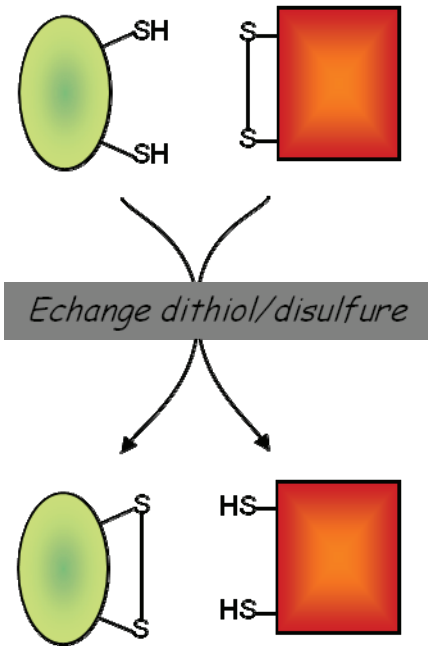

Figure 3. Echange dithiol/disulfure

Représentation schématique d'un échange dithiol/disulfure entre une protéine donneuse (forme ovale) et une protéine acceptrice (rectangulaire) d'électrons.

I.3. Importance des ponts disulfure dans les protéines

Suivant le rôle que jouent les ponts disulfure au sein des protéines, ceux-ci peuvent être classés en trois grands types (Wouters *et al*. 2010):

.Les ponts disulfure structuraux, qui assurent la stabilité des protéines,

.Les ponts disulfure allostériques, dont la formation/réduction modifie la conformation tridimensionnelle de la protéine et modifie ainsi ses fonctions enzymatiques, sans toutefois intervenir directement dans le mécanisme enzymatique de celle-ci,

.Les ponts disulfure catalytiques, qui jouent un rôle dans le mécanisme catalytique de l'enzyme.

I.4. Acteurs des échanges dithiol/disulfure

Les échanges dithiol/disulfure sont réalisés par des protéines appelées « thiol-oxydoréductases ». La grande majorité des thiol-oxydoréductases appartient à la superfamille des thiorédoxines (Trxs). Néanmoins, certaines enzymes appartiennent à d'autres familles de protéines (Ritz & Beckwith 2001; Collet & Bardwell 2002; Ortenberg & Beckwith 2003). C'est le cas des sulfhydryl oxydases, protéines impliquées dans la formation des ponts disulfure dans l'espace inter-membranaire des mitochondries (Herrmann & Köhl 2007). Bien que ces protéines contiennent également des résidus Cys impliqués dans les échanges dithiol/disulfure, leur motif catalytique et surtout leur repliement tridimensionnel sont différents. Ainsi, le fonctionnement de ces protéines est le plus souvent couplé à de petites molécules acceptrices ou donneuses d'électrons telles que le NADPH, le NADH, les flavines (FAD ou FMN), les quinones ou l'acide lipoïque (Ortenberg & Beckwith 2003). Enfin, notons que dans un grand nombre de cas, ces thiol-oxydoréductases sont susceptibles d'interagir avec des protéines de la superfamille des Trxs, comme cela est le cas dans le réticulum endoplasmique (RE), ou dans le périplasme des procaryotes (voir paragraphe V.2.c.) (Frand & Kaiser 1998; Frand & Kaiser 1999; Frand *et al*. 2000).

II. La superfamille des thiorédoxines

Dans ce chapitre nous détaillons certains aspects structuraux mais également fonctionnels des protéines à repliement Trx, une partie de ces informations a été présentée dans un chapitre d'ouvrage « *Glutaredoxin: The Missing Link Between Thiol-Disulfide Oxidoreductases and Iron Sulfur Enzymes* » fourni en annexe (Article 5, Selles *et al*. 2009).

II.1. Un repliement tridimensionnel spécifique

Par définition, les protéines appartenant à la superfamille des Trxs possèdent un ou plusieurs modules ayant un repliement de type Trx (Figure 4) (Carvalho *et al*. 2006; Pan & Bardwell 2006). Cette superfamille regroupe entre autres les Trxs, les glutarédoxines (Grxs), les protéine disulfure isomérases (PDIs), les thiol-peroxydases (Tpxs), les Dsb procaryotiques, les glutathion-S-transférases (GSTs) et les méthionine sulfoxyde réductases (MSR) (Pan & Bardwell 2006; Collet & Messens 2010). La figure 4 nous permet d'illustrer le paradigme de l'appartenance à la superfamille des Trxs. En effet, y sont représentées les structures tridimensionnelles de la Trxh1 (*Arabidopsis thaliana*), de la DsbA (*Escherichia coli*), de la GrxC1 (peuplier), de la Gpx5 (membre de la famille des Tpxs, peuplier), ainsi que de la PDI « classique » (*Saccharomyces cerevisiae*). Il est important de mentionner que les différentes protéines possèdent des similarités structurales alors que les séquences primaires peuvent présenter un très faible taux d'identité (Figure 4). Les deux seuls acides aminés strictement conservés sont la Cys catalytique en amont d'une hélice-α et une proline en configuration *cis* en amont d'un brin-β.

II.2. Caractéristiques structurales

La configuration minimale du repliement Trx consiste en un arrangement de quatre brin-β antiparallèles, formant le « cœur » de la protéine, entourés de trois hélices-α (Holmgren *et al*. 1975; Capitani *et al*. 2000; Peterson *et al*. 2005; Gruber *et al*. 2006; Collet & Messens 2010) (Figure 5). Le centre actif des protéines de la superfamille des Trxs est localisé au début de l'hélice-α1 (Ren *et al*. 2009; Pan & Bardwell 2006) (Figures 5). Il est généralement constitué de deux résidus Cys séparés par deux acides aminés variables et communément représenté sous la forme CxxC (Holmgren 1968; Shi *et al*. 1999; Kadokura *et al*. 2003). Comme nous pouvons le constater sur la figure 5, dans cette configuration, la Cys en position N-terminale (cystéine catalytique ou Cys_C) est exposée au solvant et est susceptible de réaliser des attaques nucléophiles (Kelley & Richards 1987; Peterson *et al*. 2005; Tian *et al*. 2006; Koh *et al*. 2007). La seconde Cys en position C-terminale est appelée cystéine de recyclage (Cys_R) et se trouve en général plus enfouie, tout du

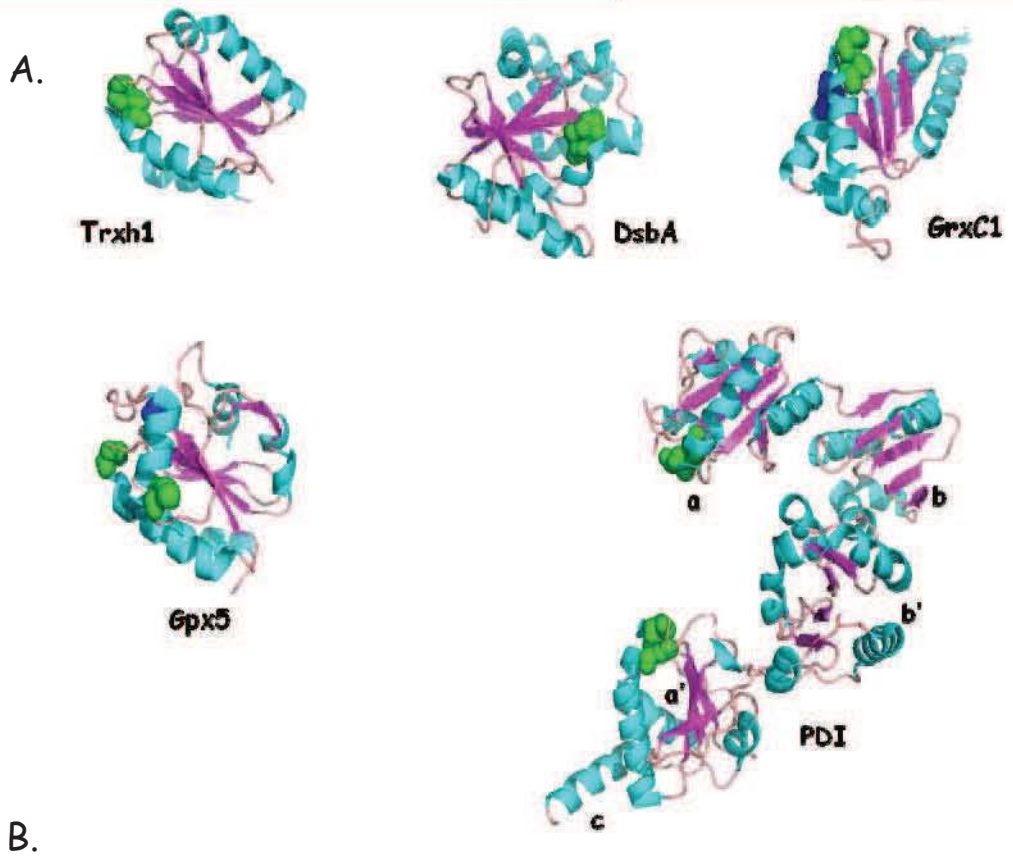

B.

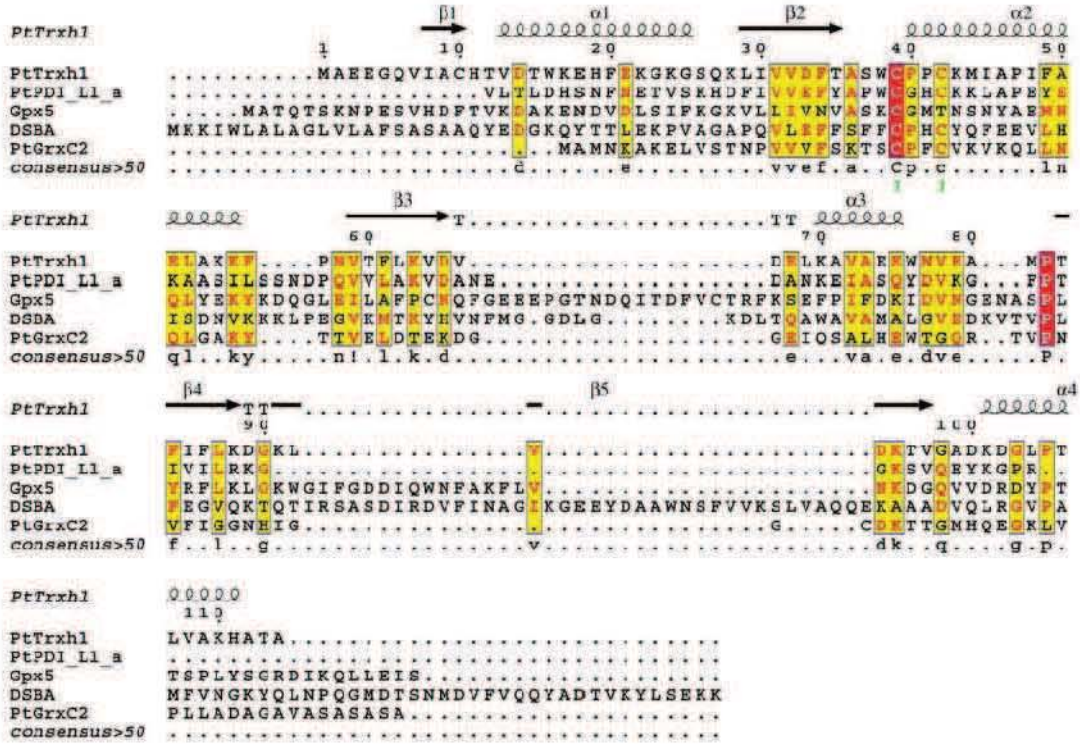

Figure 4. Le repliement thiorédoxine.

A. Représentation des structures tridimensionnelles des protéines PtTrxh1, EcDsbA, PtGrxC1, ScPDI1.1 et PtGpx5. Les sphères vertes représentent les résidus Cys impliqués dans les mécanismes catalytiques et les sphères bleues, les résidus Cys additionnels. Les indications « a », « b », « b' », « a' » et « c » mentionnées au niveau de la structure de la PDI classique de Saccharomyces représentent les modules composant la protéine. B. Alignement des séquences peptidiques des protéines PtTrxh1, PtGpx5, EcDsbA, PtGrxC2 ainsi que la séquence du module « a » de la PDI classique du peuplier.

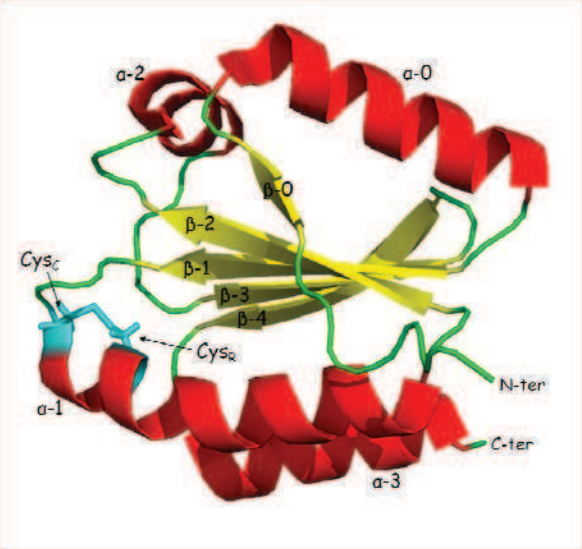

Figure 5. Structure tridimensionnelle de la protéine Trxh1 d'*Arabidopsis thaliana*, sous sa forme oxydée.

Les extrémités N-terminale et C-terminale de la protéine sont indiquées (respectivement N-ter et C-ter). Les deux Cys, en cyan, sont indiquées Cys_C et Cys_R, respectivement catalytique et résolutive. La numérotation des structures secondaires tient compte du minimum de structure requis pour le repliement Trx. Ainsi la première hélice-α et le premier brin-β sont numérotés « α-0 » et « β-0 » (PDB 1XFL; Peterson *et al.* 2005).

moins dans la forme réduite de l'enzyme. Ces deux appellations découlent directement de leurs rôles respectifs dans les mécanismes d'oxydoréduction (Figure 6) (Brandes *et al*. 1993; Navrot *et al*. 2006).

Une autre caractéristique structurale partagée par tous les membres de cette superfamille est la présence d'une proline (Pro) en configuration *cis* localisée en amont du brin-β3, l'un des consti-

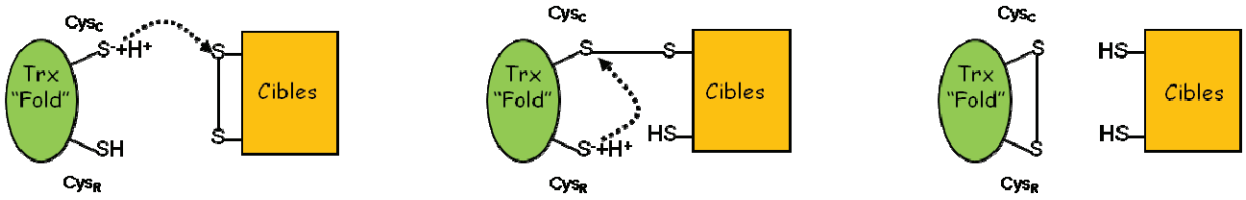

Figure 6. Schéma représentatif de l'action des cystéines catalytique (Cys_C) et résolutive (Cys_R).

La Cys_c effectue une attaque nucléophile sur le disulfure d'un substrat oxydé, pour former un disulfure intermoléculaire. La cystéine résolutive va ensuite réduire ce disulfure intermoléculaire pour aboutir à la libération du substrat sous forme réduite.

tuants du feuillet β (Peterson *et al*. 2005; Gruber *et al*. 2006; Ren *et al*. 2009). La proline est un acide aminé particulier: sa chaîne latérale, cyclique (un anneau pyrrolidone) est liée à la fois au groupe α-carboxyle et au groupe α-aminé formant ainsi une amine secondaire (Figure 7). Cette particularité a une incidence structurale. En effet, la présence de la Pro en conformation *cis* induit la formation d'un « coude » dans la chaîne polypeptidique (Figure 7). Il a été démontré que

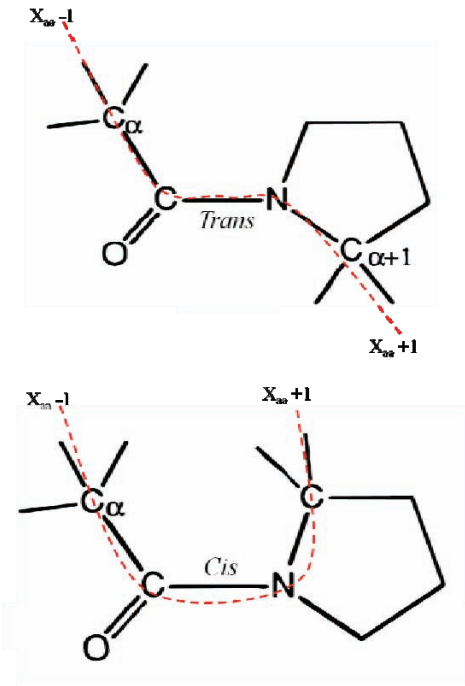

Figure 7. Le résidu proline.

Représentation schématique des conformations *trans* et *cis* de la proline. Les acides aminés précédant et suivant la proline sont indiqués par X_{aa}-1 et X_{aa}+1, respectivement. En rouge est schématisée la trajectoire de la chaîne polypeptidique autour de la proline (Schmid, 1993).

cette *cis* Pro conservée jouait un rôle dans la conformation de la protéine mais également dans la reconnaissance du substrat ainsi que dans le mécanisme catalytique (Kelley & Richards 1987; Charbonnier *et al*. 1999; Georgescu *et al*. 1998; Maeda *et al*. 2006).

II.3. Caractéristiques oxydoréductrices

Les membres de la superfamille des Trxs sont impliqués dans des processus d'échanges dithiol/disulfure via leurs résidus Cys. Nous allons détailler les facteurs déterminants de leurs activités oxydoréductrices (Pan & Bardwell 2006).

II.3.a. Le pKa de la cystéine catalytique

La sensibilité des Cys vis-à-vis de l'oxydation dépend très largement de leurs *pKa*. Le *pKa* d'une Cys isolée est de 8,3 unités pH ce qui signifie qu'à un pH de 8,3 la moitié du pool de Cys est sous forme déprotonée (S^-) (Poole *et al*. 2004; Mamathambika & Bardwell 2008). Cette forme déprotonée (ou thiolate) est la forme la plus réactive. Ainsi, on peut facilement comprendre que deux facteurs entrent en jeu dans la détermination de la réactivité de la Cys catalytique. Le *pKa*, qui, à un pH donné, définira la proportion de forme thiolate et de forme thiol et le pH, qui pour un *pKa* donné, définira la proportion de forme thiolate et de forme thiol. *In vivo*, la solution « adoptée » par toutes les protéines à repliement Trx, permettant un pool de thiolate important des Cys catalytique à pH physiologique, est de présenter un *pKa* faible compris entre 3 et 7, tandis que la Cys de recyclage possède un *pKa* avoisinant 8, plus proche des Cys « dénaturées » (Jeng

et al. 1998; Holmgren & Björnstedt 1995; Chivers *et al*. 1997b; Ma *et al*. 2007; Mamathambika & Bardwell 2008).

II.3.b. Le potentiel d'oxydoréduction du pont disulfure entre la Cys catalytique et la Cys de recyclage

Le potentiel oxydoréducteur d'un pont disulfure est une valeur empirique, déterminée à un pH et une température donnée et exprimée en volts permettant d'évaluer la proportion relative de cystines (-S-S-) ou de formes thiol (-S-H/-S-H) dans une protéine donnée. Le potentiel redox est déterminé suivant l'équation de Nernst par comparaison avec un couple de référence tel le couple glutathion réduit/glutathion oxydé (GSH/GSSG) (-240 mV à pH7). La valeur du potentiel redox entre deux résidus Cys détermine quelles réactions sont thermodynamiquement favorisées dans un environnement oxydoréducteur particulier. Cet environnement oxydoréducteur est défini par un équilibre dynamique et contrôlé de façon précise, ayant pour but d'établir l'équilibre

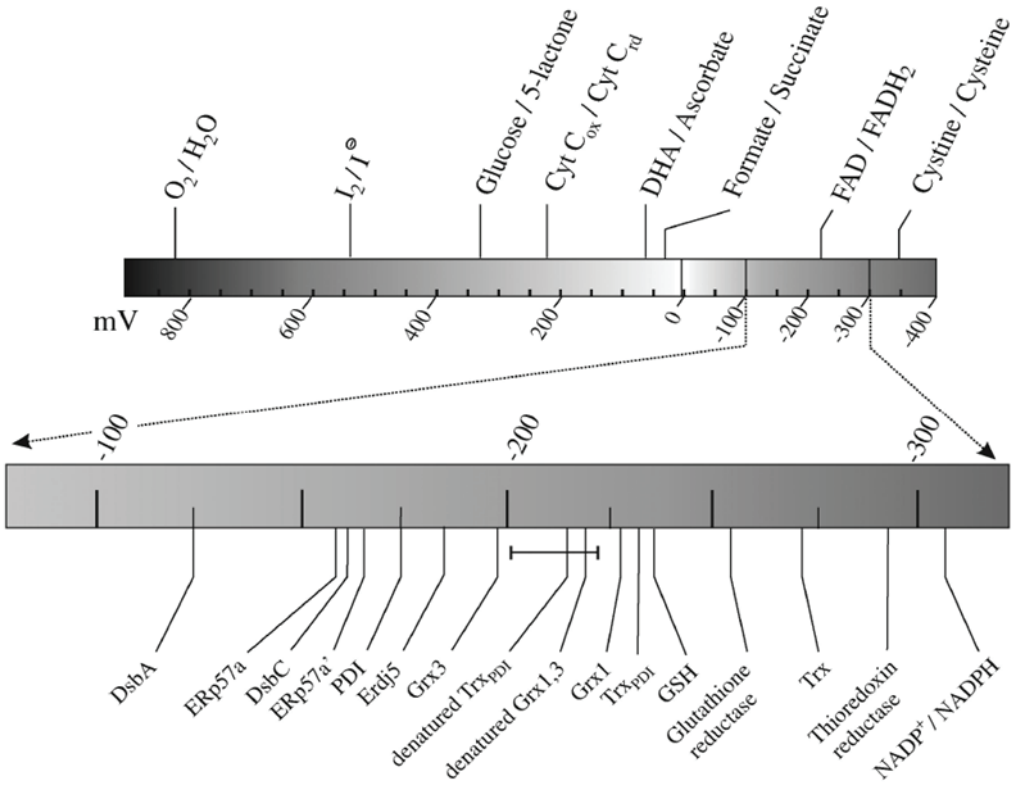

Figure 8. Schéma représentant les potentiels d'oxydoréduction des motifs CxxC de certains membres de la superfamille des Trxs catalysant des échanges dithiol/disulfure.

Sur la gauche du panneau, sont représentés les potentiels redox de protéines réalisant des réactions d'oxydation entre -100 et -200 mV alors que sur la droite sont mentionnés les potentiels redox des protéines catalysant des réactions de réduction de ponts disulfure (entre -200 et -300 mV). Les valeurs de potentiels redox pour DsbA et DsbC, Grx1 et Grx3, « denatured » Grx1 et 3 ainsi que Trx proviennent d'études menées sur *E. coli*. La valeur reportée pour la glutathion réductase provient d'une étude sur la levure *Saccharomyces cerevisiae*. Les valeurs pour la thiorédoxine réductase, ERdj5, PDI, ERp57, ERp57a et ERp57a' proviennent d'études menées sur les protéines humaines. Enfin la mention Trx_{PDI} fait référence à la Trx d'*E. coli* dont le site actif CGPC a été substitué par la séquence CGHC (Hatahet *et al.* 2009).

oxydoréducteur adéquat dans chaque compartiment cellulaire (Meyer & Dick 2010). Au sein de la cellule les différents compartiments cellulaires présentent des environnements redox différents (Meyer *et al*. 2007). Le cytosol est un environnement réducteur, présentant un potentiel redox aux alentours de -300 mV du fait de la présence de systèmes pourvoyeurs de pouvoir réducteur tels que les systèmes Trx ou Grx (Björnberg *et al*. 2006; Meyer *et al*. 2007). D'autre part, il existe au sein des cellules des compartiments plus oxydants tels que l'espace inter-membranaire des mitochondries, le réticulum endoplasmique présent chez les eucaryotes ou le périplasme chez les procaryotes (Hwang *et al*. 1992; Meyer *et al*. 2007). A pH physiologique, les ponts disulfure présents au niveau des sites actifs des protéines de la superfamille des Trxs couvrent une gamme de potentiels redox très large, pouvant aller de -122 mV jusqu'à -314 mV, pH 7,0) (Zapun *et al*. 1993; Collin *et al*. 2003; Pan & Bardwell 2006; Hatahet *et al*. 2009) (Figure 8). D'après l'équation de Nernst, les électrons, et de façon concomitante les protons H^+, suivent les potentiels redox croissants (du plus électronégatif vers le moins électronégatif). Ainsi, suivant le compartiment cellulaire où ils seront adressées et le potentiel redox de leurs ponts disulfure, les membres de la superfamille des Trxs présenteront un site actif majoritairement sous forme dithiol ou sous forme disulfure. Ce statut réduit (thiol) ou oxydé (disulfure) des sites actifs est des plus importants car il déterminera *in vivo* la capacité de la protéine à donner ou recevoir des électrons.

II.3.c. Impact des structures primaire, secondaire et tertiaire sur les caractéristiques redox

Au sein du repliement Trx, les deux caractéristiques que nous venons de décrire sont inter-dépendantes l'une de l'autre et sont fortement influencées par leurs microenvironnements dans la protéine (Wouters *et al*. 2010). Un des facteurs les plus étudiés concernant la relation *pKa*/ potentiel d'oxydoréduction est la nature des acides aminés variables du motif CxxC. Par exemple, une étude de mutagenèse dirigée sur la Trx1 d'*E. coli* a permis de montrer que différentes substitutions des acides aminés du site actif induisent une augmentation du potentiel redox. Cette augmentation est couplée à une diminution du *pKa* de la Cys catalytique (Chivers *et al*. 1997a; Mössner *et al*. 1998) (Figure 9A). Un des autres facteurs étudié a été l'acide aminé en position -1 de la *cis* Pro (Ren *et al*. 2009). Comme nous l'avons déjà mentionné, en conformation *cis* cette Pro induit la formation d'un « coude » qui, bien qu'étant éloigné du site actif dans la structure primaire, est proche de celui-ci dans la structure tridimensionnelle (Peterson *et al*. 2005; Gruber *et al*. 2006; Ren *et al*. 2009). Il a été démontré que cet acide aminé en position -1 pouvait entrer en interaction avec la Cys catalytique via des liaisons hydrogène ou hydrophobe et ainsi moduler son

pKa mais également le potentiel redox du pont disulfure (Ren *et al*. 2009) (Figure 9B). L'ensemble de ces informations indique que les caractéristiques oxydoréductrices des protéines de la superfamille des Trx sont gouvernées par deux principaux facteurs, le potentiel d'oxydoréduction du pont disulfure et le *pKa* de la Cys catalytique. Cependant, il a été démontré que le potentiel d'oxydoréduction présentait également une composante pH indépendante, c'est-à-dire indépendante du *pKa* de la Cys catalytique, laissant supposer une plus grande complexité dans l'origine des caractéristiques redox des protéines à repliement Trx (Chivers *et al*. 1997a; Wouters *et al*. 2010).

A. C_c-X_{aa}-X_{aa}-C_r

Nature des X_{aa}	Gly-Pro	Gly-His	Pro-His	Pro-Tyr
Potentiel redox du disulfure	-270	-221	-204	-194
pKa de la Cys_C	7.1	6.3	6.1	5.9

B. X_{aa}-*cis*P

	DsbA		Trx		DsbC	
Nature du X_{aa}	Val-Pro	Thr-Pro	Ile-Pro	Thr-Pro	Thr-Pro	Val-Pro
Potentiel redox du disulfure (mV)	-120	-92	-271	-226	-143	-195
pKa de la Cys_C	3.3	3.5	7	5.5	4.6	5.8

Figure 9. Impact des modifications des séquences primaires sur les caractéristiques redox des protéines à repliement Trx.

A. Illustration des modifications du potentiel redox ainsi que du *pKa* de la cystéine catalytique par substitution des acides aminés variables du motif *CxxC* chez *E. coli* Trx1. B. Illustration des modifications du potentiel redox ainsi que du *pKa* de la cystéine catalytique des motifs par substitution de l'acide aminé en position -1 de la *cis* proline (Mossner *et al*. 1998, Ren *et al*. 2009).

II.4. Les réactions catalysées

Il est communément admis que les réactions catalysées par les protéines à repliement Trx, peuvent en partie dépendre de leur environnement oxydoréducteur. En effet, en fonction du compartiment subcellulaire dans lequel les protéines sont adressées, leur activité peut être modulée. Néanmoins, il a été démontré chez la bactérie *E. coli* ou la levure S. *cerevisiae* que l'environnement oxydoréducteur n'était pas le seul facteur déterminant de l'activité des protéines (Chivers *et al*. 1996; Debarbieux & Beckwith 1998; Jonda *et al*. 1999; Debarbieux & Beckwith 2000). Des expériences de mutagenèse dirigée et d'adressage des protéines Trx1 et DsbA d'*E. coli* montrent que la protéine Trx1 adressée dans le périplasme ne peut que modérément complémenter un mutant *DsbA*. Par contre, ces auteurs ont également montré que la substitution du site actif de la Trx1 par celui de DsbA (CGPC vers CPHC) complémente totalement la délétion de DsbA (Debarbieux & Beckwith 1998; Jonda *et al*. 1999).

Dès lors, il semble clair que les aspects, que nous venons de décrire concernant les facteurs et les

caractéristiques redox des protéines à repliement Trx, sont importants dans les réactions que seront en mesure de catalyser ces protéines. Ainsi chaque famille de protéines à repliement Trx présente des caractéristiques spécifiques des réactions qu'elles sont en mesure de réaliser dans les cellules.

Il existe trois grands types de réactions catalysées par les protéines de la superfamille des Trxs (Figure 10) :

A. Les réactions de formation des ponts disulfure qui consistent à introduire un pont disulfure entre deux résidus Cys (Figure 10A),

B. Les réactions de réduction des ponts disulfure qui consistent à passer d'une forme cystine à une forme dithiol (Figure 10B),

C. Les réactions d'isomérisation des ponts disulfure qui concernent des protéines ayant plusieurs résidus Cys qui peuvent se présenter sous différentes combinaisons. Dans ce cas, l'isomérisation permet de passer d'une combinaison à une autre (Figure 10C).

Nous allons maintenant détailler certaines familles de protéines impliquées dans chaque type de réaction, mais également les protéines associées, nécessaires à leur fonctionnement.

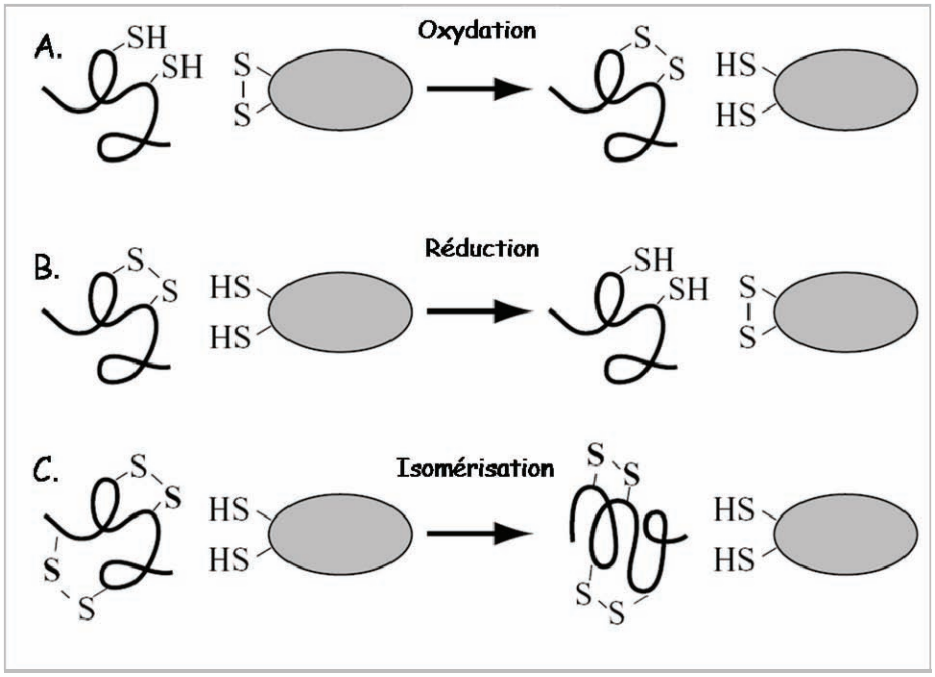

Figure 10. Représentation des réactions catalysées par les protéines de la superfamille des Trxs.
La protéine à repliement Trx est représentée par une sphère avec ses deux résidus cystéine sous forme réduite (SH/SH) ou oxydée (S-S). A. Réactions d'oxydation : la protéine à repliement Trx transfère son pont disulfure à une cible réduite. B. Réactions de réduction. C. Réactions d'isomérisation: la protéine à repliement Trx, sous forme réduite, modifie les combinaisons de disulfures sur des substrats contenant plusieurs résidus cystéine.

III. Les systèmes réducteurs impliquant des protéines à repliement thiorédoxine, exemple du système thiorédoxine

Deux grands types de systèmes réducteurs coexistent dans les cellules: le système thiorédoxine et le système glutarédoxine. Je vais principalement décrire le système Trx, cependant deux articles présentés en annexe de ce manuscrit détaillent certains aspects du système Grx (Chibani *et al*. 2010; Selles *et al*. 2009).

Les Trxs sont de petites protéines avoisinant généralement les 13 kDa initialement identifiées chez *E. coli* et impliquées dans la réduction de ponts disulfure. Comme pour la plupart des protéines à repliement Trx, cette réaction d'oxydoréduction se fait par l'intermédiaire de deux Cys présentes au niveau de leur site actif de type CxxC. Dans les Trx « classiques » possédant un site actif conventionnel, les deux acides aminés séparant les deux cystéines correspondent à une glycine (Gly) et à une proline (Pro) donnant un site actif de la forme Cys-Gly-Pro-Cys (Holmgren 1968; Jacquot *et al*. 1990; Capitani *et al*. 2000).

III.1. Une famille multigénique

Au sein des organismes non photosynthétiques, il existe généralement deux ou trois isoformes de Trxs. Chez *S. cerevisiae*, trois isoformes ont été décrites (deux cytoplasmiques et une mitochondriale), tandis que chez l'homme l'équipement en Trx se compose uniquement de deux isoformes (une cytoplasmique et l'autre mitochondriale) (Vlamis-Gardikas *et al*. 2002). Chez les organismes photosynthétiques, il existe un grand nombre d'isoformes de Trxs allant de huit chez l'algue unicellulaire *Chlamydomonas reinhardtii* à 24 chez le peuplier *Populus trichocarpa* (Chibani *et al*. 2009). De plus, les organismes photosynthétiques, et particulièrement les plantes supérieures, présentent des Trxs "atypiques" possédant des variations de séquence au niveau de leur site actif et/ou des domaines additionnels (Chibani *et al*. 2009). Si l'on considère ces séquences dites "atypiques", le groupe des Trxs végétales augmente de façon significative passant d'une vingtaine à plus de 40 représentants (Chibani *et al*. 2009).

Les Trxs dites "classiques" peuvent êtres regroupées en 7 classes, les Trxs *f*, *m*, *x*, *y* et *z* qui sont des protéines chloroplastiques, les Trxs *o* mitochondriales et les Trx *h* qui sont présentes dans différents compartiments subcellulaires comme le cytoplasme, les mitochondries, le réticulum endoplasmique ou le noyau (Gelhaye *et al*. 2005; Chibani *et al*. 2009; Meyer *et al*. 2009; Marchand *et al*. 2010; Chibani *et al*. 2011). Les Trx "atypiques", quant à elles, regroupent

les Trxs *CXXS*, *like*, *lilium*, *Clot*, *CDSP32* (pour « Chloroplastic Drought-induced Stress Protein of 32 kDa »), *HCF164* (pour « high chlorophyll fluorescence mutant »), *TDX* (pour « tetratricopeptide domain-containing thioredoxin ») et *NRX* (pour « nucleoredoxin ») (Chibani *et al*. 2009). Ainsi, chez les organismes photosynthétiques, il existe une grande variété de Trxs et parfois même une forte redondance apparente de celles-ci au sein d'un même compartiment cellulaire. Une des explications proposées est la spécificité des isoformes des Trxs vis-à-vis de leurs partenaires physiologiques aboutissant à une spécificité fonctionnelle de chacun des représentants de cette famille.

III.2. Sources de pouvoirs réducteurs

A la fin de la réaction de réduction réalisée par les Trxs, celles-ci se trouvent dans un état oxydé avec les deux Cys de leur site actif sous forme de cystine (voir figure 7). Pour pouvoir à nouveau réduire une protéine cible, les Trxs doivent être recyclées via un donneur d'électrons. Suivant le compartiment cellulaire, le pourvoyeur d'électrons des Trxs sera de différente nature. Deux systèmes réducteurs principaux des Trxs coexistent au sein des cellules végétales, le système NADPH/NADPH-thiorédoxine réductase (NTR)/Trx (Figure 11A) et le système ferrédoxine (Fdx)/ferrédoxine-thiorédoxine réductase (FTR)/Trx (Figure 11B) (Laurent *et al*. 1964; Schürmann & Jacquot 2000; Gelhaye *et al*. 2005).

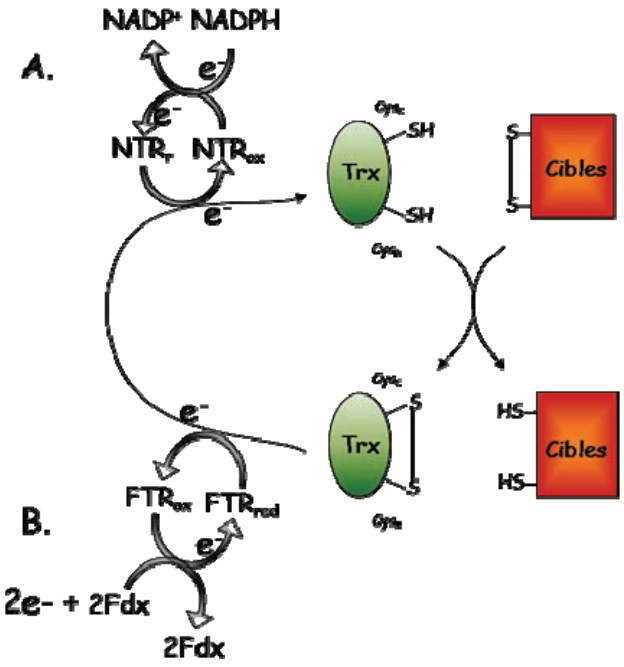

Figure 11. Les 2 principaux systèmes de régénération des thiorédoxines végétales.

A. Le système NADPH thiorédoxine réductase (NTR). B. Le système ferrédoxine/ferrédoxine-thiorédoxine réductase (Fdx/FTR).

Le NADPH va servir de donneur d'électrons pour la NTR. Cette enzyme appartient à la famille des pyridine-disulfure oxydoréductases au même titre que la lipoamide déshydrogénase, la glutathion réductase ou la mercurique réductase. La NTR est une protéine ubiquitaire présente des procaryotes aux eucaryotes supérieurs et possédant la particularité de pouvoir transférer les électrons provenant du NADPH aux Trxs via leur cofacteur flavine et un motif disulfure (Figure 12) (Lennon *et al*. 2000; Williams *et al*. 2000; Serrato *et al*. 2002). Il existe deux types de protéines NTRs qui se différencient par plusieurs facteurs, une protéine dite de haut poids moléculaire (2 sous-unités identiques d'environ 55 kDa) que l'on retrouve chez les systèmes animaux et les algues et une protéine dite de faible poids moléculaire (2 sous-unités identiques d'environ 35 kDa) que l'on retrouve chez les plantes, les champignons et les procaryotes (Arscott *et al*. 1997). Ces deux types de NTR sont actives sous forme homo-dimériques, cependant elles peuvent se distinguer, en plus de leur différence de taille, par la nature des interfaces entre chacune des deux

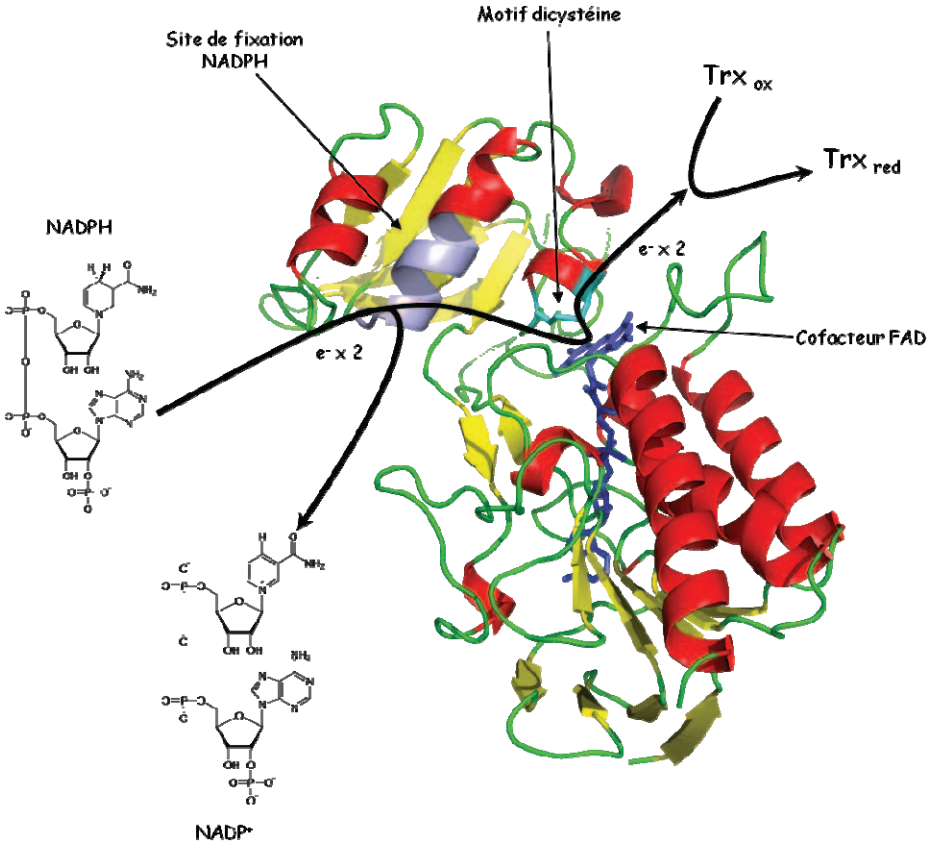

Figure 12. Structure tridimensionnelle et trajet des électrons au sein de l'isoforme B de la NTR) *d'A. thaliana* (PDB 1VDC).

La NTR est constituée de deux modules protéiques : le premier est responsable de la fixation du NADPH et le second de la fixation du cofacteur FAD (représenté en bâtonnets bleu). Lors de la fixation du NADPH sur la portion d'hélice-a représentée en violet, un pivotement des deux modules s'opère permettant la réduction du FAD par le NADPH, aboutissant à la formation de $NADP^+$ et de $FADH_2$. Par la suite le $FADH_2$ va transférer ses électrons au motif dicystéine (représenté en bâtonnets cyan) qui sera responsable de la réduction de la Trx oxydée.

sous-unités ainsi que par la présence d'une sélénocystéine dans les NTR de haut poids moléculaire (Arscott *et al*. 1997; Williams *et al*. 2000). Chez les organismes photosynthétiques, tels que *A. thaliana,* qui possèdent une NTR de faible poids moléculaire, deux isoformes sont généralement présentes, *At*NTRA et *At*NTRB. Ces isoformes réalisent la réduction des Trxs au niveau du cytoplasme et de la mitochondrie (Reichheld *et al*. 2007). Toutefois, plusieurs études, génétiques et biochimiques, ont mis en évidence l'existence d'une voie alternative de réduction de certaines Trx h par l'intermédiaire du glutathion et/ou des glutarédoxines (Gelhaye *et al*. 2003; Reichheld *et al*. 2007).

Le second système de réduction des Trxs trouve sa source de pouvoir réducteur au niveau de la chaîne de transport d'électrons chloroplastique, et plus particulièrement au niveau du photosystème I (PSI) (Figure 13) (Buchanan *et al*. 2002; Schürmann & Buchanan 2008). Les électrons du PSI vont transiter *via* deux intermédiaires pour finalement être acceptés par la Trx. Le premier de ces intermédiaires est la Fdx, petite protéine soluble de 10 kDa et présente dans le stroma des chloroplastes. Cette protéine présente la particularité de posséder un cofacteur métallique, un centre [2Fe-2S], qui transporte les électrons provenant directement du PSI, grâce notamment à un potentiel oxydoréducteur extrêmement bas (environ -420 mV à pH 7,0) (Schürmann & Buchanan 2008). Le second intermédiaire est la FTR. Cette protéine est active sous forme hétérodimérique, comprenant une sous-unité catalytique ayant un cofacteur métallique [4Fe-4S] ainsi que deux résidus Cys pouvant former un pont disulfure et une sous-unité dite variable qui est essentielle à l'assemblage de la protéine mais dont la fonction est aujourd'hui encore inconnue (Staples *et al*. 1996; Staples *et al*. 1998; Dai *et al*. 2000; Keryer *et al*. 2004). La sous-unité catalyti-

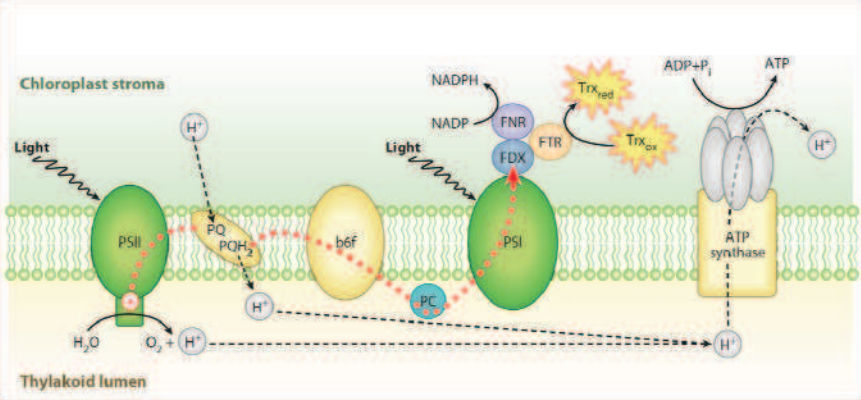

Figure 13. *Contexte physiologique de la réduction des Trxs par le système Fdx/FTR.*
En rouge est représenté le trajet des électrons au travers des différents composants de la chaîne chloroplastique de transport des électrons. Abréviations : photosystème II (PSII), plastoquinone (PQ), plastoquinone réduite (PQH_2), cytochrome b6f (b6f), plastocyanine (PC), photosystème I (PSI), ferrédoxine (FDX), ferrédoxine NADP réductase (FNR), ferrédoxine thiorédoxine réductase (FTR).

que est une petite protéine de 13 kDa, dont la séquence primaire est extrêmement conservée chez tous les organismes photosynthétiques, tandis que la sous-unité variable peut présenter de notables variations de séquence entre les espèces (Keryer *et al*. 2004). Le principe de la réduction de la Trx par le système Fdx/FTR est le suivant : la Fdx va capter un électron au niveau du PSI et le transmettre à la FTR, provoquant la réduction d'un pont disulfure sur celle-ci (Figure 14A). Un des résidus Cys de la FTR libéré du disulfure va alors attaquer le pont disulfure de la Trx oxydée et former ainsi un complexe Trx/FTR lié de façon covalente (Figure 14B). Un second électron fourni par la Fdx à la FTR permettra de réduire le complexe Trx/FTR libérant la Trx sous forme réduite (Figure 14C).

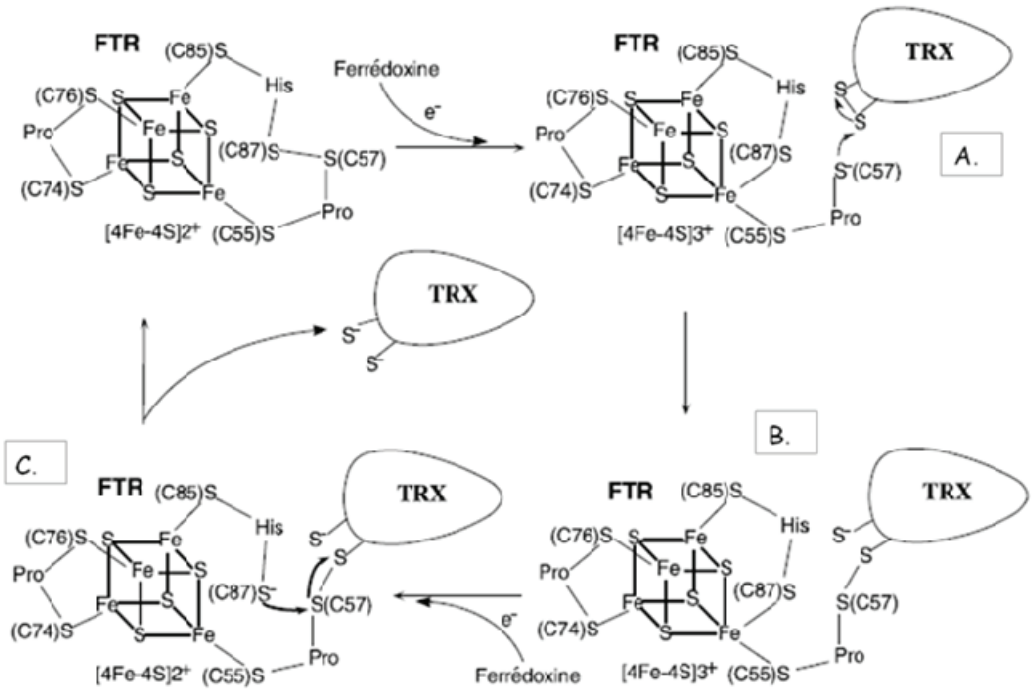

Figure 14. Mécanisme catalytique de la réduction de la thiorédoxine par le système Fdx/FTR. Les étapes du mécanisme sont détaillées dans le texte (Dai *et al*. 2007).

III.3. Partenaires, fonctions et systèmes de régulation au sein de la cellule

Les premières études sur les Trxs d'*E. coli* ont permis de mettre en évidence leur rôle dans la réduction des ponts disulfure de la ribonucléotide réductase (RNR), de la MSR, et aussi de la 3'-phosphoadénosyl sulfate réductase (PAPS réductase). Ainsi chez *E. coli*, les Trxs sont respectivement impliquées dans la biosynthèse des nucléotides, dans la réparation des dommages causés aux protéines par un stress oxydant ainsi que dans l'assimilation du sulfate (Laurent *et al*. 1964; Holmgren 1976; Arnér & Holmgren 2000; Vlamis-Gardikas *et al*. 2002). Chez les plantes, les Trx ont été découvertes lors de l'étude de la régulation du cycle de Calvin dans les phases

« d'éclairement » et « d'obscurité ». En particulier, des études portant sur des chloroplastes isolés d'épinard ont permis de montrer que plusieurs enzymes du cycle de Calvin sont régulées par la lumière de façon « redox dépendante », faisant intervenir trois facteurs, la Fdx, la FTR ainsi que la Trx (Droux *et al*. 1987).

Les Trxs peuvent réaliser deux types de régulation redox sur leurs partenaires physiologiques,

i) une réduction de ponts disulfure impliqués dans leur activité catalytique, essentielle à la régénération de la cible. C'est le cas par exemple des Tpxs et des MSRs, deux familles de protéines impliquées dans la réponse au stress oxydant et dans la détoxication des espèces actives de l'oxygène (EAOs)(Figure 15A) (Rouhier & Jacquot 2002; Broin & Rey 2003; Collin *et al*. 2003; Schürmann & Buchanan 2008; Tarrago *et al*. 2010).

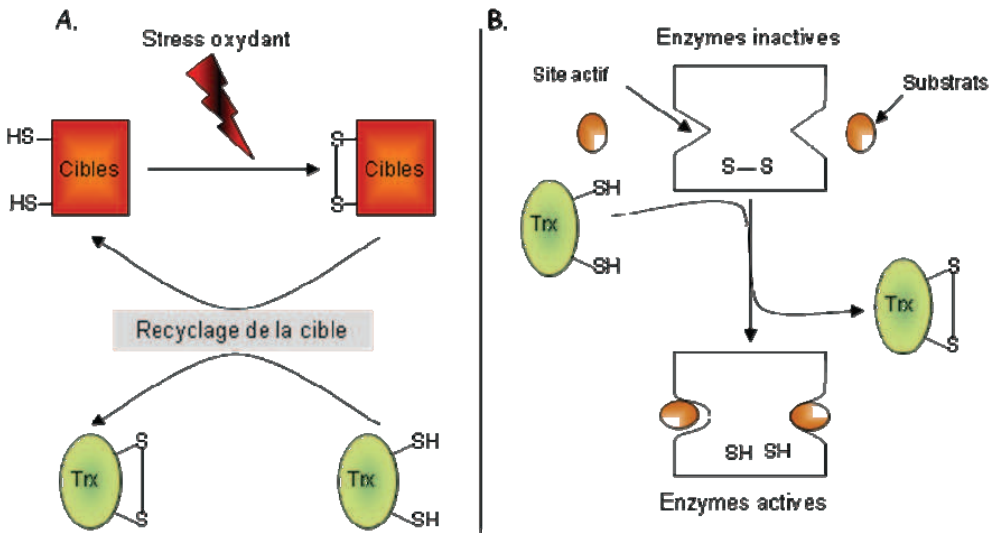

Figure 15. Les régulations redox réalisées par les thiorédoxines.
A. Recyclage de cibles en réponse à un stress oxydant. B. Régulation de l'activité des protéines par réduction d'un pont disulfure des enzymes hystérétiques.

ii) une réduction de ponts disulfure n'entrant pas dans le mécanisme catalytique de la cible mais affectant l'activité de celle-ci par modification de sa structure tridimensionnelle (cas de la malate déshydrogénase à NADP (MDH-NADP) et de la fructose-1,6-bisphosphatase (FBPase)) (Figure 15B) (Jacquot *et al*. 1984; Crawford *et al*. 1986; Johnson *et al*. 1987; Broin & Rey 2003; Meyer *et al*. 2009). Ces deux protéines sont de nature hystérétique, c'est-à-dire que leur vitesse de réduction est beaucoup plus lente que leur vitesse de catalyse. Dans ces protéines, la réduction d'un pont disulfure va induire un changement conformationnel nécessaire à la génération d'une enzyme pleinement active (Figure 15B) (Dai *et al*. 2004). C'est le cas semble t-il de la plu-

part des enzymes du cycle de Calvin (Lemaire *et al*. 2007). On peut également noter l'implication des Trxs dans l'activation allostérique de l'oxydase alternative au niveau de la chaîne de transport d'électrons mitochondriale (Umbach & Siedow 1993; Moore *et al*. 1995; Gelhaye *et al*. 2004).

Depuis ces premières découvertes, un grand nombre de protéines cibles et de processus physiologiques faisant intervenir des Trxs ont été caractérisés (Broin & Rey 2003; Meyer *et al*. 2009; Montrichard *et al*. 2009). Des études protéomiques ont rapporté plus de 500 cibles potentielles pour les Trxs végétales mais seules quelques cibles putatives ont pu être caractérisées comme telles ou confirmées *in vitro* (Balmer *et al*. 2004; Montrichard *et al*. 2009).

L'activité des Trxs peut elle-même être modifiée indirectement par la régulation de leur système de régénération. De plus, il a montré que certaines isoformes de Trxs peuvent avoir leur activité modulée par glutathionylation. La glutathionylation est une modification post-traductionnelle aboutissant à la liaison d'une molécule de glutathion sur un résidu Cys de la protéine, via une liaison covalente entre deux atomes de soufre. La glutathionylation peut résulter de plusieurs réactions dont les deux suivantes sont vraisemblablement les plus répandues:

.La réaction entre un thiol et une molécule de glutathion oxydé (GSSG) ou de nitrosoglutathion (GSNO)

.La réaction peut être la plus efficace et la plus répandue au sein des cellules vivantes se produit entre du glutathion sous forme réduite (GSH) et un pont disulfure ou une cystéine oxydée sous forme d'acide sulfénique par une espèce oxydante.

La glutathionylation a été démontrée comme étant un processus de régulation de l'activité des Trx de classe *f* ainsi que de certaines isoformes de classe *h* (Gelhaye *et al*. 2004; Michelet *et al*. 2005). Les Trxs de la classe *f* présentent la particularité de posséder une Cys additionnelle en partie C-terminale par rapport au site actif WCGPC, et il a été démontré que la liaison de glutathion sur cette Cys conduit à une forte diminution de son activité (Dai *et al*. 2004; Michelet *et al*. 2005).

IV. Rôle des thiol-peroxydases, protéines à repliement thiorédoxine, dans la réponse au stress oxydant

IV.1. Définition d'un stress oxydant

Dans des conditions physiologiques optimales, les organismes aérobies produisent des formes activées de l'oxygène (FAO). Ces FAOs peuvent être classées en trois grandes familles, les espèces activées de l'oxygène (EAO), les espèces nitrées réactives (ENR) et les espèces halogénées réactives (EHR) (Tableau 1). Ces FAOs étant produites de façon basale au sein des cellules vivantes, la régulation de leur concentration est un facteur essentiel à la définition d'un stress oxydant. Les niveaux de FAOs au sein des cellules sont donc directement dépendants des niveaux de production et des mécanismes de détoxication (Delaunay *et al*. 2002; Foyer & Noctor 2005; Halliwell & Gutteridge 2007; Moller *et al*. 2007) (Figure 16A). Un contrôle fin de l'homéostasie de ces espèces garantit une croissance et activité métabolique optimale des organismes. Cependant celle-ci peut être fortement modifiée lors d'un stress biotique ou abiotique conduisant à une accumulation d'espèces oxydantes et donc à ce que l'on définit comme un stress oxydant (Figure

Entités oxygénées réactives	
- Radicaux	- Non radicaux
Superoxyde $O_2^{\cdot-}$ Hydroxyle $OH^{\cdot}$ Peroxyle $RO_2^{\cdot}$ Alcoxyle $RO^{\cdot}$ Hydroperoxyle $HO_2^{\cdot}$	Peroxyde d'hydrogène H_2O_2 Acide hypochloreux HOCl † Ozone O_3 Oxygène singulet O_2* Acide hypobromeux HOBr †
Entités nitrées réactives	
- Radicaux	- Non radicaux
Oxyde nitrique $NO^{\cdot}$ Dioxyde de nitrogène $NO_2^{\cdot}$	Acide nitreux HNO_2 Cation nitrosyle NO^+ Anion nitrosyle NO^- Tétroxyde de dinitrogène N_2O_4 Trioxyde de dinitrogène N_2O_3 Peroxynitrite $ONOO^-$ Cation nitronium NO^{2+} Chlorure de nitryle NO_2Cl Alkyl peroxynitrate $ROONO^{\cdot}$ Anion nitroxyle $NO^{\cdot}$
Entités halogénées réactives	
	- Non radicaux
	Acide hypochloreux HOCl † Acide hypobromeux HOBr† Chlorure de nitryle NO_2Cl

Tableau 1. Les différents types de formes activées de l'oxygène.
Trois types de FAO sont rencontrés dans les cellules vivantes: les entités oxygénées (EAO), nitrées réactives (ENR) et halogénées réactives (EHR).

16B). Il est important de noter que de nombreuses études indiquent que ces molécules participent à des processus de signalisation. Dans la suite de ce manuscrit, nous allons principalement nous intéresser à la production, la détoxication ainsi qu'à la signalisation dépendante des EAOs.

IV.2. Les EAOs, nature et sites de production

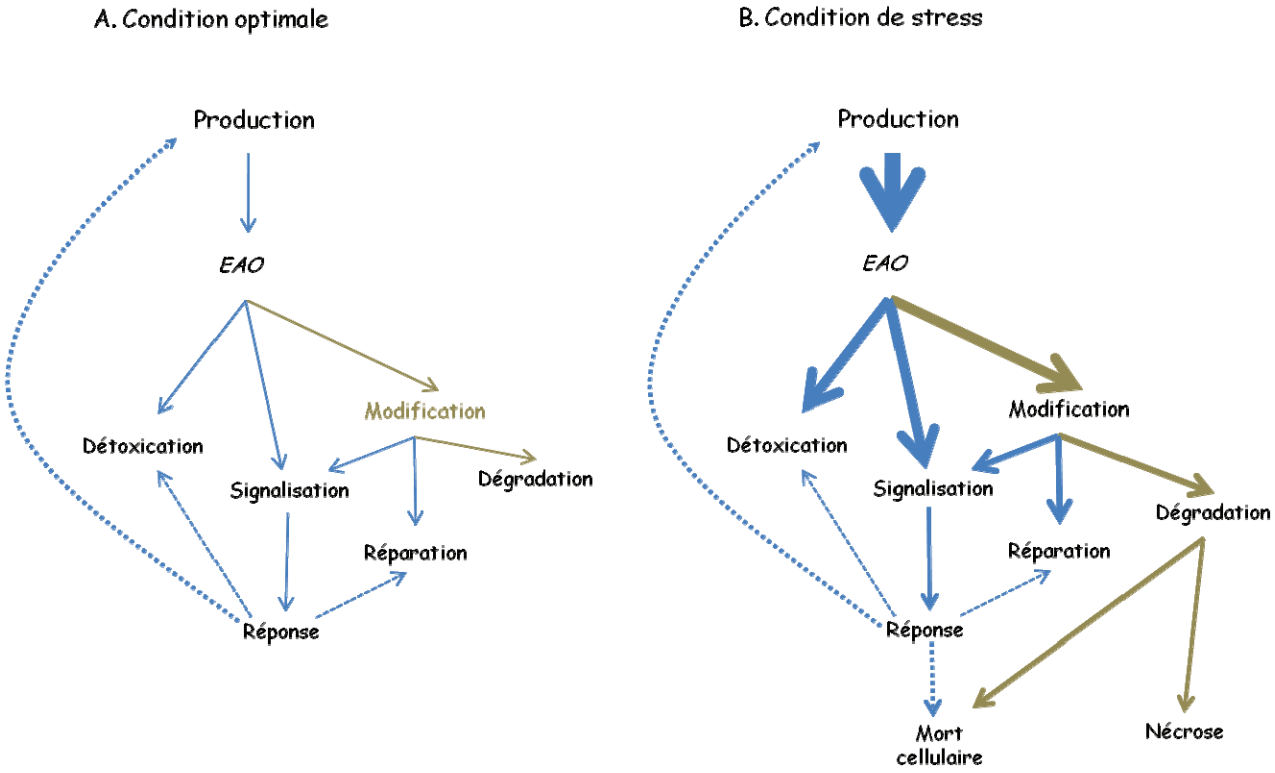

Figure 16. *Schéma de l'homéostasie des EAOs.*

A. En condition optimale ou B. lors d'un stress. L'épaisseur des flèches est proportionnelle à l'intensité du signal ou de la réponse mise en jeu. Les flèches vertes indiquent les modifications causées sur les macromolécules (Moller et al. 2007).

L'oxygène est la molécule clé à l'origine de la production des EAOs, et cela quel que soit le compartiment cellulaire dans lequel elles sont produites. Il existe différent types d'EAOs qui présentent des caractéristiques différentes en terme de pouvoir oxydant, de capacité à diffuser ou de durée de vie (Tableau 2). La figure 17 récapitule les différents types d'EAOs ainsi que leur mode de production à partir d'une molécule d'oxygène « activée » ou *oxygène singulet* ($^1O_2$). A l'état fondamental l'O_2 est sous forme triplet et cette configuration électronique (spins électroniques parallèles) lui confère une très bonne stabilité ainsi qu'une faible réactivité. Pour être activé, un réarrangement électronique (changement de spin, spins antiparallèles) doit avoir lieu et celui-ci peut être induit par un apport d'énergie (photonique ou thermique) (Figure 17). Une fois activé l'oxygène est sous forme $^1O_2$, espèce la plus réactive des EAOs. Quatre réductions mono-électroniques (captation d'un seul électron à la fois) permettront de le transformer en anion su-

Tableau 2. Propriétés des EAO (Tarrago 2009).

Propriétés	**Oxygène singulet ($^1O_2$)**	**Anion superoxyde ($O_2^{\cdot -}$)**	**Peroxyde d'hydrogène (H_2O_2)**	**Radical hydroxyl ($HO^{\cdot}$)**
$T_{1/2}$	1µs	1µs	1ms	1ns
Distance parcourue	30nm	30nm	1µm	1nm
Concentration cellulaire	?	?	µM/mM	?

peroxyde ($O_2^{\cdot -}$), en peroxyde d'hydrogène (H_2O_2), en radical hydroxyl ($HO^{\cdot}$) et finalement en eau (H_2O) (Figure 17). Les mitochondries, les chloroplastes et les peroxysomes sont les trois principaux sites de production des EAOs. Au niveau des mitochondries et des chloroplastes, la production des EAOs a lieu essentiellement durant le transfert linéaire des électrons. Les complexes I et III de la chaîne respiratoire mitochondriale sont responsables de la production d'$O_2^{\cdot -}$, qui pourront être réduits par la suite en H_2O_2 (Poyton *et al*. 2009). Dans les chloroplastes, la production d'$^1O_2$ a lieu au niveau des antennes collectrices du PSI et du PSII. Les $O_2^{\cdot -}$ sont quant à eux produits à partir du PSII et de la ferrédoxine, tandis que l'H_2O_2 est produit au niveau du complexe de dissociation de l'eau ainsi qu'à partir du PSII. Dans les peroxysomes, les EAOs sont principalement produites par des flavine oxydases (à cofacteurs FAD ou FMN) impliquées dans le cycle du glyoxylate, la β-oxydation des acides gras ou l'oxydation des isomères « D » de certains acides aminés (par exemple le D-acide aspartique ou le D-acide glutamique) (Schrader & Fahimi 2006; Antonenkov *et al*. 2010).

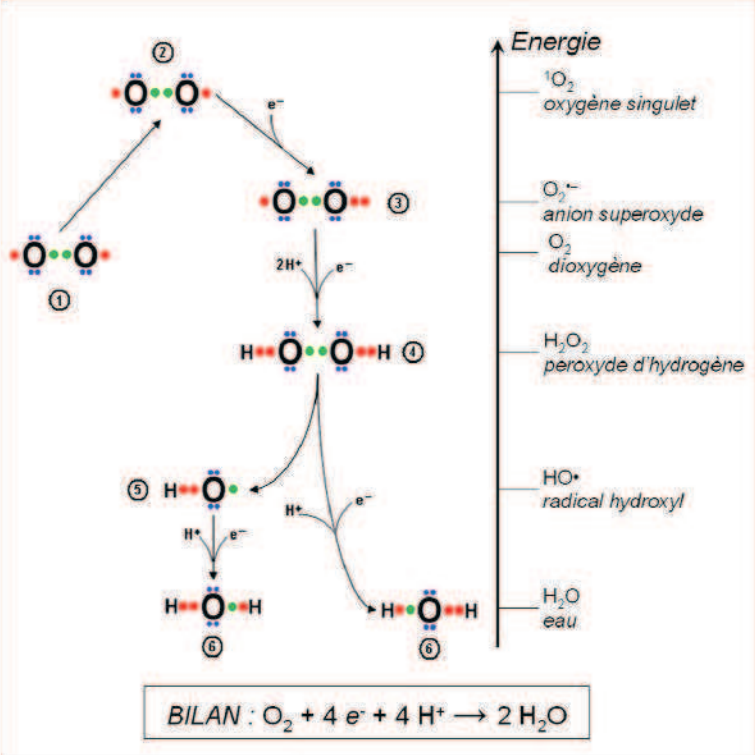

Figure 17. Les différents types d'EAO : principe de production et de réduction.

(1) L'oxygène moléculaire sous forme triplet stable va être activé sous forme d'oxygène singulet par captation d'énergie (2). Quatre réductions mono-électroniques permettront sa réduction en eau. En bleu sont représentés les électrons non liants, en rouge et vert les électrons liants.

Notons également que la production des EAOs est un des éléments du système de défense des plantes terrestres contre des attaques pathogènes. Ainsi, au cours d'un stress biotique, une forte production d'H_2O_2 a lieu au niveau de l'apoplasme des cellules infectées. En réalité, le premier sous-produit d'une attaque pathogène n'est pas l'H_2O_2 mais l'$O_2^{\cdot-}$, cependant celui-ci est très rapidement réduit en H_2O_2 (Lambeth 2004; Foyer & Noctor 2005). Deux hypothèses sont avancées quant à l'origine de cette production d'H_2O_2, l'existence de NADPH oxydases membranaires induites en réponse à un éliciteur pathogène qui vont produire de l'$O_2^{\cdot-}$ à partir d'oxygène et de NADPH, mais également la présence de peroxydases apoplastiques capables de réduire l'$O_2^{\cdot-}$ en H_2O_2 (Wojtaszek 1997; Torres 2010). L'augmentation de la concentration en molécules oxydantes dans l'apoplasme des cellules va induire une cascade de signalisation qui aboutira à la mise en place des systèmes de défense de la plante.

IV.3. La détoxication des EAOs

Suivant la nature de la molécule responsable de la réduction *sensu-stricto* des EAOs, deux grands modes de détoxication peuvent êtres décrits. Il existe des voies non-enzymatiques utilisant des molécules capables de réduire directement les EAOs et des voies enzymatiques souvent complexes. D'autre part, il existe également des protéines capables de réparer les dommages causés par les EAOs sur les lipides, l'ADN ou sur les protéines.

IV.3.a. Les systèmes de détoxication non enzymatiques

IV.3.a.1. L'acide lipoïque et dihydrolipoïque

L'acide lipoïque (AL) et dihydrolipoïque (DHAL) sont deux molécules amphiphiles (possédant à la fois un groupement hydrophile et un groupement hydrophobe) aux propriétés antioxydantes capables d'agir en milieu hydrophile ou hydrophobe (Figure 18). L'AL est en mesure de piéger $OH^{\cdot}$, $O_2^{\cdot-}$ ainsi que l'acide hypochloreux (HOCl), tandis que le DHAL est lui en mesure d'interagir avec les mêmes molécules plus le radical peroxyl ($RO_2^{\cdot}$) (Moini *et al*. 2002; Parker *et al*. 2008). De plus

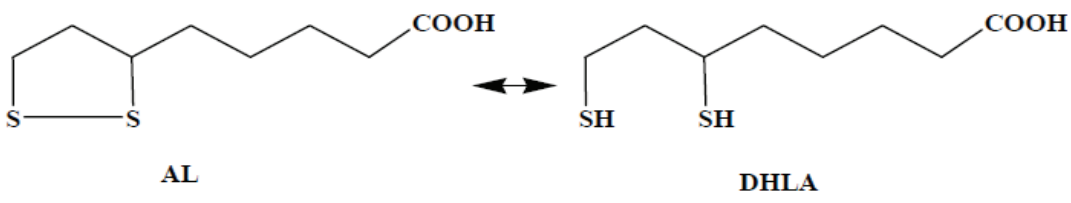

Figure 18. Structure des acides α-lipoïque (AL) et dihydrolipoïque (DHAL).

il a été démontré que le DHAL était capable de réduire le glutathion oxydé, autre molécule essentielle pour la détoxication des EAOs (voir ci-dessous; Busse *et al*. 1992).

IV.3.a.2. Les caroténoïdes

Les caroténoïdes sont des composés chimiques ayant le lycopène comme base commune, un tétraterpène constitué de 40 atomes de carbone (Figure 19). Il existe plus de 600 caroténoïdes différentiables par leur taux de cyclisation, d'insaturation et/ou d'oxydation. Les EAOs principalement ciblés par les caroténoïdes sont l'oxygène singulet et l'O_2*, néanmoins ceux-ci présentent des affinités variables vis-à-vis de ces produits (Cantrell *et al*. 2003)

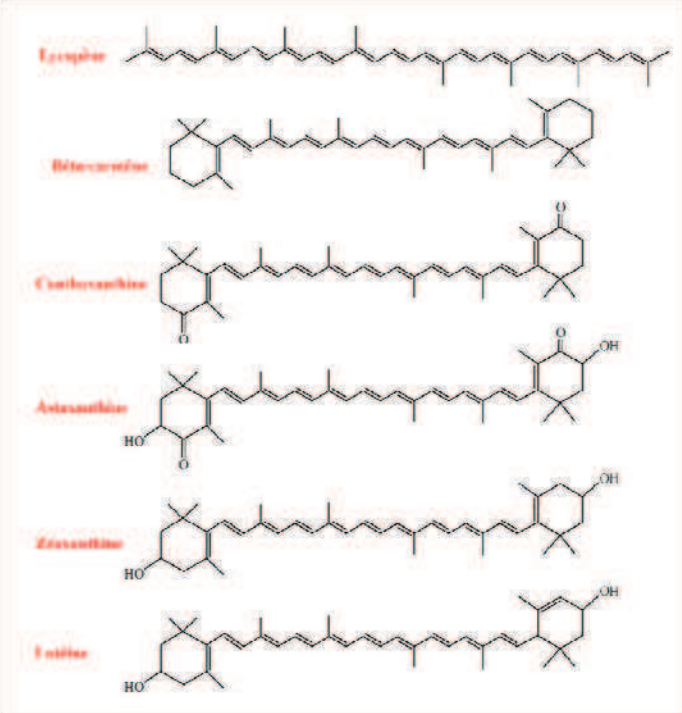

Figure 19. Structure du lycopène ainsi que quelques exemples de composés dérivant de celui-ci.

IV.3.a.3. Les flavonoïdes

Les flavonoïdes regroupent plus de 4000 types de composés polyphénoliques, spécifiques des végétaux, présentant un squelette carboné commun de deux cycles aromatiques reliés par 3 atomes de carbones (Figure 20). L'activité antioxydante des flavonoïdes se caractérise par la stabilisation de la molécule oxydante par adjonction d'un électron ou d'un proton H^+ sur celle-ci (Rice-Evans & Miller 1996)

IV.3.a.4. Le glutathion

Le glutathion est un tripeptide ubiquitaire composé d'un γ-glutamate, d'une cystéine et d'une glycine (Figure 21). Celui-ci peut se présenter sous différentes formes, citons par exemple une forme réduite où le résidu Cys présente son atome de soufre sous forme thiol (GSH) et une forme oxydée dans laquelle l'atome de soufre d'une molécule de glutathion est lié de façon cova-

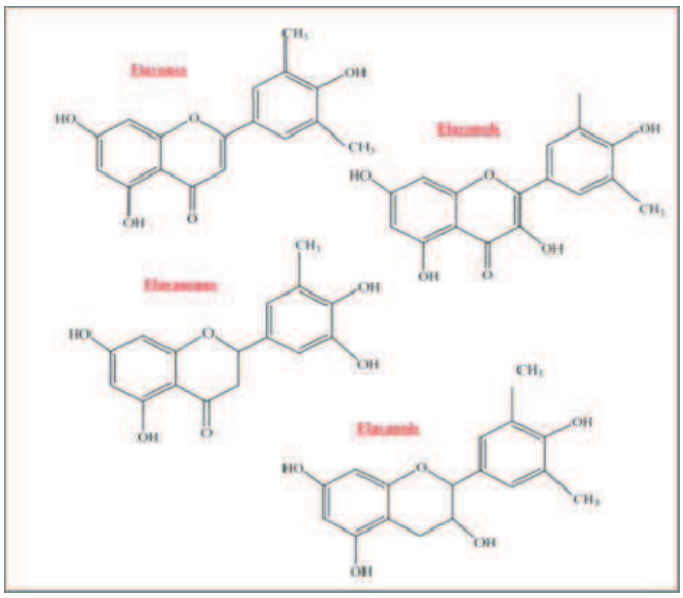

Figure 20. Structures de bases des quatre familles de flavonoïdes (Ren et al. 2003).

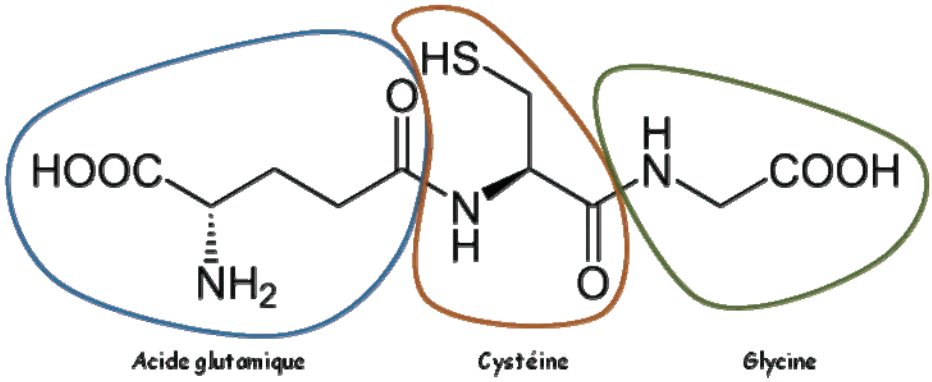

Figure 21. Structure chimique du tripeptide γ-L-glutamyl-L-cystéinylglycine.

lente avec l'atome de soufre d'une autre molécule de glutathion (GSSG). *In vivo,* plus de 90% du pool de glutathion est sous forme réduite grâce à l'action de la glutathion réductase (GR), enzyme à cofacteur FAD responsable de la réduction du GSSG par oxydation du NADPH en $NADP^+$ (Foyer & Noctor 2005; Queval *et al*. 2007). Des études *in vivo* ont pu mettre en évidence l'implication du GSH dans la prévention du stress oxydant. Ainsi, chez les plantes, la surexpression de la GR au sein des chloroplastes de peuplier induit une augmentation de la teneur en glutathion et plus particulièrement en GSH permettant une meilleur résistance à la photo-inhibition (Foyer *et al*. 1995). Inversement, des plantes où l'expression de la GR est diminuée sont plus sensibles à un traitement induisant la production d'anions superoxydes (Aono *et al*. 1993). On peut également noter que chez les mammifères, le GSH a une action antioxydante au niveau des mitochondries des cellules cardiaques. Une privation de celui-ci induisant une diminution de la synthèse d'ATP (Zhang *et al*. 1990).

En plus de son activité directe de réduction des EAOs par formation de GSSG, le GSH peut servir

de substrat pour des protéines (certaines Tpxs et Gpxs, les Grxs, les GSTs) responsables de la détoxication des EAOs.

IV.3.a.5. Les vitamines C (acide ascorbique) et E (α-tocophérol et tocotriénols)

Les composés regroupés sous le nom de vitamine E (α-tocophérol et tocotriénols) sont les principaux antioxydants des membranes lipidiques (Figure 22) (Herrera & Barbas 2001). Chez l'homme, un traitement à l'α-tocophérol induit une forte diminution du taux de peroxydation plasmatique et des LDLs (*low density lipoprotein*) (Kontush *et al*. 1996). La vitamine E étant réduite par la vitamine C (acide ascorbique), dans certaines conditions, l'action antioxydante de la vitamine E n'est possible qu'en présence d'acide ascorbique (Packer *et al*. 1979; Kontush *et al*. 1996). L'acide ascorbique est un élément essentiel de la détoxication des EAOs chez les organismes photosynthétiques. Il peut interagir directement avec $OH^{\cdot}$ ou $O_2^{\cdot -}$ (Figure 22). De plus la vitamine C est également un cofacteur essentiel à l'activité des ascorbate peroxydases (APX), enzymes à hème catalysant la réduction d'H_2O_2 en eau *via* l'oxydation de l'acide ascorbique en monodéhydroascorbate (MDHA).

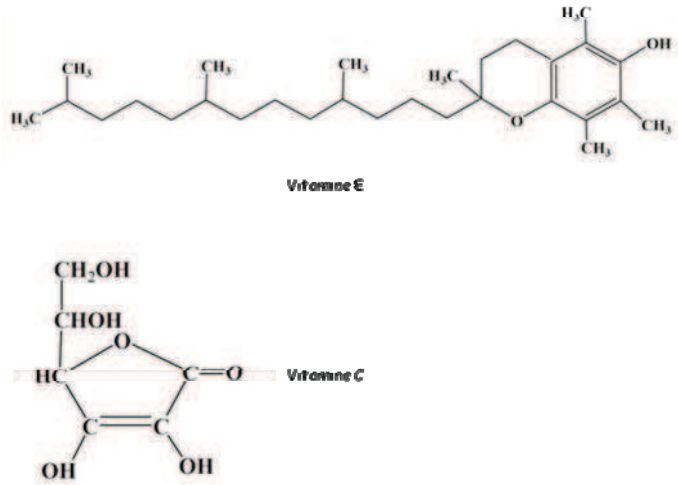

Figure 22. Structure chimique de l'acide ascorbique (vitamine E) et de la vitamine C.

IV.3.b. Les systèmes de détoxication enzymatiques impliquant des protéines à repliement thiorédoxine

Il existe une grande variété de systèmes enzymatiques de réduction des EAOs qui possèdent des spécificités différentielles. Citons par exemple des enzymes réduisant spécifiquement l'anion superoxyde telles les SOD ou les SOR qui sont des protéines à cofacteurs métalliques ou à centre fer soufre, respectivement. Dans le cas de la détoxication du peroxyde d'hydrogène nous pouvons citer des protéines à hème, longtemps supposées comme étant l'unique moyen de ré-

duction de ce type d'EAO, telles les catalases/catalase peroxydases ou ascorbate peroxydases.

En plus des différents systèmes que nous venons de citer, il existe des protéines à repliement Trx capables de réduire les EAOs. La réduction des EAOs par ces protéines à repliement Trx étant réalisé grâce à des résidus Cys conservés, ces protéines sont appelées thiol-peroxydases et feront l'objet d'une étude approfondie dans la suite de ce manuscrit (Rouhier & Jacquot 2005; Dietz 2011).

IV.3.b.1. Diversité des thiol-peroxydases et localisation subcellulaire

En fonction de leur mécanisme catalytique, directement lié au nombre de résidus Cys impliqués, de leur état d'oligomérisation, les thiol-peroxydases peuvent d'êtres divisées en six classes de peroxyrédoxines notées de A à F et en une classe de glutathion peroxydases (Gpx) (Figure 23) (Rouhier & Jacquot 2005; Dietz 2011). Les classes A à D regroupent les classes de Prxs conservées chez les organismes photosynthétiques eucaryotiques (Hofmann *et al*. 2002; Rouhier & Jacquot 2002; Rouhier & Jacquot 2005). La classe A correspond aux Prx classiques à deux résidus Cys (2-CysPrxs) et la classe B aux Prxs ne présentant qu'une seule cystéine (1-CysPrxs). Les classes C

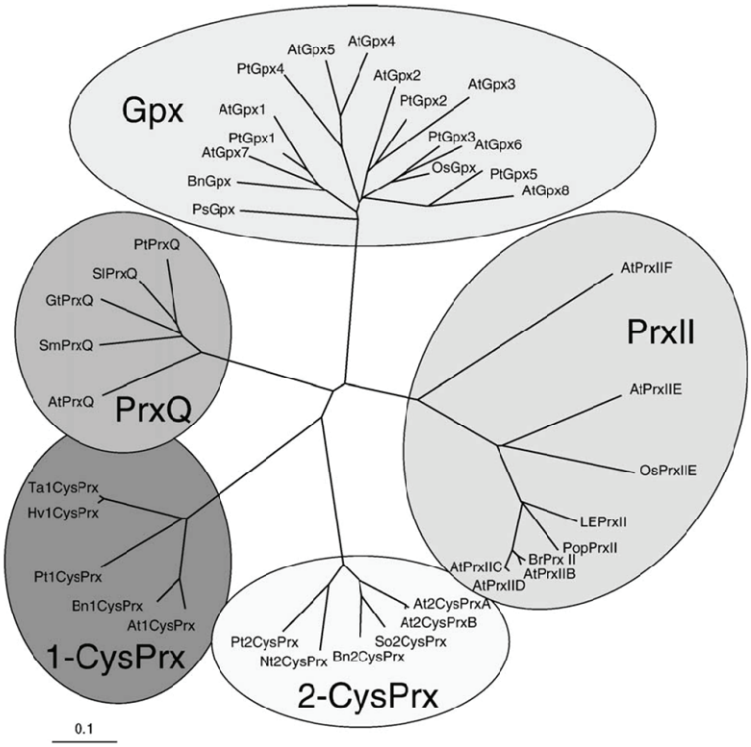

Figure 23. Relation phylogénétique des classes de thiol-peroxydases chez les organismes photosynthétiques supérieurs.

Pt, *Populus trichocarpa*; Bn, *Brassica napus*; Br, *Brassica rapa*; Ps, *Pisum sativum*; Os, *Oryza sativa*; Le, *Lycopersicon esculentum*; So, *Spinacia Oleracea*; Nt, *Nicotiana tabacum*; Hv, *Hordeum vulgare*; Ta, *Triticum aestivum*; Gt, *Gentiana triflora*; Sl, *Sedum lineare*; Sm, *Suaeda maritima subsp salsa* (Rouhier *et al*. 2005).

et D, elles, regroupent respectivement les PrxQs et les Prxs de type II. Notons que les classes C et D ont été également dénommées 2-CysPrxs atypiques, mais ce terme ne convient pas aux Prxs de type II (Hofmann *et al*. 2002; Rouhier & Jacquot 2005). Enfin, les classes E et F sont spécifiques des bactéries et de leurs homologues chez les archées, respectivement. Les Gpxs, initialement identifiées chez les mammifères, sont en mesure de réduire certaines EAOs (Mills 1957). Chez ces organismes, la réduction des molécules de peroxyde est réalisée grâce à la présence d'un résidu sélénocystéine (en guise de résidu peroxydatique) et avec l'aide d'une molécule que nous avons déjà mentionnée, le glutathion. Toutefois, il a été montré que les glutathion peroxydases de plante, qui ne comportent pas de sélénocystéine à la différence de nombreuses protéines animales, sont en réalité régénérées par des systèmes Trx dépendants. De ce fait, leur appellation de glutathion peroxydases basée sur des similitudes au niveau des séquences primaire et tertiaire est impropre car ces protéines sont en réalité des thiorédoxine-peroxydases (Sztajer *et al*. 2001; Rouhier & Jacquot 2005; Navrot *et al*. 2006; Maiorino *et al*. 2007). L'étude phylogénétique des peroxyrédoxines, sur la base des isoformes présentes chez *A. thaliana*, a montré que les plantes terrestres présentaient au minimum six protéines ayant des localisations subcellulaires variées (Rouhier & Jacquot 2005; Dietz *et al*. 2006). Ainsi, on retrouve de façon constante chez toutes les plantes terrestres une 1-CysPrx nucléaire, une Prx de type II cytosolique (AtPrxIIB), une Prx de type II mitochondriale (AtPrxIIF), une Prx de type II plastidiale (AtPrxIIE) ainsi que deux Prxs chloroplastiques, une 2-CysPrx et une PrxQ (Tableau 3) (Rouhier *et al*. 2004; Rouhier & Jacquot 2005; Dietz *et al*. 2006; Gama *et al*. 2008; Dietz 2011).

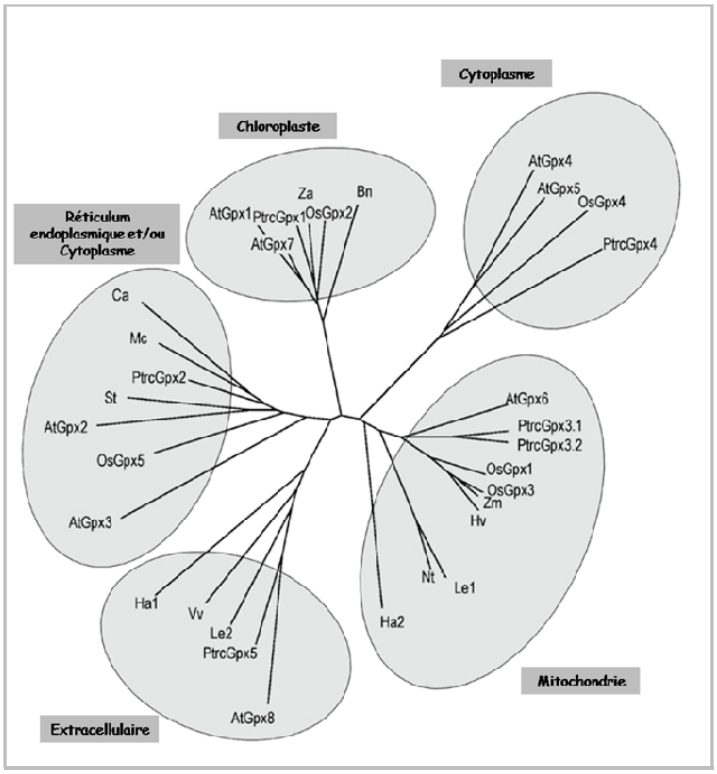

Concernant les Gpxs, à la différence de leurs homologues présents chez les mammifères, les Gpxs d'organismes photosynthétiques n'ont été étudiées que très ré-

Figure 24. Relation phylogénétique des glutathion peroxydases des organismes photosynthétiques supérieurs.

At, *A. thaliana*; Ptrc, *P. trichocarpa*; Os, *O. sativa*; Ha, *H. annuus*; Le, *L. esculentum*; Bn, *Brassica napus*; Ca, *Cicer arietinum*; Hv, *H. vulgare*; Mc, *M. charantia*; Nt, *N. tabacum*; St, *S. tuberosum*; Vv, *V. vinifera*; Za, *Z. aethiopica*; Zm, *Z. mays* (Navrot *et al*. 2006).

		Locus		
Gène	**Localisation de la protéine**	**A. thaliana**	**P. trichocarpa**	**O. sativa**
1-CysPrx	N, Cyt	At1g48130	POPTR_0008s09930	Os07g0638300 Os07g0638400
2-CysPrxA	Chl	At3g11630	POPTR_0016s07280	Os02g0537700
2-CysPrxB	Chl	At5g06290	POPTR_0006s22130 POPTR_1173s00210	-
PrxQ1	Chl	At3g23060	POPTR_0006s13980	Os06g0196300
PrxQ2	Chl	-	POPTR_0018s07400	-
PrxII A	Cyt	At1g65990	-	-
PrxII B	Cyt	At1g65980	POPTR_0001s44990	Os01g0675100*
PrxII C	Cyt	At1g65970	POPTR_0018s09030	-
PrxII D	Cyt	At1g60740	-	-
PrxII E	Chl	At3g52960	POPTR_0013s10250	Os06g0625500 Os02g0192700
PrxII F	Mit	At3g06050	POPTR_0019s04070	Os01g0266600

Tableau 3. Les gènes codant des peroxyrédoxines chez trois organismes modèles de plantes supérieures.

N, noyau ; Cyt, cytoplasme ; Chl, chloroplaste ; Mit, mitochondrie. La mention * indique que cette protéine ne possède qu'une seule cystéine, bien qu'elle appartienne aux Prxs de type II (Dietz *et al*. 2011)

cemment. De même, pour ces protéines, cinq sous-classes de Gpxs peuvent être définies chez les plantes supérieures, en fonction de leurs similarités de séquence et de leurs localisations subcellulaires variées (i.e. cytosol, plastes, mitochondries, co-adressage au réticulum endoplasmique et au cytosol et enfin extracellulaire) (Figure 24) (Margis *et al*. 2008; Navrot *et al*. 2006). Ces prédictions de localisation ont pu être confirmées expérimentalement pour les Gpx1 et Gpx3 de peuplier qui sont retrouvées au niveau du chloroplaste et pour PtGpx3 au niveau de la mitochondrie, et pour les Gpx1 et 7 d'*A. thaliana* (Navrot *et al*. 2006; Chang *et al*. 2009;). Néanmoins, les outils de prédiction subcellulaire n'apportent que des informations partielles comme le démontre l'étude d'une protéine de radis (*Raphanus sativus*). La protéine RsPHGPx, qui est l'homologue des protéines Gpx2 d'*Arabidopsis* et de peuplier, est adressée dans la mitochondrie alors que les prédictions indiquent un adressage des protéines AtGpx2 et PtGpx2 dans le réticulum endoplasmique et le cytosol (Yang *et al*. 2006).

IV.3.b.2. Les mécanismes catalytiques des thiol-peroxydases: une base commune et des modalités variées

Dans ce paragraphe, nous allons nous focaliser plus particulièrement sur les différents mécanismes réactionnels des Prxs qui peuvent se trouver sous diverses formes actives, monomériques, dimériques, décameriques et présenter un ou deux résidus cystéinyls au niveau de leurs sites actifs. La première étape est commune à tous les types de Prxs et de Gpxs d'ailleurs. Il s'agit de l'attaque nucléophile du groupement thiol de la (séléno)cystéine catalytique (ou peroxydatique) sur le composé à réduire (ROOH) (Figure 25). Un acide sulfénique (S-OH) est alors formé sur cette cystéine et une molécule d'alcool (ROH) est libérée (Figure 25). L'acide sulfénique ainsi formé est réduit selon deux voies qui dépendent du type de Prx considéré:

.L'acide sulfénique de la cystéine peroxydatique est directement attaqué par un agent réducteur (Figure 25, voie A). Ce mécanisme est valable pour les 1-CysPrxs pour lesquelles l'agent réducteur peut être une Trx, une cyclophiline, le GSH ou l'ascorbate (Kang *et al*. 1998; Pe-

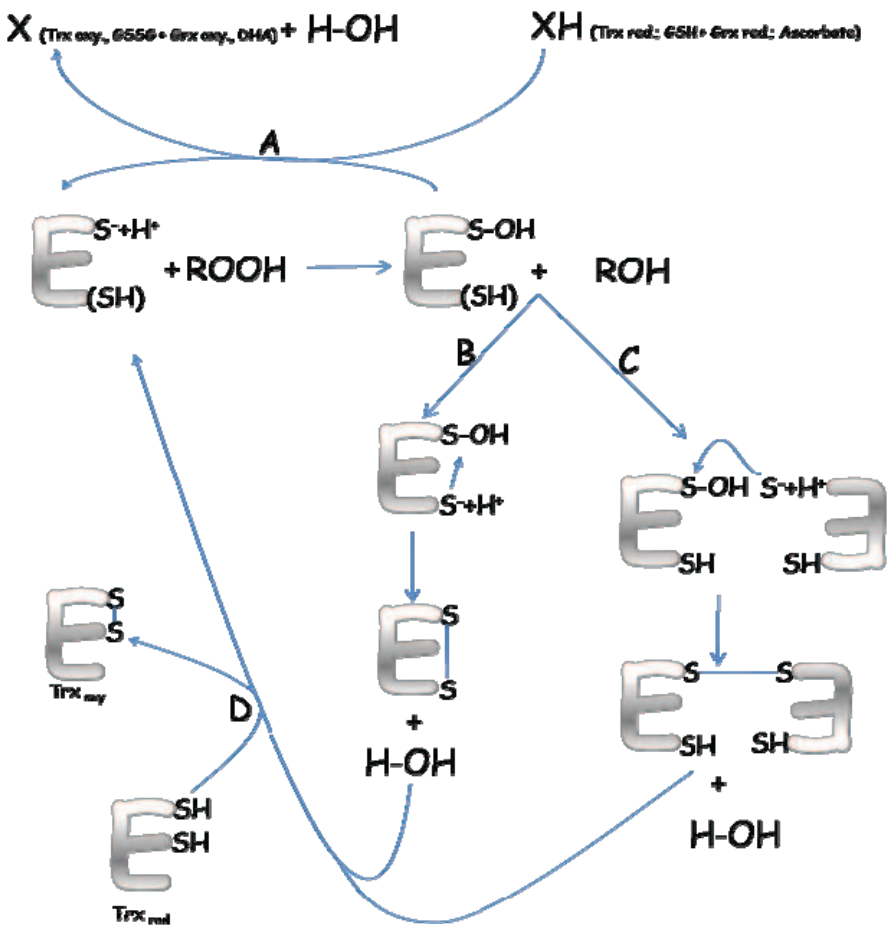

Figure 25. Les différentes voies de réduction des acides sulféniques formés sur les cystéines peroxydatiques des thiol-peroxydases.

A. Réduction par un agent réducteur externe. B. Réduction par formation d'un pont disulfure intramoléculaire. C. Réduction par formation d'un pont disulfure intermoléculaire.

drajas *et al*. 1999; Lee *et al*. 2001; Monteiro *et al*. 2007). Notons que pour certaines Prxs de type II, bien que présentant deux résidus cystéinyls très conservés, la réduction de l'acide sulfénique peut être directement réalisée par l'action du glutathion réduit suivant un mécanisme comparable aux 1-CysPrxs (Rouhier *et al*. 2001; Rouhier *et al*. 2002; Gama *et al*. 2008).

.L'acide sulfénique subit une attaque nucléophile d'un groupement thiolate appartenant à une cystéine de recyclage (Figure 25, voie B). Cette attaque induit la formation d'un pont disulfure intramoléculaire et la libération d'une molécule d'eau. Cette formation de pont disulfure intramoléculaire est rencontrée dans le mécanisme catalytique des Gpxs et des PrxQs (Rouhier *et al*. 2004; Navrot *et al*. 2006). Dans le cas des 2-CysPrxs, la cystéine de recyclage appartient à un autre monomère et un pont disulfure intermoléculaire est alors formé (Figure 25, voie C) (Poole 1996; Montemartini *et al*. 1998; Reynolds *et al*. 2002). La réduction de ces ponts disulfure s'effectue généralement grâce au système thiorédoxine (pour revue Dietz 2011).

IV.3.b.1. Caractéristiques biochimiques et structurales des Tpxs

Les thiol-peroxydases sont de petites protéines solubles (entre 17 et 25 kDa) possédant une, deux ou trois cystéines conservées suivant les classes. Ces protéines appartiennent à la superfamille des Trxs et partagent de ce fait certaines caractéristiques structurales avec ces dernières (voir paragraphe II.2.).

Le repliement typique d'une peroxyrédoxine est composé de sept brin-β entourés par cinq hélices-α (Figure 26A) (Hall *et al*. 2010a). Cependant, à la différence d'un grand nombre de protéines présentant un repliement thiorédoxine, la cystéine peroxydatique est localisée dans les premiers tours de l'hélice α2 et ne fait pas partie d'un motif di-cystéine (CxxC). La cystéine peroxydatique se situe dans un motif strictement conservé $P_{44}xxxT_{48}/SxxC_{51}$ (les acides aminés sont numérotés suivant leur position dans la séquence de la PrxIIB de peuplier) (Echalier *et al*. 2005). Les acides aminés conservés T/S forment avec la cystéine et une arginine (R_{129} dans la PrxIIB de peuplier) proche de la cystéine peroxydatique dans la structure tridimensionnelle, le site actif des peroxyrédoxines ou « triade catalytique » (Figure 26A). Cette triade est stabilisée par la présence de la Proline (P_{44}) et permet de maintenir le *pKa* de la cystéine peroxydatique à une valeur comprise entre 5 et 6 unités pH suivant les isoformes, garantissant la réactivité de celle-ci. De plus, cette triade permet également l'activation du substrat peroxydé en favorisant son positionnement au sein du site actif (Hall *et al*. 2010b).

Concernant les Gpxs, celles-ci diffèrent sensiblement des autres Tpxs, de par la stricte

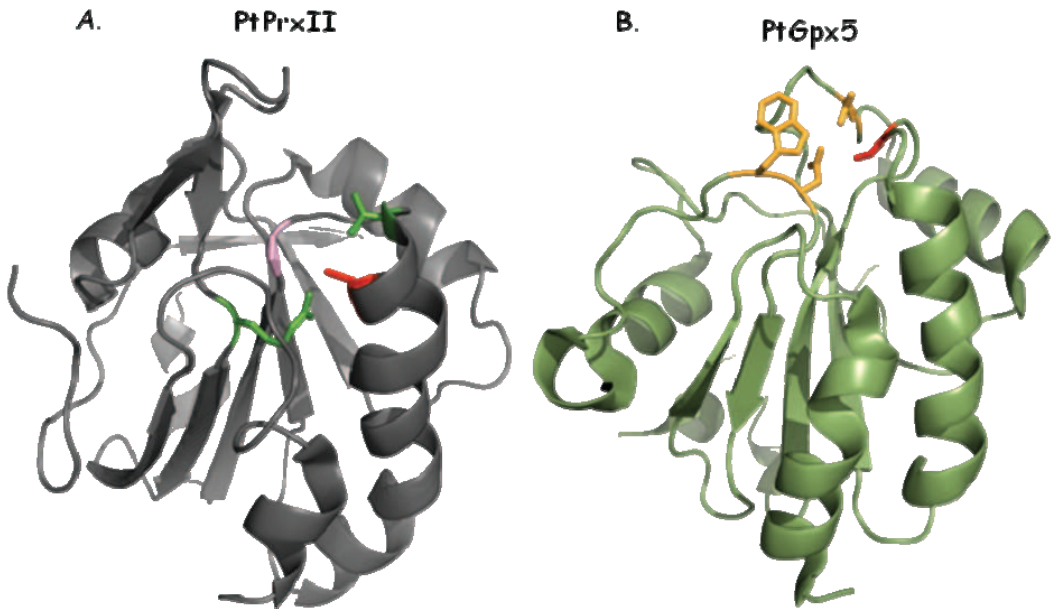

Figure 26. Structure tridimensionnelle des protéines PtPrxIIB et PtGpx5 sous forme réduite.
A. Les acides aminés importants pour la réactivité de la PrxIIB sont représentés en bâtonnet, rose pour la proline 44, vert pour les thréonine 48 et arginine 129 et rouge pour la cystéine peroxydatique 51. B. Les acides aminés composant la tétrade catalytique sont représentés en bâtonnet, jaune pour les acide glutamique 79, tryptophane 133 et asparagine 134, et rouge pour la cystéine peroxydatique 44 (Codes PDB, PtPrxIIB, 1TP9 ; PtGpx5, 2P5Q) (Echalier *et al.* 2005, Koh *et al.* 2007)

conservation de deux ou trois résidus cystéine mais également de par leur repliement composé de quatre à six brins-β et de quatre à huit hélices-α suivant les isoformes (Koh *et al*. 2007; Maiorino *et al*. 2007; Scheerer *et al*. 2007). Comme pour les Prxs, les Gpxs ne possèdent pas de motif di-cystéine mais trois motifs très conservés contenant deux des trois résidus cystéine. Le premier de ces motifs correspond à la séquence conservée NVA[S/T]xCGxT et contient la cystéine peroxydatique. Le deuxième correspond à la séquence LxFPCNQFGx[Q/E] contenant une cystéine conservée mais dont la fonction est aujourd'hui inconnue. Le troisième motif, WNFxKFL, est quant à lui retrouvé en partie C-terminale de la protéine (Figure 26B). Notons que la plupart des Gpxs, en dehors de celles des mammifères, possède une cystéine de recyclage dont la position peut légèrement varier dans la séquence primaire suivant les organismes et les isoformes. Le site actif des Gpxs est composé de différents acides aminés chargés afin de maintenir le *pKa* de la cystéine peroxydatique à une valeur entre 5 et 6 unités pH. Les acides aminés composant ce site actif sont au nombre de quatre, formant une « tétrade catalytique » (Tosatto *et al*. 2008). Dans le cas de la Gpx5 de peuplier, par exemple, ces acides aminés correspondent à la cystéine peroxydatique (C_{44}), un acide glutamique (E_{79}), un tryptophane (W_{133}) et une asparagine (N_{134}) (Figure 26B) (Koh *et al*. 2007). Notons que la Gpx5 de peuplier, ainsi que ses homologues chez d'autres organismes (ex : Gpx8 chez *Arabidopsis*) sont des cas particuliers présentant un acide

glutamique (E_{79} ou E_{76} pour PtGpx5 et AtGpx8 respectivement) au sein de leur « tétrade catalytique » tandis que la plupart des autres isoformes des eucaryotes présentent une glutamine à cette position particulière (Koh *et al*. 2007; Maiorino *et al*. 2007; Toppo *et al*. 2008; Tosatto *et al*. 2008).

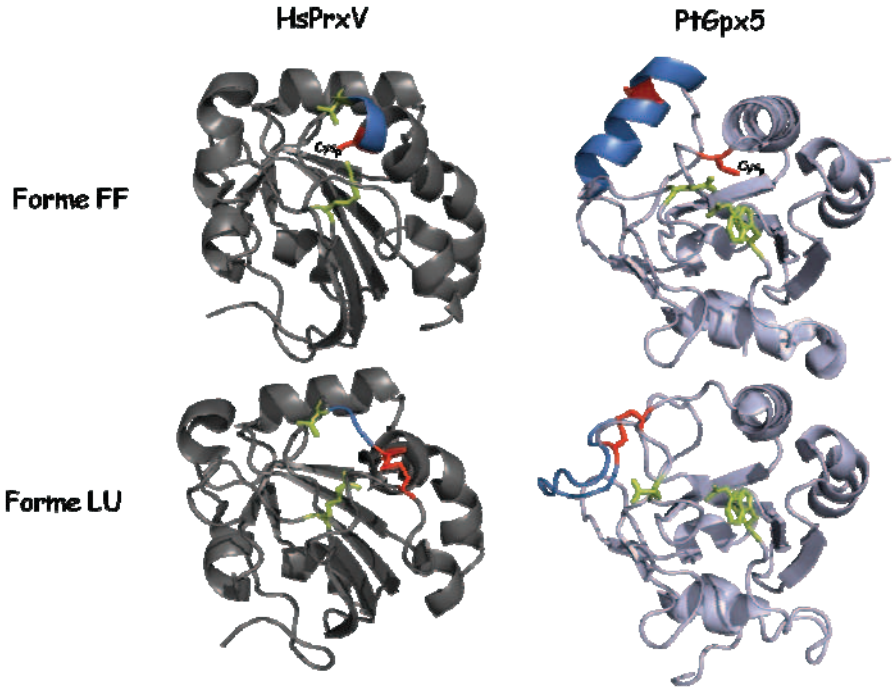

Figure 27. Changements conformationnels rencontrés des thiol-peroxydases.

Représentation des structures FF (*fully folded*) c'est-à-dire réduites et LU (*locally unfolded*) c'est-à-dire oxydées de la PrxV humaine (PDB 2VL2, chaînes A pour la FF et C pour la LU) et de la Gpx5 de peuplier (PDB 2P5Q pour la FF) et (2P5R pour la LU). Les acides aminés essentiels à la réactivité de la protéine sont représentés en bâtonnets jaunes (voir texte), et en rouge les résidus cystéinyls. Les parties de structure en bleu correspondent aux portions de protéine sujettes à des modifications de structures secondaires lors de la transition FF vers LU.

Enfin, la plupart des Tpxs présentent la particularité de posséder au moins deux conformations structurales différentes (Figure 27). Lorsque ces protéines sont sous forme réduite, elles présentent une triade ou tétrade catalytique dans une conformation optimale pour la réactivité de la cystéine peroxydatique et sont dites dans ce cas « fully folded » (FF). Par contre, lorsque les Tpxs présentent leurs cystéines peroxydatique et de recyclage sous forme de cystine, ces protéines sont dites « locally unfolded » (LU) (Koh *et al*. 2007; Hall *et al*. 2009; Hall *et al*. 2010a; Hall *et al*. 2010b). Dans la conformation LU, une hélice α est partiellement ou complètement déroulée, suivant les isoformes. Dans le cas de la protéine Gpx5 de peuplier, l'hélice α2 contenant la cystéine de recyclage est totalement déroulée tandis que pour les Prxs, ce déroulement de l'hélice α contenant la cystéine peroxydatique est partiel (Wood *et al*. 2003; Koh *et al*. 2007). Ces changements de conformation ont été très bien étudiés pour les Prxs mettant en évidence leur importance dans la fonction de ces protéines.

IV.3.b.2. Rôles physiologiques des thiol-peroxydases, plus que de simples enzymes de détoxication?

Les Tpxs sont en mesure de réduire une grande variété de substrats peroxydés, des plus simples tels le peroxyde d'hydrogène ou le peroxynitrite aux plus complexes tels les alkyl-hydroperoxydes ou lipides peroxydés. Par exemple chez les organismes photosynthétiques, il a été démontré que les Prxs chloroplastiques telles que les 2-CysPrxs et les PrxQs étaient des acteurs essentiels du maintien de l'activité photosynthétique au travers de leur activité peroxydase (Baier & Dietz 1999; Petersson *et al*. 2006; Stenbaek *et al*. 2008).

Cependant d'autres fonctions ont été caractérisées depuis quelques années pour les Tpxs (Delaunay *et al*. 2002; Wood *et al*. 2003). Tout d'abord, dans le cas des Prxs d'organismes photosynthétiques, l'exemple le plus étudié est celui des 2-CysPrxs. Trois fonctions possibles ont été proposées pour ces peroxydases : une fonction de détoxication, une fonction de chaperonne et enfin une fonction de senseur de l'état redox des cellules. Comme représenté en figure 28, les dimères de 2-CysPrx réduits sont en réalité organisés en décamères qui seraient impliqués dans la détoxication des EAOs au niveau des membranes thylacoïdiennes. Lors de la réduction d'une molécule peroxydée, le changement de conformation FF vers LU provoque une déstabilisation de la forme décamérique et la protéine se retrouve sous forme dimérique oxydée dans le stroma, lieu de son recyclage par les Trxs (CDSP32, Trx x ou NTRC) (Figure 28) (König *et al*. 2002; König *et al*. 2003;Rey *et al*. 2005; Moon *et al*. 2006; Perez-Ruiz *et al*. 2006). Cependant lors de la réduction

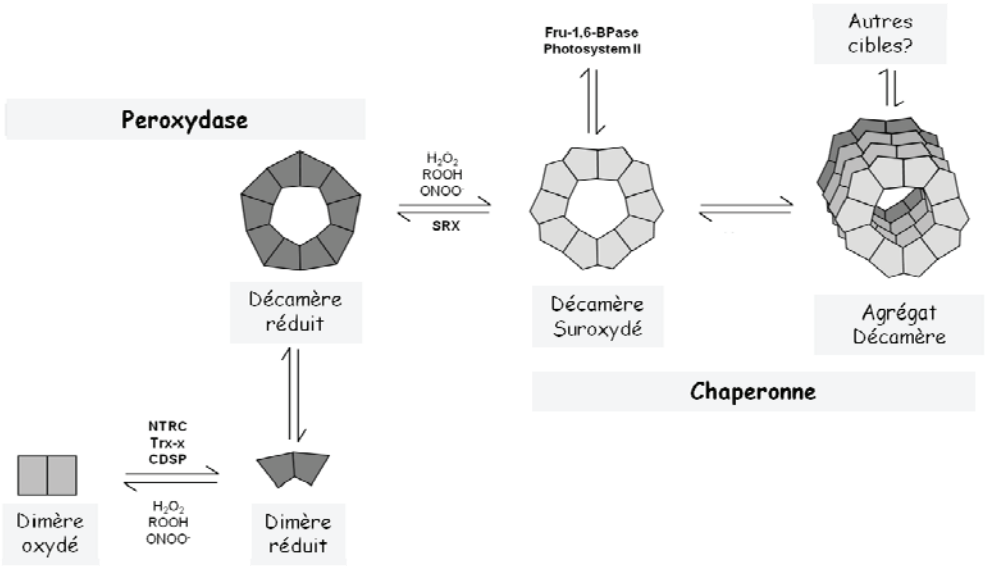

Figure 28. Fonctions physiologiques possibles de différentes formes de 2-CysPrx au sein du chloroplaste.

Les formes décamériques réduites et dimériques oxydées sont les deux formes rencontrées dans la détoxication des EAOs (partie gauche de la figure). Les formes décamériques suroxydées sous forme d'agrégats jouent très probablement un rôle de chaperonne au niveau des membranes des thylacoïdes (partie droite de la figure).

d'un peroxyde par la forme décamérique, une suroxydation de la cystéine catalytique peut avoir lieu. Ainsi, on passe d'un acide sulfénique (SOH) à un acide sulfinique (SO_2H) puis à un acide sulfonique (SO_3H). Sous ces deux dernières formes la 2-CysPrx ne peut plus être recyclée rapidement et devient par conséquent inactive. Il existe des protéines, les sulfirédoxines, capables de réduire les acides sulfiniques en acides sulféniques en présence d'ATP avec une efficacité catalytique toutefois assez lente (Rhee *et al*. 2007). Comme illustré en figure 28, les Prx inactives pour la réduction des peroxydes sont nécessairement sous forme décamérique mais elles peuvent également se présenter sous formes d'agrégats. Toutefois, ces formes inactives conservent la possibilité de fonctionner comme chaperonnes vis à vis de protéines du métabolisme carboné (FBPase) ou présentes dans le PSII (Muthuramalingam *et al*. 2009; Rhee & Woo 2010). En plus des fonctions de chaperonnes moléculaires, les 2-CysPrx suroxydées joueraient un rôle dans la signalisation en réponse aux peroxydes. En effet, il a été proposé que leur inactivation temporaire permettrait une augmentation de la concentration en peroxyde d'hydrogène conduisant à la mise en place des voies de réponses aux stress oxydant au sein du chloroplaste dans le cas des plantes (Wood *et al*. 2003). Chez *Schizosaccharomyces pombe* et *S. cerevisiae*, il a été démontré que les 2 -CysPrxs interagissent directement avec des facteurs de transcription tels que STY1 ou Pap1 (Veal *et al*. 2004; Morgan & Veal 2007).

Concernant les Gpxs, l'exemple le mieux illustré est la relation redox entre la protéine Orp1 (ScGpx3) et le facteur de transcription Yap1 connu pour être impliqué dans les voies de signalisation induites par un stress oxydant chez *Saccharomyces cerevisiae* (Delaunay *et al*. 2000; Delaunay *et al*. 2002; Ma *et al*. 2007; Takanishi *et al*. 2010). Le mécanisme d'interaction entre Orp1 et Yap1 est le suivant : la réduction d'une molécule peroxydée induit la formation d'un acide sulfénique sur la cystéine peroxydatique de Orp1 (C_{36}) (Ma *et al*. 2007). Cet acide sulfénique va être réduit non pas par la cystéine de recyclage d'Orp1 mais par une cystéine présente dans le facteur de transcription Yap1 (C_{598}), donnant lieu à la formation d'un pont disulfure intermoléculaire Orp1-Yap1 (Ma *et al*. 2007). Ce pont disulfure intermoléculaire va être à son tour réduit par l'attaque nucléophile de la cystéine 303 du facteur de Yap1, libérant Orp1 sous forme réduite et Yap1 sous forme oxydée (pont disulfure entre les C_{303} et C_{598}). La protéine Yap1 sous forme oxydée n'est plus en mesure d'être exportée hors du noyau et s'accumule dans celui-ci induisant une augmentation de la transcription des gènes impliqués dans la réponse au stress oxydant (Delaunay *et al*. 2000).

V. Les systèmes d'introduction et d'isomérisation des ponts disulfure

Comme nous l'avons déjà mentionné, la formation des ponts disulfure est un processus essentiel pour la stabilisation des protéines. Historiquement, les études menées par Anfinsen et ses collaborateurs ont longtemps laissé supposer qu'en présence d'oxygène, l'introduction des ponts disulfure était un processus ne nécessitant pas d'intervention enzymatique (Anfinsen *et al*. 1961). Néanmoins, ces réactions sont lentes et aspécifiques. Ces réactions ont lieu dans des compartiments cellulaires connus pour être oxydants tels le RE, l'espace inter-membranaire des mitochondries ou le périplasme des bactéries. Dans ces compartiments, l'introduction des ponts disulfure est dénommé « oxidative protein folding » (ou repliement redox dépendant) (Hwang *et al*. 1992; Frand *et al*. 2000; Sevier & Kaiser 2006; Meyer *et al*. 2007). Les protéines qui transitent via le RE ou le périplasme des bactéries ont pour principal but d'être sécrétées, ainsi leur repliement va leur permettre d'acquérir une meilleure stabilité, essentielle dans le milieu extracellulaire, riche en molécules oxydantes et dont l'homéostasie redox n'est pas bien contrôlée (Christis *et al*. 2008). Au niveau de l'espace inter-membranaire des mitochondries, le repliement redox dépendant des protéines est un processus important dans la synthèse d'ATP, l'exportation d'ions métalliques, la maturation des cytochromes ou la translocation des protéines au sein de la matrice (Deponte & Hell 2009). Notons l'existence de cas particuliers permettant l'introduction des ponts disulfure dans le compartiment cytoplasmique. En effet, il a été démontré que certains virus à ADN nécessitent un système efficace de formation des ponts disulfure qu'ils expriment dans le cytoplasme de leur hôte. Un autre cas intéressant concerne les bactéries thermophiles qui, grâce à un repliement redox dépendant dans leur cytoplasme, augmentent fortement la stabilité de leurs protéines. Enfin, il a été démontré que la protéine de choc thermique Hsp33, qui possède des motifs di-cystéines, est inactive sous forme réduite et que la formation de cystine est nécessaire à son activation (Ren *et al*. 1998; Jakob *et al*. 1999; Senkevich *et al*. 2000).

V.1. Le repliement redox dépendant au sein du périplasme des bactéries, le système Dsb

Le système d'introduction des ponts disulfure dans le périplasme des bactéries a été découvert chez *E. coli* grâce à l'étude de mutants (Bardwell *et al*. 1991; Kamitani *et al*. 1992). La caractérisation de la protéine codée par le locus muté a conduit à l'identification du premier représentant du système d'oxydation des ponts disulfure chez *E. coli*, la protéine DsbA, pour

« DiSulfide Bond » (Bardwell *et al*. 1991; Kamitani *et al*. 1992). Depuis ces premières découvertes, un système complexe de protéines nommé système Dsb système a été caractérisé (Kadokura *et al*. 2003; Ito & Inaba 2008; Inaba 2009). Ce système est composé de plusieurs protéines, généralement cinq appartenant ou non à la superfamille des Trxs, et responsables de l'oxydation, l'isomérisation ou la réduction de ponts disulfure. Les membres du système Dsb peuvent se scinder en deux groupes, l'un permettant l'introduction de ponts disulfure et l'autre permettant leur isomérisation (Figure 29).

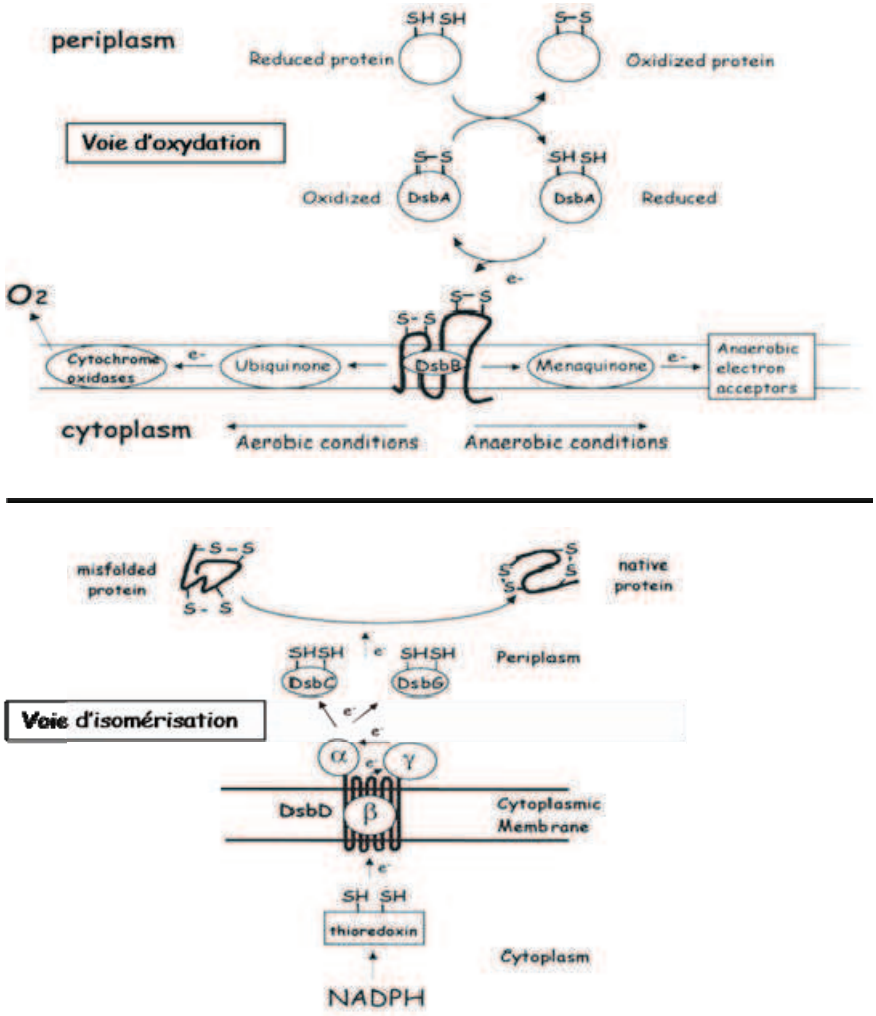

Figure 29. Schéma réactionnel représentant les voies d'introduction des ponts disulfure (en partie haute) et d'isomérisation (en partie basse) dans le périplasme des bactéries.

Ces deux voies ainsi que l'ensemble des protagonistes représentés dans ce schéma sont décrits en détail dans le texte (Collet & Bardwell, 2002).

V.1.a. La voie d'introduction des ponts disulfure

La voie d'introduction des ponts disulfure est réalisée par les protéines DsbA et DsbB, (Collet & Bardwell 2002; Kadokura *et al*. 2003; Ito & Inaba 2008; Inaba 2009). La protéine DsbA est une petite protéine soluble du périplasme à repliement Trx capable d'introduire des ponts disulfure sur des protéines réduites via son site actif di-cystéine de type CPHC. La protéine DsbA présente une caractéristique unique chez les membres de la superfamille des Trxs. Il s'agit de la protéine la plus oxydante présentant un potentiel redox de son pont disulfure catalytique autour de –80 à -125 mV (Carvalho *et al*. 2006; Lafaye *et al*. 2009). La protéine DsbB est une protéine membranaire de 20 kDa n'appartenant pas à la superfamille des Trxs (Kadokura *et al*. 2003). La protéine DsbB est en charge de ré-oxyder la protéine DsbA. En effet une fois l'oxydation d'une protéine réduite effectuée, avec transfert du pont disulfure de la protéine DsbA à sa cible, celle-ci se retrouve sous forme réduite et doit être recyclée pour effectuer un nouveau cycle d'oxydation (Figure 30). C'est la protéine DsbB qui grâce à deux motifs CxxC et à sa capacité à donner ses électrons aux quinones présentes dans les membranes du périplasme, maintient DsbA sous for-

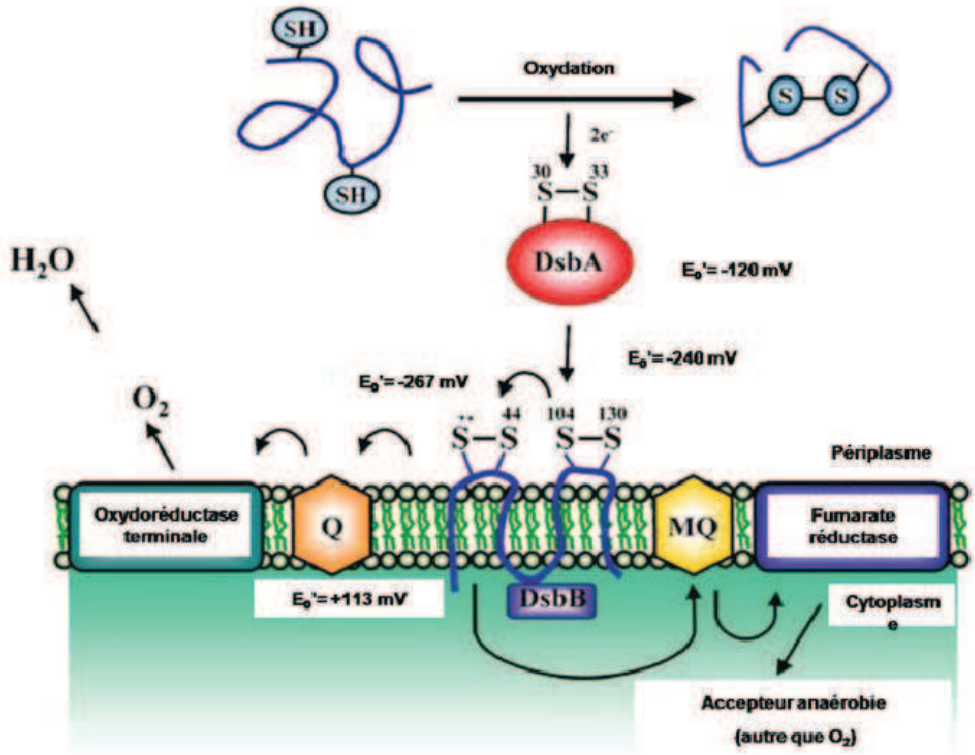

Figure 30. Schéma de l'introduction des ponts disulfure par la voie DsbB et DsbA dans le périplasme des bactéries en conditions aérobie (partie gauche) et anaérobie (partie droite).

Les potentiels d'oxydoréduction des disulfure impliqués dans le transfert des électrons des protéines DsbA (C_{30}-C_{33}) et DsbB (C_{104}-C_{130} et C_{41}-C_{44}) ainsi qu'entre les formes réduite et oxydée des quinones sont mentionnés. Les flèches indiquent le sens du trajet des électrons depuis les polypeptides à oxyder jusqu'aux accepteurs finaux, O_2 ou autres molécules en conditions aérobie et anaérobie, respectivement.

me oxydée (Figure 30). Les électrons seront ensuite acheminés vers une oxydoréductase terminale, en général un cytochrome, et seront finalement reçus par un accepteur final tel que le dioxygène (Figure 30).

V.1.b. La voie d'isomérisation des ponts disulfure

Cette voie d'isomérisation se compose de deux protéines, DsbC et DsbG, et d'une réductase DsbD. L'isomérase DsbC (dont l'expression est majoritaire) et la protéine DsbG, qui joue un rôle dans le maintient des résidus cystéinyls sous forme thiol, sont toutes deux des protéines homo-dimériques (23 kDa par monomère) formant un « V » au niveau 3D et présentant un module protéique à repliement Trx et un module de dimérisation par sous-unité (Zapun *et al*. 1995; Bessette *et al*. 1999; Depuydt et al., 2009; Depuydt et al., 2011). Ces deux protéines possèdent un site actif di-cystéinique de type CPYC, qui présente un potentiel d'oxydoréduction de -130 mV (Zapun *et al*. 1995; Bessette *et al*. 1999). Pour être en mesure d'isomériser des ponts disulfure ou de réduire les acides sulféniques, ces deux protéines doivent être sous forme réduite (Figure 31). La protéine responsable du maintien de la forme réduite des isomérases est la protéine DsbD. C'est une protéine multi-modulaire de 546 acides aminés, composée d'un « cœur » transmem-

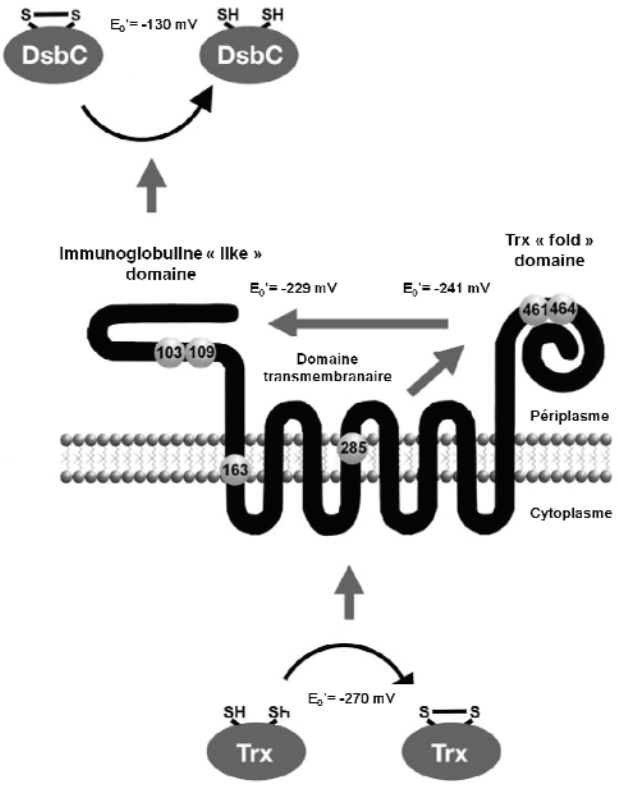

Figure 31. Schéma représentatif de l'origine des électrons nécessaires au maintien de la protéine DsbC sous forme réduite.

Les potentiel d'oxydoréduction des disulfure impliqués dans le transfert des électrons depuis la thiorédoxine (-270mV), les deux modules de DsbD (-241mV et -229mV) jusqu'à DsbC (-130mV) sont indiqués (Kadokura *et al.* 2003).

branaire comportant huit hélices transmembranaires (DsbDβ), un domaine N-terminal périplasmique avec un site de type immunoglobuline (DsbDα) et une partie C-terminale à repliement Trx (DsbDγ) (Figure 31).

Chaque domaine de la protéine DsbD comprend des résidus Cys indispensables au transfert des électrons (Figure 31) (Gordon *et al*. 2000). Pour maintenir DsbC et DsbG sous forme réduite, la protéine DsbD a besoin d'une source de pouvoir réducteur (Figure 31). Il a été démontré que ce pouvoir réducteur provenait du NADPH cytoplasmique *via* l'intermédiaire de la thiorédoxine réductase et de la Trx 1 chez *E. coli* (Figure 31) (Rietsch *et al*. 1996).

V.1.c. Le trajet des électrons, illustration d'un paradoxe thermodynamique

La description du système Dsb apporte des informations importantes sur la potentialité des réactions catalysées par les protéines à repliement Trx dans un environnement oxydoréducteur particulier. Ainsi, dans le cadre des réactions d'isomérisation, les électrons suivent les potentiels décroissants, conformément à l'équation de Nernst, à partir du NADPH jusqu'aux DsbC et

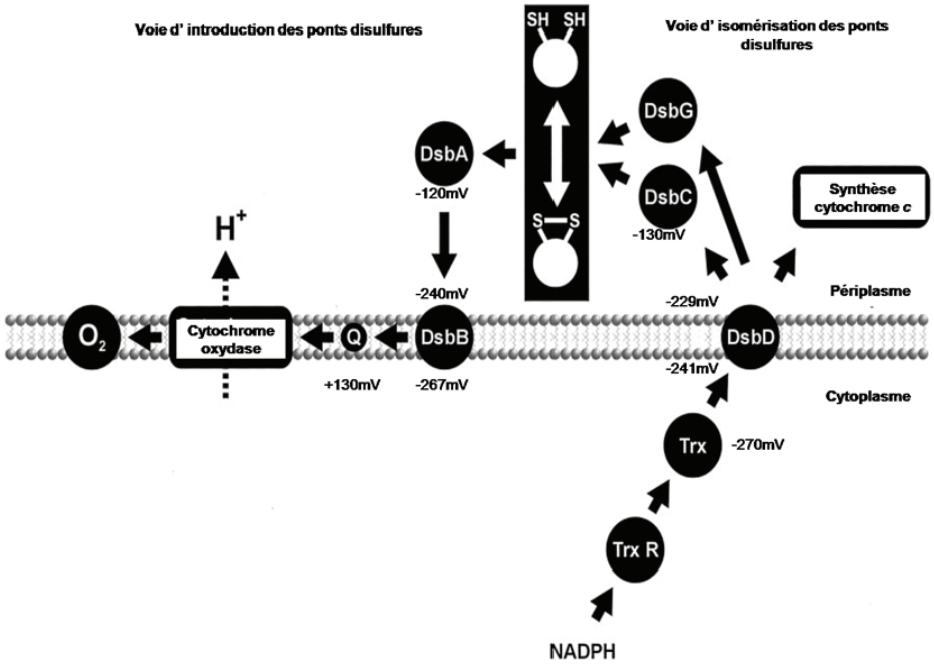

Figure 32. Trajet des électrons lors des voies d'introduction (partie gauche) et d'isomérisation (partie droite) des ponts disulfure dans le périplasme des bactéries.
Figure détaillée dans le texte (Kadokura *et al*. 2003).

DsbG (Figure 32).

Le cas des réactions d'oxydation est paradoxal. En effet, les électrons ne suivent pas le gradient des potentiels d'oxydoréduction et en particulier lors de leurs transferts entre DsbB et DsbA. L'hypothèse formulée pour expliquer cette contradiction apparente repose sur deux points prin-

cipaux (Figure 33) (Inaba & Ito 2002; Regeimbal & Bardwell 2002) :

.La formation d'un pont disulfure entre les Cys 41 et 130 de DsbB va permettre de stabiliser le complexe DsbA/DsbB, lié par un disulfure entre Cys 30_{DsbA} et $Cys104_{DsbB}$, empêchant la $Cys130_{DsbB}$ d'attaquer la liaison intermoléculaire (Figure 33),

.La présence des quinones présentant un potentiel d'oxydoréduction de +130 mV qui permettent de maintenir de façon quasi permanente les motifs di-cystéines de la DsbB sous formes de cystines.

Ainsi, malgré un bilan thermodynamique défavorable, le transfert des électrons entre les protéines DsbA et DsbB est possible. Cet exemple illustre parfaitement la complexité des échanges dithiol/disulfure. Ainsi, en plus de l'environnement oxydoréducteur global et des caractéristiques

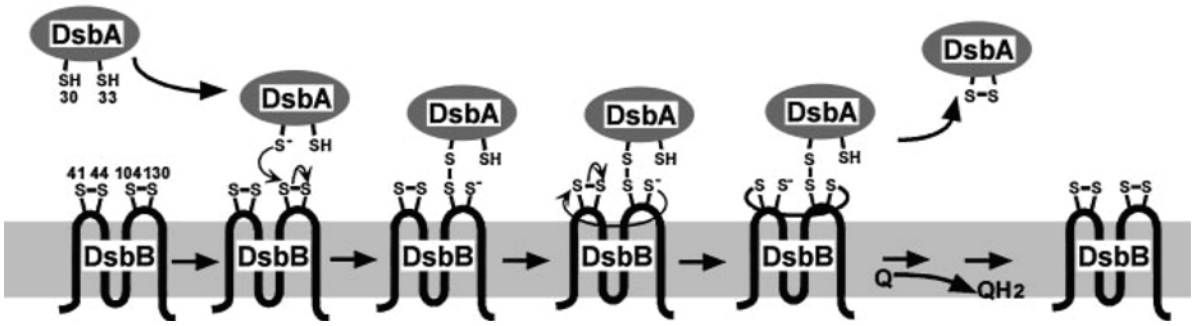

Figure 33. Schéma représentatif des successions de ponts disulfure dans la protéine DsbB lors de la formation du complexe DsbA/DsbB.

La cystéine 30 de la protéine DsbA est à l'origine d'une attaque nucléophile sur le disulfure 104/130 de la protéine DsbB, formant un pont disulfure $C30_{DsbA}/C104_{DsbB}$. La cystéine 130_{DsbB}, sous forme réduite, va alors attaquer le disulfure C41/C44 formant ainsi une cystine avec la cystéine C41. La mobilisation de la cystéine 130 de DsbB dans une liaison covalente avec la cystéine 44 permet alors à la cystéine 33_{DsbA} de résoudre le disulfure intermoléculaire $C30_{DsbA}/C104_{DsbB}$, permettant ainsi aux électrons d'aller à l'encontre des potentiels d'oxydoréduction (Kadokura *et al.* 2003).

V.1.d. Le système Dsb, conservation et variation chez les organismes procaryotiques

La description du système Dsb, présenté ci-dessus, est principalement issue d'études menées chez *E. coli*. Néanmoins, l'existence de systèmes semblables a été rapportée chez d'autres procaryotes allant de l'absence de protéines DsbA et/ou DsbB chez *Streptococcus pyogenes* (la fonction de ces protéines étant probablement remplies par des « isopeptide bond proteins ») à la coexistence de plusieurs systèmes parallèles d'introduction des ponts disulfure chez *Salmonella enterica*, *E. coli CFT073,* ou *Streptomyces coelicolor*) (Heras *et al*. 2009).

V.1.e. Rôles physiologiques

V.1.e.1. La maturation des cytochromes c

Chez les procaryotes, les cytochromes c (Cyt c) sont de petites protéines monomériques présentes dans le périplasme et possédant un cofacteur sous forme d'hème c lié de façon covalente par l'intermédiaire d'un motif di-cystéine CxxCH. Ces protéines jouent un rôle essentiel dans plusieurs processus physiologiques dont, notamment, le transfert des électrons. A la différence des eucaryotes, chez lesquels la maturation des Cyt c est réalisée par une seule protéine, la CCLH (Cytochrome C Heme Lyase), les procaryotes possèdent un système complexe de maturation appelé Ccm (Cytochrome C Maturation) (Steiner *et al*. 1996; Sanders *et al*. 2010). Ce système opère de concert avec le système Dsb dans la maturation des Cyt c (Figure 34). Tout d'abord, les

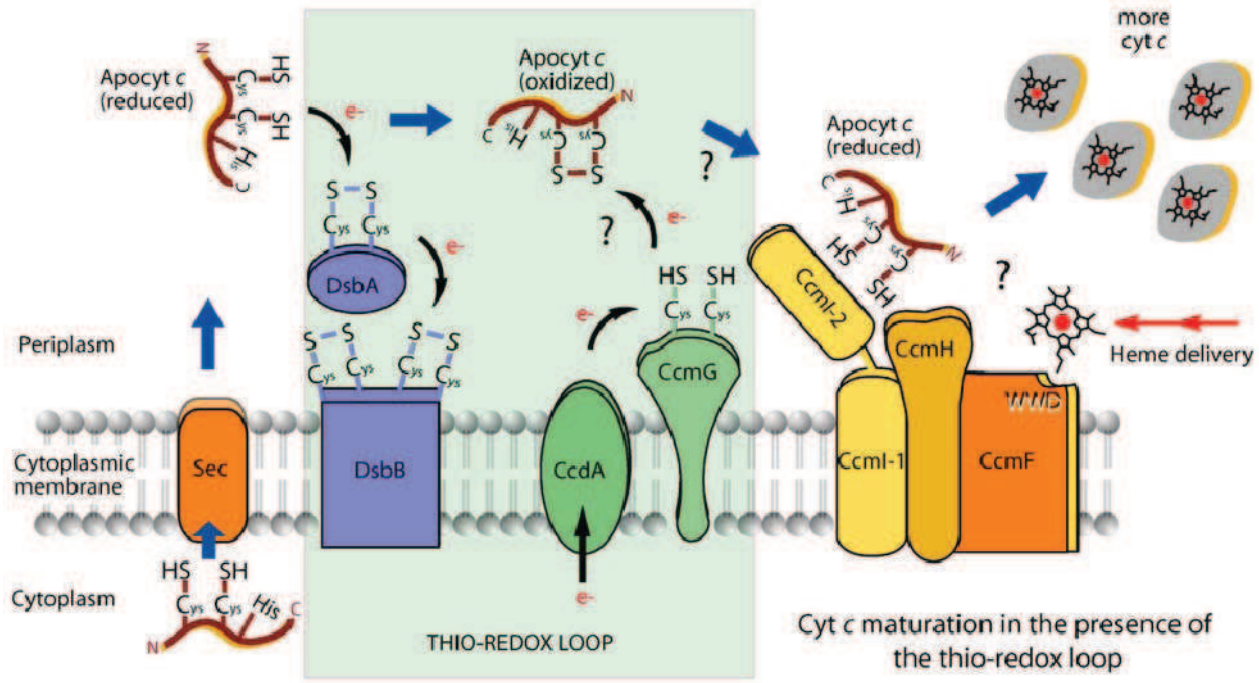

Figure 34. La voie de maturation des cytochromes c dans le périplasme des bactéries.
Après leur synthèse dans le cytoplasme, les apocytochromes c sont transportés dans le périplasme par le système Sec. La première étape de la maturation est l'oxydation du motif CxxCH des apocytochromes c par le système DsbA/DsbB. Cette oxydation est suivie d'une réduction de ce motif par la protéine Ccmg (ou DsbE). Une fois réduit, l'apocytochrome c peut interagir avec la machinerie d'incorporation des hèmes pour l'obtention de cytochromes c matures (Turkaslan *et al*. 2009).

ponts disulfure sont introduits par le le couple DsbA/DsbB qui met en jeu une oxydation des résidus Cys de l'apocytochrome c transporté au sein du périplasme (Figure 34) (Kranz *et al*. 1998). Ensuite, le motif CxxCH subit une réduction ciblée par au moins une protéine du système Ccm, la protéine CcmG, réaction nécessaire à la fixation covalente de l'hème. La protéine CcmG, liée à la membrane du périplasme, possède un module à repliement Trx et un motif di-cystéine CxxC maintenu réduit par la protéine membranaire DsbD (Di Matteo *et al*. 2010). Ainsi, cette protéine

est parfois considérée comme faisant partie du système Dsb et peut être dénommée DsbE (Figure 34) (Sanders *et al*. 2010).

V.1.e.2. Système Dsb et virulences bactériennes

Les protéines Dsb peuvent également être impliquées dans la virulence bactérienne. Dans ce cas, des études ont notamment mis en évidence l'implication de la protéine DsbA dans le repliement de différentes protéines intervenant ou supposées intervenir dans la virulence des bactéries vis-à-vis de leur hôte. La protéine DsbA intervient au niveau de trois processus :

L'adhésion

C'est le cas d'une souche d'*E. coli* uropathogénique où la mutation de DsbA inhibe la production des fibrilles responsables de sa fixation. Il a été démontré que l'intervention de DsbA dans ce phénomène est indirecte, en effet celle-ci est nécessaire au repliement d'une protéine chaperonne, la protéine PapD, qui est essentielle à l'assemblage des fibrilles (Jacob-Dubuisson *et al*. 1994).

Les systèmes de sécrétion

La protéine DsbA semble impliquée dans les systèmes de sécrétion de type II et de type III. Dans le cas de systèmes de type II, la protéine DsbA intervient dans la maturation de l'appareil de sécrétion mais également dans le repliement redox dépendant de certaines protéines transitant par celui-ci. Dans le cas des systèmes de type III, DsbA joue un rôle dans la maturation des composants du système de sécrétion (Heras *et al*. 2009).

Prolifération et mobilité

L'infection par des bactéries pathogènes nécessite qu'elles soient mobiles afin de coloniser leur hôte. Ainsi, il a été démontré que la protéine DsbA est un facteur essentiel à la maturation de la protéine FlgI (*Flagelar P ring motor protein*), composant périplasmique du système de motilité des bactéries. L'intervention des protéines DsbA et DsbB a pu être démontrée *via* l'étude de mutants *dsbA* et *dsbB* chez lesquels les bactéries étaient dans l'incapacité de produire des flagelles fonctionnels (Dailey & Berg 1993; Hayashi *et al*. 2000).

V.2. Le repliement des protéines redox-dépendant dans le réticulum endoplasmique des organismes eucaryotiques

Le réticulum endoplasmique est une structure membranaire en étroite relation avec le noyau des cellules faisant partie de la voie de sécrétion des protéines chez les eucaryotes (van Vliet *et al*. 2003). La maturation des protéines, provenant des systèmes de translocation couplés aux ribosomes, débute dès l'émergence de leurs extrémités N-terminales au sein du RE (Christis *et al*. 2008). Ce processus de maturation est complexe et regroupe un ensemble de protéines chargées de favoriser le repliement des polypeptides néo-synthétisés. Il existe quatre grands types de fonctions impliquées dans la maturation des protéines : la glycosylation, le repliement par les chaperonnes, les peptidyl-prolyl *cis-trans* isomérisations (effectuées par les cyclophilines) et les oxydoréductions (Trombetta & Parodi 2003; Christis *et al*. 2008). Le RE ayant des capacités limitées de maturation, il est nécessaire de maintenir un équilibre dynamique entre l'entrée des polypeptides néo-synthétisés et leur export ou leur dégradation. Pour cela deux voies de signalisation coexistent dans le RE :

La voie du « *contrôle qualité du RE* » (ERQC, *Endoplasmic Reticulum Quality Control*) qui s'assure que les protéines ont bien adopté leur conformation native.

La voie de « *dégradation associée au RE* » (ERAD, *Endoplasmic Reticulum Associated Degradation*) qui adresse les protéines qui ont adopté une mauvaise conformation vers les protéasomes cytoplasmiques par l'intermédiaire de réactions d'ubiquitinylation (Hegde & Ploegh 2010). Ces deux voies assurent les « sorties » du RE par sécrétion ou adressage aux protéasomes, cependant lors de stress biotiques ou abiotiques, la demande en activité de maturation peut dépasser les capacités du RE. Dans ce cas, une troisième voie est mise en œuvre. Il s'agit de la voie de « *réponse aux protéines non matures* » (UPR, *Unfolded Protein Response*). Cette voie de signalisation va pouvoir réguler l'import des protéines dans le RE par des modifications transcriptionnelles en diminuant la transcription des protéines transitant via le RE. Elle va également augmenter les capacités du RE en maturation des protéines en augmentant la transcription des acteurs du repliement des protéines.

Nous allons maintenant nous intéresser aux protéines responsables des réactions d'oxydoréduction mises en œuvre dans la maturation des protéines. Ces réactions sont principalement réalisées par deux familles multigéniques, les sulfhydryl oxydases et les protéine disulfure isomérases (Lambert & Freedman 1983; Pollard *et al*. 1998; Sevier *et al*. 2001). Dans un premier temps

nous allons décrire chaque famille de protéines séparément, puis nous détaillerons les modalités de leurs interactions dans un paragraphe spécifique.

V.2.a. Les sulfhydryl oxydases et la formation des ponts disulfure

Les sulfhydryl oxydases sont des protéines à cofacteurs catalysant spécifiquement la formation de ponts disulfure entre deux résidus Cys sous forme thiol (Figure 35A). Ces enzymes peuvent être différenciées en deux classes suivant la nature de leurs cofacteurs (Figure 35B):

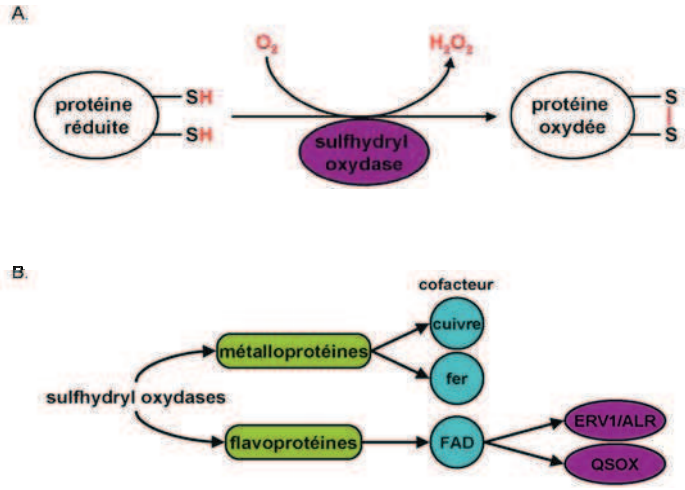

Figure 35. Les sulfhydryl oxydases.
A. Ces protéines sont en mesure de catalyser, en présence d'oxygène, la formation de ponts disulfure entre deux cystéines sous forme thiols. B. Les deux différents types de sulfhydryl oxydases définies en fonction de la nature de leurs cofacteurs.

→ Les sulfhydryl oxydases à cofacteurs métalliques (cuivre ou fer) (Janolino & Swaisgood 1975; Lash & Jones 1983),

→ Les sulfhydryl oxydases à cofacteur FAD (Lisowsky 1992).

Nous allons principalement nous intéresser aux sulfhydryl oxydases FAD dépendantes. Ces protéines à FAD peuvent également être divisées en trois sous-groupes, suivant leur organisation modulaire:

→ Les Erv/Alr

→ Les Qsoxs

→ Les EROs

V.2.a.1.Les protéines de type Erv/Alr

Les protéines Erv/Alr (Essential for Respiration and Viability/ Augmenter of Liver Regeneration) appartiennent à deux catégories. La première renferme la protéine ubiquitaire Erv1 et la protéine Alr ou HPO, orthologue de Erv1 chez l'homme (Starzl *et al*. 1979; Francavilla *et al*. 1994; Li *et al*. 2005). Erv1 est une protéine homodimérique formées de monomères de petite taille (15kDa) et adressée dans l'espace inter-membranaire des mitochondries où elle intervient dans le système d'introduction des ponts disulfure que nous détaillerons au paragraphe V.3.

Le second membre des Erv (Erv2) est spécifique aux champignons et a été identifié comme résident du RE et intervenant dans le repliement redox dépendant de certaines protéines (Sevier *et al*. 2001). Cette protéine, liée à la membrane du RE par un signal d'ancrage et un domaine transmembranaire (comme c'est le cas pour les autres résidents du RE de la famille des sulfhydryl oxydases, voir ci-dessous), réalise le transfert de disulfure grâce à deux motifs di-cystéines sous formes CxxC et CxC (Figure 36A). Bien que n'appartenant pas à la superfamille des Trxs, la structure tridimensionnelle des protéines Erv2 présente certaines caractéristiques communes avec les

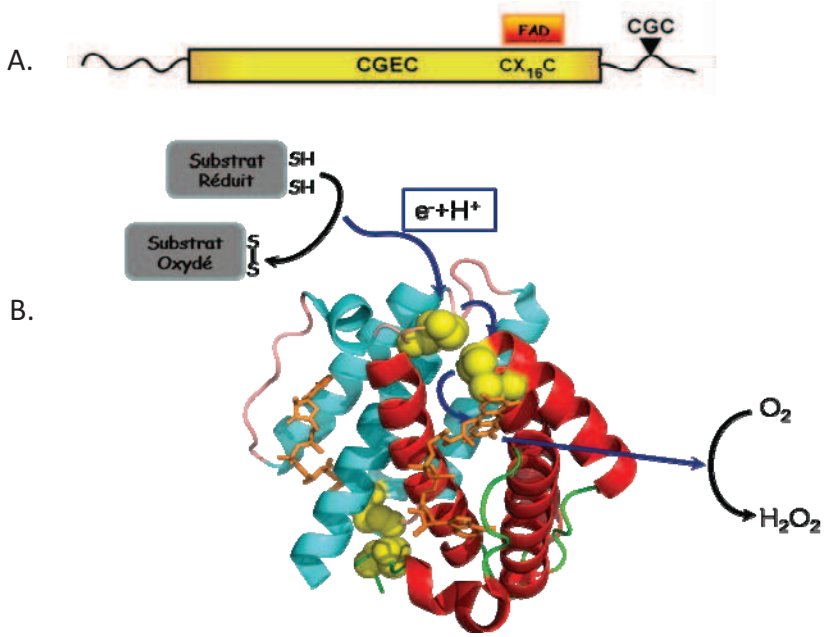

Figure 36. Caractéristiques de séquence et trajet des électrons au sein de la protéine Erv2p de Saccharomyces.

A. Représentation schématique des caractéristiques de séquence de la protéine Erv2p. Sont représentés les motifs di-cystéines catalytiques CxxC et CxC (CGEC et CGC, respectivement chez Saccharomyces) ainsi que le motif de fixation du cofacteur à flavine FAD. B. Schématisation du trajet des électrons au sein du dimère d'Erv2p (PDB 1JR8) lors de l'oxydation d'un substrat réduit. Les électrons sont tout d'abord « captés » par le motif CxC de la sous-unité A (bleu) libérant le substrat sous forme oxydée. Le motif CxC va ensuite transférer ses électrons au motif CxxC de la sous-unité B (rouge). Les électrons transiteront ensuite via le cofacteur FAD (orange) de la même sous-unité vers l'accepteur final, ici l'O_2. Les résidus cystéinyls sont représentés par des sphères jaunes.

protéines à repliement Trx. Ainsi le motif CxxC, qui est un élément central des transferts dithiol/ disulfure, y est conservé (Figure 36B). De plus, comme pour les protéines à repliement Trx, le motif di-cystéine est positionné en amont d'une hélice-α, conférant au site actif une très bonne exposition (Figure 36B). Cependant, les similitudes s'arrêtent ici. En effet la structure tridimensionnelle des protéines Erv est généralement caractérisée par le terme « paquet d'hélices » (Figure 36B). Dans cette conformation les quatre hélices-α sont arrangées de façon parallèle formant un « ballot » structural (Gross *et al*. 2002). Ce cas n'est pas unique et un exemple bien documenté de remplacement physiologique d'une protéine à architecture basée sur un tonneau β par une protéine structurée en hélice-α est le couple plastocyanine/ cytochrome c6 dans le transport photosynthétique des électrons chez les algues vertes (Redinbo *et al*. 1994).

La dimérisation de la protéine est nécessaire à son mécanisme catalytique. Les résidus Cys réduits présents sur les substrats de la protéine Erv2 sont dans un premier temps oxydés via le motif CGC de la sous-unité A (Figure 36B). Ce motif, dès lors sous forme réduite, est dans une portion de la protéine peu structurée et connue comme jouant un rôle de « navette à électrons » entre le substrat réduit et le motif catalytique CxxC de la sous-unité B (Vala *et al*. 2005). Une fois les électrons transmis au motif CxxC, qui se trouve très proche du cofacteur FAD, celui-ci va lui transmettre les électrons, et en particulier au noyau isoalloxazine, l'accepteur d'électrons transitoire (Figure 36B). Enfin le FAD transfèrera ces électrons à un accepteur final pouvant être l'oxygène moléculaire.

D'un point de vue physiologique, à ce jour, aucun partenaire cible n'a pu être identifié *in vivo*, bien qu'il ait été démontré que Erv2p était capable d'interagir *in vitro* avec la PDI de *Saccharomyces cerevisiae* (Vala *et al*. 2005; Wang *et al*. 2007).

V.2.a.2. Les protéines de type Qsox

Les protéines Qsox, pour « Quiescin Sulfhydryl Oxydase », sont des protéines multimodulaires présentes chez certains procaryotes et eucaryotes (Kodali & Thorpe 2010a). Les gènes codant les protéines Qsox, initialement identifiées au sein de cellules fibroblastiques, présentent un fort contraste de niveau d'expression lors de la transition multiplication/quiescence des cellules (d'où leur dénomination de « Quiescin Sulfhydryl Oxydase ») (Coppock *et al*. 1993). Le nombre d'isoformes présentes chez ces organismes varie de 1 à 4 (Houston *et al*. 2005; Coppock & Thorpe 2006; Heckler *et al*. 2008b; Kodali & Thorpe 2010a). Ainsi, les organismes procaryotiques ou unicellulaires (photosynthétiques ou non) ne possèdent qu'un seul gène alors que les plantes su-

périeures présentent un ou deux gènes et certains métazoaires, jusqu'à quatre gènes. Par contre, chez les champignons, aucun gène n'a pu être identifié.

V.2.a.2.α. Organisation modulaire et trajet des électrons au sein de la protéine

Suivant les organismes considérés, l'organisation modulaire des Qsoxs varie sensiblement. Ainsi chez les mammifères, les protéines Qsox sont composées de quatre à cinq modules, deux modules à repliement Trx dans la partie N-terminale, un domaine « spacer » ou HRR (« Helix rich region) et un module Erv qui possède deux motifs CxxC appelés motifs « proximal » et « distal » respectivement en fonction de leurs positions dans la séquence (Figure 37) (Coppock *et al*. 1998; Hoober *et al*. 1999). Un module d'ancrage situé en partie C-terminale de la protéine, responsable de sa localisation au niveau de la membrane du RE est également présent. Les deux modules à repliement Trx présentent des caractéristiques différentes. En effet, seul le module situé au niveau de l'extrémité N-terminale possède le motif CxxC alors que chez le protiste *Trypanosoma brucei* ou les organismes photosynthétiques, le second domaine est absent, aboutissant à une organisation modulaire de type Trx/HRR/Erv (Figure 37) (Coppock *et al*. 1998; Coppock & Thorpe 2006; Kodali & Thorpe 2010b). La présence d'un ou deux domaines Trx fusionné à un module Erv a posé la question de l'apparition de telles protéines (Coppock *et al*. 1998). L'hypothèse admise

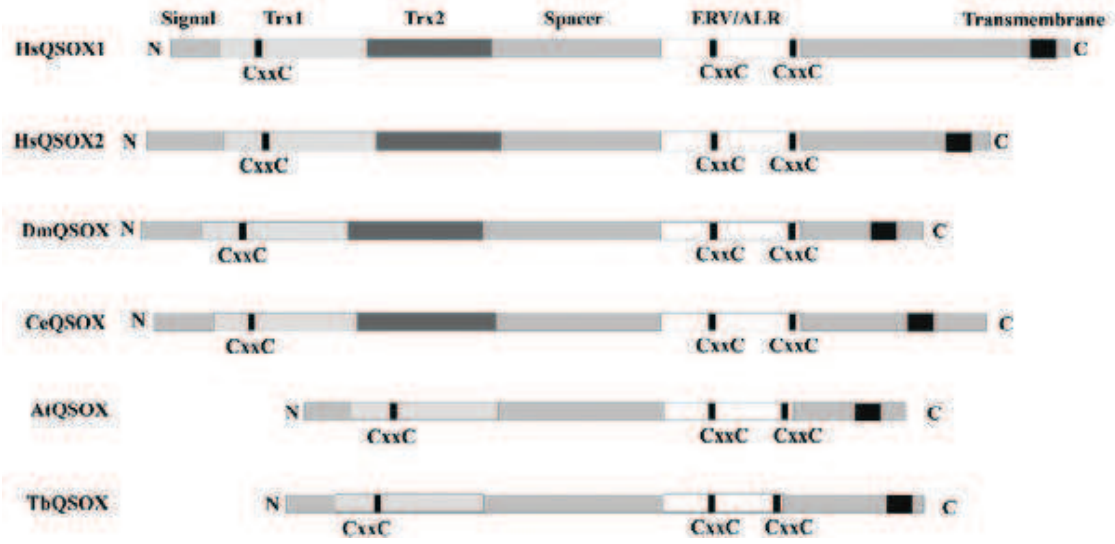

Figure 37. Organisation modulaire des protéines Qsox chez différents organismes.
HsQsox1 et HsQsox2 représentent respectivement les deux isoformes chez l'homme, DmQsox (AE003819.3) une des quatre isoformes chez *Drosophila melanogaster*, CeQsox (NP_508652.1) une des trois isoformes chez *Caenorhabditis elegans*, AtQsox (AY035175.1) une des deux isoformes chez *Arabidopsis thaliana* et TbQsox l'unique isoforme chez *Trypanosoma brucei* (Coppock &Thorpe 2006).

aujourd'hui est que le gène Qsox est le résultat d'une fusion entre deux gènes ancestraux, un gène Trx et un gène Erv. Le gène Qsox ancestral aurait subi une duplication du module Trx suivie de mutations de celui-ci, aboutissant aux gènes présents chez les mammifères (Figure 38). Récemment, une partie de cette hypothèse a pu être confirmée par obtention de la structure cristallographique du domaine Erv de la protéine humaine Qsox1 (Alon *et al*. 2010). En effet, en plus de leur identité de séquence, le domaine Erv de la protéine humaine Qsox1 et la protéine Erv1 d'*Arabidopsis* présentent de fortes homologies de structure, incluant la conservation du « ballot » structural (paragraphe V.2.a.1.) caractéristique de ces protéines et de sites d'interaction avec le cofacteur flavinique (Figure 39) (Vitu *et al*. 2006; Alon *et al*. 2010).

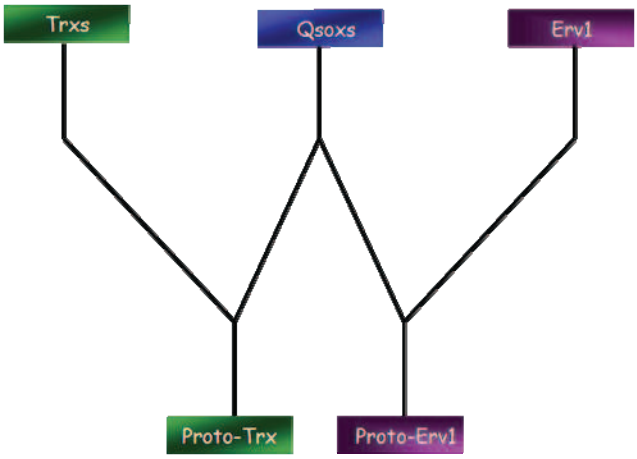

Figure 38. Hypothèse sur l'origine de l'émergence des gènes codants les protéines multimodulaires Qsox à partir des gènes ancestraux Trx et Erv1 (Coppock et al., 1998).

Figure 39. Comparaison du domaine Erv de la protéine humaine Qsox1 et de la protéine AtErv1.

A. Superposition des structures tridimensionnelles du fragment HRR/Erv de la protéine HsQsox1 (vert, PDB 3LLk) et de la protéine Erv1 d'Arabidopsis (bleu pâle, PDB 2HJ3). Les cofacteurs FAD ainsi que les ponts disulfure catalytiques CRDC et CREC sont représentés en bâtonnets rouge pour HsQsox1 et orange pour AtErv1. B. Alignement de séquences des protéines AtErv1 et du fragment Erv de la protéine HsQsox1. Les acides aminés surlignés en noir sont conservés. Les structures secondaires des protéines AtErv1 et HsQsox1 sont respectivement représentées en partie haute et basse de l'alignement de séquence.

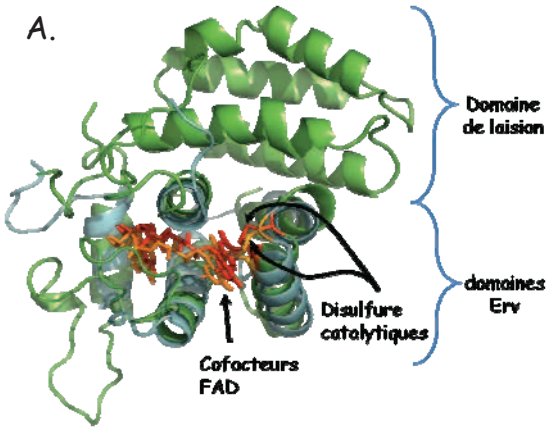

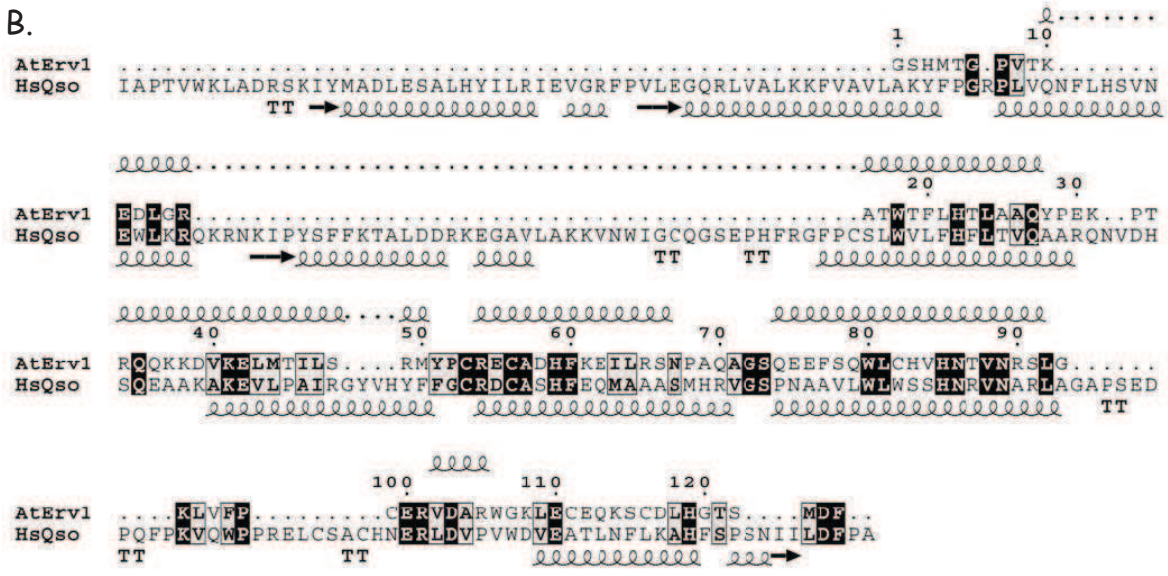

Les protéines Qsox ont été décrites comme dimériques ou monomériques suivant l'organisme considéré (Hoober *et al*. 1999; Jaje *et al*. 2007; Heckler *et al*. 2008a). Ainsi, selon l'état d'oligomérisation des protéines, deux séquences de transfert d'électrons ont été proposées (Figure 40). La première étape, correspondant à une étape d'oxydation du substrat protéique réduit via le motif CxxC du module Trx est commune pour les deux types de protéines. Dans le cas des protéines dimériques, les électrons vont être transférés au motif CxxC "distal" du domaine Erv de la même sous-unité. Les électrons transiteront ensuite par le motif CxxC "proximal" et le FAD de la seconde sous-unité pour terminer leur trajet vers l'accepteur final d'électrons, l'oxygène moléculaire. Dans le cas des protéines monomériques, le module Trx transfère les électrons directement au motif "proximal" du domaine Erv, puis au FAD (Figure 40) (Heckler *et al*. 2008a). Dans ce cas, le motif CxxC "distal" n'interviendrait pas dans le transfert des électrons. De plus, la résolution structurale de la protéine Qsox1 humaine (forme monomérique), indique que l'arrangement tridimensionnel du fragment Erv n'est pas compatible avec un mécanisme catalytique faisant intervenir le motif di-cystéine distal. Toutefois, les données structurales et mécanistiques indiquent que ce motif, strictement conservé chez toutes les Qsoxs, pourrait avoir un rôle dans la régulation de l'activité de la protéine ou dans la stabilisation de sa structure tridimensionnelle (Heckler *et al*. 2008a; Heckler *et al*. 2008b; Alon *et al*. 2010).

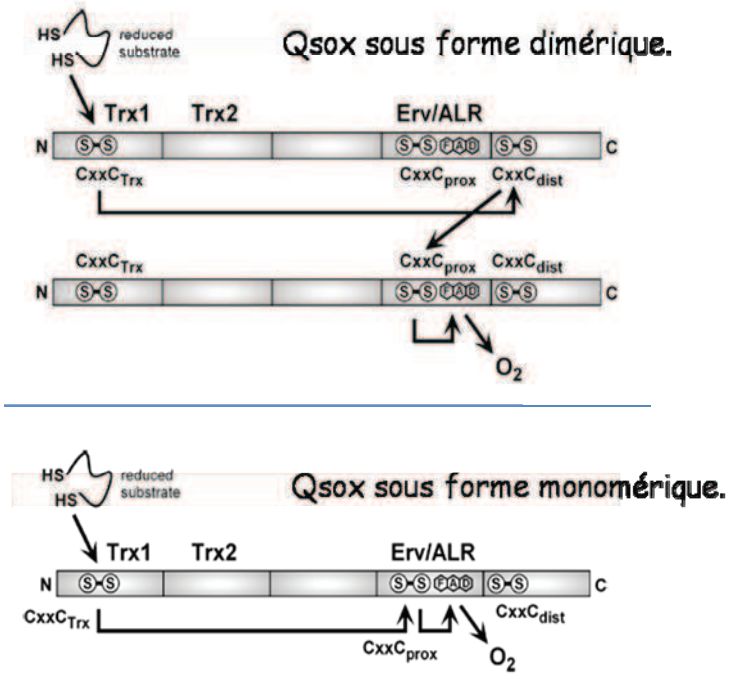

Figure 40. Trajet des électrons au sein de la protéine Qsox humaine suivant son état d'oligomérisation.
Figure détaillé dans le texte (Heckler *et al*. 2008a).

V.2.a.2.β. Localisation subcellulaire et rôle physiologique des protéines Qsox

Malgré la présence d'un module d'ancrage dans les 2 Qsoxs de mammifères, leur localisation subcellulaire n'est pas identique. Ainsi, la Qsox1 est liée aux membranes du RE, à l'appareil de Golgi ainsi qu'aux vésicules de sécrétion (Mairet-Coello *et al*. 2004; Tury *et al*. 2004). Une fraction du pool de protéine Qsox1 humaine peut être sécrétée, du fait de sa présence dans des surnageants de culture de fibroblastes (Coppock *et al*. 2000). La seconde isoforme (Qsox2/SOXN), a pu être, quant à elle, détectée au niveau du cytoplasme mais également au niveau de la membrane nucléaire (Wittke *et al*. 2003). Chez les organismes photosynthétiques, des expériences d'expression transitoire dans des cellules d'épiderme de tabac ont d'autre part montré que la protéine Qsox2 (QSO2) d'*Arabidopsis* est localisée au niveau de la paroi cellulaire. Enfin, lorsque Qsox2 est exprimée chez la levure, une fraction du pool de protéine est sécrétée (Alejandro *et al*. 2007).

Nous détaillerons dans un autre paragraphe les hypothèses concernant le rôle des Qsoxs au sein du RE. Comme nous l'avons mentionné précédemment, les Qsoxs présentent différentes localisations subcellulaires possibles et les résultats que nous présenterons dans ce paragraphe concernent les Qsoxs non résidentes du RE. Très peu de données *in vivo* ont été décrites à ce jour au sujet des Qsoxs, mais néanmoins, deux études majeures permettent d'avancer quelques hypothèses quant à la fonction des protéines Qsoxs, notamment chez les mammifères. Ainsi, une étude de transformants menée sur de cellules de neuroblastomes a pu démontrer l'implication de la protéine Qsox2 humaine dans la voie de signalisation de l'apoptose (Wittke *et al*. 2003). Il a également été rapporté que la protéine Qsox1 joue un rôle dans la signalisation de l'apoptose cellulaire en réponse à un stress oxydant, mais également de protection contre ces stress (Morel *et al*. 2007). Dès lors, ces deux protéines (Qsox1 et Qsox2) semblent présenter des rôles antagonistes dans la signalisation de l'apoptose, Qsox1 montrant des capacités de prévention de l'apoptose lors de sa surexpression alors que la protéine Qsox2 augmente la sensibilité des cellules vis-à-vis de celle-ci (Wittke *et al*. 2003; Morel *et al*. 2007). Ces fonctions *a priori* opposées concernent des protéines qui présentent des localisations subcellulaires différentes et probablement des partenaires eux aussi différents. On peut donc émettre l'hypothèse que leurs fonctions antagonistes seraient le résultat d'interactions avec des cibles spécifiques.

Chez les organismes photosynthétiques, seule une étude du mutant Qsox2 d'Arabidopsis a été décrite. Cette protéine semblerait être impliquée dans la régulation de l'homéostasie cationique, au niveau de la paroi cellulaire (systèmes d'efflux du potassium, indépendamment du sys-

tème SKOR) (Gaymard *et al*. 1998; Alejandro *et al*. 2007).

V.2.a.3. Les protéines de type ERO

Le gène codant une protéine appelée ERO, pour Endoplasmic Reticulum Oxidoreductin, a été découvert à la fin des années 90 par deux équipes travaillant sur la régulation du statut redox du RE de la levure *Saccharomyces cerevisiae* (Frand & Kaiser 1998; Pollard *et al*. 1998). Grâce à des approches génétiques, ces deux équipes ont mis en évidence l'importance de ce locus dans le maintien du pouvoir oxydant du RE. En effet, des mutants de la levure *Saccharomyces cerevisiae* dépourvus de leur gène ERO présentent une hypersensibilité à un traitement au dithiothreitol (DTT) tandis que la surexpression de ce même gène confère une résistance au DTT (Figure 41) (Frand & Kaiser 1998; Pollard *et al*. 1998). A l'instar des protéines Erv2p de champignons et contrairement aux protéines de type Qsoxs, les EROs sont spécifiquement adressées au RE, qui est à ce jour leur seule localisation subcellulaire décrite (Frand & Kaiser 1998; Pollard *et al*. 1998). Les EROs sont représentés chez tous les eucaryotes, cependant leur nombre varient suivant les espèces. Ainsi chez *Saccharomyces cerevisiae* ou le nématode *Caenorhabditis elegans*, on ne retrouve qu'un seul gène, tandis que chez beaucoup d'autres eucaryotes, deux gènes codant deux isoformes des protéines EROs sont retrouvés (Cabibbo *et al*. 2000; Frand *et al*. 2000; Dixon *et al*. 2003). Initialement découverte chez *Saccharomyces*, cette protéine a été dénommée ERO1p (Pollard *et al*. 1998). Cette dénomination a été conservée chez les organismes présentant plusieurs isoformes. Ainsi chez l'homme et les mammifères en général, les deux isoformes d'ERO sont appelées ERO1-α et ERO1-β (ou ERO1-Lα et ERO1-Lβ) (Cabibbo *et al*. 2000; Pagani *et al*. 2000). Néanmoins, la nomenclature des gènes présents chez *Arabidopsis* diffère quelque peu puisque les deux gènes ont été dénommé AERO1 et AERO2 (pour Arabidopsis Endoplasmic Reticulum Oxidoreductin) (Dixon *et al*. 2003).

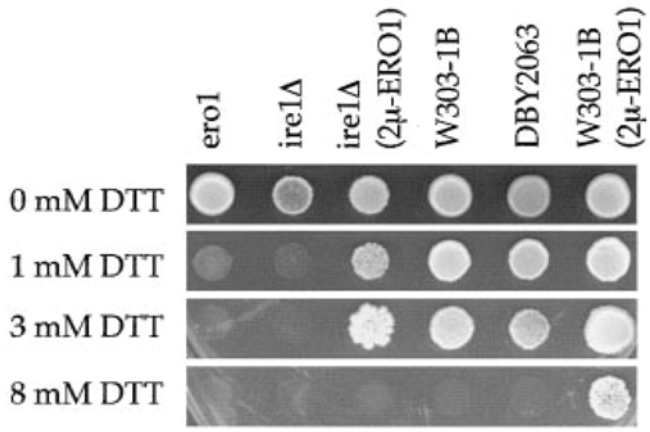

Figure 41. La sensibilité de souches de levure à un stress réducteur est dépendante du niveau d'expression du gène ERO1.

Différentes souches de levure soumises à des traitements au DTT. Les souches *ero1* et *ire1Δ* sont respectivement délétées pour le gène ERO1 et IRE1, ce dernier codant une kinase transmembranaire indispensable à la mise en place des réponses du réticulum endoplasmique lors d'un stress (UPR). Les souches W303-1B et DBY2063 sont les souches parentales des mutants *ero1* et *ire1Δ*, respectivement. La mention 2μ-ERO1 indique une souche contenant un plasmide multicopie du gène ERO1 (Pollard *et al*. 1998).

V.2.a.3.α. Caractéristiques biochimiques et structurales des EROs

Les EROs sont des flavoprotéines monomériques avoisinant les 60 kDa mais ne présentant pas d'identité de séquence avec les deux autres membres des sulfhydryl oxydases (Erv/Qsoxs). Ces protéines, comme toutes les sulfhydryl oxydases, possèdent des cystéines strictement conservées leur permettant de réaliser des réactions d'oxydation. Cependant, suivant les organismes et les différentes isoformes considérées, le nombre de Cys présentes peut varier. Ainsi les protéines humaines ERO1-α et ERO1-β présentent, respectivement, 15 et 14 résidus Cys, ERO1p 14 résidus Cys, et les isoformes AERO1 et AERO2 d'*Arabidopsis* 18 résidus Cys (Figure 42) (Dixon

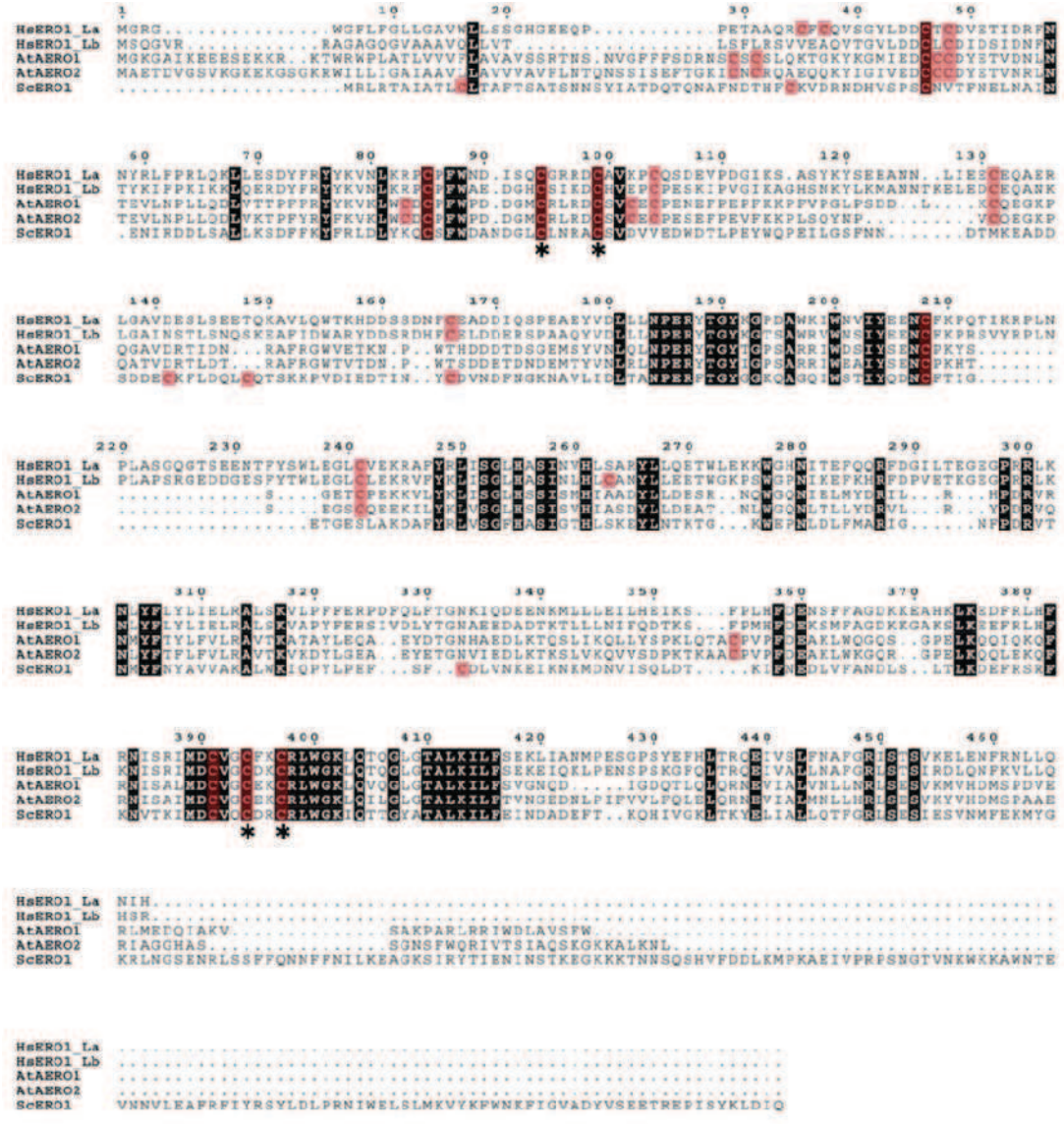

Figure 42. Alignement de séquences primaires des protéines EROs issues de différents organismes.

Sont représentées les séquences des deux isoformes des protéines ERO humaine HsERO1-La et HsERO1-Lβ (accessions NP_055399.1 et NP_063944.3, respectivement). Les deux isoformes d'Arabidopsis AtAERO1 et AtAERO2 (accessions AT1G72280 et AT2G38690, respectivement), et la protéine ERO1 de Saccharomyces (accession D6W0F5) sont présentées. Les acides aminés strictement conservés sont surlignés en noir et les résidus cystéinyls en rouge. Les astérisques indiquent les résidus cystéinyls essentiels à l'activité de la protéine.

La numérotation est différente de celle reportée dans le texte du à l'alignement de séquence.

et al. 2003). Tous ces résidus ne sont pas impliqués dans les réactions d'oxydation catalysées par les EROs. Seuls 4 résidus Cys (en position 100, 105, 352 et 355) sont impliqués dans le transfert d'électrons dans la protéine ERO1p (Figure 42) (Frand & Kaiser 2000). Ces 4 résidus Cys forment 2 ponts disulfure, respectivement entre les Cys 100 et 105 et les Cys 352 et 355, à l'origine d'un mode d'action qui pourrait être comparable aux autres protéines de la famille des sulfhydryl oxydases (et particulièrement des protéines Erv voir paragraphe V.2.a.1.). Le pont disulfure 100-105 est responsable de l'oxydation du substrat et forme ce que l'on nomme « une navette à électrons » (Figure 42). Le second pont disulfure (formé entre les Cys 352 et 355), va accepter les électrons provenant de la « navette » (ré-oxydant celle-ci) et les transmettre au FAD. Comme cela a déjà été mentionné pour les autres sulfhydryl oxydases, le FAD transmettra alors les électrons à l'oxygène moléculaire.

Les protéines ERO1p et ERO1-α humaine présentent des caractéristiques structurales similaires aux autres membres de la famille des sulfhydryl oxydases (Gross *et al*. 2004; Inaba *et al*. 2010). Ainsi ces protéines sont riches en structures secondaires et particulièrement en hélices-α (Figure 43A). La chaine polypeptidique des EROs, à la différence des Qsoxs, forme un unique module protéique. Le mode de liaison entre les protéines EROs et leur cofacteur FAD est tout à fait comparable à celui précédemment rapporté pour les protéines Erv/Qsoxs. En effet, 4 hélices-α forment le « ballot structural » caractéristique du site de liaison des sulfhydryl oxydases avec le FAD (Figure 43A). Cependant, ce site de liaison est réparti entre les parties N- et C-terminale de la protéine au niveau des hélices-α 2, 3, 7 et 8 à la différence de la protéine Erv2p dans laquelle le « ballot structural » est présent dans les hélices-α 1, 2, 3 et 4 (Figure 43B). Une autre caractéristique commune aux EROs et à Erv/Qsox concerne la présence de deux ponts disulfure essentiels au mécanisme catalytique. Dans la protéine ERO1p, ces deux ponts disulfure se trouvent dans des environnements structuraux propices à leurs fonctions. Ainsi, le pont disulfure 100/105 se trouve dans une région à faible taux de structure secondaire indispensable à sa mobilité, tandis que le disulfure 352/355 se trouve à proximité du noyau isoalloxazine, l'accepteur d'électrons du FAD (Figure 43C-E)

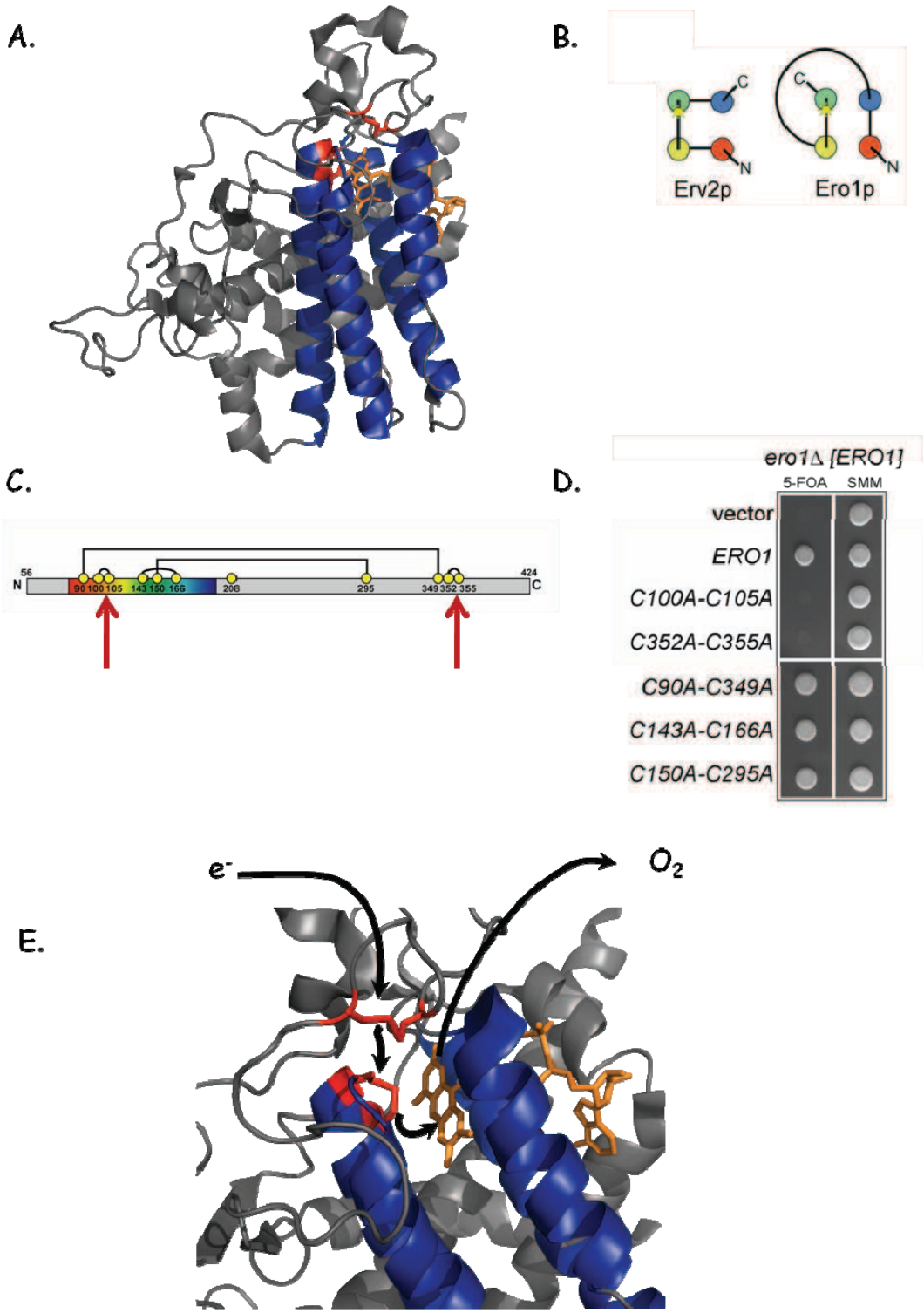

Figure 43. *Caractéristiques structurales et fonctionnelles de la protéine ERO1p.*

A. Structure tridimensionnelle de la protéine ERO1p de Saccharomyces (PDB 1RQ). Les résidus cystéinyls impliqués dans le transfert des électrons sont représentés en bâtonnets rouges et le cofacteur FAD en orange. Les hélices-a colorées en bleu forment « le ballot structural », structure tridimensionnelle commune à toutes les sulfhydryl oxydases et nécessaire à la fixation du cofacteur FAD. B. Comparaison du « ballot structural » que l'on retrouve dans les protéines Erv2p et ERO1p de Saccharomyces (figure détaillé dans le texte) (Gross et al., 2002). C. Les différents disulfure que l'on retrouve dans la protéine ERO1p, les flèches rouges indiquent la position des disulfure catalytiques (Sevier et al., 2007). D. Implications fonctionnelles des différents disulfure de la protéine ERO1p par complémentation de souches déficientes de levure pour le gène ERO1 (D'après Sevier et al., 2007). E. Organisation structurale des disulfure catalytiques de la protéine ERO1p, les résidus cystéine sont représentés en bâtonnets rouges et le cofacteur FAD en orange. Les flèches noires indiquent le transfert des électrons depuis le substrat réduit à l'accepteur final d'électrons l'oxygène moléculaire.

Les EROs présentent une caractéristique unique parmi les protéines de la famille des sulfhydryl oxydases puisque leur activité est elle-même régulée d'une façon redox dépendante suivant l'accessibilité ou la disponibilité du pont disulfure 100-105 (Figure 44) (Sevier *et al*. 2007; Inaba *et al*. 2010).

En ce qui concerne la protéine ERO1p, il a été démontré que deux ponts disulfure (90/349 et 150/295) intervenaient dans la régulation de son activité (Figure 44A). Cependant, il a été démontré que le pont disulfure 150/295 jouait le rôle le plus important (Sevier *et al*. 2007). Au niveau structural, ces deux ponts disulfure permettent de lier la région flexible N-terminale, conte-

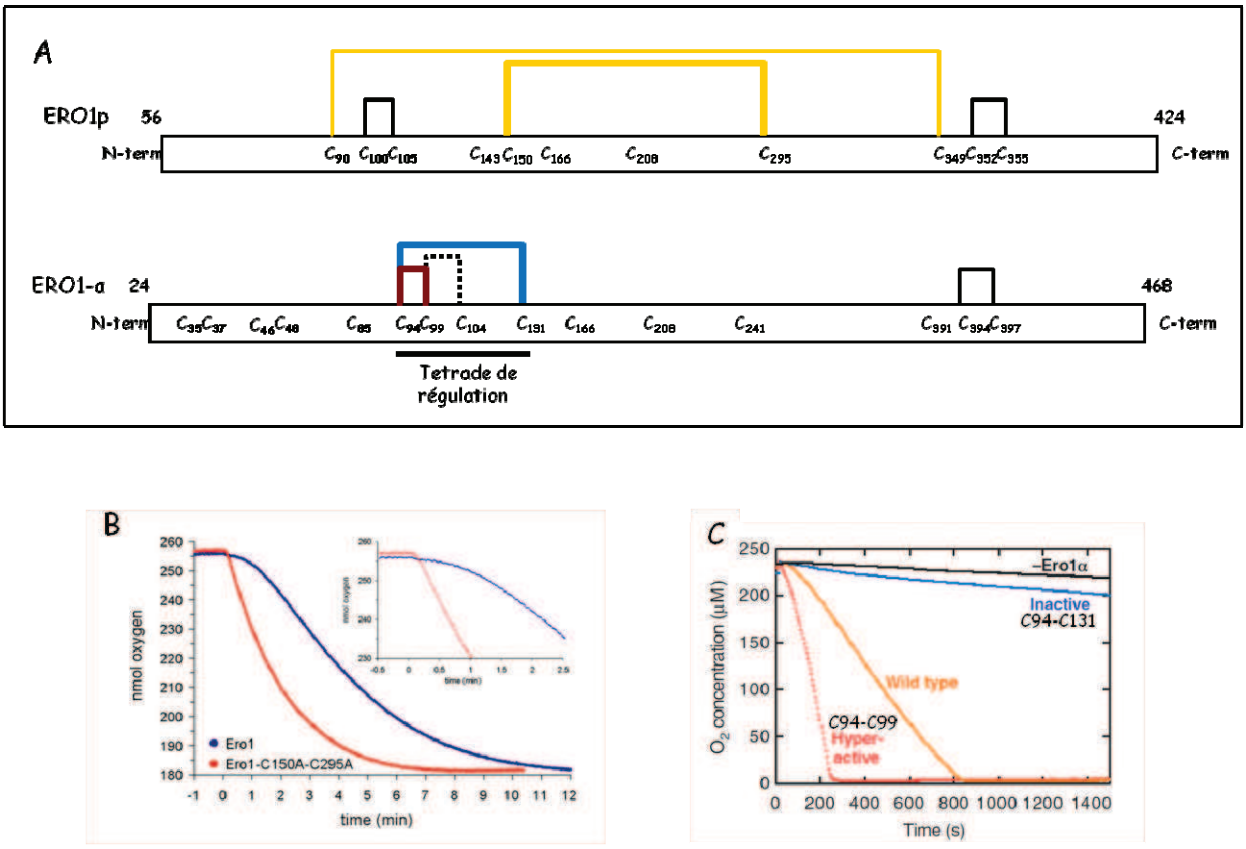

Figure 44. Rôles des cystéines régulatrices des protéines ERO1.

A. Représentation schématique des ponts disulfure impliqués dans le mécanisme catalytique des protéines ERO1p et ERO1-α (en noir) et dans la régulation de leur activité (différentes couleurs suivant leurs implications). Pour la protéine ERO1p les disulfure régulateurs sont représentés en jaune, l'intensité du trait indique leur importance relative (épais = forte importance, fin = faible importance ; D'après Sevier et al., 2007). Dans le cas de la protéine ERO1-α le disulfure responsable du transfert des électrons au cofacteur FAD est représenté en noir tandis que les disulfure possibles au sein de la tétrade de régulation présentent le code couleur de la partie *C*. Lors de la formation des disulfure *C94-C99* et *C94-C131* la protéine est respectivement hyperactive ou inactive. En pointillés est représenté le possible disulfure formé dans la configuration *C94-C131* entre les cystéines 99 et 104 (Inaba et al., 2010). *B.* Oxydation de Trxs réduites par deux mutants de la protéine ERO1p (Sevier et al., 2007). L'indication *ERO1-C150A-C295A* correspond à une double mutation cystéine pour alanine. *C.* Oxydation de la PDI humaine par la protéine ERO1-α en présence de 10mM de glutathion réduit. Les indications *C94-C99* et *C94-C131* correspondent aux disulfure présents dans la protéine (Inaba *et al*. 2010).

nant le pont 100-105, à la partie riche en hélices-α contenant le pont disulfure 352-355 (Figure 44A). Ainsi, lorsque les deux ponts disulfure sont formés, la mobilité du fragment protéique contenant le pont 100-105 se trouve diminuée. Au contraire, lorsque les cystéines 90/349 et 150/295 sont sous forme réduite, le segment N-terminal de la protéine est plus mobile, permettant ainsi une meilleure interaction entre les deux ponts disulfure catalytiques (Figure 44B).

Dans le cas de la protéine humaine ERO1-α, le mécanisme de régulation de l'activité de la protéine semble plus complexe et ne serait pas le résultat de simples formations/réductions de ponts disulfure régulateurs, mais d'échanges au sein d'une tétrade de résidus cystéine (Figure 44A et C) (Appenzeller-Herzog *et al*. 2008a; Inaba *et al*. 2010). Suivant les combinaisons de disulfure entre les résidus en position 94, 99, 104 et 131, la protéine peut être inactive (pont disulfure entre les cystéines 94 et 131) ou hyperactive (pont disulfure entre les cystéines 94 et 99, figure 44A et C) (Inaba *et al*. 2010). De plus, le pont disulfure C94-C131, responsable majoritaire de l'inactivation de la protéine ERO1-α, présente un potentiel d'oxydoréduction avoisinant les -275 mV, ce qui le rend stable dans le contexte oxydoréducteur du réticulum endoplasmique (Baker *et al*. 2008; Meyer & Dick 2010). *In vivo*, la réduction de ces ponts disulfure régulateurs pourrait intervenir grâce à un partenaire protéique non identifié maintenu sous forme réduite au sein du RE ou grâce au GSH (Sevier & Kaiser 2008).

V.2.a.4. Redéfinition du statut redox du RE

Le crible physiologique ayant permis l'identification des protéines EROs a dès le début laissé supposer que les protéines EROs jouent un rôle majeur dans le maintien du statut redox du RE (Frand & Kaiser 1998; Pollard *et al*. 1998). L'importance des EROs dans ce processus a depuis été confirmée chez différents organismes, aboutissant à la reformulation de certaines hypothèses quant à l'origine du pouvoir oxydant du RE (Kadokura & Beckwith 2001; Appenzeller-Herzog *et al*. 2008a; Enyedi *et al*. 2010; Tavender & Bulleid 2010).

Il est communément admis que les protéines extracellulaires, donc transitant par le RE et les autres organelles de la voie de sécrétion, doivent être sous forme oxydée pour assurer leur stabilité. De ce fait, la communauté scientifique a longtemps accepté l'hypothèse selon laquelle la voie de sécrétion était une voie d'oxydation. Au début des années 90, de nombreuses études allant dans ce sens ont montré, d'après des quantifications intracellulaires des pools respectifs de GSH et de GSSG, que le RE était un environnement oxydant du fait de son plus faible ratio GSH/GSSG par rapport aux autres compartiments (Hwang *et al*. 1992). Ainsi la nécessité pour les organismes de produire des protéines oxydées était tout à fait compatible avec les données concer-

nant les concentrations en GSH et GSSG au sein des voies de sécrétion. Néanmoins, la découverte des EROs a radicalement modifié cette perception de l'origine du pouvoir oxydant du RE. En effet, aujourd'hui, la fonction des pool de GSH/GSSG est radicalement opposée. Il a été proposé que la concentration en GSH du RE était suffisante pour maintenir certaines oxydoréductases sous forme réduite, leur réduction étant nécessaire à leur fonction au sein du RE (Tu *et al*. 2000; Chakravarthi *et al*. 2006; Sevier & Kaiser 2008). Une autre hypothèse avancée est l'importance du GSH du RE dans la prévention d'un stress oxydant. En effet la surexpression de la protéine ERO, qui induit de par son activité un stress oxydant (voir ci-dessous), induit une diminution du pool de GSH du RE (Sevier & Kaiser 2008).

V.2.a.5. Les sulfhydryl oxydases: sources de molécules oxydantes

L'introduction de cystines sur des protéines cibles via les protéines de la famille des sulfhydryl oxydases (Erv2/Qsox/ERO) est couplée avec la consommation de dioxygène et la formation de peroxyde d'hydrogène. Le bilan de cette réaction globale est qu'une molécule d'oxygène va accepter deux électrons et deux protons provenant des deux cystéines pour former une molécule d'H_2O_2 et un pont disulfure selon un ratio de 1:1. Ainsi, l'introduction de ponts disulfure par les sulfhydryl oxydases est source de stress oxydant dans le RE. Bien que des systèmes de détoxication d'H_2O_2 existent dans ce compartiment, la régulation de l'activité des EROs est un processus essentiel au maintien de l'intégrité du RE (Tavender *et al*. 2008; Tavender & Bulleid 2010). Les études corrélant l'activité des sulfhydryl oxydases et le statut redox du RE concernent essentiellement les protéines EROs, et il a été démontré que la surexpression ou la déplétion par RNAi de la protéine ERO1-α induisent de fortes modifications de concentrations en H_2O_2 du RE (Enyedi *et al*. 2010). Ce type de changement n'a pu être identifié pour Erv2p ou Qsoxs. Ceci est peut être dû à leur spécificité de substrat comme cela a été proposé, impliquant une production réduite de molécules oxydantes.

V.2.b. Les protéine disulfure isomérases, protéines responsables de la formation et de l'isomérisation des ponts disulfure

Les premières études révélant l'existence de facteurs favorisant le repliement redox dépendant ont été réalisées au début des années 60 sur des extraits bruts ou fractionnés de foie de rat (Goldberger *et al*. 1963). Anfinsen et coll. ont mis en évidence la présence d'un ou de plusieurs facteurs favorisant la réactivation de la ribonucléase A (RNAse A), protéine contenant 4 ponts disulfure nécessaires à son activité. Le ou les facteurs responsables de la catalyse de la réactivation de la RNAse furent enrichis par purification de microsomes, c'est-à-dire par l'isolement de l'ensemble des structures membranaires des cellules chez différents organismes (Goldberger *et al*. 1963; Givol *et al*. 1964). Les protéines les plus abondantes de ces fractions avoisinent les 60 kDa, représentant jusqu'à 0,8% de l'ensemble des protéines solubles des cellules (Freedman *et al*. 1994). Ces protéines sont les protéine disulfure isomérases (en anglais disulfide isomerases, PDI). Les PDIs appartiennent à la superfamille des Trxs du fait de la présence de plusieurs modules protéiques présentant des homologies de structure avec les Trxs (Figure 45) (Lundström &

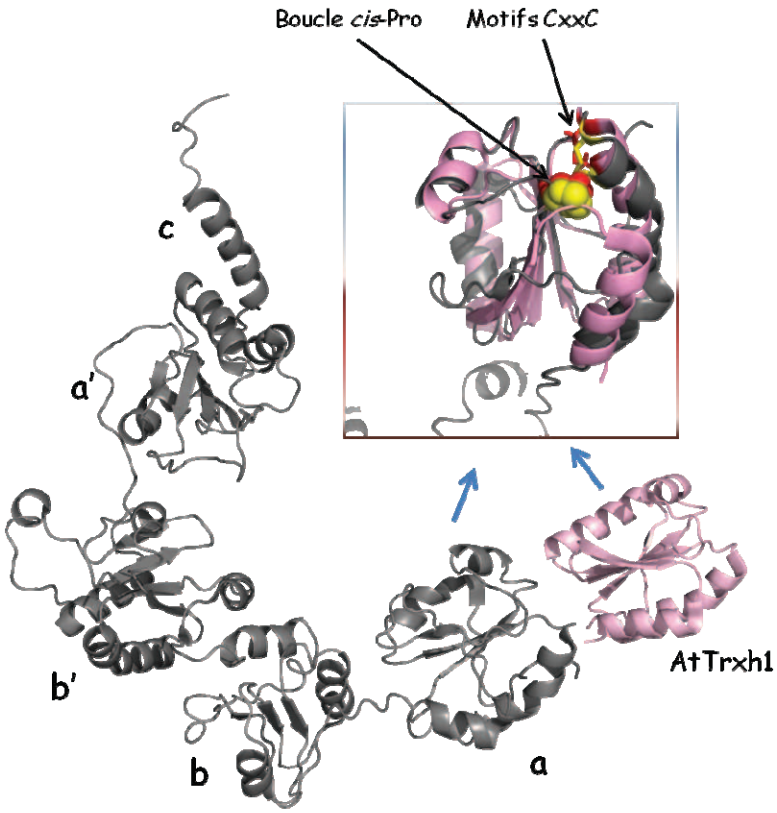

Figure 45. Comparaison des structures tridimensionnelles des protéines Trxh1 d'*Arabidospsis* (PDB 1XFL) et de la PDI1p de Saccharomyces (PDB 3BOA).

AtTrxh1 est représenté en rose pâle et ScPDI1p en gris. Les lettres présentes le long de la structure de la PDI indiquent les modules protéiques. La superposition des structures de la Trxh1 et du module « a » de PDI est également représenté dans l'encadré. Les motifs dicystéine (ici sous forme de cystines) et la boucle de la *cis*-Proline sont représentés, respectivement, en bâtonnets et en sphères de couleurs différentes (rouge pour la Trxh1 et jaune pour la PDI).

Holmgren 1990; Krause & Holmgren 1991; Carvalho *et al*. 2006; Kozlov *et al*. 2010b). Ces protéines présentes chez tous les eucaryotes sont codées par une famille multigénique comprenant de 3 à 6 gènes chez les champignons ascomycètes ou basidiomycètes, 19 gènes chez l'homme ou 13 gènes chez Arabidopsis (Norgaard *et al*. 2001; Houston *et al*. 2005; Appenzeller-Herzog & Ellgaard 2008b; Duplessis *et al*. 2011).

V.2.b.1.Caractéristiques des PDIs chez les organismes photosynthétiques

Article 1. Comparative genomic study of protein disulfide isomerases from photosynthetic organisms

Benjamin Selles, Jean-Pierre Jacquot, Nicolas Rouhier.

Genomics 97(1): 37-50 (2011)

Cet article présente une étude phylogénétique de la famille multigénique des PDIs à partir de l'analyse de 24 génomes d'organismes photosynthétiques. Les organismes sélectionnés pour cette étude sont représentatifs des grandes variabilités de physiologie que l'on peut rencontrer chez les autotrophes. Cette analyse revêt de l'importance car la plupart des études précédentes sur les PDIs de plantes ne concernaient le plus souvent que quelques membres ou quelques espèces (Lemaire & Miginiac-Maslow 2004; Houston *et al*. 2005; Kamauchi *et al*. 2008; Lu & Christopher 2008; Wadahama *et al*. 2008; Iwasaki *et al*. 2009). De plus, aucune classification adéquate n'avait pu émerger de ces différentes études. Ainsi la première partie de notre étude consista, sur la base des travaux réalisés sur *Glycine max* à mettre en place un système de classification des PDIs adaptable à l'ensemble des organismes photosynthétiques qu'ils soient unicellulaires ou pluricellulaires. Nous avons également abordé les différents rôles physiologiques des PDIs ainsi que la signification possible de la présence de modules protéiques additionnels chez les PDIs des organismes photosynthétiques. Enfin nous avons réalisé une modélisation de la structure tridimensionnelle de certaines isoformes provenant de plantes terrestres ou aquatiques puisqu'aucune donnée structurale n'est à ce jour disponible.

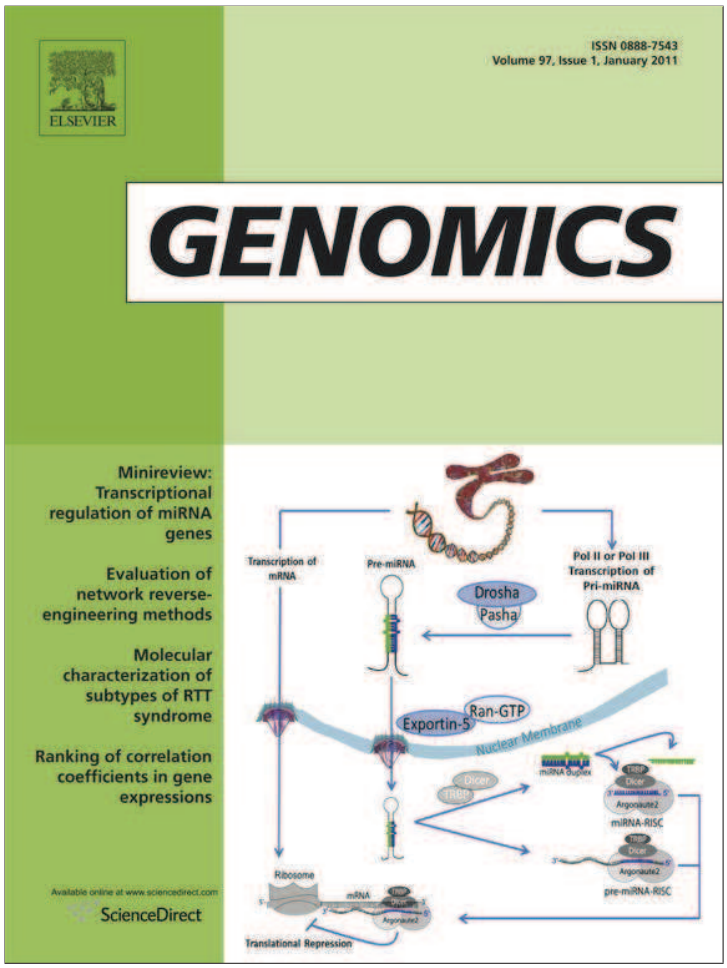

Genomics 97 (2011) 37–50

Contents lists available at ScienceDirect

Genomics

journal homepage: www.elsevier.com/locate/ygeno

Comparative genomic study of protein disulfide isomerases from photosynthetic organisms

Benjamin Selles, Jean-Pierre Jacquot, Nicolas Rouhier *

Unité Mixte de Recherches 1136 INRA Nancy University, Interactions Arbre-Microorganismes, IFR 110 EFABA, Faculté des Sciences BP 239 54506 Vandoeuvre Cedex, France

ARTICLE INFO

Article history:
Received 18 June 2010
Accepted 7 October 2010
Available online 14 October 2010

Keywords:
Photosynthetic organisms
Phylogenomic
Protein disulfide isomerase
Protein folding
Endoplasmic reticulum

ABSTRACT

Protein disulfide isomerases (PDIs) are eukaryotic oxidoreductases essential for oxidative protein folding. Their diversity in photosynthetic organisms was assessed by analyzing 24 sequenced genomes belonging to algal, lycophyte, bryophyte and angiosperm phyla. This phylogenetic analysis led to an updated classification into 9 classes (PDI-A to -F, -L, -M and -S) which differed by the number of Trx domains and the presence of additional domains (*D*, *COPII*, *J* and *ARMET*). From an evolutionary perspective, the distribution and protein architecture of PDIs differ considerably between algae and terrestrial plants, 5 PDI classes are common whereas 1 is specific to terrestrial plants and 3 to algae. Some algal PDI-Fs possess selenocysteine residues. The PDI family is larger in mammals (19 members in human) than in land plants (around 10 members) and *Saccharomyces cerevisiae* (5 members). However, PDIs from photosynthetic organisms display an important structural and functional diversity considering their association to specific protein domains.

1. Introduction

The oxidation of cysteine residues leading to the formation of disulfide bridges is an essential process for protein folding, for the regulation of enzyme catalytic activity or for protein–protein interactions. In eukaryotes, the major compartment in which newly synthesized polypeptide chains are folded is the endoplasmic reticulum (ER), an oxidizing compartment due in part to a lower reduced over oxidized glutathione (GSH/GSSG) ratio than in other sub-cellular compartments [1,2]. Protein disulfide isomerases (PDIs) are considered as major catalysts for protein folding in the ER [3]. PDIs are very versatile enzymes as they are able to catalyze *in vitro* thiol oxidation reactions and disulfide reduction or isomerisation, depending on their redox states. PDIs that are found in an oxidized form most likely function as thiol oxidases, whereas PDIs functioning as isomerases need to be in a reduced state [4]. In the former case, a protein named ERO1 (endoplasmic reticulum oxidoreductase) accepts electrons from reduced PDIs to regenerate an oxidized form. In the latter case, it has been proposed that GSH serves to maintain those PDIs reduced [5]. It is worth mentioning that another class of thiol oxidases called QSOX (quiescin sulfhydryl oxidases) is also expressed in the ER [6]. This apparent redundancy is most likely explained by a different specificity *vs* target proteins, as already observed inside the PDI family [7]. Other sulfhydryl oxidases, called Erv1, with sequence features close to QSOX, form together with MIA40 an oxidative folding system in the inter-membrane space of the mitochondria [8]. Interestingly, in prokaryotes and in particular in cyanobacteria, oxidative protein folding is performed by another subgroup of proteins called DSB proteins for disulfide bond proteins [9]. This includes several proteins devoted either to disulfide oxidation or isomerisation with some of them, DsbA and C, belonging to the thioredoxin (Trx) superfamily, as they possess the characteristic so-called Trx fold, $\alpha1\beta2\alpha2\beta3\beta4\alpha3\alpha4$, consisting of a central pleated β-sheet surrounded by α-helices [10].

Trxs are usually single domain proteins with a WC[G/P]PC active site and which catalyze disulfide reductase reactions because of their low redox potential, around −300 mV [10]. On the contrary, PDIs are generally multi-domain proteins, belonging to the thioredoxin superfamily as it is composed of several Trx domains [11]. Classical PDIs (EC 5.3.4.1) have five domains named *a*–*b*–*b*′–*a*′–*c*. The *a* and *a*′ domains represent Trx domains and usually display two cysteines included in a *WCGHC* active site motif. The different chemical nature of the two middle residues of the CxxC motif, compared to Trxs, is one of the major determinants making PDIs better catalysts for disulfide bond formation as they possess a higher redox potential, generally situated around −150 mV. The *b* and *b*′ domains, although sharing some structural similarity with a Trx domain, do not possess the specific active site motif. Finally, a short and acidic amino acid sequence, referred to as the *c* domain, is present in the C-terminal part, as well as an ER retention signal composed of four amino acids, generally [K/H/N]DEL [12–14]. Besides this typical architecture, other representatives differ by the number of *a* and *b* modules, by the presence and the position of the *c*

* Corresponding author.
E-mail address: nrouhier@scbiol.uhp-nancy.fr (N. Rouhier).

0888-7543/$ – see front matter © 2010 Elsevier Inc. All rights reserved.
doi:10.1016/j.ygeno.2010.10.001

domain, by the presence of additional domains and more specifically for proteins containing *a* domains by the Trx active site sequences. Hence, in eukaryotes, PDIs are encoded by multigenic families. To date, phylogenetic analyses have been essentially conducted in mammals and in *Saccharomyces cerevisiae* [15,16]. In mammals, PDIs have been initially classified into four main classes based on the number and the position of the Trx modules in the sequence [17]. Class 1 contains classical PDIs (*a*–*b*–*b*′–*a*′–*c* architecture) presented above. PDIs from class 2 also possess two *a* modules repeated in tandem in the N-terminal part usually followed by the *b* and *c* domains leading to an *a*°–*a*–*b*–*c* organization. PDIs from classes 3 and 4 both possess three Trx modules. The domain organization for class 3 PDIs is *a*°–*a*–*b*–*a*′ whereas it is of the form *a*–*a*′–*a*″ for class 4 PDIs. PDIs initially identified in yeast and containing a single Trx module, constitute class 5 [17,18]. A recent and exhaustive investigation of PDIs in human reported the existence of 19 members, four PDIs in class 1, one in class 2, one in class 3, three in class 4, eight in class 5 and two PDI members with no catalytic cysteine residues [15]. In *S. cerevisiae*, five PDIs are distributed into classes 1 (Pdi1 and Eug1) and 5 (Mpd1, Mpd2 and Eps1) [16]. Functional studies showed that only Pdi1 is essential for viability [3,16].

Regarding photosynthetic organisms, comparative genomic studies devoted to the exhaustive identification of PDI isoforms have been performed with only a limited number of organisms, i.e. *Arabidopsis thaliana*, *Oryza sativa*, *Zea mays*, *Triticum aestivum* and *Chlamydomonas reinhardtii* [19–22]. From these studies, according to the classification described above, all members are distributed into the classes 1, 2 and 5. However, except for two studies which described the complete set of *Arabidopsis* PDIs [19,20], all other studies were not exhaustive. Moreover, the nomenclature used was not homogeneous and from the PDI domain organization, it cannot be extended to all sequenced photosynthetic organisms, especially algae. For these reasons, a large scale genomic study is still required to understand the distribution and evolution of PDI family in completely sequenced photosynthetic organisms. We have included in this study 24 photosynthetic eukaryote organisms with different lifestyles including algae (diatoms, red and green algae), bryophytes, lycophytes and angiosperms. Furthermore, PDI sequences containing additional protein domains were not much investigated before and this detailed description could provide new tracks regarding the physiological role of such particular PDI isoforms. Finally, the structure–function relationship of these PDIs was evaluated by modelling some of these PDIs against the recently solved 3D structures of mammalian or yeast PDIs.

2. Results and discussion

2.1. An improved classification is needed for PDIs from photosynthetic organisms

As mentioned previously, only a few reports have deeply analyzed the PDI gene content in photosynthetic organisms, leading to distinct nomenclatures (Table 1) [19,20,22]. PDI isoforms were formerly assigned to classes 1, 2 and 5 and numbered consecutively. Hence, *Arabidopsis* isoforms were named PDI1.1 to 1.6, PDI2.1 to 2.3 and PDI5.1 to 5.4 [20]. This nomenclature is indeed adapted for *Arabidopsis* PDI members. However, as it does not take into account the variability in PDI domain organization observed in other organisms, this classification is not adequate for all plant species possessing a different number of PDI in a given class. As an example, in *A. thaliana*, class 1 can be divided into three different subclasses based on the phylogenetic analysis, PDI1.1 grouping with 1.2, PDI1.3 with 1.4 and PID1.5 with 1.6. For a species such as *O. sativa* which possesses 3 isoforms orthologous to AtPDI1.1 and 1.2, this nomenclature would require to denominate them OsPDI1.1, 1.2 and 1.3, whereas OsPDI1.3 is not a true ortholog of AtPDI1.3, having a different domain arrangement. The biggest problem concerns PDIs belonging to class 2 which exhibit two types of modular organizations *a*°–*a*–*D* and *a*°–*a*–*b*–*c*. *Arabidopsis* possesses only one member with an *a*°–*a*–*D* arrangement (AtPDI2.1) and two members with an *a*°–*a*–*b*–*c* arrangement (AtPDI2.2 and AtPDI2.3). Other land plants such as poplar, soybean or maize possess two or four representatives with an *a*°–*a*–*D* organization and one or two representatives with an *a*°–*a*–*b*–*c* organization. Thus, despite having the same number of isoforms, the distribution of PDIs into the different classes differs between species, making the nomenclature not adapted to most recent genomic data.

More recently, an alternative PDI classification, which does not take into account protein domain organization either, was proposed [22]. *A. thaliana* PDIs have been numbered from 1 to 12, the PDIs 1 to 6 correspond to class 1 and display an *a*–*b*–*b*′–*a*′ organization, the PDIs 7, 8 and 12 represent the class 5 (*a*–*x*) and PDIs 9 to 11 the class 2 (*a*°–*a*–*x*). The same problems arise with this nomenclature because isoforms exhibiting different modular organizations will have the same denomination [22]. Very recently, d'Aloisio and colleagues renamed the PDI classes from PDIL1 to 8 with multiple sequences in the same class being numbered consecutively. Although this classification does not present major drawbacks, it splits the PDI with an *a*–*b*–*b*′–*a*′ domain organization into 3 classes, it does not include classes found in other photosynthetic organisms such as algae and it is a bit confusing with the nomenclature used by Urade and colleagues, who have assigned a letter for some *Glycine max* PDI classes and each isoform is numbered consecutively [23–26]. For example, classical PDIs have been named PDI-L and each subclass discriminated by a number. PDI-L1 corresponds to proteins with an *a*–*b*–*b*′–*a*′ arrangement and PDI-L2 and 3 to proteins with a *c*–*a*–*b*–*b*′–*a*′ organization. The major difference between the latter two subclasses lies in the redox active sites of the Trx domains [23,24]. Two isoforms belonging to PDI-L3 subclass have been denominated PDI-L3a and PDI-L3b [23]. Concerning PDI from class 2, those with an *a*°–*a*–*D* modular organization have been named PDI-S and those with an *a*°–*a*–*b*–*c* modular organization PDI-M [25,26]. Using this classification, all isoforms can be numbered in any species regardless of the number of representatives in each class. Basically, we have kept the current PDI-L, -M and -S classes and we propose to denominate the other classes with a similar code letter, from PDI-A to PDI-F, and to attribute a number for each isoform.

2.2. Updated classification for PDIs in photosynthetic organisms

Previous genomic studies identified 13 PDI members in *A. thaliana*, 12 in *O. sativa* and *Z. mays*, 9 in *T. aestivum*, 5 in *C. reinhardtii* and 3 in *Physcomitrella patens* [19–22,27]. From this set of annotated PDI genes, we have extended this inventory, by blast search, to 24 recently sequenced photosynthetic organisms, 11 other *algae* (*Cyanidioschyzon merolae*, *Phaeodactylum tricornutum*, *Thalassiosira pseudonana*, *Ostreococcus lucimarinus*, *Ostreococcus tauri*, *Ostreococcus RCC809*, *Micromonas pusilla CCMP1545*, *Micromonas* sp. *RCC299*, *Volvox carteri*, *Coccomyxa* sp. *C-169* and *Chlorella* sp. *NC64A*) and 9 land plants, the lycophyte *Selaginella moellendorffii*, the moss *P. patens* sp. *patens*, and 7 angiosperms, 1 monocot (*Sorghum bicolor*), and 6 dicots (*G. max*, *Vitis vinifera*, *Populus trichocarpa*, *Manihot esculenta*, *Mimulus guttatus* and *Cucumis sativus*). The selection of these organisms with different lifestyles could also help explain the evolution of PDI sequences across the green lineage. For the PDI sequence mining, we have considered as a major criterion the presence of at least one Trx module, classically with a [Y/F]APWCGHC active site motif. However, we have tolerated some amino acid substitutions in the active site sequence for proteins presenting a noticeable sequence identity outside this region. In this respect, it is interesting to note that no thioredoxin, glutaredoxin or nucleoredoxin sequence has been identified in the course of this genomic analysis. On the contrary, protein sequences having a noticeable similarity with PDIs, but possessing additional domains not reported before in other organisms, have been identified. Last but not least, considering that PDIs are usually targeted to the ER through

Table 1
Classification of PDIs from terrestrial plants.

A. thaliana AGI numbers	Classification from Houston et al.	Classification from Lu et al.	Classification from d'Aloisio et al.	Proposed classification	Human orthologs	Yeast orthologs	Module composition
At1g21750	PDI 1.1	PDI 5	PDIL1-1	PDI-L1	ERp57/PDI/PDIp/PDILT	PDI1p	*a–b–b′–a′*
At1g77510	PDI 1.2	PDI 6	PDIL1-2				
At3g54960	PDI 1.3	PDI 1	PDIL2-1	PDI-L2			*c–a–b–b′–a′*
At5g60640	PDI 1.4	PDI 2	PDIL2-2				
At1g52260	PDI 1.5	PDI 3	PDIL3-1	PDI-L3		Eug1p	*c–a–b–b′–a′*
At3g16110	PDI 1.6	PDI 4	PDIL3-2				
At2g47470	PDI 2.1	PDI 11	PDI-L4-1	PDI-S	No	No	*a°–a–D*
At1g04980	PDI 2.2	PDI 10	PDIL5-1	PDI-M	P5	No	*a°–a–b–c*
At2g32920	PDI 2.3	PDI 9	PDIL5-2				
At1g35620	PDI 5.2	PDI 8	PDIL7-1	PDI-B	TMX3	Eps1	*a–b–b′*
At3g20560	PDI 5.3	PDI 12	PDIL8-1	PDI-C	No	No	*a-COPII*
At4g27080	PDI 5.4	PDI 7	PDIL8-2				
At1g07960	PDI 5.1	–	PDIL6-1	PDI-A	ERp18	No	*a*

Three different classifications have been proposed for *Arabidopsis* PDIs, by Houston et al., by Lu et al. and by d'Aloisio et al., but they do not take into account the diversity existing in other organisms, especially algae. The proposed classification extends the denomination used for *Glycine max* PDI-L, -S and -M [23–26]. For a more comprehensive view, orthologs from yeast and human have been included [15,77]. It is important to note that, for this reason, all yeast and human PDI have not been mentioned here. In particular, concerning the PDI-S class, the closest human PDI, named ERp29, displays a *b–D* domain organization, whereas there is no ortholog in *S. cerevisiae* though it is found in most ascomycetes or basidiomycetes.

a N-terminal targeting sequence and possess a C-terminal retention signal, the presence of both signals has been analyzed carefully. However, it is important to note that these N-terminal extensions are, in general, the most variable parts and that they are very often missed by automatic annotation procedures. For these reasons, some targeting sequences may have been missed also during our manual curation. This analysis led to the identification of 237 annotated and mostly complete PDI sequences in the 24 selected organisms (available as Supplementary material).

The phylogenetic tree, constructed using these PDI sequences, as well as our careful analysis of protein primary structure allowed us to identify several major clades which contain isoforms with a distinct protein domain organization (Fig. 1). The 6 classes containing sequences from land plants are consistent with those described previously [19]. The biggest clade is composed of classical PDIs (*a–b–b′–a′*), forming a single class, PDI-L, which is itself divided into three different subclasses (PDI-L1 to 3) differing by the protein size, by the presence of an acidic N-terminal extension (*c*) and/or by variations in the active site sequences (Fig. 2). These three subclasses have been distinguished in a previous phylogenomic study conducted on land plants exclusively and named PDIL1 to 3 [19]. Although the other branches are sometimes less well defined, probably because of a lower number of representatives, they clearly correspond to eight different classes. Two classes comprise PDIs generally exhibiting two Trx modules (*a°–a*) repeated in the N-terminal part followed by an additional redox inactive domain, either a *b* domain for PDI-M or a *D* domain for PDI-S. The *D* domain is very similar to the one found in the C-terminal part of metazoan ERp28/ERp29 proteins. The 6 other classes (PDI-A to -F) contain PDIs with a single Trx module associated or not with additional domains (Figs. 1 and 2). PDI-A class is specific to land plants, PDI-B class is present in all terrestrial plants and only in stramenopiles, PDI-C class is found both in algae and land plants and PDI-D to -F classes are only present in algae (Table 2). The PDI-A class contains the shortest PDI representatives. It is composed of PDIs with a single Trx domain without any additional domains (Fig. 2). The PDI-B class includes PDIs with an *a–b–b′* organization. The PDI-C class is composed of proteins which possess a C-terminal *COPII* domain found in mammalian proteins involved in ER to Golgi vesicle trafficking (ERGIC-32) and shown to interact with Erv44 and Erv46 proteins (Fig. 2) [28]. The PDI-D class includes proteins constituted by a N-terminal *J* domain fused to a Trx domain and an *ARMET* (arginine rich, mutated in early stage tumors) domain at the C-terminus (Fig. 2). The *J* domain is similar to the one present in DnaJ chaperones which is involved in the interaction with Hsp70. The *ARMET* domain was initially described in mammals as a small protein localized in the ER and up-regulated during unfolded protein response (UPR) [29,30]. The PDI-E class contains PDIs presenting similarity with mammalian TMX proteins and exhibiting a conserved trans-membrane domain at the C-terminus, except one representative from prasinophyte (MpPDI-E2). Finally, the PDI-F class contains proteins formed by a Trx domain followed by an unusually long α-helix in the C-terminal part (Fig. 2). A few sequences with no marked similarity with the classes defined previously, have been denominated PDI-x. However, due to the presence of one or two Trx domains with a WCGHC active site and a slightly modified ER retention signal (RDEL in several of them), they are considered as true potential PDIs.

As already proposed for higher plant thioredoxins and glutaredoxins, one of the criteria to classify genes into classes is to consider the position of introns and the number of exons in the genomic sequences [31,32]. Except for *P. patens*, which exhibits marked differences in the number of exons, the PDI gene organization is overwhelmingly conserved within each land plant group, supporting the proposed classification (data not shown). For instance, with a few exceptions and as observed for *T. aestivum* PDI genes, genes coding for PDI-L1 are formed by 10 exons, by 12 exons for PDL-L2 and L3, by 9 exons for PDI-M, by 11 exons for PDI-S, by 4 exons for PDI-A, by 5 exons for PDI-B and by 15 exons for PDI-C (Fig. 2) [19]. However, this criterion cannot be used for algal PDI genes which diverge strikingly in this respect.

Being involved in the protein oxidative folding of eukaryote proteins, PDIs should be localized in the ER, in the Golgi or in intermediate compartments. As expected, the subcellular localization for all these proteins is predicted to be the either ER or secretory pathways which basically correspond to the same prediction depending on the nomenclature used by each software (Table 3). With the exception of PDI-C sequences, all sequences from other PDI classes exhibit a N-terminal signal peptide of *ca* 20 to 30 amino acids, which is consistent with the analysis of wheat PDIs [19]. In addition, PDI-Ls possess regular C-terminal ER retention signals formed by the last four amino acids, most often KDEL. PDI-A, -F and -M present slightly modified but recognizable sequences. PDI members of other classes do not have clear retention signals raising the question of their final destination. It is of course largely possible that these proteins either enter or are retained in the ER by unknown targeting sequences and mechanisms. It is interesting to note that the plant PDIs which have been shown to be localized either in plastids or in mitochondria, belong to the PDI-L class and possess both the N-terminal signal peptide and retention signal (see paragraph 8 for further details) [33–35].

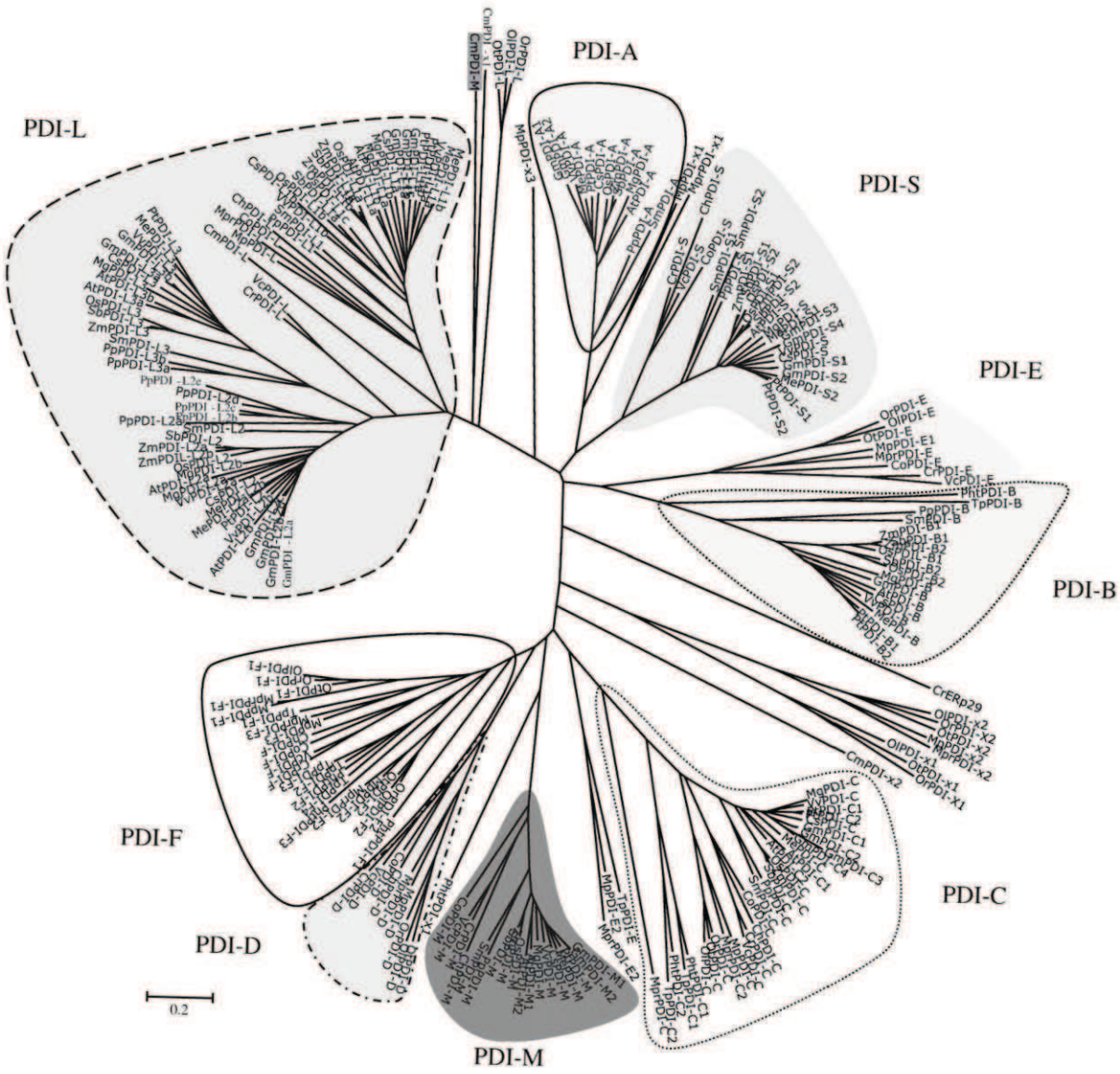

Fig. 1. Unrooted phylogenetic tree of PDIs from photosynthetic organisms. The analysis was performed using MEGA 4 using the neighbor-joining method. Branch lengths are proportional to phylogenetic distances. The name of the protein is composed of the two-letter code for the species, except for *P. tricornutum* (Pht) and *Micromonas* sp. *RCC299* (Mpr) followed by the PDI numbering adopted in this study.

In summary, from the phylogenetic tree, the gene organization and the sequence characteristics, PDIs from photosynthetic organisms can be grouped into 9 classes, each corresponding to a distinct domain organization. Note that the PDI-L class is divided into 3 subclasses. From their primary sequence and prediction programs, most of these PDIs should be localized in the ER constituting an impressive set of chaperones and/or oxidases, which is consistent with the high number of secreted or membrane proteins requiring disulfide bonds for their structural or functional integrity. Each class will be discussed separately in the following sections of this manuscript.

2.3. The PDI-L class: classical PDIs with a–b–b′–a′ domain organization

In land plants, the number of PDI-L usually ranges from 3 in *S. moellendorffii* to 6 in most dicots, whereas algae usually possess only one representative, except the two diatoms, *P. tricornutum* and *T. pseudonana*, which do not possess any member (Table 2). *P. patens* and *G. max* represent particular cases with 8 and 9 PDI-L including 5 and 4 isoforms respectively of the PDI-L2 type, most likely arising from several duplication events specific to these organisms.

From this phylogenetic analysis and in agreement with the work conducted in *G. max*, this class is divided into three subclasses called PDI-L1, L2 and L3. The difference between PDI-L1 and L2 subclasses is the presence of a *c* domain in the N-terminal part of PDI-L2. In both subclasses, the active site sequence of the *a* and *a′* domains is usually YAPWCGHC, with some variations encountered in a few representatives (Fig. 2 and Supplementary Fig. 7). In particular, *Ostreococcus* PDI-Ls surprisingly display a modified YAPWDGHS for the *a* domain, very likely redox inactive, whereas the active site of the *a′* domain (YAPWCRTC), which is divergent compared to usual sequences, contains the two cysteine residues. In PDI-L3, the *c* domain is present but the active sites of the Trx domains have been subjected to various changes, being of the A[P/S]WCXXS and [T/A/S]PWCXXC form for the *a* and *a′* domain respectively.

PDI-Ls from rhodophyte (*C. merolae*), prasinophyte (*M. pusilla CCMP1545*, *M.* sp. *RCC299*, *O. tauri*, *O. lucimarinus* and *O.* sp. *RCC809*) and chlorophyte (*Coccomyxa* sp. *C-169* and *Chlorella* sp. *NC64A*) do not exhibit the N-terminal *c* domain and cluster either with PDI-L1 or form isolated branches as is the case for the 3 *Ostreoccocus* PDI-Ls (Fig. 1). On the contrary, the two other chlorophytes analyzed,

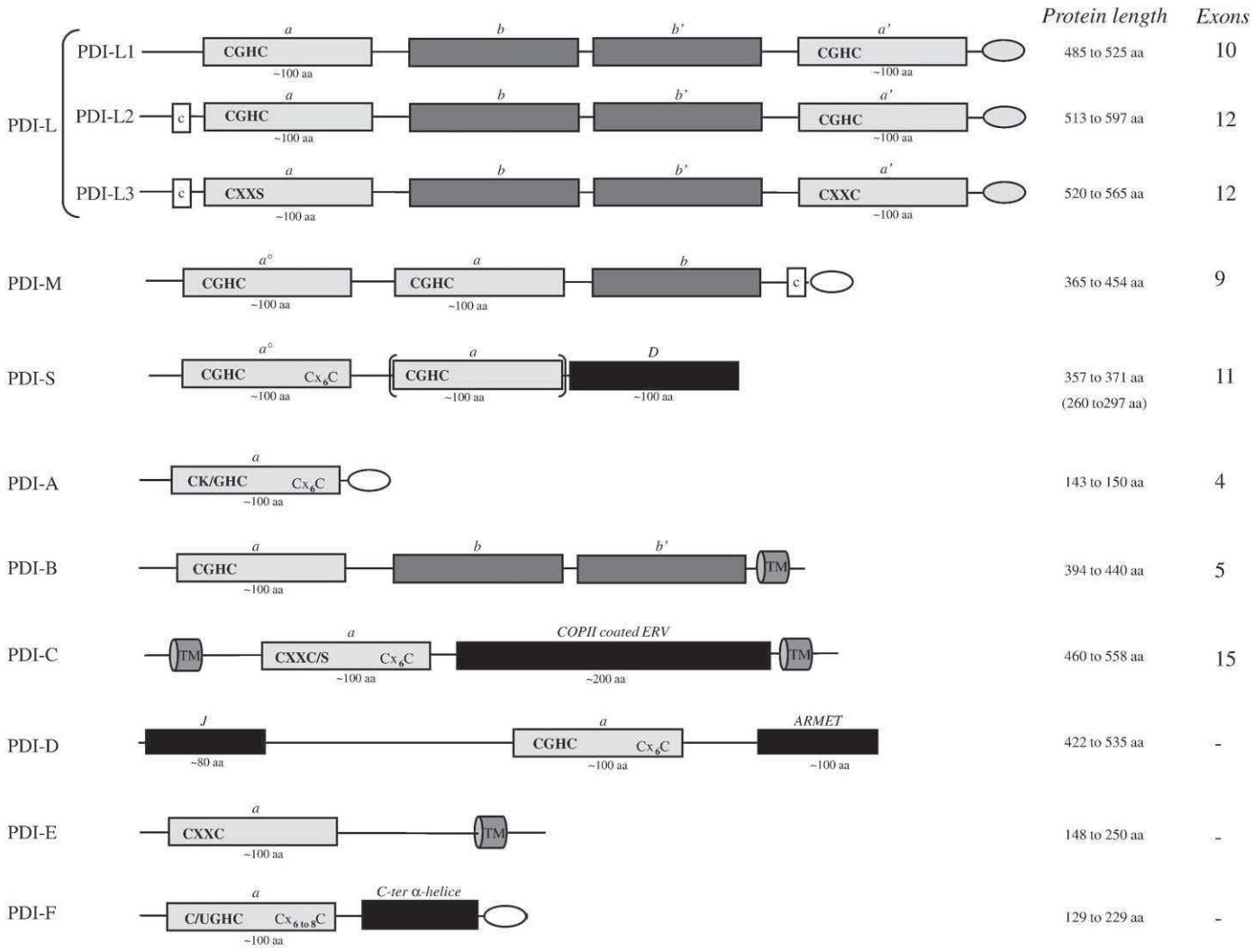

Fig. 2. Domain organization of PDIs from photosynthetic organisms. The protein domains (*a*, *b*, *c*, *D*, *J*, *COPII*, *ARMET*) and approximate sizes, as well as active site sequences and the conserved Cx_6C motif have been depicted for each PDI class. In addition, we have indicated predicted trans-membrane domains and the helical extension for the PDI-F class. The N-terminal signal peptide of around 20 to 30 amino acids, which is present in most PDIs except PDI-C, has not been represented. The classical C-terminal ER retention signal (KDEL) found in PDI-L is represented by a gray circle whereas in PDI-A, -F, -M classes, it is represented by a white circle as only some PDIs possess this potential ER retention signals and as the sequence is very often slightly modified. For PDI-S, algae (*a*°–*D*) possess only a single *a* domain compared to land plants (*a*°–*a*–*D*).

C. reinhardtii and *V. carteri*, possess the acidic extension and rather belong to the PDI-L2 subclass (Table 2). From this gene occurrence, we can speculate that the PDI-L class constitutes a monophyletic group and that the ancestral PDI-L isoform exhibited the *a*–*b*–*b*′–*a*′ architecture with canonical Trx active sites in the *a* domains but without the *c* domain. During chlorophyte evolution, the *c* domain may have been acquired by specific algae. The 3 PDI-L subclasses found in terrestrial plants most likely derive from this gene related to PDI-L2. Subsequently, PDI-L1 might have lost this *c* domain and PDI-L3 accumulated some mutations visible in particular in the Trx active site sequences of the *a* and *a*′ domains. The sequence identities are in the range 28 to 90% for PDI-L1, 33 to 90% for PDI-L2 and 32 to 94% for PDI-L3. The sequence identity between subclasses may support this evolutionary picture. Indeed, the closest subclasses are PDI-L2 and PDI-L3 with an overall 23 to 35% identity, then PDI-L1 and PDI-L2 with 22 to 28% identity and finally the more divergent classes are PDI-L1 and PDI-L3 with 17 to 21% identity.

Comparing these PDIs with human and *S. cerevisiae* representatives, there are some variations concerning the domain organization. The closest human members, human PDI (P4HB, accession number P07237) and human ERp57 (PDIA3, accession number P30101), differ from those identified in plants; the *c* domain is positioned in the C-terminal part in human PDI, whereas the C-terminal extension is constituted by basic residues in human ERp57. Human PDI1p (PDIA2, accession number Q13087) and human PDILT (PDILT, accession number Q8N807) also display an *a*–*b*–*b*′–*a*′ modular organization but possess divergent active sites CGHC/CTHC and SKQS/SKKC, respectively. The only human PDI member presenting a N-terminal *c* domain is human ERP72 (PDIA4, accession number 13667) but it possesses an additional Trx module, having the following domain organization *c*–*a*°–*a*–*b*–*b*′–*a*′. In yeast, yeast PDI1p (accession number 2B5E), is similar to human PDI, exhibiting a C-terminal *c* domain [36]. On the other hand, Eug1p does not possess this domain and it exhibits atypical CXXS active site motifs for the *a* and *a*′ domains [37].

2.4. The a°–a–b domain organization of PDI-M class

In the PDI-M family (*a*°–*a*–*b*–*c*), only one isoform is found in chlorophytes, in rhodophytes and in all land plants except *A. thaliana*, *C. sativus* and *G. max* which possess 2 members most likely arising from species-specific duplication events (Table 2). A careful analysis of *A. thaliana* and *G. max* genomes using the Plant Genome Duplication Database (http://chibba.agtec.uga.edu) indicated some synteny, i.e. co-localization of genes on chromosomes of related species. Indeed,

Table 2
Gene content and distribution of PDIs.

		PDI classes												
		L			M	S	A	B	C	D	E	F	Other	Total
		1	2	3										
Dicots	*Populus trichocarpa*	2	1	1	1	2	1	2	2	0	0	0	0	12
	Arabidopsis thaliana	2	2	2	2	1	1	1	2	0	0	0	0	13
	Glycine max	3	4	2	2	4	2	1	4	0	0	0	0	22
	Vitis vinifera	2	2	1	1	1	1	1	1	0	0	0	0	10
	Manihot esculenta	2	2	1	1	2	1	1	1	0	0	0	0	11
	Mimulus guttatus	2	2	1	1	1	1	1	1	0	0	0	0	10
	Cucumis sativus	2	1	1	2	1	1	1	1	0	0	0	0	9
Monocots	*Sorghum bicolor*	2	1	1	1	2	1	2	1	0	0	0	0	11
	Oryza sativa	3	1	1	1	2	1	2	1	0	0	0	0	12
	Zea mays	2	2	1	1	2	1	2	1	0	0	0	0	12
Lycophytes	*Selaginella moellendorffii*	1	1	1	1	2	1	1	1	0	0	0	0	9
Bryophytes	*Physcomitrella patens* ssp.	1	5	2	1	1	1	1	1	0	0	0	0	13
Chlorophytes	*Chlamydomonas reinhardtii*	0	1	0	1	2°	0	0	1	1	1	1	0	8
	Volvox carteri	0	1	0	1	1	0	0	1	1	1	1	0	7
	Coccomyxa sp. *C-169*	1	0	0	1	1	0	0	1	1	1	1	0	7
	Chlorella sp. *NC64A*	1	0	0	1	1	0	0	1	1	0	1	0	6
Prasinophytes	*Micromonas pusilla*	1	0	0	0	0	0	0	1	1	2	3*	3	11
	Micromonas sp. *RCC299*	1	0	0	0	0	0	0	2	1	2	3*	2	11
	Ostreococcus lucimarinus	1	0	0	0	0	0	0	1	1	1	2*	2	8
	Ostreococcus sp. *RCC809*	1	0	0	0	0	0	0	1	1	1	2*	2	8
	Ostreococcus tauri	1	0	0	0	0	0	0	1	1	1	2*	2	8
Stramenopiles	*Phaeodactylum tricornutum*	0	0	0	0	0	0	1	2	0	0	3	1	7
	Thalassiosira pseudonana	0	0	0	0	0	0	1	2	0	1	4*	0	8
Rhodophytes	*Cyanidioschyzon merolae*	1	0	0	1	0	0	0	0	0	0	0	2	4

The 237 PDI sequences, collected from 24 selected photosynthetic organisms and annotated, have been divided into 9 classes (PDI-A to -F, -L, -M, -S) according to the Trx module organization, to the presence of additional domains and more generally to the sequence identity. Superscript for *Chlamydomonas reinhardtii* PDI-S indicates the presence of a *b–D* isoform. The asterisk indicates the presence of selenoproteins. Because they are too divergent, a few algal sequences, which do not cluster in defined classes (see Fig. 1), have not been integrated in any class and described as other.

the genome areas surrounding AtPDI-M1, and AtPDI-M2, GmPDI-M1 and GmPDI-M2, as well as the isoforms from *V. vinifera* (VvPDI-M) and *P. trichocarpa* (PtPDI-M) exhibit many common genes suggesting that the appearance of a second member in *A. thaliana* and *G. max* results from duplication events specific to these species. Similar syntenic relationships have been observed in monocots for all wheat and rice paralogs [19]. Overall, it also supports the fact that genome duplication and rearrangements are key factors in evolution and occurred widely in plants [38]. On the other hand, the observation that PDI-M are not found in prasinophytes and stramenopiles, suggests that these PDIs emerged recently. However, the presence of a PDI-M in *C. merolae* with an *a°–a–b* organization but which clusters separately, leads us to propose 2 distinct hypotheses: i) a PDI-M representative was originally present in the ancestor of all eukaryote photosynthetic organisms but it has been lost in prasinophytes and stramenopiles or ii) the PDI-M isoform appeared in chlorophytes by combinatorial shuffling of protein domains and independently or by gene transfer in *C. merolae* [39].

Table 3
Prediction of the putative sub-cellular localizations of higher plant PDIs.

PDI classes	YLoc	Sherloc	TargetP
PDI-A (13)	SP: 10, C: 2 (1), M: 1 (1)	ER: 13	SP: 11, M:2 (2)
PDI-B (16)	SP: 12, C: 4 (1), P:1	ER: 14, C: 1, Extra: 1	SP: 15, M: 1 (1)
PDI-C (17)	P: 7 (1), M: 4 (3), SP: 3 (2), N: 3	ER: 10 (8), G: 4 (4), C: 3 (2)	Other: 17
PDI-L1 (24)	SP: 22, N: 2	ER: 23, C: 1	SP: 23, other: 1
PDI-L2 (24)	SP: 23, N: 1	ER: 23, C: 1	SP: 23, C: 1
PDI-L3 (15)	SP: 10 (3), N: 3 (1), C: 2 (2)	ER: 15	SP: 15
PDI-M (14)	SP: 10, P: 3, M: 1	ER: 13, M: 1 (1)	SP: 14
PDI-S (21)	SP: 15, C: 6	ER: 21	SP: 21

The possible sub-cellular localization of all PDI isoforms from land plants was summarized from predictions achieved with three servers, TargetP, Yloc, and Sherloc. From our experience, these are the best tools for proteins targeted to the ER, while Wolfpsort and Psort are not useful for this purpose. For each class, the numbers of isoforms analyzed is indicated between parentheses. For a given isoform, only the best score has been retained. However, the number of sequences for which the probability is below 50% has been indicated between parentheses. Abbreviations are: SP: secretory pathways (including ER targeting), P: plastids, M: mitochondria, N: nucleus, C: cytosol, G: Golgi apparatus, and Extra: extracellular.

All PDI-M isoforms exhibit a strictly conserved *WCGHC* active site in the *a* domain, and a few variations in the three amino acids preceding the active site, FANWCGHC in *S. moellendorffii* and *P. patens* and VASWCGHC in *C. merolae* instead of the usual [Y/F]APWCGHC. Regarding the *a′* domain, all isoforms display an [Y/F]APWCGHC active site sequence with the exception of *C. merolae* (YAPWCGAC) (Supplementary Fig. 8). Considering the absence of a *b* domain in PDI-M compared to PDI-L, these proteins are slightly shorter, ranging usually from 365 to 454 amino acids compared to the 485–597 amino acids found in PDI-L. Excluding *C. merolae* which presents only 17 to 20% identity with all other sequences, the identity ranges from 35 to 97% between viridiplantae members. The presence of a C-terminal transmembrane domain in *C. merolae* PDI-M suggests that this sequence has indeed evolved independently as proposed above.

Concerning the presence of PDI-M orthologs in other kingdoms, only one PDI, referred to as the P5 isoform, is present in mammals [15]. While there is no ortholog in *S. cerevisiae*, PDI-M isoforms were identified in various completely sequenced ascomycetes or basidiomycetes (our observation) [15].

2.5. The PDI-S class: proteins with an a°–a–D domain organization

In land plants, PDI-S members exhibit two N-terminal Trx modules, with a strictly conserved YAPWCGHC active site sequence both in the *a°* and *a* domains, with one exception for *S. moellendorffii* PDI-S2 which exhibits a FINSCGAC active site in the *a°* domain (Supplementary Fig. 9). These Trx modules are coupled with a *D* domain in the C-terminus, generally leading to an *a°–a–D* modular organization. It is worth mentioning that PDI-S are absent in rhodophytes, prasinophytes and stramenopiles and that chlorophytes display PDI-S with an *a–D* domain

organization, suggesting that proteins of this class emerged in this phylum. The additional *D* domain presents an α-helical conformation and a peptide/protein binding site. However, its importance is not clear as mammalian PDI mutants lacking this extension are still able to bind client proteins indicating that the Trx domain of ERp29/ERp28 is sufficient for protein interaction [40]. Some evolutionary features concerning the arrangement of PDI-S domains and their distribution merit development.

From the sequence identity, the *a* domain of algal PDI-S is very similar to both the *a*° (39% identity) and *a* (37% identity) modules of terrestrial PDI-S. However, as a Cx_6C motif conserved in the *a*° module of PDI-S from land plants is not present in the *a* domain of algal PDI-S, the ancestral Trx domain present in PDI-S is probably the *a* domain. Thus, it is tempting to speculate that the additional Trx domain in PDI-S from land plants originates from a duplication of the Trx domain which was inserted in frame before the original domain. It has already been observed that such multimodular proteins can be created by duplication of single domains [41]. Interestingly, *C. reinhardtii* also possesses an isoform with a *b–D* arrangement, similar to the mammalian ERp29/ERp28 supporting the view that this organism retained some genes of metazoan origin [11,42,43].

Regarding the number of PDI-S members, as there is only one isoform in most chlorophytes and *P. patens*, but 2 members in *S. moellendorffii* and most land plants, the more plausible hypothesis is that a duplication event arose after the split between bryophytes and lycophytes. The presence of only 1 gene in some dicots and 4 genes in *G. max* is likely explained by gene loss or duplication respectively (Table 2). As for PDI-M, the questioning of the Plant Genome Duplication Database, both for dicot and monocot PDI-M, indicates that the genomic area surrounding these genes is indeed conserved. The sequence identity ranges from 41 to 89% between terrestrial plant isoforms, from 42 to 70% between *V. carteri*, *Coccomyxa* sp. and *C. reinhardtii* isoforms and from 18 to 33% between algal and terrestrial plant PDI-S. In fungi, PDI-S orthologs with an *a*°*–a–D* domain organization have been identified in most ascomycetes and basidiomycetes but not in *S. cerevisiae*, whereas as indicated before mammals possess *b–D* isoforms (Table 1) [16].

2.6. PDI isoforms with only one Trx module

PDI-A constitute the simplest PDIs, presenting only one Trx module and no additional domain. Hence, these are the smallest PDIs, exhibiting a protein length of *ca* 150 amino acids. Except for *G. max*, which possesses two isoforms probably arising from duplication, all other organisms possess only one isoform (Table 2). Compared to *P. patens* and *S. moellendorffii*, which present a canonical FAPWCGHC active site sequence, higher plant representatives exhibit a divergent but highly conserved C[V/L]PWCKHC active site sequence (Supplementary Fig. 1). The last four C-terminal amino acids are quite variable in these PDIs, in particular for monocot PDI-As (LEAD, LQAD and LQDS) and for *S. moellendorffii* (NDSL) and *P. patens* (AAVL), raising the question of their retention to ER.

The PDI-B class includes PDIs with an *a–b–b′* modular organization. All land plants, except poplar and the 3 monocots analyzed which have 2 members, possess 1 isoform (Table 2). The presence of only one PDI-B isoform in the less evolved organisms, the moss *P. patens* and the lycophyte *S. moellendorffii*, suggests that specific duplication events occurred in monocots after the split with dicots and in poplar. In algae, only the two stramenopiles *P. tricornutum* and *T. pseudonana* present a member of the PDI-B class which exhibits the same sequence features than terrestrial plant isoforms. These proteins usually exhibit a conserved YAPWCGHC active site sequence, with a few variations for the first amino acid following the catalytic cysteine residue in *Populus* (YAPWCTHC), in *Selaginella* (YAPWCSHC) and in *Physcomitrella* (YAPWCKHC) isoforms (Supplementary Fig. 2). These representatives present a protein length in the same range than PDI-M (394 to 440 compared to 365 to 454 amino acids), but significantly shorter compared to PDI-L (around 500 amino acids) due to the absence of the *a′* domain. PDI-B members do not possess the classical ER retention signal although the four last residues are often charged residues. Nevertheless, all isoforms possess a putative transmembrane domain of about 25 amino acids near the C-terminus end, which is followed, except in *Selaginella*, by a region enriched in charged residues (Fig. 2 and Supplementary Fig. 2).

The next class, called PDI-C, is present in all photosynthetic organisms selected, except the rhodophyte *C. merolae*. Two isoforms are present in diatoms, in *Micromonas* sp. *RCC299* and in some dicots as *P. trichocarpa* and *A. thaliana*, whereas only 1 member is found in other organisms analyzed (Table 2). Note the specific case of *G. max* with 4 members. Again, as for PDI-A and -B, the presence of only one gene in most organisms suggests that some duplication occurred in specific organisms from a single ancestor. The proteins, which have been successfully reconstituted, have a size ranging from 460 to 558 amino acids, a [H/N/F/Y]A[P/S/N]WCX[W/H][C/S] active site sequence. In fact, two active site cysteines are found in algae, in one of the two *Arabidopsis* members and in two of the four soybean isoforms, whereas all other representatives possess a CXXS active site, raising the question of the catalytic mechanism used by these PDIs (Supplementary Fig. 3). Regarding their modular organization, in addition to the Trx domain, PDI-C present two predicted membrane anchoring domains in the N- and C-terminal parts as well as a *COPII* coated Erv domain in the C-terminal part. As previously mentioned, this additional *COPII* coated Erv domain is found in human ERGIC-32 (ERGIC1) and yeast Erv46p proteins, two proteins involved in the trafficking between ER and Golgi apparatus [28]. Indeed, in these organisms, a compartment, called ERGIC (endoplasmic reticulum-Golgi intermediate compartment), functions in the delivery of secreted proteins from the ER-exit site (ERES) to the Golgi [44]. It is known that human PDIs such as PDI and ERp44 act in concert with ERGIC proteins, in particular human ERGIC-53 (LMAN1) for the trafficking of client proteins such as SUMF1 (sulfatase modifying factor 1) being involved in a sort of quality control process [45]. The localization of these PDI-Cs is uncertain, as there are no N-terminal signal peptides predicted and no clear retention signals which would indicate that they reside in the ER. However, the presence of both the trans-membrane domains and the *COPII* coated Erv domain could indicate that PDI-C isoforms are anchored in the ER membranes. In plants, the trafficking machinery differs significantly and Golgi stacks might interact with ERES without ERGIC [46]. Altogether, it is tempting to hypothesize that the absence of this compartment in plants could be compensated by the presence of specific PDIs with a *COPII* coated Erv domain which could ensure the quality control process of client proteins during vesicle trafficking.

The 3 next classes are absent in land plants and found specifically in algae, though not present in the rhodophyte *C. merolae*. The PDI-D class contains proteins composed of 422 to 535 amino acids. These proteins display a central Trx module with the canonical YAPWCGHC active site sequence (Fig. 2 and Supplementary Fig. 4). The Trx module is flanked by two additional modules, the N-terminal *J* domain generally found in DnaJ/Hsp40 protein family and the C-terminal *ARMET* domain also found as an ER protein responding to the UPR stress [30,47]. DnaJ proteins are known to interact with Hsp70/DnaK, stimulating its ATPase activity and facilitating substrate binding [48]. Hsp70/DnaK are nucleotide-dependent molecular chaperones composed of two domains, the N-terminal domain is a nucleotide-binding site whereas the C-terminal one is a hydrophobic protein binding domain. The *J* domain of DnaJ is capable to increase the ATPase activity of the N-terminal part of DnaK proteins, particularly through a HPD tripeptide also present in these PDI-D sequences [49]. DnaJ proteins can be divided into three different types depending on the presence or absence of three characteristic regions [50]. The type I is composed of the *J* domain, a glycine/phenylalanine (G/F)-rich region that might

help to position the *J* domain for its interaction with DnaK and a cysteine-rich region (C) that mediates zinc binding. The type II only contains the *J* and G/F domains and the type III the *J* domain only [50,51]. The *J* domain of algal PDI-D is of type II suggesting that PDI-D conserved the capacity to modulate Hsp70/DnaK chaperone activity (Fig. 2).

The ARMET protein is an 18 kDa secreted protein which responds to the UPR stress and controls cell proliferation and cell death [47]. As Grp78, an Hsp70 protein, it is regulated at the transcriptional level by an ERSE (endoplasmic reticulum stress response element) *cis*-element found in its promoter sequence, indicating a possible role in quality control of proteins in the ER [29]. These proteins possess two CxxC motifs, in the N- and C-terminal parts of the protein, and two other $Cx_{10}C$ elements which form four structural disulfide bonds [29]. PDI-D only have the C-terminal CXXCXEK motif strictly conserved in ARMET proteins.

The PDI-E class regroups algal proteins with a size comprised between 148 and 250 amino acids and homologous to mammalian TMX (thioredoxin-related trans-membrane protein). Thus, they constitute one of the smallest PDI type with PDI-A and -F. Only one representative is found in chlorophytes, rhodophytes and prasinophytes with the exception of *M. pusilla* and *Micromonas* sp. *RCC299* which present 2 members. A PDI-E sequence was also identified in *T. pseudonana* but not in *P. tricornutum* and in *C. merolae* raising the question of the occurrence of this PDI class in all algae. The domain architecture consists of a N-terminal Trx domain with variable active site sequences, YAxWC[G/K]HC for most prasinophytes (except the additional sequences found in the two species of *Micromonas*) and YAPWCx[H/E]C for chlorophytes and for *T. pseudonana* (Supplementary Fig. 5). In addition, one putative trans-membrane domain is found in the C-terminal part followed by a C-terminal region enriched in charged amino acids, two characteristics shared with PDI-B and mammalian TMX3 PDIs exhibiting an a–b–b′ modular organization (Fig. 2) [15]. However, the identity between PDI-E and PDI-B or TMX3 ranges from 17 to 21% and from 15 to 17% respectively.

The last class, called PDI-F, is found in all algae analyzed except the rhodophyte *C. merolae* (Table 2). Chlorophytes have only 1 member, prasinophytes 2 or 3 members, and stramenopiles 3 to 4 isoforms (Table 2). The size of these PDI-F isoforms is generally around 200 amino acids with an organization into two domains, a N-terminal Trx domain associated to a long α-helix positioned in the C-terminal part, the protein ending by a putative ER retention signal (Supplementary Fig. 6). Among these PDI-Fs, a careful analysis of the primary sequences indicates that two subtypes can be differentiated. The proteins from chlorophytes are 129 to 139 amino acids long, and they also present typical active site sequences but lack the C-terminal α-helix and the putative ER retention signal, thus resembling in this respect PDI-A sequences. The 19 other isoforms display a protein length ranging from 191 to 229 amino acids and the α-helical C-terminal domain and only some of them possess a recognizable ER retention signal (KDEL, KTEL and NDEL) (Fig. 2 and Supplementary Fig. 6). It is worth mentioning that these α-helical extensions are not predicted to be trans-membrane domains. Regarding the active site sequences, 12 sequences belonging to all algal divisions exhibit the [F/Y]APWCGHC canonical sequence, FQPWCGHC in the case of *P. tricornutum* PDI-F1. In the 7 isoforms remaining (OtPDI-F1, OlPDI-F1, OrPDI-F1, MpPDI-F1, MprPDI-F1, MprPDI-F2 and TpPDI-F3), a leucine replaces the aromatic residue in position −3 of the catalytic cysteine, which is itself strikingly replaced by a putative selenocysteine (Sec, U), forming a LAPWUGHC active site. Among photosynthetic organisms, selenoproteins have only been found in algae such as *C. reinhardtii*, *C. merolae*, *P. tricornutum*, *Ostreococcus* sp. or *Emiliania huxleyi* with some PDI members predicted in the last three organisms [52,53]. In order to determine whether PDI selenoproteins are widespread among algae, we performed some blast searches on various other sequenced organisms. We identified 10 supplementary sequences in some animals of the chordate phylum (*Ciona intestinalis* and *Branchiostoma floridae*), in other stramenopiles (*Aureococcus anophagefferens* and *Fragilariopsis cylindrus*), in some dinoflagellates (*Karenia brevis* and *Karlodinium micrum*) and in haptophytes (*Prymnesium parvum*, *Isochrysis galbana* and *E. huxleyi*). All sequences share the LAPWUGHC active site sequence, the α-helical C-terminal domain and present 29 to 70% sequence identity.

For these sequences, the presence of putative selenocysteine insertion sequence (SECIS) elements generally found in the 3′ UTR of mRNA sequences was analyzed using SECISearch 2.19 [54]. A SECIS was identified for 8 out of the 17 sequences but only the 3 haptophyte PDI-Fs presented a significant score. The PDI-F from *E. huxleyi*, formerly named EhSEP2, was effectively shown to be a selenoprotein, though, at that time, no typical SECIS element was found in the mRNA [55]. Although no SECIS element was clearly identified for the other sequences, the presence of ESTs supports their existence and would indicate that the SECIS elements contained in these sequences possess atypical features.

Interestingly, the analysis of PDI-F from prasinophytes, which are thought to be the most primitive organisms in the green lineage, might help revealing which of the selenoprotein or the cysteine-containing protein is the ancestor. During the manual curation of these genes, we have observed three different genomic organizations. The genes encoding selenoproteins are constituted either by a single exon or by two exons. The borders of these exons code for the active site, the LAP sequence being encoded by the first one, the UGHC by the second one and the W by both exons. On the contrary, all Cys-containing PDI-F encoding genes are encoded by two exons, keeping the same exon borders. Hence, considering that Sec insertion is a rather complex process requiring a Sec insertion machinery and SECIS element in the 3′ untranslated region which should limit the probability for Cys to Sec exchange, one can hypothesize that the ancestral isoform of the PDI-F class was originally a selenoprotein encoded gene formed by a single exon. Some intron insertion should have arisen in these genes before Sec to Cys replacement.

Another important factor for the maintenance of these selenoproteins in some organisms is their living environment. From genome and selenoproteome analyses, it has been concluded that selenoproteins have been favoured or selected in organisms living in specific ecological niches such as aquatic environment where selenium is abundant, whereas it has not been favoured or lost in organisms living in environments where selenium abundance is low or in organisms which do not possess the specific machinery for Sec incorporation [52].

2.7. Why do PDIs from photosynthetic organisms possess additional domains?

In mammals, the diversity in the PDI family is essentially linked to the number and the position of *a* and *b* domains, with PDI possessing from 0 to 4 *a* domains and 0 to 2 *b* domains. In photosynthetic organisms, the variations also originate from the presence of additional domains (*D*, *COPII*, *J* and *ARMET*). The *D* domain is specifically and commonly found in PDIs from various kingdoms. It has been identified in mammalian (ERp28/29) and fungal PDIs, except *S. cerevisiae*, as well as in many other eukaryotes [15,16]. However, a strong variability in the nature and the number of Trx domains associated to this domain is observed, being either *b–D*, *a–D* or *a°–a–D*. On the contrary, *COPII* and *J* domains are present exclusively in other fusion proteins from various eukaryotic organisms such as human ERGIC-32 or yeast Erv46p. ARMET is found as an isolated protein in mammals but is absent in most photosynthetic organisms, although some orthologs have been identified in stramenopiles (*P. tricornutum* and *T. pseudonana*) or alveolata organisms. Overall, the presence of PDI classes containing fusion proteins is apparently more common in photosynthetic organisms compared to non-photosynthetic organisms as only human ERdj5 (DNAJC10) possesses a type I *J* domain [15,16]. It is striking that algal and mammalian PDIs do not have the same type of *J* domain.

Usually, the fusion of protein domains is indicative of a functional or physical relationship between the proteins. It is supposed to provide a significant evolutionary advantage for example for the coordinated recruitment of both proteins and/or for their functioning. One of the best documented examples in the redox field comes from the simultaneous observation that glutaredoxins can serve as reductants for a class of peroxiredoxin called Prx II by characterizing isolated proteins from poplar and fusion proteins found in cyanobacteria and some pathogenic bacteria [56,57]. Alternatively, the appearance of hybrid proteins might also contribute to the acquisition of specific functions or properties during evolution. Extrapolating from the role of ERGIC proteins, this suggests in particular that PDI-Cs, which possess a *COPII* domain, might participate to the protein trafficking from ER to Golgi. By analogy to the roles described in other organisms, we could also hypothesize that the presence of an *ARMET* and a *J* domain in PDI-Ds could confer them the capacity to specifically interact with HSP70 protein family and to play a role during an ER stress.

2.8. Physiological roles of PDI from photosynthetic organisms

To date, only few studies have been performed to understand the physiological roles of plant PDIs. The most documented function for PDIs is their involvement in seed germination and development. Indeed, many seed storage proteins, which constitute essential components during these processes, are synthesized in the ER as precursors and then transported into vacuoles for their processing into mature proteins. In addition, these are cysteine-rich proteins, thus requiring a disulfide isomerase system to be properly folded. A former work, conducted in rice, identified a PDI as a protein required for the processing of the proglutelin precursor into mature glutelin in the endosperm [58]. In *A. thaliana*, the abundance of two PDIs (AtPDI-L1a and 1b) increases in a mutant affected in the transport of storage protein precursors between the ER and Golgi complex, thus accumulating the precursors of two major storage proteins, 2S albumin and 12S globulin, in dry seeds [59]. Biochemical and co-immunoprecipitation studies achieved with *G. max* PDI-L1, PDI-L2, PDI-S or PDI-M indicated that these PDIs are interacting with the main storage proteins called proglycinin, precursors of glycinin, or β-conglycinin, in seeds and in particular in cotyledons [24–26]. All these results suggest that the formation/isomerisation of disulfide bonds and/or the chaperone activity of PDIs are crucial for the maturation, transport and storage of proteins found in the seeds and in particular in endosperm cells [60]. In the same line, some *Arabidopsis* PDI-S mutant (At2g47470, formerly PDI2.1) showed smaller siliques and a reduced number of seeds originating from a delay in embryo sac maturation and from the disruption of pollen tube guidance [61]. However, these defects have been attributed to the gain of function of some PDI truncated versions, formed from residual truncated transcripts. This gain of function is observed when the truncated PDIs contain at least one of the two Trx modules with its redox active cysteines. On the contrary, no reproductive phenotypes were observed for *Arabidopsis* PDI-L1a, -M2, and -C1 (also known as PDIL1.1, PDIL2.3 and PDIL5.3) insertion lines. This work also showed that PDI-S is able to complement a yeast PDI null mutant, likely indicating that it exhibits an oxidoreductase activity *in vivo* [61]. Consistent with these observations, mRNA or protein levels of various PDIs (PDI-L, PDI-M and PDI-S) have been shown to accumulate in inflorescences and seeds [24–26,62].

Another function identified for PDI-L isoforms is their implication in the chloroplastic translational regulation [63]. The *C. reinhardtii* PDI-L isoform, CrPDI-L, (formerly referred to as RB60) is dual-targeted both to the ER and to the chloroplast using a single targeting sequence [64,65]. However, it is cleaved upon translocation into the ER, whereas it remains intact after import into the chloroplast. The acidic region present in this targeting sequence seems to be necessary for thylakoid binding. As this N-terminal part does not possess the characteristics of a plastidial transit peptide and as the C-terminal KDEL signal is present, the prediction programs indicate that all PDI-L sequences are presumably localized in the ER. However, the identification of *A. thaliana* PDI-Ls in a proteome study of the thylakoid fraction and the immunolocalization of AtPDI-L2a at the stromal-starch interface of leaf chloroplasts suggest that the presence of PDI in plastids is not restricted to *C. reinhardtii* and that, on the contrary, it could constitute a general feature of plants [33,34]. In algae, this chloroplastic PDI was primarily shown to regulate in a redox manner, during light/dark transition, the translation of psbA mRNA, by belonging to a protein complex that binds with high affinity to the 5′-untranslated region of this mRNA. More precisely, it has been shown that RB60 is able to modulate the mRNA binding capacity of one of the component of this complex, RB47, through a redox process involving the active site cysteine residues of the Trx domains [63,66]. Regarding AtPDI-L2a, it was proposed that it might be involved in the redox regulation of enzymes of the starch metabolism [33]. Interestingly, a thylakoid membrane located protein, called CYO1, likely required for thylakoid biogenesis in cotyledons but with no sequence similarity with PDIs, possesses an *in vitro* protein disulfide isomerase activity, extending the possible set of disulfide isomerases [67]. In *P. patens*, it is interesting to note that the construction of three knock-out mutants for three PDI-L genes did not apparently generate a developmental defect under normal autotrophic growth conditions [27]. As *P. patens* possesses 8 genes in the PDI-L class, it is likely that some redundancy exists between them.

Besides their contribution to ER stress, some studies have also established a link between PDIs and stress response. The transcript levels of a wheat PDI-L have been shown to increase at the early time points (from 3 to 12 h after inoculation) both in resistant and susceptible plants infected by the pathogen fungus, *Mycosphaerella graminicola*, but this induction is much higher in pathogen-treated resistant lines [68]. This behaviour, very similar to the one observed for pathogenesis-related (PR) proteins, suggests that this PDI constitutes a defence-response gene activated very early which might contribute to the general plant defence system through the regulation of the redox state of other defence proteins. This has indeed been established for cyclotides. These are small circular disulfide-rich peptides found in plants of the rubiaceae and violaceae families, serving as defence molecules. It has been shown that a PDI-L from *Oldenlandia affinis* expressed during the biosynthesis of cyclotides, can assist the oxidative folding of kalata B1 to form its three disulfide bonds [69]. Oxidative stress treatments of *Arabidopsis* cell culture allowed the identification of AtPDI-L2a as a protein induced in mitochondria in response to hydrogen peroxide or menadione [35]. The authors have postulated that this PDI could regulate, under oxidizing conditions, the redox state of damaged or newly synthesized mitochondrial proteins through their isomerase or reductase activity. Finally, the study of knock-out mutants for AtPDI-L1a, referred to as PDI5, indicates that it regulates the timing of programmed cell death in the endothelial cells of developing seeds likely by inhibiting some cysteine proteases during their trafficking to vacuoles [62]. In this manner, it would control the transition from protein storage vacuoles to lytic vacuoles, a step occurring during programmed cell death.

2.9. 3D structure modelling of plant PDIs

Probably because of their size and their modular organization, only 6 3D structures have been determined by NMR or X-ray crystallography for whole PDIs from *S. cerevisiae* or *H. sapiens*: yeast PDI1p (PDB 2B5E), yeast Mpd1p (PDB 3ED3), human ERp29 (PDB 2QC7) human ERp44 (PDB 2R2J), human ERp57 (PDB 3F8U) and human ERp18 (TXNDC12, PDB2K8V) [36,40,70–73]. The other structural data concern single or double PDI modules. For example, for complex isoforms such as human ERp72 exhibiting a *c*–*a*°–*a*–*b*–*b*′–*a*′

modular organization, the structure of the *a*° (PDB 2DJ1), *a* (PDB 2DJ3), *a*′ (PDB 2DJ2), *a*°–*a* (PDB 3DIV) modules were obtained separately. As there are no structures for plant enzymes and as some of them share a similar domain organization, 3D structure modelling has been achieved when sufficient identity existed with proteins whose structure is solved. As expected, all *a* or *b* domains of PDIs from photosynthetic organisms modelled individually present a typical Trx fold with the essential secondary structure elements conserved formed by a central pleated β-sheet surrounded by α helices. In addition, their N-terminal active site Cys or Sec for some PDI-F isoforms are located at the beginning of the α1 helix of the Trx fold and the strictly conserved *cis*-proline, found in all oxidoreductases with a Trx fold, is spatially close to the active site disulfide (data not shown). Note that many eukaryote oxidoreductases have an additional N-terminal α helix completing the Trx fold and, as a consequence, the position of the N-terminal active site Cys is often considered to be the beginning of the α2 helix.

The available structures of two orthologs, yeast PDI1p (PDB 2B5E) and human ERp57 (PDB 3F8U), has allowed us to predict the three-dimensional structure of PDI-L isoforms from photosynthetic organisms, focusing on *P. trichocarpa* PDI-L1a and *O. tauri* PDI-L isoforms in which the N-terminal catalytic Cys residue in the *a* module is replaced by an aspartic acid. For PDI-L2 and -L3, the N-terminal acidic extension is never modelled. Overall, both PDI-Ls exhibit the classical U-shaped structure formed by four Trx modules (Supplementary Figs. 10 and 11 and data not shown) [36,70]. In OlPDI-L, the aspartic acid replacing the catalytic Cys in the *a* domain is modelled at a structural position equivalent to the N-terminal Cys (Supplementary Fig. 11). However, despite an apparent classical 3D structure, some amino acids essential for the catalytic mechanism (proton transfer charge) (E/[K/R]) or pKa modulation [R] are absent in the *a* or *a*′ modules of OlPDI-L but present in PtPDI-L1a. Although that OlPDI-L displays 73 to 77% sequence identity with higher plant PDI-L1 isoforms, the lack of a catalytic Cys residue in the *a* domain and the absence of some other essential amino acids could indicate that these proteins present unusual catalytic properties and might not be efficient isomerases and/or oxidases. Instead they could have specific functions such as chaperones.

Another important aspect for the PDIs with an *a*–*b*–*b*′–*a*′ or *a*–*b*–*b*′ organization comes from a detailed structural analysis of the substrate binding sites of various mammalian PDIs which indicated that they have developed different characteristics for substrate recruitment [74]. At least two different situations have been described, human PDI and human ERp44, as well as human PDI1p and PDILT, display a hydrophobic pocket in the *b*′ module, with 8 residues distributed between the α1- and α3-helices composing this hydrophobic cavity. On the other hand, human ERp72 and human ERp57 do not contain such hydrophobic pocket. Instead, their substrate binding sites consists of several charged residues, which preclude the binding of hydrophobic model peptides *in vitro*. The resolution of the ERp57 structure in complex with tapasin, a chaperone serving as peptide cargo led to the hypothesis that this charged area is actually essential for the recruitment of intermediary chaperones rather than for the direct binding of peptides [70]. This exemplifies how subtle structural differences in the non-catalytic domains of several PDIs might define specialized roles in oxidative folding. Using this established list of key residues found in the *b*′ domain, we have analyzed the sequences from the PDI-L and PDI-B classes as these are the only two classes having a *b*′ domain. Interestingly, PDI-L1 and -L2 globally share the hydrophobic residues, with 6 hydrophobic residues strictly aligned with those of mammalian isoforms. On the contrary, PDI-L3 and PDI-B lack many of these residues suggesting that they do not exhibit the hydrophobic patch. Although none of the plant isoforms strictly possess the patch of charged residues observed in human ERp72 and human ERp57, PDI-B proteins present several negatively charged amino acids in this area, that are not conserved in other plant or mammalian isoforms. These two properties (absence of hydrophobic pocket and a negatively charged patch) might indicate that PDI-B present specific features regarding substrate or intermediary chaperones recruitment.

With the available structures of the human ERp72 *a*°–*a* modules (PDB 3IDV) and of the *a*° domain of the mammalian P5 isoform (PDB 2DML), similar modelling and superpositions have been performed for the *Arabidopsis* and poplar PDI-S and PDI-M, which share an identity ranging from 29 to 35% in the *a*°–*a* area. The amino acid sequence alignment of these proteins with several mammalian P5 and ERp72 sequences allowed us to localize the additional N-terminal acidic extension present only in ERp72 (Supplementary Fig. 12). Moreover, another major difference resides in an amino acid insertion rich in glycine and charged residues, found in all plant PDI-M and mammalian P5, but not in PDI-S and ERP72, and which is located immediately before the linker observed between the *a*° and *a* modules of ERp72 *a*°–*a* fragment (Supplementary Fig. 13). The models obtained for poplar PDI-M and PDI-S and mammalian P5 using the structure of ERp72 *a*°–*a* fragment as a template suggest that this additional sequence may form two additional β-strands after the C-terminal extremity of the *a*° modules of both plant PDI-M and mammalian P5 but not of plant PDI-S, as expected from the primary sequence (Supplementary Fig. 12). In ERp72, it was proposed that the catalytic *a*°, *a* and *a*′ domains could form a substrate binding site and that the *a*°–*a* linker, formed by several proline residues, though presenting a somewhat rigid conformation in the crystal structure, might actually be quite mobile in solution [75]. The presence of two putative additional β-strands in plant PDI-M and mammalian P5 isoforms in the *a*°–*a* linker region presumably indicates that it could contribute both to some specific domain arrangement and/or substrate specificity. More generally, it also points to the importance of the linker areas (*a*–*b*, *b*–*b*′ or *a*–*a*) in PDIs.

Finally, the availability of complete 3D structures for *Drosophila* ERp28, also known as Wind (PDB 1OVN), and human ERp29 (PDB 2QC7) exhibiting the *b*–*D* modular organization allowed us to construct models for two *Chlamydomonas* PDIs, CrPDI-S and CrERp29 (*a*–*D* and *b*–*D* modular organization respectively). As expected, both isoforms present two protein domains, the N-terminal *a* or *b* domain exhibits a Trx fold, whereas the C-terminal *D* domain has an all helical structure composed of five α-helices (Figs. 3A and B). Both the *Drosophila* ERp28 and the human ERp29 are homodimers. The dimerization site, for which the following residues, $_{37}$GxLxxDxxxxxKxxxK$_{52}$, are the most important contributors, is exclusively located on the *b* domain. The peptide binding site of the *b* domain is formed near the so-called tyrosine cluster, essentially by the following residues: $_{59}$KxDxxYPYGEKQxxF$_{73}$ (human ERp29 numbering). In the *D* domain, the peptide binding site is formed by the $_{221}$ExxRxxKL$_{228}$ motif and Leu241. Although the protein is dimeric and some residues of the D domain have been demonstrated to participate to substrate binding, it appears that a monomeric *b* domain is sufficient *in vitro* for the binding a client proteins [40]. In general, most of the residues (or at least their nature or their capacity to form similar interactions) forming the dimer interface and the two peptide binding sites are conserved in algal ERp29 sequences. On the other hand, comparing several ERp28/29 sequences with chlorophyte PDI-S sequences indicates that the *b* binding motif is obviously not conserved as it actually aligns with the classical WCGHC active site. Incidentally, this has led to propose that mutations accumulated into the *b* domain from an original Trx domain led to the acquisition of a substrate binding site [76]. The best conservation is observed for the residues forming the peptide binding site of the *D* domain, whereas the amino acids involved in dimerization are less conserved. Altogether, these observations could indicate that algal PDI-S and maybe higher plants PDI-S might not be dimeric proteins and could only use the *D* peptide binding site for substrate recognition.

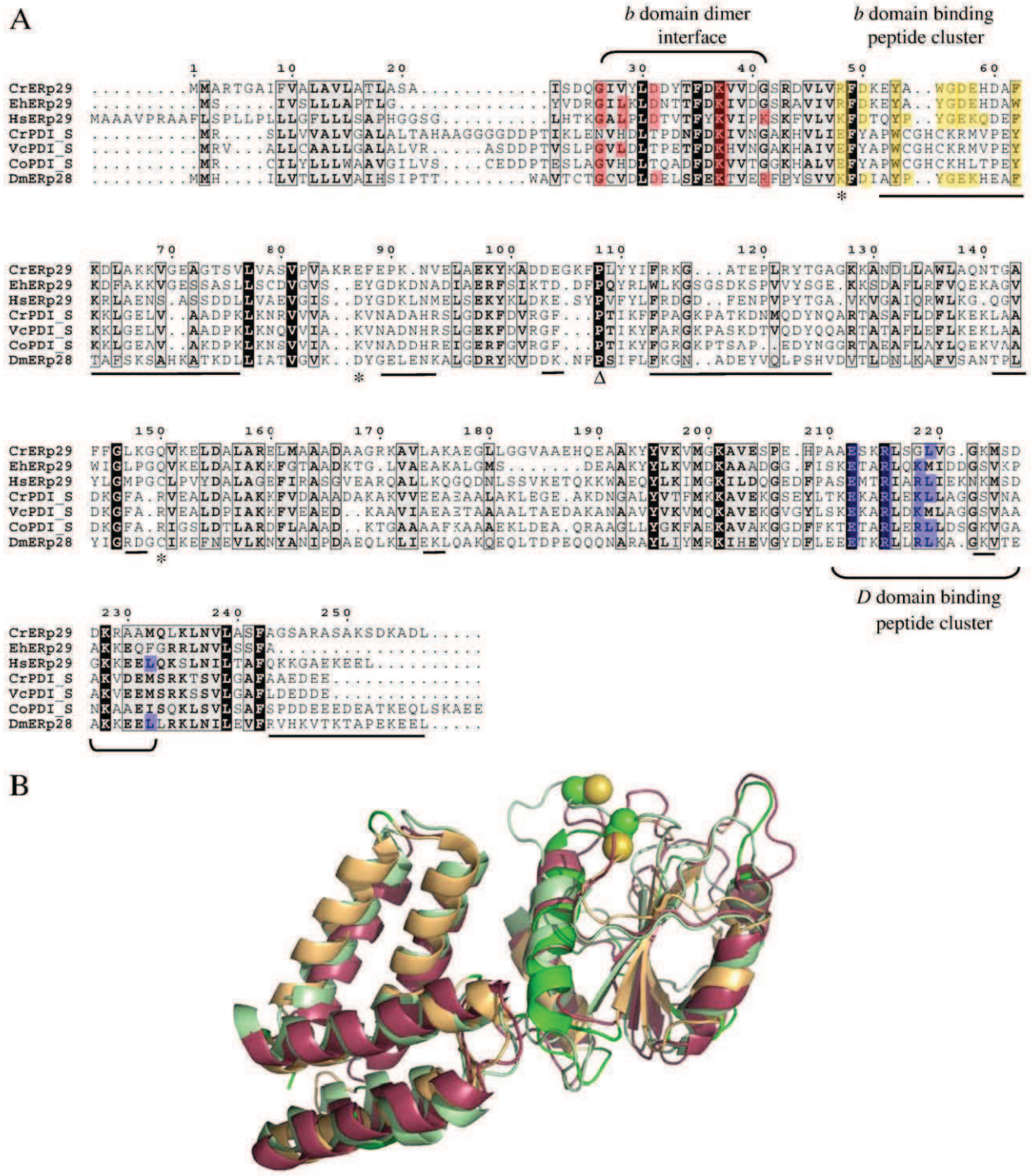

Fig. 3. Amino acid sequence alignment and three-dimensional structure prediction of PDI-S and ERp29 isoforms from *Chlamydomonas reinhardtii*. A. Sequence alignment of human ERp29 (NP_006808) with *Drosophila melanogaster* ERp28 (1OVN), *C. reinhardtii* and *E. huxleyi* (estExtDG_fgenesh_newKGs_kg.C_1670029) ERp29 isoforms and *C. reinhardtii*, *V. carteri* and *Coccomyxa* sp. *C169* PDI-S isoforms. Amino acids in dark background are strictly conserved, those in gray background have a functional homology. The asterisks indicate the position of amino acids essential for the catalytic mechanism (proton transfer charge) (E/[K/R]) or pKa modulation (see the text for more detail). The triangle shows the position of *cis*-proline residue. Amino acids proved to participate to ERp29 dimerization, to the peptide binding cluster of the *b* and *D* domains are colored respectively in red, yellow and blue. The underlined sequences indicate protein region that do not align in three-dimensional structure predictions (see part B). B. Superposition of 3D structures of ERp28 from *Drosophila* (1OVN) in pale yellow, of modelled CrPDI-S in pale green and modelled CrERp29 in brown. The portions of proteins from DmERp28, CrERp29 and CrPDI-S, that do not match each to another, have been represented in green and are underlined in part A. Cys residues are represented as spheres.

2.10. Concluding remarks

The present study, performed with a large variety of eukaryote photosynthetic organisms has allowed us to identify PDI sequences in organisms with various lifestyles and to classify them into 9 distinct classes, confirming the complexity of the PDI family and extending our knowledge of this protein family. The differences essentially lie in the number and the position of Trx modules, their active site sequence and the presence of additional protein domains. Only 5 classes are present both in terrestrial and aquatic photosynthetic organisms, but none of them is present in all organisms analyzed. The most widespread PDI class is PDI-C with members found in all phyla

except in the rhodophyte *C. merolae*. Nevertheless, this suggests that these classes might have a general physiological role. On the contrary, it is worth mentioning that land plants and algae differ significantly both in the number of PDIs and in their domain organization. Hence, PDI classes specific for some phyla could have specific functions in some organisms. However, that does not mean this is not an essential function. Only few genetic, biochemical or structural studies have been conducted on plant PDIs to date. Such inventory should help to understand the specificity or possibly redundancy between isoforms in a given organism. Obviously, due to the diverse functions identified to date for PDIs by biochemical studies, i.e. oxidase, isomerase, reductase or chaperone activity, genetic and physiological studies will be required to further characterize the *in vivo* function of each PDI member in photosynthetic organisms.

3. Material and methods

3.1. Bioinformatic genome analysis: sequence annotation, phylogenetic analyses

The PDI sequences retrieved by text and Blast searches from the *P. trichocarpa* whole genome database (version 1.1) at the U.S. Department of Energy Joint Genome Institute (JGI) (http://genome.jgi-psf.org/Poptr1_1/Poptr1_1.home.html) have been first corrected. The curated poplar amino acid sequences were used to search against 23 other genomes from photosynthetic organisms using BLASTP or TBLASTN. The genomes are available at the following websites, for *A. thaliana* (http://www.arabidopsis.org/), *O. sativa* (http://rice.plantbiology.msu.edu/), *V. vinifera* (http://www.genoscope.cns.fr/spip/Vitis-vinifera-whole-genome.html), *S. bicolor* (http://genome.jgi-psf.org/Sorbi1/Sorbi1.home.html), *G. max* (http://www.phytozome.net/soybean), *M. esculenta* (version 1.0) (http://genome.jgi-psf.org/cassava/cassava.home.html), *C. sativus* (version 1.0) (http://genome.jgi-psf.org/cucumber/cucumber.home.html), *M. guttatus* (version 1.0) (http://genome.jgi-psf.org/mimulus/mimulus.home.html), *P. patens* subsp. *patens* (version 1.1) (http://genome.jgi-psf.org/Phypa1_1/Phypa1_1.home.html), *S. moellendorffii* (version 1.0) (http://genome.jgi-psf.org/Selmo1/Selmo1.home.html), *C. reinhardtii* (version 3.0) (http://genome.jgi-psf.org/Chlre3/Chlre3.home.html), *O. lucimarinus* (version 2.0) (http://genome.jgi-psf.org/Ost9901_3/Ost9901_3.home.html), *O. tauri* (version 2.0) (http://genome.jgi-psf.org/Ostta4/Ostta4.home.html), *Ostreococcus RCC809* (version 2.0) (http://genome.jgi-psf.org/OstRCC809_1/OstRCC809_1.home.html), *Coccomyxa* sp. *C-169* (version 1.0) (http://genome.jgi-psf.org/Chlvu1/Chlvu1.home.html), *V. carteri* (version 1.0) (http://genome.jgi-psf.org/Volca1/Volca1.home.html), *Chlorella* sp. *NC64A* (http://genome.jgi-psf.org/ChlNC64A_1/ChlNC64A_1.home.html), *T. pseudonana* (http://genome.jgi-psf.org/Thaps3/Thaps3.home.html), *P. tricornutum* (http://genome.jgi-psf.org/Phatr2/Phatr2.home.html), *C. merolae* (http://merolae.biol.s.u-tokyo.ac.jp/blast/blast.html), *M. pusilla* CCMP1545 (http://genome.jgi-psf.org/MicpuC2/MicpuC2.home.html), and *Micromonas* sp. *RCC299* (version 3.0) (http://genome.jgi-psf.org/MicpuN3/MicpuN3.home.html). Whenever possible, all the incomplete sequences have been correctly annotated based on available ESTs and manual inspection of the genomic sequences. All protein sequences and corresponding accession numbers used in this article can be found in the databases mentioned above and as supplementary material. Amino acid sequence alignments were done using CLUSTALW and imported into the Molecular Evolutionary Genetics Analysis (MEGA) package version 4.1. Phylogenetic analyses were conducted using the neighbor-joining (NJ) method implemented in MEGA, with the pairwise deletion option for handling alignment gaps, and with the Poisson correction model for distance computation. Bootstrap tests were conducted using 1000 replicates. Branch lengths are proportional to phylogenetic distances.

3.2. Determination of protein sequence features

The presence of protein domains was predicted with Pfam server (http://pfam.sanger.ac.uk/). The presence of putative targeting sequences in higher plant PDIs was evaluated using several softwares: TargetP (http://www.cbs.dtu.dk/services/TargetP/), SignalP (http://www.cbs.dtu.dk/services/SignalP/), YLoc (http://www-bs.informatik.uni-tuebingen.de/Services/YLoc/webloc.cgi) and SherLoc2 (http://www-bs.informatik.uni-tuebingen.de/Services/SherLoc2). Because of the known variability in the targeting sequence properties of algal proteins, they have not been analyzed. The presence of trans-membrane regions was evaluated using two programs: TMHMM (http://www.cbs.dtu.dk/services/TMHMM/) and TMPro (http://flan.blm.cs.cmu.edu/tmpro/). In addition, in order to discriminate between ER targeting signals and trans-membrane domains, the sequences were also analyzed by Phobius (http://phobius.sbc.su.se/). The presence of SECIS element in algal PDI-F was analyzed with the SECISearch 2.19 software (http://genome.unl.edu/SECISearch.html).

3.3. Computational prediction of secondary and tertiary structures

Secondary structure prediction was achieved using the 12 different algorithms found in the consensus secondary structure prediction tool found at http://npsa-pbil.ibcp.fr/cgi-bin/npsa_automat.pl?page=/NPSA/npsa_seccons.html. 3D structure modelling was performed using two online servers: $(PS)^2$ (http://ps2.life.nctu.edu.tw.html) and SwissModel Automatic Modelling Mode (http://swissmodel.expasy.org/workspace/index.php?func=modelling_simple1.html). PDB files of solved structures were obtained at the RCSB Protein Data Bank (http://www.pdb.org/pdb/home/home.do.html). The drawing and superposition of 3D structures were done using the PyMOL software (http://www.pymol.org.html).

Acknowledgments

The authors gratefully acknowledge Andreas Meyer (Heidelberg Institute of Plant Sciences, University of Heidelberg) for the critical reading of the manuscript.

Appendix A. Supplementary data

Supplementary data to this article can be found online at doi:10.1016/j.ygeno.2010.10.001.

References

[1] C. Hwang, A.J. Sinskey, H.F. Lodish, Oxidized redox state of glutathione in the endoplasmic reticulum, Science 257 (1992) 1496–1502.
[2] A.J. Meyer, T. Brach, L. Marty, S. Kreye, N. Rouhier, J.P. Jacquot, R. Hell, Redox-sensitive GFP in *Arabidopsis thaliana* is a quantitative biosensor for the redox potential of the cellular glutathione redox buffer, Plant J. 52 (2007) 973–986.
[3] R. Farquhar, N. Honey, S.J. Murant, P. Bossier, L. Schultz, D. Montgomery, R.W. Ellis, R.B. Freedman, M.F. Tuite, Protein disulfide isomerase is essential for viability in *Saccharomyces cerevisiae*, Gene 108 (1991) 81–89.
[4] A.R. Frand, C.A. Kaiser, Ero1p oxidizes protein disulfide isomerase in a pathway for disulfide bond formation in the endoplasmic reticulum, Mol. Cell 4 (1999) 469–477.
[5] A.R. Frand, C.A. Kaiser, The ERO1 gene of yeast is required for oxidation of protein dithiols in the endoplasmic reticulum, Mol. Cell 1 (1998) 161–170.
[6] C. Thorpe, K.L. Hoober, S. Raje, N.M. Glynn, J. Burnside, G.K. Turi, D.L. Coppock, Sulfhydryl oxidases: emerging catalysts of protein disulfide bond formation in eukaryotes, Arch. Biochem. Biophys. 405 (2002) 1–12.
[7] C.E. Jessop, R.H. Watkins, J.J. Simmons, M. Tasab, N.J. Bulleid, Protein disulphide isomerase family members show distinct substrate specificity: P5 is targeted to BiP client proteins, J. Cell Sci. 122 (2009) 4287–4295.
[8] M. Rissler, N. Wiedemann, S. Pfannschmidt, K. Gabriel, B. Guiard, N. Pfanner, A. Chacinska, The essential mitochondrial protein Erv1 cooperates with Mia40 in biogenesis of intermembrane space proteins, J. Mol. Biol. 353 (2005) 485–492.
[9] B. Heras, S.R. Shouldice, M. Totsika, M.J. Scanlon, M.A. Schembri, J.L. Martin, DSB proteins and bacterial pathogenicity, Nat. Rev. Microbiol. 7 (2009) 215–225.
[10] J.P. Jacquot, E. Gelhaye, N. Rouhier, C. Corbier, C. Didierjean, A. Aubry, Thioredoxins and related proteins in photosynthetic organisms: molecular basis for thiol dependent regulation, Biochem. Pharmacol. 64 (2002) 1065–1069.

[11] D.M. Ferrari, H.D. Soling, The protein disulphide-isomerase family: unravelling a string of folds, Biochem. J. 339 (Pt 1) (1999) 1–10.
[12] J.C. Edman, L. Ellis, R.W. Blacher, R.A. Roth, W.J. Rutter, Sequence of protein disulphide isomerase and implications of its relationship to thioredoxin, Nature 317 (1985) 267–270.
[13] R.B. Freedman, T.R. Hirst, M.F. Tuite, Protein disulphide isomerase: building bridges in protein folding, Trends Biochem. Sci. 19 (1994) 331–336.
[14] J. Kemmink, N.J. Darby, K. Dijkstra, M. Nilges, T.E. Creighton, The folding catalyst protein disulfide isomerase is constructed of active and inactive thioredoxin modules, Curr. Biol. 7 (1997) 239–245.
[15] C. Appenzeller-Herzog, L. Ellgaard, The human PDI family: versatility packed into a single fold, Biochim. Biophys. Acta 1783 (2008) 535–548.
[16] P. Norgaard, V. Westphal, C. Tachibana, L. Alsoe, B. Holst, J.R. Winther, Functional differences in yeast protein disulfide isomerases, J. Cell Biol. 152 (2001) 553–562.
[17] S. Kanai, H. Toh, T. Hayano, M. Kikuchi, Molecular evolution of the domain structures of protein disulfide isomerases, J. Mol. Evol. 47 (1998) 200–210.
[18] H. Tachikawa, W. Funahashi, Y. Takeuchi, H. Nakanishi, R. Nishihara, S. Katoh, X.D. Gao, T. Mizunaga, D. Fujimoto, Overproduction of Mpd2p suppresses the lethality of protein disulfide isomerase depletion in a CXXC sequence dependent manner, Biochem. Biophys. Res. Commun. 239 (1997) 710–714.
[19] E. d'Aloisio, A.R. Paolacci, A.P. Dhanapal, O.A. Tanzarella, E. Porceddu, M. Ciaffi, The protein disulfide isomerase gene family in bread wheat (*T. aestivum* L.), BMC Plant Biol. 10 (2010) 101.
[20] N.L. Houston, C. Fan, J.Q. Xiang, J.M. Schulze, R. Jung, R.S. Boston, Phylogenetic analyses identify 10 classes of the protein disulfide isomerase family in plants, including single-domain protein disulfide isomerase-related proteins, Plant Physiol. 137 (2005) 762–778.
[21] S.D. Lemaire, M. Miginiac-Maslow, The thioredoxin superfamily in *Chlamydomonas reinhardtii*, Photosynth. Res. 82 (2004) 203–220.
[22] D.P. Lu, D.A. Christopher, Endoplasmic reticulum stress activates the expression of a sub-group of protein disulfide isomerase genes and AtbZIP60 modulates the response in *Arabidopsis thaliana*, Mol. Genet. Genomics 280 (2008) 199–210.
[23] K. Iwasaki, S. Kamauchi, H. Wadahama, M. Ishimoto, T. Kawada, R. Urade, Molecular cloning and characterization of soybean protein disulfide isomerase family proteins with nonclassic active center motifs, FEBS J. 276 (2009) 4130–4141.
[24] S. Kamauchi, H. Wadahama, K. Iwasaki, Y. Nakamoto, K. Nishizawa, M. Ishimoto, T. Kawada, R. Urade, Molecular cloning and characterization of two soybean protein disulfide isomerases as molecular chaperones for seed storage proteins, FEBS J. 275 (2008) 2644–2658.
[25] H. Wadahama, S. Kamauchi, M. Ishimoto, T. Kawada, R. Urade, Protein disulfide isomerase family proteins involved in soybean protein biogenesis, FEBS J. 274 (2007) 687–703.
[26] H. Wadahama, S. Kamauchi, Y. Nakamoto, K. Nishizawa, M. Ishimoto, T. Kawada, R. Urade, A novel plant protein disulfide isomerase family homologous to animal P5 — molecular cloning and characterization as a functional protein for folding of soybean seed-storage proteins, FEBS J. 275 (2008) 399–410.
[27] E. Meiri, A. Levitan, F. Guo, D.A. Christopher, D. Schaefer, J.P. Zryd, A. Danon, Characterization of three PDI-like genes in *Physcomitrella patens* and construction of knock-out mutants, Mol. Genet. Genomics 267 (2002) 231–240.
[28] L. Breuza, R. Halbeisen, P. Jeno, S. Otte, C. Barlowe, W. Hong, H.P. Hauri, Proteomics of endoplasmic reticulum-Golgi intermediate compartment (ERGIC) membranes from brefeldin A-treated HepG2 cells identifies ERGIC-32, a new cycling protein that interacts with human Erv46, J. Biol. Chem. 279 (2004) 47242–47253.
[29] N. Mizobuchi, J. Hoseki, H. Kubota, S. Toyokuni, J. Nozaki, M. Naitoh, A. Koizumi, K. Nagata, ARMET is a soluble ER protein induced by the unfolded protein response via ERSE-II element, Cell Struct. Funct. 32 (2007) 41–50.
[30] X.B. Qiu, Y.M. Shao, S. Miao, L. Wang, The diversity of the DnaJ/Hsp40 family, the crucial partners for Hsp70 chaperones, Cell. Mol. Life Sci. 63 (2006) 2560–2570.
[31] Y. Meyer, F. Vignols, J.P. Reichheld, Classification of plant thioredoxins by sequence similarity and intron position, Meth. Enzymol. 347 (2002) 394–402.
[32] N. Rouhier, J. Couturier, J.P. Jacquot, Genome-wide analysis of plant glutaredoxin systems, J. Exp. Bot. 57 (2006) 1685–1696.
[33] D.P. Lu, D.A. Christopher, Immunolocalization of a protein disulfide isomerase to *Arabidopsis thaliana* chloroplasts and its association with starch biogenesis, Int. J. Plant Sci. 167 (2006) 1–9.
[34] J.B. Peltier, G. Friso, D.E. Kalume, P. Roepstorff, F. Nilsson, I. Adamska, K.J. van Wijk, Proteomics of the chloroplast: systematic identification and targeting analysis of lumenal and peripheral thylakoid proteins, Plant Cell 12 (2000) 319–341.
[35] L.J. Sweetlove, J.L. Heazlewood, V. Herald, R. Holtzapffel, D.A. Day, C.J. Leaver, A.H. Millar, The impact of oxidative stress on *Arabidopsis* mitochondria, Plant J. 32 (2002) 891–904.
[36] G. Tian, S. Xiang, R. Noiva, W.J. Lennarz, H. Schindelin, The crystal structure of yeast protein disulfide isomerase suggests cooperativity between its active sites, Cell 124 (2006) 61–73.
[37] C. Tachibana, T.H. Stevens, The yeast EUG1 gene encodes an endoplasmic reticulum protein that is functionally related to protein disulfide isomerase, Mol. Cell. Biol. 12 (1992) 4601–4611.
[38] A.L. Hufton, G. Panopoulou, Polyploidy and genome restructuring: a variety of outcomes, Curr. Opin. Genet. Dev. 19 (2009) 600–606.
[39] J. Huang, J.P. Gogarten, Ancient gene transfer as a tool in phylogenetic reconstruction, Meth. Mol. Biol. 532 (2009) 127–139.
[40] N.N. Barak, P. Neumann, M. Sevvana, M. Schutkowski, K. Naumann, M. Malesevic, H. Reichardt, G. Fischer, M.T. Stubbs, D.M. Ferrari, Crystal structure and functional analysis of the protein disulfide isomerase-related protein ERp29, J. Mol. Biol. 385 (2009) 1630–1642.
[41] A.K. Bjorklund, D. Ekman, A. Elofsson, Expansion of protein domain repeats, PLoS Comput. Biol. 2 (2006) e114.
[42] E. Liepinsh, M. Baryshev, A. Sharipo, M. Ingelman-Sundberg, G. Otting, S. Mkrtchian, Thioredoxin fold as homodimerization module in the putative chaperone ERp29: NMR structures of the domains and experimental model of the 51 kDa dimer, Structure 9 (2001) 457–471.
[43] S.S. Merchant, S.E. Prochnik, O. Vallon, E.H. Harris, S.J. Karpowicz, G.B. Witman, A. Terry, A. Salamov, L.K. Fritz-Laylin, L. Marechal-Drouard, W.F. Marshall, L.H. Qu, D.R. Nelson, A.A. Sanderfoot, M.H. Spalding, V.V. Kapitonov, Q. Ren, P. Ferris, E. Lindquist, H. Shapiro, S.M. Lucas, J. Grimwood, J. Schmutz, P. Cardol, H. Cerutti, G. Chanfreau, C.L. Chen, V. Cognat, M.T. Croft, R. Dent, S. Dutcher, E. Fernandez, H. Fukuzawa, D. Gonzalez-Ballester, D. Gonzalez-Halphen, A. Hallmann, M. Hanikenne, M. Hippler, W. Inwood, K. Jabbari, M. Kalanon, R. Kuras, P.A. Lefebvre, S.D. Lemaire, A.V. Lobanov, M. Lohr, A. Manuell, I. Meier, L. Mets, M. Mittag, T. Mittelmeier, J.V. Moroney, J. Moseley, C. Napoli, A.M. Nedelcu, K. Niyogi, S.V. Novoselov, I.T. Paulsen, G. Pazour, S. Purton, J.P. Ral, D.M. Riano-Pachon, W. Riekhof, L. Rymarquis, M. Schroda, D. Stern, J. Umen, R. Willows, N. Wilson, S.L. Zimmer, J. Allmer, J. Balk, K. Bisova, C.J. Chen, M. Elias, K. Gendler, C. Hauser, M.R. Lamb, H. Ledford, J.C. Long, J. Minagawa, M.D. Page, J. Pan, W. Pootakham, S. Roje, A. Rose, E. Stahlberg, A.M. Terauchi, P. Yang, S. Ball, C. Bowler, C.L. Dieckmann, V.N. Gladyshev, P. Green, R. Jorgensen, S. Mayfield, B. Mueller-Roeber, S. Rajamani, R.T. Sayre, P. Brokstein, et al., The *Chlamydomonas* genome reveals the evolution of key animal and plant functions, Science 318 (2007) 245–250.
[44] C. Appenzeller-Herzog, H.P. Hauri, The ER-Golgi intermediate compartment (ERGIC): in search of its identity and function, J. Cell Sci. 119 (2006) 2173–2183.
[45] A. Fraldi, E. Zito, F. Annunziata, A. Lombardi, M. Cozzolino, M. Monti, C. Spampanato, A. Ballabio, P. Pucci, R. Sitia, M.P. Cosma, Multistep, sequential control of the trafficking and function of the multiple sulfatase deficiency gene product, SUMF1 by PDI, ERGIC-53 and ERp44, Hum. Mol. Genet. 17 (2008) 2610–2621.
[46] Y.D. Yang, R. Elamawi, J. Bubeck, R. Pepperkok, C. Ritzenthaler, D.G. Robinson, Dynamics of COPII vesicles and the Golgi apparatus in cultured *Nicotiana tabacum* BY-2 cells provides evidence for transient association of Golgi stacks with endoplasmic reticulum exit sites, Plant Cell 17 (2005) 1513–1531.
[47] A. Apostolou, Y. Shen, Y. Liang, J. Luo, S. Fang, Armet, a UPR-upregulated protein, inhibits cell proliferation and ER stress-induced cell death, Exp. Cell Res. 314 (2008) 2454–2467.
[48] F. Hennessy, W.S. Nicoll, R. Zimmermann, M.E. Cheetham, G.L. Blatch, Not all J domains are created equal: implications for the specificity of Hsp40-Hsp70 interactions, Protein Sci. 14 (2005) 1697–1709.
[49] L.H. Chamberlain, R.D. Burgoyne, The molecular chaperone function of the secretory vesicle cysteine string proteins, J. Biol. Chem. 272 (1997) 31420–31426.
[50] P.M. Cunnea, A. Miranda-Vizuete, G. Bertoli, T. Simmen, A.E. Damdimopoulos, S. Hermann, S. Leinonen, M.P. Huikko, J.A. Gustafsson, R. Sitia, G. Spyrou, ERdj5, an endoplasmic reticulum (ER)-resident protein containing DnaJ and thioredoxin domains, is expressed in secretory cells or following ER stress, J. Biol. Chem. 278 (2003) 1059–1066.
[51] M.E. Cheetham, A.J. Caplan, Structure, function and evolution of DnaJ: conservation and adaptation of chaperone function, Cell Stress Chaperones 3 (1998) 28–36.
[52] A.V. Lobanov, D.E. Fomenko, Y. Zhang, A. Sengupta, D.L. Hatfield, V.N. Gladyshev, Evolutionary dynamics of eukaryotic selenoproteomes: large selenoproteomes may associate with aquatic life and small with terrestrial life, Genome Biol. 8 (2007) R198.
[53] S.V. Novoselov, M. Rao, N.V. Onoshko, H. Zhi, G.V. Kryukov, Y. Xiang, D.P. Weeks, D.L. Hatfield, V.N. Gladyshev, Selenoproteins and selenocysteine insertion system in the model plant cell system, *Chlamydomonas reinhardtii*, EMBO J. 21 (2002) 3681–3693.
[54] G.V. Kryukov, S. Castellano, S.V. Novoselov, A.V. Lobanov, O. Zehtab, R. Guigo, V.N. Gladyshev, Characterization of mammalian selenoproteomes, Science 300 (2003) 1439–1443.
[55] T. Obata, Y. Shiraiwa, A novel eukaryotic selenoprotein in the haptophyte alga *Emiliania huxleyi*, J. Biol. Chem. 280 (2005) 18462–18468.
[56] N. Rouhier, E. Gelhaye, P.E. Sautiere, A. Brun, P. Laurent, D. Tagu, J. Gerard, E. de Fay, Y. Meyer, J.P. Jacquot, Isolation and characterization of a new peroxiredoxin from poplar sieve tubes that uses either glutaredoxin or thioredoxin as a proton donor, Plant Physiol. 127 (2001) 1299–1309.
[57] B. Vergauwen, F. Pauwels, F. Jacquemotte, T.E. Meyer, M.A. Cusanovich, R.G. Bartsch, J.J. Van Beeumen, Characterization of clutathione amide reductase from *Chromatium gracile*. Identification of a novel thiol peroxidase (Prx/Grx) fueled by glutathione amide redox cycling, J. Biol. Chem. 276 (2001) 20890–20897.
[58] Y. Takemoto, S.J. Coughlan, T.W. Okita, H. Satoh, M. Ogawa, T. Kumamaru, The rice mutant esp2 greatly accumulates the glutelin precursor and deletes the protein disulfide isomerase, Plant Physiol. 128 (2002) 1212–1222.
[59] L. Li, T. Shimada, H. Takahashi, H. Ueda, Y. Fukao, M. Kondo, M. Nishimura, I. Hara-Nishimura, MAIGO2 is involved in exit of seed storage proteins from the endoplasmic reticulum in *Arabidopsis thaliana*, Plant Cell 18 (2006) 3535–3547.
[60] Y. Kawagoe, K. Suzuki, M. Tasaki, H. Yasuda, K. Akagi, E. Katoh, N.K. Nishizawa, M. Ogawa, F. Takaiwa, The critical role of disulfide bond formation in protein sorting in the endosperm of rice, Plant Cell 17 (2005) 1141–1153.
[61] H. Wang, L.C. Boavida, M. Ron, S. McCormick, Truncation of a protein disulfide isomerase, PDIL2-1, delays embryo sac maturation and disrupts pollen tube guidance in *Arabidopsis thaliana*, Plant Cell 20 (2008) 3300–3311.
[62] C. Andeme Ondzighi, D.A. Christopher, E.J. Cho, S.C. Chang, L.A. Staehelin, *Arabidopsis* protein disulfide isomerase-5 inhibits cysteine proteases during trafficking to vacuoles before programmed cell death of the endothelium in developing seeds, Plant Cell 20 (2008) 2205–2220.

[63] J. Kim, S.P. Mayfield, The active site of the thioredoxin-like domain of chloroplast protein disulfide isomerase, RB60, catalyzes the redox-regulated binding of chloroplast poly(A)-binding protein, RB47, to the 5′ untranslated region of psbA mRNA, Plant Cell Physiol. 43 (2002) 1238–1243.
[64] A. Levitan, T. Trebitsh, V. Kiss, Y. Pereg, I. Dangoor, A. Danon, Dual targeting of the protein disulfide isomerase RB60 to the chloroplast and the endoplasmic reticulum, Proc. Natl Acad. Sci. USA 102 (2005) 6225–6230.
[65] T. Trebitsh, E. Meiri, O. Ostersetzer, Z. Adam, A. Danon, The protein disulfide isomerase-like RB60 is partitioned between stroma and thylakoids in *Chlamydomonas reinhardtii* chloroplasts, J. Biol. Chem. 276 (2001) 4564–4569.
[66] T. Alergand, H. Peled-Zehavi, Y. Katz, A. Danon, The chloroplast protein disulfide isomerase RB60 reacts with a regulatory disulfide of the RNA-binding protein RB47, Plant Cell Physiol. 47 (2006) 540–548.
[67] H. Shimada, M. Mochizuki, K. Ogura, J.E. Froehlich, K.W. Osteryoung, Y. Shirano, D. Shibata, S. Masuda, K. Mori, K. Takamiya, *Arabidopsis* cotyledon-specific chloroplast biogenesis factor CYO1 is a protein disulfide isomerase, Plant Cell 19 (2007) 3157–3169.
[68] S. Ray, J.M. Anderson, F.I. Urmeev, S.B. Goodwin, Rapid induction of a protein disulfide isomerase and defense-related genes in wheat in response to the hemibiotrophic fungal pathogen *Mycosphaerella graminicola*, Plant Mol. Biol. 53 (2003) 701–714.
[69] C.W. Gruber, M. Cemazar, R.J. Clark, T. Horibe, R.F. Renda, M.A. Anderson, D.J. Craik, A novel plant protein-disulfide isomerase involved in the oxidative folding of cystine knot defense proteins, J. Biol. Chem. 282 (2007) 20435–20446.
[70] G. Dong, P.A. Wearsch, D.R. Peaper, P. Cresswell, K.M. Reinisch, Insights into MHC class I peptide loading from the structure of the tapasin-ERp57 thiol oxidoreductase heterodimer, Immunity 30 (2009) 21–32.
[71] M.L. Rowe, L.W. Ruddock, G. Kelly, J.M. Schmidt, R.A. Williamson, M.J. Howard, Solution structure and dynamics of ERp18, a small endoplasmic reticulum resident oxidoreductase, Biochemistry 48 (2009) 4596–4606.
[72] E. Vitu, E. Gross, H.M. Greenblatt, C.S. Sevier, C.A. Kaiser, D. Fass, Yeast Mpd1p reveals the structural diversity of the protein disulfide isomerase family, J. Mol. Biol. 384 (2008) 631–640.
[73] L. Wang, S. Vavassori, S. Li, H. Ke, T. Anelli, M. Degano, R. Ronzoni, R. Sitia, F. Sun, C.C. Wang, Crystal structure of human ERp44 shows a dynamic functional modulation by its carboxy-terminal tail, EMBO Rep. 9 (2008) 642–647.
[74] G. Kozlov, P. Maattanen, D.Y. Thomas, and K. Gehring, A structural overview of the PDI family of proteins. FEBS J 277 (2010) 3924–3936.
[75] G. Kozlov, S. Azeroual, A. Rosenauer, P. Maattanen, A.Y. Denisov, D.Y. Thomas, and K. Gehring. Structure of the catalytic a(0)a fragment of the protein disulfide isomerase ERp72. J. Mol. Biol. 401 (2010) 618–25.
[76] A. Pirneskoski, P. Klappa, M. Lobell, R.A. Williamson, L. Byrne, H.I. Alanen, K.E. Salo, K.I. Kivirikko, R.B. Freedman, L.W. Ruddock, Molecular characterization of the principal substrate binding site of the ubiquitous folding catalyst protein disulfide isomerase, J. Biol. Chem. 279 (2004) 10374–10381.
[77] L. Ellgaard, L.W. Ruddock, The human protein disulphide isomerase family: substrate interactions and functional properties, EMBO Rep. 6 (2005) 28–32.

V.2.b.2.Les PDIs : oxydoréductases « à tout faire »

Les données mécanistiques des protéines de la famille des PDIs concernent principalement les PDIs appartenant à la classe L (Selles *et al*. 2011). Ces protéines ont été caractérisées chez différents organismes tels que l'homme, la levure ou certains organismes photosynthétiques. Elles sont capables de réaliser tous les types de réaction, réduction, formation et isomérisation de ponts disulfure (Figure 46) (Hatahet *et al*. 2009). Comme schématisé dans la figure 46, les réactions catalysées par les PDIs dépendront de leur état d'oxydation. Ainsi une PDI sous forme oxydée sera en mesure d'introduire des ponts disulfure sur une protéine cible réduite grâce à son potentiel d'oxydoréduction élevé (Figure 46A). Sous forme réduite, du fait de son faible *pKa* (4.8) la cystéine catalytique est en mesure de faire une attaque nucléophile sur le disulfure de sa cible (Figure 46B) (Karala *et al*. 2009). Cette attaque nucléophile est la première étape, commune aux réactions de réduction et d'isomérisation de ponts disulfure (Figure 46B-C).

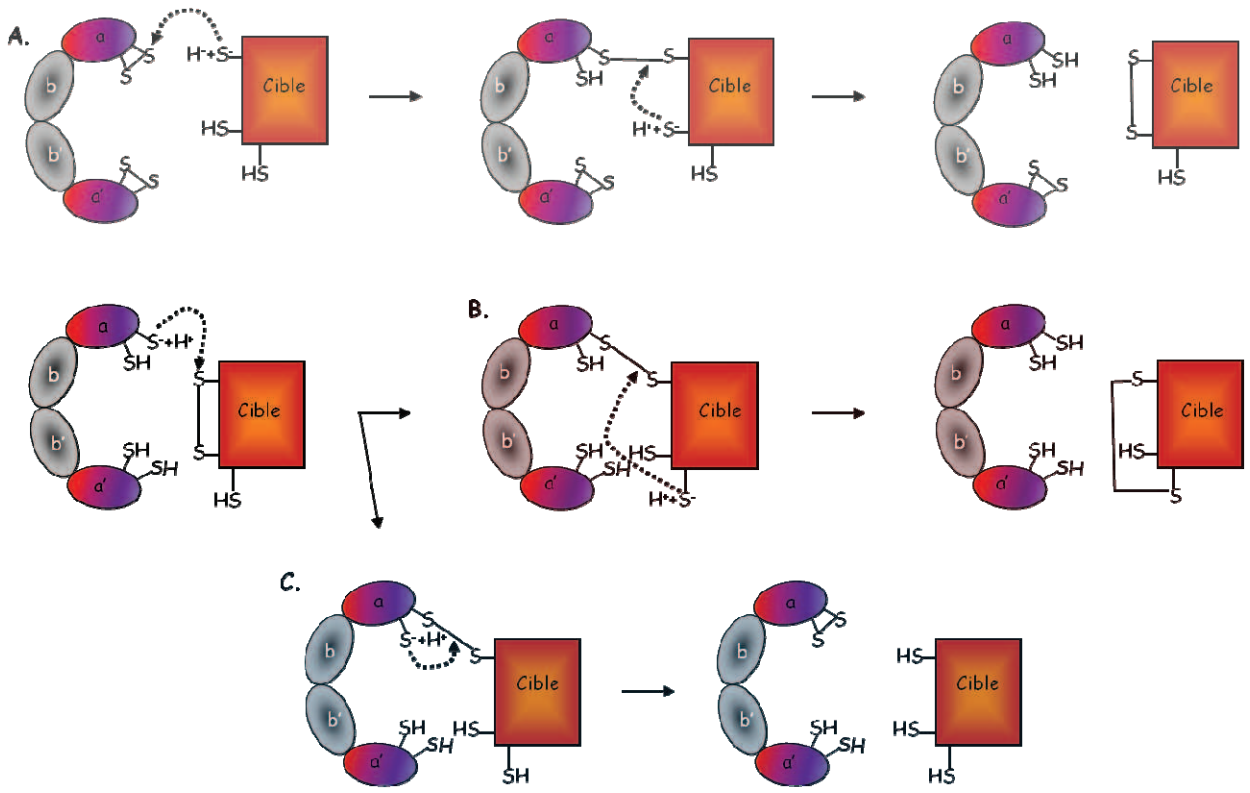

Figure 46. Les réactions catalysées par les PDIs.
A. Les réactions d'oxydation. B. Les réactions d'isomérisation. C. Les réactions de réduction.

V.2.b.3. Implication des différents modules de la PDI dans les réactions redox

Toutes les réactions représentées dans le mécanisme catalytique illustré en figure 46 sont l'œuvre d'un unique module possédant le motif CGHC. Ce choix de représentation est arbitraire. En effet, les données concernant la contribution respective des module *a* et *a'* dans les réactions d'oxydation, d'isomérisation ou de réduction ne permettent généralement pas de différencier l'action de ces 2 modules. Néanmoins, sur la base des expériences menées sur la PDI humaine, la protéine PDI1p de levure ainsi que sur son homologue chez *Humicola insolens,* il a été avancé que les modules redox actifs *a* et *a'* pouvaient présenter certaines spécificités vis-à-vis des réactions d'oxydation ou de réduction (Figure 47) (Tian *et al*. 2006; Karala *et al*. 2009; Serve *et al*. 2010). Ainsi le motif CGHC du module *a* de la PDI1p, qui présente un potentiel redox bas (environ -188 mV) serait responsable de la réduction des ponts disulfure non natifs tandis que le motif CGHC du module *a'* serait lui responsable de réactions d'oxydation grâce à son potentiel redox plus élevé (environ -152 mV) (Tian *et al*. 2006; Serve *et al*. 2010). Bien que moins importantes, les différences de potentiel redox des modules *a* et *a'* de la protéine humaine ERp57 vont également dans le même sens (-167 et 156 mV, respectivement) (Frickel *et al*. 2004).

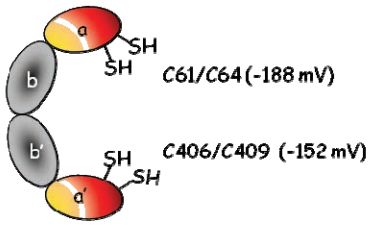

Organisations modulaires	Mutations	rRNAse (%)	sRNAse (%)
a-b-b'-a'	-	100	100
a-b-b'	Δ a'	43	58
a-b	Δ b'-a'	27	20
b-b'-a'	Δ a	63	84
b'-a'	Δ a-b	67	60
a-b-b'-a'	C64A	48	69
a-b-b'-a'	C409A	56	82
a-b-b'-a'	C61S/C64S	46	62
a-b-b'-a'	C406S/C409S	14	29
a-b-b'-a'	C64S/C409S	18	73

Figure 47. Implication des modules catalytiques « a » et « a' » dans la maturation de la RNAse A.

Les résultats des activités des différents mutants sont exprimés en pourcentages par rapport à l'activité de la protéine sauvage. Deux conditions sont testées pour la maturation de la RNAse, une condition ou la RNAse est réduite (rRNAse A) et une condition ou les disulfure de la RNAse sont dans une mauvaise conformation (ou « Scramble », sRNAse A). Dans les deux cas, en absence de PDI, l'activité de la RNAse est nulle (Tian *et al.* 2006).

En ce qui concerne les modules redox inactifs (*b* et *b'*) il a été démontré que ceux-ci jouaient un rôle de reconnaissance vis-à-vis des substrats ou partenaires protéiques. En effet les modules *a* et *a'* sont en mesure de réaliser des réactions redox *in vitro*, néanmoins ces réactions ne concernent que de petits peptides. Pour réaliser des réactions d'oxydoréduction sur des polypeptides complexes, la PDI classique nécessite la présence d'au moins un module inactif *b* ou *b'* (Figure 47) (Tian *et al*. 2006). Des expériences de mutagenèse ont montré que le module *b'* jouait un rôle prépondérant dans les interactions PDI/substrats. Ces données d'activité *in vitro* ont été confirmées par l'obtention de la structure tridimensionnelle des fragments *b-b'* des protéines humaines PDI et ERp57 mais également par cartographie des sites de fixation de peptides (Kozlov *et al*. 2006; Nguyen *et al*. 2008; Byrne *et al*. 2009; Denisov *et al*. 2009). Dans le cas des protéines PDI1p de *Saccharomyces* et PDI humaine, l'interaction avec leurs substrats se fait via une poche hydrophobe principalement localisée au niveau du module *b*' (Denisov *et al*. 2009). En ce qui concerne la protéine humaine ERp57, qui possède une plus grande variété de substrats que la PDI classique, l'interaction avec la calnexine, une chaperonne chargée d'augmenter son affinité avec ses substrats, se réalise également au niveau du module *b'* (Kozlov *et al*. 2006; Jessop *et al*. 2009b; Coe & Michalak 2010). Néanmoins, la nature biochimique du site d'interaction entre ERp57 et la calnexine diffère de façon significative par rapport au site d'interaction PDI1p/ substrats. En effet, la protéine ERp57 présente une région fortement chargée au niveau de son module *b'* qui est responsable du recrutement de protéines chaperonnes (Kozlov *et al*. 2006).

V.2.c. Interaction des protéines responsables de la maturation au sein du RE

Dans les paragraphes précédents, nous avons décrit les caractéristiques des familles de protéines identifiées à ce jour dans la maturation redox dépendante des protéines néo-synthétisées. Nous allons maintenant tenter de faire l'état des lieux de leurs interactions. La figure 48 synthétise l'ensemble des informations relatives aux interactions entre les sulfhydryl oxydases, les PDIs ainsi que d'autres protéines associées. Ainsi, 3 grandes voies peuvent être définies suivant le rôle tenu par les PDIs :

(i) La voie d'oxydation/isomérisation dépendante des protéines ERO1 qui se divise en deux étapes. Une étape d'oxydation dans laquelle la PDI transfère son (ou ses) ponts disulfure aux polypeptides non matures (Figure 48 rectangle vert). La PDI se trouve dès lors sous forme réduite et peut isomériser son substrat si celui est oxydé de façon non native, ou subir une réoxydation de la part de la protéine ERO1 pour à nouveau transférer des ponts disulfure à des ci-

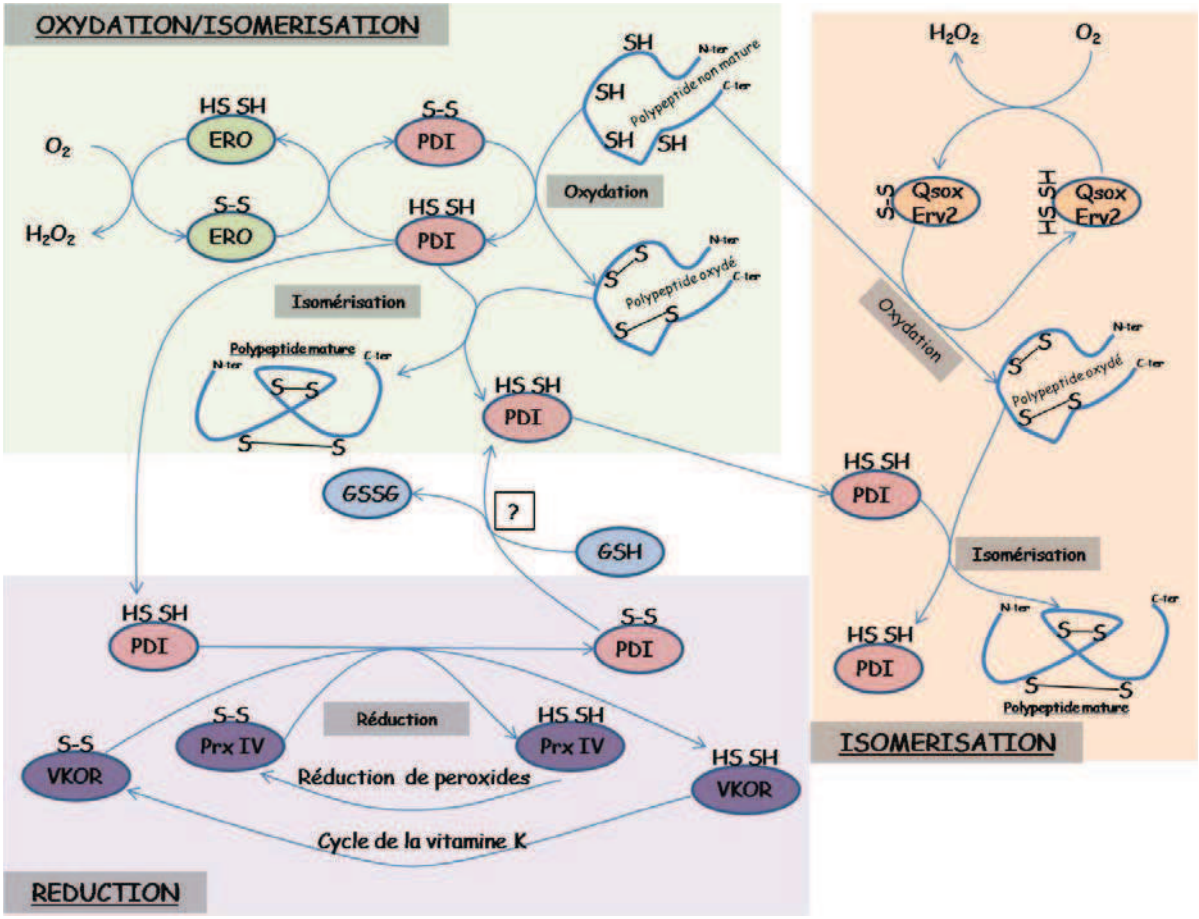

Figure 48. Les voies thiol dépendantes de maturation des protéines au sein du RE.
Figure détaillée dans le texte.

bles réduites (Figure 48 rectangle vert).

(ii) La voie d'isomérisation dépendante des protéines Qsoxs ou Erv2p. Dans cette voie, la PDI est sous forme réduite et va isomériser un polypeptide qui a été oxydé par les protéines Qsoxs ou Erv2p (Figure 48 rectangle orange). En effet, les PDIs ne sont pas des substrats physiologiques de ces sulfhydryl oxydases, tandis que les protéines Qsoxs sont capables d'oxyder la RNAse A. Ceci suggère que les Qsoxs et Erv2p transfèrent leurs ponts disulfure directement à des cibles, les PDIs sous forme réduite réalisant les réactions d'isomérisation nécessaires à l'obtention de leurs formes matures.

(iii) La voie de réduction. Très récemment, il a été démontré que les PDIs sous forme réduite pouvaient être ré-oxydées sans l'intervention des sulfhydryl oxydases (Figure 48 rectangle violet). Dans ce cas les accepteurs d'électrons peuvent être la Prx IV ou la vitamine K époxyde réductase (VKOR) (Wajih *et al*. 2007; Tavender & Bulleid 2010).

La vitamine K est un cofacteur aromatique essentiel à certaines enzymes responsables de

modifications post-traductionnelles, telles la γ-glutamyl carboxylase impliquée dans la carboxylation d'acides glutamiques en acide γ-carboxy-glutamiques (Tie & Stafford 2008). La vitamine K qui est exclusivement produite par les cyanobactéries et les organismes photosynthétiques est connue pour jouer un rôle de transporteur d'électrons durant la photosynthèse. Cette molécule présente 3 niveaux d'oxydation :quinone époxyde, quinone et quinol mais seule la forme quinol est un cofacteur efficace. La VKOR est une enzyme présentant un domaine à repliement Trx responsable de sa réduction via son site actif de forme CxxC permettant les réactions de carboxylation. Ainsi, chez les mammifères, l'existence de complexes PDI/VKOR dans le RE a été établie, la PDI étant le pourvoyeur d'électrons nécessaires aux étapes de réduction des quinones époxydes en quinols (Wajih *et al*. 2007). Le cas de la Prx IV est très intéressant. En effet, il a été démontré que la Prx IV humaine, résidente du RE, était en mesure d'accepter les électrons provenant de diverses isoformes de PDIs et quelquefois de façon beaucoup plus efficace que la protéine ERO1-α (Tavender *et al*. 2008; Tavender & Bulleid 2010). L'existence de cette voie alternative d'oxydation des PDIs, indépendante des protéines EROs, est également appuyée par des expériences *in vivo* de mutants des protéines ERO1-α et β dans lesquels aucun phénotype clair n'a pu être mis en évidence (Zito *et al*. 2010). Enfin, comme nous l'avons déjà mentionné, l'oxydation des PDIs par les sulfhydryl oxydases est source de peroxyde d'hydrogène. L'oxydation des PDIs via une thiol-peroxydase est un mécanisme élégant couplant à la fois le maintien de l'homéostasie en molécules oxydantes du RE et la maturation redox dépendante des protéines.

V.3. Le repliement des protéines dans l'espace inter-membranaire des mitochondries

Les mitochondries sont des structures membranaires intracellulaires (ou organites) essentielles à la physiologie des cellules eucaryotes. Ces organites sont composés de 4 compartiments, les membranes externes et internes, l'espace inter-membranaire et la matrice. Bien que les mitochondries soient le fruit ultime d'une endosymbiose, il y a environ 1,8 à 2 milliards d'années, impliquant à l'origine vraisemblablement une cellule eucaryote et une α-protéobactérie, un nombre très discret de protéines restent codées par le génome mitochondrial (de l'ordre du 1% des protéines totales) (Bihlmaier *et al*. 2008). Pour l'essentiel, les protéines mitochondriales sont codées par l'ADN nucléaire, traduites au niveau des ribosomes dans le cytosol et elles doivent être adressées aux mitochondries. Deux systèmes d'adressage coexistent, suivant la destination des polypeptides émergeant des ribosomes, la matrice ou l'espace inter-membranaire (IMS) (Riemer *et al*. 2010).

V.3.a. L'adressage au sein de la matrice

Les précurseurs protéiques à destination de la matrice présentent le plus souvent une séquence d'adressage N-terminale qui leur permettra de transiter via les translocases de la membrane externe (TOM, *Translocase of the Outer Membrane*) mais également *via* les translocases de la membrane interne (TIM, *Translocase of the Inner Membrane*). Le passage à travers les membranes externes, internes mais également au niveau de l'IMS est possible grâce à la consommation d'ATP ainsi qu'aux différences de potentiel membranaire. Arrivées à destination de la matrice, leur séquence d'adressage sera clivée pour obtention d'une protéine mature (Figure 49) (Koehler 2004).

V.3.b. L'adressage au sein de l'IMS

Dans le cas des polypeptides adressés à l'espace inter-membranaire, la plupart de ces protéines ne possèdent pas la séquence d'adressage classique des protéines de la matrice et peuvent être adressées à ce compartiment suivant différentes modalités (Herrmann & Hell 2005). Trois grandes classes de protéines de l'IMS (I, II et III) sont définies suivant le mécanisme d'import utilisé (Figure 49) (Koehler 2004; Herrmann & Hell 2005; Riemer *et al*. 2010). Nous allons plus particulièrement nous intéresser au processus d'import des protéines de classe II dans l'IMS. Ces protéines de petite taille (6 à 13 kDa) présentent la particularité de pouvoir transiter du cytosol vers l'IMS sans aide extérieure lorsqu'elles sont sous forme dépliée.

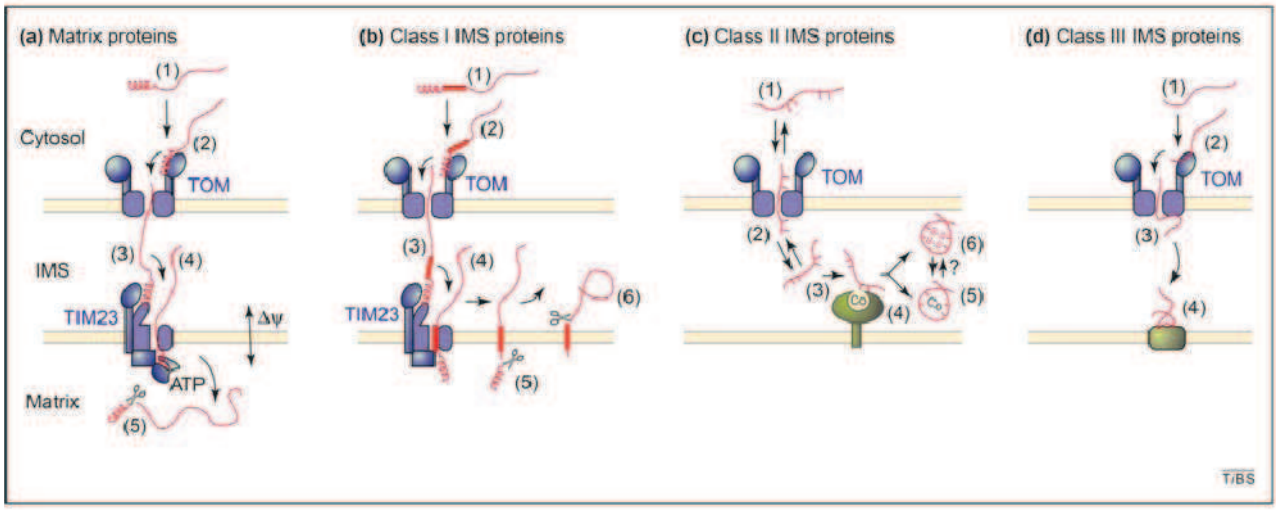

Figure 49. Les différentes modalités d'importation des protéines au sein des compartiments des mitochondries.

A. Transport ATP dépendant à travers les membranes et l'espace inter-membranaire des mitochondries des protéines depuis le cytosol vers la matrice.

(1) Les protéines de la matrice codées sous formes de pré-protéines par le noyau des cellules sont synthétisées au niveau des ribosomes dans le cytoplasme. (2) Les séquences d'adressage de ces pré-protéines vont être reconnues spécifiquement par un système de la membrane externe (complexe TOM) chargé de leur faire franchir la membrane externe. (3) Dans l'espace inter-membranaire, leurs séquences d'adressage seront reconnues par un autre système de translocation, celui-ci présent dans la membrane interne, le système TIM. (4) Grâce à la différence de potentiels entre l'IMS et la matrice (représenté par ΔΨ) ainsi qu'à la consommation d'ATP, ces pré-protéines vont transiter à travers la membrane interne vers la matrice. (5) Enfin la protéolyse des séquences d'adressage des pré-protéines est l'étape finale de leur maturation.

B. Adressage des pré-protéines de classe I dans l'IMS.

(1) Ces précurseurs possèdent une séquence d'adressage bipartite composée d'une hélice-a et d'un module transmembranaire. (2) Reconnaissance par le système TOM. (3) Reconnaissance par le système TIM. (4) Incorporation du domaine transmembranaire dans la membrane interne de la mitochondrie. (5) Protéolyse de la séquence d'adressage orientée dans la matrice. (6) Protéolyse du domaine transmembranaire pour obtenir une protéine mature au sein de l'IMS.

C. Adressage des pré-protéines de classe II dans l'IMS.

(1) Les prés-protéines de classe II présentent la particularité de pouvoir transiter à travers le système TOM sans processus de reconnaissance spécifique. (2) Ainsi elles sont en équilibre entre le cytosol et l'IMS. (3) Pour être retenue dans l'IMS elles doivent êtres reconnues par des systèmes de modification post-traductionnelle. (4) Ces systèmes peuvent introduire des cofacteurs ((5) cas de la SOD) ou des ponts disulfure (6) les empêchant de passer à travers le système TOM.

D. Adressage des protéines de classe III dans l'IMS.

(1) Ces protéines ne présentent pas de séquences d'adressage. (2) Cependant elles sont reconnues spécifiquement par le système TOM. (3) La membrane externe franchie, elles seront stabilisées par des sites de fixation protéique dans l'IMS (4) (Herman & Hell 2005).

V.3.c. Le repliement redox dépendant des protéines de classe II est nécessaire à leur localisation dans l'IMS

La rétention de ces protéines dans l'IMS est soumise à une étape de repliement redox dépendant. Cette maturation redox est l'œuvre d'un système composé de deux protéines, la protéine Mia40 (*Mitochondrial Inter-membrane space import and Assembly*) et la sulfhydryl oxydase Erv1 (Mesecke *et al*. 2005). La protéine Mia40 est une protéine reliée à la membrane interne via

un module hydrophobe, avec un domaine protéique orienté vers l'IMS présentant des résidus cystéinyls conservés. Ces résidus Cys forment trois motifs : un motif catalytique CPC responsable de l'oxydation des substrats dans l'IMS et deux motifs Cx_9C formant deux ponts disulfure structuraux. Ces trois motifs sont conservés chez tous les représentants de cette protéine chez les champignons, plantes ou mammifères (Herrmann & Köhl 2007). La protéine Mia40 est responsable de l'oxydation de substrats réduits au sein de l'IMS et elle est régénérée (ré-oxydée) par la sulfhydryl oxydase Erv1.

Les protéines Erv1, Erv1p *et al*r présentent des structures tridimensionnelles assez proches de la protéine Erv2p de *Saccharomyces* que nous avons décrite précédemment (Figure 50, paragraphe III.2.a.1) (Gross *et al*. 2002; Vitu *et al*. 2006). La différence majeure réside dans la localisation et la nature de la navette à électrons (Hofhaus *et al*. 2003; Vitu *et al*. 2006; Daithankar *et al*. 2010). Trois cas de figure sont possibles suivant la protéine considérée. Ainsi, la protéine Erv1 d'*Arabidopsis* possède une navette à électrons sous la forme Cx_4C en partie C-terminale (Figure 50) (Vitu *et al*. 2006). Dans le cas des protéines Erv1p et Alr, un motif CxxC en partie N-terminale a été démontré comme essentiel à l'oxydation de Mia40, bien que sa fonction de navette à électrons ne soit pas clairement établie (Figure 50) (Hofhaus *et al*. 2003; Daithankar *et al*. 2010).

V.3.d. Les cibles du système Mia40-Erv1 et leurs rôles physiologiques

La protéine Mia40, qui tire son potentiel oxydant de la protéine Erv1, est connue pour oxyder des protéines présentant certains types de motifs di-cystéines, les motifs Cx_3C et des motifs Cx_9C en tandem (Tableau 4) (Chacinska *et al*. 2004; Gabriel *et al*. 2007; Gebert *et al*. 2008; Longen *et al*. 2009; Reddehase *et al*. 2009; Endo *et al*. 2010). Ces motifs sont présents dans des protéines ayant des rôles physiologiques assez variés. Nous pouvons citer par exemple la maturation des cytochrome oxydases (présentant un motif Cx_9C en tandem), la morphologie des mitochondries (Mdm35, Cx_9C), la maturation et le transport des protéines (les protéines Tims, Cx_3C) ainsi que certaines protéines de fonction inconnue (Cmc4, Mic14, Mic17 ; Cx_9C) (Tableau 4). Notons également qu'il a été démontré que le couple Mia40/Erv1 intervient dans la maturation d'une enzyme de détoxication des EAOs, une superoxyde dismutase, bien que celle-ci ne présente pas de motif di-cystéine particulier (Reddehase *et al*. 2009).

Des études de mutants chez la levure ont pu mettre en évidence que la protéine Mia40p et la protéine Erv1p sont essentielles à la viabilité des mitochondries ainsi qu'à la maturation des protéines à centre fer/soufre du cytoplasme (Lisowsky 1992; Lange *et al*. 2001; Rissler *et al*. 2005; Terziyska *et al*. 2005). Néanmoins, la situation chez les organismes photosynthétiques varie sensi-

Protéines	Motifs ciblés par Mia40/Erv1	Fonctions
Cox17	Double Cx_9C	Maturation des cytochromes c oxydases
Cmc1		
Cmc2		
Cmc3/Coa4		
Cmc4		
Mic14		Inconnue
Mic17		Inconnue
Mdm35		Morphologie mitochondriale
Tim8	Cx_3C	Transport Protéique
Tim9		
Tim12		
Tim13		
RIP1/RIESK FeS	autres	Fonction du cytochrome bc1
Qcr6		
Sod1		Peroxydase
Ccs1		Maturation de la Sod1

Tableau 4. Protéines ciblées et motifs responsables de l'interaction avec le couple Mia40/Erv1 dans l'espace inter-membranaire des mitochondries (Endo *et al.* 2010).

blement. En effet, chez *Arabidopsis* la protéine Mia40 n'est pas essentielle au maintien des mitochondries et le phénotype de mutants pour le gène Mia40 n'est que très peu marqué. Par contre, le gène Erv1 est essentiel et aucune lignée homozygote délétée pour ce gène n'a pu être obtenue (Carrie *et al*. 2010). Il semblerait donc que le couple Mia40/Erv1 présente des caractéristiques spécifiques suivant les organismes considérés. D'ailleurs, la protéine AtErv1 n'est pas en mesure de complémenter un mutant Erv1p (Levitan *et al*. 2004). Une des hypothèses avancées est la nature de la navette à électron de la protéine Erv1 chez les organismes photosynthétiques, qui diffère significativement de celle que l'on retrouve dans la protéine Erv1p de levure. Ainsi chez les organismes photosynthétiques, Erv1 serait en mesure, grâce à son motif Cx_4C en partie C-terminale, d'oxyder directement la plupart des protéines cibles contenues dans l'IMS.

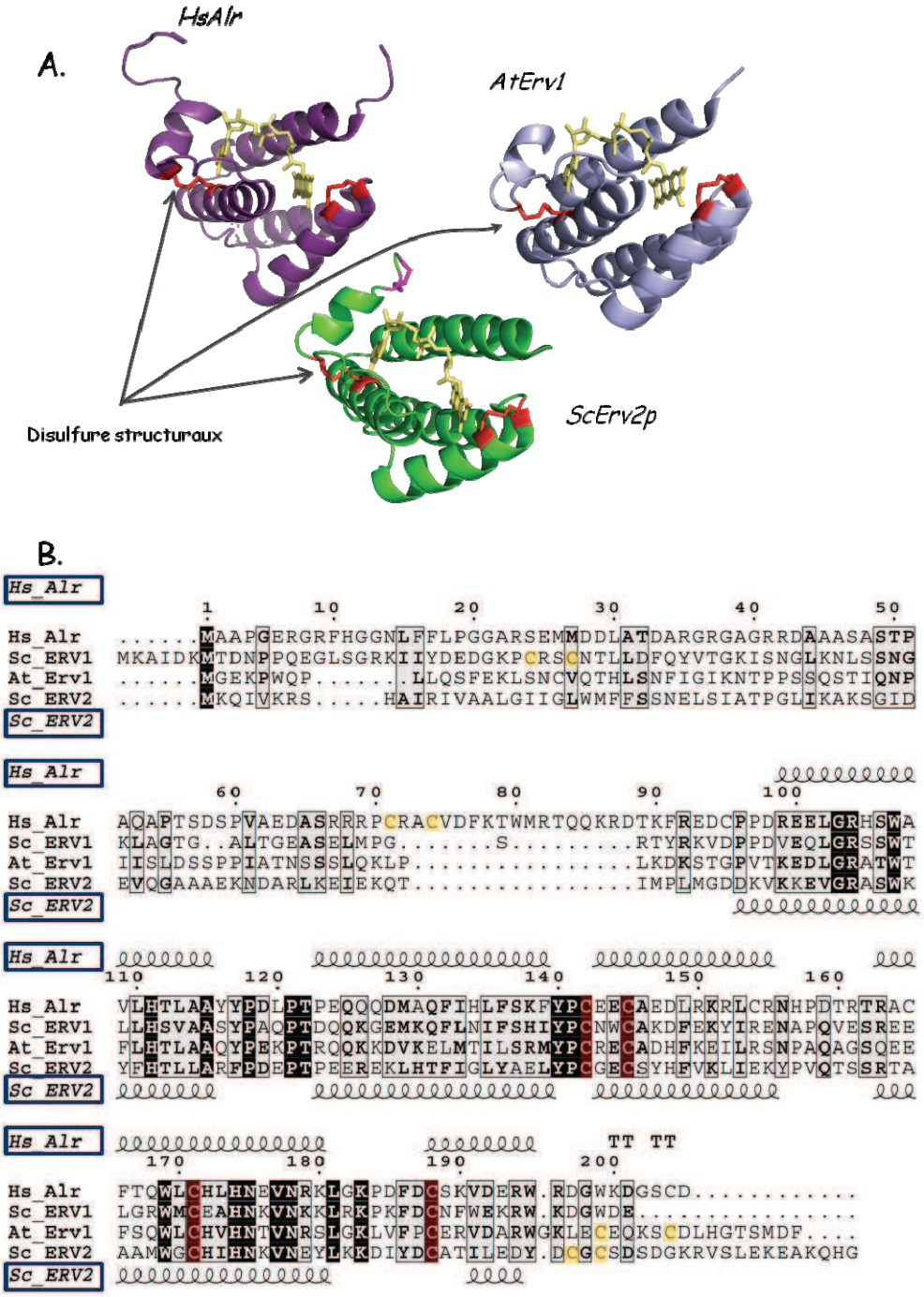

Figure 50. Comparaison des séquences et des structures tridimensionnelles des protéines Erv.

A. Structures 3D des protéines Alr humaine en mauve (PDB 3MBG), Erv1 d'Arabidopsis en gris (2HJ3) et de la protéine Erv2p de Saccharomyces en vert (1JR8). Les cofacteurs FAD sont représentés en bâtonnets jaunes et les disulfure présents en rouge. Pour la protéine Erv2p le disulfure en violet est le motif CGC, seule navette à électrons présente dans les trois structures. B. Alignement des séquences des protéines HsAlr (NP_005253.3), ScErv1p (NP_011543.2), ScErv2p (NC_001148.3) et AtErv1 (AT1G49880). Les acides aminé strictement conservés sont surlignés en noir, en rouge les deux disulfure présents dans les trois structures et en jaune les motifs dicystéines faisant office de navette à électrons. En partie haute et basse sont respectivement représentés les structures secondaires des protéines HsAlr (PDB 3MBG) et ScErv2p (PDB 1JR8).

Problématiques et objectifs

Mon travail de thèse avait pour objectif de caractériser biochimiquement deux familles de protéines appartenant à la superfamille des Trxs, les glutathion peroxydases et les protéine disulfure isomerases.

En se basant sur la structure cristallographique de la Gpx5 de peuplier, le premier volet de ce travail était d'étudier plusieurs aspects du mécanisme réactionnel : déterminer le ou les facteurs impliqués dans la transition structurale entre les formes réduite et oxydée, caractériser certains acides aminés important pour le mécanisme réactionnel mais également comprendre les modalités d'interaction avec les Trxs. Dans cette optique, j'ai tout d'abord réalisé un important travail de mutagenèse dirigée ciblant des acides aminés potentiellement impliqués dans ces mécanismes.

L'étude biochimique, enzymatique et spectroscopique de ces mutants nous a permis d'éclaircir certains aspects mécanistiques du fonctionnement de la Gpx5.

Concernant les PDIs, très peu d'études biochimiques ont été effectuées sur des PDIs de plantes et ce sujet est totalement nouveau au sein de notre laboratoire.

Suite à une analyse phylogénétique des PDIs d'organismes photosynthétiques mettant en évidence les spécificités » des PDIs de plantes et proposant une nouvelle classification, cinq isoformes du peuplier, les PDI-A, -L1a, -L3, -C et -M ont été sélectionnées en vue de leur caractérisation biochimique. Après purification des protéines recombinantes, les spécificités catalytiques de chaque isoforme soluble ont été étudiées grâce à la détermination de leurs activités oxydase, isomérase et réductase. En raison de son organisation particulière (a°-a-b), une analyse plus poussée de l'isoforme PDI-M a par ailleurs été effectuée, afin de déterminer l'implication de chaque domaine catalytique dans les activités détectées.

Les résultats les plus significatifs de mon travail de thèse sont regroupés dans deux articles en préparation (Articles 2 et 3), formant les deux chapitres de la partie résultats de ce manuscrit.

Résultats

I Article 2: Catalytic mechanism and oxidative inactivation of the poplar thioredoxin-dependent glutathione peroxidase 5

Benjamin Selles, Martin Hugo, Madia Trujillo, Vaibhav Srivastava, Gunnar Wingsle, Jean-Pierre Jacquot, Rafael Radi, Nicolas Rouhier

Sur la base de a description de la structure tridimensionnelle de la protéine Gpx5 de peuplier (Koh et al. 2007), ainsi que la détermination de certaines étapes du cycle catalytique de la protéine PtGpx3 (Navrot et al. 2006), nous avons procédé à une analyse approfondie des caractéristiques biochimiques de la PtGpx5. Pour cette étude, les propriétés spectroscopiques, enzymologiques et biochimiques de la protéine WT et de nombreux variants protéiques générés par mutagenèse dirigée, ont été analysées afin de détailler finement certaines étapes du mécanisme réactionnel : formation de l'acide sulfénique, changement structural entre formes réduites et oxydées, régénération par les Trxs. Par ailleurs, ce travail a permis de montrer la dimérisation de la Gpx5 n'est pas obligatoire pour son activité mais pourrait jouer un rôle dans la reconnaissance de certains substrats. Nous avons également démontré que la Gpx5 était en mesure de réduire les peroxynitrites, activité qui avait été uniquement décrite pour les Prxs ou Gpxs à sélénocystéine. Enfin, la démonstration que la cystéine peroxydatique de la Gpx5 peut subir une suroxydation conduisant à l'inactivation de la protéine, laisse supposer que certaines Gpxs de plantes pourrait jouer un rôle dans la perception et/ou la signalisation d'un stress oxydant, de manière sensiblement identique au rôle connu pour les 2-CysPrxs.

Catalytic mechanism and oxidative inactivation of the poplar thioredoxin-dependent glutathione peroxidase 5

Benjamin Selles[1], Martin Hugo[2], Madia Trujillo[2], Vaibhav Srivastava[3], Gunnar Wingsle[3], Jean-Pierre Jacquot[1], Rafael Radi[2], Nicolas Rouhier[1*]

Addresses

[1] Unité Mixte de Recherches 1136 Nancy University-INRA, Interactions Arbres-Microorganismes, IFR 110, EFABA 54506 Vandoeuvre-lès-Nancy cedex, France.

[2] Departamento de Bioquímica, and Center for Free Radical and Biomedical Research, Facultad de Medicina, Universidad de la República, 11800 Montevideo, Uruguay.

[3] Department of Forest Genetics and Plant Physiology, Swedish University of Agricultural Sciences, Umeå Plant Science Center, 90183 Umeå, Sweden.

Running head: catalytic mechanism of poplar Gpx5

[*]**Address correspondence to Nicolas Rouhier,** UMR 1136 Nancy University-INRA, Interactions Arbres Microorganismes, 54506 Vandoeuvre-lès-Nancy Cedex, France. Phone: ++383684225, Email: nrouhier@scbiol.uhp-nancy.fr

Contrary to selenocysteine-dependent glutathione peroxidases (Secys-Gpx), which are truly regenerated by glutathione, cysteine-containing glutathione peroxidases (Cys-Gpx) are recycled by thioredoxins and thus constitute thioredoxin-dependent glutathione peroxidase-like proteins. Using poplar Gpx5 as a model for Cys-Gpx, the role of several residues important either for the catalytic mechanism or the conformational arrangement has been explored. Here, we demonstrate that the conformational changes observed during the transition from the reduced to the oxidized form of PtGpx5 are primarily determined by the oxidation of the peroxidatic cysteine into sulfenic acid. Besides, mass spectrometry analyses demonstrated for the first time that plant Cys-Gpx could be subjected to over-oxidation of their peroxidatic cysteine into sulfinic or sulfonic acids. This suggests that some isoforms could have dual functions potentially acting in peroxide and peroxynitrite detoxification and/or as a mediator of H_2O_2 or peroxynitrite signalling as proposed for 2-Cys peroxiredoxins.
Exploring the role of Glu79 in PtGpx5, which replaces the Gln usually found in Gpx catalytic tetrad, pointed to its possible involvement in substrate selectivity. Indeed, although its redox properties (redox midpoint potential of the catalytic disulfide Cys44-Cys92 and *pKa* of Cys44) were not modified, an E79Q variant exhibited significantly improved kinetic parameters ($K_{peroxide}$ and k_{cat}) with the bulky tert-butyl hydroperoxide. The enzymatic characterization of the monomeric Y151R variant demonstrated that PtGpx5 does not act as an obligate homodimer. Regarding the Trx-mediated recycling, we provide evidence that the conserved Phe90 is important for Trx recognition and that PtGpx5 regeneration occurs via the formation of a transient disulfide between the catalytic cysteine of Trx and the resolving cysteine of Gpx5.

Introduction

In plants, various metabolic pathways or physiological processes such as photosynthesis and respiration produce reactive oxygen species (ROS) in different sub-cellular compartments as mitochondria, chloroplasts or peroxisomes (1). ROS can be different species as singlet oxygen, hydroxyl radicals, superoxide radical anions ($O_2^{\bullet-}$) or hydrogen peroxide (H_2O_2). On the other hand, plants produce nitric oxide ($^{\bullet}NO$) by several possible pathways, but the best and unambiguously characterized pathway so far is dependent on nitrite and requires nitrate reductases (2). Regardless its origin, $^{\bullet}NO$ can lead to reactive nitrogen species (RNS) formation, such as the oxidizing and nitrating species peroxynitrite[1], a peroxide formed *in vivo* from the diffusion-controlled reaction between $^{\bullet}NO$ and $O_2^{\bullet-}$ (3,4). Some of these ROS and RNS are known to be signalling molecules, being involved in apoptosis, cell proliferation or biotic and abiotic stress responses, but at the same time they are toxic compounds leading to random or targeted oxidation of DNA and proteins or to lipid peroxidation with associated potential drastic modifications of the physico-chemical properties of these macromolecules (1,5-7) Reactive species are continuously produced by cells, but in particular conditions, such as those occurring during environmental constraints, their concentrations can increase dramatically and lead to conditions of oxidative or nitro-oxidative stress (6,8). All organisms and particularly plants have developed a wide range of detoxification processes to tightly control cellular ROS and peroxynitrite concentrations (9,10). Among these scavenging enzymes are thiol-dependent peroxidases (Tpxs), which use a reactive cysteine residue to reduce various types of peroxides (from hydrogen peroxide to phospholipid hydroperoxides and peroxynitrite) (11). Several mammalian, protozoa and bacterial Tpxs have also been reported to reduce peroxynitrite to nitrite, although the peroxynitrite reductase activity of plant Tpxs have been investigated only for a few of them (10,12,13). Whatever the substrate reduced, the regeneration of the sulfenic acid formed during catalysis is dependent on thiol compounds, usually glutathione or thiol-containing proteins such as thioredoxins (Trxs), glutaredoxins (Grxs) or tryparedoxins. Five classes of thiol peroxidases have been defined in plants, grouping both the so-called

[1] The term peroxynitrite is used to refer to both peroxynitrite anion ($ONOO^-$) and its conjugated acid, peroxynitrous acid (ONOOH, *pKa* = 6.6-6.8).

glutathione peroxidases (Gpx) and peroxiredoxins (Prx), themselves separated into 1-Cys Prx, 2-Cys Prx, type II Prx and Prx Q subgroups (14). Regarding the Gpx class, they are usually monomeric or tetrameric enzymes distributed into two major types, depending on the presence of a selenocysteine (SeCys-Gpx) or cysteine (Cys-Gpx) as the catalytic residue (15,16). SeCys-Gpxs are present in mammals or algae such as *Chlamydomonas reinhardtii*, whereas Cys-Gpxs are found in non vertebrate organisms such as bacteria, fungi, insects and plants. Despite being denominated as glutathione peroxidases, most, if not all, Cys-Gpxs are in fact regenerated by Trxs but not or very poorly by glutathione (14,17-19). Cys-Gpxs usually contain 3 conserved Cys residues, but only two of these Cys are essential for the catalytic and regeneration mechanisms (18) The catalytic mechanism employed by Cys-Gpxs is a two-step process. The first step consists in a nucleophilic attack of the substrate by the most N-terminal cysteine defined as the catalytic or peroxidatic Cys (Cys_P), which is concomitant with the formation of a sulfenic acid on this residue and with the release of a water or of an alcohol molecule, depending on the nature of the substrate. Then, the most C-terminal cysteine named resolving or recycling Cys (Cys_R) attacks the sulfenic acid moiety forming an intramolecular disulfide (18,20-22). Then, the recycling of the reduced active form usually proceeds via a dithiol-disulfide exchange with Trxs. *In vitro*, under steady-state conditions, the efficiency of the overall reaction is determined by the rate-limiting step. For enzymes of the methionine sulfoxide reductase family, which are using an analogous reaction mechanism, it has been demonstrated that the rate-limiting step is attributed to the reduction by Trx and more precisely to the dissociation of both partners (23). As observed for some other thiol peroxidases such as 2-Cys Prx and for some methionine sulfoxide reductases, the transition from the reduced to the oxidized form in the dimeric poplar Gpx5 (PtGpx5) is accompanied by an important conformational change (23-26). Previous studies on Gpxs have defined that three residues Glu/Gln, Trp and Asn, govern the reactivity of Cys_P essentially by lowering its *pKa* value, forming a catalytic tetrad (16,20-22,27). Although the residues are different, the principle is very similar to Prxs, where a Thr and an Arg activate Cys_P and a Pro stabilizes the active site pocket (15,24).

Based on its previously solved 3D structure, an in-depth biochemical and enzymatic analysis was performed on PtGpx5 to dissect different steps of the catalytic and Trx-dependent recycling mechanisms. This analysis shed light on four important properties of this Cys-Gpx: i) it is efficiently reduced by Trx both in monomeric and dimeric forms, iii) the conformational changes observed during the transition from the reduced to the oxidized form of PtGpx5 are dependent on the oxidation state of Cys_P, iii) which is susceptible to overoxidation into sulfinic or sulfonic forms, and iv) an engineered enzyme, where one of the residues of the catalytic tetrad, Glu79 is replaced by a Gln, is a better catalyst for the reduction of complex hydroperoxides.

Experimental procedures

Cloning, production and purification of recombinant proteins

The cloning of PtGpx5 (POPTR_0001s09280) into pET-3d was described previously (18). Several variants (E79Q, D89K, F90E and Y151R) have been obtained by PCR-based site-directed mutagenesis using two complementary mutagenic primers (Supplemental Table 1). Culture and purification conditions were similar to the procedures described for PtGpx5 WT (18).

Peroxide and protein quantitation

The concentration of H_2O_2 stock solutions was measured at 240 nm (ε_{240} = 43.6 $M^{-1}cm^{-1}$) (28). Peroxynitrite concentration was determined at alkaline pH at 302 nm (ε_{302} = 1670 $M^{-1}cm^{-1}$) (4). Protein concentrations were measured spectrophotometrically using a molar extinction coefficient at 280 nm of 20065 M^{-1} cm^{-1} for PtGpx5 WT, the single cysteine mutants and the E79Q, D89K, F90E variants, 19940 M^{-1} cm^{-1} for the double cysteine mutants and 18575 M^{-1} cm^{-1} for PtGpx5 Y151R, as determined from their primary sequences (http://www.expasy.ch/tools/protparam.html). The concentration of horse radish peroxidase (HRP) was determined by its absorption at the Soret band (ε_{403} = 1.02 x 10^5 M^{-1} cm^{-1} (29).

Steady-state activity measurement

The Trx-dependent peroxidase activity of WT and mutated PtGpx5 was measured using a NADPH-coupled spectrophotometric method at 25°C as described previously (18). The assays were carried out in a total volume of 500 µL containing TE buffer (30 mM Tris-HCl, pH 8.0, 1 mM EDTA), 200 µM NADPH, 1 µM *Arabidopsis thaliana* NTRB, 25 µM poplar Trxh1, 200 nM PtGpx5 and varying peroxide concentrations. The catalytic parameters for one substrate have been obtained by varying its concentration at saturating concentrations of the other substrate (typically between 1 and 100 µM for Trxh1, and between 40 µM and 12 mM for the peroxides, either H_2O_2, *tert*-butyl hydroperoxide (*t*-BOOH) and cumene hydroperoxide (COOH)). The decrease in absorbance was followed at 340 nm. The peroxidase activity was determined after subtracting the spontaneous reduction rate observed in the absence of PtGpx5, and the number of µmole of NADPH oxidized per second per µmole of enzyme (i.e. turnover number, s^{-1}) was calculated using the molar extinction coefficient of NADPH (ε_{340} = 6.23 mM^{-1} cm^{-1}). Two to three independent experiments were performed at each substrate concentration. The k_{cat} and K_m values of PtGpx5 for Trxh1 (K_{Trx}) or peroxides ($K_{peroxide}$) have been calculated by non-linear regression using GraFit (Erithacus Software). Inactivation of PtGpx5 and Arabidopsis 2-Cys Prx (50 nM and 1.5 µM, respectively) were evaluated under the same conditions using H_2O_2 concentrations ranging from 50 µM to 2.5 mM by monitoring the mean speed of NADPH oxidation between 30 seconds and 1 minute after addition of thiol peroxidases.

PtGpx5 thiol reduction and alkylation

The enzyme was reduced immediately before use by incubation with 1 mM DTT for 30 min at 4 °C. Excess reductant was removed by gel filtration using a HiTrap column (Amersham Bioscience) and UV-Vis detection at 280 nm. Samples were extensively purged with argon once collected. For protein thiol alkylation, pre-reduced PtGpx5 was incubated with N-ethylmaleimide (NEM) (10 mM) for 30 min at 4 °C, and excess NEM was removed as described for DTT.

Pre-steady state investigation of the oxidative part of PtGpx5 catalytic cycle

All pre-steady state kinetic measurements were made using a stopped-flow apparatus with a mixing time of 1.1 ms and coupled with spectrophotometric and fluorimetric detection (Applied Photophysics SV20). Experiments were performed in sodium phosphate buffer 100 mM plus 0.1 mM DTPA (to minimize transition metal ion dependent chemistry), pH 7.4 and 25 ºC, unless otherwise indicated.

The kinetics of H_2O_2-mediated PtGpx5 oxidation was studied by two pre-steady state approaches. The first one was a direct determination that made use of the increase in PtGpx5 intrinsic, tryptophan-dependent fluorescence intensity that occurred upon enzyme oxidation. Reduced enzyme (2 µM) was rapidly mixed with different concentrations of H_2O_2 in excess. The time courses of total fluorescence increase (λ_{ex} = 295 nm) were followed and experimental curves were fitted to increasing exponentials from which observed rate constants (k_{obs}) were determined. From the slope of the plot of k_{obs} values versus H_2O_2 concentrations, the rate constant of H_2O_2-mediated PtGpx5 oxidation at pH 7.4 and 25º C was determined. The second approach was an indirect, competition method described previously (30). Briefly, we investigated the ability of reduced PtGpx5 to inhibit HRP oxidation to compound I by H_2O_2, a reaction with a reported rate constant (k_{HRP}) of 1.7 x 10^7 $M^{-1}s^{-1}$ (31). The time courses of compound I formation from the reaction of 2 µM HRP and 0.65 µM H_2O_2 in the absence or presence of 28.5 µM reduced PtGpx5 were followed at 398 nm ($\Delta\varepsilon_{398}$ = 4.2 x 10^4 M^{-1} cm^{-1} (32)). Experimental traces were fitted to exponential curves from which observed rate constants at each PtGpx5 concentration were obtained. Since the observed rate constants (k_{obs}) relates to the rate constant of H_2O_2-mediated oxidation of HRP ($k_{H2O2/HRP}$) and to the rate constant of H_2O_2-mediated oxidation of PtGpx5 ($k_{H2O2/PtGpx5}$) by

$k_{obs} = k_{H2O2/HRP}$ x [HRP]+ $k_{H2O2/PtGpx5}$ x [PtGpx5], the plot of k_{obs} versus PtGpx5 concentration allowed calculation of both $k_{H2O2/HRP}$ as the y-intercept and $k_{H2O2/PtGpx5}$ as the slope or the plot.

The kinetics of peroxynitrite-mediated PtGpx5 oxidation was also investigated by two pre-steady state approaches. Firstly, we tried a direct approach, following the initial rate of peroxynitrite decomposition in the absence or

presence of reduced PtGpx5 at 310 nm as previously reported for other thiol-containing proteins (33). However, the reaction rate was too fast to be accurately followed by this methodology. Therefore, we tried an indirect, competition approach, by determining the inhibitor effect of increasing reduced PtGpx5 concentrations on peroxynitrite-mediated HRP oxidation to compound I in a similar way as above indicated for the determination of the kinetics of PtGpx5 oxidation by H_2O_2.

Pre-steady state investigation of the reductive part of PtGpx5 catalytic cycle

The kinetics of the reactions of oxidized PtGpx5 with GSH, thioredoxin h1 (Trxh1) and thioredoxin h5 (Trxh5) were investigated by a direct fluorescence approach, where reduced PtGpx5 was firstly oxidized by treatment with an almost equimolar H_2O_2 concentration (~ 0.8:1, in order to get the enzyme to be oxidized in a controlled way and avoid overoxidation) followed by mixing with different concentrations of reductant in excess. The time courses of total fluorescence intensity change (λ_{ex} = 295 nm) were fitted to exponential curves and k_{obs} values of fluorescence change plotted versus reductant concentration. From the slopes of the latter plots, the rate constants of PtGpx5 reaction with GSH, Trxh1 or Trxh5 at pH 7.4 and 25 ºC were determined.

Detection of sulfenic acid with NBD-Cl

NBD-Cl (4-Chloro-7-nitro-2,1,3-benzoxadiazole) was used to detect the formation of sulfenic acids on purified proteins after an H_2O_2 treatment. 100 mM stock solutions of NBD-Cl were prepared in DMSO and stored in the dark at -20 °C. The recombinant proteins were reduced by incubation with 5 mM DTT for 1 h at 25 °C. After reduction, proteins were subjected to successive dilution/concentration steps in TE buffer by ultrafiltration in order to remove excess DTT. Then, 50 µM reduced proteins were oxidized by incubation in 500 µl reaction mixtures with various concentrations of H_2O_2, from 250 µM to 5 mM. 250 µM of NDB-Cl was added after 1 min and the reaction mixture incubated in the dark for 1 h at 25°C. The proteins were separated from excess NBD-Cl by precipitation for 15 min on ice with 10% TCA (v/v). After centrifugation (15 min 13000 rpm), the pellets were washed with 1 mL of TCA 2%. After another centrifugation step (15 min, 13000 rpm), proteins were resuspended in 500 µL of Tris-HCl 1M 2% SDS for 30 minutes and their UV-visible spectra were recorded on a Cary 50 spectrophotometer (Varian).

ESI-MS analysis of oxidized and reduced PtGpx5

Solutions of PtGpx5 WT or C73/92S at 100 µM were either reduced by 150 µM DTT or oxidized in the presence of a mixture of either 150 µM, 1.5 mM or 7.5 mM of both DTT and H_2O_2 for 5 min at room temperature. High-resolution ESI-MS spectra of treated and untreated proteins were obtained on a Bruker microTOF-Q spectrometer (Bruker Daltonik, Bremen, Germany), equipped with Apollo II electrospray ionization source with ion funnel, operated in the negative ion mode. The concentrated sample (around 100 µL of the 100 µM solution) in formic acid was injected at a flow rate of 10-20 µl min^{-1}. The potential between the spray needle and the orifice was set to 4.5 kV. Before each run the instrument was calibrated externally with the Tunemix™ mixture (Agilent Technologies) in quadratic regression mode. Data were treated with the DataAnalysis software (Bruker).

Determination of the oligomerization state

The oligomerization state of WT and mutated Gpxs was analyzed by size-exclusion chromatography on a Superose 12 HR 10/30 column connected to a FPLC system (Pharmacia Fine Chemicals, Uppsala, Sweden). 200 µL of proteins at 10 $mg \cdot ml^{-1}$ were loaded on the column equilibrated in 50 mM Tris HCl pH 8.0 containing 150 mM NaCl and 1 mM EDTA. The flow rate was fixed at 0.25 $ml \cdot min^{-1}$ and detection was recorded at 280 nm. The column was calibrated by loading 100µl bovine milk lactoserum (34).

Determination of the midpoint redox potential

Oxidation-reduction titrations, using the fluorescence of adducts formed between the protein and mBBr, were carried out at ambient temperature as described previously (18). The 500 µl reaction mixtures contained 100 µg protein in 100 mM HEPES-NaOH buffer, pH 7.0, containing defined mixtures of oxidized and reduced DTT to set the ambient potential (Eh) with an overall concentration in DTT of 2 mM. After 2 h incubation at 25°C,

excess mBBr was added and incubated in the dark for 1 h. mBBr labelled proteins were precipitated with TCA 20% (v/v), incubated 15 min on ice and centrifuged 15 min at 13000 rpm. Pellets were washed with 1 volume of 2% TCA by centrifugation (15 min, 13000 rpm) and then resuspended in 300 µl Tris-HCl 1 M, SDS 2% during 30 min. Protein solutions were then diluted to a final volume of 2.2 ml and mBBr fluorescence emission was recorded between 400 and 500 nm using a Cary Eclipse spectrofluorimeter after excitation at 350 nm.

pK_a of Gpx sulfhydryl groups

The reaction of (2-pyridyl)dithiobimane (PDT-bimane) with cysteine forms pyridine-2-thione, which has a maximum absorption wavelength at 343 nm. The stock solution of PDT-bimane was made in DMSO, and the concentration was determined using the absorbance extinction coefficient at 380 nm, ε_{380} = 5000 M^{-1} cm^{-1} in ethanol. Reactions were started by the addition of PDT-bimane to a final concentration of 25 µM into a cuvette containing 10 µM pre-reduced proteins in 500 µl of sodium citrate or phosphate buffer ranging from pH 3.0 to 8.0. After rapid mixing, the absorbance at 343 nm was recorded over 120 min with a Varian Cary 50 spectrophotometer. Absorbance data were approximately fitted to an exponential with the GraFit (Erithacus Software) program and the $t_{½}$ (the time to reach half-maximal reactivity as monitored by half-maximal release of pyridyl-2-thione) at each pH was determined. Those values were plotted against pH using sigmoidal curve fit in GraphPad Prism 5.

Circular dichroism

Circular dichroism (CD) spectra of the different enzymes (25 µM in phosphate buffer 10 mM pH 7.1), either reduced by DTT or oxidized by almost equimolar H_2O_2 concentration, were recorded at 25°C in a quartz cuvette (1-mm path length) between 200 to 250 nm with a bandwidth of 10 nm using a Jobin-Yvon CD6 spectropolarimeter. The mean residue molar ellipticity [θ] was expressed in deg cm^2 $dmol^{-1}$.

In gel digestion and mass spectrometry analysis of PtGpx5-Trxh1 heterodimer

The formation of heterodimers between PtGpx5 and poplar Trxh1 C42S was accomplished by incubating a pre-reduced Trxh1 C42S and native (oxidized) Gpx5 at 1µg/µl in 50 µl of 50 mM Tris HCl pH 8.0 for 1 hour at room temperature. Pre-reduced Trxh1 C42S was obtained after reduction of 500 µM protein using 10 mM DTT for 30 minutes and desalting on a Sephadex G-25 column. Around 7.5µg of each protein was loaded on non reducing SDS PAGE. The gel band corresponding to PtGpx5-Trxh1 heterodimer was excised and digested in-gel as described in (35). Briefly, all the selected bands were washed, reduced and alkylated with DTT and iodoacetamide (IAM), respectively or only alkylated without reduction. At last, bands were digested in-gel with sequencing grade modified trypsin (Promega/SDS Biosciences) or chymotrypsin (Roche). The resulting peptides were extracted, dried and dissolved in 0.1% formic acid for mass spectrometric analysis.

Peptide analysis was done by reverse-phase liquid chromatography electrospray ionization-tandem mass spectrometry, as described in (36), using a nanoACQUITY ultra-performance liquid chromatography (UPLC) system coupled to a QTOF mass spectrometer (Q-TOF Ultima; Waters Corp.). Raw data were processed by ProteinLynx Global Server (version 2.2.5) software for database searches. Proteins were identified by an in-house Mascot server and the Mascot Daemon application (version 2.1.6; Matrix Science; www.matrixscience.com) using the Populus protein database. The following settings were used for the database search: trypsin or chymotrypsin specific digestion with one missed cleavage allowed, carbamidomethylated Cys, oxidized Met, dioxidized and trioxidized Cys in variable mode, peptide tolerance of 80 ppm, and fragment tolerance of 0.1 D. Peptides with Mascot ion scores exceeding the threshold for statistical significance ($P < 0.05$) were selected.

Results

We previously determined the involvement of two cysteines (Cys44 and Cys92, formerly Cys107 and 155 taking into account the plastidial targeting sequence) out of the three conserved cysteines in the catalytic and regeneration mechanisms of plant Cys-Gpxs using PtGpx3 as a model (18).Moreover, we have been able to solve the 3D structure of PtGpx5, a paralog isoform, in both reduced

and oxidized forms, which confirmed first that Cys44 and Cys92 of PtGpx5 are the Cys_P and Cys_R respectively and which indicated that a large conformational change, i.e. unwinding of the beginning of the α1 helix and of the whole α2 helix, occurs in order to bring the two distant cysteine residues together to form an intramolecular disulfide bond (25). This change in oxidation state is also associated to a modification of the intrinsic fluorescence of the protein and to a shift observable in non reducing SDS PAGE (18). In this study, we have generated different mutated PtGpx5 proteins, replacing first individually all cysteines by serines (Gpx5 C44S, C73S, and C92S variants), and then combining two mutations to generate protein variants in which only Cys_P (C73/92S) or Cys_R (C44/73S) remained. In addition, with the aim of dissecting the catalytic cycle we have generated other mutated proteins on residues presumably involved in dimerization (Y151R), in Trx recognition (F90E), in the reactivity of Cys_P (E79Q) and in the instability of helix α2 (D89K).

Substrate specificities of PtGpx5

Using activity measurements achieved under steady-state conditions, we have first confirmed that, as previously reported for some plant Gpxs, the recombinant form of PtGpx5 cannot reduce peroxides using glutathione as reducing substrate (data not shown) (17,18,37). The kinetic parameters of PtGpx5 have thus been determined using a NADPH/NTR/Trxh1 reduction system and various peroxides. The catalytic efficiency (k_{cat}/K_m) of PtGpx5 toward these peroxides is quite variable with values of 133, 78 and 3 $x10^3$ $M^{-1}.s^{-1}$, for H_2O_2, COOH and t-BOOH respectively (Table 1). The marked difference observed with *t*-BOOH (difference of a factor 25 to 45 compared with the other peroxides tested) essentially correlates with a difference in the apparent substrate affinity, with K_m values of 32 and 81 µM for H_2O_2 and COOH and 1.9 mM for *t*-BOOH. The comparison of these values with those determined previously for two different Cys-Gpxs from photosynthetic organisms, PtGpx3 and *Chlamydomonas reinhardtii* GpxH (CrGpxH), indicates that all three enzymes have very similar properties, t-BOOH being the poorest substrate in all cases (Table 1) (18,38). Concerning the two poplar paralogs, although PtGpx3 has a slightly better turnover number, around 10 s^{-1} vs 5 s^{-1} for PtGpx5, the much better apparent affinity of PtGpx5 for H_2O_2 (K_m value of 32 µM vs 545 µM for PtGpx3), generates a difference in catalytic efficiency (k_{cat}/K_m) by a factor of 6 for this substrate. On the other hand, although CrGpxH had the highest catalytic efficiency towards the organic hydroperoxides tested, PtGpx5 was almost equally efficient as CrGpxH towards H_2O_2 reduction (Table 1).

We took advantage of the fact that, similarly to PtGpx3, PtGpx5 exhibits fluorescence changes between the reduced and the oxidized state, to study the kinetic of H_2O_2 reduction independently of the presence of the recycling system. The addition of H_2O_2 in excess to reduced PtGpx5 caused a rapid increase in its intrinsic fluorescence intensity that did not occur when an enzyme mutated at the peroxidatic cysteine residue PtGpx5 C44S was used (Fig. 1A inset). Addition of increasing concentrations of H_2O_2 led to a linear dose-dependent increase in the observed rate constants of PtGpx5 intrinsic fluorescence change (Fig. 1A), indicating that the bimolecular reaction between the enzyme and the oxidant was the rate-limiting step of the process leading to the change observed in tryptophan fluorescence. From the slope of the plot, a second-order rate constant of 5 ± 1 $x10^4$ M^{-1} s^{-1} at pH 7.4 and 25 ºC was determined. These results were confirmed by measuring the inhibition of HRP compound I formation by PtGpx5. Indeed, reduced PtGpx5 (28.5 µM) caused only a marginal decrease on the yield of HRP (2 µM) oxidation to compound I by H_2O_2 (0.65 µM) and a slight increase in the k_{obs} of the process[2] that is consistent with a rate constant of ~$1x10^5$ M^{-1} s^{-1} (Supplemental Fig. 1).

Regarding the apparent affinity of PtGpx5 toward poplar Trxh1, a K_m value of 5.2 µM was obtained in steady-state conditions, slightly better than the one determined with PtGpx3 (12 µM). This led to a k_{cat}/K_m of 1.33

[2] from 23 s^{-1} in the absence of PtGpx5 (consistent with a rate constant value of H_2O_2-mediated HRP oxidation of 1.2 x 10^7 M^{-1} s^{-1} in agreement with previously reported data (ref)) to 27.7 s^{-1}, i.e. 4.7 s^{-1} increase in observed rate constant of HRP-compound I formation, that divided into PtGpx5 concentration (28.5 µM) indicated a rate constant value of H_2O_2-mediated PtGpx5 oxidation of approximately 1 x 10^5 M^{-1} s^{-1} at pH 7.4 and 25 ºC.

$x10^6$ M^{-1} s^{-1}. Using intrinsic fluorescence measurement, the kinetic of GSH or Trx oxidation by PtGpx5 was measured by mixing oxidized PtGpx5 or reduced PtGpx5 (as a control) with varying amounts of GSH or pre-reduced Trxh1 or Trxh5. These substrates led to changes in PtGpx5 intrinsic fluorescence intensity that fitted to exponential curves, and observed rate constants of the process were linearly dependent on the reductant concentration, indicating that the bimolecular reaction was rate-limiting the process leading to the observed change in protein fluorescence. With this method, the second order rate constants of PtGpx5 reduction were 56 ± 5 M^{-1} s^{-1} , 1.00 ± 0.02 $x10^6$ M^{-1} s^{-1} and 4.3 ± 0.04 x 10^5 M^{-1} s^{-1} for GSH, Trxh1 and Trxh5 respectively (Fig. 1B to D). As GSH proved to be inefficient in activity assays conducted under steady-state conditions, this change of fluorescence likely reflects the formation of a mixed disulfide between GSH and the remaining free cysteine.

Next, the capacity of PtGpx5 to reduce peroxynitrite, a known substrate of some thiol peroxidases was assessed. When reduced PtGpx5 (10 µM) was mixed with peroxynitrite (15 µM), a decrease in the initial peroxynitrite concentration measured at 310 nm was observed (Supplemental Fig. 2A). This decrease happened in the first 100 ms before the spontaneous decomposition of peroxynitrite, which indicates a very fast reaction with reduced PtGpx5 but was too fast for initial rate of peroxynitrite decay to be followed by stopped flow techniques (mixing time of our apparatus is 1.1 ms). When pre-incubating the reduced enzyme with the thiol alkylating agent N-ethylmaleimide (5 mM NEM during 30 minutes), peroxynitrite fast reduction was significantly diminished (Supplemental Fig. 2B). The fact that the total change in absorbance at 310 nm is still a bit lower in the presence of alkylated enzyme may be due to partial alkylation of thiols under this condition. In this context, the second-order rate constant of reaction of PtGpx5 with peroxynitrite was determined by a competition approach as described in (30). As expected, reduced PtGpx5 inhibited the yield of peroxynitrite-dependent formation of HRP-Compound I (Fig. 2 inset) and caused a dose-dependent increase in the observed rate constant of HRP-compound I formation (Fig. 2). From the y-intercept of the plot, a second-order rate constant of peroxynitrite-mediated HRP oxidation of 3 x 10^6 at pH 7.4 and 25 ºC was obtained, in agreement with previously reported data (39). From the slope of the plot, a second-order rate constant of 1.4 x 10^6 M^{-1} s^{-1} for the PtGpx5 oxidation by peroxynitrite at pH 7.4 and 25 ºC was determined.

Overoxidation of the peroxidatic cysteine of PtGpx5

Activity measurements achieved under steady-state conditions with H_2O_2 indicated that the rate of the reaction catalyzed by Gpx5 decreased with time although substrate amounts were not limiting, suggesting that some enzyme inactivation occurred (data not shown). Hence, we have established a dose-dependent response by increasing the concentrations of H_2O_2 from 50 µM to 2.5 mM and using, for comparison, a 2-Cys Prx from *A. thaliana*, as this class of thiol-peroxidases is known to be sensitive to overoxidation (40). For both proteins, a significant loss of activity was observed (Fig. 3). Although some inactivation of 2-Cys Prx was detected at lower oxidant concentrations (visible at 500 µM H_2O_2) compared to PtGpx5, both proteins lost about 60% of activity at a concentration of 2.5 mM. It has been demonstrated for 2-Cys Prxs that this inactivation coincides with the overoxidation of Cys_P into sulfinic (SO_2H) or sulfonic (SO_3H) acids. As PtGpx5 is purified in an oxidized form, the molecular mass of Gpx5 was analyzed by mass spectrometry, after incubating the protein in the presence of a mixture of DTT and H_2O_2 at different concentrations. In the presence of DTT, only one peak with a molecular mass of 19,281 Da was detected. This is consistent with the theoretical mass of PtGpx5 with a cleaved N-terminus methionine. Following H_2O_2 incubation, two other protein peaks (19,313 and 19,330 Da), presenting mass increments of ~32 or ~49 Da, have been detected likely indicating the presence of 2 or 3 additional oxygen atoms and suggesting that one or several cysteines have been overoxidized.

In order to identify whether the cysteines are indeed the target of oxidation and which of the two cysteines involved in the catalytic mechanism is the most sensitive, the redox state of the Cys44 and Cys92 was analyzed using the C73/92S and C44/73S variants respectively by incubating reduced proteins with different peroxide concentrations

(250 µM, 500 µM and 5 mM) during 1 min. Subsequently, the proteins were incubated with NBD-Cl, a compound which reacts with thiol groups and sulfenic acids but not with sulfinic or sulfonic forms. The covalent attachment of NBD-Cl generates an absorption band centered at 350 nm upon reaction with thiol groups, whereas it is centered at 415 nm upon reaction with sulfenic acids. Following reaction with NBD-Cl, the absorption spectra of both reduced mutant proteins exhibited the expected absorption band at 415 nm (Fig. 4). From the absorbance, the levels of NBD-Cl adducts detected are consistent with the full alkylation of all cysteines. A treatment of the C73/92S mutant with 250 µM H_2O_2 led to the appearance of the absorption band specific to the reaction of NBD-Cl with sulfenic acids, indicating that Cys44 or Cys_P is readily oxidized to a sulfenic form. The decrease or the disappearance of this signal upon treatment with 500 µM and 5 mM H_2O_2 respectively, likely indicates that Cys_P is over-oxidized to sulfinic or sulfonic acid forms. Consistently, mass spectrometry analysis of the C73/92S treated with 5 mM DTT, 50 µM H_2O_2 and 1 mM H_2O_2 identified protein species with molecular masses of 19249 Da, 19266 Da (+17 Da) and 19281 Da (+32 Da) respectively. For the C44/73S variant, no oxidation has been observed on Cys_R whatever the H_2O_2 concentration used.

pKa of the catalytic cysteines and midpoint redox potential of the catalytic disulfide

The catalytic efficiency of thiol-dependent oxidoreductases largely depends on the reactivity of the catalytic cysteine which is usually made more acidic by the protein environment and on the midpoint redox potential (E_m) of the catalytic disulfide if any. In order to investigate the redox properties of PtGpx5, both parameters have been determined. The midpoint redox potential (E_m) of the catalytic disulfide was determined with DTT in various dithiol-disulfide ratios. After prolonged incubation, monobromobimane, a fluorescent thiol probe, can react with free thiol groups. Titration data were fitted by non-linear regression to the Nernst equation setting the value of n at 2, as expected for a disulfide/dithiol two-electron transfer process (Fig. 5A). Average E_m of three independent experiments was -286 ± 5mV at pH 7.0. Independently from consideration regarding substrate recognition, this Em value is clearly more adapted for a fast reduction by the more electronegative thioredoxin but not glutathione.

The pK_a of the thiol groups of Cys44 and Cys92 has been measured using a thiol-cleavable fluorophore, named PDT-bimane based on the fact that the thiolate, deprotonated form of cysteine only weakly reacts with this compound (41). From the plot of the $t1/2$ of half-maximal release of pyridyl-2-thiolate against pH, the pKa of Cys44 (Cys_P) is 5.23 ± 0.02 and the pKa of Cys92 (Cys_P) is 7.66 ± 0.09 (Fig. 5B).

Residues forming the catalytic tetrad in Gpx have been shown to be essential components for Gpx reactivity in particular by maintaining a low pKa value for Cys_P (16,20,22,27). Amino acid sequence comparisons indicate that, beyond Cys_P and among the three other residues, the one in position 79 of PtGpx5 or in equivalent position in other Gpxs is the most variable, most SeCys-Gpxs or Cys-Gpxs possess a Gln, whereas PtGpx5 has a Glu. Hence, we have explored whether this variation could influence protein reactivity by measuring first both the pKa of Cys_P and the redox potential of the catalytic disulfide in the E79Q variant. However, both parameters were not significantly altered with a pKa of Cys_P of 5.32 ± 0.06 and an E_m value of -281 ± 5 mV (Figs. 5A and B). Regarding peroxide reduction, the E79Q mutation only slightly affected the affinity and turnover number for H_2O_2 and COOH compared to the WT enzyme, whereas it had a dramatic effect on the apparent affinity for t-BOOH (Table 1). The decrease of the K_m value from 1.91 mM for Gpx5 WT to 58 µM for E79Q variant largely contributes to the increase of the catalytic activity for t-BOOH by a factor of 50 (147 x10^3 *vs* 3 x10^3 M^{-1} s^{-1}). Strikingly, in this variant, the K_m values toward the different peroxides are very close, being comprised between 54 to 58 µM. This suggests that Glu79 is important for peroxide recognition, maybe playing some role in determining substrate preference.

Unwinding of helix α2 is promoted by the oxidation of Cys_P

From the structural comparison of the reduced vs oxidized form of PtGpx5, a noticeable conformational change has been noted for the formation of the intramolecular

disulfide, consisting in the bowing of the loop that connects β1 and α1 (where Cys_P is located) by about 90% and the unwinding of the helix α2 (where Cys_R is located) (25). In addition, it has been proposed that this helix-coil transition could be linked to a helical instability conferred by the thiolate form of Cys_P and by two negatively charged residues (Asp85 and Asp89) located on the same face of three helical turns. We hypothesized that the mutation of one of these residues could block the unwinding of helix α2. However, the substitution of the Asp89 by a residue with an opposite charge (D89K variant) had no impact on the kinetic parameters, likely indicating that none of the different steps of the catalytic mechanism, in particular the formation of the disulfide, are appreciably affected (Table 1).

Next, to figure out whether the oxidation of Cys_P or the formation of the disulfide causes this structural rearrangement, the secondary structure content of PtGpx5 and some of the cysteinic mutants was analyzed using circular dichroism. Figure 6A shows the spectra of PtGpx5 WT either in the reduced or in the oxidized state. Although the α-helical and β-sheet contents deduced from these spectra do not correspond to the percentage obtained from the 3D structure, the strong modification of the spectrum for the oxidized form at 222 nm, confirmed the variation in α-helical content of PtGpx5 depending on its redox state (Fig. 6A). Recently, the same difficulties for correlating secondary structure content between CD spectra and 3D structure have been encountered for a glutathione peroxidase-like tryparedoxin peroxidase (42). Hence, since for unknown reasons the percentage of secondary structures cannot be determined accurately, only the qualitative aspects will be considered in these experiments. Similar experiments have been performed with the C73/92S and C44/73S variants (Figs. 6B and C). Whereas similar modifications have been obtained in the CD spectra of the C73/92S variant in the reduced or oxidized forms, there was no change in the variant retaining only Cys92 and where Cys44 is absent. These data clearly show that the unwinding of helix α2 is governed by the change of the redox state of the catalytic residue, presumably the formation of the sulfenic acid but not the formation of the intramolecular disulfide bridge.

Dimerization is not required for Gpx5 functioning

In either reduced or oxidized crystal structure of PtGpx5, Tyr151 is found at the interface between the two subunits of the dimer, in a position possibly contributing to its stabilization. Thus, in order to explore its role, a Y151R variant was produced and its oligomerization state evaluated by analytical gel filtration in comparison to the WT enzyme. The WT enzyme migrates as two different forms with differential abundance. The first one, representing about 5% of loaded proteins, exhibits a retention time of 46.64 min corresponding to an apparent mass of 95.2 kDa. The second one, representing 95% of loaded proteins, displays a retention time of 51.64 min corresponding to an apparent mass of 41.7 kDa. Hence, from the theoretical mass of 19.2 kDa, these results confirmed that Gpx5 is essentially in a dimeric form, while the minor form likely corresponds to a small fraction of tetramers. Contrary to PtGpx5 WT and to other variants tested, the majority (95%) of the Y151R variant elutes with a retention time (56.23 min) corresponding to a monomer, whereas a minor form (5%) still corresponds to a dimer. Regarding the kinetic parameters, this mutation altered the affinity and the catalytic efficiency for the reduction of COOH compared to WT Gpx5 (0.739 mM and 5 $M^{-1}.s^{-1}$ vs 0.081 mM and 7.8 $M^{-1}.s^{-1}$) and it also affected to a lesser extent the apparent affinity for *t*-BOOH (Table 1). On the other hand, no significant difference was observed between WT or Y151R proteins regarding kinetic parameters for H_2O_2 and the apparent affinity for Trxh1, with K_m values for the latter of 5.2 µM and 3.7 µM respectively. Overall, these data point out to two important properties of Gpx5, the dimeric form is not required for its interaction with Trxh1, but it might be important for the reduction of some complex or big peroxides such as those with an aromatic cycle.

Role of Phe90 and Cys92 in the interaction with Trx

From molecular docking experiments, we previously built two complex models for the interaction between Trxh1 and PtGpx5 with a transient intermolecular disulfide bond formed between the catalytic Cys39 of poplar Trxh1 and either Cys44 (Cys_P, complex1) or Cys92 (Cys_R, complex2) of the oxidized

PtGpx5 (25). Although both complexes were found structurally possible, complex 2 proved to be more stable from the calculated free energy. In addition, in both cases, the aromatic ring of Phe90 was found to interact perpendicularly with its edge pointing towards the Trp of the active site Trxh1 ($_{38}$WCPPC$_{42}$ active site). A F90E variant, substituting the aromatic side chain by a negatively charged residue has been constructed and analyzed. The apparent affinity of the F90E mutant for Trxh1 is substantially modified with a K_m value of 25.4 µM compared to the value of 5.2 µM obtained with PtGpx5 WT (Table 1). Besides, in order to identify which of Cys_P or Cys_R of PtGpx5 forms the transient disulfide with Cys39 of Trxh1, we have formed heterocomplexes between a Trxh1 C42S variant and oxidized PtGpx5 (Fig. 7). In order to separate the PtGpx5-Trxh1 adduct from the monomeric forms, the mixture was separated on non-reducing SDS-PAGE and the band corresponding to this adduct (present in lane xx in Fig. 7) was analyzed by mass spectrometry after in-gel digestion. The gel band was cut into small pieces (~ 1 mm size) and divided in two separate pools. One pool was first treated with DTT to reduce all disulfide bonds within the protein adduct followed by IAM treatment to block all Cys residues (carbamidomethylation), whereas the other pool was not treated with DTT but only IAM, meaning that only free Cys should be carbamidomethylated and Cys residues involved in the covalent adduct remain unaffected. The tryptic peptide of PtGpx5 containing Cys44 was present in the two samples, whereas the tryptic peptide of PtGpx5 containing Cys92 and the one of Trxh1 containing Cys39 were present only in the first sample. For reasons presumably related to peptide separation or detection, these two latter peptides supposed to be covalently linked in sample 2 were not detected. Hence, peptides extracted from this second pool and originally treated with IAM only, were further analyzed by mass spectrometry after treating them with DTT and again with IAA. In this case, both peptides absent in the non-reduced sample were now detected, confirming that the covalent adduct is formed between Cys39 of Trxh1 and Cys92 of PtGpx5. The peptide spectra with their corresponding sequences are shown in supplemental Fig. 3.

Discussion

Plant Cys-Gpxs belong to multigenic families (from 5 to 8 members in plants) and constitute, based on their reductant specificity, an additional class of thioredoxin peroxidase, although they have a primary and tertiary structure resembling glutathione-dependent Secys-Gpxs. Although PtGpx5 is predicted to be secreted, thus presumably residing in the apoplast, there are other predicted or confirmed paralogs in other subcellular compartments e.g. cytosol, plastids and mitochondria. In all these compartments, there are evidence for the presence of H_2O_2 and potentially for $ONOO^-$ taking into account the presence of superoxide anion and nitric oxide production sites and their possible diffusible. In this study, we have demonstrated using steady-state and pre-steady state activity measurement that PtGpx5 possesses catalytic efficiencies in the 10^6, 10^5, 10^4 and 10^3 M^{-1} s^{-1} range toward $ONOO^-$, H_2O_2, COOH and *t*-BOOH, respectively. To our knowledge, this is the first demonstration that Cys-Gpxs, and in particular plant isoforms, are competent for peroxynitrite reduction, constituting an alternative system to the previously described peroxynitrite reductase activity of the plastidial 2-Cys Prx and Prx IIE (12,13). The values of catalytic efficiency for the reduction of $ONOO^-$ and H_2O_2 are in the same range as those previously described for some Cys-Gpxs and Prxs (21,30,43,44). Finally, from the comparison of the activity measurements conducted in steady-state or pre-steady state conditions and because the change in fluorescence was linearly dependent on the oxidant concentration, we have learned that the Gpx oxidation but not Trx mediated recycling was rate limiting the process. In this respect, it seems to be different from methionine sulfoxide reductases, although the catalytic mechanisms between both protein families are similar (23).

Dimerization is important for organic peroxide reduction but is not essential

The dimeric organisation of PtGpx5 contrasts with the homotetrameric organisation of Secys-Gpxs (mammalian Gpx1, Gpx2, Gpx3) or the monomeric nature of mammalian Gpx4, *D. melanogaster* Gpx, yeast Orp1/Gpx3 and *Trypanosoma brucei* PxII and PxIII (21,22,45-47). It was previously proposed that

a monomeric state is required for the interaction with Trxs (21). The Trx-dependent recycling of the dimeric PtGpx5 indicates that this assumption is also valid for plant dimeric Cys-Gpxs. However, contrary to as *E. coli* Tpx for example, PtGpx5 is not an obligate homodimer since a monomeric Y151R variant exhibited the same affinity for Trxh1 as the WT enzyme (24). This variant has nevertheless an impaired activity specifically with the complex substrates presenting a benzene cycle (COOH) or ramified carbon chain (*t*-BOOH), but not H_2O_2, which could indicate that the native dimeric organisation of plant CysGpxs might be more essential for peroxide than for Trx recognition. Quite similarly, a single amino acid substitution affecting the decameric organisation of *Salmonella typhimurium* AhpC showed that the dimeric form is less efficient for peroxide reduction (48).

Reactivity of Cys_P and conservation of the catalytic tetrad between Secys- and Cys-Gpxs

The hallmark of most Secys- or Cys-Gpxs is the presence of the so-called catalytic tetrad formed by Cys44, Glu79, Trp133 and Asn134 (PtGpx5 numbering). These residues are thought to modulate Cys_P reactivity by stabilizing the deprotonated form of Cys_P thus decreasing its *pKa* and stabilizing the the transition state of the reaction (15,49). However, in some enzymes, their mutation does not abolish completely enzyme activity and in some 3D structures, they are not simply located in the active site (22,37,50,51). Instead, in *T. brucei* PxIII, three conserved Lys are important for substrate binding (peroxide or tryparedoxin) (50).

Except the replacement of the Gln by a Glu in PtGpx5 as well as in some specific plant orthologs, the residues forming the catalytic tetrad are conserved in plant Cys-Gpxs. In human Gpx4, the substitution of this Gln81 by a Glu drastically decreased the activity of a Gpx4 Secys to Cys variant by a factor 5 (46). Interestingly, the opposite substitution in PtGpx5 resulted in an increased catalytic efficiency from a factor 2 for H_2O_2 to a factor 50 for *t*-BOOH. This result is in agreement with computational predictions indicating that an acidic amino acid in the catalytic tetrad of Gpxs would decrease enzyme reactivity (15,16).

In the case of *t*-BOOH, the E79Q substitution enhances the apparent substrate affinity, decreasing the K_m by a factor 30, but it does modify both the midpoint redox potential and the *pKa* of Cys_P. This suggests that the nature of this residue is important for the accessibility of some organic hydroperoxides inside the active site pocket. Regarding the *pKa* value measured for Cys_P in PtGpx5 (5.23), it is in the range of those determined for other Tpxs such as *S. typhimurium* AhpC, yeast Tsa1 and Tsa2, *Xylella fastidiosa* PrxQβ or yeast Orp1/Gpx3 (20,30,43,44,52,53). However, it is worth mentioning that decreasing the *pKa* of the thiol group below 6.4, where 90 % of the enzyme would be deprotonated anyway, would not necessarily be a good idea, since thiolates with the lower *pKa* are less nucleophilic than others (49). Instead, the specialized and efficient peroxidase activity of Prxs is thought to be achieved through transition state stabilization.

The formation of the sulfenic acid is responsible of the PtGpx5 conformational rearrangement

It has been observed that the transition between the reduced and oxidized forms of several Prxs and of some Cys-Gpxs is accompanied by a helix to coil transition, with the partial or total unravelling of one or two α-helices in order to bring the two cysteines at the right distance for the formation of the disulfide bridge (24,25,43). In this respect, this is very similar to other enzymes using a cysteine-based catalytic mechanism such as methionine sulfoxide reductases and arsenate reductases (26,54). However, a number of crystal or NMR structures obtained for reduced or oxidized Cys-Gpxs does not apparently follow this statement. For example, the structure of oxidized and reduced *T. brucei* PxIII are very similar and there is no sign of structural rearrangement (50). Strikingly, the resolution of the 3D structure of *T. brucei* PxII, which is nearly identical to the PxIII isoform and of *T. cruzy* Gpx1, indicated that, in the reduced state, the cysteines are indeed very distant (45,51). These discrepancies have been tentatively explained by the structural plasticity required for these enzymes and by the fact that they can adopt multiple conformations that exchange on the µs-ms timescale.

In the case of PtGpx5, following an aerobic purification, the protein is found in an oxidized state and a reduced enzyme is very

rapidly re-oxidized without any oxidative treatment indicating that the enzyme is more stable in the oxidized state. However, an unresolved question in the case of PtGpx5 was to know whether the binding of the substrate is sufficient to promote the unwinding of the α2 helix, or whether the formation of the sulfenic acid is required. In the present analysis, we have demonstrated, using circular dichroism, that the oxidation of Cys_P triggered α2-helix unwinding. Indeed, a mutated variant, where only Cys_P (Cys44) remains, presents the same variation of the CD spectra observed for the reduced and oxidized WT enzyme, whereas a mutated protein where Cys_P is absent does not exhibit any variation in α-helical content. Similar findings were obtained for a bacterial PrxQ (43).

Recently, it was suggested, from the structural analysis of a C76S mutated version of *T. brucei* PxIII, that the conserved Cys (Cys76 in PxIII, Cys73 in PtGpx5) residue, which does not impact catalytic activity, might be important for the occurrence of these conformational changes (42). Indeed, in this mutant, no drastic conformational change seems to be required for Cys_P-Cys_R disulfide formation. However, in the case of PtGpx5, the C73S variant still exhibit redox-dependent conformational changes as assessed by gel shift migration and by its fluorescence properties (data not shown).

The Trx-dependent regeneration of Cys-Gpxs

Previous studies on the Tpx-Trx interaction showed that in the case of the Cys-Gpx from *D. melanogaster* and of *T. brucei* PxIII, an intermediate heterocomplex formed between the two partners involved the catalytic cysteine of Trx and Cys_R of Tpx (21,22). In contrast, in the case of poplar Prx II or *Mycobacterium tuberculosis* thioredoxin peroxidase, the transient complex involved also the catalytic cysteine of Trx but Cys_P of Tpx (55,56). Using a pre-reduced Trx mutated on the second active site cysteine, stable dead-end intermediates have been obtained by reaction with an oxidized PtGpx5. Mass spectrometry analysis of the heterocomplex indicated that, in the case of this plant Cys-Gpx, the disulfide is formed between Cys92 or Cys_R of PtGpx5 and the catalytic cysteine of Trxh1. Besides, the mutational analysis of Phe90 confirmed its implication for Trx recognition. This residue is conserved in most Cys-Gpxs but absent in glutathione-dependent Secys-Gpxs. Further structural studies of the heterocomplex would be necessary to precisely define the contact area between the two partners.

Physiological relevance of the sulfenic, sulfinic and sulfonic acid forms detected on poplar Gpx5

Besides their peroxidase activity, it has been shown that some thiol-peroxidases display peroxide signalling functions. This has been well illustrated recently by showing that yeast cells lacking the eight Tpxs (5 Prxs and 3 Cys-Gpxs) have lost their ability to regulate gene expression in response to H_2O_2 (57). For instance, the Tpx-dependent perception of peroxide by AP1 transcription factors in several yeast species has been very well documented. In *S. cerevisiae*, the detailed characterization of the Orp1/Gxp3-dependent activation of Yap1 or of the Ahp1-dependent activation of Cad1/Yap2 occurs through a redox relay consisting in the conversion of the sulfenic acid generated on these Tpxs from their reaction with H_2O_2 or peroxidized lipids respectively, into an intramolecular disulfide on AP1 transcription factors (20,58-60). In the case of Yap1, the formation of the disulfide is thought to mask the nuclear export signal thus promoting its nuclear activity (61). In *Schizosaccharomyces pombe,* a similar mechanism likely occurs for the Tpx1-dependent activation of Pap1 at low H_2O_2 levels (62). However, at higher peroxide concentration, the inactivation of Tpx1 by oxidation of its catalytic cysteine to a sulfinic acid prevents such redox relay (62). Whether this regulation occurs also for ScGpx3 is not known. In this context, the observation of irreversible cysteine oxidation forms on a plant Cys-Gpx could be physiologically relevant and could provide an additional potential mediator for H_2O_2 signalling pathways, although no similar AP1-dependent regulation mechanism has been described so far in plants. Instead, it has been shown that *A. thaliana* Gpx3, by physically interacting with a protein phosphatase 2C named ABI2 (ABA INSENSITIVE2), can regulate the redox state and thus the activity of ABI2, likely relaying the H_2O_2 signal coupled to the abscisic acid (ABA) signalling in response to drought stress (63).

A crucial point for such regulation, especially for Tpxs usually using a recycling cysteine in their catalytic mechanism, is the lifetime of the sulfenic acid moiety as it is usually considered as a short lived species. All enzymes implicated so far are of the 2-Cys Prx or Cys-Gpx type. Interestingly, the formation of the inter- or intramolecular disulfide bridge formed during the regeneration of these enzymes, is accompanied by a structural rearrangement in order to bring the two cysteines at the right distance for the formation of the disulfide bridge. Hence, the stability of the sulfenic acid in these proteins might certainly be explained, at least partly, by the rate of this step Incidentally, it is also likely responsible of the Cys_P overoxidation observed when H_2O_2 concentration increases (64). Alternatively, sulfenic acids can be stabilized by specific protein environment. The chemical trapping of the sulfenic acid intermediate in a WT Tpx has only been achieved recently for yeast Gpx3, supporting the view that the protein context is important and that not all Tpx could act as peroxide sensor (60).

Besides their peroxidase and redox sensor roles, Prxs also undergo a functional change upon overoxidation of their catalytic cysteines, e.g. they acquire a molecular chaperone activity subsequent to the formation of high molecular weight complexes. In plants, Tpx overoxidation has been observed both for 2-Cys Prx and 1-Cys Prx (40,65). Concerning the 2-Cys Prx, it has been shown that the redox state of the protein affected its subcellular localisation, with the reduced or overoxidized decameric forms being attached to the thylakoids and the oxidized dimeric form being released in the stroma for Trx reduction (40). Overall, all these observations support the view that the ability of Cys-Gpxs to adopt different redox states (reduced, oxidized or overoxidized) in response to different oxidative conditions could dramatically modify their biochemical properties and thus their physiological role and interaction network.

References

1. **Foyer, C.H. and Noctor, G. (2005) Redox homeostasis and antioxidant signaling: a metabolic interface between stress perception and physiological responses. *Plant Cell*, 17, 1866-1875.**
2. **Gupta, K.J., Fernie, A.R., Kaiser, W.M. and van Dongen, J.T. (2011) On the origins of nitric oxide. *Trends Plant Sci*, 16, 160-168.**
3. **Beckman, J.S., Beckman, T.W., Chen, J., Marshall, P.A. and Freeman, B.A. (1990) Apparent hydroxyl radical production by peroxynitrite: implications for endothelial injury from nitric oxide and superoxide. *Proc Natl Acad Sci U S A*, 87, 1620-1624.**
4. **Radi, R., Beckman, J.S., Bush, K.M. and Freeman, B.A. (1991) Peroxynitrite oxidation of sulfhydryls. The cytotoxic potential of superoxide and nitric oxide. *J Biol Chem*, 266, 4244-4250.**
5. **Apel, K. and Hirt, H. (2004) Reactive oxygen species: metabolism, oxidative stress, and signal transduction. *Annu Rev Plant Biol*, 55, 373-399.**
6. **Neill, S., Desikan, R. and Hancock, J. (2002) Hydrogen peroxide signalling. *Curr Opin Plant Biol*, 5, 388-395.**
7. **Pacher, P., Beckman, J.S. and Liaudet, L. (2007) Nitric oxide and peroxynitrite in health and disease. *Physiol Rev*, 87, 315-424.**
8. **Peluffo, G., Calcerrada, P., Piacenza, L., Pizzano, N. and Radi, R. (2009) Superoxide-mediated inactivation of nitric oxide and peroxynitrite formation by tobacco smoke in vascular endothelium: studies in cultured cells and smokers. *Am J Physiol Heart Circ Physiol*, 296, H1781-1792.**
9. **Rouhier, N., Koh, C.S., Gelhaye, E., Corbier, C., Favier, F., Didierjean, C. and Jacquot, J.P. (2008) Redox based anti-oxidant systems in plants: biochemical and structural analyses. *Biochim Biophys Acta*, 1780, 1249-1260.**
10. **Trujillo, M., Ferrer-Sueta, G. and Radi, R. (2008) Peroxynitrite detoxification and its biologic implications. *Antioxid Redox Signal*, 10, 1607-1620.**
11. **Rouhier, N. and Jacquot, J.P. (2002) Plant peroxiredoxins: alternative hydroperoxide scavenging enzymes. *Photosynth Res*, 74, 259-268.**
12. **Romero-Puertas, M.C., Laxa, M., Matte, A., Zaninotto, F., Finkemeier, I., Jones, A.M., Perazzolli, M., Vandelle, E., Dietz, K.J. and Delledonne, M. (2007) S-nitrosylation of peroxiredoxin II E promotes peroxynitrite-mediated tyrosine nitration. *Plant Cell*, 19, 4120-4130.**
13. **Sakamoto, A., Tsukamoto, S., Yamamoto, H., Ueda-Hashimoto, M., Takahashi, M., Suzuki, H. and Morikawa, H. (2003) Functional complementation in yeast reveals a protective role of chloroplast 2-Cys peroxiredoxin against reactive nitrogen species. *Plant J*, 33, 841-851.**
14. **Rouhier, N. and Jacquot, J.P. (2005) The plant multigenic family of thiol peroxidases. *Free Radic Biol Med*, 38, 1413-1421.**
15. **Flohe, L., Toppo, S., Cozza, G. and Ursini, F. (2010) A Comparison of Thiol Peroxidase Mechanisms. *Antioxid Redox Signal*.**
16. **Tosatto, S.C., Bosello, V., Fogolari, F., Mauri, P., Roveri, A., Toppo, S., Flohe, L., Ursini, F. and Maiorino, M. (2008) The catalytic site of glutathione peroxidases. *Antioxid Redox Signal*, 10, 1515-1526.**
17. **Herbette, S., Lenne, C., Leblanc, N., Julien, J.L., Drevet, J.R. and Roeckel-Drevet, P. (2002) Two GPX-like proteins from Lycopersicon esculentum and Helianthus annuus are antioxidant enzymes with phospholipid hydroperoxide**

glutathione peroxidase and thioredoxin peroxidase activities. *Eur J Biochem*, 269, 2414-2420.

18. **Navrot, N., Collin, V., Gualberto, J., Gelhaye, E., Hirasawa, M., Rey, P., Knaff, D.B., Issakidis, E., Jacquot, J.P. and Rouhier, N. (2006) Plant glutathione peroxidases are functional peroxiredoxins distributed in several subcellular compartments and regulated during biotic and abiotic stresses. *Plant Physiol*, 142, 1364-1379.**
19. **Tanaka, T., Izawa, S. and Inoue, Y. (2005) GPX2, encoding a phospholipid hydroperoxide glutathione peroxidase homologue, codes for an atypical 2-Cys peroxiredoxin in Saccharomyces cerevisiae. *J Biol Chem*, 280, 42078-42087.**
20. **Ma, L.H., Takanishi, C.L. and Wood, M.J. (2007) Molecular mechanism of oxidative stress perception by the Orp1 protein. *J Biol Chem*, 282, 31429-31436.**
21. **Maiorino, M., Ursini, F., Bosello, V., Toppo, S., Tosatto, S.C., Mauri, P., Becker, K., Roveri, A., Bulato, C., Benazzi, L. *et al.* (2007) The thioredoxin specificity of Drosophila GPx: a paradigm for a peroxiredoxin-like mechanism of many glutathione peroxidases. *J Mol Biol*, 365, 1033-1046.**
22. **Schlecker, T., Comini, M.A., Melchers, J., Ruppert, T. and Krauth-Siegel, R.L. (2007) Catalytic mechanism of the glutathione peroxidase-type tryparedoxin peroxidase of Trypanosoma brucei. *Biochem J*, 405, 445-454.**
23. **Boschi-Muller, S., Gand, A. and Branlant, G. (2008) The methionine sulfoxide reductases: Catalysis and substrate specificities. *Arch Biochem Biophys*, 474, 266-273.**
24. **Hall, A., Sankaran, B., Poole, L.B. and Karplus, P.A. (2009) Structural changes common to catalysis in the Tpx peroxiredoxin subfamily. *J Mol Biol*, 393, 867-881.**
25. **Koh, C.S., Didierjean, C., Navrot, N., Panjikar, S., Mulliert, G., Rouhier, N., Jacquot, J.P., Aubry, A., Shawkataly, O. and Corbier, C. (2007) Crystal structures of a poplar thioredoxin peroxidase that exhibits the structure of glutathione peroxidases: insights into redox-driven conformational changes. *J Mol Biol*, 370, 512-529.**
26. **Rouhier, N., Kauffmann, B., Tete-Favier, F., Palladino, P., Gans, P., Branlant, G., Jacquot, J.P. and Boschi-Muller, S. (2007) Functional and structural aspects of poplar cytosolic and plastidial type a methionine sulfoxide reductases. *J Biol Chem*, 282, 3367-3378.**
27. **Maiorino, M., Aumann, K.D., Brigelius-Flohe, R., Doria, D., van den Heuvel, J., McCarthy, J., Roveri, A., Ursini, F. and Flohe, L. (1995) Probing the presumed catalytic triad of selenium-containing peroxidases by mutational analysis of phospholipid hydroperoxide glutathione peroxidase (PHGPx). *Biol Chem Hoppe Seyler*, 376, 651-660.**
28. **Claiborne, A., Miller, H., Parsonage, D. and Ross, R.P. (1993) Protein-sulfenic acid stabilization and function in enzyme catalysis and gene regulation. *FASEB J*, 7, 1483-1490.**
29. **Schonbaum, G.R. and Lo, S. (1972) Interaction of peroxidases with aromatic peracids and alkyl peroxides. Product analysis. *J Biol Chem*, 247, 3353-3360.**
30. **Ogusucu, R., Rettori, D., Munhoz, D.C., Netto, L.E. and Augusto, O. (2007) Reactions of yeast thioredoxin peroxidases I and II with hydrogen peroxide and peroxynitrite: rate constants by competitive kinetics. *Free Radic Biol Med*, 42, 326-334.**

31. Dolman, D., Newell, G.A. and Thurlow, M.D. (1975) A kinetic study of the reaction of horseradish peroxidase with hydrogen peroxide. *Can J Biochem*, 53, 495-501.
32. Hayashi, Y. and Yamazaki, I. (1979) The oxidation-reduction potentials of compound I/compound II and compound II/ferric couples of horseradish peroxidases A2 and C. *J Biol Chem*, 254, 9101-9106.
33. Trujillo, M., Ferrer-Sueta, G. and Radi, R. (2008) Kinetic studies on peroxynitrite reduction by peroxiredoxins. *Methods Enzymol*, 441, 173-196.
34. Girardet, J.M., Saulnier, F., Gaillard, J.L., Ramet, J.P. and Humbert, G. (2000) Camel (camelus dromedarius) milk PP3: evidence for an insertion in the amino-terminal sequence of the camel milk whey protein. *Biochem Cell Biol*, 78, 19-26.
35. Srivastava, V., Srivastava, M.K., Chibani, K., Nilsson, R., Rouhier, N., Melzer, M. and Wingsle, G. (2009) Alternative splicing studies of the reactive oxygen species gene network in Populus reveal two isoforms of high-isoelectric-point superoxide dismutase. *Plant Physiol*, 149, 1848-1859.
36. Bylesjo, M., Nilsson, R., Srivastava, V., Gronlund, A., Johansson, A.I., Jansson, S., Karlsson, J., Moritz, T., Wingsle, G. and Trygg, J. (2009) Integrated analysis of transcript, protein and metabolite data to study lignin biosynthesis in hybrid aspen. *J Proteome Res*, 8, 199-210.
37. Jung, B.G., Lee, K.O., Lee, S.S., Chi, Y.H., Jang, H.H., Kang, S.S., Lee, K., Lim, D., Yoon, S.C., Yun, D.J. *et al.* (2002) A Chinese cabbage cDNA with high sequence identity to phospholipid hydroperoxide glutathione peroxidases encodes a novel isoform of thioredoxin-dependent peroxidase. *J Biol Chem*, 277, 12572-12578.
38. Fischer, B.B., Dayer, R., Schwarzenbach, Y., Lemaire, S.D., Behra, R., Liedtke, A. and Eggen, R.I. (2009) Function and regulation of the glutathione peroxidase homologous gene GPXH/GPX5 in Chlamydomonas reinhardtii. *Plant Mol Biol*, 71, 569-583.
39. Floris, R., Piersma, S.R., Yang, G., Jones, P. and Wever, R. (1993) Interaction of myeloperoxidase with peroxynitrite. A comparison with lactoperoxidase, horseradish peroxidase and catalase. *Eur J Biochem*, 215, 767-775.
40. Konig, J., Lotte, K., Plessow, R., Brockhinke, A., Baier, M. and Dietz, K.J. (2003) Reaction mechanism of plant 2-Cys peroxiredoxin. Role of the C terminus and the quaternary structure. *J Biol Chem*, 278, 24409-24420.
41. Mansoor, S.E. and Farrens, D.L. (2004) High-throughput protein structural analysis using site-directed fluorescence labeling and the bimane derivative (2-pyridyl)dithiobimane. *Biochemistry*, 43, 9426-9438.
42. Muhle-Goll, C., Fuller, F., Ulrich, A.S. and Krauth-Siegel, R.L. (2010) The conserved Cys76 plays a crucial role for the conformation of reduced glutathione peroxidase-type tryparedoxin peroxidase. *FEBS Lett*, 584, 1027-1032.
43. Horta, B.B., de Oliveira, M.A., Discola, K.F., Cussiol, J.R. and Netto, L.E. (2010) Structural and biochemical characterization of peroxiredoxin Qbeta from Xylella fastidiosa: catalytic mechanism and high reactivity. *J Biol Chem*, 285, 16051-16065.
44. Trujillo, M., Clippe, A., Manta, B., Ferrer-Sueta, G., Smeets, A., Declercq, J.P., Knoops, B. and Radi, R. (2007) Pre-steady state kinetic characterization of human peroxiredoxin 5: taking advantage of Trp84 fluorescence increase upon oxidation. *Arch Biochem Biophys*, 467, 95-106.

45. **Alphey, M.S., Konig, J. and Fairlamb, A.H. (2008) Structural and mechanistic insights into type II trypanosomatid tryparedoxin-dependent peroxidases. *Biochem J*, 414, 375-381.**
46. **Scheerer, P., Borchert, A., Krauss, N., Wessner, H., Gerth, C., Hohne, W. and Kuhn, H. (2007) Structural basis for catalytic activity and enzyme polymerization of phospholipid hydroperoxide glutathione peroxidase-4 (GPx4). *Biochemistry*, 46, 9041-9049.**
47. **Zhang, W.J., He, Y.X., Yang, Z., Yu, J., Chen, Y. and Zhou, C.Z. (2008) Crystal structure of glutathione-dependent phospholipid peroxidase Hyr1 from the yeast Saccharomyces cerevisiae. *Proteins*, 73, 1058-1062.**
48. **Parsonage, D., Youngblood, D.S., Sarma, G.N., Wood, Z.A., Karplus, P.A. and Poole, L.B. (2005) Analysis of the link between enzymatic activity and oligomeric state in AhpC, a bacterial peroxiredoxin. *Biochemistry*, 44, 10583-10592.**
49. **Ferrer-Sueta, G., Manta, B., Botti, H., Radi, R., Trujillo, M. and Denicola, A. (2010) Factors Affecting Protein Thiol Reactivity and Specificity in Peroxide Reduction. *Chem Res Toxicol*.**
50. **Melchers, J., Diechtierow, M., Feher, K., Sinning, I., Tews, I., Krauth-Siegel, R.L. and Muhle-Goll, C. (2008) Structural basis for a distinct catalytic mechanism in Trypanosoma brucei tryparedoxin peroxidase. *J Biol Chem*, 283, 30401-30411.**
51. **Patel, S., Hussain, S., Harris, R., Sardiwal, S., Kelly, J.M., Wilkinson, S.R., Driscoll, P.C. and Djordjevic, S. (2010) Structural insights into the catalytic mechanism of Trypanosoma cruzi GPXI (glutathione peroxidase-like enzyme I). *Biochem J*, 425, 513-522.**
52. **Bryk, R., Griffin, P. and Nathan, C. (2000) Peroxynitrite reductase activity of bacterial peroxiredoxins. *Nature*, 407, 211-215.**
53. **Nelson, K.J., Parsonage, D., Hall, A., Karplus, P.A. and Poole, L.B. (2008) Cysteine pK(a) values for the bacterial peroxiredoxin AhpC. *Biochemistry*, 47, 12860-12868.**
54. **Messens, J. and Silver, S. (2006) Arsenate reduction: thiol cascade chemistry with convergent evolution. *J Mol Biol*, 362, 1-17.**
55. **Rouhier, N., Gelhaye, E. and Jacquot, J.P. (2002) Glutaredoxin-dependent peroxiredoxin from poplar: protein-protein interaction and catalytic mechanism. *J Biol Chem*, 277, 13609-13614.**
56. **Trujillo, M., Mauri, P., Benazzi, L., Comini, M., De Palma, A., Flohe, L., Radi, R., Stehr, M., Singh, M., Ursini, F. *et al.* (2006) The mycobacterial thioredoxin peroxidase can act as a one-cysteine peroxiredoxin. *J Biol Chem*, 281, 20555-20566.**
57. **Fomenko, D.E., Koc, A., Agisheva, N., Jacobsen, M., Kaya, A., Malinouski, M., Rutherford, J.C., Siu, K.L., Jin, D.Y., Winge, D.R. *et al.* (2011) Thiol peroxidases mediate specific genome-wide regulation of gene expression in response to hydrogen peroxide. *Proc Natl Acad Sci U S A*, 108, 2729-2734.**
58. **Delaunay, A., Pflieger, D., Barrault, M.B., Vinh, J. and Toledano, M.B. (2002) A thiol peroxidase is an H2O2 receptor and redox-transducer in gene activation. *Cell*, 111, 471-481.**
59. **Iwai, K., Naganuma, A. and Kuge, S. (2010) Peroxiredoxin Ahp1 acts as a receptor for alkylhydroperoxides to induce disulfide bond formation in the Cad1 transcription factor. *J Biol Chem*, 285, 10597-10604.**
60. **Paulsen, C.E. and Carroll, K.S. (2009) Chemical dissection of an essential redox switch in yeast. *Chem Biol*, 16, 217-225.**

61. Wood, M.J., Storz, G. and Tjandra, N. (2004) Structural basis for redox regulation of Yap1 transcription factor localization. ***Nature*****, 430, 917-921.**

62. Vivancos, A.P., Castillo, E.A., Biteau, B., Nicot, C., Ayte, J., Toledano, M.B. and Hidalgo, E. (2005) A cysteine-sulfinic acid in peroxiredoxin regulates H2O2-sensing by the antioxidant Pap1 pathway. ***Proc Natl Acad Sci U S A*****, 102, 8875-8880.**

63. Miao, Y., Lv, D., Wang, P., Wang, X.C., Chen, J., Miao, C. and Song, C.P. (2006) An Arabidopsis glutathione peroxidase functions as both a redox transducer and a scavenger in abscisic acid and drought stress responses. ***Plant Cell*****, 18, 2749-2766.**

64. Wood, Z.A., Poole, L.B. and Karplus, P.A. (2003) Peroxiredoxin evolution and the regulation of hydrogen peroxide signaling. ***Science*****, 300, 650-653.**

65. Pulido, P., Cazalis, R. and Cejudo, F.J. (2009) An antioxidant redox system in the nucleus of wheat seed cells suffering oxidative stress. ***Plant J*****, 57, 132-145.**

Footnotes/ Acknowledgements

Abbreviations

GSH, reduced glutathione; Trx, thioredoxin.

Keywords : glutathione peroxidase, overoxidation, peroxynitrite, redox properties, site-directed mutagenesis, thiol peroxidase

Figure legends

Figure 1. Kinetics of reaction of PtGpx5 with H_2O_2, GSH and PtTrxh1.
(A) Reduced PtGPx5 (2 µM) was rapidly mixed with different concentrations of H_2O_2, time courses of total fluorescence intensity changes (λ_{ex} = 295 nm) were fitted to exponential curves and observed rate constants of fluorescence change thus obtained were plotted versus oxidant concentrations. The inset shows the time course of fluorescence change observed by mixing H_2O_2 (80 µM) with wild type enzyme (PtGPx5 wt, 2 µM) or H_2O_2 (100 µM) with the enzyme mutated at the peroxidatic cysteine residue (PtGPx5 C44S, 2 µM). (B) Oxidized PtGPx5 (2 µM) was mixed with different GSH concentrations in excess and the time courses of total fluorescence intensity decrease were fitted to exponentials. Observed rate constants of the process were plotted versus GSH concentration. (C and D) Oxidized PtGPx5 (1 µM) was mixed with different reduced PtTrxh1 (C) or PtTrxh5 (D) concentrations in excess and time courses of total fluorescence intensity decrease were fitted to exponentials. Observed rate constants of fluorescence change were plotted versus thioredoxin concentration.

Figure 2. Kinetics of ONOOH reduction by PtGpx5.
Peroxynitrite (1.2 µM) in NaOH 10 mM was rapidly mixed with HRP (5 µM) in the absence or presence of increasing concentrations of reduced PtGPx5 in sodium phosphate buffer 100 mM pH 7 plus 0.1 mM dtpa. Final pH measured at the outlet was 7.4 ± 0.1. The time courses of HRP-compound I formation were followed at the Soret band. The inset shows the experimental traces corresponding to HRP-compound I formation without PtGPx5 (control) and with 7.3 µM reduced PtGPx5. Experimental data were fitted to exponentials from which observed rate constants of HRP-compound I formation were determined. The latter were plotted versus PtGPx5 concentrations.

Figure 3. Inhibition of the peroxidase activity of PtGpx5 by increasing H_2O_2 concentration
The peroxidase activity of PtGpx5 was measured under steady-state conditions using the Trx reduction system by measuring the rate of NAPDH oxidation between 30 seconds and 1 minute after addition of thiol peroxidases. Results are represented as a percentage of the maximal activity (100%) obtained at 50µM H_2O_2 for At2-Cys Prx and at 500µM H_2O_2 for PtGpx5.

Figure 4. Oxidation state of Cys_P and Cys_R in response to an H_2O_2 treatment
UV/visible absorption spectra of PtGpx5 C73/92S (A) and C44/73S (B) treated or not with various H_2O_2 concentrations during 1 minute and reacted with NBD-Cl.

Figure 5. Redox properties of PtGpx5
A. Determination of the midpoint redox potential (E_m) of the catalytic disulfide in Gpx5 WT (black circle) and in E79Q variant (black triangles).
The titration was carried out using DTT_{red}/DTT_{ox} as redox couple reference with a total DTT concentration of 2 mM and with a redox equilibration time of 2 h. Free protein thiols are labeled by mBBr. Values are the means ± SD of three replicates.
B. Determination of the pKa of the peroxidatic (Cys_P) and resolving (Cys_R) cysteines of Gpx5.
Reaction of PtGpx5 C44/73S (black squares), C73/92S (black circles) or C73/C92S/E79Q (grey circles) with PDT-Bimane was monitored at 343 nm at pH values ranging from 3.0 to 8.0. Each curve was fitted to an exponential and $T_{1/2}$ (time for half reaction) plotted as a function of pH were fitted to a sigmoidal curve. From this plot, sulfhydryl pK_a values of 5.23±0.02 and 5.32±0.06 were determined for Cys44 in the PtGpx5 C73/92S or C73/C92S/E79Q variant respectively and a value of 7.68±0.09 for Cys92 in the PtGpx5 C44/73S variant.

Figure 6. Redox-dependent conformational changes
Circular dichroism (CD) was used to evaluate the variations in α-helix content in PtGpx5 WT (A), C73/92S (B) or C44/73S (C). Spectra were recorded in 10 mM phosphate buffer pH 7.1 with 25 µM protein either reduced by 150 µM of DTT (dotted lines) or oxidized by 75 µM H_2O_2 (continuous lines).

Figure 7. SDS-PAGE showing heterodimer formation between PtGpx5 and Trxh1 C42S.
Lanes 1 and 4: Trxh1 C42S, lanes 2 and 5: PtGpx5 and lanes 3 and 6: mixture of oxidized PtGpx5 and Trxh1 C42S. Lanes 1 to 3 correspond to reducing conditions and 4 to 6 to non reducing conditions. The monomers and heterodimer are indicated by arrows.

	H_2O_2			*t*-BOOH			COOH			Trxh1
	K_m (µM)	k_{cat} (s^{-1})	k_{cat}/K_m ($M^{-1}.s^{-1}x10^4$)	K_m (mM)	k_{cat} (s^{-1})	k_{cat}/K_m ($M^{-1}.s^{-1}x10^4$)	K_m (µM)	k_{cat} (s^{-1})	k_{cat}/K_m ($M^{-1}.s^{-1}x10^4$)	K_m (µM)
PtGpx3[a]	545	11	2	1.41	9.1	0.64	239	13	5.3	12
CrGpxH[a]	54 ± 5	7.4 ± 0.2	13.7 ± 0.49	0.73 ± 0.11	11.3 ± 0.7	1.6 ± 0.6	63 ± 11	8.9 ± 0.4	14.1 ± 3.3	-
PtGpx5	32 ± 0.12	4 ± 0.13	13.3 ± 0.6	1.91 ± 0.2	6 ± 0.86	0.3 ± 0.03	81 ± 19	6 ± 0.3	7.8 ± 1.4	5.2 ± 0.7
PtGpx5 E79Q	56 ± 0.9	13 ± 2.4	24.0 ± 1.4	0.058 ± 0.007	9 ± 1.5	14.7 ± 3.7	54 ± 6	14 ± 3.8	26.9 ± 5.1	3.9 ± 2.6
PtGpx5 D89K	80 ± 2.5	9 ± 0.9	11.7 ± 2.4	4.383 ± 1.8	9 ± 2.3	0.2 ± 0.06	95 ± 17	5 ± 1.2	5.5 ± 0.57	4.2 ± 1.1
PtGpx5 Y151R	18 ± 0.5	5 ± 0.01	24.9 ± 0.81	7.366 ± 1.44	6 ± 2.8	0.08 ± 0.006	739 ± 24	4 ± 0.52	0.5 ± 0.08	3.7 ± 0.5
PtGpx5 F90E	60 ± 6.8	8 ± 1.4	13.4 ± 2.04	4.78 ± 1.4	5 ± 0.6	0.1 ± 0.05	60 ± 2.3	6 ± 0.03	9.9 ± 0.33	25.4 ± 2.8

Table 1. Steady-state kinetic parameters of mutated or WT PtGpx5 and comparison with PtGpx3 and CrGpxH.
Values for the different peroxides were obtained using poplar Trxh1 as electron donor and as described in the experimental procedures. [a]Values for PtGpx3 and CrGpxH have been extracted from (18,38).

Supplemental figures

Figure 1. Kinetics of H_2O_2-mediated PtGpx5 oxidation by a competition approach
The time course of HRP-compound I formation by reaction of H_2O_2 (0.65 μM) with HRP (5 μM) in the absence (black trace) or presence of reduced PtGpx5 (28.5 μM)(red trace), in sodium phosphate buffer 100 mM plus 0.1 mM DTPA, pH 7.4 and 25 ºC was followed at the Soret band.

Figure 2. Rapid reduction of peroxynitrite by reduced PtGpx5
Peroxynitrite (20 μM) in NaOH 10 mM was rapidly mixed with none (black line, control), reduced PtGpx5 (10 μM))(red line, $_{red}$PtGpx5) or with alkylated PtGpx5 (10 μM)(blue line, PtGpx5-NEM) in sodium phosphate buffer 100 mM plus 0.1 mM DTPA pH 7.0 and 25 ºC and peroxynitrite decay was measured at 310 nm. Final pH measured at the outlet was 7.4 ± 0.1.

Figure 3. Mass spectrometry analysis of trypsin digested heterodimers
Peptide spectra containing the cysteine residues of PtGpx5 after the following treatments: **A.** Protein pool treated with DTT and IAM. B. Protein pool treated with IAM only. C. Protein pool initially treated by IAM only was further treated with DTT and IAM.

A

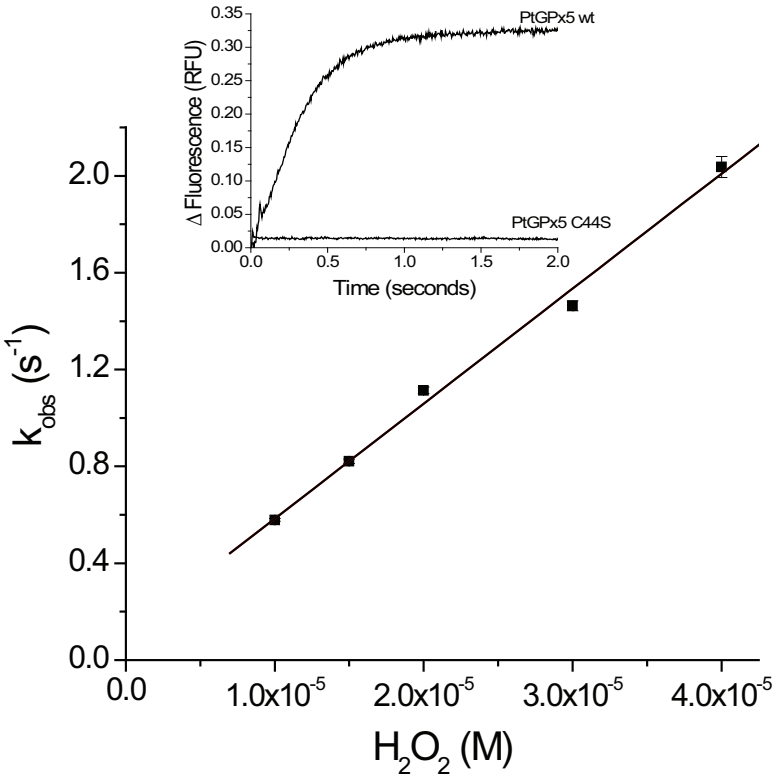

B

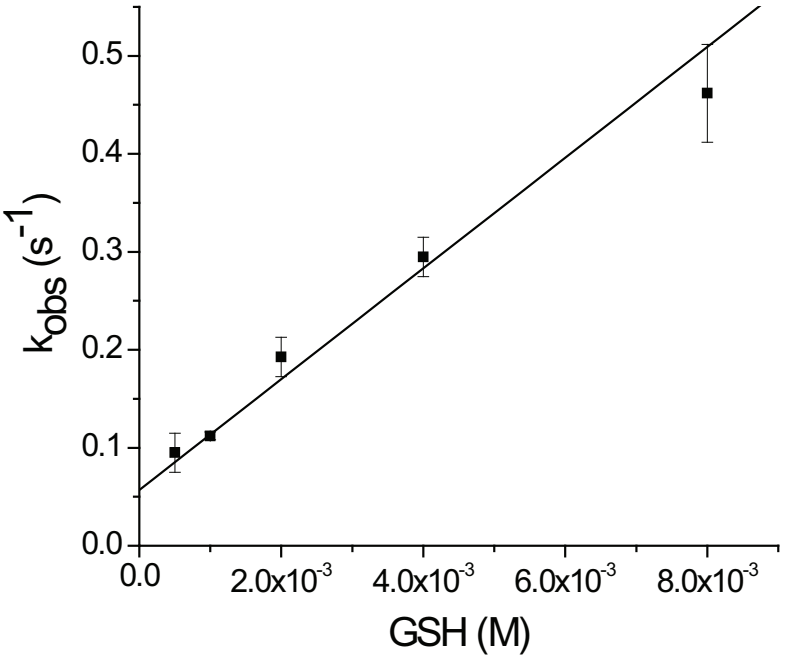

Figure 1A & B

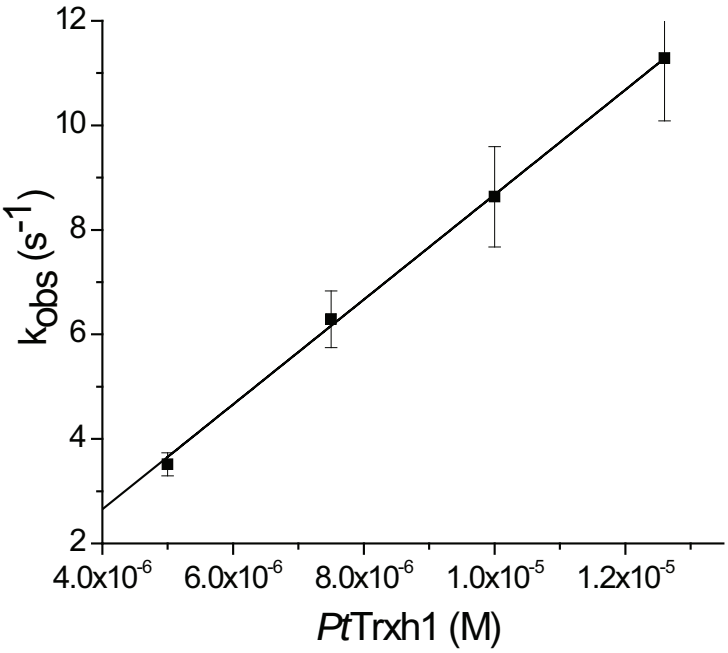

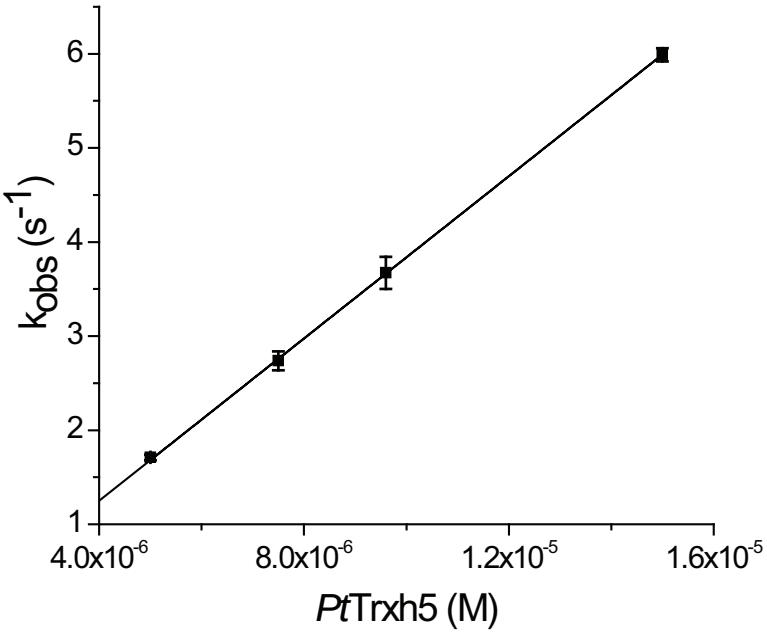

Figure 1C and D

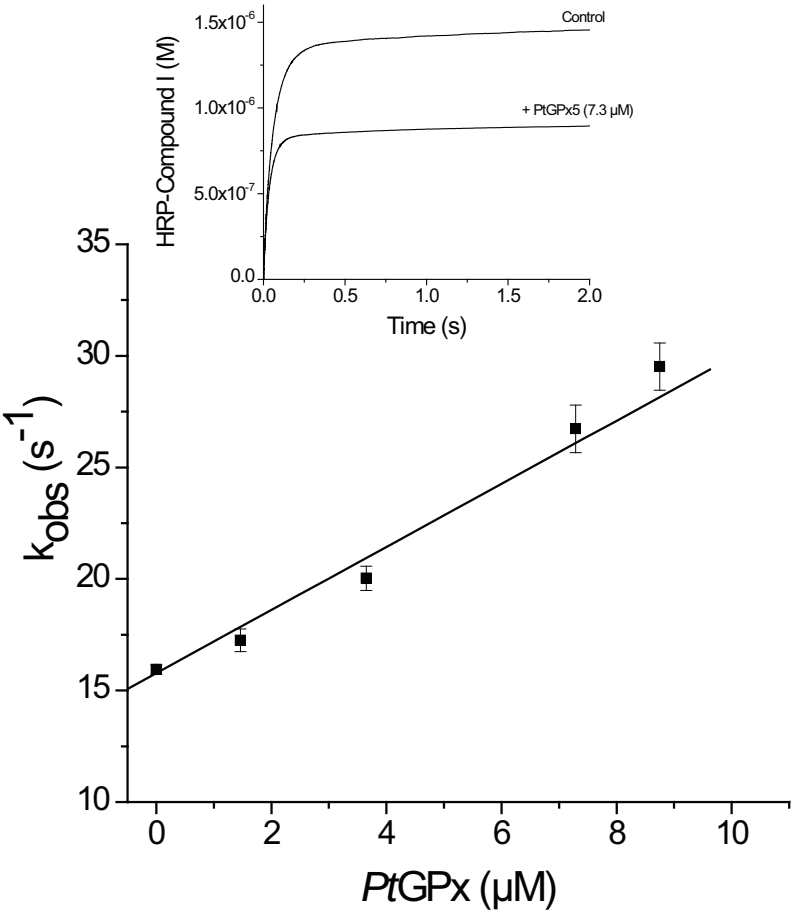
HRP-Compound I (M)
1.5x10-6
1.0x10-6
5.0x10-7
0.0
Control
+ PtGPx5 (7.3 µM)
0.0
0.5
1.0
1.5
2.0
Time (s)
kobs (s-1)
35
30
25
20
15
10
0
2
4
6
8
10
PtGPx (µM)

Figure 2

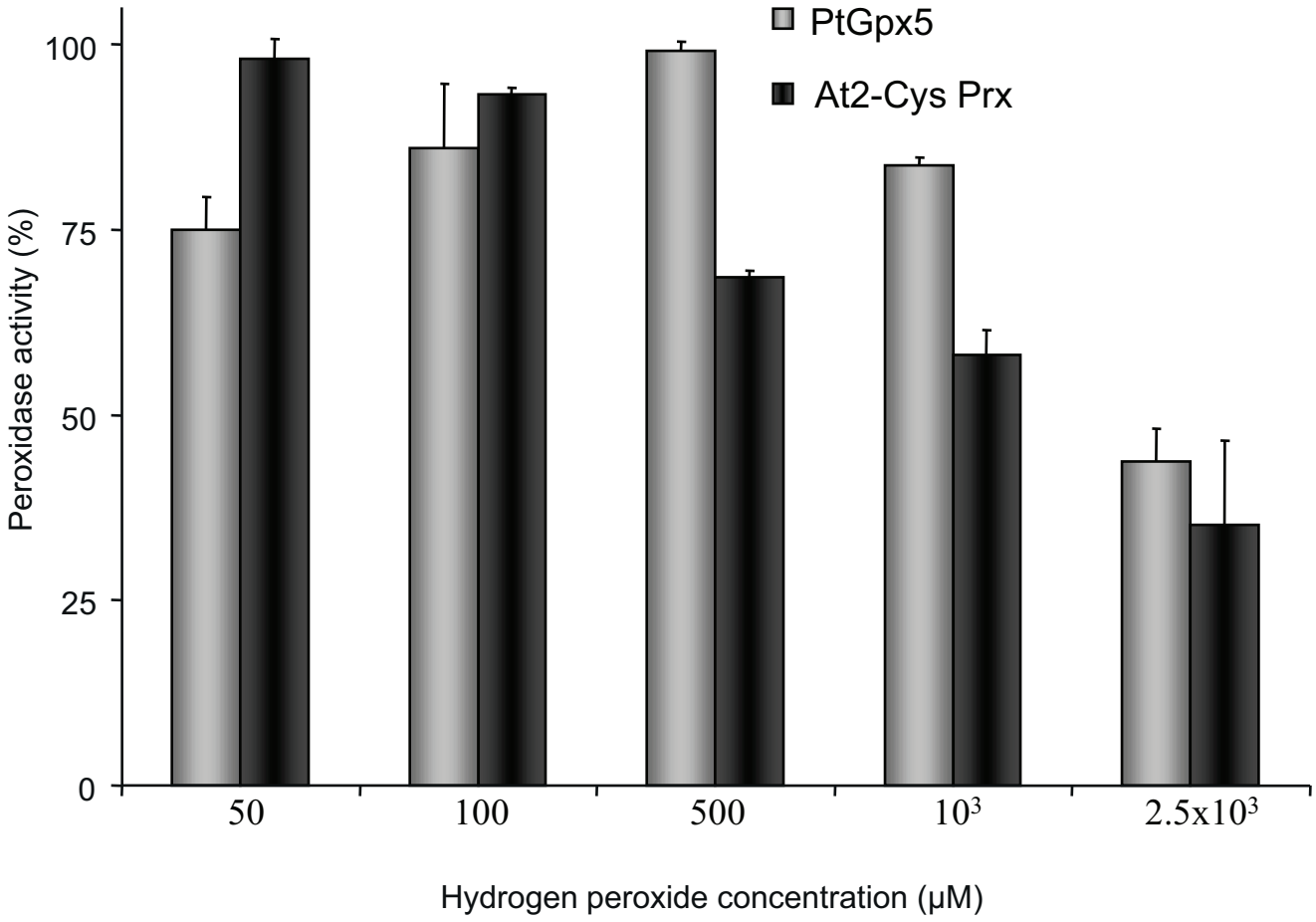
PtGpx5
At2-Cys Prx
Peroxidase activity (%)
100
75
50
25
0
50
100
500
10³
2.5x10³
Hydrogen peroxide concentration (µM)

Figure 3

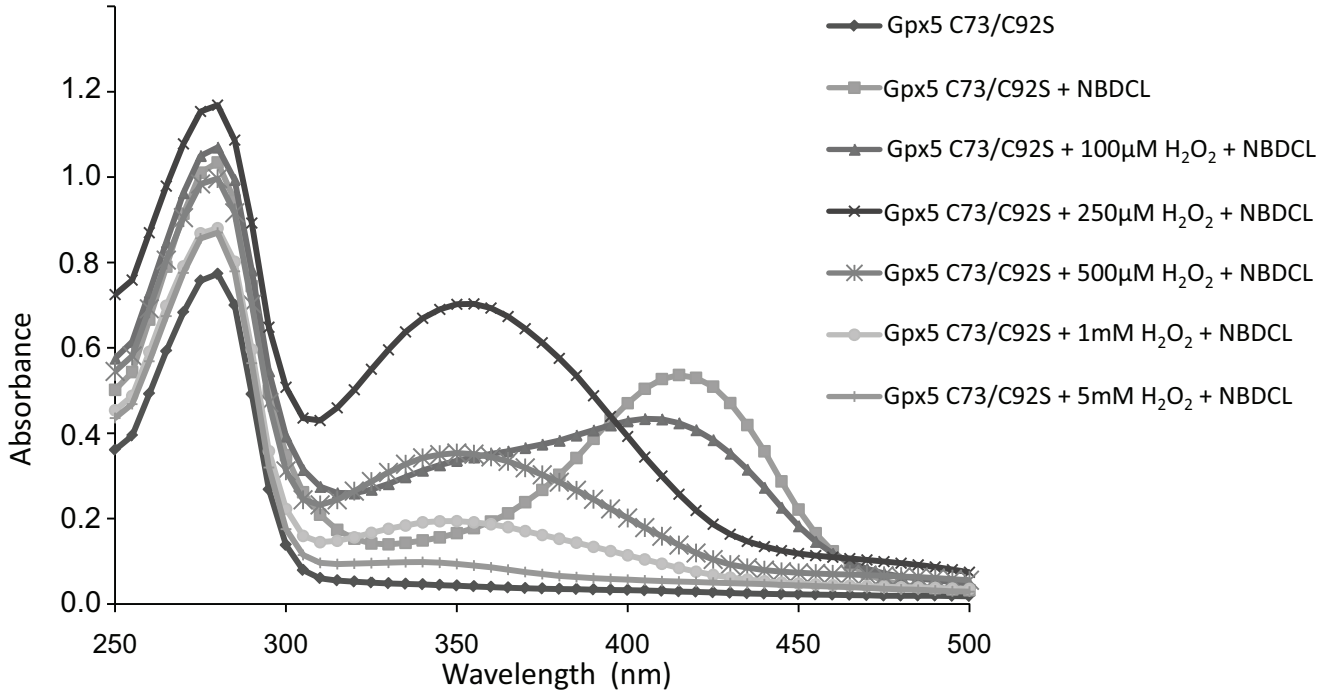
Gpx5 C73/C92S
Gpx5 C73/C92S + NBDCL
Gpx5 C73/C92S + 100µM H_2O_2 + NBDCL
Gpx5 C73/C92S + 250µM H_2O_2 + NBDCL
Gpx5 C73/C92S + 500µM H_2O_2 + NBDCL
Gpx5 C73/C92S + 1mM H_2O_2 + NBDCL
Gpx5 C73/C92S + 5mM H_2O_2 + NBDCL
Absorbance
Wavelength (nm)

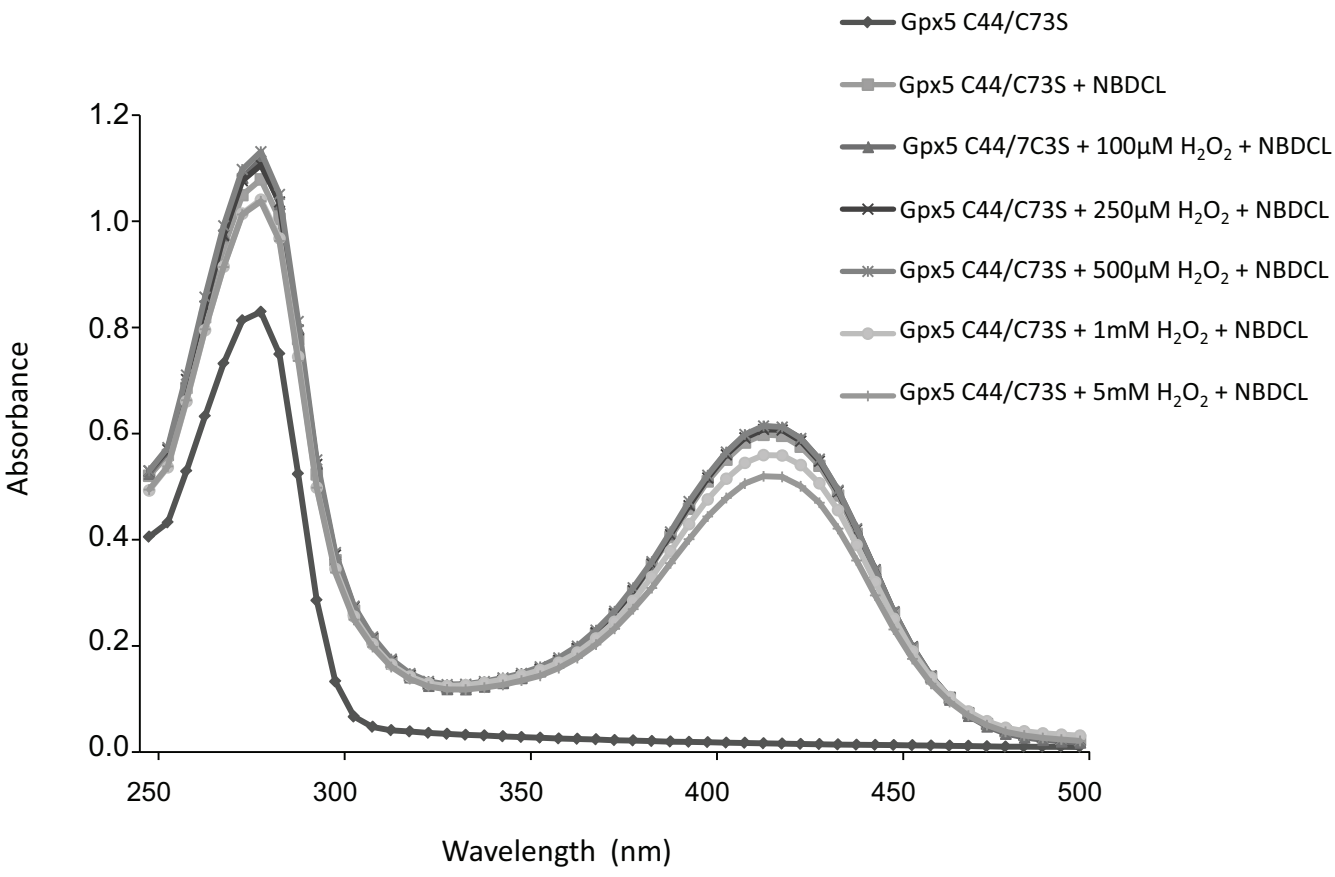
Gpx5 C44/C73S
Gpx5 C44/C73S + NBDCL
Gpx5 C44/7C3S + 100µM H_2O_2 + NBDCL
Gpx5 C44/C73S + 250µM H_2O_2 + NBDCL
Gpx5 C44/C73S + 500µM H_2O_2 + NBDCL
Gpx5 C44/C73S + 1mM H_2O_2 + NBDCL
Gpx5 C44/C73S + 5mM H_2O_2 + NBDCL
Absorbance
Wavelength (nm)

Figure 4

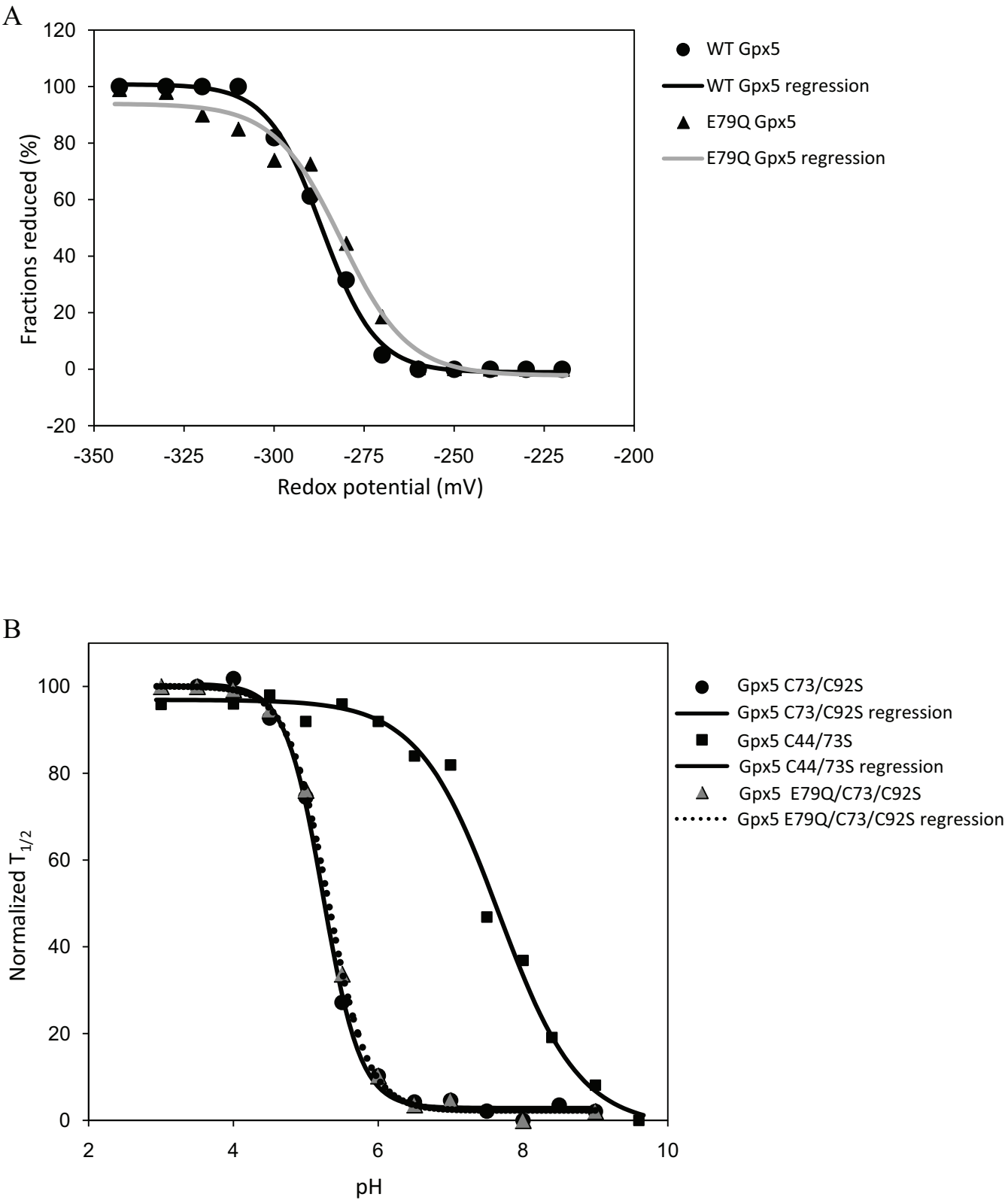
A
120
100
80
60
40
20
0
-20
Fractions reduced (%)
-350
-325
-300
-275
-250
-225
-200
Redox potential (mV)
WT Gpx5
WT Gpx5 regression
E79Q Gpx5
E79Q Gpx5 regression
B
100
80
60
40
20
0
Normalized $T_{1/2}$
2
4
6
8
10
pH
Gpx5 C73/C92S
Gpx5 C73/C92S regression
Gpx5 C44/73S
Gpx5 C44/73S regression
Gpx5 E79Q/C73/C92S
Gpx5 E79Q/C73/C92S regression

Figure 5

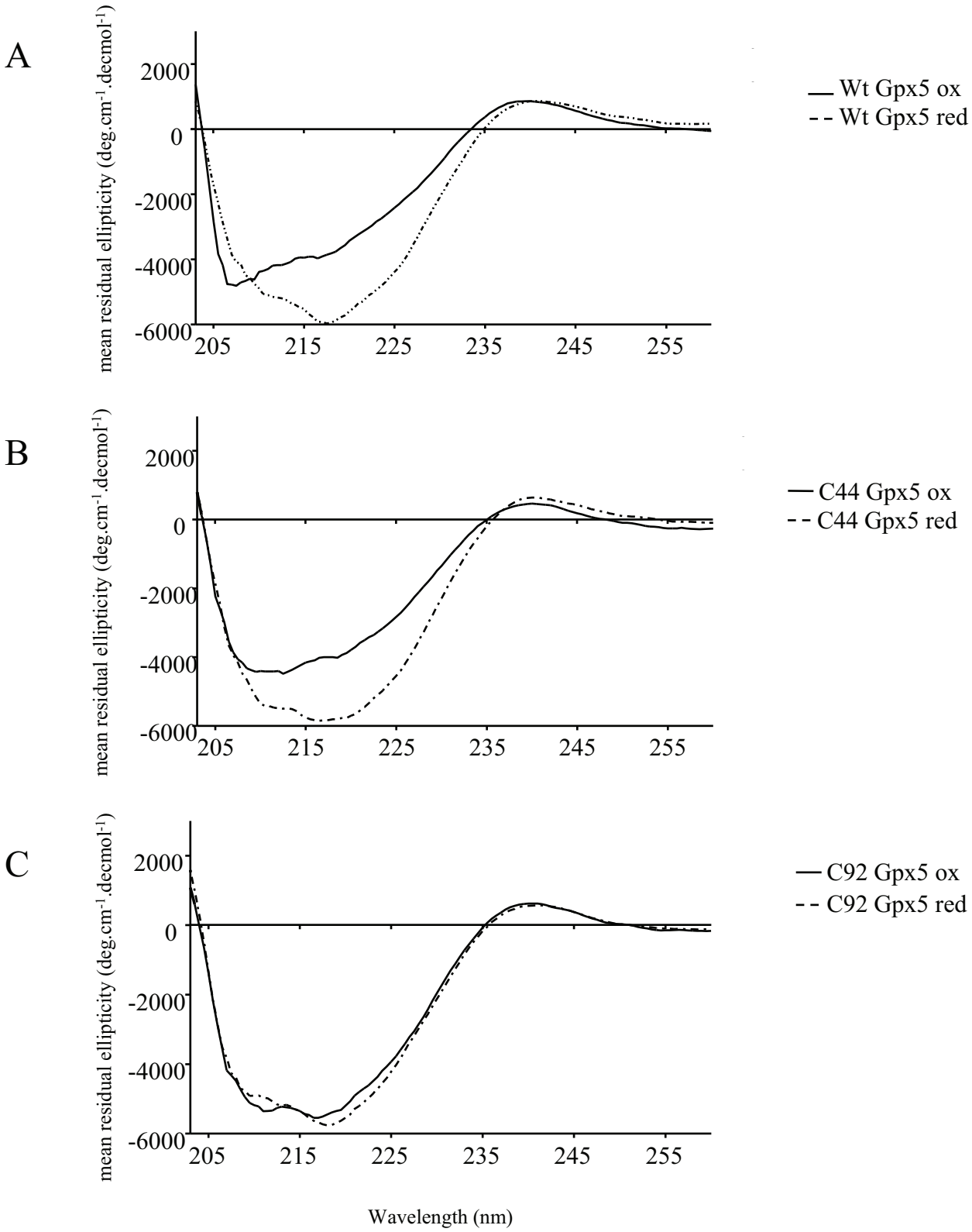
A
B
C
mean residual ellipticity (deg.cm-1.decmol-1)
2000
0
-2000
-4000
-6000
205
215
225
235
245
255
Wt Gpx5 ox
Wt Gpx5 red
C44 Gpx5 ox
C44 Gpx5 red
C92 Gpx5 ox
C92 Gpx5 red
Wavelength (nm)

Figure 6

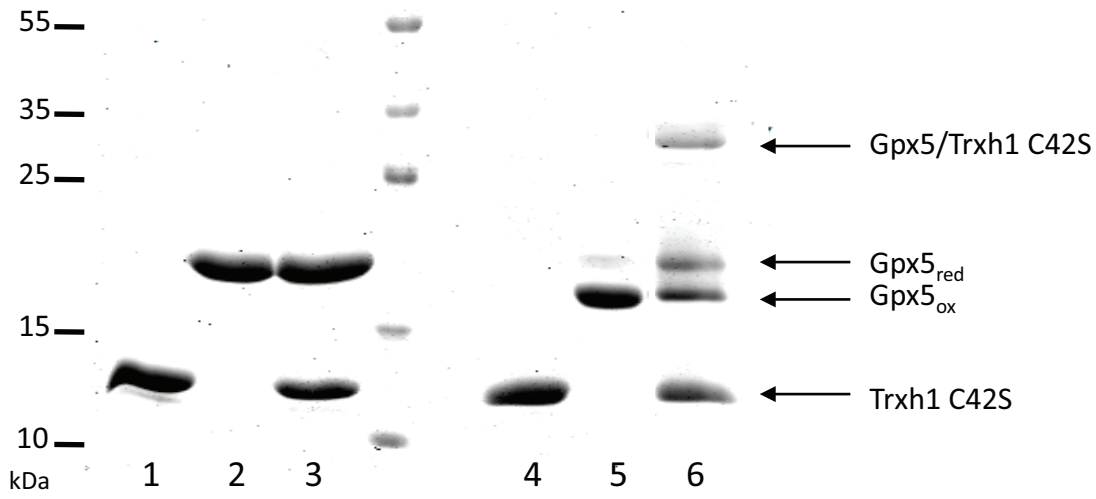
55
35
25
15
10
kDa
1
2
3
4
5
6
Gpx5/Trxh1 C42S
Gpx5red
Gpx5ox
Trxh1 C42S

Figure 7

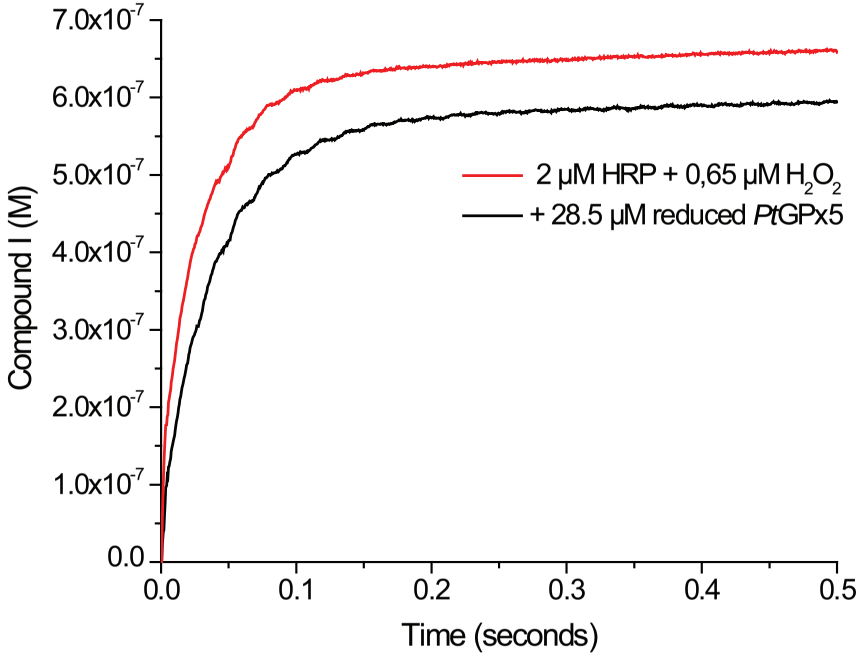

Suppl Figure 1

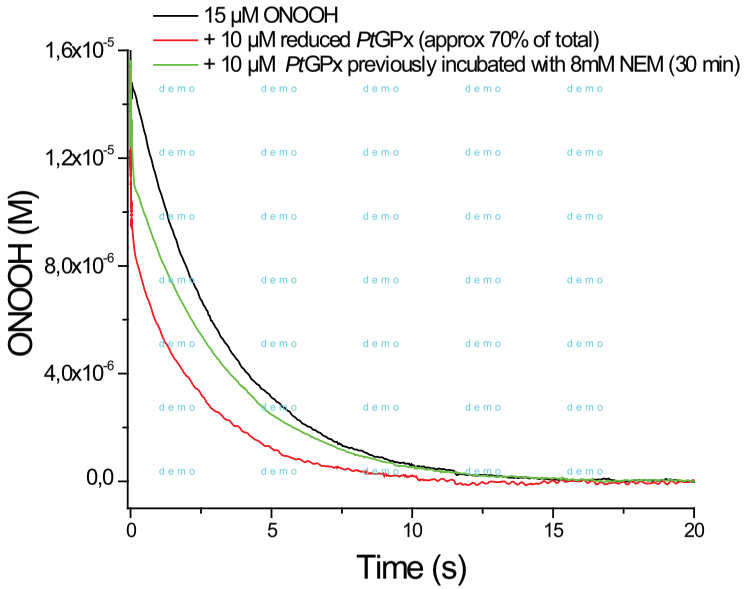

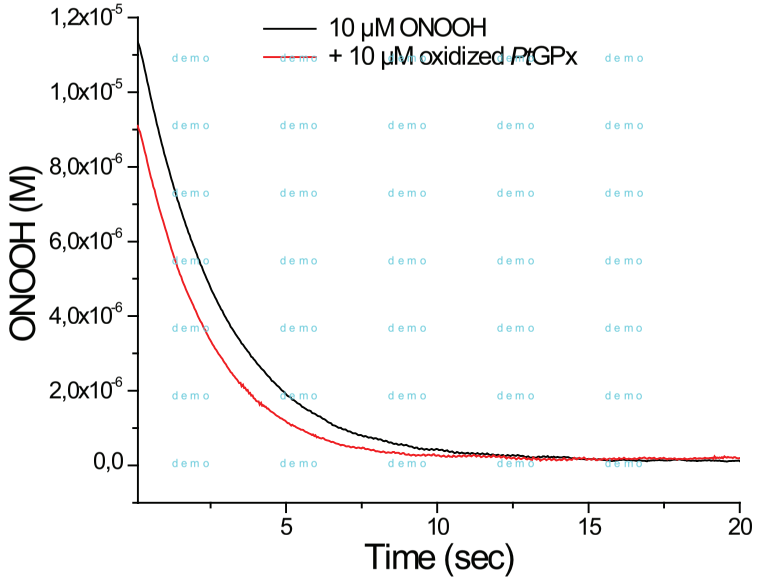

Suppl Figure 2

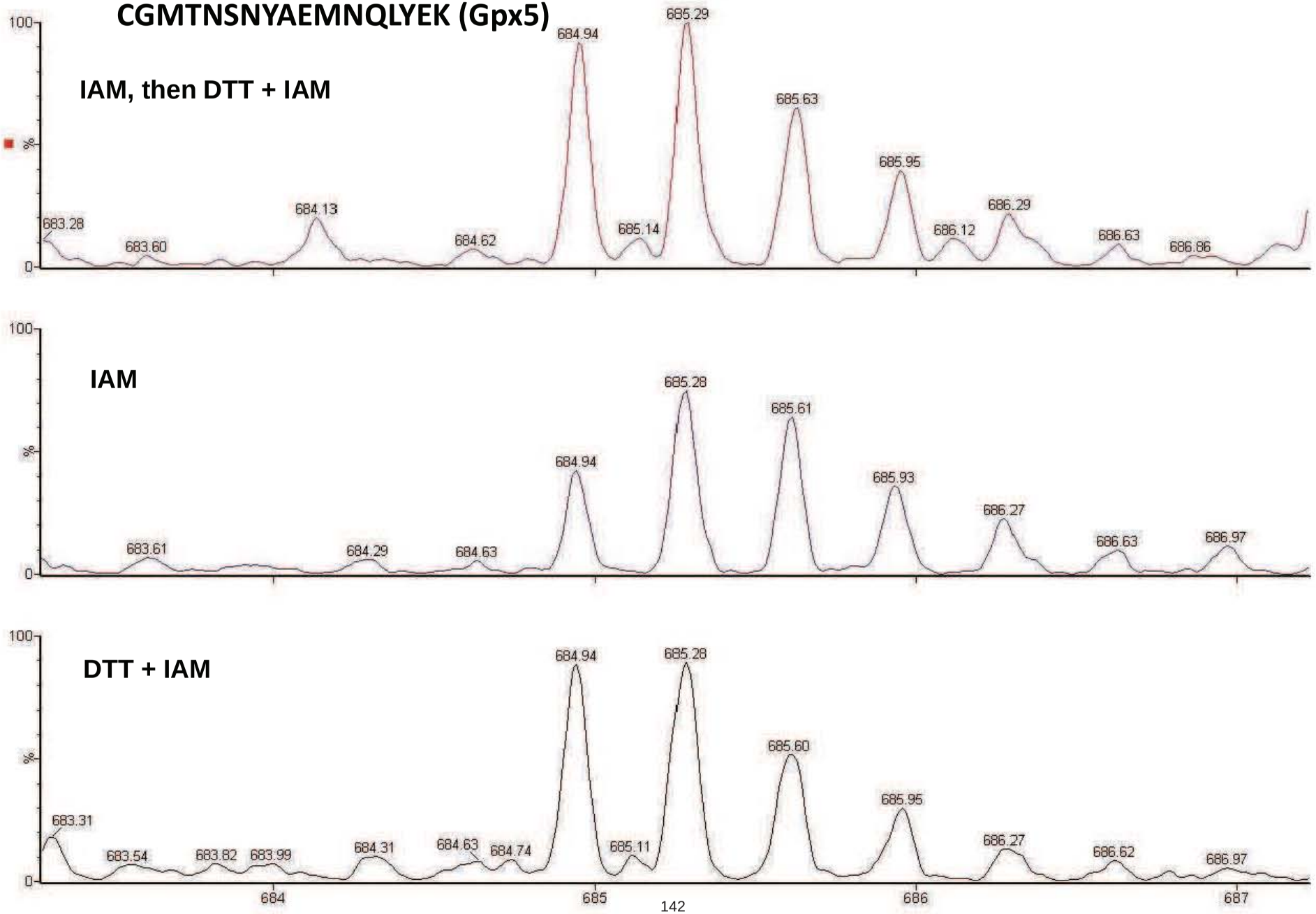

Suppl Figure 3A

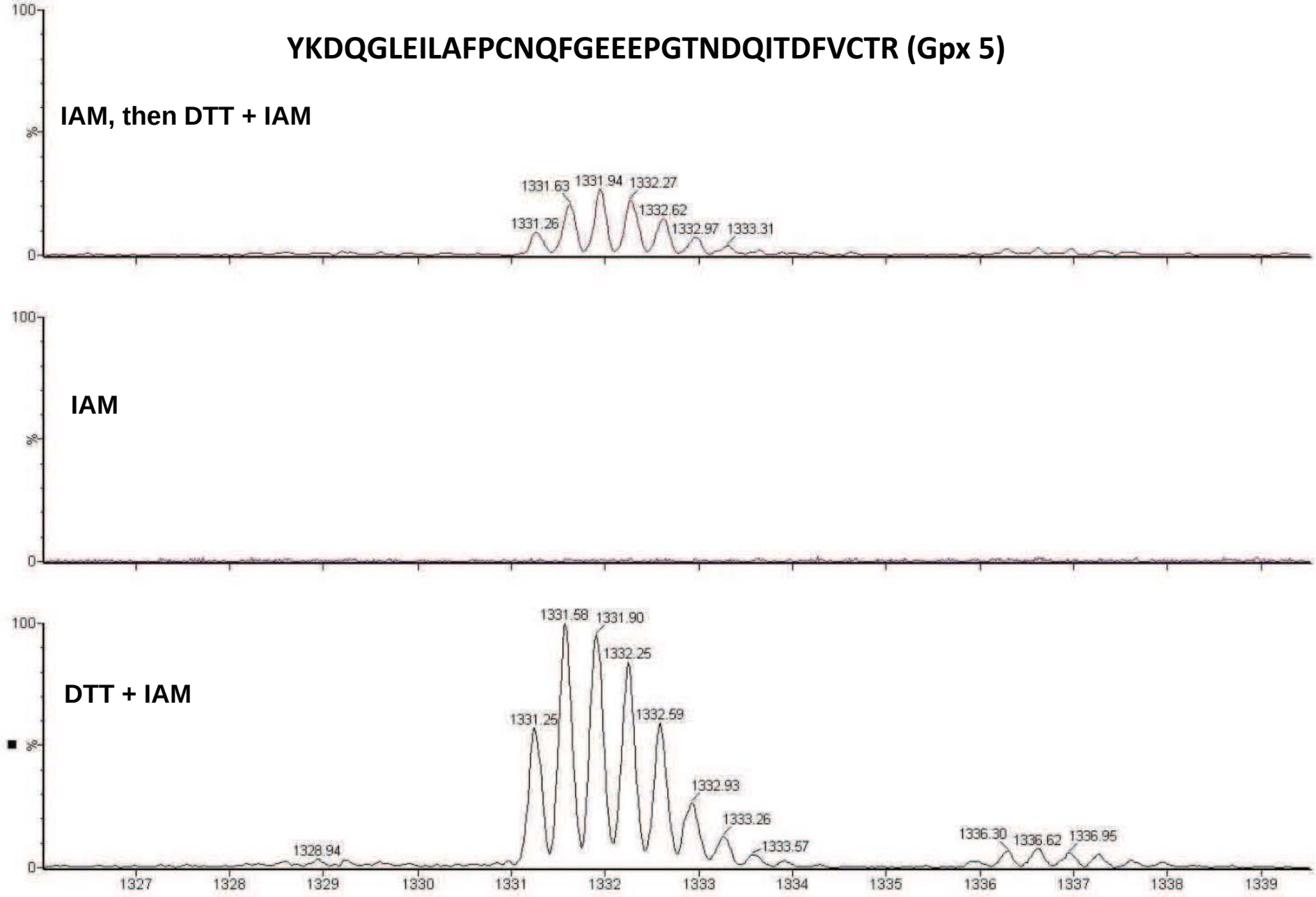

Suppl Figure 3B

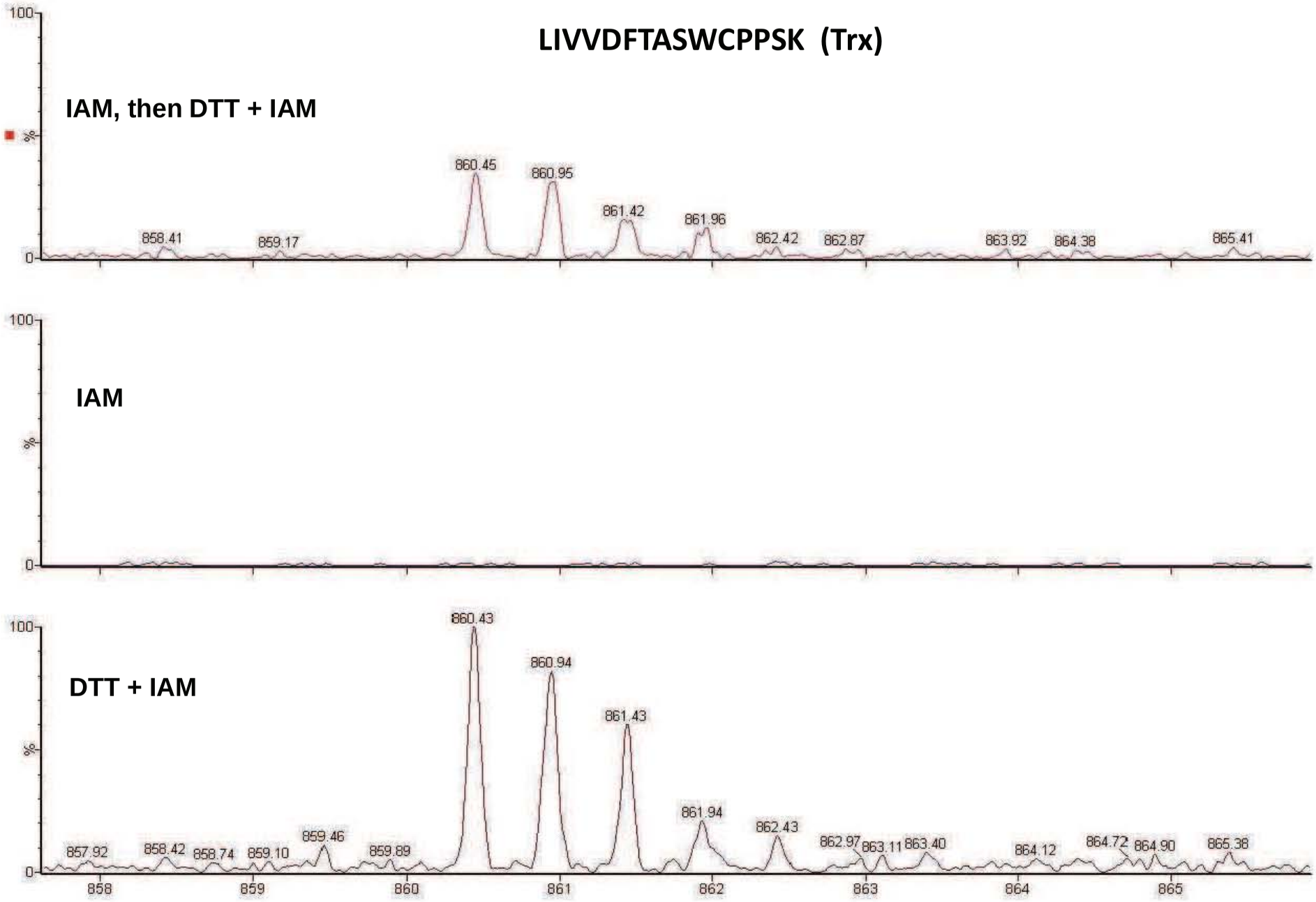

Suppl Figure 3C

II Article 3: Biochemical characterization of three poplar PDI isoforms with different domain organizations: emphasis on the oxidoreductase properties of PDI-M

Benjamin Selles, Jean-Pierre Jacquot, Nicolas Rouhier

Cet article présente la caractérisation biochimique de trois isoformes du peuplier, appartenant à trois classes de PDIs présentant des organisations modulaires distinctes. Les isoformes des classes L et M (PDI-L1a et PDI-M) présentent deux modules catalytiques de type a qui sont respectivement séparés par deux modules b ou associés en tandem, tandis que l'isoforme de la classe A (PtPDI-A) est composé d'un seul module a. Malgré la présence d'un motif CxxC présentant un potentiel d'oxydoréduction classique de -170 mV, aucune activité enzymatique n'a été identifiée pour la PDI-A, suggérant soit que la protéine n'a aucune activité oxydase, isomérase ou réductase soit que les substrats utilisés ne sont pas adaptés et que cette protéine possède des substrats très spécifiques. Concernant les 2 autres PDIs, les PDI-L1a et -M sont toutes deux réduites par la NTR et sont capables d'oxyder une forme réduite de RNAse A dénaturée et de réduire l'insuline, la PDI-L1a étant systématiquement plus efficace. Par contre, la PDI-M est le seule isoforme à pouvoir activer une malate déshydrogénase à NADP chloroplastique, une enzyme habituellement régulée par les Trxs. Par ailleurs, la caractérisation de variants protéiques mutés sur l'un ou l'autres des sites actifs indique que le module *a°* de la PDI-M catalyse préférentiellement des réactions d'oxydation, en accord avec un potentiel d'oxydoréduction de -170 mV, tandis que le module a est plus efficace dans la catalyse de réactions de réduction et possède un potentiel d'oxydoréduction de -190 mV.

Biochemical characterization of three poplar PDI isoforms with different domain organizations: emphasis on the oxidoreductase properties of PDI-M.

Selles B, Jacquot JP, Rouhier* N.

Addresses
Unité Mixte de Recherches 1136 Nancy University-INRA, Interactions Arbres-Microorganismes, IFR 110, EFABA 54506 Vandoeuvre-lès-Nancy cedex, France.

***Address correspondence to Nicolas Rouhier,** UMR 1136 Nancy University-INRA, Interactions Arbres Microorganismes, 54506 Vandoeuvre-lès-Nancy Cedex, France. Phone: ++383684225, Email: nrouhier@scbiol.uhp-nancy.fr

Protein disulfide isomerases are usually multi-modular redox catalysts able to perform the reduction, creation or isomerisation of disulfide bonds. We present here the expression, purification and biochemical characterization of three poplar PDI isoforms. PDI-A is characterized by a single catalytic Trx module. Despite having a presumed WCKHC active forming a disulfide with a redox midpoint potential of -170 mV, no *in vitro* reductase or oxidase/isomerase activity has been detected for this protein, suggesting that it might have very specific partners. The other PDI investigated displays two catalytic or so-called *a* domains, with an *a-b-b'-a'* and *a°-a-b* organisation respectively for PDI-L1a and PDI-M. Using a battery of non-physiological redox substrates as insulin, NADPH thioredoxin reductase (NTR), NADP malate dehydrogenase (MDH-NADP), peroxiredoxins or RNAse A, both proteins were found to be able to catalyze oxidation or reduction reactions with PDI-L1a being more efficient in most cases, except that it is not able at all to activate MDH-NADP, contrary to PDI-M. To evaluate the contribution of each catalytic domain of PDI-M in these redox reactions, similar activity assays have been performed with full-length proteins where the dicycsteinic motif at each *a* domain has been independently mutated. Each module was found to perform specific reactions, the *a°* module preferentially catalyzing oxidation and the *a* module reduction. These results are consistent with the measured redox potentials of -170 mV and -190 mV for the *a°* and *a* modules respectively. The proximity of the two catalytic domains and their different properties raise the question of the structural or mechanistic relationship between these two adjacent *a* domains.

Introduction

Oxidative protein folding is an essential process, occurring generally in oxidizing sub-cellular compartments, and which is required, in particular, for the maturation and assembly of newly synthesized secreted and membrane proteins In the periplasm of prokaryotes, the proteins responsible for the creation and isomerisation of disulfide bonds belong to the Dsb (DiSulfide Bonds) protein family. This protein family is composed of several members referred to as DsbA to DsbL. The major actors, conserved in many bacteria, are the DsbA-DsbB couple which is involved in oxidation reactions, the DsbC-DsbD couple in isomerisation reactions, DsbE or CcmG in cytochrome c maturation and DsbG to the reduction of sulfenic acids [1,2]. In eukaryotes, the proteins responsible of the oxidative protein folding are essentially found in the endoplasmic reticulum and in the intermembrane mitochondrial space. In the former compartment, the proteins involved principally belong to the endoplasmic reticulum oxidase (ERO) and protein disulfide isomerase (PDI) protein families (ref). However, proteins named quiescin sulfhydryl oxidases (QSOX) and displaying oxidase activity *in vitro* are also present in this compartment but their exact physiological role is unknown (ref). In the intermembrane mitochondrial space, the oxidation of cysteines is ensured by a pair of protein Mia40 and Erv1, a flavoprotein of the sulfhydryl oxidase family (ref).

All PDIs, as well as some Dsb members, belong to the thioredoxin (Trx) superfamily displaying a common structural fold named the Trx fold [3,4]. All PDIs possess at least one Trx domain referred to as *a* or *b* domain and consisting of about 100 amino acids which adopt a Trx fold. However, modules *a* exhibit a catalytic active site (more frequently WCGHC), whereas modules *b* do not possess catalytic centers, but instead are

thought to be important for substrate recognition (ref). The isoforms usually differ by the number and the positions of the *a* and *b* domains and by the active site sequence of the *a* domains. In addition, in a few cases, additional domains, likely conferring specific functions to the isoforms possessing it, have been evolutionary added. The so-called classical PDI isoforms, which are present in all eukaryotic organisms, possess four modules with an *a-b-b'-a'* organisation. PDIs constitute a multigenic family composed of 5 genes in yeast and up to 20 genes in human [5,6]. In photosynthetic organisms, PDIs cluster into 9 classes (A, B, C, D, E, F, L, M and S), 3 are specific to algae, 1 is specific to land plants and 5 are present in both phyla [7-13]. Higher plants possess around 10 members but very little is known regarding their biochemical and physiological properties. Some soybean PDI isoforms belonging to classes L, M and S play essential roles in seed and pollen maturation and development [10-13]. The plastidial form of a *Chlamydomonas reinhardtii* PDI-L, is involved in the redox-dependent transcriptional regulation in the chloroplast [14]. A maize PDI-A protein is accumulated is response to an ER stress,,but, in contrast to classical PDIs, they might not reside in the ER or only transiently [9].

The aim of this study was to compare the biochemical properties of three poplar PDIs (PDI-A, PDI-L1, PDI-M) exhibiting different domain organisation and belonging to three different classes, by examining in particular their *in vitro* reductase and oxidase/isomerase activities using both physiological or non-physiological substrates. For poplar PDI-M, a deeper analysis was performed using proteins mutated for their active site cysteines in order to investigate the catalytic mechanism used by this protein during oxidation or reduction of disulfide bonds. The data indicates that, although the redox potentials of the two modules of PDI-M are very close and seem to be interdependent, each Trx module could perform specific reactions, the *a* domain being competent for reduction and the *a°* domain for oxidation.

Material and methods

Cloning, site-directed mutagenesis, production and purification of recombinant proteins

The sequences encoding poplar PDI-L1a (POPTR_0002s08260), PDI-M (POPTR_0014s15820), PDI-A (POPTR_0009s00990) in the Phytozome portal, http://www.phytozome.net/), amplified from leaf cDNAs of *Populus trichocarpa* x *nigra* for PtPDI-L1a and PtPDI-M and of *Populus tremula* x *tremuloides* for PtPDI-A, have been cloned into pET3d for PDI-L1a or into pET-15b for PDI-M and PDI-A. In order to express the mature forms of each protein, the 21, 23 and 24 most N-terminal amino acids, corresponding to the putative ER targeting sequence, were truncated, in PtPDI-L1a, PtPDI-M and PtPDI-A respectively. The primers used for cloning and site-directed mutagenesis (PDI-A $K_{56}G$, $C_{51}V_{52}/Y_{51}A_{52}$, PDI-M $C_{36}/C_{39}S$ and $C_{165}/C_{168}S$ are listed in supplemental Table I. Recombinant plasmids were used to transform the *Escherichia coli* BL21(DE3) strain. The culture and purification conditions were as described in [15]. Briefly, the purification consisted of a succession of ammonium sulphate precipitation, ACA44 gel filtration and DEAE Sephacel chromatography. After dialysis against TE buffer (30 mM Tris–HCl, pH 8.0, 1 mM EDTA), protein concentrations were determined using a molar extinction coefficient at 280 nm of 39100 M^{-1} cm^{-1} for PtPDI-L1a, 55265 M^{-1} cm^{-1} for PtPDI-M, 55140 M^{-1} cm^{-1} for PtPDI-M(*a*) double mutant, 55140 M^{-1} cm^{-1} for PtPDI-M(*a°*) double mutant, 21220 M^{-1} cm^{-1} for PtPDI-A and 21220 M^{-1} cm^{-1}.for PDI-A K56G proteins.

Determination of the midpoint redox potential

Oxidation-reduction titrations using the fluorescence of adducts formed between the protein and mBBr were carried out at ambient temperature as described previously [16,17]. The 500µl reaction mixtures contained 100 µg protein in 100 mM HEPES-NaOH buffer, pH 7.0, containing defined mixtures of oxidized and reduced glutathione to set the ambient potential (Eh) with an overall concentration in glutathione of 2 mM. After 2 h incubation at 25°C, excess mBBr was added and incubated in the dark for 1 h. mBBr labelled proteins were precipitated with TCA 20% (v/v), incubated 15 min on ice and centrifuged 15 min at 13000 rpm. Pellets were washed with 1 volume of 2% TCA by centrifugation (15 min, 13000 rpm) and then resuspended in 300 µl Tris-HCl 1 M, SDS 2% during 30 min. Protein solutions were then diluted to a final volume of 2.2 ml and mBBr fluorescence emission was measured between 400 and 500 nm using a Cary Eclipse spectrofluorimeter after excitation at 350 nm.

RNAse A oxidative refolding

RNAse A reduction and denaturation was performed in 200µl 100 mM Tris-HCl pH 8.0 containing 6 M guanidine, 73 mM DTT and 7.3 mM native bovine RNAse A (Sigma Aldrich), for 1h at 37°C. Excess DTT was removed with a desalting column (Sephadex G25) equilibrated with Tris-HCl 30mM pH8, 1mM EDTA and 1% acetic acid. The RNAse A concentration was determined using an extinction coefficient of 9800 M^{-1}. cm^{-1}. The effective reduction of RNAse A was confirmed with DTNB (5,5'-dithio-bis-2-nitrobenzoic acid, 13600 M^{-1} cm^{-1}) by measuring a ratio of 8 thiol per RNAse A molecule. RNAse A refolding was assessed by incubating 50µM of reduced and denatured RNAse A for 15 minutes in a 300µl mixture containing Tris-HCl 30 mM pH 8.0, 1 mM EDTA, 1 mM GSH, 0.2 mM GSSG with or without 3 µM PDIs. For RNAse A activity measurement, 50 µl of refolding mixture were added every 5 minutes to 450µl Tris-HCl 30 mM pH 8.0, 1 mM EDTA containing 2.5 mM cCMP (cytidine 2',3'-cyclic monophosphate). RNAse A recovered activity was estimated by following the augmentation of absorbance at 296 nm resulting from the hydrolysis of cCMP to CMP [18].

Insulin and DTNB reductase activities

Insulin reduction was measured using 5 µM proteins as in [19]. The non-enzymatic reduction of insulin by DTT was used as a control. The ability of PDIs to catalyze the reduction of DTNB (5,5′-dithio-bis-2-nitrobenzoic acid) in presence of *A. thaliana* NTRB (AtNTRB) was measured at 25°C by monitoring the increase in absorbance at 412 nm caused by the release of thionitrobenzoate (TNB^-). The reaction medium contained 30 mM Tris-HCl, pH 8.0, 2 mM EDTA, 200 µM NADPH, 2 µM AtNTRB, 100 µM DTNB and 0.2 µM PDIs.

PDI-mediated recycling of 2-CysPrx

The PDI-dependent recycling of 2-CysPrx was measured using a NADPH-coupled spectrophotometric method at 25°C as described previously [20]. The assays were carried out in a total volume of 500 µL containing TE buffer (30 mM Tris-HCl, pH 8.0, 1 mM EDTA), 200 µM NADPH, 1 µM *Arabidopsis thaliana* NTRB, 5 µM At2-CysPrx, 100 µM H_2O_2 and 2.5 µM PDIs. The decrease in absorbance was followed at 340 nm. The 2-CysPrx activity was determined after subtracting the spontaneous reduction rate observed in the absence of PDIs.

NADP-malate dehydrogenase (NADP-MDH) activation

NADP-MDH from *Sorghum bicolor* was purified as described in [21]. The activity test was modified from [21]. The activation mixture (200 µl) contained 500 µM DTT, 5 µM PDI or Trx xx used as a control and

10 µg recombinant NADP-MDH in 100 mM Tris-HCl, pH 8.0 buffer. It was incubated at 25°C for 15 min. Every 5 minutes, an aliquot of 20 µL was added to 480 µl of standard reaction mixture containing 100 mM Tris-HCl, pH 8.0, 189 µM oxaloacetate, and 800 µM NADPH. The rate of activation was measured by following the decrease in absorbance at 340 nm.

Results

Protein sequence characteristics

In order to analyse the biochemical features of PDIs with different domain organisation, three proteins (PtPDI-L1a, PtPDI-M and PtPDI-A shortened as PDI-L1a, PDI-M and PDI-A) belonging to the PDI-L, -M and -A classes and devoid of their putative N-terminal ER targeting sequence have been produced in E. *coli* and purified to homogeneity. PDI-L1a and PDI-M are multimodular proteins composed of 4 and 3 domains respectively but both proteins possess two *a* domains containing the conventional WCGHC redox active site sequence (Figs 1A and B). On the contrary, PDI-A exhibits only one protein domain with a modified WCKHC active site motif, as its higher plant orthologs. Outside the active site, there are 5 other strictly conserved residues, a Phe and a Leu in position -5 and +6 compared to the catalytic Cys, as well as in the C-terminal part, the *cis*-Pro conserved in all oxidoreductases having a Trx fold, a Tyr and an Arg. This Arg was proposed to modulate the *pKa* of the C-terminal active-site cysteine, necessary for PDI reoxidation step, by moving into and out of the active-site, depending on the catalytic step [22]. From studies conducted on *E. coli* Trx, two other residues, a Glu and a Lys, highlighted in figure 1A, are involved in the modulation of the N-terminal active site cysteine *pKa* [23]. Whereas they are strictly conserved in PDI-L1a (E_{52}/K_{86} and E_{397}/K_{431}), only the Glu is conserved in the two *a* domains of PDI-M, the Lys being replaced by an alanine (A_{85}) and a histidine (H_{213}) in the *a*° and *a* Trx modules respectively, and none of them are conserved in PDI-A.

Oxidoreductase activity of poplar PDI isoforms

The classical test used for measuring PDI activity, i.e. the oxidative refolding of reduced and denatured RNAse A, has been used for the three poplar isoforms. PDI-L1a is the most efficient protein, as, after 15 min, it allowed the recovery of *ca* 90% of the activity relatively to the activity observed with native RNAse A (Fig. 2A). In contrast, after 15 min, the RNAse A activity recovery is only 60% in the presence of PDI-M and the kinetics obtained with PDI-A is similar to the control experiment achieved by omitting PDI, indicating that PDI-A does not promote RNAse A refolding. The differences observed in this test raised the question of the functionality of PDI-A and/or could point out the possibility that some PDIs have developed specific properties.

The capacity of these PDIs to catalyze the reduction of disulfide bridges instead of promoting their formation was next analyzed by measuring insulin reduction, which is accompanied by its precipitation as measured at 650 nm. In this test, PDI-L1a is the most efficient protein, even more efficient than poplar Trxh1, with the reduction starting after 0.5 and 4 minutes respectively (Fig. 2B). PDI-M can also perform insulin reduction but, as for the previous assay, it is less efficient than PDI-L1a or Trxh1, but more than PDI-A which is not able at all to reduce insulin. Considering the presence of two Trx modules in PDI-L1a and PDI-M, the better reducing activity of PDI-L1a but not of PDI-M compared to Trx h1 could suggest that both catalytic domains of PDI-L1a, but only one of PDI-M possess reductase activity. Moreover, independently of the speed of the reaction, the fact that the turbidity in inferior in the case of both PDIs compared to Trx h1

might indicate that all disulfide bridges are not efficiently reduced by PDIs.

Finally, since a variety of PDI can be efficiently reduced by a NADPH/ NADPH thioredoxin reductase (NTR) system and although it is presumably not the physiological reductant of ER-targeted PDIs, we wanted to determine whether the PDIs are reduced by the *A. thaliana* NTR using DTNB as electron acceptor. Such system would be extremely convenient afterward for measuring the capacity of PDIs to reduce usual Trx targets [24]. Also in this test, PDI-La1 is more efficient than PDI-M and PDI-A is inactive (Fig. 2C). Considering the size of the proteins (NTR is an homodimer of 55 kDa and PDI-L, -M and PDI-A are monomers of 53, 44 and 15 kDa respectively), the difference observed between PDIs might not concern to steric hindrance problems but more likely could originate from ionic or hydrophobic interactions. Actually it was proposed that Trxs interact with NTR proteins via a hydrophobic area positioned in one side of the disulfide bond and with its target proteins by an ionic patch on the other site of active site [25]. It was reported for the *a* domain of human PDI protein that a hydrophobic area surround the active site of these Trx module [26]. Hence we can speculate that PDI-L1a proteins interact with NTR in a comparable way of Trxs, meanwhile the lack of obvious difference in amino acids sequences composition and structural data concerning PDI-M and PDI-A cannot allow us to conclude regarding PDI isoforms specificities toward NTR protein (Fig 1).

As PDI-A is inactive in all assays, but possesses a particular active site sequence, a protein variant, named PDI-A $K_{56}G$, has been produced to modify the WCGKC active site into WCGHC. We have first investigated the redox potential of this mutant compared to the WT protein. The E_m value of PDI-A was determined at -170 mV ± 5 mV, whereas the one measured for PDI-A $K_{56}G$ is -150 mV ± 5 mV (Fig. 3A). Next, we wondered whether the increase of *ca* 20 mV by substituting the positively charged Lys to a glycine possibly conferred some oxidoreductase activity to the protein. However, the protein was still found inactive in all assays used previously (RNAse refolding, insulin and DTNB reduction).

In depth biochemical characterization of PDI-M

Besides structural considerations, the redox properties of oxidoreductases are mostly governed by the pKa of the catalytic cysteines and the midpoint redox potential of the catalytic disulfides. The latter parameter was evaluated for PDI-M by producing two protein variants corresponding to the full-length protein but where the dicysteinic WCGHC motif of each *a* domain was substituted by a WSGHS motif. The PtPDI-M variant, where Cys_{165} and Cys_{168} of the *a* domain were mutated, was referred to as PtPDI-M(*a*°) and the one where Cys_{36} and Cys_{39} of the *a*° domain were mutated to as PtPDI-M(*a*). Using these variants, E_m values of -170 mV± 5 mV and of -190 mV ± 5 mV have been determined for the *a*° and *a* catalytic disulfides respectively (Fig. 3B). These midpoint redox potentials are close to those reported in the literature for homologous proteins and are fully consistent with a functioning in oxidative protein folding [27].

In the following parts, we have investigated, using these variants, the contribution of each catalytic domain to the PDI-M activity using essentially the same activity assays, i.e. RNAse A oxidative refolding, insulin reduction, NADP-malate dehydrogenase activation and 2-CysPrx regeneration. In the refolding assay of denatured and reduced RNAse A, PDI-M(*a*°) present a comparable efficiency as PDI-M, whereas PDI-M(*a*) exhibits only 50 to 60 % activity compared to WT (Fig. 4). The fact that the N-terminal *a*° module of PDI-M has an activity similar to the WT, suggests that it is likely the only or major contributor of

the activity measured with the WT protein. However, in its absence, the second domain can partly substitute it.

The conclusions obtained from the insulin reduction assay are slightly different, as the wild type protein is the most efficient form in this case (Fig. 5). Regarding the contribution of the modules, PDI-M(*a*) is more efficient than PDI-M(*a*°). This indicate that, in the presence of DTT, the *a* module is more efficient for insulin reduction than *a*°. Moreover, the fact that PDI-M activity approximately corresponds to the sum of activities of both domains, suggest that both domains contributed to the reduction activity though with different efficiencies.

The ability of PDI-M to reduce known Trx targets could be more easily evaluated if it is reduced itself by a NADPH/NTR system as electron supplier. PDI-M(*a*°) has equivalent ability to reduce DTNB as the WT in the presence of NTR, whereas PDI-M(*a*) was very porrly reduced by NTR (Figure 6A). This was further confirmed by performing insulin reduction with NADPH/NTR as electron supplier. As expected, the PDI-M(*a*) protein is inactive in this condition, whereas it was active with DTT. On the other hand, PDI-M(*a*°) reduces insulin in presence of NADPH/NTR, but less efficiently than PtPDI-M (Figure 6B). Hence, from these experiments, it seems clear that the active site thioredoxin modules of PDI-M proteins are asymmetrically targeted by NTR. The DTNB reduction monitored is mostly due to the reduction of the *a*° module, with equivalent activities for PDI-M and PDI-M(*a*°) in contrast with the insulin reduction for which the activity of PDI-M(*a*°) does not reach that of PDI-M. These data indicate that despite the fact that NTR does not reduce the PDI-M *a* module, the double serine mutation of this module has an impact on insulin reduction via the *a*° module.

To take advantage of the asymmetric reduction of PDI-M modules by NTR, we tested the reduction of peroxiredoxins by PtPDI-M protein in presence of NTR system. Very recently it was shown that an ER targeted human 2-CysPrx (PrxIV) can accept electrons from P5 and ERp46 PDI isoforms [28]. In this respect and despite the absence of characterization of such proteins in plant ER , we tested the biochemical capability of PDI-M to reduce plant chloroplastic Arabidopsis 2-CysPrx (At2-CysPrx). As shown in figure 7, PDI-M is able to promote the reduction of hydrogen peroxide via the regeneration of At2-CysPrx in the presence of NADPH NTR as electron donor. The same experiment performed with the two PDI-M variants resulted in significant loss of activity, with ca 10 and 50 % remaining activity compared to wild type for PDI-M(*a*) and PDI-M(*a*°), respectively. The quasi absence of activity for PDI-M(*a*) was expected due to the incapacity of NTR to sustain its regeneration. The loss of activity observed for PDI-M(*a*°) is more unexpected as the *a*° module is as efficiently reduced as PDI-M by the NTR system. This could demonstrate that, as for insulin reduction, the mutation of the *a* module active site impacts *a*° module functioning.

Next, activation of NADPH malate dehydrogenase (NADP-MDH) was tested as an additional substrate for measuring reduction properties of PDI-M in comparison to PtTrxh1 used as a positive control (Fig. 8). This is a well characterized redox-regulated chloroplastic protein, catalyzing the conversion of oxaloacetate to malate in the presence of NADPH and involved in the malate shuttle or in the C4 pathway of CO_2 fixation in some tropical plants. Surprisingly, taking into account the unfavourable thermodynamic barrier (NADP-MDH possesses disulfides with very negative redox potential, around -300 mV), PDI-M is able to activate the NADP-MDH. However, this activation is less efficient than with PtTrxh1 (around 40% of the

PtTrxh1 activity at identical concentrations). In this kind of experiments, we observed that PtPDI-A (data not shown) and the more classical PtPDI-L1a cannot activate NADP-MDH in the presence of DTT (Figure 8). The two PDI-M domains present different activities toward oxidized NADP-MDH, PtPDI-M(*a*) is slightly more active than wild type for NADP-MDH activation (close to 50% compared to PtTrxh1), whereas PtPDI-M(*a*°) is less active than wild type (less than 20% compared to PtTrxh1) (Figure 8). These data are in accordance with the reduction of insulin in presence of DTT in which the *a* module active site is a more efficient reductant. Nevertheless, in contrast with insulin reduction with DTT as electron donor, NADP-MDH reduction by PtPDI-M(*a*) proteins is equivalent to PtPDI-M, indicating that the mutation of the *a*° module did not impact this reaction in presence of DTT as electron supplier. The activity of PtPDI-M(*a*°) may represent a residual activity obtained due to the mutation of the *a* module active site.

Discussion

Protein disulfide isomerases are versatile catalysts of redox reactions. *In vivo* they perform the reduction, creation and/or isomerisation of disulfide bonds. In connection with those different redox reactions, PDIs are generally multi modular proteins and the modification of their module arrangements can lead to alteration of their activities [29,30]. These changes can be very large, indicating that a given protein module could possess a "specific" function. As an example the *b'* module of mammalian ERp57 or PDI proteins, which is redox inactive, is essential for substrate or chaperone partner recruitment [5,31,32]. In this study we report a comparative biochemical characterization of plant PDIs belonging to three different classes.

Redox properties of the single module PDI-A

We have first examined the properties of an atypical mono-module PDI isoform, PDI-A. The E_m value measured for PtPDI-A (-170 mV) is in the same range, indicating that the PtPDI-A midpoint redox potential is compatible with oxidation reactions. Indeed, proteins involved in oxidation reaction exhibit redox potentials ranging from less than -100 mV, for some prokaryotic DsbA proteins, to -180 mV for *a* modules of classical PDIs [29,33]. Additionally, the conserved arginine residue encountered in active Trx modules of PDI proteins and which is proposed to be involved in the reoxidation of PDI CGHC motif, by modulating the *pKa* value of the C-terminal cysteine residue, is present [22]. Together, these data indicate that PtPDI-A could potentially be an efficient oxidoreductase. Nevertheless no activity of any sort can be measured. A first, unlikely but possible explanation could be that we have cleaved the transit peptide of the sequence at an unfavourable position, eliminating some residues essential for activity or stability in the N-terminus part of the protein. More reasonably is the hypothesis that this absence of reactivity is linked to unusual sequence features. First the active site encountered in PDI-A displays some potential important differences though conserved in PDI-A orthologs (FCVPWCKHC instead of [Y/F]APWCGHC, figure 1). The presence of an additional cysteine residue coupled with a valine instead of the classical alanine-proline couple could slow down disulfide reduction or creation. However, a PDI-A CV to YA variant did not exhibit any additional activity (data not shown). Similarly, we have demonstrated that the atypical WCKHC, though influencing the midpoint redox potential, was not responsible for the absence of activity. Another feature that can putatively explain the absence of activity concerns the residues supposedly in charge of stabilizing the deprotonated form of the

catalytic cysteine by lowering its pKa [23]. As previously mentioned, this protein exhibits a Lys and a Glu charged pair (K_{49} and E_{84}), instead of classical D/E and K couple (D_{26}/K_{57} in the case of *E. coli* Trx1 and E_{52}/K_{86} or E_{397}/K_{431} respectively for the *a* and *a'* module of the classical PtPDI-L1a (Figure 1). In *E. coli* Trx1, it was shown that these two amino acids are not equally involved in *E. coli* Trx1 reactivity, since Asp26 is more important than Lys_{57}, probably due to its ionisable lateral chain *pka* [23]. Whereas the Asp to Glu substitution in classical and non-classical PDIs is conservative, PtPDI-A exhibits a charge inversion with a Lys in place of the Asp residue [34,35]. The *pKa* of an isolated Lys was reported to be around 10 pH unit whereas isolated Asp or Glu present *pKa* around 4 pH unit and D26 has a *pKa* between 7 and 9 depending on the oxidation state of *E. coli* Trx [34,35]. The amino acid change at this position thus could explain at least partially the inactivity of PtPDI-A in our test conditions. However, as these variations are naturally present, the inactivity of PDI-A with classical redoxin and PDI substrates, raises the question of the physiological role and partners of this protein. Considering the DKDL C-terminal sequence, quite distant from classical ER retention signals (very often KDEL or KEEL), the question of its subcellular localization is not solved. From the redox potential of the catalytic disulfide, it is nevertheless expected that this protein is redox active. If this protein possesses highly specific physiological partners, we may not have used proper partners yet for our *in vitro* assays. It is worth mentioning that such small mono domain PDI, as human ERp18 has previously been shown to exhibit an oxidase activity on synthetic peptides [36]. However, despite their comparable modular organisation, PDI-A and ERp18 are not true orthologs, exhibiting only *ca* 15 % sequence identity.

Does the domain organisation confer different biochemical properties?

The second aim of the study was the biochemical characterization of a poplar PDI-M isoform possessing an *a°-a-b* domain organisation quite different from the *a-b-b'-a'* of the classical and well characterized PDI-Ls. In particular, this organisation of the catalytic domains in tandem raises the question of their respective contribution for protein reactivity and of their possible connectivity, which is in fact one of unresolved question for most types of PDIs, although such cooperativity has been proposed based on the U shape arrangement of the four thioredoxin domains of the yeast PDI1p, very similar to DsbC or DsbG [31]. In addition to the characterization of WT PDI-L and -M, we analyzed the respective involvement of the two active Trx modules (*a°* and *a*) of PDI-M in reduction reactions with insulin, 2-CysPrx and NADP-MDH or oxidation reactions with NTR and RNAse-A. Regarding oxidation reactions, it was previously reported that some PDIs can act as oxidants of NTR or in other words that NTR can reduce PDIs [24].

Except for the NADP-MDH activation assay, where the PDI-L1a is not active at all, it is always more efficient than PDI-M in all other assays measuring the reductase or oxidase properties. This better efficiency, in particular in reduction assays, could be explained by the strict conservation of the charged amino acids required for decreasing the pKa of the N-terminal catalytic cysteine (Figure 1). Indeed, the two *a* modules of PDI-L1a possess the usual Glu and Lys residues, whereas both domains of PDI-M contains the Glu but an Ala or a His in the *a°* and *a* modules respectively (Figure 1). The fact that PDI-L1a is inactive toward NADP-MDH, whereas PDI-M proteins exhibit noticeable activities could arise from their natural capacity to interact with non folded or folded proteins respectively. Indeed, it

was shown for mammalian enzymes that PDI-L proteins interact directly with misfolded or unfolded proteins by the intervention of a hydrophobic patch in the *b'* module, whereas P5 proteins, the mammalian PDI-M orthologs, are partners of the BiP chaperone, a folded protein, which is thought to bring misoxidized/misfolded proteins to P5 for their correct oxidative folding [37]. Hence, by analogy and despite a lower "intrinsic" reductase activity compared to PtPDI-L1a, PtPDI-M can interact with and promote the activation of native proteins such as NADP-MDH [37]. Altogether, the parallel between PDI-L and PDI-M/P5 seems to indicate that common thermodynamic forces govern activities of different PDI classes during oxidative protein folding, notwithstanding different substrate specificities and modular organisation [37].

The physiological significance of these opposed oxidase/reductase properties is an important issue The *in vivo* measurement of the redox state of an endogenous PDI in HEK-293 cells was performed recently, showing a mixture of fully reduced (50%), fully oxidzed (16%) and partially oxidized on the a or a' module (18/15%) [38]. These results suggested first that neither of the two domains in human PDI might exclusively catalyze substrate oxidation or reduction, but also that this redox is adequate for both reactions. This potential dual function has been nicely illustrated recently by demonstrating that several PDI can reduce ER resident proteins as 2-CysPrx (PrxIV) or vitamin K epoxide reductase [28,39-41]. These alternative routes of PDI oxidation independently from ERO1, which is a source of H_2O_2 production, have been proposed to decrease reactive oxygen species formation in the ER [42].

Is there a specific contribution of each catalytic domain of multi-domain PDIs?

Although we did not achieve similar experiments with plant PDI-L, it was well documented that the *a'* module (the C-terminal one) of these PDIs, which presents the highest redox potential (*ca* -150 mV), possesses a preponderant oxidase activity toward reduced and scrambled RNAse A [29]. Similarly, we demonstrate for PDI-M that the *a°* module, having the most oxidant di-cysteine motif (redox potential of -150 mV), is more efficient for oxidation reaction than the *a* module, allowing a recovery of RNase A activity, similar to the WT enzyme. This is very comparable to their orthologous mammalian counterparts called P5 isoforms, for which the *a°* module (the N-terminal one) is also the main actor in oxidative refolding of reduced or scrambled RNAse A [43]. In addition, the *a°* module can efficiently oxidize NTR contrary to the *a* module. The incapacity of the *a* module to oxidize NTR is thus more probably due to unfavourable protein/protein interactions rather than thermodynamic factors, since the redox potential of both domains are not very different. In any case, it prevented to estimate, for this domain, the reduction of Trx targets proteins in a couple assay requiring the NADPH-NTR system.

On the other hand, we have observed that the *a* module of PDI-M is the most efficient for reduction reactions (insulin, NADP-MDH) (Figure xx). Taking advantage of the oxidation of NTR by the PDI-M(*a°*) module we have demonstrated that the *a°* module is not as efficient as the WT PDI-M for insulin reduction and 2-CysPrx reduction. This difference of activity could indicate that the presence of a redox active *a* module is needed for a maximal efficiency, possibly because there might be a "cross talk" between the *a* and *a°* module during insulin or 2-CysPrx reduction that uses NTR oxidation (Figure 7c). However, we cannot exclude that amino acid substitutions in a specific active site Trx module could modify redox properties and/or capability of the other di-

cysteine motif, leading to alterations in catalysis.

References

1 Inaba K (2009) Disulfide bond formation system in Escherichia coli. *J. Biochem* **146**, 591-597.

2 Depuydt M, Leonard SE, Vertommen D, Denoncin K, Morsomme P, Wahni K, Messens J, Carroll KS & Collet JF (2009) A periplasmic reducing system protects single cysteine residues from oxidation. *Science* **326**, 1109-11.

3 Collet J-F & Messens J (2010) Structure, Function and Mechanism of Thioredoxin Proteins. *Antioxid Redox Signal*.

4 Pedone E, Limauro D, D'Ambrosio K, De Simone G & Bartolucci S (2010) Multiple catalytically active thioredoxin folds: a winning strategy for many functions. *Cell. Mol. Life Sci* **67**, 3797-3814.

5 Kozlov G, Määttänen P, Thomas DY & Gehring K (2010) A structural overview of the PDI family of proteins. *FEBS J* **277**, 3924-3936.

6 Appenzeller-Herzog C & Ellgaard L (2008) The human PDI family: versatility packed into a single fold. *Biochim Biophys Acta* **1783**, 535-48.

7 Lemaire SD & Miginiac-Maslow M (2004) The thioredoxin superfamily in Chlamydomonas reinhardtii. *Photosyn. Res* **82**, 203-220.

8 Selles B, Jacquot J-P & Rouhier N (2010) Comparative genomic study of protein disulfide isomerases from photosynthetic organisms. *Genomics*.

9 Houston NL, Fan C, Xiang JQ, Schulze JM, Jung R & Boston RS (2005) Phylogenetic analyses identify 10 classes of the protein disulfide isomerase family in plants, including single-domain protein disulfide isomerase-related proteins. *Plant Physiol* **137**, 762-78.

10 Wadahama H, Kamauchi S, Ishimoto M, Kawada T & Urade R (2007) Protein disulfide isomerase family proteins involved in soybean protein biogenesis. *FEBS J* **274**, 687-703.

11 Wadahama H, Kamauchi S, Nakamoto Y, Nishizawa K, Ishimoto M, Kawada T & Urade R (2008) A novel plant protein disulfide isomerase family homologous to animal P5 - molecular cloning and characterization as a functional protein for folding of soybean seed-storage proteins. *FEBS J* **275**, 399-410.

12 Kamauchi S, Wadahama H, Iwasaki K, Nakamoto Y, Nishizawa K, Ishimoto M, Kawada T & Urade R (2008) Molecular cloning and characterization of two soybean protein disulfide isomerases as molecular chaperones for seed storage proteins. *FEBS J* **275**, 2644-58.

13 Iwasaki K, Kamauchi S, Wadahama H, Ishimoto M, Kawada T & Urade R (2009) Molecular cloning and characterization of soybean protein disulfide isomerase family proteins with nonclassic active center motifs. *FEBS J* **276**, 4130-41.

14 Kim J & Mayfield SP (2002) The active site of the thioredoxin-like domain of chloroplast protein disulfide isomerase, RB60, catalyzes the redox-regulated binding of chloroplast poly(A)-binding protein, RB47, to the 5' untranslated region of psbA mRNA. *Plant Cell Physiol* **43**, 1238-43.

15 Couturier J, Didierjean C, Jacquot J-P & Rouhier N (2010) Engineered mutated glutaredoxins mimicking peculiar plant class III glutaredoxins bind iron-sulfur centers and possess reductase activity. *Biochemical and Biophysical Research Communications* **403**, 435-441.

16 Hirasawa M, Schurmann P, Jacquot JP, Manieri W, Jacquot P, Keryer E, Hartman FC & Knaff DB (1999) Oxidation-reduction properties of chloroplast thioredoxins, ferredoxin:thioredoxin reductase, and thioredoxin f-regulated enzymes. *Biochemistry* **38**, 5200-5.

17 Krimm I, Lemaire S, Ruelland E, Miginiac-Maslow M, Jaquot JP, Hirasawa M, Knaff DB & Lancelin JM (1998) The single mutation Trp35-->Ala in the 35-40 redox site of Chlamydomonas reinhardtii thioredoxin h affects its biochemical activity and the pH dependence of C36-C39 1H-13C NMR. *European journal of biochemistry / FEBS* **255**, 185-95.
18 Lyles MM & Gilbert HF (1991) Catalysis of the oxidative folding of ribonuclease A by protein disulfide isomerase: dependence of the rate on the composition of the redox buffer. *Biochemistry* **30**, 613-619.
19 Couturier J, Koh CS, Zaffagnini M, Winger AM, Gualberto JM, Corbier C, Decottignies P, Jacquot JP, Lemaire SD, Didierjean C & Rouhier N (2009) Structure-function relationship of the chloroplastic glutaredoxin S12 with an atypical WCSYS active site. *The Journal of biological chemistry* **284**, 9299-310.
20 Navrot N, Collin V, Gualberto J, Gelhaye E, Hirasawa M, Rey P, Knaff DB, Issakidis E, Jacquot J-P & Rouhier N (2006) Plant glutathione peroxidases are functional peroxiredoxins distributed in several subcellular compartments and regulated during biotic and abiotic stresses. *Plant Physiol* **142**, 1364-1379.
21 Issakidis E, Lemaire M, Decottignies P, Jacquot JP & Miginiac-Maslow M (1996) Direct evidence for the different roles of the N- and C-terminal regulatory disulfides of sorghum leaf NADP-malate dehydrogenase in its activation by reduced thioredoxin. *FEBS Lett* **392**, 121-124.
22 Lappi AK, Lensink MF, Alanen HI, Salo KEH, Lobell M, Juffer AH & Ruddock LW (2004) A conserved arginine plays a role in the catalytic cycle of the protein disulphide isomerases. *J. Mol. Biol* **335**, 283-295.
23 Dyson HJ, Jeng MF, Tennant LL, Slaby I, Lindell M, Cui DS, Kuprin S & Holmgren A (1997) Effects of buried charged groups on cysteine thiol ionization and reactivity in Escherichia coli thioredoxin: structural and functional characterization of mutants of Asp 26 and Lys 57. *Biochemistry* **36**, 2622-2636.
24 Lundström-Ljung J, Birnbach U, Rupp K, Söling HD & Holmgren A (1995) Two resident ER-proteins, CaBP1 and CaBP2, with thioredoxin domains, are substrates for thioredoxin reductase: comparison with protein disulfide isomerase. *FEBS Lett* **357**, 305-308.
25 Eklund H, Cambillau C, Sjöberg BM, Holmgren A, Jörnvall H, Höög JO & Brändén CI (1984) Conformational and functional similarities between glutaredoxin and thioredoxins. *EMBO J* **3**, 1443-1449.
26 Kemmink J, Darby NJ, Dijkstra K, Nilges M & Creighton TE (1996) Structure determination of the N-terminal thioredoxin-like domain of protein disulfide isomerase using multidimensional heteronuclear 13C/15N NMR spectroscopy. *Biochemistry* **35**, 7684-7691.
27 Hatahet F, Ruddock LW, Ahn K, Benham A, Craik D, Ellgaard L, Ferrari D & Ventura S (2009) Protein disulfide isomerase: a critical evaluation of its function in disulfide bond formation. *Antioxid. Redox Signal* **11**, 2807-2850.
28 Tavender TJ, Springate JJ & Bulleid NJ (2010) Recycling of peroxiredoxin IV provides a novel pathway for disulphide formation in the endoplasmic reticulum. *EMBO J* **29**, 4185-4197.
29 Tian G, Xiang S, Noiva R, Lennarz WJ & Schindelin H (2006) The crystal structure of yeast protein disulfide isomerase suggests cooperativity between its active sites. *Cell* **124**, 61-73.
30 Chambers JE, Tavender TJ, Oka OBV, Warwood S, Knight D & Bulleid NJ (2010) The reduction potential of the active site disulfides of human protein disulfide isomerase limits oxidation of the enzyme by Ero1α. *J. Biol. Chem* **285**, 29200-29207.

31 Kozlov G, Maattanen P, Schrag JD, Pollock S, Cygler M, Nagar B, Thomas DY & Gehring K (2006) Crystal structure of the bb' domains of the protein disulfide isomerase ERp57. *Structure* **14**, 1331-1339.
32 Maattanen P, Kozlov G, Gehring K & Thomas DY (2006) ERp57 and PDI: multifunctional protein disulfide isomerases with similar domain architectures but differing substrate-partner associations. *Biochem. Cell Biol* **84**, 881-889.
33 Lafaye C, Iwema T, Carpentier P, Jullian-Binard C, Kroll JS, Collet J-F & Serre L (2009) Biochemical and structural study of the homologues of the thiol-disulfide oxidoreductase DsbA in Neisseria meningitidis. *J. Mol. Biol* **392**, 952-966.
34 Thurlkill RL, Grimsley GR, Scholtz JM & Pace CN (2006) pK values of the ionizable groups of proteins. *Protein Sci* **15**, 1214-1218.
35 Menchise V, Corbier C, Didierjean C, Saviano M, Benedetti E, Jacquot JP & Aubry A (2001) Crystal structure of the wild-type and D30A mutant thioredoxin h of Chlamydomonas reinhardtii and implications for the catalytic mechanism. *Biochem J* **359**, 65-75.
36 Alanen HI, Williamson RA, Howard MJ, Lappi A-K, Jäntti HP, Rautio SM, Kellokumpu S & Ruddock LW (2003) Functional characterization of ERp18, a new endoplasmic reticulum-located thioredoxin superfamily member. *J. Biol. Chem* **278**, 28912-28920.
37 Jessop CE, Watkins RH, Simmons JJ, Tasab M & Bulleid NJ (2009) Protein disulphide isomerase family members show distinct substrate specificity: P5 is targeted to BiP client proteins. *J. Cell. Sci* **122**, 4287-4295.
38 Appenzeller-Herzog C & Ellgaard L (2008) In vivo reduction-oxidation state of protein disulfide isomerase: the two active sites independently occur in the reduced and oxidized forms. *Antioxid. Redox Signal* **10**, 55-64.
39 Tavender TJ, Sheppard AM & Bulleid NJ (2008) Peroxiredoxin IV is an endoplasmic reticulum-localized enzyme forming oligomeric complexes in human cells. *Biochem. J* **411**, 191-199.
40 Wajih N, Hutson SM & Wallin R (2007) Disulfide-dependent protein folding is linked to operation of the vitamin K cycle in the endoplasmic reticulum. A protein disulfide isomerase-VKORC1 redox enzyme complex appears to be responsible for vitamin K1 2,3-epoxide reduction. *J. Biol. Chem* **282**, 2626-2635.
41 Schulman S, Wang B, Li W & Rapoport TA (2010) Vitamin K epoxide reductase prefers ER membrane-anchored thioredoxin-like redox partners. *Proc. Natl. Acad. Sci. U.S.A* **107**, 15027-15032.
42 Gross E, Kastner DB, Kaiser CA & Fass D (2004) Structure of Ero1p, source of disulfide bonds for oxidative protein folding in the cell. *Cell* **117**, 601-610.
43 Kikuchi M, Doi E, Tsujimoto I, Horibe T & Tsujimoto Y (2002) Functional analysis of human P5, a protein disulfide isomerase homologue. *J. Biochem* **132**, 451-455.

Legend to figures

Table 1. Oligonucleotide sequences used for cloning and mutagenesis.

Figure 1. Sequence characteristics and domain organisation of selected poplar PDI isoforms.

A. Modular organisation of the PDI isoforms, PtPDI-L1a, PtPDI-M and PtPDI-A. Rectangle in light grey and dark grey indicate redox active (*a°*, *a'* or *a*) and inactive (*b* or *b'*) Trx modules, respectively. Letter surrounding redox active Trx modules indicate the nature of amino acids involved in redox properties or biochemical features. The conserved arginine (R) is represented in the most C-terminal part of Trx like modules, whereas the charged amino acid pairs are mentioned in the N-terminal and the central parts of Trx modules. Classical (KDEL) or unusual (DKDL) ER retention signals are represented in light grey and white egg-shaped form, respectively. B. Sequence alignment of active Trx like modules from PDI-L1a, PDI-M and PDI-A isoforms belonging to At, *Arabidopsis thaliana* (AtPDI-A, At1g07960; AtPDI-L1a, At1g21750; AtPDI-M1, At1g04980; AtPDI-M2, At2g32920); Pp, *Physcomitrella patens* (PpPDI-A, 168026171 ; PpPDI-L1, 168027645 ; PpPDI-M, 168057362); Pt, *Populus trichocarpa* (PtPDI-A, POPTR_0009s00990; PtPDI-L1a, POPTR_0002s08260; PtPDI-M, POPTR_0014s15820) and Zm, *Zea mays* (ZmPDI-A, GRMZM2G073628; ZmPDI-L1a, AY739284; ZmPDI-M, AY739290) organisms. Trx modules were delimited according Pfam only database (http://pfam.sanger.ac.uk/) and alignments were built using ClustalW algorithm at the NPSA web portal (http://npsa-pbil.ibcp.fr). Output of this alignment was made with the ESprit web portal (http://espript.ibcp.fr/ESPript/cgi-bin/ESPript.cgi). Amino acids strictly conserved appear in black, whereas partially conserved amino acids are indicated in light gray. Cysteines presumably involved in the catalytic mechanism are indicated with stars, other essential amino acids are indicated by triangles.

Figure 2. Oxidoreductase activity of poplar PDI isoforms.

A. ***Oxidative refolding of RNAse A***, results are represented in percent compared to native RNAse A activity as positive control (nRNAse A; diamonds, dotted line), reduced RNAse A (rRNAse A; squares, solid line), PtPDI-L1a (circle, solid line), PtPDI-M (triangles, solid line) and PtPDI-A (crosses, dotted line). For RNAse A preparation and details see material and methods. B. ***PDIs are efficient reducers of insulin***, insulin reduction was assessed using

5 µM of various PDIs or PtTrxh1 as positive control by measuring the turbidity at 650 nm caused by the precipitation of reduced insulin. PtTrxh1 (triangles), PtPDI-L1a (diamonds), PtPDI-M (crosses), PtPDI-A (circles) and DTT alone (squares). C. ***PDIs can accept electron form NTR B protein***, DTNB reduction was followed at 412 nm in presence of NADPH, NTR alone (black solid line) or with PtPDI-L1a (black dotted line), PtPDI-M (grey dotted line) or PtPDI-A (grey solid line). See material and methods for details.

Figure 3. Redox titration of selected poplar PDI isoforms.

A. Midpoint redox potential of wild type (solid line) and $K_{56}G$ substitution mutant (dotted line) CGHC active site disulfide of PtPDI-A proteins. B. Midpoint redox potential of *a* (solid line) and *a*° (dotted line) modules with CGHC active site disulfide from PtPDI-M protein. B. The titration was carried out using a total glutathione concentration of 2 mM in the redox buffer and with a redox equilibration time of 2 h. Free protein thiols are labeled by mBBr.

Figure 4. Oxidative refolding of reduced and denatured RNAse A by PtPDI-M wild type and mutants.

Result are represented in percent compared to native RNAse A as positive control (nRNAse A; diamonds, dotted line), reduced RNAse A (rRNAse A; squares, solid line), PtPDI-M (triangles, solid line), PtPDI-M(*a*°) (crosses, solid line) and PtPDI-M(*a*) (crosses, dotted line).

Figure 5. Involvement of *a*° and *a* modules in insulin reduction.

Insulin reduction was assessed using 5 µM of PtTrxh1 as positive control or PtPDI-M wild type and mutants, by measuring the turbidity at 650 nm caused by the precipitation of reduced insulin. PtTrxh1 (grey squares), PtPDI-M (black squares), PtPDI-M(*a*°) (triangles), PtPDI-M(*a*) (crosses) or DTT alone (open diamonds).

Figure 6. Involvement of *a*° and *a* modules in electron transfer from NTR to DTNB and insulin.

A. DTNB reduction followed at 412 nm in presence of NADPH, NTR alone (grey dotted line) or with PtPDI-M (black solid line), PtPDI-M(*a*°) (black dotted line) or PtPDI-M(*a*) (solid grey line). See material and methods for details. B. Insulin reduction assessed using NADPH/NTR as electron donor using 5 µM of PtPDI-M (black solid line), PtPDI-M(*a*°) (grey solid line) or PtPDI-M(a) (black dotted line) by measuring the turbidity at 650 nm caused by the precipitation of reduced insulin.

Figure 7. 2-CysPrx peroxidase activity during recycling by PtPDI-M protein.

2-CysPrx reduction was assessed by following NADPH oxidation (160µM) at 340 nm in presence of NTR (2µM), 2-CysPrx (5µM), H_2O_2 (100µM) and 2.5 µM of PtPDI-M, PtPDI-M(*a*°) or PtPDI(*a*). Results are represent in percent compared to PtPDI-M activity.

Figure 8. NAPD-malate dehydrogenase activation.

PtTrxh1 was used as positive control (solid line, diamond) and results are represented as percent compared to Trxh1 reactivation, DTT alone (solid line, squares), PtPDI-L1a (solid line, triangles) PtPDI-M dotted line, crosses), PtPDI-M(a°) (dotted line circle) PtPDI-M(a) dotted line, open circles). The activity of NADP-MDH protein was followed at 340 nm. See material and methods for more details.

Table 1.

PtPDI-L1a for	5′CCCCCCATGGCTGAGGATGAATCAAAGGAGTAC 3′
PtPDI-L1a rev	5′CCCCGGATCCTCAAAGTTCATCTTTAGCTGT 3′
PtPDI-M for	5′CCCCCCCCCATATGCTATATGGGCCTTCATCTCCT 3′
PtPDI-M rev	5′CCCCGGATCCTTATAACTCATCCTTGCTTCC 3′
PtPDI-M C36/39S for	5′GCACCATGGTCTGGGCACTCTAAAGCTCTC
PtPDI-M C36/39S rev	5′GAGAGCTTTAGAGTGCCCAGACCATGGTGC3′
PtPDI-M C165S/168 S for	5′GCACCTTGGTCGGGTCACTCTAAGAAACTGGCT3′
PtPDI-M C165/168S rev	5′AGCCAGTTTCTTAGAGTGACCCGACCAAGGTGC3′
PtPDI-A for	5′CCCCCCCCCATATGGTTATAACCCTAACTCCT 3′
PtPDI-A rev	5′CCCCGGATCCTCACAAATCTTTATCATAGCC 3′
PtPDI-A K56G for	5′TGTGTTCCCTGGTGTGGGCATTGTAAGAATTTG 3′
PtPDI-A K56G rev	5′CAAATTCTTACAATGCCCACACCAGGGAACACA 3′
PtPDI-A CV/YA for	5′TGGTTTGTCAAATTTTATGCTCCCTGGTGT 3′
PtPDI-A CV/YA rev	5′ACACCAGGGAGCATAAAATTTGACAAACCA 3′

A.

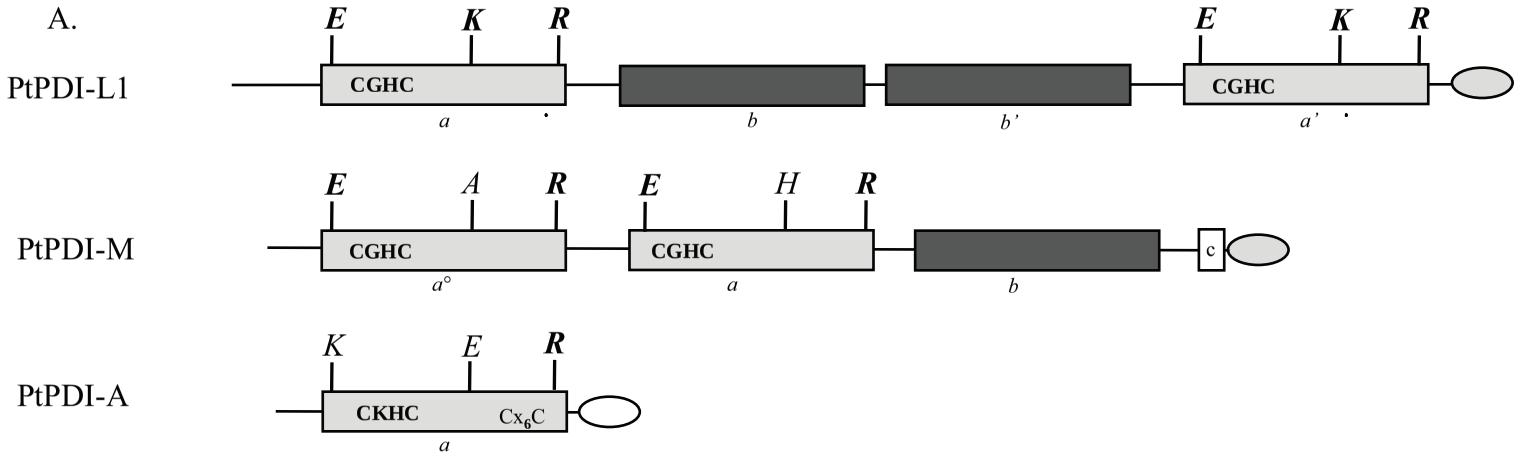
PtPDI-L1
E
K
R
CGHC
a
b
b'
CGHC
a'
PtPDI-M
E
A
R
CGHC
a°
E
H
R
CGHC
a
b
c
PtPDI-A
K
E
R
CKHC
Cx6C
a

B.

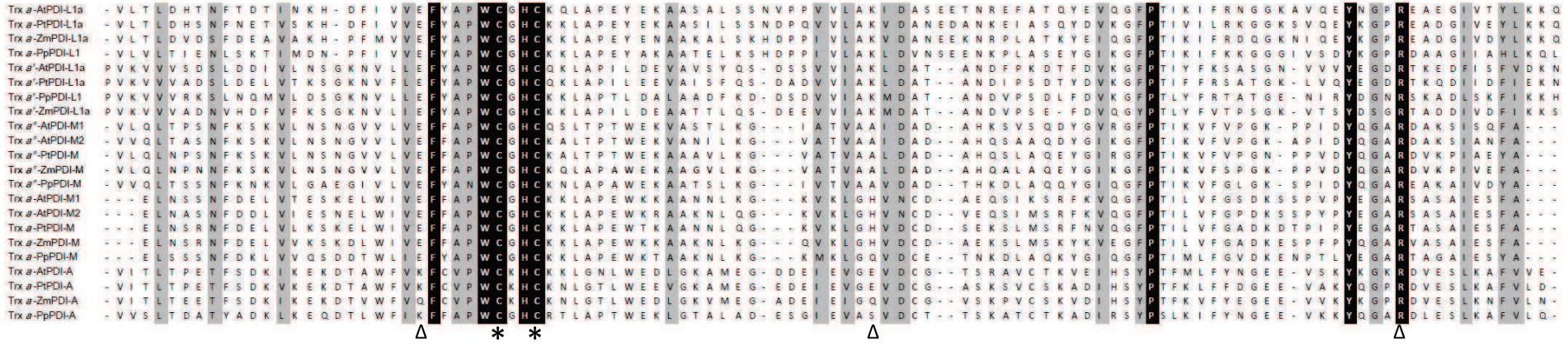
Trx a-AtPDI-L1a
Trx a-PtPDI-L1a
Trx a-ZmPDI-L1a
Trx a-PpPDI-L1
Trx a'-AtPDI-L1a
Trx a'-PtPDI-L1a
Trx a'-PpPDI-L1
Trx a'-ZmPDI-L1a
Trx a°-AtPDI-M1
Trx a°-AtPDI-M2
Trx a°-PtPDI-M
Trx a°-ZmPDI-M
Trx a°-PpPDI-M
Trx a-AtPDI-M1
Trx a-AtPDI-M2
Trx a-PtPDI-M
Trx a-ZmPDI-M
Trx a-PpPDI-M
Trx a-AtPDI-A
Trx a-PtPDI-A
Trx a-ZmPDI-A
Trx a-PpPDI-A

Figure 1

Figure 2

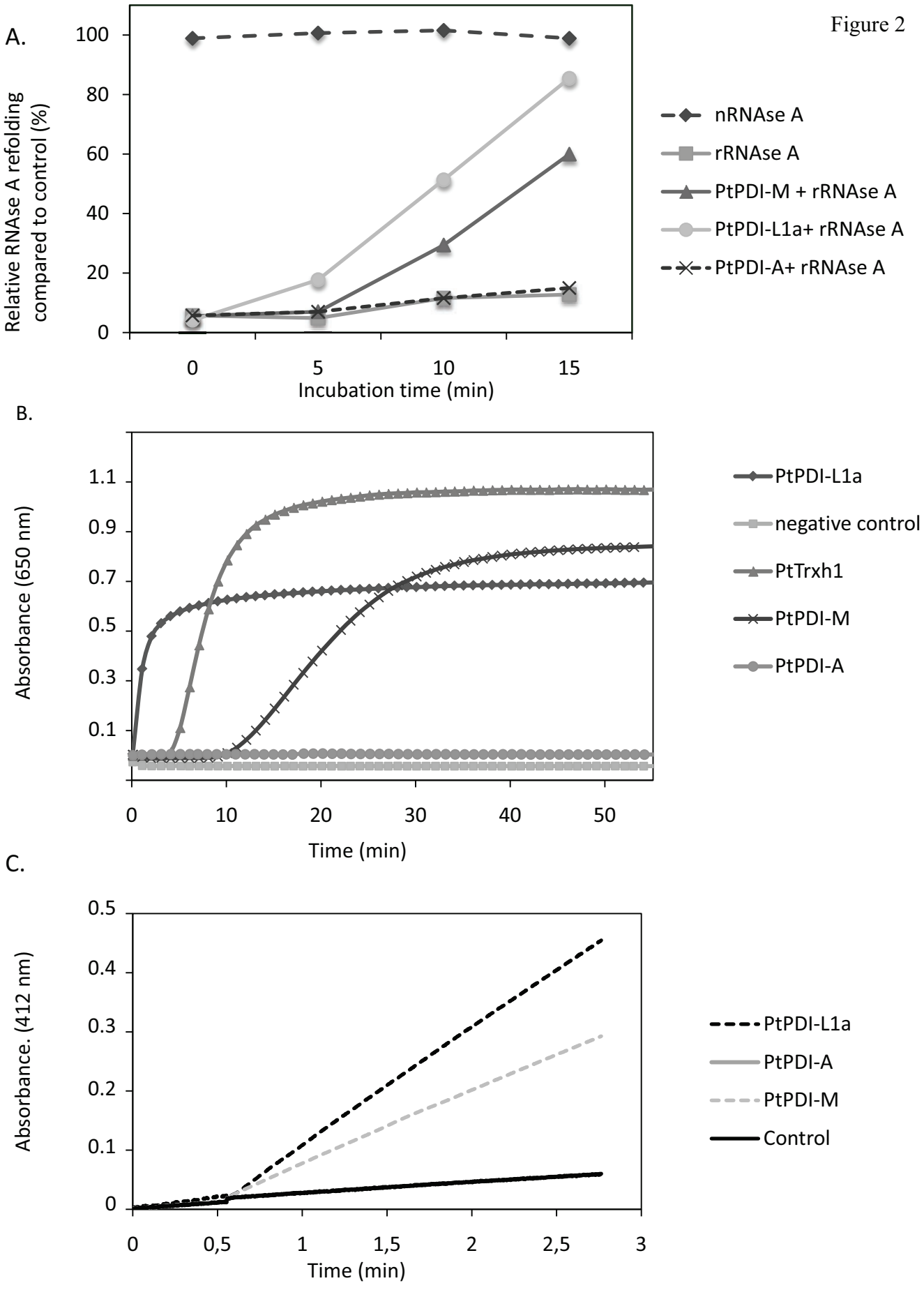
A.
Relative RNAse A refolding compared to control (%)
100
80
60
40
20
0
0
5
10
15
Incubation time (min)
nRNAse A
rRNAse A
PtPDI-M + rRNAse A
PtPDI-L1a+ rRNAse A
PtPDI-A+ rRNAse A
B.
Absorbance (650 nm)
1.1
0.9
0.7
0.5
0.3
0.1
0
10
20
30
40
50
Time (min)
PtPDI-L1a
negative control
PtTrxh1
PtPDI-M
PtPDI-A
C.
Absorbance. (412 nm)
0.5
0.4
0.3
0.2
0.1
0
0
0,5
1
1,5
2
2,5
3
Time (min)
PtPDI-L1a
PtPDI-A
PtPDI-M
Control

A.

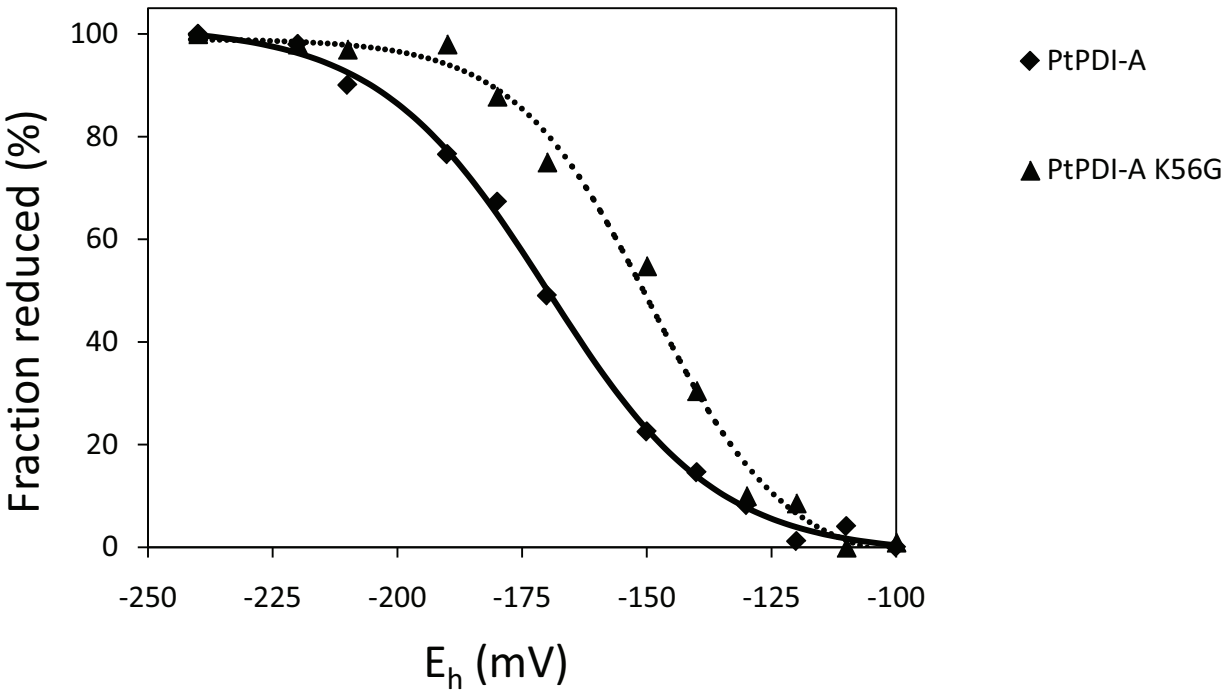
100
80
60
40
20
0
Fraction reduced (%)
-250
-225
-200
-175
-150
-125
-100
E_h (mV)
PtPDI-A
PtPDI-A K56G

B.

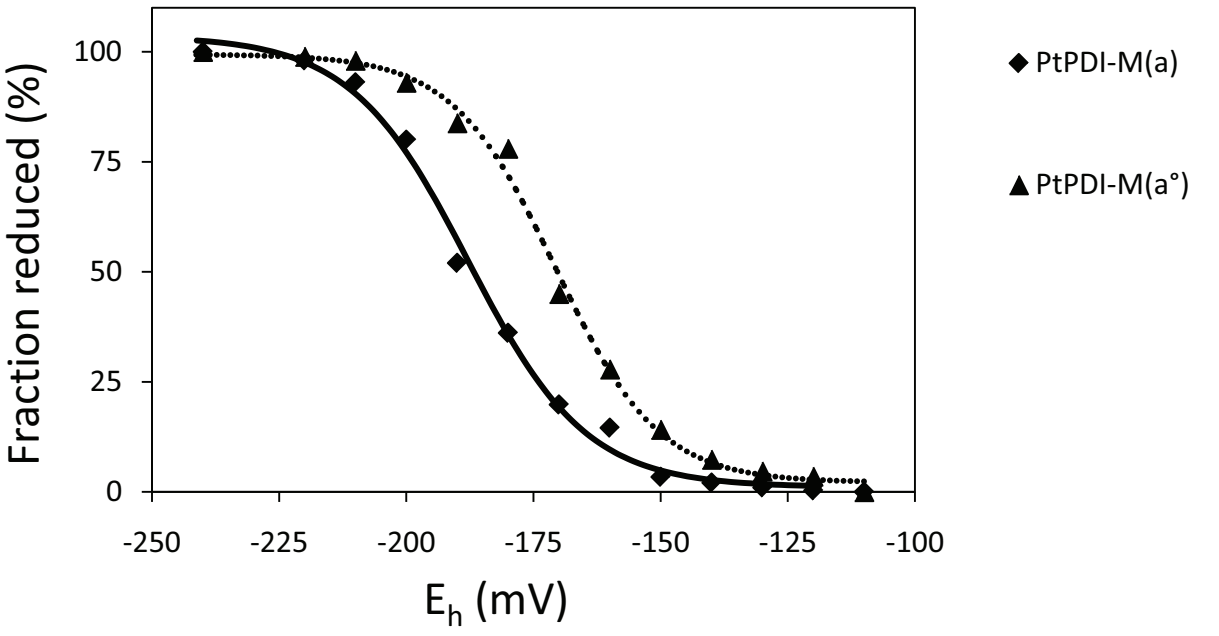
100
75
50
25
0
Fraction reduced (%)
-250
-225
-200
-175
-150
-125
-100
E_h (mV)
PtPDI-M(a)
PtPDI-M(a°)

Figure 3

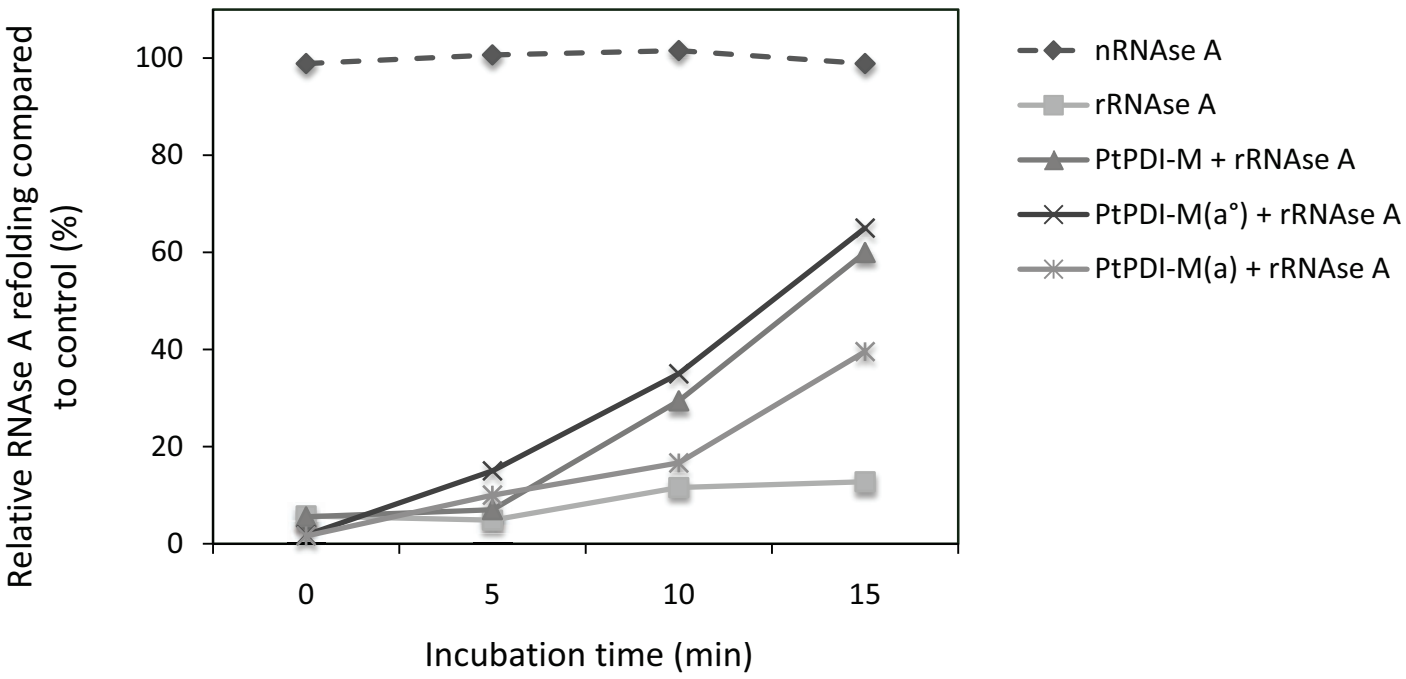
Relative RNAse A refolding compared to control (%)
100
80
60
40
20
0
0
5
10
15
Incubation time (min)
nRNAse A
rRNAse A
PtPDI-M + rRNAse A
PtPDI-M(a°) + rRNAse A
PtPDI-M(a) + rRNAse A

Figure 4

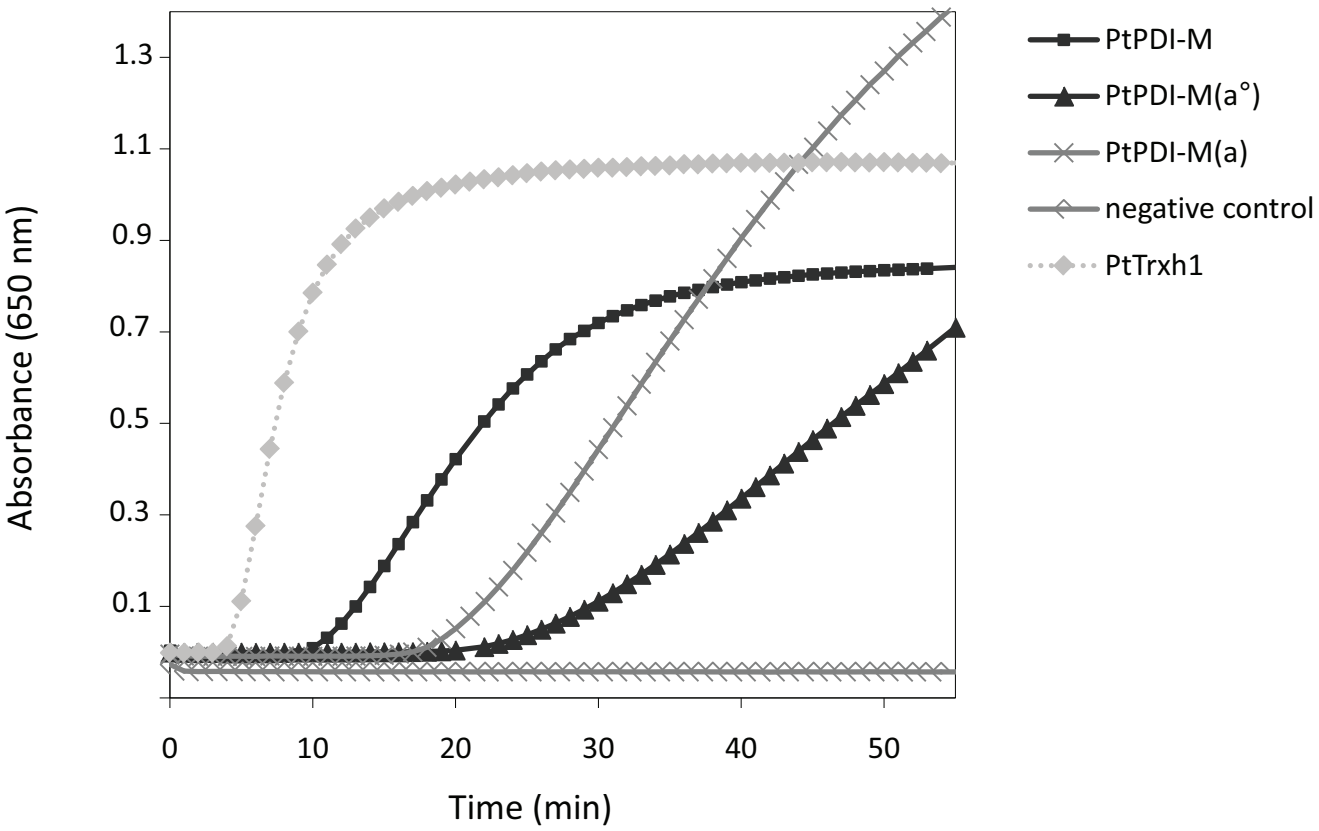
Absorbance (650 nm)
1.3
1.1
0.9
0.7
0.5
0.3
0.1
0
10
20
30
40
50
Time (min)
PtPDI-M
PtPDI-M(a°)
PtPDI-M(a)
negative control
PtTrxh1

Figure 5

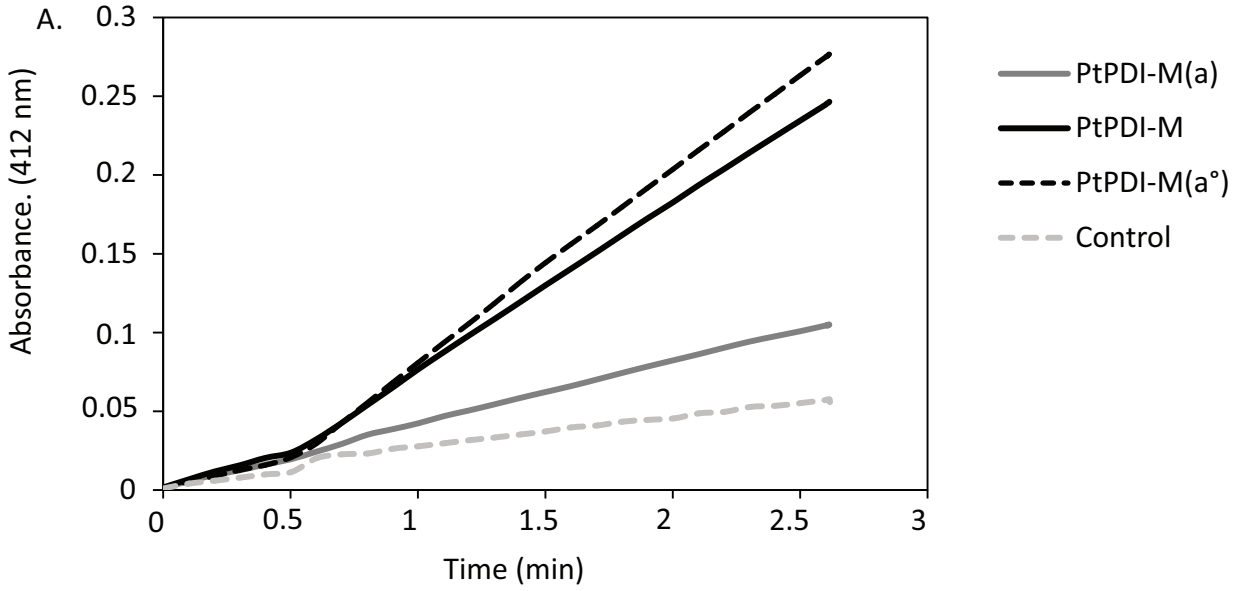
A.
Absorbance. (412 nm)
0.3
0.25
0.2
0.15
0.1
0.05
0
0
0.5
1
1.5
2
2.5
3
Time (min)
PtPDI-M(a)
PtPDI-M
PtPDI-M(a°)
Control

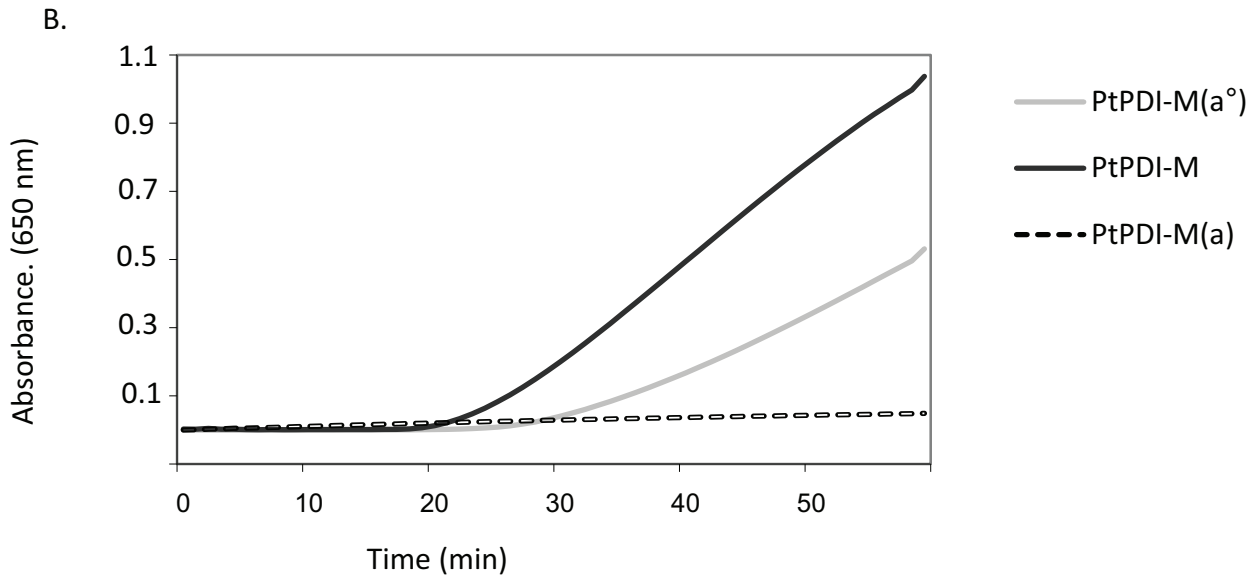
B.
Absorbance. (650 nm)
1.1
0.9
0.7
0.5
0.3
0.1
0
10
20
30
40
50
Time (min)
PtPDI-M(a°)
PtPDI-M
PtPDI-M(a)

Figure 6

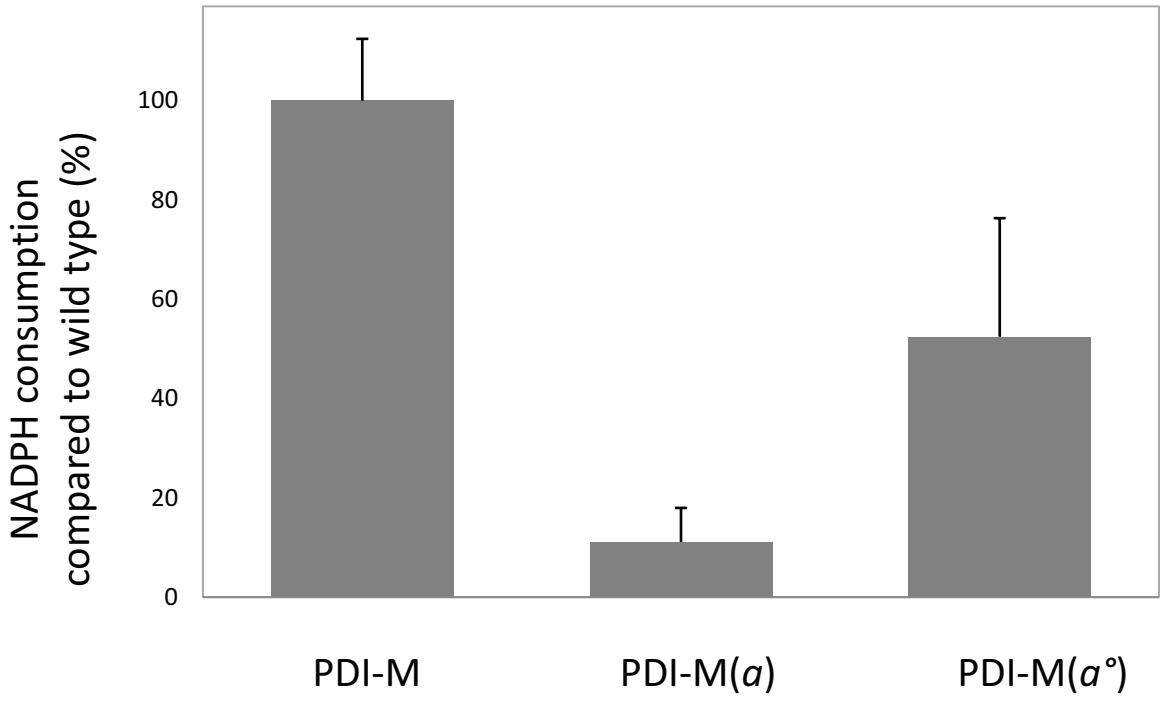
NADPH consumption compared to wild type (%)
100
80
60
40
20
0
PDI-M
PDI-M(a)
PDI-M(a°)

Figure 7

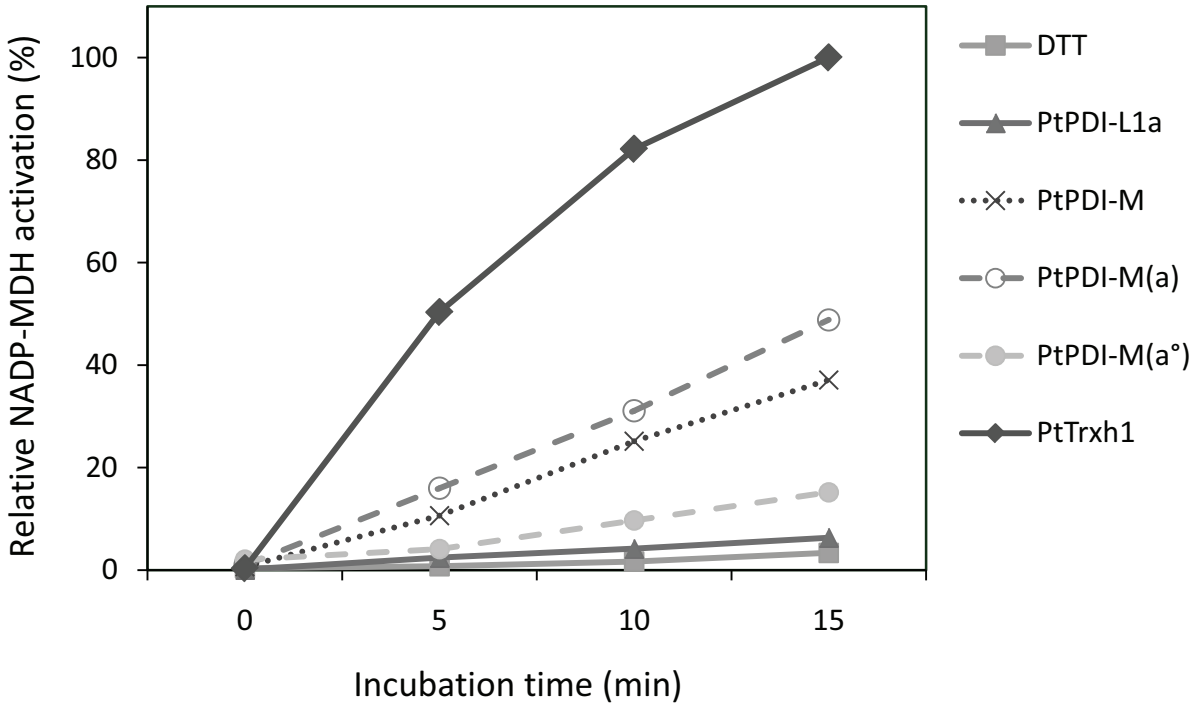
Relative NADP-MDH activation (%)
100
80
60
40
20
0
0
5
10
15
Incubation time (min)
DTT
PtPDI-L1a
PtPDI-M
PtPDI-M(a)
PtPDI-M(a°)
PtTrxh1

Figure 8

Discussions & perspectives

Les travaux présentés dans ce manuscrit, fruits de mes trois années de thèse, s'inscrivent dans la thématique de l'équipe «Réponse aux stress et régulation redox» visant à caractériser les relations structure-fonction de deux familles de protéines impliquées dans les réactions redox et appartenant à la superfamille des Trxs, les glutathion peroxydases et les protéine disulfure isomérases. Comme expliqué dans l'introduction, les Gpxs sont classées comme des enzymes glutathion-dépendantes sur la base de leur séquence primaire et tertiaire mais les Cys-Gpxs sont en fait régénérées par le système Trx. L'étude sur les Gpxs, préalable à mon arrivée, avait clairement démontré l'implication de deux résidus cystéines conservés dans leurs mécanismes catalytiques ainsi que l'accumulation de certaines isoformes lors d'un stress métallique induit par un traitement au cadmium (Navrot *et al.* 2006). De plus, l'obtention de la structure tridimensionnelle de la Gpx5 de peuplier a apporté des informations essentielles quant aux changements de conformation de cette protéine lors de son cycle catalytique et aux bases structurales de son interaction avec les Trxs (Koh *et al.* 2007). Concernant les PDIs, qui représentent un nouveau champ d'étude pour notre laboratoire, les données phylogénétiques, fonctionnelles, biochimiques et structurales ont principalement été obtenues chez *S. cerevisiae* et chez les mammifères mais au contraire, très peu de données existent pour les organismes photosynthétiques.

Ainsi, ce travail de thèse a consisté à approfondir nos connaissances sur les processus biochimiques impliqués dans la réactivité des Gpxs vis-à-vis des ses substrats (peroxides ou Trxs), mais également à initier l'étude des PDIs.

I. Dissection des caractéristiques mécanistiques et biochimiques de la Gpx5 de peuplier

I.1. La tétrade catalytique des Gpxs, plus qu'un modulateur du pKa de la Cys_P

Le site actif des Cys-Gpxs ou SeCys-Gpxs, également définis sous le terme tétrade catalytique, est généralement composé d'une Cys_P ou $SeCys_P$, d'une Gln, d'un Trp et d'une Asn. Les trois derniers acides aminés cités ont été proposés comme essentiels au maintien du faible p*Ka* du résidu peroxydatique (Maiorino *et al.* 1995, 1998; Schlecker *et al.* 2007; Scheerer *et al.* 2007). Néanmoins, quelques isoformes possèdent un Glu à la place de la Gln (Navrot *et al.* 2006; Koh *et al.* 2007; Maiorino *et al.* 2007b). Un travail de mutagenèse dirigée comparant la réactivité des protéines sauvage (Glu_{79}) et mutante (Gln_{79}), a permis de montrer que la présence d'une Gln pouvait constituer un avantage dans la réduction de certains peroxydes organiques tels que le *t*-butyl hydroperoxyde (Article 2). Du fait de l'absence de modification du potentiel d'oxydoréduction, du p*Ka* de la Cys_P, et malgré la spécificité de l'impact de cette substitution sur un substrat non physiologique, une hypothèse que nous pouvons avancer pour expliquer cette meilleure efficacité catalytique concerne le rôle de la fonction carboxy-amide permettant une meilleure polarisation de la liaison peroxyl (ROOH → $RO^{\delta+}$-$O^{\delta-}$H) facilitant ainsi sa réduction par la Cys_P (Toppo *et al.* 2009; Flohé *et al.* 2010). Cependant, une étude sur la SeCys Gpx4 humaine, une isoforme glutathion dépendante et préalablement mutée $SeCys_P$ → Cys_P, a montré que la substitution de la Gln (Gln_{81} pour la Gpx4) par une Asn diminue fortement la réactivité de la protéine (Scheerer *et al.* 2007). Les différences notables entre la Gpx5 et la Gpx4 humaine laissent toutefois croire que la caractérisation de la substitution Glu_{79} → Asn chez la Gpx5 apporterait des informations sur le fonctionnement de la tétrade catalytique. Par contre, la mutation de la Gln par un Glu dans cette Gpx4 humaine engendre bien des effets opposés à ceux observés avec la Gpx5, à savoir une diminution de l'efficacité catalytique d'un facteur 6 pour le *t*-BOOH (Scheerer *et al.* 2007).

Afin de poursuivre l'étude de cette position spécifique au sein de la tétrade catalytique, il serait donc intéressant de :

(i) Evaluer l'impact de la mutation Glu_{79} → Gln sur la réduction d'autres peroxydes tels les peroxynitrites ou les lipides peroxydés.

(ii) Substituer l'acide glutamique par un acide aspartique ou une asparagine, permettant de confirmer l'importance du groupement carboxy-amide.

(iii) Substituer l'acide glutamique par un acide aminé biochimiquement très différent et incapable de former des liaisons hydrogène (alanine ou glycine) pour confirmer que ce résidu est important pour les caractéristiques redox de la protéine (p*Ka* essentiellement).

Le *pKa* de la Cys_P a été mesuré dans de nombreuses thiol-peroxydases. Il est généralement compris entre 5.2 et 6.3 (Tableau 5). Dans tous les cas, cette valeur de *pKa* signifie que la Cys_P sera majoritairement sous forme déprotonée à pH physiologique. Cette valeur se situe dans la même gamme que les thiorédoxines, réducteurs parmi les plus efficaces mais est bien supérieure aux valeurs déterminées pour les Grxs par exemple. Il a été démontré récemment que pour les thiol-peroxydases, le *pKa* est bien sur important pour la capacité de ces enzymes à réduire des peroxydes, mais l'environnement protéique de cette cystéine et en particulier la formation d'un état de transition suite à la fixation du substrat est un autre paramètre essentiel (Ferrer-Sueta *et al.* 2011).

	Thiol-peroxidase	efficacité catalytique (M^{-1} s^{-1})	pKa de la Cys_P	Refs.
Saccharomyces cerevisiae	Tsa1	~10^7	5,4	Ogusucu et al. 2007
	Tsa2	~10^7	6,3	
Salmonella typhimurium	AhpC	~10^7	5,8	Nelson et al. 2008
Mycobacterium tuberculosis	AhpE	~10^5	5,2	Hugo et al. 2009
Xylella fastidiosa	PrxQβ	~10^7	6,2	Horta et al. 2010
Homo sapiens	Prx5	~10^5	5,2	Trujillo et al. 2007
Homo sapiens	Prx2	~10^7	5<pKa<6	Peskin et al. 2007
Drosophila melanogater	Gpx	~10^6	7,2*	Tossato et al. 2009
Populus trichocarpa	Gpx5	~10^5	5,2	Article 2

(*) prédiction

Tableau 5. Relation entre le *pKa* et l'efficacité catalytiques pour différentes Tpxs.

I.2. La dualité de fonction de la Cys_P

I.2.a. Rôle de la Cys_P dans les modifications structurales

Le travail sur l'état d'oxydation de la Cys_P a conduit à évaluer son importance dans la transition conformationnelle entre les formes réduite et oxydée de la Gpx5, que l'on retrouve chez un grand nombre de Tpxs (Koh *et al.* 2007; Maiorino *et al.* 2007a; Hall *et al.* 2009; Horta *et al.* 2010). Plusieurs hypothèses ont été envisagées concernant les causes de ce réarrangement. Cela pourrait provenir soit de la fixation du peroxyde soit de l'oxydation de la cystéine qui pourrait consti-

tuer un facteur déstabilisant de l'hélice-α2. D'ailleurs, sur la base de la structure de la Gpx5 de peuplier, il a été proposé que l'ionisation de la Cys_R (Cys_{92}), couplée à la présence de deux résidus Asp (Asp_{85} et Asp_{89}) sur 3 boucles successives de l'hélice-α2 formaient un motif (Cys-S^-/Asp-O^-/ Asp-O^-) fortement électronégatif jouant un rôle prépondérant dans la déstabilisation de l'hélice-α2 lors du mécanisme catalytique (Koh *et al.* 2007).

Pour répondre à ces deux principales hypothèses, un travail de mutagenèse sur différents acides aminés a été réalisé.

(i) La substitution de l'Asp_{89} par une Lys n'a modifié ni l'activité, ni le contenu en hélice-α de la Gpx5 (Article 2 et résultats non montrés). Il serait toutefois important d'étudier le rôle possible du centre chargé Cys_R/Asp_{85}/Asp_{89} dans la transition structurale par production d'un double mutant pour ces deux Asp.

(ii) La fixation du substrat sur un mutant pour la Cys_P (Cys_{44}/Cys_{73} → Ser) n'a pas induit de changements du contenu en hélice-α. Par contre, grâce à deux mutants (Cys_P/Cys_{73} → Ser et Cys_{73}/Cys_{92} → Ser), nous avons montré que l'oxydation de la Cys_P provoquait le changement conformationnel, de façon analogue à une PrxQ de *Xyllela fastidiosa* et une 1-CysPrx, AhpE, de *Mycobacterium tuberculosis* (Article 2, Hugo *et al.* 2009; Horta *et al.* 2010). Ce mécanisme semble ainsi pouvoir être étendu à plusieurs membres de la famille des thiol-peroxydases.

Dans ce contexte, il est important de mentionner que les données bibliographiques concernant les structures tridimensionnelles des Gpxs et des protéines de type Gpx, tels les tryparédoxine peroxydases de *Trypanosoma brucei* sont assez contradictoires. Dans la forme réduite de la PxII de *T. brucei* obtenue par cristallographie, l'hélice-α2 est présente alors que dans la forme réduite de la PxIII, une enzyme différant par seulement 1 résidu, la forme réduite ne présente pas cette hélice et les auteurs indiquent qu'ils n'observent pas de réarrangement conformationnel entre les formes réduites et oxydées (Melchers *et al.* 2007; Alphey *et al.* 2008). De plus, dans le cas de la forme réduite de la PxIII, les résidus formant la tétrade catalytique ne sont pas positionnés de manière adéquate pour la catalyse (Melchers *et al.* 2007). L'hélice-α2 n'a pas non plus été observée dans la forme réduite de la Gpx1 de *T. cruzi* mais le site actif dans ce cas n'est pas très bien défini et la protéine a été pré-oxydée par du t-BOOH et adopte une structure typique d'une forme oxydée (Patel *et al.* 2010). Les auteurs ont suggéré que le pont disulfure a été clivé par les rayons x. Finalement, de manière contradictoire à ce qui a été publié précédemment, l'étude d'un mutant Cys_{76} → Ser (résidu cystéinyl conservé chez certaines Gpxs mais non impliqué dans le mécanisme catalytique chez les isoformes de plantes) de la PxIII de *T. brucei* par des expérien-

ces de dichroisme circulaire indiquent que l'hélice-α2 est bien présente dans les formes réduites de l'enzyme WT et du mutant C76S (Muhle-Goll *et al.* 2010). Tous ces résultats semblent indiquer qu'une plasticité/flexibilté assez importante existe pour ces enzymes. Outre la forme oxydée, il se peut que plusieurs états réduits puissent exister et que, selon l'enzyme et l'organisme, la forme la plus « stable » ou la forme qui cristallise soit différente. Globalement, on peut proposer que les structures observées représentent différents états transitoires des Cys-Gpxs. Il pourrait exister une forme réduite désorganisée, en tous les cas où le site actif n'est trop bien défini et la tétrade catalytique n'est pas correctement positionnée (observée pour la PxIII). L'arrivée du substrat pourrait provoquer une réorganisation du site actif pour obtenir une forme enzymatiquement compétente de la protéine (observée pour la Gpx5). Puis la réduction du substrat, accompagnée de l'oxydation de la cystéine peroxydatique, contribue au changement conformationnel comme nos expériences le suggèrent. Bien que nos résultats ne semblent pas indiquer qu'il puisse exister deux formes de Gpx5 sous forme réduite, des études dynamiques par RMN sur la protéine de peuplier pourraient permettre de mettre en évidence plusieurs conformations à l'état réduit.

I.2.b. L'état d'oxydation de la Cys_P, un indice en faveur d'une multiplicité de fonctions des Gpxs de plantes?

Un des autres aspects étudiés dans ce travail est la susceptibilité de la protéine Gpx5 à l'inactivation, processus jusqu'à présent décrit seulement pour certains types de Prxs (Yang *et al.* 2002; König *et al.* 2003; Wood *et al.* 2003; Pascual *et al.* 2010). La perte d'activité observée pour la Gpx5 suite à la formation d'un acide sulfinique ou sulfonique sur la Cys_P, est un phénomène comparable à celui observé pour les 2-CysPrxs (Figure 51A) (König *et al.* 2003; Pascual *et al.* 2010). Chez les plantes, l'inactivation transitoire de la 2-CysPrx chloroplastique a été démontrée comme ayant un impact sur sa fonction puisque la forme S-O_2H (inactive) provoque une modification de l'état d'oligomérisation de la protéine et promeut une fonction chaperonne vis-à-vis de protéines impliquées dans la photosynthèse ou le métabolisme carbonée. De plus, par analogie à la théorie «*hydroperoxide floodgate*» établie pour les 2-CysPrxs eucaryotiques, on peut proposer que l'inactivation des Cys-Gpxs eucaryotiques pourrait jouer un rôle dans la signalisation en réponse au peroxyde d'hydrogène, en provoquant une accumulation limitée dans le temps et dans l'espace de ce produit qui permettrait aux cellules de mettre en place les voies de réponse à un stress oxydant (Wood *et al.* 2003) Parmi les Prxs, il a été montré que l'inactivation était spécifique des 2-CysPrxs eucaryotiques contenant dans leurs séquences deux motifs structuraux GGLG et YF qui réduisent la mobilité de l'hélice-α en C-terminale de la protéine (Wood *et al.* 2003; Pas-

cual *et al.* 2010). Ceci est à l'origine une demi-vie plus longue de la forme S-OH de la Cys_P augmentant la probabilité d'une suroxydation sous forme S-O_2H. Le fait que cette Gpx de plante peut être suroxydée ouvre donc potentiellement des perspectives nouvelles sur la fonction physiologique des Gpxs chez les organismes photosynthétiques.

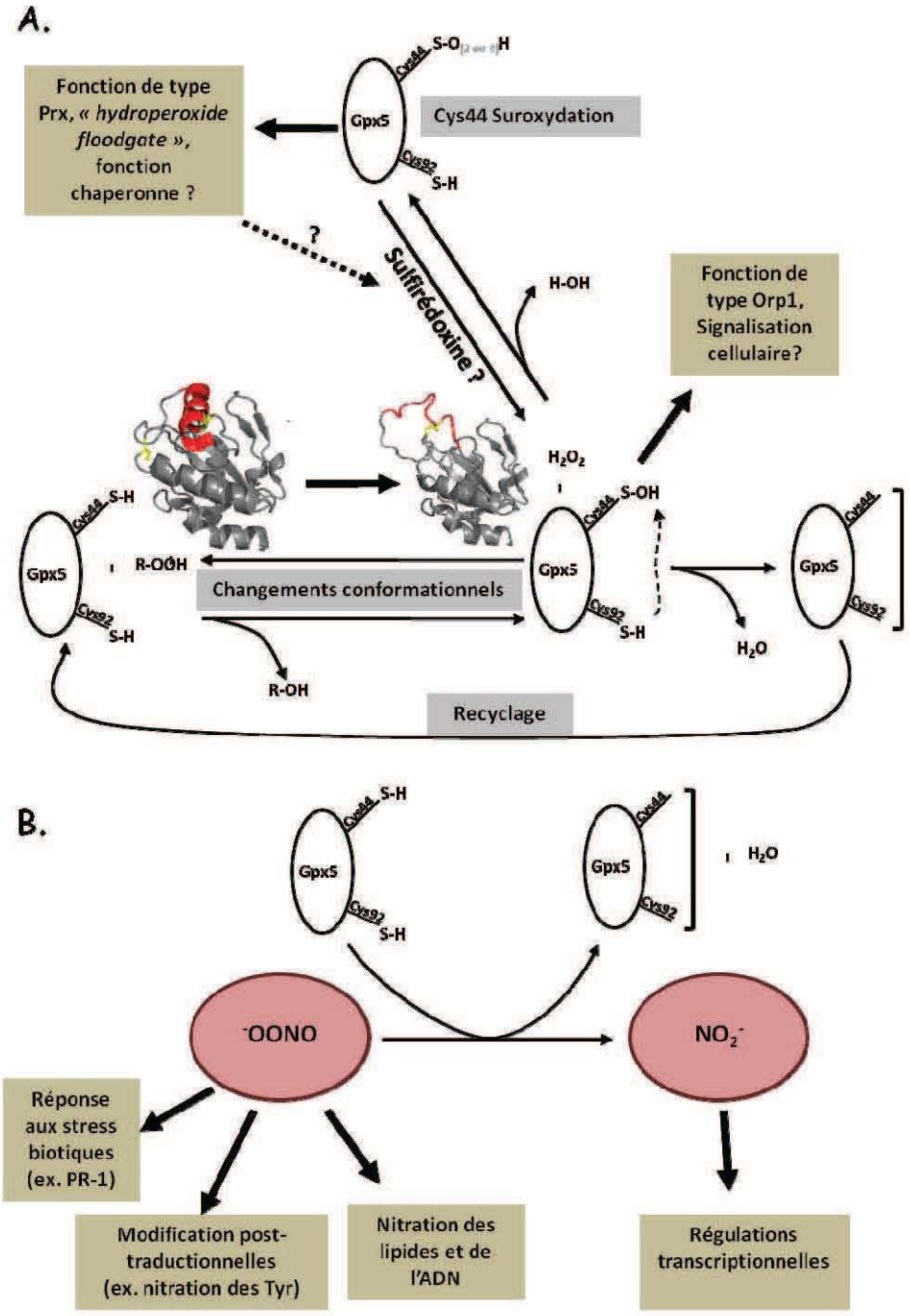

Figure 51. Bilan de mon travail sur la Gpx5 de peuplier.
A. Schéma du mécanisme catalytique de la Gpx5 de peuplier mentionnant l'implication de l'oxydation de la Cys_P comme étape essentielle du changement de conformation. Sont également représentés les différents états de la Cys_P (sulfénique et sulfinique/sulfonique) et les rôles physiologiques déterminés pour d'autres Tpxs. B. Implications fonctionnelles et physiologiques de la détoxication des péroxynitrites par la Gpx5 de peuplier.

Par ailleurs, plusieurs Tpxs peuvent interagir avec et réguler la localisation subcellulaire et donc l'activité de facteurs de transcription de la famille AP1 (Delaunay *et al.* 2000; Vivancos *et al.* 2005; Bozonet *et al.* 2005; Iwai *et al.* 2010). En particulier, l'interaction YAP1/Gpx3 (Orp1) chez *Saccharomyces* a été finement détaillée. L'acide sulfénique formé sur la Cys_P après réduction d'une molécule de peroxyde est réduit par une cystéine de YAP1 plutôt que par la Cys_R de Gpx3 (Figure 51A) (Delaunay *et al.* 2000; Ma *et al.* 2007; Paulsen & Carroll 2009). Cette liaison intermoléculaire sera elle-même réduite par une autre cystéine de YAP1, aboutissant à la formation d'un pont disulfure intramoléculaire sur le facteur de transcription, empêchant l'export du facteur de transcription hors du noyau et provoquant une forte augmentation de la transcription des gènes de réponse au stress oxydant (Delaunay *et al.* 2000). Le changement conformationnel observé entre les formes réduites et oxydées des Gpxs est certainement à l'origine d'une durée de vie plus longue de l'acide sulfénique qui pourrait favorisé dans certaines conditions sa réduction par YAP1 plutôt que par la cystéine de recyclage.

Les futurs travaux qu'il serait intéressant de réaliser concernant l'état d'oxydation de la Cys_P et les rôles physiologiques des Gpxs de plantes se répartissent en plusieurs axes:

(i) Confirmer que l'inactivation par suroxydation est commune aux Cys-Gpxs et rechercher les facteurs structuraux liés à cette inactivation et en particulier ceux liés au déroulement de l'hélice-α2.

(ii) Etudier l'état d'oligomérisation de la Gpx5 *in vitro* et *in vivo* en réponse à des oxydants et ainsi déterminer si, comme décrit pour les 2-CysPrxs, l'état d'oxydation de la Cys_P pouvait avoir un impact sur la formation d'oligomères en relation avec une fonction différente de la protéine (fonction de chaperonnes). Nous pourrions également déterminer si, même en absence d'oligomères, cette protéine est en mesure d'avoir une activité chaperonne sous forme inactive.

(iii) Conformément à l'hypothèse de l'«*hydroperoxide floodgate*», l'implication des Gpxs dans des processus de signalisation cellulaire nécessite que leur inactivation soit transitoire. Ainsi, il est indispensable de savoir si les Cys-Gpx suroxydées peuvent être régénérées par les sulfirédoxines (Biteau *et al.* 2003). L'isoforme de peuplier est disponible au laboratoire pour ce genre de tests. En parallèle, il faut étudier si ce cycle de suroxydation/régénération se produit *in vivo* en situation de stress par exemple.

(iv) Bien qu'à ce jour aucun facteur de transcription de type YAP1 n'a été caractérisé chez les plantes supérieures, plusieurs protéines (MSR, PDI) interagissant de manière redox avec

des Cys-Gpxs ont d'ores et déjà été identifiées (Kho *et al.* 2006; Lee *et al.* 2008). D'autres partenaires pourraient être identifiés par des approches de chromatographies d'affinité ou par co-immunoprcéipitation. Cette recherche de protéines cibles pourrait donc apporter des indications sur la possibilité pour les isoformes de plantes d'avoir un rôle analogue à la Gpx3 de levure.

I.3. Les modalités d'interaction entre la Gpx5 et la Trxh1.

Bien qu'il ait été proposé ou démontré pour certaines Prxs de type II, 1-Cys Prx ou PrxQ/BCP, que la régénération de l'enzyme était le résultat de l'attaque de la Cys_P par les Grxs ou Trxs, le recyclage de la Gpx5 s'effectue à l'aide d'une cystéine de recyclage de manière tout à fait comparable à celui rapporté pour la Gpx de la Drosophile (DmGPx) (Jeong *et al.* 2000; Rouhier *et al.* 2002; Maiorino *et al.* 2007a; Trujillo *et al.* 2007). La construction de deux modèles Gpx5-Trxh1 où la cystéine catalytique de la Trx est respectivement en complexe avec la Cys_P ou la Cys_R de la Gpx5, a permis de proposer que la formation d'un pont intermoléculaire avec la Cys_R est la forme la plus favorable en terme de calcul d'énergie libre (Koh *et al.* 2007). La formation de complexes hétérodimériques, associée à l'analyse par spectrométrie de masse des fragments obtenus après digestion trypsique, a confirmé cette hypothèse.

Sur cette même base de modélisation, Koh et collaborateurs ont proposé que le résidu Phe_{90} pourrait interagir avec le Trp_{37} de la Trxh1, utilisée comme modèle, permettant de stabiliser le complexe Gpx5/Trxh1 (Koh *et al.* 2007). L'importance de ce résidu a ainsi été vérifiée, par substitution par un Glu. Ainsi, bien que le recyclage de la Gpx5 par la Trxh1 dans un mutant Phe_{90}àGlu est toujours possible, une forte diminution de l'affinité (Km augmenté d'un facteur 5) entre les deux protéines a été observée (Article 2). Deux autres acides aminés ont été proposés comme stabilisateur du complexe Gpx5/Trxh1, la Pro_{81} de la Gpx5 ou la Pro_{39} de la Trxh1 (Koh *et al.* 2007). La mutation de ces résidus, seuls ou en combinaison, nous permettrait d'affiner nos connaissances sur l'interaction de la Gpx5 avec la Trxh1.

Un autre aspect concerne l'efficacité de recyclage de la Gpx5 par les Trxs. Le fait que les valeurs d'efficacité catalytique obtenues en conditions « *steady state* » et pré-« *steady state* » soient similaires indique que l'étape limitante de la réaction est l'oxydation de la Gpx mais pas le recyclage de la Gpx5 par le système Trx. De ce point de vue, la régénération de la Gpx5 par la Trx semble présenter des différences notables comparées à d'autres Prxs et aux MSRs. Dans le cas de la protéine bactérienne AhpC, l'oxydation de la protéine se déroule à une vitesse de 56 s^{-1} alors que les tests de réduction effectués en conditions « *steady state* » indiquent une vitesse de 10 s^{-1},

signifiant que l'étape de réduction par les Trx est limitante (Poole et Ellis, 1996; Parsonage *et al.* 2005, 2008). Des donnés encore plus précises ont été obtenues pour les MSRs, enzymes qui utilisent un mécanisme catalytique très similaire. Le mécanisme catalytique de ces enzymes peut également se décomposer en trois étapes, (1) réduction du substrat et formation d'un acide sulfénique sur la cystéine catalytique (2) formation d'un pont disulfure intramoléculaire s'accompagnant d'un réarrangement conformationnel et (3) régénération par la Trx (Boschi-Muller *et al.* 2008). Il a été démontré que l'étape (1) présentait un k_{cat} de 790 s^{-1} et de 85 s^{-1} pour les MSRA et MSRB de *N. meningitidis*, et que l'étape de réduction de ces 2 enzymes par la Trx présente un k_{cat} de 50 s^{-1} et de 5 s^{-1} lors de conditions cinétiques où l'enzyme effectue un seul cycle catalytique (Boschi-Muller *et al.* 2008). Cependant, les tests en conditions « *steady-state* » révèlent des k_{cat} de 3 s^{-1} et 1 s^{-1} respectivement pour ces 2 mêmes enzymes indiquant que l'étape limitante de la régénération des MSR par les Trxs se produit après le transfert des électrons depuis la Trx vers la MSR et concerne donc la dissociation du complexe MSR/Trx (Boschi-Muller *et al.* 2008).

I.4. Les rôles physiologiques des Gpxs dans la réponse au stress oxydant.

Les différentes études concernant les fonctions physiologiques des Gpxs de plantes démontrent que celles-ci sont impliquées dans les réponses à divers stress biotiques ou abiotiques. Par exemple, il a été démontre que les gènes codant pour l'ensemble des Gpxs chez *A. thaliana* étaient régulés de façon différentielle en réponse à différents stress biotiques mais également à différentes hormones végétales (Rodriguez Milla *et al.* 2003). De nombreuses données concernent le rôle des Gpxs dans le contexte photosynthétique. Il a été démontré, par des études transcriptionnelles de mutants KO ou de sur-expresseurs chez Arabidopsis (Gpx1 et Gpx7), Chlamydomonas (Gpxh) ou *Lycopersicum esculentum* (Cys-Gpx de mammifère), que les Gpxs jouaient un rôle dans le maintien de l'activité photosynthétique en réponse à différents stress abiotiques, et plus particulièrement en réponse à la production d'$^1O_2$ lors d'un stress photooxydant (Herbette *et al.* 2005; Fischer *et al.* 2006; Fischer *et al.* 2009; Chang *et al.* 2009). De plus, la délétion des deux isoformes chloroplastiques indique que ces protéines ont vraisemblablement un rôle développemental puisque le double mutant présente une morphologie altérée des cellules foliaires et des chloroplastes (Chang *et al.* 2009). Hors du contexte chloroplastique, l'étude de lignées KO ou de sur-expresseur pour la Gpx3 d'Arabidopsis démontre la double fonction de cette protéine, d'une part dans l'homéostasie des EAOs et d'autre part dans la signalisation ABA dépendante grâce a une interaction physique avec ABI2, une protéine phosphatase (Miao *et al.* 2006).

La capacité des Gpxs de plantes à réduite *in vitro* certaines ENRs telles que $OONO^-$ est un indice

supplémentaire en faveur d'un rôle plus étendue que la détoxication des EAOs, comme cela a été démontré pour certaines Prxs de plantes, humaines, bactériennes ou de levures (Bryk *et al.* 2000; Dubuisson *et al.* 2004; Ogusucu *et al.* 2007; Romero-Puertas *et al.* 2007; Trujillo *et al.* 2007; Horta *et al.* 2009). Les $OONO^-$ et le NO sont connus comme des molécules provoquant des modifications post-traductionnelles telles que la nitrosylation de résidus cystéine, qui a été démontré comme possible inactivateur de l'activité des Prxs de type II, ou la nitration des résidus tyrosine, interférant de ce fait potentiellement avec la signalisation cellulaire par phosphorylation (Figure 51B) (Schopfer *et al.* 2003; Romero-Puertas *et al.* 2007). Les auteurs ont démontré que le NO était en mesure de réguler l'activité de détoxication de la PrxIIE par S-nitrosylation aboutissant à son inactivation, provoquant ainsi une augmentation de la concentration intracellulaire en $OONO^-$ (Romero-Puertas *et al.* 2007). Ainsi, au même titre que certains types d'EAOs, cette molécule oxydante est aujourd'hui proposée comme molécule signal et toute enzyme régulant les niveaux de peroxynitrite se retrouve indirectement liée à ces phénomènes (Alamillo & García-Olmedo 2001; Romero-Puertas *et al.* 2007; Arasimowicz-Jelonek & Floryszak-Wieczorek, 2011).

L'étude de mutants de plantes (KO., K.Down ou sur-expresseurs) pour les différentes Gpxs représente certainement une étape incontouranble et complémentaire à la caractérisation biochimique effectuée au cours de ce travail de thèse. Seule la combinaison de ces différentes approches permettrait d'avoir une vision d'ensemble des rôles fonctionnelles des Gpxs de plantes que ceux-ci soient restreints à la détoxication des EAOs et ENRs ou soient étendus aux processus de signalisation cellulaire.

II. Les PDIs chez les organismes photosynthétiques

II.1. Analyse phylogénétique et classification

L'avancée principale de l'étude phylogénétique a été la mise en place d'une nomenclature adaptable à l'ensemble des organismes photosynthétiques que nous avions sélectionnés (Article 1). En effet, trois études majeures avaient déjà proposé différentes nomenclatures des PDIs (Houston *et al.* 2005; Lu & Christopher, 2008; d'Aloisio *et al.* 2010). Néanmoins, deux de ces études ne considéraient que les plantes supérieures, et parfois même un pool de PDI incomplet (Houston *et al.* 2005; Lu & Christopher, 2008). La dernière étude en date, publiée par d'Aloisio et coll., la semaine précédent la soumission de notre article, prenait en considération un ensemble d'organismes assez variés pour établir une classification robuste (d'Aloisio *et al.* 2010). Cependant, cette étude présentait une nouvelle nomenclature qui ne tenait pas compte du travail effectué sur les PDIs de *Glycine max* (Wadahama *et al.* 2007; Kamauchi *et al.* 2008; Wadahama *et al.* 2008; Iwasaki *et al.* 2009). Nous avons donc choisi de conserver la nomenclature appliquée aux protéines caractérisées et de l'étendre à l'ensemble des PDIs des organismes photosynthétiques. Nous avons identifié 9 classes de PDIs chez ces organismes (A, B, C, D, E, F, L, M et S). Les classes L, M et S correspondent aux classes de protéines définies par Urade et coll. (Wadahama *et al.* 2007; Kamauchi *et al.* 2008; Wadahama *et al.* 2008; Iwasaki *et al.* 2009). Néanmoins ces 9 classes ne sont pas présentes chez tous les organismes photosynthétiques, les classes A et B étant spécifiques des plantes terrestres tandis que les classes D, E et F sont spécifiques des algues (Article 1).

En plus de la mise en place de cette classification, cette analyse a permis de montrer que deux classes de PDIs (L et C) sont présentes chez tous les organismes photosynthétiques verts des prasinophytes aux arbres (Article 1). Les PDI-L sont les protéines majoritaires avec une organisation modulaire de type *a-b-b'-a'*. Il a été proposé que RB60 (ou CrPDI-L, appartenant à la sous-classe 2) jouait un rôle de régulation redox pour la transcription du gène *psbA* codant pour une protéine constituante du photosystème II (Fromm *et al.* 1985; Trebitsh *et al.* 2000). De plus, il a également été proposé chez Arabidopsis, que la protéine AtPDI-L2a serait en mesure d'exercer une régulation redox dépendante des protéines impliquées dans la biogenèse des granules d'amidon foliaires (Lu & Christopher, 2006). Ainsi, la présence de certaines isoformes de la classe L chez les organismes photosynthétiques pourrait être en relation avec le maintien de la photosynthèse au sein du chloroplaste mais également avec les processus d'assimilation du carbone.

Concernant les protéines de la classe C qui sont composées de deux modules protéiques, un module à repliement Trx et un module de type COPII (pour ***CO**ated **P**rotein*). Ce module est spécifique de protéines impliquées dans le transport vésiculaire entre le RE et le Golgi (van Vliet *et al.* 2003; Appenzeller-Herzog et Hauri, 2006). Chez les mammifères, ce module se retrouve dans des protéines intégrées aux membranes du compartiment ERGIC (« ***E**ndoplasmic **R**eticulum to **G**olgi **I**ntermediate **C**ompartment* ») (Breuza *et al.* 2004; Hanton *et al.* 2005; Appenzeller-Herzog & Hauri, 2006). Ce compartiment, qui est absent chez les organismes photosynthétiques, est une structure vésiculaire dynamique chargée de stocker les protéines subissant les mouvements rétrograde ou antérograde depuis le RE vers le Golgi (Hanton *et al.* 2005; Appenzeller-Herzog & Hauri, 2006). Chez les mammifères et les champignons, aucune protéine de fusion comparable aux PDI-C n'a pu être identifiée, laissant supposer que ce type de protéine est spécifique des organismes photosynthétiques. De plus chez l'homme, il a été démontré que certaines PDIs (la protéine PDI ainsi que ERp44) agissaient de concert avec des protéines de type ERGIC (ERGIC 53) dans la répartition de la protéine SUMF1 (pour ***SU**lfatase **M**odifying **F**actor **1***) au sein de la voie de sécrétion mais également dans la régulation redox dépendante de l'activité de celle-ci (Fraldi *et al.* 2008). SUMF1 est une protéine à activité sulfatase dont la mutation est impliquée dans certaines pathologies humaine (Cosma *et al.* 2003). Ainsi, au sein de la voie de sécrétion spécifique des organismes photosynthétiques, c'est-à-dire en absence de compartiment ERGIC, la fusion entre un module de type PDI et un module COPII pourrait être un avantage déterminant dans la régulation redox dépendante de l'activité de certaines cibles mais également dans la régulation de leur répartition entre le RE, le Golgi ou la sécrétion de celle-ci.

La définition claire et précise de la diversité des PDIs chez les organismes réalisant la photosynthèse est une étape essentielle dans la compréhension de cette famille de protéines. Celle-ci nous a permis de sélectionner certains représentants pouvant présenter un intérêt particulier du fait de leur conservation chez les organismes photosynthétiques. De plus, la disponibilité croissante de génomes séquencés de divers organismes des différents règnes du vivant permettra, à l'avenir, de sélectionner des isoformes de PDIs présentant des distributions atypiques, pouvant révéler ainsi les spécificités de ces organismes et/ou protéines dans la maturation redox dépendante.

II.2. Caractérisation biochimique de trois isoformes de PDIs de peuplier

Suite à cette étude phylogénétique, les séquences codant pour cinq isoformes appartenant à quatre classes distinctes ont été clonées (Figure 52) (PtPDI-L1a, PtPDI-L3, PtPDI-A, PtPDI-C et

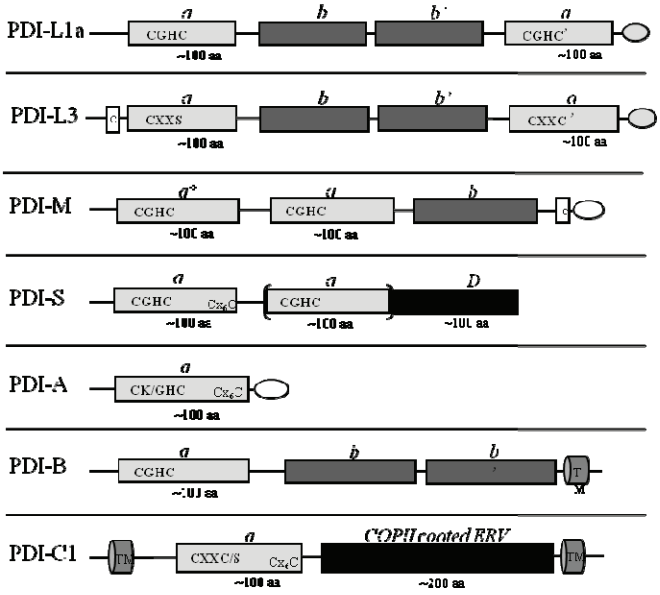

			Réduction		Oxydation	
Clonage	*Production*	*Purification*	*Insuline*	*MDH*	*NTR*	*RNAse A*
Oui	Oui	Oui	++	-	++	++
Oui	X	/	/	/	/	/
Oui	Oui	Oui	+	+	+	+
Non	/	/	/	/	/	/
Oui	Oui	Oui	-	-	-	-
Non	/	/	/	/	/	/
Oui	Oui	X	/	/	/	/

Figure 52. Les isoformes des PDIs du peuplier étudiées durant mon travail de thèse.

A. Les différentes classes de PDIs rencontrées chez le peuplier, caractérisées par des organisations modulaires distinctes. B. Tableau récapitulatif des étapes de clonage, de production, de purification des 5 isoformes sélectionnées, ainsi que les tests d'activités auxquels ils ont été soumis. Les mentions Oui ou Non correspondent au choix des isoformes dans notre étude, X correspond a un échec dans l'étape considérée, un – à une absence d'activité. Lorsqu'une activité a pu être mesurée (mention +), le nombre de + correspond à l'importance relative de l'activité entre les différents isoformes des PDIs.

PtPDI-M) (Article 3 et résultats non montrés). Trois de ces protéines ont pu être purifiées à homogénéité (PtPDI-L1a, PtPDI-A et PtPDI-M). Ainsi, un des futurs objectifs concernant l'étude comparative des PDIs sera de réussir à purifier les deux isoformes restantes et en particulier la protéine PtPDI-C qui pourrait présenter des caractéristiques biochimiques et fonctionnelles propres aux organismes photosynthétiques (Article 1).

II.2.a. Propriétés des protéines sauvages vis-à-vis de tests classiques d'activité PDI

Nous avons procédé à la caractérisation biochimique des isoformes que nous avons réussi à purifier dans le cadre de tests classiques des protéines dites « redoxines » (Figure 52). Tout d'abord notons qu'aucune activité enzymatique n'a pu être mise en évidence pour la protéine PtPDI-A. Dans l'article 3, nous proposons deux hypothèses pouvant expliquer cette absence d'activité :

(i) le site de clivage de la séquence d'adressage pourrait être mal défini ce qui pourrait donc avoir un impact sur la stabilité et/ou l'activité de la protéine.

(ii) l'absence d'activité enzymatique envers des substrats classiques pourrait provenir d'une forte spécificité naturelle vis-à-vis de ses substrats physiologiques.

Les résultats obtenus pour les protéines PtPDI-L1a et PtPDI-M sont cohérents avec les données déjà publiées sur leurs homologues chez les mammifères chez lesquels la PDI classique présente une bien meilleure activité de maturation que la protéine P5 (ou CaBP1, homologue des PDI-M) (Article 3, Kramer *et al.* 2001; Kikuchi *et al.* 2002). L'origine de cette meilleure activité peut être expliquée par au moins deux hypothèses :

(i) premièrement, la PDI classique interagit avec ses substrats non repliés grâce à une surface hydrophobe principalement localisée au niveau du module *b'* (Maattanen *et al.* 2006; Kozlov *et al.* 2010b). A ce jour, aucune donnée n'a confirmé la présence de cette surface hydrophobe dans les PDI-M ou les P5. De plus, des tests d'activités chaperonne ont montrés que la protéine P5 présentait une faible voire aucune activité de ce type quels que soient les substrats utilisés (Kramer *et al.* 2001; Kikuchi *et al.* 2002).

(ii) deuxièmement, nous avons déterminé les potentiels d'oxydoréduction des deux motifs CGHC de la protéine la PtPDI-M. Ces résultats indiquent que la PtPDI-M présente des potentiels d'oxydoréduction sensiblement plus réducteurs que les PDIs classiques (Article 3).

Ainsi, l'absence probable de sites de fixation de peptides hydrophobes, couplée à des potentiels d'oxydoréduction moins favorables à des réactions d'oxydation, peuvent expliquer la plus faible activité de la protéine PtPDI-M comparé à la PtPDI-L1a dans la maturation de la RNAse A ou l'oxydation de la NTR.

Les résultats concernant les réactions de réduction sont plus paradoxaux, en effet nous avons démontré que la PtPDI-L1a était plus efficace dans la réduction de l'insuline que la PtPDI-M. D'un autre côté, la PtPDI-L1a n'est pas en mesure de réduire la NADP-MDH tandis que la PtPDI -M présente une activité atteignant 40% de celle relevée pour une Trx (PtTrxh1, Article 3). Une des hypothèses que nous pouvons avancer pour expliquer cette différence est la nature des partenaires de ces deux protéines ainsi que leur mode d'action. La protéine P5 a été proposée comme partenaire d'une protéine chaperonne, appelée BiP et chargée de recruter des substrats non matures (Jessop *et al.* 2009a). Ce type d'interaction a déjà été proposé pour certaines PDIs et démontré pour la protéine ERp57 qui interagit avec la calnexine par le biais d'interaction ioniques

(Frickel *et al.* 2002, 2004; Jessop *et al.* 2009b). Il a également été proposé que la protéine P5 était spécialisée dans la réduction des ponts disulfure des protéines non matures (Jessop *et al.* 2009a). Ainsi cette spécialisation des protéines P5, orthologues des PDI-M, dans l'interaction avec des protéines natives pourrait expliquer l'efficacité de cette protéine chez le peuplier en comparaison avec la PtPDI-L1a dans la réduction de la NADP-MDH.

Une des clés de la caractérisation précise des spécificités de substrat des PDIs repose sur l'obtention de données structurales (Kozlov *et al.* 2010b). Malheureusement, aucun cristal n'a pu être obtenu à ce jour pour la PtPDI-L1a. Une des perspectives qui s'offrent à nous est la production et la purification de combinaisons de modules Trxs, en particulier de la PtPDI-M pour laquelle aucune donnée structurale, même partielle n'est aujourd'hui disponible. Deux aspects paraissent très importants dans cette protéine pour son interaction avec ses substrats. Les spécificités de substrat pourraient être définies par l'orientation des centres redox actifs (*a°-a*) par rapport au module *b* et/ou par le mode de liaison entre les modules *a°* et *a*, retrouvé également dans la protéine ERp72 (Kozlov *et al.* 2010a). Toutefois, sur la base de prédictions de structures (Article 1), le mode de liaison entre les module *a°* et *a* des P5 et des PDI-M semble être sensiblement différent de celui rencontré pour la protéine ERp72 de par la présence de deux brins β additionnels (Article 1; Kozlov *et al.* 2010a).

Enfin, bien que des expériences de complémentation fonctionnelle de levure ou d'*E. coli* ont été réalisées pour les protéines classiques et pour la protéine P5 des mammifères, de telles expériences pourront êtres réalisés pour les isoformes du peuplier. Plus particulièrement, la complémentation de l'oxydase strict DsbA ou de l'isomérase DsbC chez la bactérie *E. coli* pourrait apporter des informations sur l'activité de la PDI-A qui possède un seul domaine Trx lui conférant plus potentiellement ce type d'activité oxydase ou isomérase.

II.2.b. Recherche des spécificités des deux modules Trx *a°* et *a* de la protéine PtPDI-M

Un des aspects controversés concernant la caractérisation biochimique des PDIs est la recherche de spécificités attribuées à chacun des modules (Article 1; Appenzeller-Herzog & Ellgaard, 2008c). Sur la base des expériences décrites dans l'article 3 sur les mutants de la PtPDI-M, les modules *a°* et *a* de cette protéine semblent présenter des spécificités vis-à-vis des réactions d'oxydation ou de réduction (Figure 53). En effet, le module *a°* est le facteur majoritaire dans la maturation de la RNAse-A mais également dans l'oxydation de la NTR (Article 3; Kramer *et al.* 2001; Kikuchi *et al.* 2002). Au contraire, le motif CGHC du module *a* est plus efficace dans la ré-

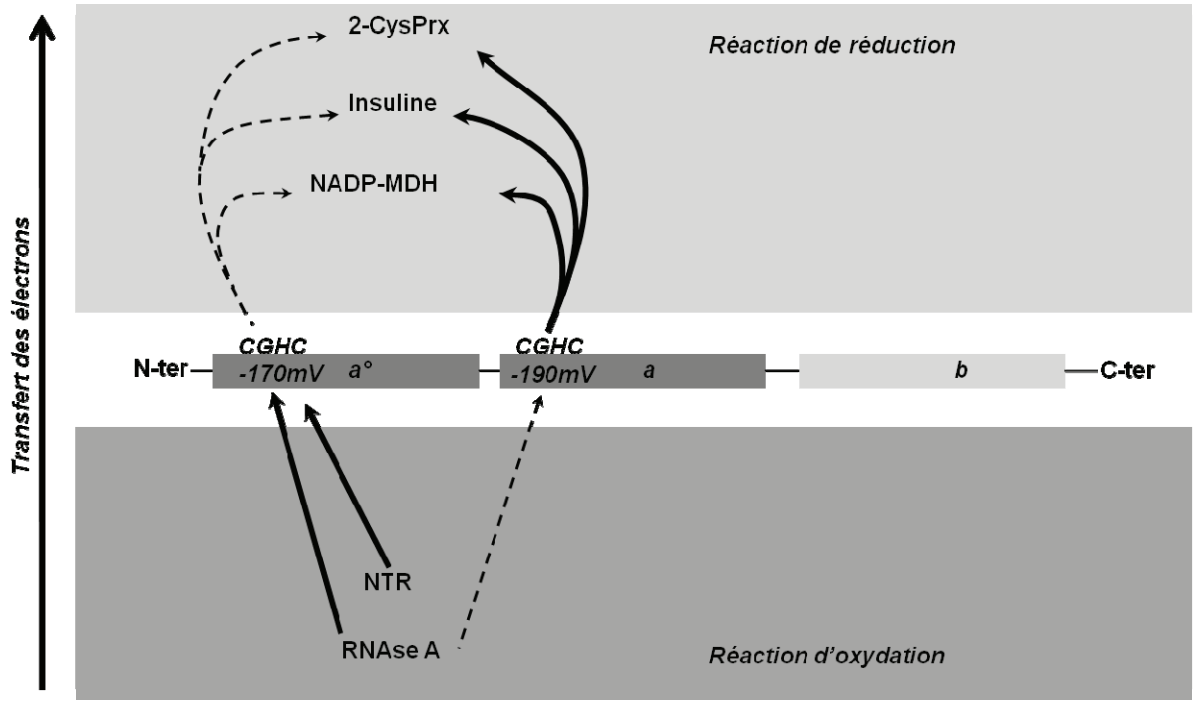

Figure 53. Les spécificités redox des modules *a°* et *a* de la protéine PDI-M du peuplier.

duction de l'insuline en présence de DTT, dans l'activation de la MDH mais également dans le recyclage des 2-CysPrxs (Article 3). Ces spécificités de catalyse pourraient provenir de caractéristiques biochimiques liées à des variations dans la nature des acides aminés chargés de moduler le *pKa* de la Cys_C dans les protéines de la famille des Trxs (voir discussion article 3).

Pour répondre à ce point, une étude de mutagenèse dirigée consistant à inter-convertir les caractéristiques de séquences des modules respectifs pourrait nous éclairer sur leurs rôles dans la catalyse. Alternativement, si les spécificités ne sont pas propres aux séquences des modules mais à leur position dans la protéine, nous pourrions également produire une protéine avec les modules *a°* et *a* inter-changés dans la séquence.

Outre ces aspects, nous avons pu mettre en évidence que la mutation d'un des modules avait un impact sur l'activité du second, comme illustré par les tests NTR dans la réduction de l'insuline ou de la 2-CysPrx (Article 3). Ainsi, bien que nos résultats ne puissent catégoriquement indiquer qu'il y ait un transfert d'électrons entre le module *a°* et *a*, un challenge actuel est de mettre en évidence un possible dialogue moléculaire entre ceux-ci. Nous avons tenté de mettre en évidence ce transfert en réalisant les tests en présence des deux mutants simultanément mais ces résultats n'étaient pas concluants (résultats non montrés). Une des explications concernant l'absence de dialogue moléculaire entre les protéines PtPDI-M(*a°*) et PtPDI-M(*a*) lors de nos tests,

pourrait provenir du fait que ces échanges sont intramoléculaires, rendant difficile leur mise en évidence entre deux protéines séparées. Une des possibilités serait de produire les module *a°* et *a* séparément et d'évaluer leur capacité a échanger leurs électrons. Cette expérience nous permettrait de nous affranchir des contraintes d'encombrement spatial dues à la présence de plusieurs modules Trxs dans un même polypeptide.

II.2.c. La versatilité des réactions catalysées *in vitro* par les PDIs, un aperçu de leur activité *in planta* ?

Depuis l'émergence des techniques de biologie moléculaire, les différentes réactions catalysées par les PDIs ont pu être déterminées *in vitro*. Ainsi depuis les expériences de Holmgren et coll. nous savons que les PDIs sont en mesure de catalyser certaines réactions longtemps supposées comme spécifiques des Trxs (Lundström & Holmgren, 1990). Néanmoins, du fait de leur localisation dans la RE et de leur implication dans la maturation des protéines non matures, les donnés biochimiques vis-à-vis de cette famille de protéine concernaient principalement des réactions d'oxydation ou d'isomérisation (Darby *et al.* 1998; Kramer *et al.* 2001; Kikuchi *et al.* 2002; Tian *et al.* 2006). De ce fait, peu d'informations sur les propriétés réductases intrinsèques aux motifs CGHC des PDIs étaient connues. De plus, les études de protéomiques systématiques sur différents compartiments subcellulaires a permis de montrer que les PDI étaient présentes aux niveaux des chloroplastes, des mitochondries, des noyaux, de la vacuole ou des membranes plasmiques des cellules, laissant entrevoir une grande plasticité de localisation subcellulaire et potentiellement de fonctions physiologiques (Sweetlove *et al.* 2002; Friso *et al.* 2004; Heazlewood *et al.* 2004; Kleffmann *et al.* 2004; Bayer *et al.* 2006; Jaquinod *et al.* 2007; Mitra *et al.* 2009). Originellement proposées comme résiduelles due aux similarités entre les Trx et les PDIs, l'activité réductase des PDIs, parfois importante, présente aujourd'hui un intérêt tout particulier puisqu'elle pourrait être importante physiologiquement pour la réduction de différents substrats (Lundström & Holmgren 1990; Wajih *et al.* 2007; Tavender, Springate, *et al.* 2010; Nguyen *et al.* 2011). Ainsi, l'étude systématique des interactions possibles des PDIs avec des partenaires connus des rédoxines, comme nous le proposons dans notre article 3 avec la NADP-MDH, pourrait apporter des informations complémentaires sur leurs possibles fonctions physiologiques.

Annexes

Article 4

Obligate biotrophy features unraveled by the genomic analysis of rust fungi

Obligate biotrophy features unraveled by the genomic analysis of rust fungi

Sébastien Duplessis[a,1,2], Christina A. Cuomo[b,1,2], Yao-Cheng Lin[c], Andrea Aerts[d], Emilie Tisserant[a], Claire Veneault-Fourrey[a], David L. Joly[e,3], Stéphane Hacquard[a,4], Joëlle Amselem[f], Brandi L. Cantarel[g], Readman Chiu[h], Pedro M. Coutinho[g], Nicolas Feau[e,5], Matthew Field[h], Pascal Frey[a], Eric Gelhaye[a], Jonathan Goldberg[b], Manfred G. Grabherr[b], Chinnappa D. Kodira[b,6], Annegret Kohler[a], Ursula Kües[i], Erika A. Lindquist[d], Susan M. Lucas[d], Rohit Mago[j], Evan Mauceli[b], Emmanuelle Morin[a], Claude Murat[a], Jasmyn L. Pangilinan[d], Robert Park[k], Matthew Pearson[b], Hadi Quesneville[f], Nicolas Rouhier[a], Sharadha Sakthikumar[b], Asaf A. Salamov[d], Jeremy Schmutz[d], Benjamin Selles[a], Harris Shapiro[d], Philippe Tanguay[e], Gerald A. Tuskan[d,l], Bernard Henrissat[g], Yves Van de Peer[c], Pierre Rouzé[c], Jeffrey G. Ellis[j], Peter N. Dodds[j], Jacqueline E. Schein[h], Shaobin Zhong[m,7], Richard C. Hamelin[e], Igor V. Grigoriev[d], Les J. Szabo[m,n,1], and Francis Martin[a,1]

[a]Unité Mixte de Recherche 1136, Institut National de la Recherche Agronomique/Nancy Université, Interactions Arbres/Micro-organismes, Centre de Nancy, 54280 Champenoux, France; [b]Broad Institute of Massachusetts Institute of Technology and Harvard University, Cambridge, MA 02142; [c]Department of Plant Systems Biology, Vlaams Instituut voor Biotechnologie, B-9052 Ghent, Belgium; [d]US Department of Energy Joint Genome Institute, Walnut Creek, CA 94598; [e]Natural Resources Canada, Ste-Foy, QC, Canada G1V 4C7; [f]Institut National de la Recherche Agronomique, Unité de Recherche Génomique Info, 78026 Versailles Cedex, France; [g]Unité Mixte de Recherche 6098, Centre National de la Recherche Scientifique–Universités Aix-Marseille I and II, Marseille, France; [h]Genome Sciences Centre, British Columbia Cancer Agency, Vancouver, BC, V5Z 4S6 Canada; [i]Division of Molecular Wood Biotechnology and Technical Mycology, Büsgen-Institute, University of Göttingen, Büsgenweg, 37077 Göttingen, Germany; [j]Commonwealth Scientific and Industrial Research Organization, Plant Industry, Canberra, ACT 2601, Australia; [k]Plant Breeding Institute Cobbitty, University of Sydney, Camden, NSW 2570, Australia; [l]Biosciences Division, Oak Ridge National Laboratory, Oak Ridge, TN 37831-6422; [m]Department of Plant Pathology, University of Minnesota, St. Paul, MN 55108; and [n]Cereal Disease Laboratory, Agricultural Research Service, US Department of Agriculture, St. Paul, MN 55108

Edited by Paul Schulze-Lefert, Max Planck Institute for Plant Breeding Research, Cologne, Germany, and approved March 31, 2011 (received for review January 5, 2011)

Rust fungi are some of the most devastating pathogens of crop plants. They are obligate biotrophs, which extract nutrients only from living plant tissues and cannot grow apart from their hosts. Their lifestyle has slowed the dissection of molecular mechanisms underlying host invasion and avoidance or suppression of plant innate immunity. We sequenced the 101-Mb genome of *Melampsora larici-populina*, the causal agent of poplar leaf rust, and the 89-Mb genome of *Puccinia graminis* f. sp. *tritici*, the causal agent of wheat and barley stem rust. We then compared the 16,399 predicted proteins of *M. larici-populina* with the 17,773 predicted proteins of *P. graminis* f. sp *tritici*. Genomic features related to their obligate biotrophic lifestyle include expanded lineage-specific gene families, a large repertoire of effector-like small secreted proteins, impaired nitrogen and sulfur assimilation pathways, and expanded families of amino acid and oligopeptide membrane transporters. The dramatic up-regulation of transcripts coding for small secreted proteins, secreted hydrolytic enzymes, and transporters *in planta* suggests that they play a role in host infection and nutrient acquisition. Some of these genomic hallmarks are mirrored in the genomes of other microbial eukaryotes that have independently evolved to infect plants, indicating convergent adaptation to a biotrophic existence inside plant cells.

comparative genomics | plant pathogen | basidiomycete | evolution | rust disease

Rust fungi (Pucciniales, Basidiomycota) are a diverse group of plant pathogens composed of more than 120 genera and 6,000 species, and are one of the most economically important groups of pathogens of native and cultivated plants (1, 2). *Puccinia graminis*, the causal agent of stem rust, has caused devastating epidemics wherever wheat is grown (3), and a new highly virulent strain (Ug99) threatens wheat production worldwide (4). Similarly, epidemics of poplar leaf rust, caused by *Melampsora* spp., is a major constraint on the development of bioenergy programs based on domesticated poplars (5) as a result of the lack of durable host resistance (6, 7). Rust fungi are obligate biotrophic parasites with a complex life cycle that often includes two phylogeneticaly unrelated hosts (2). They have evolved specialized structures, haustoria, formed within host tissue to efficiently acquire nutrients and suppress host defense responses (8). Molecular features driving adaptations to an obligate biotrophic association with plant hosts are unknown. Whether the convergent biotrophic adaptation observed in bacterial parasites (9) and other lineages of microbial eukaryotes (e.g., microsporidia) (10) has led to functional specializations at the genome level (i.e., gene gain or loss, regulation of gene expression) remains to be determined. The recent report of the genome sequence of *Blumeria graminis*, an ascomycete biotroph pathogen responsible for barley powdery mildew, revealed a genome size expansion caused by transposon proliferation concomitant with dramatic reduction in gene content, i.e., genes encoding sugar-cleaving enzymes, transporters and assimilatory enzymes for inorganic nitrate and sulfur (11). Similarly, gene losses

Author contributions: S.D., C.A.C., G.A.T., I.V.G., L.J.S., and F.M. designed research; S.D., C.A.C., Y.-C.L., A.A., E.T., C.V.-F., D.L.J., S.H., J.A., B.L.C., R.C., P.M.C., N.F., M.F., P.F., E.G., J.G., M.G.G., C.D.K., A.K., U.K., E.A.L., S.M.L., R.M., E. Mauceli, E. Morin, C.M., J.L.P., M.P., H.Q., N.R., S.S., A.A.S., J.S., B.S., H.S., P.T., B.H., J.G.E., P.N.D., J.E.S., R.C.H., I.V.G., L.J.S., and F.M. performed research; R.P., Y.V.d.P., P.R., and S.Z. contributed new reagents/analytic tools; S.D., C.A.C., Y.-C.L., A.A., E.T., C.V.-F., D.L.J., S.H., J.A., B.L.C., R.C., P.M.C., N.F., M.F., P.F., E.G., J.G., M.G.G., C.D.K., A.K., U.K., E.A.L., S.M.L., R.M., E. Mauceli, E. Morin, C.M., J.L.P., M.P., H.Q., N.R., S.S., A.A.S., J.S., B.S., H.S., P.T., B.H., J.G.E., P.N.D., J.E.S., R.C.H., I.V.G., L.J.S., and F.M. analyzed data; and S.D., C.A.C., Y.-C.L., C.V.-F., D.L.J., S.H., N.F., P.F., A.K., U.K., C.M., N.R., P.T., B.H., P.N.D., R.C.H., I.V.G., L.J.S., and F.M. wrote the paper.

The authors declare no conflict of interest.

This article is a PNAS Direct Submission.

Data deposition: The sequences reported in this paper have been deposited in the GenBank database [accession nos. AECX00000000 (*M. larici-populina* 98AG31) and AAWC01000000 (*Puccinia graminis* f. sp. *tritici*)]; the data reported in this paper have been deposited in the Gene Expression Omnibus (GEO) database, www.ncbi.nlm.nih.gov/geo [accession nos. GSE23097 (*M. larici-populina* 98AG31) and GSE25020 (*Puccinia graminis* f. sp. *tritici*)].

Freely available online through the PNAS open access option.

[1]To whom correspondence may be addressed. E-mail: duplessi@nancy.inra.fr, cuomo@broadinstitute.org, les.szabo@ars.usda.gov, or fmartin@nancy.inra.fr.

[2]S.D. and C.A.C. contributed equally to this work.

[3]Present address: Agriculture and Agri-Food Canada, Pacific Agri-Food Research Centre, Summerland, BC, Canada V0H 1Z0.

[4]Present address: Max Planck Institute for Plant Breeding Research, 50829 Cologne, Germany.

[5]Present address: Unité Mixte de Recherche Biodiversity, Genes and Communities 1202, Institut National de la Recherche Agronomique, 33612 Cestas, France.

[6]Present address: Roche 454 Life Sciences, Branford, CT 06405.

[7]Present address: Department of Plant Pathology, North Dakota State University, Fargo, ND 58102.

This article contains supporting information online at www.pnas.org/lookup/suppl/doi:10.1073/pnas.1019315108/-/DCSupplemental.

Table 1. Assembly statistics for the dikaryotic genome of *M. larici-populina* (*Mlp*) 98AG31 and *P. graminis* f. sp. *tritici* (*Pgt*) CDL75-36–700-3, race SCCL

Parameter	*Mlp**	*Pgt*
Sequence coverage	6.9	12
Scaffold total, Mb	101.1	88.6
Scaffolds	462	392
Scaffold N50 length, Mb†	1.1	0.97
Scaffold N50†	27	30
Assembly in scaffolds > 50 kb, %	96.5	97.1
Contig sequence total, Mb	97.7	81.5
Contigs	3,254	4,557
Contig N50 length, kb†	112.3	39.5
Contig N50†	265	546
Base quality ≥ Q40, %	98.3	96.3
Gap content, %	3.4	8
GC content, %	41	43.3
Protein coding genes	16,399	17,773
Mean coding sequence length, nt	1,565	1,075
Mean exon number per gene	4.92	4.7
Mean exon length, nt	247	175
Mean intron length, nt	118	133
Mean intergenic length, nt	4,356	3,328
tRNAs	253	428

*Statistics for Mlp are based on the "main genome scaffolds" of the assembly; the "repetitive," "excluded," and "altHaplotype" scaffolds for Mlp (Dataset S1, Table S2) were not included.

†The N50 metric corresponds to the *N* largest scaffolds required to capture half of the total sequence. The N50 length is that of the smallest scaffold in the N50 set.

were observed in the genome of the oomycete *Hyaloperonospora arabidopsidis*, a biotroph parasite infecting *Arabidopsis thaliana*, as well as the diversification of genes encoding RXLR effector-like secreted proteins (12). Despite their phylogenetic distance, these two pathogens forming haustoria seem to share striking adaptation convergences to biotrophy. To determine the genetic features underlying pathogenesis and biotrophic ability of rust pathogens, we report here the genome sequences of the rust fungi *Melampsora larici-populina* and *P. graminis* f. sp. *tritici*.

Results and Discussion

Genome Sequencing, Gene Family Annotation, and Expression Analysis. We have sequenced the dikaryotic genomes of the poplar leaf rust fungus, *M. larici-populina*, and of the wheat stem rust fungus, *P. graminis* f. sp. *tritici*, by a Sanger whole-genome shotgun strategy (*SI Text, Genome Sequencing and Assembly*). The overall assembly sizes of the haploid genomes of *M. larici-populina* and *P. graminis* f. sp. *tritici* are 101.1 Mb and 88.6 Mb, respectively (Table 1). These genomes are much larger than the other sequenced basidiomycete genomes (13, 14), but no evidence for whole-genome duplication or large-scale dispersed segmental duplications was observed. The expanded size results from a massive proliferation of transposable elements (TEs), which account for nearly 45% of both assembled genomes (Figs. S1 and S2 and Dataset S1, Tables S3 and S4). Class I LTR retroelements are more abundant in *P. graminis* f. sp. *tritici*, whereas class II terminal inverted repeat (TIR) DNA transposons are prominent in *M. larici-populina*. Timing of TE activity by using sequence divergence of extant copies suggests that a major wave of retrotransposition in the *M. larici-populina* and *P. graminis* f. sp. *tritici* lineages occurred more than 1 Mya (*SI Text, Repeat Analysis*).

We predicted 16,399 and 17,773 protein-coding genes in *M. larici-populina* and *P. graminis* f. sp. *tritici*, respectively. The size of these proteomes is similar to the symbiotic basidiomycete *Laccaria bicolor* (14), but strikingly larger than the corn smut fungi *Ustilago maydis* and *Sporisorium reilianum*, two nonobligate pathogenic biotrophs that encode only approximattely 6,500 proteins (15, 16). Among the predicted proteins, only 41% and 35% in *M. larici-populina* and *P. graminis* f. sp. *tritici*, respectively, showed significant sequence similarity to documented proteins (BLASTP E-value $\leq 10^{-5}$; *SI Text, Gene Prediction and Annotation* and Fig. S3). To investigate protein evolution in *M. larici-populina* and *P. graminis* f. sp. *tritici*, we constructed families containing both orthologues and paralogues from a diverse set of ascomycetous and basidiomycetous fungi (*SI Text, Multigene Families and Evolutionary Analysis of Multigene Families*). The two genomes shared 3,984 orthologous Tribe-MCL families, which comprised 7,959 *P. graminis* f. sp. *tritici* genes and 7,875 *M. larici-populina* genes; 26% of the predicted protein families were lineage-specific, whereas 774 gene families were unique to these two rust fungi. Expansion of protein family sizes was prominent in both *M. larici-populina* and *P. graminis* f. sp. *tritici* (Fig. 1, Fig. S4, and Dataset S1, Tables S6–S8); several expanded protein families are lineage-specific, suggesting that important protein-coding innovation occurred in these lineages. Of the 5,045 *M. larici-populina* genes that have an orthologue in *P. graminis* f. sp. *tritici* (best reciprocal BLASTP hit, E-value $\leq 10^{-5}$), very few showed conservation of neighboring orthologues, suggesting there is little synteny between the genomes (*SI Text, Lack of Genome Duplication and Synteny Between* M. larici-populina *and* P. graminis *f. sp.* tritici, and Fig. S5). This is likely because of the expansion of the TE and massive reshuffling of the genomes as a result of recombination between TEs. In addition, within the rust fungi, *M. larici-populina* and *P. graminis* f. sp. *tritici* represent very divergent phylogenetic lineages (1). Gene family expansions also occurred in those genes

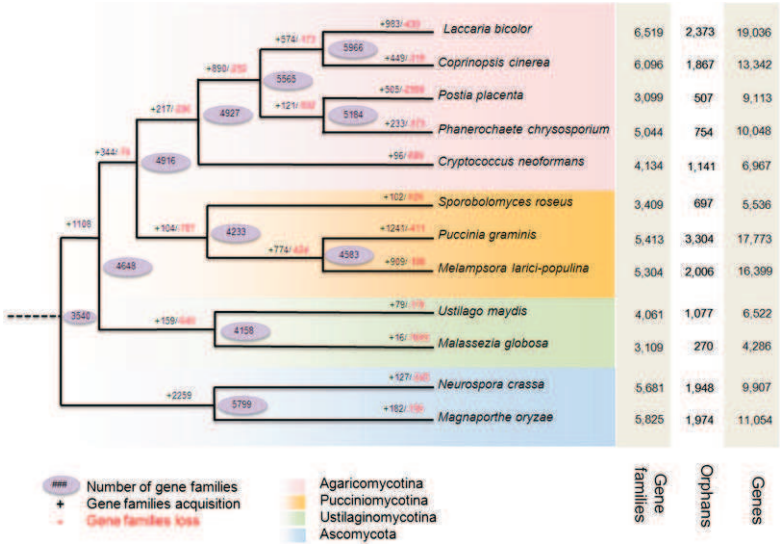

Fig. 1. Predicted pattern of gene families gain and loss in representative fungal genomes. The figure represents the total number of protein families in each species or node estimated by Dollo parsimony principle. The numbers on the branches of the phylogenetic tree correspond to expanded (*Left*, black), contracted (*Right*, red), or inferred ancestral (oval) protein families along each lineage by comparison with the putative pan-proteome. For each species, the number of gene families, orphan genes, and the total gene number are indicated on the right.

coding for oligopeptide membrane transporters (OPTs; Dataset S1, Table S18), copper/zinc superoxide dismutase (SOD; Dataset S1, Table S23), different types of glycosyl hydrolases, lipases, and peptidases, and several groups of predicted signaling genes, including kinases and transcription factors (Figs. S4 and S6–S8). Several gene families encoding leucine-rich repeat domain-containing proteins were expanded (Fig. S4*A*), and are potentially involved in protein–protein interactions in rust fungi. Different types of helicases are also represented in expanded gene families of rust fungi and could allow for an increased capability for DNA maintenance and repair. Strikingly, both rust fungi have expanded lineage-specific gene families encoding zinc-finger proteins (Fig. S4*B*), with significantly overrepresented nucleic acid binding and zinc ion binding gene ontology terms in both genes sets, which represent potential transcription factors (*SI Text*, *Multigene Families and Evolutionary Analysis of Multigene Families*, and Dataset S1, Tables S7 and S8). These results suggest that rust fungi possess a diverse potential to regulate and repair nucleic acid; targeted work will be required to decipher the roles of these proteins during the interaction with plant hosts. Although proliferation of TEs might have contributed to the expansion of gene families in rust fungi, no specific localization of particular gene families was identified in TE-rich regions of rust genomes, such as reported for effectors in other plant pathogens (17,18, 19) (*SI Text*, *Multigene Families and Evolutionary Analysis of Multigene Families*).

Seventy and 54% of the predicted genes of *M. larici-populina* and *P. graminis* f. sp. *tritici*, respectively, were detected by custom microarray transcript profiling of resting and germinating urediniospores, as well as infected leaves (*SI Text*, *Whole-Genome Exon Oligoarrays*). A significant proportion of the detected transcripts (18%) is differentially expressed (fold ratio ≥ 10.0; $P < 0.05$) in infected leaves, whereas only approximately 8.0% are specifically expressed *in planta* (*SI Text*, *Whole-Genome Exon Oligoarrays*). Transcripts coding for secreted peptidases and lipases, transporters of hexoses, amino acids, and oligopeptides, and carbohydrate-cleaving enzymes, such as chitin deacetylases and cutinases (Tables 2 and 3 and Dataset S1, Tables S12 and S16), are strikingly enriched (≥10-fold) *in planta*. However, the most highly up-regulated transcripts *in planta* (≥100-fold) are mainly comprised of lineage-specific transcripts, including those coding for small secreted proteins (SSPs; Fig. 2 and Dataset S1, Tables S10 and S14). These *in planta*-induced, lineage-specific genes are likely involved in the specific relationship established between these rust fungi and their respective hosts.

Rust Fungi Secretomes Contain Species-Specific Candidate Effectors. Microbial pathogens have evolved highly advanced mechanisms to engage their hosts in intimate contact and sabotage host immune responses by secreting effector proteins into host cells to target regulators of defense (20–22). Most SSPs that are specifically produced during plant infection are likely to be effectors that manipulate host cells to facilitate parasitic colonization, such as by suppressing plant innate immunity or enhancing nutrient availability (21). *In silico* gene prediction and manual annotation of SSP genes in *M. larici-populina* genome identified a set of 1,184 SSPs (*SI Text*, *Effector/Secretome*, and Dataset S1, Table S17), of which 74% are lineage-specific. *P. graminis* f. sp. *tritici* contains a similar number of 1,106 SSP genes, of which 84% are lineage-specific. In *M. larici-populina*, a total of 812 SSPs are organized in 169 families of two to 111 members (Dataset S1, Table S17); the largest family contains a highly conserved 10-cysteine pattern (Fig. S6*A*). In *P. graminis* f. sp. *tritici*, a total of 593 SSPs are or-

Table 2. Selection of *M. larici-populina* (*Mlp*) genes strongly up-regulated during poplar leaf infection

		Best BLAST hit		Expression level		96 hpi/urediniospores	
Mlp ID	Function	*Pgt* ID	GenBank accession no.	96 hpi	Urediniospores	Fold-change	*P* value
89465	Aspartic peptidase A1, secreted	PGTG_10570	XP_001881739	44,063	38*	1159.6	3.42×10^{-5}
94889	Lipase, secreted	PGTG_15782	XP_749106	27,318	36*	758.9	1.72×10^{-4}
123524	SSP, RTP homologue	PGTG_18022	ABS86408	49,354	68*	725.8	8.53×10^{-4}
106755	Glycosyl hydrolase, GH16, secreted	No hit	No hit	25,530	57*	447.9	7.42×10^{-5}
88574	Oligopeptide transporter, OPT	PGTG_17016	XP_001394363	38,726	88*	440.1	1.40×10^{-4}
86448	Transporter, AEC (Auxin Efflux Carrier) family	PGTG_06747	XP_759229	17,984	42*	428.2	1.33×10^{-4}
112330	α-Glycosidase, secreted, GH47	PGTG_09507	XP_001881296	14,561	41*	355.2	3.92×10^{-5}
36184	Amino acid permease, PIG2 homologue	PGTG_15547	XP_001873273	10,319	34*	303.5	2.10×10^{-4}
95696	Alanine aminotransferase	PGTG_07510	XP_001837651	11,018	37*	297.8	3.84×10^{-4}
53832	Thiamin biosynthesis enzyme, THI4 homologue	PGTG_01304	Q9UVF8	52,910	194	272.8	1.14×10^{-4}
39287	SSP, Cro r I homologue	No hit	AAF87492	7,916	30*	263.9	0.026
64764	SSP, HESP-376 homologue	No hit	No hit	7,596	35*	217.1	1.26×10^{-3}
89463	Subtilisin protease S8A, secreted	PGTG_18581	XP_001877576	18,072	87*	207.8	1.15×10^{-4}
40379	Sugar transporter HXT1, MFS	PGTG_15147	XP_001874568	12,387	61*	203.1	2.64×10^{-4}
91040	β-Glycosidase, endoglucanase, GH5	PGTG_17056	XP_001875020	7,212	36*	200.4	5.13×10^{-4}
124202	Secreted protein, AvrM-B homologue	No hit	ABB96259	3,764	27*	139.5	4.12×10^{-4}
67013	Thiamin biosynthesis enzyme THI1 homologue	PGTG_10151	ABK96768	35,825	274	130.8	1.51×10^{-4}
48366	Carotenoid ester lipase, secreted	PGTG_13346	XP_001875752	14,890	121	123.1	1.26×10^{-3}
40488	Chitin deacetylase, CE4	PGTG_09635	XP_774611	3,704	39*	95	1.10×10^{-3}
109896	Secreted protein related to plant expansins	PGTG_19856	XP_771894	4,998	52*	96.2	4.34×10^{-3}
60884	Glycosyltransferase GT18	PGTG_01151	XP_001884748	3,889	41*	94.9	8.36×10^{-4}
87910	Oligopeptide transporter, OPT	PGTG_15138	XP_001834544	12,366	160	77.3	6.03×10^{-5}
39227	Zinc transporter, CDF	PGTG_14264	CAE00445	3,210	43*	74.7	5.67×10^{-3}
25498	Chitin deacetylase, CE4	PGTG_09635	XP_774611	4,541	61*	74.5	3.41×10^{-3}
55212	SSP, HESP-735 homologue	No hit	ABB96276	2,221	33*	67.4	5.20×10^{-4}

Up-regulation in poplar infected leaves is assessed by comparing transcripts profiles to those from resting urediniospores. Poplar leaves were infected by *M. larici-populina* urediniospores and left for 96 hours postinoculation (hpi) under controlled conditions. At this stage, poplar rust pathogen has formed many haustoria in planta and sporulation has not yet occurred. Expression values are the means of three biological replicates for 96 hpi and urediniospores. Based on statistical analysis of normalized fluorescence levels, a gene was considered significantly regulated if it met two criteria (1): *t* test *P* value, 0.05 (ArrayStar; DNAStar); infected poplar leaves at 96 hpi versus urediniospores fold change > 10. Genes were selected on the basis of homology to a function, and hypothetical proteins or genes without homology of unknown function (exception of SSPs homologues of candidate rust pathogen effectors) were discarded. The complete list of significantly regulated genes is detailed in Dataset S1, Table S12.
*Below background expression level.

ganized in 164 families of two to 44 members and the largest family contains a highly conserved eight-cysteine pattern (Fig. S6*B*). Four of these proteins show evidence of haustorial expression in wheat rust, providing additional evidence that they are potentially effectors. This expansion of SSP genes in rust fungi is striking as SSP families account for approximately 10% of the expanded families in both rust genomes. Between 50% and 56% of the lineage-specific SSP genes are supported by ESTs or expression detected on the custom oligoarrays, which provide evidence to support these predicted genes of unknown function; additional genes could be specifically expressed during the sexual phase of the lifecycle (23), which was not explored here. Both *M. larici-populina* and *P. graminis* f. sp. *tritici* require an alternate host to complete their lifecycle and achieve sexual reproduction, and successful infection of the alternate host may involve a different set of SSP genes. Homologues of known effectors from *Melampsora lini*, such as haustorially expressed secreted proteins (HESPs) and the avirulence factors *AvrM*, *AvrL567*, *AvrP123*, and *AvrP4* from the flax rust fungus *M. lini* (8, 21), and the rust-transferred protein RTP1 from the bean rust pathogen (22), are present among highly up-regulated *M. larici-populina* transcripts (Table 2 and Dataset S1, Tables S10–S12). Interestingly, whereas 19 of the 21 *M. lini* HESPs (24) showed significant similarity to *M. larici-populina* SSP genes (BLASTP E-value $\leq 10^{-5}$), only nine showed similarity to *P. graminis* f. sp. *tritici* SSP genes, suggesting the presence of effector genes conserved in the Melampsoraceae and not shared within the Pucciniales order. By contrast, homologues of *Uromyces fabae RTP1* were detected in the poplar and the wheat rust genomes—three and seven, respectively—indicating the presence of conserved effectors families in the Pucciniales. Recently, [Y/F/W]xC motifs were reported in the N-terminal region of secreted proteins in the ascomycete *B. graminis*, an obligate biotroph of wheat, as well as in *Puccinia* spp. (25). Systematic search for these motifs in the poplar leaf and the wheat stem rust fungi showed that they were indeed abundant in SSPs but not restricted to the N-terminal region as in *B. graminis* (Fig. S6*A*; *SI Text*, *Effector/Secretome*). These motifs were also present in nonsecreted proteins related to zinc binding and nucleic acid binding (*SI Text*, *Effector/Secretome*), suggesting these motifs are also conserved in other cysteine-rich proteins. At least 43% of *M. larici-populina* and 40% of *P. graminis* f. sp. *tritici* SSPs are expressed in infected leaves. In *P. graminis* f. sp. *tritici*, PGTG_17547 matches the highest number of haustorial ESTs, and is similar in sequence to a predicted secreted protein (ADA54575) from the wheat stripe rust fungus, *Puccinia striiformis* (25); this protein is lineage-specific, sharing no significant similarity with proteins outside the Pucciniales. In both rust species, one highly *in planta*-expressed SSP [PGTG_13212, Joint Genome Institute (JGI) ID no. 85525] is similar in sequence to HESP-735 from the flax rust pathogen (24) (Dataset S1, Tables S12 and S14). SSPs are highly overrepresented in the mostly highly induced genes; 50 and 29 SSPs belong to the top 100 most highly transcriptionally up-regulated in infected poplar and wheat leaves compared with *M. larici-populina* and *P. graminis* f. sp. *tritici* urediniospores, respectively (Fig. 2 and Dataset S1, Tables S10 and S14). Most up-regulated SSP transcripts *in planta* were lineage-specific, as only 16% have an orthologue in both rust species, suggesting that these sequences are evolving at a very high rate. The specific location remains to be determined, whether up-regulated SSPs are expressed in infection hyphae and/or haustoria, and whether they remain in the cell wall or extrahaustorial matrix or are adressed to specific compartments of the host cell where they interact with their target proteins as shown for avirulence proteins in *M. lini* (8, 21). Similarly, some of the predicted SSP genes not expressed in urediniospores or *in planta* could act as specialized effectors during infection of the alternate host.

Table 3. Selection of *P. graminis* f. sp. *tritici* (*Pgt*) genes strongly up-regulated during wheat infection

		Best BLAST hit		Expression levels		Wheat/urediniospores	
Pgt ID	Function	*Mlp* ID	GenBank accession no.	Wheat	Urediniospores	Fold-change	*P* value
PGTG_12502	Amino acid permease	113062	No hit	31,670	68*	467.2	0.004
PGTG_15174	Differentiation-related protein Infp	No hit	AAD38996	23,002	50*	466.3	0.002
PGTG_07532	Amino acid permease	113062	No hit	13,666	47*	293.8	0.005
PGTG_07938	Invertase	44167	CAG26671	18,901	70*	271	3.63×10^{-4}
PGTG_17720	Zinc finger, C2H2 type	No hit	No hit	31,604	175	180.9	0.004
PGTG_16569	Multicopper oxidase, secreted	112024	BAG50320	18,825	114*	166.6	0.012
PGTG_15026	Lipase	96073	XP_001273241	21,088	229	92.4	1.22×10^{-6}
PGTG_10570	Aspartic protease, secreted	89871	No hit	3,493	46*	76.1	0.04
PGTG_05667	Cu/Zn SOD, secreted	73483	XP_002418001	10,257	138*	74.7	0.004
PGTG_11683	Major intrinsic protein	106246	No hit	8,738	118*	74.6	4.73×10^{-4}
PGTG_19191	Serine carboxypeptidase, secreted	49959	EEY14780	6,156	86*	71.8	0.017
PGTG_11725	Endo-1,4-β-glucanase, secreted, GH5	47207	AAR29981	6,503	100*	65.3	0.038
PGTG_08842	Thiamine monophosphate synthase/TENI	63716	No hit	7,343	117*	63.1	7.47×10^{-4}
PGTG_10915	Major intrinsic protein	89561	No hit	41,747	686	61	0.006
PGTG_05491	MFS sugar transporter, putative	86594	XP_002480590	28,494	478	59.8	0.006
PGTG_15162	Endo-β-mannanase, GH5	86044	ABR27262	6,992	123*	57.3	0.009
PGTG_02527	Chitin synthase N-terminal, GT2	73345	ABB70409	33,954	766	44.4	8.40×10^{-4}
PGTG_06309	Plasma membrane (H+) ATPase	44104	CAA05841	10,443	272	38.5	0.003
PGTG_01889	Lipase, secreted	91294	No hit	13,249	348	38.2	9.55×10^{-4}
PGTG_15889	Aspartic peptidase A1	34644	XP_001880663	4,880	128*	38.2	0.019
PGTG_15122	Chitinase, GH18	75188	CAQ51152	15,175	415	36.6	2.63×10^{-4}
PGTG_12200	MFS monocarboxylate transporter	86626	XP_001267950	1,636	49*	34	0.012
PGTG_15888	Aspartic peptidase A1	34644	XP_001880663	2,159	77*	28.2	0.021
PGTG_18584	Hexose transporter HXT1	38418	CAC41332	8,629	378	22.9	0.006

Up-regulation in infected wheat is assessed by comparing transcripts profiles to those from resting urediniospores. Wheat leaves were infected by *P. graminis* f. sp. *tritici* urediniospores and left for 8 d after inoculation under controled conditions. At this stage, wheat rust pathogen has started to sporulate and macroscopic flecking are visible. Expression values are the means of three biological replicates for 8 dpi and urediniospores. Based on statistical analysis of normalized fluorescence levels, a gene was considered significantly regulated if it met two criteria (1): *t* test *P* value, 0.05 (using mattes in Matlab); infected wheat at 8 dpi versus urediniospores fold-change > 10. Genes were selected on the basis of homology to a function, and hypothetical proteins or genes without homology of unknown function were discarded. The complete list of significantly regulated genes is detailed in Dataset S1, Table S16.
*Below background expression level.

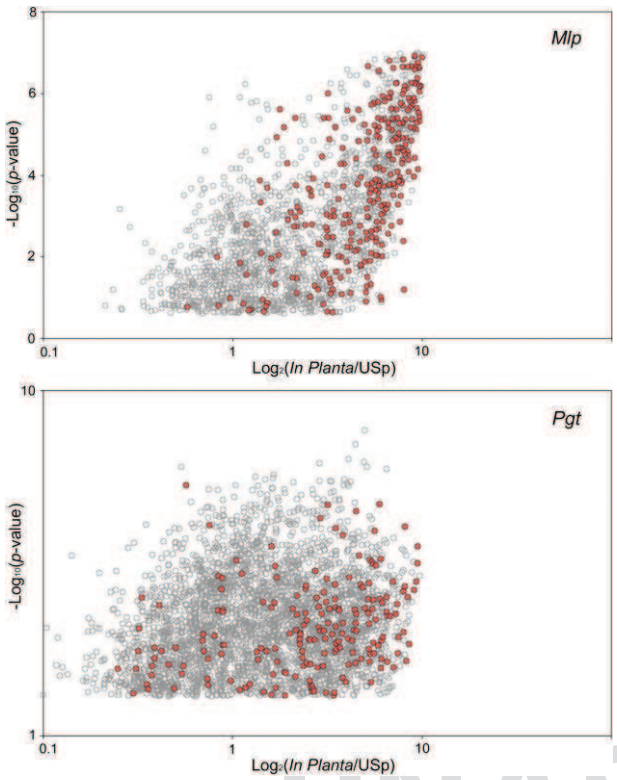

Fig. 2. Expression profiling of candidate rust effector genes. Global gene expression in infected poplar or wheat leaves (*in planta*) versus resting urediniospores (USp) in *M. larici-populina* (Mlp, *Top*) and *P. graminis* f. sp. *tritici* (Pgt, *Bottom*). Log_2-fold change ratio of significantly induced genes *in planta* compared with resting urediniospores plotted versus the *P* value. Gray circles, significantly *in planta*-induced genes; red circles, SSP encoding genes.

Rust Fungi Carbohydrate-Active Enzymes Set. Gene families encoding host-targeted, hydrolytic enzymes acting on plant biopolymers, such as proteinases, lipases, and several sugar-cleaving enzymes (carbohydrate-active enzymes; CAZymes) (26), are highly up-regulated in both rust pathogen transcriptomes *in planta* (Tables 2 and 3 and Dataset S1, Tables S12 and S16), suggesting that the invading hypha is penetrating the host cells by using these degrading enzymes. The comparison of the glycoside hydrolase (GH), glycosyltransferases (GTs), polysaccharide lyase (PL), and carbohydrate esterase (CE) of 21 sequenced fungi (Fig. S8) revealed that *M. larici-populina* and *P. graminis* f. sp. *tritici* have a relatively smaller set of GH-encoding genes (173 and 158 members, respectively; *SI Text*, *Annotation of Putative CAZymes*, and Dataset S1, Table S19); this content is similar to that in the basidiomycete symbiont *L. bicolor* (14), but much fewer than in hemibiotrophic or necrotrophic phytopathogens (e.g., *Magnaporthe oryzae*) and saprotrophs (including *Neurospora crassa*; *Coprinopsis cinerea*; *Schizophyllum commune*) (27). This set of CAZymes is strikingly larger than the repertoire of the biotroph *U. maydis* (100 members) (15). In evolving a biotrophic lifestyle, the rust fungi have lost several secreted hydrolytic GH and PL enzymes acting on plant cell wall (PCW) polysaccharides (Fig. S8) and they are lacking the cellulose-binding carbohydrate-binding module 1 (CBM1). However, they show a moderate expansion of a few GHs cleaving plant celluloses and hemicelluloses (e.g., GH7, GH10, GH12, GH26, and GH27) compared with the biotroph *U. maydis* or the hemibiotroph *M. oryzae*. These enzymes, together with *in planta* up-regulated and expanded α-mannosidase (GH47) and β-1,3-glucanase (GH5) transcripts (Dataset S1, Tables S12 and S16), may play a key role in the initial stages of host colonization, i.e., penetration of the parenchyma cells. A different set of enzymes, induced chitin deacetylases (CE4) present in *P. graminis* f. sp. *tritici*, *M. larici-populina*, and the symbiont *L. bicolor* (14), are likely involved in fungal cell wall remodeling and may play a role in the alteration of the fungal cell wall surface during infection to conceal invading hypha from the host (28).

Expanded Rust Transporters Gene Families Are Expressed During Host Infection. Acquisition of nutrients, including carbohydrates and amino acids, is crucial to the success of rust pathogen biotrophic interactions established by invading hyphae forming haustoria within the host plant (21, 29, 30). The repertoire of membrane transporters (*SI Text*, *Transporters*, and Dataset S1, Table S18) in *M. larici-populina* and *P. graminis* f. sp. *tritici* contains homologues of the hexose transporter HXT1, amino acid transporters AAT1, AAT2, and AAT3, and H^+-ATPases from the bean rust pathogen (*U. fabae*), known to be highly up-regulated during the interaction with its host plant. In addition, *M. larici-populina* and *P. graminis* f. sp. *tritici* genomes display an increased genetic potential for peptide uptake with 22 and 21 OPT genes, respectively, whereas other basidiomycete genomes contain only five to 16 OPT genes (Dataset S1, Table S18). OPT genes that are transcriptionally up-regulated *in planta* (Dataset S1, Tables S12 and S16), are likely involved in the transport of peptides released by the action of the induced proteinases (aspartic peptidase, subtilisin) expressed in infected leaf tissues. The Major Facilitator Superfamily (MFS) gene family is reduced in the *M. larici-populina* and *P. graminis* f. sp. *tritici* genomes compared with other basidiomycetes (Dataset S1, Table S18), but many MFS transcripts are, however, highly expressed *in planta* including two HXT1 homologues. Consistent with *in planta* expression of *M. larici-populina* and *P. graminis* f. sp. *tritici* invertase genes (Dataset S1, Tables S12 and S16), no homologue of the sucrose transporter Srt1 recently described in *U. maydis* (29) was identified, supporting the preferential uptake of host hexoses by invading rust pathogen hyphae (30). The increased activity of membrane transporters provides the needed fuel for the high primary metabolism activity observed in the invading rust fungi (Dataset S1, Tables S12 and S16). Strikingly, both rust fungi showed expansion of genes encoding auxin efflux carriers compared with other basidiomycetes (*SI Text*, *Transporters*), several of which are strongly expressed during plant infection. In addition, homologues of *U. maydis* auxin synthesis genes are also expressed during host infection. The potential for synthesis of auxin-like compounds that could regulate plant growth or development, as well as the expansion of strongly expressed auxin efflux carriers in rust fungi, suggests that fungal auxins could affect host hormone signaling and defense response or PCW integrity during rust infection.

Nitrate and Sulfate Assimilation Pathway Deficiencies in Rust Fungi. Based on the inability of rust fungi to grow in vitro, we hypothesized that the *M. larici-populina* and *P. graminis* f. sp. *tritici* genomes may lack genes typically present in saprotrophic basidiomycetes. Major anabolic pathways of primary metabolism were manually inspected for potential deficiencies. Although the enzymes of the NH_4^+ assimilation pathway were identified, several genes involved in nitrate assimilation were lacking in both rust pathogen genomes; the nitrate/nitrite porter and the nitrite reductase are missing from the nitrate assimilation gene cluster found in other fungi (31). Loss of another pathway was specific to one of the genomes; genes required to perform the primary sulfate assimilation were identified in *M. larici-populina* whereas they were not found in *P. graminis* f. sp. *tritici*. The latter fungus lacks both α- and β-subunits of sulfite reductase (SiR), whereas the *M. larici-populina* β-subunit of SiR is missing the transketolase domain present in other fungal SiRs. The apparent incapacitation of nitrate and sulfate assimilation pathways in both rust fungi is consistent with their obligate biotrophic lifestyle, as they depend on reduced nitrogen (NH_4^+ or amino acids) and sulfur from plant cells. These metabolic deficiencies have also been found in other plant pathogens that represent two independent evolutionary lineages of obligate biotrophy in the oomycete (*H. arabidopsidis*) and ascomycete (*B. graminis*) lineages (11, 12).

Conclusions

Little is known about how obligate biotrophic rust fungi invade their hosts and avoid or suppress defense responses. The genome sequences of the poplar leaf and wheat stem rust fungi provide

an unparalleled opportunity to address questions related to the obligate biotrophic lifestyle. The genetic changes that brought about the evolution of obligate biotrophy from nonbiotrophic progenitors remain obscure. Our comparisons of *M. larici-populina* and *P. graminis* f. sp. *tritici* to other saprotrophic, pathogenic, and symbiotic basidiomycetes indicate that developmental innovations in the rust fungi lineages did not involve major changes in the ancestral repertoire of conserved proteins with known function. However, gene family expansions observed for OPT, auxin efflux carriers, SOD, and signaling elements could reflect specific adaptations to this extreme parasitic lifestyle of these fungi. Similarly, lineage-specific gene families encoding zinc finger proteins, which may act as transcription factors during plant–rust interactions, suggest that these allow for different transcriptional programs in the two fungi. Analysis of these genomes revealed that the largest innovation of gene content encompasses the large set of lineage-specific, expanding gene families, which may enable developmental innovation and adaptation. Further, our analysis shows that the colonization of the host leaf, differentiation of pathogenic structures, and control of the plant immune system can be associated with a large-scale invention of lineage-specific proteins. For example, the rich repertoire of candidate effector-like SSPs could underlie the coevolution and adaptation of these obligate pathogens to the plant immune system. In contrast to obligate bacterial biotrophs and microsporidial fungal parasites, which frequently undergo gene loss and genome compaction (9, 10), the rust pathogen genomes are among the largest fungal genomes sequenced so far, as a result of expanded gene families and massive proliferation of TEs. No large-scale gene loss was observed in *M. larici-populina* and *P. graminis* f. sp. *tritici*, but some losses of clear impact, including the deletion of genes apparently not essential for the obligate biotrophic lifestyle (nitrate and sulfur assimilation), and a reduced set of PCW polysaccharide degrading enzymes, are genomic hallmarks of rust fungi, and, more broadly, of biotrophic pathogens as a group (11, 12). A deeper understanding of the complex array of the factors, including effector-like SSPs, affecting host–pathogen interactions and coevolution could enable efficient targeting of parasite-control methods in agricultural and forest ecosystems.

Materials and Methods

Genome Sequencing, Assembly, and Annotation. The dikaryotic *M. larici-populina* 98AG31 and *P. graminis* f. sp. *tritici* CDL 75–36-700–3 (race SCCL) strains (*SI Text, Background Information*) were sequenced by whole-genome sequencing and were assembled into predicted 101.1-Mb and 88.6-Mb genomes, respectively (*SI Text, Genome Sequencing and Assembly*). The protein-coding genes were predicted with a combination of automated gene callers, ESTs produced from each rust fungus, and filtering dubious genes with similarity to TEs (*SI Text, Gene Prediction and Annotation*). In total, the gene sets included 16,399 and 17,773 predicted genes for *M. larici-populina* and *P. graminis* f. sp. *tritici*, respectively; these were the basis for multigene family analyses. The *M. larici-populina* genome sequence can be accessed at http://jgi.doe.gov/Melampsora and the *P. graminis* f. sp. *tritici* genome sequence can be accessed at http://www.broadinstitute.org/annotation/genome/puccinia_group/MultiHome.html.

Microarray Analysis of Gene Expression in Urediniospores and Rust-Infected Plants. For both *M. larici-populina* and *P. graminis* f. sp. *tritici*, gene expression was assessed in resting and in vitro germinating urediniospores of the sequenced rust strains, as well as in respective host plant tissues at late stages of infection, by using specific custom 70-mer oligoarrays (*SI Text, Whole-Genome Exon Oligoarrays*). Methods for RNA isolation, probe synthesis and hybridization, and data capture and analyses are described in *SI Text, Whole-Genome Exon Oligoarrays*, and the data can be accessed in the Gene Expression Omnibus (GEO) database (GSE23097 for *M. larici-populina* and GSE25020 for *P. graminis* f. sp. *tritici*).

ACKNOWLEDGMENTS. We thank M.-P. Oudot-LeSeq for the initial *M. larici-populina* TE annotation; B. Hilselberger for database construction, C. Commun and H. Niculita-Hirzel for the annotation of the *M. larici-populina* secretome and mating-type genes, respectively; and Jerry Johnson for technical assistance. The work conducted on *M. larici-populina* by the Joint Genome Institute of the US Department of Energy is supported by the Office of Science of the US Department of Energy under Contract DE-AC02-05CH11231. This project was also funded by grants from the Institut National de la Recherche Agronomique and the Région Lorraine Council (to F.M. and S.D.) and a grant from Natural Resources Canada (to R.C.H.), The sequencing of *P. graminis* f. sp. *tritici* was funded by the US National Science Foundation and conducted by the Broad Institute Sequencing Platform. The work of Y.-C.L., P.R., and Y.V.d.P. was supported by Interuniversity Attraction Pole P6/25 (BioMaGNet).

1. Aime MC, et al. (2006) An overview of the higher level classification of Pucciniomycotina based on combined analyses of nuclear large and small subunit rDNA sequences. *Mycologia* 98:896–905.
2. Cummins GB, Hiratsuka Y (2004) *Illustrated Genera of Rust Fungi* (APS Press, St. Paul) 3rd Ed.
3. Leonard KJ, Szabo LJ (2005) Stem rust of small grains and grasses caused by *Puccinia graminis*. *Mol Plant Pathol* 6:99–111.
4. Stokstad E (2007) Plant pathology. Deadly wheat fungus threatens world's breadbaskets. *Science* 315:1786–1787.
5. Rubin EM (2008) Genomics of cellulosic biofuels. *Nature* 454:841–845.
6. Duplessis S, Major I, Martin F, Séguin A (2009) Poplar and pathogen interactions: insights from *Populus* genome-wide analyses of resistance and defense gene families and gene expression profiling. *Crit Rev Plant Sci* 28:309–334.
7. Gérard PR, Husson C, Pinon J, Frey P (2006) Comparison of genetic and virulence diversity of *Melampsora larici*-populina populations on wild and cultivated poplar and influence of the alternate host. *Phytopathology* 96:1027–1036.
8. Dodds PN, et al. (2009) Effectors of biotrophic fungi and oomycetes: Pathogenicity factors and triggers of host resistance. *New Phytol* 183:993–1000.
9. Ochman H, Moran NA (2001) Genes lost and genes found: Evolution of bacterial pathogenesis and symbiosis. *Science* 292:1096–1099.
10. Corradi N, Pombert JF, Farinelli L, Didier ES, Keeling PJ (2010) The complete sequence of the smallest known nuclear genome from the microsporidian *Encephalitozoon intestinalis*. *Nat Commun* 1:77.
11. Spanu PD, et al. (2010) Genome expansion and gene loss in powdery mildew fungi reveal tradeoffs in extreme parasitism. *Science* 330:1543–1546.
12. Baxter L, et al. (2010) Signatures of adaptation to obligate biotrophy in the *Hyaloperonospora arabidopsidis* genome. *Science* 330:1549–1551.
13. Cuomo CA, Birren BW (2010) The fungal genome initiative and lessons learned from genome sequencing. *Methods Enzymol* 470:833–855.
14. Martin F, et al. (2008) The genome of *Laccaria bicolor* provides insights into mycorrhizal symbiosis. *Nature* 452:88–92.
15. Kämper J, et al. (2006) Insights from the genome of the biotrophic fungal plant pathogen *Ustilago maydis*. *Nature* 444:97–101.
16. Schirawski J, et al. (2010) Pathogenicity determinants in smut fungi revealed by genome comparison. *Science* 330:1546–1548.
17. Haas B, et al. (2009) Genome sequence and analysis of the Irish potato famine pathogen Phytophthora infestans. *Nature* 461:393–398.
18. Raffaele S, et al. (2010) Genome evolution following host jumps in the Irish potato famine pathogen lineage. *Science* 330:1540–1543.
19. Rouxel T, et al. (2011) Effector diversification within compartments of the Leptosphaeria maculans genome affected by repeat-induced point mutations. *Nature Commun* 2:202.
20. Panstruga R, Dodds PN (2009) Terrific protein traffic: the mystery of effector protein delivery by filamentous plant pathogens. *Science* 324:748–750.
21. Ellis JG, Rafiqi M, Gan P, Chakrabarti A, Dodds PN (2009) Recent progress in discovery and functional analysis of effector proteins of fungal and oomycete plant pathogens. *Curr Opin Plant Biol* 12:399–405.
22. Voegele RT, Hahn M, Mendgen K (2009) The uredinales: cytology, biochemistry, and molecular biology. *The Mycota V: Plant Relationships*, ed Deising HB (Spinger, Berlin), pp 69–98.
23. Xu J, et al. (2011) Gene discovery in EST sequences from the wheat leaf rust fungus Puccinia triticina sexual spores, asexual spores and haustoria, compared to other rust and corn smut fungi. *BMC Genomics* 12:161.
24. Catanzariti A-M, Dodds PN, Lawrence GJ, Ayliffe MA, Ellis JG (2006) Haustorially expressed secreted proteins from flax rust are highly enriched for avirulence elicitors. *Plant Cell* 18:243–256.
25. Godfrey D, et al. (2010) Powdery mildew fungal effector candidates share N-terminal Y/F/WxC-motif. *BMC Genomics* 11:317.
26. Cantarel BL, et al. (2009) The Carbohydrate-Active EnZymes database (CAZy): An expert resource for Glycogenomics. *Nucleic Acids Res* 37(Database issue): D233–D238.
27. Ohm RA, et al. (2010) Genome sequence of the model mushroom *Schizophyllum commune*. *Nat Biotechnol* 28:957–963.
28. El Gueddari NE, Rauchhaus U, Moerschbacher BM, Deising HB (2002) Developmentally regulated conversion of surface-exposed chitin to chitosan in cell walls of plant pathogenic fungi. *New Phytol* 156:103–112.
29. Wahl R, Wippel K, Goos S, Kämper J, Sauer N (2010) A novel high-affinity sucrose transporter is required for virulence of the plant pathogen *Ustilago maydis*. *PLoS Biol* 8:e1000303.
30. Voegele RT, Struck C, Hahn M, Mendgen K (2001) The role of haustoria in sugar supply during infection of broad bean by the rust fungus *Uromyces fabae*. *Proc Natl Acad Sci USA* 98:8133–8138.
31. Slot JC, Hibbett DS (2007) Horizontal transfer of a nitrate assimilation gene cluster and ecological transitions in fungi: a phylogenetic study. *PLoS ONE* 2:e1097.

Article 5

Glutaredoxin: The Missing Link Between Thiol-Disulfide Oxidoreductases and Iron Sulfur Enzymes

Glutaredoxin: The Missing Link Between Thiol-Disulfide Oxidoreductases and Iron Sulfur Enzymes

BENJAMIN SELLES, NICOLAS ROUHIER, KAMEL CHIBANI, JEREMY COUTURIER, FILIPE GAMA AND JEAN-PIERRE JACQUOT[1]

Unité Mixte de Recherches 1136 INRA UHP Interactions Arbre-Microorganismes, IFR 110 EFABA, Ecosystèmes Forestiers, Agroressources, Bioprocédés et Alimentation, Faculté des Sciences, Nancy Université, BP 239, 54506 Vandoeuvre Cedex, France

I. Introduction 406
II. Iron-Containing Enzymes 407
A. Di-Iron Centers 407
B. Hemes 407
C. ISC and Iron Sulfur Proteins 408
D. Current Mechanism of ISC Assembly in Plant Plastids and Mitochondria 411
III. Thiol-Disulfide Oxidoreductases 412
A. The Thioredoxin Model 413
B. PDIs Derive from Thioredoxins 416
C. Glutaredoxins are Glutathione-Dependent Proteins Derived from Thioredoxins 419
IV. Early Experiments Suggesting a Link Between Iron Sulfur Enzymes and Redoxins 421
V. Glutaredoxins Bind ISCs 423
VI. Glutaredoxins Help Transfer ISCs in Apoproteins 426
VII. Concluding Remarks 427
References 427

[1]Corresponding author: Email: j2p@scbiol.uhp-nancy.fr

Advances in Botanical Research, Vol. 52 0065-2296/09 $35.00

DOI: 10.1016/S0065-2296(09)52013-7

ABSTRACT

The CXXC motif is present in many disulfide oxidoreductases as thioredoxins, glutaredoxins, and protein disulfide isomerases. It is also present in several metal-binding structures including hemoproteins and iron sulfur proteins. Although the 3D structure of ferredoxins and thioredoxins is radically different, the presence of this motif in both proteins suggests that thioredoxins and their derivatives might be able to accommodate iron sulfur centers (ISCs) as well. Several studies have indeed proven the presence of metals, such as iron or zinc, in thioredoxin-like structures either as natural products or after mutagenesis as in *Escherichia coli* thioredoxin 1. Moreover, it was recently demonstrated that some glutaredoxin species with CGYC or CGFS active sites can assemble a [2Fe–2S] ISC in a homodimer. Quite surprisingly, the ligands are the glutaredoxin catalytic cysteine and an external glutathione molecule. As a yeast CGFS glutaredoxin is thought to be involved in the transfer of preassembled ISCs from scaffold to acceptor apoproteins, this suggests that glutaredoxins are involved in these pathways through their own capacity to assemble such centers and transfer them efficiently. Altogether, these data provide firm evidence that glutaredoxins are a link between the world of thiol-disulfide reductases and iron sulfur enzymes.

I. INTRODUCTION

A large number of biochemical reactions require the participation of metals, including the mitochondrial and plastidial electron transfer chains, the metabolic pathways leading to the assimilation of nitrogen or sulfur, the synthesis of ribosomes, or the process of DNA repair, to cite only a few of these processes. Overwhelmingly, the metal ligands in proteins are histidine (through its nitrogen atom) and methionine and cysteine residues via their sulfur atom. Occasionally, acidic residues as aspartate or glutamate are also encountered. Metals as diverse as copper, molybdenum, iron, manganese, zinc, and nickel or even vanadium and cadmium (Lane *et al.*, 2005; Messerschmidt and Wever, 1996) are assembled into apoproteins via post-translational reactions. With a few exceptions, most metalloenzymes play a redox role, transferring electrons to neighboring proteins or chemical compounds by shifting back and forth between reduced and oxidized states. The microenvironment of the metal is extremely important in determining the redox potential of the metallic structures and hence, their reactivity. Among the many metalloenzymes, iron-containing enzymes play a prominent role in biology, and thus we discuss thereafter more extensively the organization of these metallic centers in macromolecules.

II. IRON-CONTAINING ENZYMES

Several types of iron-containing structures are present in proteins, the more frequently encountered being the di-iron centers, the hemes, and the iron sulfur centers (ISCs). It has been proposed that ISCs are the most primitive structures, as the primitive earth atmosphere is thought to have contained reduced sulfur and iron, the necessary components for ISC assembly (Milner-White and Russell, 2005). Interestingly, the Nest theory assumes the importance of glycine residues in early iron sulfur-binding peptides (see later the glutaredoxin (Grx) requirements for iron sulfur binding). It is postulated that hemes appeared later in evolution.

A. DI-IRON CENTERS

Di-ferric iron centers are present in a number of proteins, most notably ribonucleotide reductase (RNR), a key enzyme necessary for the biosynthesis of deoxyribonucleotides. In aerobic type RNR, the two irons are μ-oxo-linked and coordinated to the protein via ligands that include four carboxylic residues and two histidines. The di-iron site is close to the Tyr radical of the enzyme and serves for the generation and stabilization of the radical. Unlike the situation of cytochromes of the *c* type and of iron sulfur proteins, there is no direct link between this di-iron site in RNR and thioredoxin (Trx) except that RNR is an enzyme that requires thioredoxin or glutaredoxin for its catalytic activity (Avval and Holmgren, 2009). The regeneration of the active form of RNR involves the successive reduction of disulfide bonds, one situated at the C-terminus with the sequence CESGAC is more specifically the thioredoxin or glutaredoxin target (Persson *et al.*, 1997). Interestingly, some model compounds have been created where the two iron atoms are not oxo-linked but rather dithiolate bridged (Borg *et al.*, 2004).

B. HEMES

Several types of hemes are present in proteins, including the a, b, and c classes. All hemes are inserted posttranslationally into the apoproteins but their binding differs depending on the class considered. The a and b hemes are noncovalently attached, and are bound mostly via hydrophobic bonds. On the other hand, the c-type hemes are linked via thioether bonds that include two vicinal cysteine residues separated by two amino acids with the general formula CXXCH. The two X residues are variable, for example, in

horse heart cytochrome *c*, the attachment sequence is CAQC (Abriata *et al.*, 2009). It is CAAC in *Chlamydomonas reinhardtii* cytochrome *c*6 (Merchant and Bogorad, 1987), CSQC in chicken cytochrome *c* (Chan and Margoliash, 1966), and CANC in cytochrome *f* either from *Mastigocladus laminosus* or from *C. reinhardtii* (Baniulis *et al.*, 2008). In all c-type cytochromes, the iron atom in the center of the heme possesses two axial ligands, a histidine, and a methionine. It is well known that spacing two cysteines with two amino acids results in having the two sulfur atoms in close proximity in the 3D space, and thus in the possibility of creating a disulfide bond between the two cysteines following translation of the polypeptide. This is probably the reason why heme assembly requires the participation of thioredoxin-like molecules, for example, CCMH for *Arabidopsis thaliana* mitochondrial cytochrome *c* (Meyer *et al.*, 2005). In this case, the thioredoxin-like protein is required for the reduction of the disulfide prior to heme assembly.

C. ISC AND IRON SULFUR PROTEINS

1. Nature of the center

There are many types of ISCs in proteins, from the most simple type containing a single iron and no heterosulfur (rubredoxin-like) to more complex structures as [2Fe–2S] centers (chloroplastic ferredoxin, chloroplastic, and mitochondrial Rieske protein, mitochondrial adrenodoxin), [3Fe–4S] centers (e.g., in aconitase), and [4Fe–4S] centers (e.g., in chloroplastic photosystem I, nitrite reductase, sulfite reductase, glutamate oxoglutarate aminotransferase, and also in mitochondrial complex I) (Sazanov and Hinchliffe, 2006).

2. Nature of the ligands, position in the primary structure, and the CXXC motif

Except for the Rieske protein in which the ISC is ligated via two cysteines and two histidines, the amino acid ligands for ISCs are overwhelmingly cysteines and the ligation involves the sulfur atom of the side chain. In the rubredoxin mono iron type, the ligands coordinate with the iron atom in a tetrahedral organization. Interestingly for the *Clostridium pasteurianum* rubredoxin, the four cysteines are organized in two pairs separated by two amino acids with the sequences CTVC and CPLC (Mathieu *et al.*, 1992). In [2Fe–2S] ISCs, the four coordinating sulfur atoms are in the same plane than the two iron atoms, but in addition there are two inorganic sulfur atoms (also called labile sulfur) linking the two irons above and below the above defined plane. In [3Fe–4S] and [4Fe–4S] centers, the iron atoms and the hetero sulfur atoms are alternating in a cubane-like structure, the iron atoms being themselves covalently bound via the sulfur atoms of the ligand cysteines. In chloroplastic

ferredoxins, the position of the cysteines is conserved across species (in position 38, 43, 46, and 76 in *C. reinhardtii*) with a pair of cysteines in a CXXC motif which is absolutely conserved (Stein *et al.*, 1993). In general, the positions of the cysteine ligands are quite variable depending on which enzyme is considered, but examples abound where a CXXC motif is necessary for the binding of either [2Fe–2S] or [4Fe–4S] ISCs (Amman *et al.*, 2004; Brandt, 2006; Bych *et al.*, 2008; Raux-Deery *et al.*, 2005; Song and Lee, 2008; Yabe *et al.*, 2008; Zhang *et al.*, 2008). The remark concerning the cysteine spacing in cytochrome *c* and their potential oxidation into a disulfide after protein synthesis and before heme insertion obviously also applies to the many ISC-containing proteins with the CXXC motifs. Overall, nearly all of the ISC-containing proteins contain multiple iron atoms (except for the rubredoxin-type) and sometimes even multiple ISCs are present in a single poplypeptide, as in PsaC of photosystem I (Takahashi *et al.*, 1991). Nevertheless, although they contain multiple iron atoms, the ISCs are able to transfer only one electron at a time, this being possibly related to the position of the iron atoms in the 3D structure. For example, for a spinach chloroplastic ferredoxin (pdb accession number 1A70), it is indeed clear that one of the iron atoms is located closer to the surface of the protein and the other more deeply buried and thus unable to participate in electron transfer reactions (Binda *et al.*, 1998).

3. *Pathways where iron sulfur enzymes are required*

It has been briefly mentioned that nitrite reductase and glutamate synthase contain an ISC, and that nitrogen assimilation requires the participation of iron sulfur enzymes (Swamy *et al.*, 2005). Likewise, the iron sulfur-containing sulfite reductase, an enzyme with high analogy to nitrite reductase, and APS reductase are involved in sulphate assimilation (Hirasawa *et al.*, 2004; Kim *et al.*, 2006). As noted above the electron transfer chains of mitochondria and chloroplasts contain multiple ISCs (Complex I, II, and III in mitochondria, and cytochrome *b6f* and PSI in chloroplasts). The energetic metabolism and formation of ATP are thus dependent on these enzymes and so is the carbon assimilation in plants. In the cytosol, one enzyme involved in leucine biosynthesis, isopropylmalate isomerase (Leu1p) also contains an ISC (Sipos *et al.*, 2002). Scaffold proteins such as CnfU, a key iron sulfur cluster biosynthetic scaffold that is required for biogenesis of ferredoxin and photosystem I in chloroplasts also contain ISCs (Yabe *et al.*, 2008). This is also the case for the proteins Dre2, Nar1, and SirB which are involved in cytosolic iron sulfur biogenesis and siroheme biosynthesis, respectively (Raux-Deery *et al.*, 2005; Song and Lee, 2008; Zhang *et al.*, 2008). These examples are certainly not exhaustive but are demonstrative of how essential

these structures are for central metabolism, be it carbon, nitrogen, or sulfur metabolisms (and autotrophy in plants) or amino acid biosynthesis and iron sulfur assembly.

4. 3D structure of [2Fe–2S]-containing ferredoxins

Experiments described subsequently in this chapter have indicated that the thioredoxin and glutaredoxin molecules can harbor ISCs of the [2Fe–2S] type, either in "natural" proteins or in engineered mutagenized versions of the proteins and thus become "ferredoxin-like," so we describe here the 3D structure of most well-known ferredoxins from cyanobacteria or chloroplasts. These proteins are extremely well conserved with 96–99 amino acids in their mature form and the ligand cysteines in invariant positions. The protein is held together by several β-strands forming a β-sheet at the back of the molecule (Fig. 1). To the front of the molecule, three short α-helices surround the iron sulfur cluster, with one of the iron atoms positioned closer to the surface and thus better suited for transferring electrons. In the three helices lie key acidic residues that are required for protein–protein interaction (Binda *et al.*, 1998; Jacquot *et al.*, 1997). Other types of structures harboring a low potential [2Fe–2S] center are thioredoxin-like proteins present in bacteria such as *Azotobacter vinelandii*, *C. pasteurianum*, and *Chlorobium tepidum* (Meyer, 2001). Interestingly, these proteins form dimers, each

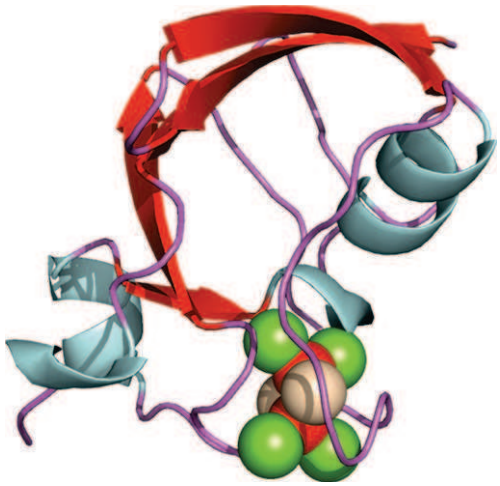

Fig. 1. Crystal structure of the E92K mutant of [2Fe–2S] ferredoxin I from *Spinacia oleracea* (Binda *et al.*, 1998; pdb accession number 1A70). Sulfur atoms belonging to cysteine residues 38, 43, 46, and 76 are represented by green spheres, iron atoms by red, and labile sulfur atoms by yellow.

monomer having a half "thioredoxin-like" architecture with a central pleated β-sheet surrounded by α-helices (Fig. 2) (Yeh *et al.*, 2000). In the dimer, the two β-sheets face one another and two of the helices surrounding them in more traditional thioredoxins are missing.

D. CURRENT MECHANISM OF ISC ASSEMBLY IN PLANT PLASTIDS AND MITOCHONDRIA

Two of the three bacterial ISC assembly systems, nif, suf, and isc have been retained in photosynthetic eukaryote organisms, the suf machinery being present in plastids and the isc machinery in mitochondria. In addition, nonplant eukaryotes possess an ISC export machinery and a cytosolic

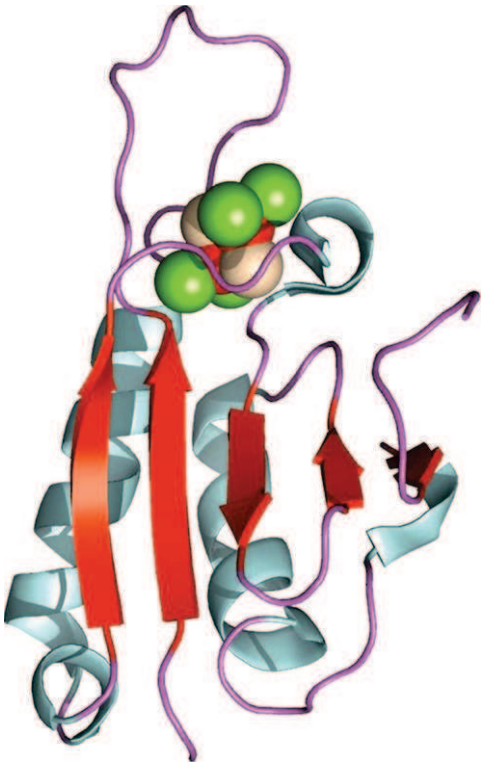

Fig. 2. Crystal structure of a thioredoxin-like [2Fe–2S] ferredoxin from *Aquifex aeolicus* (Yeh *et al.*, 2000; pdb 1F37). Sulfur atoms belonging to cysteine residues 9, 22, 55, and 59 are represented by green spheres, iron atoms by red and labile sulfur atoms by yellow.

assembly machinery for cytosolic and nuclear FeS proteins (Lill and Mühlenhoff, 2008). Based on the conservation of the proteins involved in the two latter systems, it is likely that these pathways also exist in plants (Balk and Lobreaux, 2005). It has been suggested from genetic studies in yeast that Grx5 is involved in the transfer of preassembled clusters from Isu proteins to acceptor proteins (Muhlenhoff *et al.*, 2003). As most Grxs from mammals, plants, and cyanobacteria can complement the defects associated with the deletion of Grx5 in yeast, this suggests that they fulfil similar functions in their respective organelles (Molina-Navarro *et al.*, 2006; Picciocchi *et al.*, 2007; Rouhier *et al.*, 2008). The latest developments concerning the involvement of Grxs in plant ISC biogenesis will be described in a subsequent section.

III. THIOL-DISULFIDE OXIDOREDUCTASES

The family of oxidoreductases includes disulfide reductases called thioredoxins, glutaredoxins, disulfide oxidases, or isomerases belonging to the sulfhydryl oxidase (SOX) and protein disulfide isomerase (PDI) families. Grxs, Trxs, and PDIs belonging to the large Trx superfamily possess many features in common, the active site, the 3D structure, the reaction mechanism. They are all ubiquitous or nearly ubiquitous redox proteins with conserved redox-active sites CXXC/S possessing generally oxidoreductase activity in dithiol-disulfide exchange reactions (Holmgren, 1985). The major difference lies in the redox potential of their active pair of cysteines, Trxs having a more electronegative redox potential than Grxs and even more than PDI. Furthermore, Chivers and collaborators have shown that the modification of the CXXC motif and consequently of the redox potential can modify the oxidoreductase properties of the protein. For example, a *Sc*Trx mutant with a higher redox potential can efficiently replace *Sc*PDI1 null mutant (Chivers *et al.*, 1996, 1997).

Photosynthetic and nonphotosynthetic organisms contain a large number of genes encoding these three classes of enzymes, for example, in poplar, around 40 Trx- and Grx-encoding genes and 13 PDI encoding genes (Chibani *et al.*, 2009; Couturier *et al.*, 2009b; Houston *et al.*, 2005; Morel *et al.*, 2008). All these proteins have variable subcellular localizations. In eukaryotic cells, Trxs and Grxs are rather present in compartments with a reducing environment, whereas PDI and SOX are present in compartments supposed to have an oxidizing environment. For example, PDIs are mostly found in the endoplasmic reticulum and their function is to fold properly other proteins via cysteine rearrangement.

A. THE THIOREDOXIN MODEL

1. *Active-site sequence*

Most frequently, Trxs have a highly conserved classical dicysteinic CXXC active-site sequence (overwhelmingly WC[G/P]PC), comprising two vicinal cysteines separated by two variable amino acids. Besides, in plants, several genomic studies have highlighted the presence of thioredoxin-like proteins with dicysteinic or monocysteinic active sites (CXXS), but little is known about their biochemical properties (Chibani *et al.*, 2009; Gelhaye *et al.*, 2004; Meyer *et al.*, 2007). In fact, Serrato and colleagues have demonstrated that some *Arabidopsis* CXXS Trxs have a disulfide reductase activity (Serrato *et al.*, 2008).

2. *Redox potential and reaction mechanism*

In Trxs containing a pair of cysteine residues, both cysteines play different roles. The first cysteine is involved in the nucleophilic attack on disulfide bonds present in target proteins, leading to the formation of a disulfide bond between the target protein and Trx. The second cysteine, called the backup/resolving or recycling cysteine, subsequently cleaves the disulfide formed between Trx and its target. In general, Trxs with a conventional active site WCGPC, have a low redox potential comprised between − 270 and − 330 mV compared to the other redoxins (Bréhélin *et al.*, 2004; Collin *et al.*, 2003). The two residues located between the two cysteines in the active-site motif are important in controlling the redox properties of the proteins. Changing one residue of the active site by site-directed mutagenesis affects the redox potential of the protein. For example, swapping the proline to histidine in the *Escherichia coli* Trx active-site sequence induces a higher redox potential (− 235 mV) than the wild type (Krause *et al.*, 1991). This mutation confers the ability to function as a disulfide isomerase and also has an impact on its interaction with folding protein substrates (Eklund *et al.*, 1991; Holmgren, 1995). Recently, it has also been demonstrated that the residue preceding the *cis* Pro conserved in all Trx superfamily members is crucial in determining the redox potential of the oxidoreductases (Ren *et al.*, 2009). A recent study showed that atypical chloroplastic Trxs called Trx-lilium from *Arabidopsis* with CGSC, CGGC, or CASC active sites display higher redox potentials between −237 and −240 mV, suggesting they cannot reduce all the usual Trx partners but that they could instead have specific functions (Dangoor *et al.*, 2009).

3. *Subcellular localization and physiological roles*

Thioredoxins are involved in a wide variety of fundamental biological functions including dithiol hydrogen donation to RNR, regulation of the activity of photosynthetic enzymes including fructose-1,6-bisphosphatase and

NADP malate dehydrogenase and of some eukaryotic transcription factors (Schürmann and Buchanan, 2008; Schürmann and Jacquot, 2000). In addition, it has been recently well documented that thioredoxins serve as regenerating systems for peroxiredoxins (Prx) and methionine sulfoxide reductases, enzymes in which the catalytic cysteine becomes oxidized into a sulfenic acid residue upon catalysis (Rouhier *et al.*, 2001, 2007a, 2008). In addition to these well-described interactions, the list of Trx targets involved in many metabolic pathways and cellular processes is growing with their identification by proteomic studies (for a review see Montrichard *et al.*, 2009 and also the paper by Nishiyama and Hisabori in this issue). There are multiple Trx isoforms localized in different compartments such as the cytosol (h), chloroplast (f, m, x, y, CDSP32, lilium), mitochondria (o, h2), nucleus (nucleoredoxin), apoplasm (h), endoplasmic reticulum (s), and Trxs with unknown localization (Trx-like and clot) (Alkhalfioui *et al.*, 2008; Chibani *et al.*, 2009; Meyer *et al.*, 2006). In chloroplasts, Trxs are essentially reduced by ferredoxin via ferredoxin-thioredoxin reductase (FTR), whereas cytosolic or mitochondrial Trxs are reduced by NADPH via a NADPH-Trx reductase (NTR) (Jacquot *et al.*, 2009). An alternative chloroplastic Trx reduction pathway involves NADPH and the hybrid enzyme NTRC (it contains a built-in Trx module in the C-terminal part of a NTR module). This protein might be specifically devoted to the reduction of some Prx types. A recent review summarizes the evolution and properties of thioredoxin reductases in photosynthetic organisms (Jacquot *et al.*, 2009).

4. 3D structures of thioredoxins

The first 3D Trx structure is the one of the *E. coli* Trx1 and it has been solved by X-ray crystallography (Holmgren *et al.*, 1975). Subsequently, several structures of Trxs from different organisms have been determined, and they display a high degree of homology, most of these proteins being rather homogeneous in length with ca. 110–120 amino acid residues (Fig. 3). Trx structures are also described in this volume in a chapter by Hägglund and colleagues. All Trx structures have a well-conserved hydrophobic core and most amino acid variants are located on the surface of the protein, affecting surface patches only locally. Thioredoxins and glutaredoxins are characterized by a common fold, the thioredoxin fold, which is a central five stranded β-sheet flanked by three or four α-helices and a CXXC active-site motif. The secondary elements are in the order β1, α1, β2, α2, β3, α3, β4, β5, α4. The conserved redox-active site forms the link between the second β-strand and the subsequent α2 helix, and the cysteines are located at the N-terminus of the helix and rather exposed at the surface of the molecule, especially the catalytic one (Dai *et al.*, 2000; Mössners *et al.*, 1998). Concerning plant Trxs, the

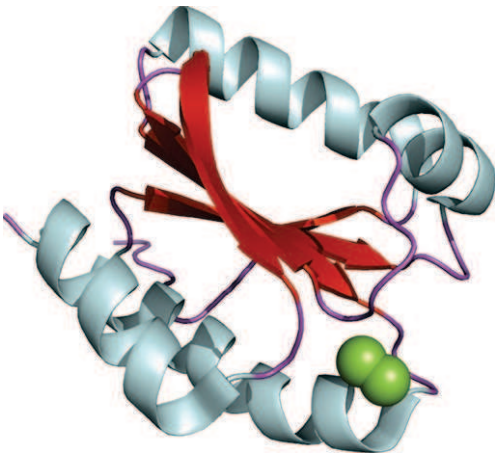

Fig. 3. Crystal structure of thioredoxin h1 from *Arabidopsis thaliana* (Peterson *et al.*, 2005; pdb 1XFl). Sulfur atoms belonging to cysteine residues 40 and 43 are represented in spheres (green in the web version).

structures of some Trxs f, m, and h have been determined in several organisms and solved by X-ray crystallography and NMR. The crystal structure of recombinant spinach Trx m has been solved in the oxidized and reduced state at 2.1 and 2.3 Å resolution, respectively (Capitani *et al.*, 2000). The structure of *C. reinhardtii* thioredoxin *m* has been solved by NMR and it is very similar to the spinach protein (Lancelin *et al.*, 2000). The spinach Trx f structure shares much similarity with the m, however, the f protein is more positively charged with some of these charges surrounding the active site where they must be instrumental in orientating the protein correctly upon interaction with its targets. Despite their structural similarities, a striking difference is the presence of a conserved third Cys73 in the C-terminal part of the f sequence. This cysteine is structurally exposed on the surface of the structure, 9.7 Å away from the first Cys of the active site (Brandes *et al.*, 1993; del Val *et al.*, 1999). Thus, the overall structure of the spinach Trx f and m does not differ markedly from the *E. coli* model (Schürmann and Buchanan, 2008). The structures of h-type Trxs have been determined for *C. reinhardtii,* barley, *A. thaliana*, and poplar enzymes (Coudevylle *et al.*, 2005; Koh *et al.*, 2008; Maeda *et al.*, 2008; Menchise *et al.*, 2001; Peterson *et al.*, 2005). In general, the h structure presents one major difference compared to other thioredoxins, namely an elongated α1 helix. Analysis of the 3D-structure of the *C. reinhardtii h* together with calorimetric studies showed that thioredoxin h has a much reduced thermal stability compared to thioredoxin m and has more similarity to the mammalian protein-type (Lemaire *et al.*, 2000;

Richardson *et al.*, 2000; Stein *et al.*, 1995). This is in agreement with the phylogenetic analyses that proposed an eukaryotic origin for thioredoxin f and h and a prokaryotic origin for thioredoxin m (Meyer *et al.*, 2002). These hypotheses were recently strengthened in a study reporting the effect of applying force to individual thioredoxin molecules from various sources (Perez-Jimenez *et al.*, 2009). A recent study has allowed the comparison of structures of two barley Trx h isoforms (Trxh1 and Trxh2). Barley Trx h1 and h2 have been solved in the oxidized state at 1.7 Å and Trxh2 in the reduced state at 2 Å resolution. The Trxh1 Arg101 can play a particularly crucial role in the association with target proteins by forming electrostatic interactions with a protein motif bound in the substrate-binding loop motif. The presence of Arg101 in Trxh1 and the uncharged Ile107 in Trxh2 may therefore give rise to differential isoform interactions with some redox patterns (Hagglund *et al.*, in this issue; Maeda *et al.*, 2008).

B. PDIs DERIVE FROM THIOREDOXINS

PDIs are generally multidomain proteins sharing structural and amino acid sequence similarities with thioredoxins (Ferrari and Söling, 1999). ''Classical'' PDI are constituted by five independent domains (a-b-b′-a′-c). The a, a′, b, and b′ domains have homologies to thioredoxins, while the a and a′ domains generally possess the CXXC active site, the b and b′ domains do not. The c domain is a short, acidic amino acid sequence (Edman *et al.*, 1985; Freedman *et al.*, 1994; Kemmink *et al.*, 1999). Most PDI also share an endoplasmic reticulum retention signal (K/HDEL) at the C-terminal end (Freedman *et al.*, 1994). Other classes of PDI differ from the ''classical'' representative member by the number and distribution of active and inactive TRX modules and the presence of additional domains sharing no similarity with Trxs (Appenzeller-Herzog and Ellgaard, 2008). Concerning plants, PDIs were first detected in higher plants at the end of the 1970s (Grynberg *et al.*, 1977) and then in the photosynthetic alga *C. reinhardii* (Myllylä *et al.*, 1989). Some comparative genomic studies performed on different photosynthetic organisms (*C. reinhardii*, *A. thaliana*, *Oryza sativa*, *Zea mays*) highlighted the complexity of the plant PDI family, similar to the situation in mammals and yeast (Houston *et al.*, 2005; Lemaire and Miginiac-Maslow, 2004).

1. Active site

The plant PDIs characterized so far generally possess one or two TRX active domains with a catalytic WCGHC motif that can be extended to the EFYAPW*CGHC*K/Q sequence, based on amino acid sequence comparisons

(Houston *et al.*, 2005; Lemaire and Miginiac-Maslow, 2004; Xu *et al.*, 2002). However, as for the thioredoxin and glutaredoxin families, a large variability exists concerning the amino acids present between the cysteines and even the number of cysteines in the catalytic modules leading to CxxS or SxxC active-site motifs (Maattanen *et al.*, 2006). Although plants have such isoforms, none of them has been characterized yet. As mentioned before, an *Arabidopsis* atypical thioredoxin h with a CXXS active site has been shown to catalyze isomerization of scrambled RNAse (Serrato *et al.*, 2008). This study suggests the existence of plants atypical PDI with efficient isomerase activity.

2. Redox potential

The global redox potential of PDI is around − 175 mV, with values ranging from − 188 mV for the a domain to − 155 mV for the a′ domain. These data are coherent with the fact that the redox state of the two modules can be different, the active site of the a domain being natively oxidized while the one of the a′ domain is reduced (Tian *et al.*, 2006). The prokaryotic periplasmic oxidase, DsbA, which has a function similar to eukaryotic PDI has a redox potential of around − 130 mV. This could explain why PDIs, which have a redox potential similar to Grxs, can also be efficient reductases (Hawkins *et al.*, 1991; Wunderlich and Glockshuber, 1993).

3. Subcellular localization and physiological role

As mentioned previously, PDIs are generally residents of the endoplasmic reticulum and they present all features required and sufficient for its targeting and retention into the ER. Nevertheless it was shown that RB60, a *C. reinhardtii* PDI member with a KDEL retention signal was partitioned between the stroma and thylakoids of chloroplasts (Trebitsh *et al.*, 2001). Concerning their physiological role, PDI is probably one of the most versatile members of the thioredoxin superfamily as it is able to catalyze *in vitro* disulfide oxidation, reduction, and isomerization (Kaska *et al.*, 1990; Myllylä *et al.*, 1989; Shorrosh *et al.*, 1993; Wadahama *et al.*, 2007). Some data obtained *in vivo* with mammalian and yeast PDI confirmed oxidase and isomerase activities (Frand and Kaiser, 1999; Laboissiere *et al.*, 1995), and also chaperone activities in the absence of an active Trx domain (Song and Wang, 1995).

4. 3D structures of PDIs

The 3D structures of some nonplant eukaryotic PDI members have been solved, essentially from human and yeast (Fig. 4). Only a few of them represent whole proteins (*Hs*ERp29, *Hs*ERp18, *Sc*PDI1p, and *Sc*Mpd1 with respective pdb accession numbers: 2QC7, 1SEN, 2B5E, 3ED3) while some others only describe isolated protein domains (Barak *et al.*, 2009; Rowe

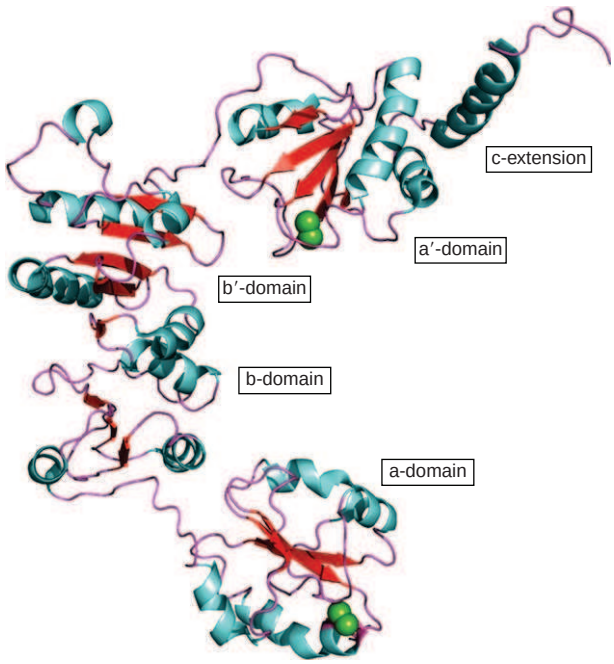

Fig. 4. Crystal structure of protein disulfide isomerase *Sc*PDI1p from Baker's yeast *Saccharomyces cerevisiae* (Tian *et al.*, 2006; pdb accession number 3BOA). Active Trx domains are named a and a′, inactive Trx domain b and b′ and acidic C-terminal extension c. Sulfur atoms belonging to cysteines 43, 46, 388, and 391 are represented by green spheres.

et al., 2009; Tian *et al.*, 2006; Vitu *et al.*, 2008). These four proteins vary by the domain composition, the number of "active" Trx modules, and exemplify various PDI classes. Here, we will focus our attention on the 3D structure of *Saccharomyces cerevisiae* PDI1p, a "classical" PDI. This protein is composed of the four domains a, a′, b, and b′ with thioredoxin fold. The four Trx domains and the acidic C-terminal tail of *Sc*PDI form a twisted "U" shape with active sites (CGHC) of active TRX domain (a-a′) facing each other at the end of the U branch. As in thioredoxins, each active site is located at the N-terminal side of the second α-helix. The inactive Trx domain (b-b′), forming the base of the "U," is present at the same relative position as the hydrophobic patch forming a continuous hydrophobic surface at the inside face of the "U." This hydrophobic "pocket" seems to be important for substrate recognition, particularly when PDI acts as a folding and chaperone protein (Kozlov *et al.*, 2006; Zheng and Gilbert, 2001). The connections between the Trx modules are different. The noncatalytic b and b′ modules are connected by a sequence of 17 amino acid residues in an

extended conformation susceptible to rigidity. The link between a-b and b′-a′ domains are shorter and presumably more flexible, suggesting that PDI can accommodate diverse substrates (Tian *et al.*, 2006).

C. GLUTAREDOXINS ARE GLUTATHIONE-DEPENDENT PROTEINS DERIVED FROM THIOREDOXINS

1. *Active-site sequence*

Glutaredoxins are ubiquitous proteins present in most prokaryotes and eukaryotes (Couturier *et al.*, 2009b; Fernandes and Holmgren, 2004). They were initially categorized, based on the active-site sequence, into two groups, a dithiol (CPY/FC motif) and a monothiol (CGFS motif) subgroup (Rodríguez-Manzaneque *et al.*, 1999). In plants, these two types of Grxs represent what we defined as class I and II, respectively. Classes I and II have been further divided into several subgroups called Grx C1, C2, C3, C4, and C5/S12 for class I and GrxS14, S15, S16, and S17 for class II. The specificity of these subgroups has been detailed previously (Couturier *et al.*, 2009b; Rouhier *et al.*, 2004a, 2006). A third Grx class, which contains proteins with a CCxx active-site motif, was also identified specifically in terrestrial plants (Lemaire, 2004; Rouhier *et al.*, 2004a), see the chapter by Li and Zachgo in this volume concerning the Roxy protein of this group. More recently, it has been demonstrated, notably in eukaryotic photosynthetic organisms, that there is a fourth class comprising multidomain proteins containing in their N-terminal part one Grx module with atypical active sites (essentially, CRDC in higher plants and CPHC in algae) (Couturier *et al.*, 2009b). Moreover, genome analysis of cyanobacterial genomes identified two new Grx classes composed of multidomain proteins containing a Grx domain with atypical active site, either CP[W/Y]G in class V, or CPWC/S in class VI (Couturier *et al.*, 2009b). With some exceptions, Grxs from other kingdoms fit well with the above-defined classification.

2. *Redox potential and mechanism*

Basically, whatever the organism considered, half of the Grxs possess a CxxC active site whereas the remaining sequences have a CxxS active site. Hence, this sequence property makes Grxs very efficient in reducing glutathionylated proteins (the topic of the chapter by Gao and colleagues in this volume). Only in a few cases, has it been shown that Grxs reduce intra- or intermolecular disulfide bonds on target proteins. For the reduction of protein-glutathione adducts, two distinct mechanisms have been elucidated, a monothiol or a dithiol one. In both cases, the N-terminal cysteine of the active site is employed for reducing mixed disulfides between glutathione and the target protein.

The striking difference between the two mechanisms is the involvement of a second cysteine for solving the intermediate disulfide bridge in the case of dithiol mechanism, whereas a glutathione molecule is used for solving the intermediate disulfide bridge in the case of monothiol mechanism. Until recently, the Grxs were considered as glutathione (GSH)-dependent oxidoreductases, but the identification of some Grxs in organisms lacking glutathione, especially in Gram negative bacteria, the identification of fusion proteins between FTR and Grx modules and the biochemical evidence that some Grxs from various sources are reduced by NADPH- or ferredoxin-dependent thioredoxin reductases have moderated this assumption (Jacquot *et al.*, 2009; Johansson *et al.*, 2004; Jordan *et al.*, 1997; Reynolds *et al.*, 2002; Zaffagnini *et al.*, 2008). These observations also suggest that Grxs derived from a Trx ancestor by the acquisition of a glutathione binding site, but some of these Grxs, although possessing the necessary residues, kept the possibility to be regenerated by thioredoxin reductases. This is exemplified by the human Grx2, which is reduced both by GSH and NTR, depending on the protein oxidation state that has been generated during its catalytic cycle (Johansson *et al.*, 2004). A redox potential can be measured for Grxs with two cysteine residues involved in the formation of a disulfide bridge. This led to the conclusion that Grxs are less efficient reductants than Trxs as they possess redox potential values around − 170 mV at pH 7 for poplar GrxC4 and GrxC1, compared to values around − 300 mV for thioredoxins (Rouhier *et al.*, 2007b). In the case of a class II Grx (*C. reinhardtii* Grx3 possessing a CGFS active site), a disulfide bond is formed during its catalytic cycle between the active-site cysteine and a cysteine positioned in the C-terminal part. A lower redox potential has been measured for this protein (around − 323 mV at pH 7.9), explaining that this protein is reduced by FTR but not by glutathione (Zaffagnini *et al.*, 2008). Assuming this is a two-electron process, the value at pH 7, extrapolated from the one at pH 7.9, would be − 269 mV, still much more negative than those determined for classical Grxs with regular dithiol active sites.

3. Subcellular localization and function

There are multiple Grx isoforms localized in different compartments, such as the cytosol, chloroplast, mitochondria, nucleus, and probably apoplasm (Rouhier *et al.*, 2008). The functions of Grxs in plants have been reviewed recently and are detailed in the chapter by Li and Zachgo. Basically, these proteins emerged as stress response proteins involving either their specific deglutathionylation activity or not. They are involved in some developmental processes such as petal development and most likely participate in iron sensing and/or iron sulfur biogenesis (reviewed in Rouhier *et al.*, 2008). Indeed, they are able to reduce dehydroascorbate and are involved in the

regeneration of thiol-dependent antioxidant enzymes, especially type II peroxiredoxins and methionine sulfoxide reductases (Msr) (Rouhier *et al.*, 2001, 2002, 2004b, 2007a; ; Tarrago *et al.*, 2009; Vieira dos Santos *et al.*, 2007). Normally, they do not reduce the same Msr and Prx classes than Trxs.

4. 3D structure of Grxs

Grx structures from various organisms have been solved both by NMR and X-ray crystallography. In general, most X-ray determined structures have been obtained with mutated proteins on the second active-site cysteine which allowed the irreversible binding of a glutathione molecule on the first active-site cysteine, most likely stabilizing the protein. The solved Grx structures (Grx1, 2, 3, and 4 from *E. coli*, pig, and human Grxs, Grxs from viruses) generally indicate a monomeric organization and the arrangement of secondary structures is quite similar to Trx structures, with β-strands forming a β-sheet flanked by several α-helices. Interestingly, some eukaryotic Grxs possess two supplementary α-helices in the N- and C-terminal regions compared to most prokaryotic Grxs. Several of the nonphotosynthetic 3D structures of Grx are discussed in the following reviews (Fernandes and Holmgren, 2004; Qin *et al.*, 2000). To date, three structures of plant Grxs (poplar GrxC1, C4, and S12) have been solved, GrxC1 and GrxC4 existing in a monomeric and a dimeric form, whereas GrxS12 exists only in the monomeric form (Figs. 4 and 5) (Couturier *et al.*, 2009a; Feng *et al.*, 2006; Noguera *et al.*, 2005; Rouhier *et al.*, 2007b). These different studies have notably demonstrated that dimeric GrxC1 bridges an iron sulfur cluster, whereas dimeric GrxC4 cannot ligate such a cluster due to the presence of an active-site proline residue (Glycine in GrxC1). The negative impact of another conserved *cis* proline residue for ISC incorporation into disulfide oxidoreductases has also been described by Su and colleagues (Su *et al.*, 2007). Some differences exist between the dimers of GrxC1 and GrxC4, since in GrxC4 the monomers are arranged in a head-to-tail orientation, while in GrxC1 the monomers are in a mirrored conformation. We discuss in more detail in the next section the arrangement of the iron sulfur cluster insertion in glutaredoxins as it is relevant to the function in iron sulfur assembly and to the CXXC motif described throughout this chapter.

IV. EARLY EXPERIMENTS SUGGESTING A LINK BETWEEN IRON SULFUR ENZYMES AND REDOXINS

Early experimental evidence for a connection between the thioredoxin world and proteins of the iron sulfur world originated from the laboratory of Jacques Meyer. As explained above Meyer and colleagues have isolated an

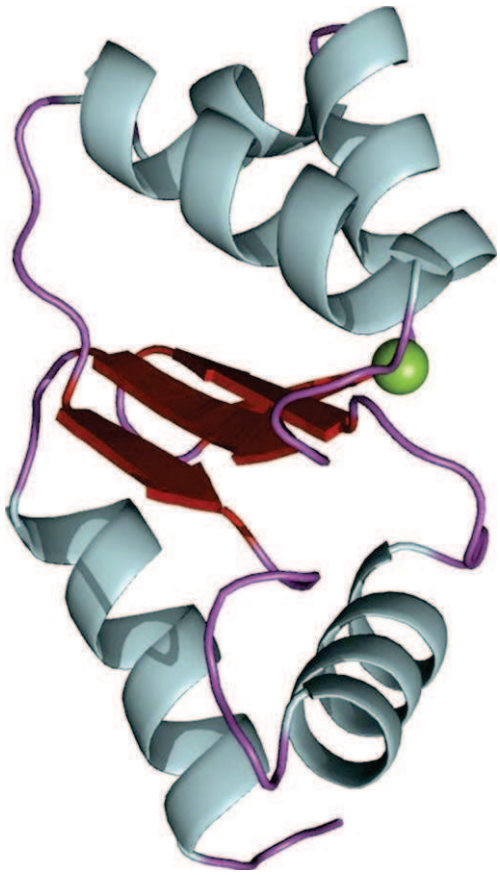

Fig. 5. RMN structure of *Populus tremula* GrxC4 exhibiting a CPYS active site (Noguera *et al.*, 2005). The sulfur atom belonging to cysteine 27 is shown as a sphere (green in the web version).

unusual ferredoxin from *Aquiflex aeolicus* that they have named ferredoxin of the third kind. Instead of having an architecture similar to traditional ferredoxins, this protein incorporates a [2Fe–2S] center in a thioredoxin-like molecule which forms dimers, each monomer containing an ISC (Fig. 2; Yeh *et al.*, 2000, 2002). Similar proteins have been identified in *C. pasteurianum*, *A. vinelandii*, and *C. tepidum* (Meyer, 2001). These studies have been instrumental in indicating that a thioredoxin fold could incorporate an ISC.

That thioredoxin was able to incorporate metals was also recognized in several other instances. In 2003, Collet and colleagues have observed that *E. coli* thioredoxin 2, an elongated form of thioredoxin, can bind zinc with a high affinity. Compared to traditional thioredoxins, Trx2 contains an

N-terminal extension with two CxxC motifs (CTHC and CGRC) that provide the zinc binding site (Collet *et al.*, 2003). The presence of this zinc center influences the reactivity and redox properties of the protein (El Hajjaji *et al.*, 2009).

Another approach that has led to the incorporation of metals in thioredoxin was through rational design and site-directed mutagenesis. In a pioneering work, Hellinga and colleagues have introduced a series of mutations in *E. coli* thioredoxin allowing the insertion of metals as copper or mercury (Hellinga *et al.*, 1991). Likewise, the substitution of W28 and I75 in *E. coli* thioredoxin into cysteines has led to the creation of a rubredoxin-like center with one iron atom linked to four cysteines (Benson *et al.*, 1998). Similar strategies have led to the creation of a mononuclear Cys2His2Zinc binding site in *E. coli* thioredoxin (Wisz *et al.*, 1998) and to the incorporation of a variety of transition metals with possible gain of enzymatic function (e.g., superoxide dismutase activity linked to zinc insertion) (Benson *et al.*, 2000).

In the present context of discussing the CXXC motif in redoxins and iron sulfur proteins, the most significant achievement has been the introduction of a [2Fe–2S] into *E. coli* thioredoxin by manipulating the WCGPC active-site sequence and altering it into a WCACA active site (Fig. 6.) (Masip *et al.*, 2004). This has been achieved by random mutagenesis and the structure of the CACA mutant has suggested that an exposure of a second cysteine (it is generally buried) allows the bridging of a 2Fe–2S cluster into a homodimer, the sulfur atoms of the two cysteines of each subunit serving as ligands to the iron atoms (Collet *et al.*, 2005).

Except for the bacterial ferredoxins of the third kind, all of the experiments described above create *de novo* artificial metal-containing thioredoxins by rational design and site-directed mutagenesis and it was unclear whether these manipulations were related to the ability of molecules with a thioredoxin fold to bind ISCs *in vivo*.

V. GLUTAREDOXINS BIND ISCs

The simultaneous observation that two glutaredoxins, one human with a SCSYC active-site sequence and the other from poplar with a YCGYC active site sequence, were able to bind [2Fe–2S] clusters *in vitro* and *in vivo* was a remarkable discovery (Feng *et al.*, 2006, Lillig *et al.*, 2005; Rouhier *et al.*, 2007b). Site-directed mutagenesis, together with the elucidation of the 3D structure of the two proteins, has indicated that the ISC is inserted at the interface of dimers with only the first Cys of the active site being a ligand. Remarkably, in the two structures, the additional ligands are two external

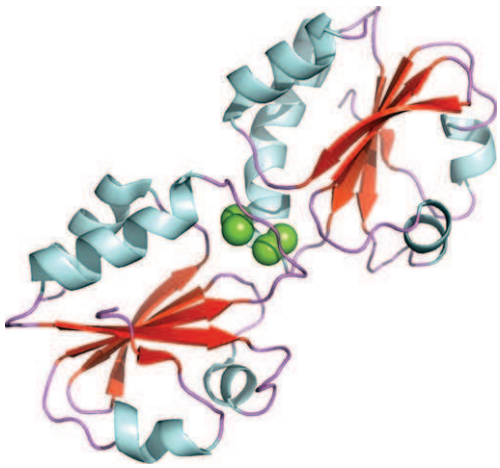

Fig. 6. Crystal structure of the *E. coli* Trx A CACA mutant dimer (Collet *et al.*, 2005; pdb 1ZCP). Sulfur atoms belonging to protein cysteine residues 32 and 34 are shown as green spheres.

glutathione molecules situated in *trans* with respect to the ISC (Fig. 7.; Johansson *et al.*, 2007; Rouhier *et al.*, 2007b). Further investigations with poplar Grxs (GrxC1, YCGYC active site; GrxC2, YCPFC active site; GrxC3, YCPYC active site; GrxC4, YCPYC active site; and GrxS12, WCSYS active site) have established that the ISC assembly in these structures requires a Tyr or another small amino acid residue before the first Cys residue and a small amino acid (Gly or Ser but not Pro) after the first Cys of the active site. On the other hand, the second Cys of the active site is dispensable, and as a consequence, Grxs with a CGFS active site sequence could accommodate an ISC in a dimer as poplar GrxC1 (Rouhier *et al.*, 2007b). This finding is remarkable in many respects, (i) it shows that glutaredoxins which possess a thioredoxin fold are able to incorporate an ISC, thereby providing a link between disulfide oxidoreductases and iron sulfur proteins; (ii) it indicates that the prediction of the binding of an ISC to a given polypeptide is complex. So far, it has essentially been based on sequence comparisons and the presence of CXXC motifs in proteins or conserved Cys and His for the Rieske type ISC. The possibility for CGFS Grxs to incorporate ISC in a homodimer with external glutathione molecules as ligands would have been impossible to predict in this context; (iii) it brings forth a hypothesis that glutaredoxins of the CGFS type can actually be involved in reactions related to iron homeostasis rather than in redox reactions. Many CGFS Grxs (*E. coli* Grx4, yeast Grx5 and, *A. thaliana* and polar GrxS14 and S16) characterized so far are indeed able to bind a labile

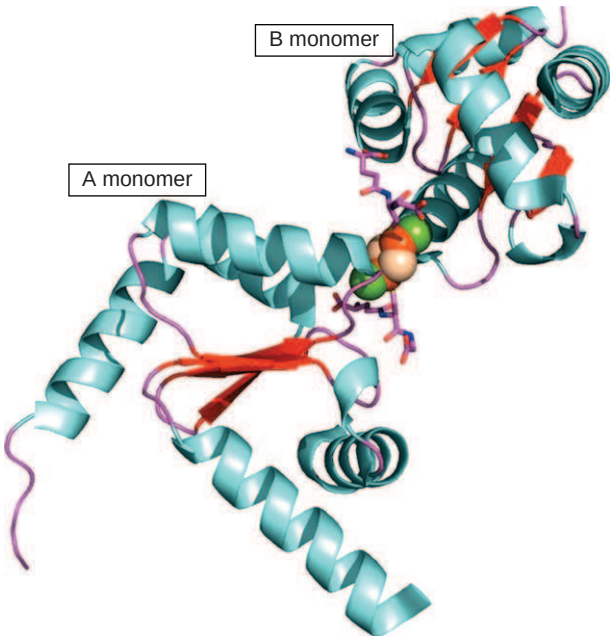

Fig. 7. Crystal structure of the holo form of glutaredoxin C1 from *Populus Tremula X Tremuloides* (Rouhier *et al.*, 2007b; pdb 2E7P). Sulfur atoms belonging to protein cysteine residues 30 and 33 of each monomer (A and B) are shown as green spheres, iron atoms as red, labile sulfur atoms as yellow and glutathione in stick.

[2Fe–2S] cluster when overexpressed in *E. coli*, presumably, as in GrxC1, with the catalytic cysteines and external glutathione molecules, but some differences in the spectroscopic signature of these proteins suggest that the cluster environment might be different (Bandyopadhyay *et al.*, 2008; Picciocchi *et al.*, 2007). No structure for ISC-containing CGFS Grxs has been solved yet. The recent biochemical and structural characterization of the *A. thaliana* CNFU scaffold protein indicated that the protein, similar to Grxs, bridged an all cysteinyl-ligated and labile [2Fe–2S] cluster into a dimer but that the ligands are two cysteines of each monomer comprised in a CXXC motif (Yabe *et al.*, 2008).

The study of Grxs from various sources led to the characterization of other ISC-containing Grxs, as the yeast Grx6 or the *Trypanosoma brucei* Grx1 (Comini *et al.*, 2008; Mesecke *et al.*, 2008). Considering that different Grxs, located in various subcellular compartments, can incorporate ISCs with variable stabilities, different putative roles have been proposed. First, based on the observation that GSH can stabilize the cluster in human Grx2 and poplar GrxC1, it has been proposed that the cluster might, similar to some

bacterial ISC-containing transcription factors, serve as a redox sensor, which would respond to cellular variation in the GSH/GSSG ratio (Lillig *et al.*, 2005; Rouhier *et al.*, 2007b). Alternatively, these ISC-containing Grxs could sense the iron status of a given compartment or of the cells. It has been shown in yeast that Grx3 and 4 can regulate the iron regulon in response to the cellular iron status through their interaction with the transcriptional activator Aft1 (Kumánovics *et al.*, 2008; Ojeda *et al.*, 2006). Last but not least, additional evidence indicates that CGFS Grxs participate in the ISC assembly (see Section VI).

VI. GLUTAREDOXINS HELP TRANSFER ISCs IN APOPROTEINS

The first evidence for a role of Grxs in ISC assembly came from the study of the yeast null *grx5* mutant strain (Rodríguez-Manzaneque *et al.*, 2002). In this mutant, the activity of two mitochondrial enzymes requiring iron sulfur clusters, aconitase and succinate dehydrogenase, was considerably decreased, whereas the content and activity of cytochrome *c*, a heme-containing protein is not affected. Other deficiencies include inability to grow in respiratory conditions and iron accumulation in their mitochondria. The latter observation might be responsible for the hypersensitivity of this Δ*grx5* mutant to external oxidants. It has been proposed later, still in yeast, based on the accumulation in this mutant of high amount of Fe/S clusters bound to the Isu1p scaffold protein that this mitochondrial Grx5 would help in the transfer of preassembled clusters from scaffold to acceptor proteins (Muhlenhoff *et al.*, 2003). With a few exceptions, almost all CGFS Grxs, either from prokaryotes or eukaryotes, are able to complement the yeast Grx5 deleted strain, suggesting that they could play similar roles in their own cells (Bandyopadhyay *et al.*, 2008; Molina *et al.*, 2004; Molina-Navarro *et al.*, 2006). The presence of a labile ISC in many CGFS Grxs and the possibility of the poplar chloroplastic monothiol Grx, GrxS14, to efficiently transfer intact [2Fe–2S] cluster to chloroplastic *Synechocystis* apoferredoxin, then supported the view that CGFS Grxs could also act directly as scaffold proteins (Bandyopadhyay *et al.*, 2008). The fact that GrxC1, which contains a more stable cluster and a different active site, was not able to transfer its cluster suggests that only Grxs with CGFS active sites and containing a labile cluster could be involved in ISC biogenesis (Bandyopadhyay *et al.*, 2008). The presence of CGFS Grxs in all cellular compartments (chloroplast, mitochondria, cytosol), where an ISC assembly machinery exists, supports the hypothesis that the function of these Grxs is conserved. Nevertheless, as

many scaffold proteins of the SUF, NFU, or ISC types have already been characterized in chloroplasts and mitochondria, one may wonder what the roles of these Grxs would be (for an exhaustive list, see Balk and Lobreaux, 2005). In addition, it is not known whether other Grxs with less classical active sites can also incorporate a cluster, whether all Grxs containing a labile cluster can transfer it to various acceptor proteins. Clearly, there is a pressing need to investigate if Grxs can transfer their cluster to other acceptor proteins and if some specificity exists for these reactions, both *in vitro* and *in vivo*.

VII. CONCLUDING REMARKS

At first sight, disulfide oxidoreductases and iron sulfur proteins have little in common, for example, the 3D architecture of ferredoxin is radically different from those of thioredoxin, both having a pleated β-sheet, central in thioredoxin but in the back of the molecule for ferredoxin and the arrangement of the α-helices is completely different. Nevertheless, they have in common to possess CxxC motifs that participate either in disulfide/dithiol exchange (thioredoxin) or in ISC binding (ferredoxin). The recent advances made with glutaredoxins in animal, plant, and bacterial systems have finally firmly connected these two separate worlds. The observation that some glutaredoxins bind ISCs in a way that has never been observed before for other ISC-containing proteins, together with the capacity to transfer those centers with high efficiency to apoferredoxin have absolutely transformed our vision of this research domain. Much remains to be done, however, for example, it is not known if Grxs are able to bind ISCs different from the [2Fe–2S] type. Can they bind [4Fe–4S] centers for example? Would they be able to transfer those? What about more complex proteins such as nitrogenase that contains both iron sulfur and iron molybdenum centers? All these questions are still unanswered and much remains to be done to further clarify the role that glutaredoxins play in ISC synthesis and assembly.

REFERENCES

Abriata, L. A., Cassina, A., Tórtora, V., Marín, M., Souza, J. M., Castro, L., Vila, A. J. and Radi, R. (2009). Nitration of solvent-exposed tyrosine 74 on cytochrome *c* triggers heme iron-methionine 80 bond disruption. Nuclear magnetic resonance and optical spectroscopy studies. *The Journal of Biological Chemistry* **284**, 17–26.

Alkhalfioui, F., Renard, M., Frendo, P., Keichinger, C., Meyer, Y., Gelhaye, E., Hirasawa, M., Knaff, D. B., Ritzenthaler, C. and Montrichard, F. (2008).

A novel type of thioredoxin dedicated to symbiosis in legumes. *Plant Physiology* **148**, 424–435.

Amman, K., Lezhneva, L., Wanner, G., Herrmann, R. G. and Meurer, J. (2004). ACCUMULATION OF PHOTOSYSTEM ONE1, a member of a novel gene family, is required for accumulation of [4Fe-4S] cluster-containing chloroplast complexes and antenna proteins. *The Plant Cell* **16**, 3084–3097.

Appenzeller-Herzog, C. and Ellgaard, L. (2008). The human PDI family: Versatility packed into a single fold. *Biochimica et Biophysica Acta* **4**, 535–548.

Avval, F. Z. and Holmgren, A. (2009). Molecular mechanisms of thioredoxin and glutaredoxin as hydrogen donors for Mammalian s phase ribonucleotide reductase. *The Journal of Biological Chemistry* **284**, 8233–8240.

Balk, J. and Lobreaux, S. (2005). Biogenesis of iron sulfur proteins in plants. *Trends in Plant Science* **10**, 324–331.

Bandyopadhyay, S., Gama, F., Molina-Navarro, M. M., Gualberto, J. M., Claxton, R., Naik, S. G., Huynh, B. H., Herrero, E., Jacquot, J. P., Johnson, M. K. and Rouhier, N. (2008). Chloroplast monothiol glutaredoxins as scaffold proteins for the assembly and delivery of [2Fe-2S] clusters. *EMBO Journal* **27**, 1122–1133.

Baniulis, D., Yamashita, E., Zhang, H., Hasan, S. S. and Cramer, W. A. (2008). Structure–function of the cytochrome *b6f* complex. *Photochemistry and Photobiology* **84**, 1349–1358.

Barak, N. N., Neumann, P., Sevvana, M., Schutkowski, M., Naumann, K., Malešević, M., Reichardt, H., Fischer, G., Stubbs, M. T. and Ferrari, D. M. (2009). Crystal structure and functional analysis of the protein disulfide isomerase-related protein ERp29. *Journal of Molecular Biology* **385**, 1630–1642.

Benson, D. E., Wisz, M. S., Liu, W. and Hellinga, H. W. (1998). Construction of a novel redox protein by rational design: Conversion of a disulfide bridge into a mononuclear iron sulfur center. *Biochemistry* **37**, 7070–7076.

Benson, D. E., Wisz, M. S. and Hellinga, H. W. (2000). Rational design of nascent metalloenzymes. *Proceedings of the National Academy of Sciences of the United States of America* **97**, 6292–6297.

Binda, C., Coda, A., Aliverti, A., Zanetti, G. and Mattevi, A. (1998). Structure of the mutant E92K of [2Fe-2S] ferredoxin I from *Spinacia oleracea* at 1.7 A resolution. *Acta Crystallographica. Section D, Biological Crystallography* **54**, 1353–1558.

Borg, S. J., Behrsing, T., Best, S. P., Razavet, M., Liu, X. and Pickett, C. J. (2004). Electron transfer at a dithiolate-bridged diiron assembly: Electrocatalytic hydrogen evolution. *Journal of the American Chemical Society* **126**, 16988–16999.

Brandes, H. K., Larimer, F. W., Geck, M. K., Stringer, C. D., Schürmann, P. and Hartman, F. C. (1993). Direct identification of the primary nucleophile of thioredoxin f. *Journal of Biological Chemistry* **268**, 18411–18414.

Brandt, U. (2006). Energy converting NADH:quinone oxidoreductase (complex I). *Annual Review of Biochemistry* **75**, 69–92.

Bréhélin, C., Laloi, C., Setterdahl, A. T., Knaff, D. B. and Meyer, Y. (2004). Cytosolic, mitochondrial thioredoxins and thioredoxin reductases in *Arabidopsis thaliana*. *Photosynthesis Research* **79**, 295–304.

Bych, K., Kerscher, S., Netz, D. J., Pierik, A. J., Zwicker, K., Huynen, M. A., Lill, R., Brandt, U. and Balk, J. (2008). The iron sulfur protein Ind1 is required for effective complex I assembly. *EMBO Journal* **27**, 1736–1746.

Capitani, G., Markovic-Housley, Z., del Val, G., Morris, M., Jansonius, J. N. and Schürmann, P. (2000). Crystal structures of two functionally different thioredoxins in spinach chloroplasts. *Journal of Molecular Biology* **302**, 135–154.

Chan, S. K. and Margoliash, E. (1966). Amino acid sequence of chicken heart cytochrome *c*. *The Journal of Biological Chemistry* **241**, 507–515.

Chibani, K., Wingsle, G., Jacquot, J. P., Gelhaye, E. and Rouhier, N. (2009). Comparative genomic study of the thioredoxin family in photosynthetic organisms with emphasis on *Populus trichocarpa*. *Molecular Plant* **2**, 308–322.

Chivers, P. T., Laboissière, M. C. and Raines, R. T. (1996). The CXXC motif: Imperatives for the formation of native disulfide bonds in the cell. *EMBO Journal* **15**, 2659–2667.

Chivers, P. T., Prehoda, K. E. and Raines, R. T. (1997). The CXXC motif: A rheostat in the active site. *Biochemistry* **36**, 4061–4066.

Collet, J. F., D'Souza, J. C., Jakob, U. and Bardwell, J. C. (2003). Thioredoxin 2, an oxidative stress-induced protein, contains a high affinity zinc binding site. *The Journal of Biological Chemistry* **14**, 45325–45332.

Collet, J. F., Peisach, D., Bardwell, J. C. and Xu, Z. (2005). The crystal structure of TrxA (CACA): Insights into the formation of a [2Fe-2S] iron sulfur cluster in an *Escherichia coli* thioredoxin mutant. *Protein Science* **14**, 1863–1869.

Collin, V., Issakidis-Bourguet, E., Marchand, C., Hirasawa, M., Lancelin, J. M., Knaff, D. B. and Miginiac-Maslow, M. (2003). The *Arabidopsis* plastidial thioredoxins: New functions and new insights into specificity. *The Journal of Biological Chemistry* **278**, 23747–23752.

Comini, M. A., Rettig, J., Dirdjaja, N., Hanschmann, E. M., Berndt, C. and Krauth-Siegel, R. L. (2008). Monothiol glutaredoxin-1 is an essential iron sulfur protein in the mitochondrion of African trypanosomes. *The Journal of Biological Chemistry* **283**, 27785–27798.

Coudevylle, N., Thureau, A., Hemmerlin, C., Gelhaye, E., Jacquot, J. P. and Cung, M. T. (2005). Solution structure of a natural CPPC active site variant, the reduced form of thioredoxin h1 from poplar. *Biochemistry* **44**, 2001–2008.

Couturier, J., Koh, C. S., Zaffagnini, M., Winger, A. M., Gualberto, J. M., Corbier, C., Decottignies, P., Jacquot, J. P., Lemaire, S. D., Didierjean, C. and Rouhier, N. (2009a). Structure–function relationship of the chloroplastic glutaredoxin S12 with an atypical WCSYS active site. *The Journal of Biological Chemistry* **284**, 9299–9310.

Couturier, J., Jacquot, J. P. and Rouhier, N. (2009b). Evolution and diversity of glutaedoxins in photosynthetic organisms. *Cellular and Molecular Life Sciences* **66**, 2539–2557.

Dai, S., Schwendtmayer, C., Johansson, K., Ramaswamy, S., Schürmann, P. and Eklund, H. (2000). How does light regulate chloroplast enzymes? Structure–function studies of the ferredoxin/thioredoxin system. *Quarterly Reviews of Biophysics* **33**, 67–108.

Dangoor, I., Peled-Zehavi, H., Levitan, A., Passand, O. and Danon, A. (2009). A small family of chloroplast atypical thioredoxins. *Plant Physiology* **149**, 1240–1250.

del Val, G., Maurer, F., Stutz, E. and Schürmann, P. (1999). Modification of the reactivity of spinach chloroplast thioredoxin *f* by site-directed mutagenesis. *Plant Science* **149**, 183–190.

Edman, J. C., Ellis, L., Blacher, R. W., Roth, R. A. and Rutter, W. J. (1985). Sequence of protein disulfide isomerase and implications of its relationship to thioredoxin. *Nature* **317**, 267–270.

Eklund, H., Gleason, F. K. and Holmgren, A. (1991). Structural and functional relations among thioredoxins of different species. *Proteins Structure Function and Genetics* **11**, 13–28.

El Hajjaji, H., Dumoulin, M., Matagne, A., Colau, D., Roos, G., Messens, J. and Collet, J. F. (2009). The zinc center influences the redox and thermodynamic properties of *Escherichia coli* thioredoxin 2. *Journal of Molecular Biology* **386**, 60–71.

Feng, Y., Zhong, N., Rouhier, N., Hase, T., Kusunoki, M., Jacquot, J. P., Jin, C. and Xia, B. (2006). Structural insight into poplar glutaredoxin C1 with a bridging iron sulfur cluster at the active site. *Biochemistry* **45**, 7998–8008.

Fernandes, A. P. and Holmgren, A. (2004). Glutaredoxins: Glutathione-dependent redox enzymes with functions far beyond a simple thioredoxin backup system. *Antioxidants and Redox Signaling* **6**, 63–74.

Ferrari, D. M. and Söling, H.-D. (1999). The protein disulfide isomerase family: Unravelling a string of folds. *Biochemical Journal* **339**, 1–10.

Frand, A. R. and Kaiser, C. A. (1999). ERO1p oxidizes protein disulfide isomerase in a pathway for disulfide bond formation in the endoplasmic reticulum. *Molecular Cell* **4**, 469–477.

Freedman, R. B., Hirst, T. R. and Tuite, M. F. (1994). Protein disulfide isomerase: Building bridges in protein folding. *Trends in Biochemical Sciences* **19**, 331–336.

Gelhaye, E., Rouhier, N. and Jacquot, J.-P. (2004). The thioredoxin h system of higher plants. *Plant Physiology and Biochemistry* **42**, 265–271.

Grynberg, A., Nicolas, J. and Drapron, R. (1977). Presence of a protein disulfide isomerase (EC 5.3.4.1) in wheat germ. *Comptes Rendus de l'Académie des Sciences Série D Sciences Naturelles* **284**, 235–238.

Hawkins, H. C., de Nardi, M. and Freedman, R. B. (1991). Redox properties and cross-linking of the dithiol/disulfide active sites of mammalian protein disulfide isomerase. *The Biochemical journal* **275**, 341–348.

Hellinga, H. W., Caradonna, J. P. and Richards, F. M. (1991). Construction of new ligand binding sites in proteins of known structure. II. Grafting of a buried transition metal binding site into Escherichia coli thioredoxin. *Journal of Molecular Biology* **222**, 787–803.

Hirasawa, M., Nakayama, M., Hase, T. and Knaff, D. B. (2004). Oxidation-reduction properties of maize ferredoxin: Sulfite oxidoreductase. *Biochimica et Biophysica Acta* **1608**, 140–148.

Holmgren, A. (1985). Thioredoxin. *Annual Review of Biochemistry* **54**, 237–271.

Holmgren, A. (1995). Thioredoxin structure and mechanism: Conformational changes on oxidation of the active-site sulfhydryls to a disulfide. *Structure* **3**, 239–243.

Holmgren, A., Söderberg, B. O., Eklund, H. and Brändén, C. I. (1975). Three-dimensional structure of *Escherichia coli* thioredoxin-S2 to 2.8 A resolution. *Proceedings of the National Academy of Sceinces of the United States of America* **72**, 2305–2309.

Houston, N. L., Fan, C., Xiang, Q.-Y., Schulze, J. M., Jung, R. and Boston, R. S. (2005). Phylogenetic analyses identify 10 classes of the protein disulfide isomerase family in plants, including single-domain protein disulfide isomerase-related proteins. *Plant Physiology* **137**, 762–778.

Jacquot, J. P., Stein, M., Suzuki, A., Liottet, S., Sandoz, G. and Miginiac-Maslow, M. (1997). Residue Glu-91 of *Chlamydomonas reinhardtii* ferredoxin is essential for electron transfer to ferredoxin-thioredoxin reductase. *FEBS Letters* **400**, 293–296.

Jacquot, J. P., Eklund, H., Rouhier, N. and Schürmann, P. (2009). Thioredoxin reductases in photosynthetic organisms. *Trends in Plant Science* **14**, 336–343.

Johansson, C., Lillig, C. H. and Holmgren, A. (2004). Human mitochondrial glutaredoxin reduces *S*-glutathionylated proteins with high affinity accepting electrons from either glutathione or thioredoxin reductase. *The Journal of Biological Chemistry* **279**, 7537–7543.

Johansson, C., Kavanagh, K. L., Gileadi, O. and Oppermann, U. (2007). Reversible sequestration of active site cysteines in a 2Fe-2S-bridged dimer provides a mechanism for glutaredoxin 2 regulation in human mitochondria. *The Journal of Biological Chemistry* **282**, 3077–3082.

Jordan, A., Aslund, F., Pontis, E., Reichard, P. and Holmgren, A. (1997). Characterization of *Escherichia coli* NrdH. A glutaredoxin-like protein with a thioredoxin-like activity profile. *The Journal of Biological Chemistry* **272**, 18044–18050.

Kaska, D. D., Kivirikko, K. I. and Myllylä, R. (1990). Purification and characterization of protein disulfide-isomerase from unicellular alga *Chlamidomonas reinhardii*. *The Biochemical journal* **268**, 63–68.

Kemmink, J., Dijkstra, K., Mariani, M., Scheek, R. M., Penka, E., Nilges, M. and Darby, N. J. (1999). The structure in solution of the b domain of protein disulfide isomerase. *Journal of Biomolecular NMR* **13**, 357–368.

Kim, S. K., Rahman, A., Conover, R. C., Johnson, M. K., Mason, J. T., Gomes, V., Hirasawa, M., Moore, M. L., Leustek, T. and Knaff, D. B. (2006). Properties of the cysteine residues and the iron sulfur cluster of the assimilatory 5'-adenylyl sulfate reductase from *Enteromorpha intestinalis*. *Biochemistry* **45**, 5010–5018.

Koh, C. S., Navrot, N., Didierjean, C., Rouhier, N., Hirasawa, M., Knaff, D. B., Wingsle, G., Samian, R., Jacquot, J. P., Corbier, C. and Gelhaye, E. (2008). An atypical catalytic mechanism involving three cysteines of thioredoxin. *The Journal of Biological Chemistry* **283**, 23062–23072.

Kozlov, G., Maattanen, P., Schrag, J. D., Pollock, S., Cygler, M., Nagar, B., Thomas, D. Y. and Gehring, Kalle (2006). Crystal structure of the bb domains of the protein disulfide isomerase ERp57. *Structure* **14**, 1331–1339.

Krause, G., Lundstrom, J., Barea, J. L., Pueyo de la Cuesta, C. and Holmgren, A. (1991). Mimicking the active site of protein disulfide-isomerase by substitution of proline 34 in *Escherichia coli* thioredoxin. *The Journal of Biological Chemistry* **266**, 9494–9500.

Kumánovics, A., Chen, O. S., Li, L., Bagley, D., Adkins, E. M., Lin, H., Dingra, N. N., Outten, C. E., Keller, G., Winge, D., Ward, D. M. and Kaplan, J. (2008). Identification of *FRA1* and *FRA2* as genes involved in regulating the yeast iron regulon in response to decreased mitochondrial iron sulfur cluster synthesis. *The Journal of Biological Chemistry* **16**, 10276–10286.

Laboissiere, M. C., Sturley, S. L. and Raines, R. T. (1995). The essential function of protein disulfide isomerase is to unscramble non-native disulfide bonds. *The Journal of Biological Chemistry* **270**, 28006–28009.

Lancelin, J. M., Guilhaudis, L., Stein, M., Krimm, I., Blackledge, M. J., Marion, D. and Jacquot, J. P. (2000). NMR Structures of thioredoxin *m* from the green alga *Chlamydomomas reinhardtii*. *Proteins Structure Function and Genetics* **41**, 334–349.

Lane, T. W., Saito, M. A., George, G. N., Pickering, I. J., Prince, R. C. and Morel, F. M. (2005). Biochemistry: A cadmium enzyme from a marine diatom. *Nature* **435**, 42.

Lemaire, S. D. (2004). The glutaredoxin family in oxygenic photosynthetic organisms. *Photosynthesis Research* **3**, 305–318.

Lemaire, S. D. and Miginiac-Maslow, M. (2004). The thioredoxin superfamily in *Chlamydomonas reinhardii*. *Photosynthesis Research* **82**, 203–220.

Lemaire, S. D., Richardson, J. M., Goyer, A., Keryer, E., Lancelin, J. M., Makhatadze, G. I. and Jacquot, J. P. (2000). Primary structure determinants of the pH- and temperature-dependent aggregation of thioredoxin. *Biochimica et Biophysica Acta (BBA)—Protein Structure and Molecular Enzymology* **2**, 311–323.

Lill, R. and Mühlenhoff, U. (2008). Maturation of iron sulfur proteins in eukaryotes: Mechanisms, connected processes, and diseases. *Annual Review of Biochemistry* **77**, 669–700.

Lillig, C. H., Berndt, C., Vergnolle, O., Lönn, M. E., Hudemann, C., Bill, E. and Holmgren, A. (2005). Characterization of human glutaredoxin 2 as iron sulfur protein: A possible role as redox sensor. *Proceedings of the National Academy of Sciences of the United States of America* **102**, 8168–8173.

Maattanen, P., Kozlov, G., Gehring, K. and Thomas, D. Y. (2006). Erp57 and PDI: Multifunctional protein disulfide isomerase with similar domain architectures but differing substrate-partner associations. *Biochemistry and Cell Biology* **84**, 881–889.

Maeda, K., Hägglund, P., Finnie, C., Svensson, B. and Henriksen, A. (2008). Crystal structures of barley thioredoxin h isoforms HvTrxh1 and HvTrxh2 reveal features involved in protein recognition and possibly in discriminating the isoform specificity. *Protein Science* **17**, 1015–1024.

Masip, L., Pan, J. L., Haldar, S., Penner-Hahn, J. E., DeLisa, M. P., Georgiou, G., Bardwell, J. C. and Collet, J. F. (2004). An engineered pathway for the formation of protein disulfide bonds. *Science* **303**, 1185–1189.

Mathieu, I., Meyer, J. and Moulis, J. M. (1992). Cloning, sequencing and expression in *Escherichia coli* of the rubredoxin gene from *Clostridium pasteurianum*. *Biochemical Journal* **285**, 255–262.

Menchise, V., Corbier, C., Didierjean, C., Saviano, M., Benedetti, E., Jacquot, J. P. and Aubry, A. (2001). Crystal structure of the wild-type and D30A mutant thioredoxin h of *Chlamydomonas reinhardtii* and implications for the catalytic mechanism. *Biochemical Journal* **359**, 65–75.

Merchant, S. and Bogorad, L. (1987). The Cu(II)-repressible plastidic cytochrome *c*. Cloning and sequence of a complementary DNA for the pre-apoprotein. *The Journal of Biological Chemistry* **262**, 9062–9067.

Mesecke, N., Mittler, S., Eckers, E., Herrmann, J. M. and Deponte, M. (2008). Two novel monothiol glutaredoxins from *Saccharomyces cerevisiae* provide further insight into iron sulfur cluster binding, oligomerization, and enzymatic activity of glutaredoxins. *Biochemistry* **47**, 1452–1463.

Messerschmidt, A. and Wever, R. (1996). X-ray structure of a vanadium-containing enzyme: Chloroperoxidase from the fungus *Curvularia inaequalis*. *Proceedings of the National Academy of Sciences of the United States of America* **93**, 392–396.

Meyer, J. (2001). Ferredoxins of the third kind. *FEBS Letters* **30**, 1–5.

Meyer, Y., Vignols, F. and Reichheld, J. P. (2002). Classification of plant thioredoxins by sequence similarity and intron position. *Methods in Enzymology* **347**, 394–402.

Meyer, E. H., Giegé, P., Gelhaye, E., Rayapuram, N., Ahuja, U., Thöny-Meyer, L., Grienenberger, J. M. and Bonnard, G. (2005). AtCCMH, an essential component of the c-type cytochrome maturation pathway in *Arabidopsis*

mitochondria, interacts with apocytochrome *c*. *Proceedings of the National Academy of Sciences of the United States of America* **102**, 16113–16118.

Meyer, Y., Riondet, C., Constans, L., Abdelgawwad, M. R., Reichheld, J. P. and Vignols, F. (2006). Evolution of redoxin genes in the green lineage. *Photosynthesis Research* **89**, 179–192.

Meyer, Y., Siala, W., Bashandy, T., Riondet, C., Vignols, P. and Reichheld, J. P. (2007). Glutaredoxins and thioredoxins in plants. *Biochimica et Biophysica Acta* **1783**, 589–600.

Milner-White, E. J. and Russell, M. J. (2005). Sites for phosphates and iron sulfur thiolates in the first membranes: 3 to 6 residue anion-binding motifs (nests). *Origins of Life and Evolution of the Biosphere* **35**, 19–27.

Molina, M. M., Bellı, G., de la Torre, M. A., Rodriguez-Manzaneque, M. T. and Herrero, E. (2004). Nuclear monothiol glutaredoxins of *Saccharomyces cerevisiae* can function as mitochondrial glutaredoxins. *The Journal of Biochemistry* **50**, 51923–51930.

Molina-Navarro, M. M., Casas, C., Piedrafita, L., Bellí, G. and Herrero, E. (2006). Prokaryotic and eukaryotic monothiol glutaredoxins are able to perform the functions of Grx5 in the biogenesis of Fe/S clusters in yeast mitochondria. *FEBS Letters* **580**, 2273–2280.

Montrichard, F., Alkhalfioui, F., Yano, H., Venseld, W. H., Hurkmand, W. J. and Buchanan, B. B. (2009). Thioredoxin targets in plants: The first 30 years. *Journal of Proteomics* **72**, 452–474.

Morel, M., Kohler, A., Martin, F., Gelhaye, E. and Rouhier, N. (2008). Comparison of the thiol-dependent antioxidant systems in the ectomycorrhizal *Laccaria bicolor* and the saprotrophic *Phanerochaete chrysosporium*. *New Phytologist* **180**, 391–407.

Mössners, E., Huber-Wunderlich, M. and Glockshuber, R. (1998). Characterization of *Escherichia coli* thioredoxin variants mimicking the active-sites of other thiol/disulfide oxidoreductases. *Protein Science* **7**, 1233–1244.

Muhlenhoff, U., Gerber, J., Richhardt, N. and Lill, R. (2003). Components involved in assembly and dislocation of iron sulfur clusters on the scaffold protein Isu1p. *EMBO Journal* **22**, 4815–4825.

Myllylä, R., Kaska, D. D. and Kivirikko, K. I. (1989). The catalytic mechanism of the hydroxylation reaction of peptidylproline and lysine does not require protein disulfide-isomerase activity. *The Biochemical Journal* **263**, 609–611.

Noguera, V., Walker, O., Rouhier, N., Jacquot, J. P., Krimm, I. and Lancelin, J. M. (2005). NMR reveals a novel glutaredoxin–glutaredoxin interaction interface. *Journal of Molecular Biology* **353**, 629–641.

Ojeda, L., Keller, G., Muhlenhoff, U., Rutherford, J. C., Lill, R. and Winge, D. R. (2006). Role of glutaredoxin-3 and glutaredoxin-4 in the iron regulation of the Aft1 transcriptional activator in *Saccharomyces cerevisiae*. *The Journal of Biological Chemistry* **281**, 17661–17669.

Perez-Jimenez, R., Li, J., Kosuri, P., Sanchez-Romero, I., Wiita, A. P., Rodriguez-Larrea, D., Chueca, A., Holmgren, A., Miranda-Vizuete, A., Becker, K., Cho, S. H. Beckwith, J. *et al*. (2009). Diversity of chemical mechanisms in thioredoxin catalysis. *Nature Structural and Molecular Biology* **16**, 890–896.

Persson, A. L., Eriksson, M., Katterle, B., Pötsch, S., Sahlin, M. and Sjöberg, B. M. (1997). A new mechanism-based radical intermediate in a mutant R1 protein affecting the catalytically essential Glu441 in *Escherichia coli* ribonucleotide reductase. *The Journal of Biological Chemistry* **272**, 31533–31541.

Peterson, F. C., Lytle, B. L., Sampath, S., Vinarov, D., Tyler, E., Shahan, M., Markley, J. L. and Volkman, B. F. (2005). Solution structure of thioredoxin *h*1 from *Arabidopsis thaliana*. *Protein science* **8**, 2195–2200.

Picciocchi, A., Saguez, C., Boussac, A., Cassier-Chauvat, C. and Chauvat, F. (2007). CGFS-type monothiol glutaredoxins from the cyanobacterium *Synechocystis* PCC6803 and other evolutionary distant model organisms possess a glutathione-ligated [2Fe-2S] cluster. *Biochemistry* **46**, 15018–15026.

Qin, J., Yang, Y., Velyvis, A. and Gronenborn, A. (2000). Molecular views of redox regulation: Three-dimensional structures of redox regulatory proteins and protein complexes. *Antioxidants and Redox Signaling* **2**, 827–840.

Raux-Deery, E., Leech, H. K., Nakrieko, K. A., McLean, K. J., Munro, A. W., Heathcote, P., Rigb, S. E., Smith, A. G. and Warren, M. J. (2005). Identification and characterization of the terminal enzyme of siroheme biosynthesis from *Arabidopsis thaliana*: A plastid-located sirohydrochlorin ferrochelatase containing a 2FE-2S center. *The Journal of Biological Chemistry* **280**, 4713–4721.

Ren, G., Stephan, D., Xu, Z., Zheng, Y., Tang, D., Harrison, R. S., Kurz, M., Jarrott, R., Shouldice, S. R., Hiniker, A., Martin, J. L. Heras, B. *et al*. (2009). Properties of the thioredoxin fold superfamily are modulated by a single amino acid residue. *The Journal of Biological Chemistry* **284**, 10150–10159.

Reynolds, C. M., Meyer, J. and Poole, L. B. (2002). An NADH-dependent bacterial thioredoxin reductase-like protein in conjunction with a glutaredoxin homologue form a unique peroxiredoxin (AhpC) reducing system in *Clostridium pasteurianum*. *Biochemistry* **41**, 1990–2001.

Richardson, J. M., III, Lemaire, S. D., Jacquot, J. P. and Makhatadze, G. I. (2000). Difference in the mechanisms of the cold and heat induced unfolding of thioredoxin h from *Chlamydomonas reinhardtii*: Spectroscopic and calorimetric studies. *Biochemistry* **39**, 11154–11162.

Rodríguez-Manzaneque, M. T., Ros, J., Cabiscol, E., Sorribas, A. and Herrero, E. (1999). Grx5 glutaredoxin plays a central role in protection against protein oxidative damage in *Saccharomyces cerevisiae*. *Molecular and Cellular Biology* **19**, 8180–8190.

Rodríguez-Manzaneque, M. T., Tamarit, J., Bellí, G., Ros, J. and Herrero, E. (2002). Grx5 is a mitochondrial glutaredoxin required for the activity of iron/sulfur enzymes. *Molecular Biology of the Cell* **4**, 1109–1121.

Rouhier, N., Gelhaye, E., Sautiere, P. E., Brun, A., Laurent, P., Tagu, D., Gerard, J., de Fay, E., Meyer, Y. and Jacquot, J. P. (2001). Isolation and characterization of a new peroxiredoxin from poplar sieve tubes that uses either glutaredoxin or thioredoxin as a proton donor. *Plant Physiology* **127**, 1299–1309.

Rouhier, N., Gelhaye, E. and Jacquot, J. P. (2002). Glutaredoxin dependent peroxiredoxin from poplar: Protein–protein interaction and catalytic mechanism. *The Journal of Biological Chemistry* **277**, 13609–13614.

Rouhier, N., Gelhaye, E. and Jacquot, J. P. (2004a). Plant glutaredoxins: Still mysterious reducing systems. *Cellular and Molecular Life Science* **61**, 1266–1277.

Rouhier, N., Gelhaye, E., Gualberto, J., Jordy, M. N., de Fay, E., Hirasawa, M., Duplessis, S., Lemaire, S., Frey, P., Martin, F., Manieri, W. Knaff, D. B. *et al*. (2004b). Poplar peroxiredoxin Q: A thioredoxin-linked chloroplast antioxidant functional in pathogen defense. *Plant Physiology* **134**, 1027–1038.

Rouhier, N., Vieira Dos Santos, C., Tarrago, L. and Rey, P. (2006). Plant methionine sulfoxide reductase A and B multigenic families. *Photosynthesis Research* **89**, 247–262.

Rouhier, N., Kauffmann, B., Tete-Favier, F., Paladino, P., Gans, P., Branlant, G., Jacquot, J. P. and Boschi-Muller, S. (2007a). Functional and structural aspects of poplar cytosolic and plastidial type a methionine sulfoxide reductases. *The Journal of Biological Chemistry* **282**, 3367–3378.

Rouhier, N., Unno, H., Bandyopadhyay, S., Masip, L., Kim, S. K., Hirasawa, M., Gualberto, J. M., Lattard, V., Kusunoki, M., Knaff, D. B., Georgiou, G. Hase, T. *et al*. (2007b). Functional, structural, and spectroscopic characterization of a glutathione-ligated [2Fe-2S] cluster in poplar glutaredoxin C1. *Proceedings of the National Academy of Sciences of the United States of America* **104**, 7379–7384.

Rouhier, N., Lemaire, S. and Jacquot, J. P. (2008). The role of glutathione in photosynthetic organisms: Emerging functions for glutaredoxins and glutathionylation. *Annual Reviews of Plant Biology* **59**, 143–166.

Rowe, M. L., Ruddock, L. W., Jurgen, G. K., Schmidt, M., Williamson, R. A. and Howard, M. J. (2009). Solution structure and dynamics of ERp18, a small endoplasmic reticulum resident oxidoreductase. *Biochemistry* **2**, 4596–4606.

Sazanov, L. A. and Hinchliffe, P. (2006). Structure of the hydrophilic domain of respiratory complex I from *Thermus thermophilus*. *Science* **31**, 1430–1436.

Schürmann, P. and Buchanan, B. B. (2008). The ferredoxin/thioredoxin system of oxygenic photosynthesis. *Antioxidants and Redox Signaling* **10**, 1235–1274.

Schürmann, P. and Jacquot, J. P. (2000). Plant thioredoxin systems revisited. *Annual Review of Plant Physiology and Plant Molecular Biology* **51**, 371–400.

Serrato, A. J., Guilleminot, J., Meyer, Y. and Vignols, F. (2008). AtCXXS: Atypical members of the *Arabidopsis thaliana* thioredoxin h family with a remarkably high disulfide isomerase activity. *Physiologia Plantarum* **133**, 611–622.

Shorrosh, B. S., Subramaniam, J., Schubert, K. R. and Dixon, R. A. (1993). Expression and localisation of plant protein disulfide isomerase. *Plant Physiology* **103**, 719–726.

Sipos, K., Lange, H., Fekete, Z., Ullmann, P., Lill, R. and Kispal, G. (2002). Maturation of cytosolic iron sulfur proteins requires glutathione. *The Journal of Biological Chemistry* **277**, 26944–26949.

Song, D. and Lee, F. S. (2008). A role for IOP1 in mammalian cytosolic iron sulfur protein biogenesis. *The Journal of Biological Chemistry* **283**, 9231–9238.

Song, J.-L. and Wang, C. C. (1995). Chaperon-like activity of protein disulfide-isomerase in the refolding of rhodanese. *European Journal of Biochemistry/FEBS Journal* **231**, 312–316.

Stein, M., Jacquot, J. P. and Miginiac-Maslow, M. (1993). A cDNA clone encoding *Chlamydomonas reinhardtii* preferredoxin. *Plant Physiology* **102**, 1349–1350.

Stein, M., Jacquot, J. P., Jeannette, E., Decottignies, P., Hodges, M., Lancelin, J. M., Mittard, V., Schmitter, J. M. and Miginiac-Maslow, M. (1995). *Chlamydomonas reinhardtii* thioredoxins: Structure of the genes coding for the chloroplastic *m* and cytosolic *h* isoforms; expression in *Escherichia coli* of the recombinant proteins, purification and biochemical properties. *Plant Molecular Biology* **28**, 487–503.

Su, D., Berndt, C., Fomenko, D. E., Holmgren, A. and Gladyshev, V. N. (2007). A conserved cis-proline precludes metal binding by the active site thiolates in members of the thioredoxin family of proteins. *Biochemistry* **46**, 6903–6910.

Swamy, U., Wang, M., Tripathy, J. N., Kim, S. K., Hirasawa, M., Knaff, D. B. and Allen, J. P. (2005). Structure of spinach nitrite reductase: Implications for multi-electron reactions by the iron sulfur:siroheme cofactor. *Biochemistry* **44**, 16054–16063.

Takahashi, Y., Goldschmidt-Clermont, M., Soen, S. Y., Franzén, L. G. and Rochaix, J. D. (1991). Directed chloroplast transformation in *Chlamydomonas reinhardtii*: Insertional inactivation of the psaC gene encoding the iron sulfur protein destabilizes photosystem I. *EMBO Journal* **10**, 2033–2040.

Tarrago, L., Laugier, E., Zaffagnini, M., Marchand, C., Le Maréchal, P., Rouhier, N., Lemaire, S. D. and Rey, P. (2009). Regeneration mechanisms of *Arabidopsis thaliana* methionine sulfoxide reductases B by glutaredoxins and thioredoxins. *The Journal of Biological Chemistry* **284**, 18963–18971.

Tian, G. G., Xiang, S., Noiva, R., Lennarz, W. and Schindelin, H. (2006). The crystal structure of yeast protein disulfide isomerase suggest cooperativity between its active sites. *Cell* **124**, 61–73; Erratum in: Cell (2006). 124, 1085-1088.

Trebitsh, T., Meiri, E., Ostersetzeri, O., Adami, Z. and Danon, A. (2001). The protein disulfide isomerase-like RB60 is partitioned between stroma and thylakoids in *Chlamydomonas reinhardtii* chloroplasts. *The Journal of Biological Chemistry* **7**, 4564–4569.

Vieira Dos Santos, C., Laugier, E., Tarrago, L., Massot, V., Issakidis-Bourguet, E., Rouhier, N. and Rey, P. (2007). Specificity of thioredoxins and glutaredoxins as electron donors to two distinct classes of *Arabidopsis* plastidial methionine sulfoxide reductases B. *FEBS Letters* **581**, 4371–4376.

Vitu, E., Gross, E., Greenblatt, H. M., Sevier, C. S., Kaiser, C. A. and Fass, D. (2008). Yeast Mpd1p reveals the structural diversity of the protein disulfide isomerase family. *Journal of Molecular Biology* **384**, 631–640.

Wadahama, H., Kamauchi, S., Ishimoto, M., Kawada, T. and Urade, R. (2007). Protein disufide isomerase family proteins involved in soybean protein biogenesis. *The FEBS Journal* **274**, 687–703.

Wisz, M. S., Garrett, C. Z. and Hellinga, H. W. (1998). Construction of a family of Cys2His2 zinc binding sites in the hydrophobic core of thioredoxin by structure-based design. *Biochemistry* **37**, 8269–8277.

Wunderlich, M. and Glockshuber, R. (1993). *In vivo* control of redox potential during protein folding catalyzed by bacterial protein disulfide-isomerase (DsbA). *The Journal of Biological Chemistry* **268**, 24547–24550.

Xu, Z.-J., Ueda, K., Masuda, K., Ono, M. and Inoue, M. (2002). Molecular characterization of a novel protein disulfide isomerase in carrot. *Gene* **284**, 225–231.

Yabe, T., Yamashita, E., Kikuchi, A., Morimoto, K., Nakagawa, A., Tsukihara, T. and Nakai, M. (2008). Structural analysis of *Arabidopsis* CnfU protein: An iron sulfur cluster biosynthetic scaffold in chloroplasts. *Journal of Molecular Biology* **381**, 160–173.

Yeh, A. P., Chatelet, C., Soltis, S. M., Kuhn, P., Meyer, J. and Rees, D. C. (2000). Structure of a thioredoxin-like [2Fe-2S] ferredoxin from *Aquifex aeolicus*. *Journal of Molecular Biology* **300**, 587–595.

Yeh, A. P., Ambroggio, X. I., Andrade, S. L., Einsle, O., Chatelet, C., Meyer, J. and Rees, D. C. (2002). High resolution crystal structures of the wild type and Cys-55–>Ser and Cys-59–>Ser variants of the thioredoxin-like [2Fe-2S] ferredoxin from *Aquifex aeolicus*. *The Journal of Biological Chemistry* **13**, 34499–34507.

Zaffagnini, M., Michelet, L., Massot, V., Trost, P. and Lemaire, S. D. (2008). Biochemical characterization of glutaredoxins from *Chlamydomonas reinhardtii* reveals the unique properties of a chloroplastic CGFS-type glutaredoxin. *The Journal of Biological Chemistry* **283**, 8868–8876.

Zhang, Y., Lyver, E. R., Nakamaru-Ogiso, E., Yoon, H., Amutha, B., Lee, D. W., Bi, E., Ohnishi, T., Daldal, F., Pain, D. and Dancis, A. (2008). Dre2, a conserved eukaryotic Fe/S cluster protein, functions in cytosolic Fe/S protein biogenesis. *Molecular and Cellular Biology* **28**, 5569–5582.

Zheng, J. and Gilbert, H. F. (2001). Discrimination between native and non-native disulfides by protein disulfide isomerase. *The Journal of Biological Chemistry* **276**, 15747–15752.

Article 6

The chloroplastic thiol reducing systems: dual functions in the regulation of carbohydrate metabolism and regeneration of antioxidant enzymes, emphasis on the poplar redoxin equipment

Photosynth Res (2010) 104:75–99
DOI 10.1007/s11120-009-9501-8

REVIEW

The chloroplastic thiol reducing systems: dual functions in the regulation of carbohydrate metabolism and regeneration of antioxidant enzymes, emphasis on the poplar redoxin equipment

Kamel Chibani · Jérémy Couturier · Benjamin Selles · Jean-Pierre Jacquot · Nicolas Rouhier

Received: 17 July 2009 / Accepted: 12 October 2009 / Published online: 10 November 2009

Abstract The post-translational modification consisting in the formation/reduction of disulfide bonds has been the subject of intense research in plants since the discovery in the 1970s that many chloroplastic enzymes are regulated by light through dithiol–disulfide exchange reactions catalyzed by oxidoreductases called thioredoxins (Trxs). Further biochemical and proteomic studies have considerably increased the number of target enzymes and processes regulated by these mechanisms in many sub-cellular compartments. Recently, glutathionylation, a modification consisting in the reversible formation of a glutathione adduct on cysteine residues, was proposed as an alternative redox regulation mechanism. Glutaredoxins (Grxs), proteins related to Trxs, are efficient catalysts for deglutathionylation, the opposite reaction. Hence, the Trxs- and Grxs-dependent pathways might constitute complementary and not only redundant regulatory processes. This article focuses on these two multigenic families and associated protein partners in poplar and on their involvement in the regulation of some major chloroplastic processes such as stress response, carbohydrate and heme/chlorophyll metabolism.

Keywords Chloroplast · Glutaredoxin · Photosynthesis · Stress · Thioredoxin

Kamel Chibani, Jérémy Couturier, and Benjamin Selles have equally contributed to the writing of this review.

K. Chibani · J. Couturier · B. Selles · J.-P. Jacquot · N. Rouhier (✉)
Unité Mixte de Recherches 1136 INRA-Nancy Université, Interactions Arbre-Microorganismes IFR 110 EFABA, 54506 Vandoeuvre-lès-Nancy Cedex, France
e-mail: nrouhier@scbiol.uhp-nancy.fr

Over the last decades, *Arabidopsis thaliana* has become the leading plant model, in particular for genetic studies. In general, it is a good model for elucidating the roles of thioredoxins (Trxs) and glutaredoxins (Grxs) and their interactions with target enzymes. Nevertheless, genomic analyses have proven that other plant species have different gene contents, some species either lacking some isoforms or having additional and specific isoforms. In addition, when we compare herbaceous dicotyledonous plants to cereals or trees, for example, some developmental aspects are very different and sometimes specific. Compared to *A. thaliana*, poplar is a perennial plant and seasonality, wood formation and flowering are important processes to consider which are likely to be unique in this model (Jansson and Douglas 2007). The possibility to form different types of symbiosis (endo or ectomycorrhiza with fungi or nodule formation with bacteria) also constitutes specific traits of some plants. Poplar has recently become a woody plant model, in particular, because its genome of modest size has been fully sequenced and annotated, and in addition, many expressed sequence tags are available. Moreover, it is growing rapidly and some poplar species can be transformed easily and propagated vegetatively. In this review, we are focusing on the equipment of poplar plastids in small proteins of the redoxin family, i.e., Trxs, Grxs, and ferredoxins (Fdxs), which are essential for the regulation of most processes in this organelle. Both Trxs and Grxs are regulating the activity or folding of many target proteins by reducing one or several disulfide bonds. Many of the target proteins have been identified in a single species, very often *Arabidopsis thaliana*, but it is anticipated that when the cysteines involved in the redox regulation mechanism are conserved in poplar sequence orthologs, the relevant mechanisms should also be present in poplar.

The chloroplastic thioredoxin system: thioredoxin isoforms and reduction pathways

Compared to bacteria and other eukaryotes which have a lower number of Trx isoforms, plants have an extended Trx system consisting of several isoforms localized in different sub-cellular compartments such as the chloroplast, the mitochondria, the cytosol, the nucleus, the apoplast, or the endoplasmic reticulum (Alkhalfioui et al. 2008; Chibani et al. 2009; Gelhaye et al. 2005; Meyer et al. 2005). In plants, unlike bacteria and animals, Trxs have been grouped based on their primary structures, biochemical properties, and sub-cellular localizations. Phylogenetic analyses of sequenced photosynthetic organisms led to the distribution of Trxs in about 20 major classes: f, m, x, y, o, h, s, CDSP32 (chloroplast drought-induced protein of 32 kDa), TDX (tetratricopeptide domain-containing Trxs), CiTrx (Cf-9 interacting Trxs), Nrx (nucleoredoxins), HCF164, Trx CxxS, Trx-like1, Trx-like2, Trx-lilium1, Trx-lilium2, Trx-lilium3, Clot and NTRC (NADPH Trxs reductase C; Alkhalfioui et al. 2008; Chibani et al. 2009; Meyer et al. 2008). They include proteins with classical WCGPC or WCPPC active sites but also with atypical CxxC/S active sites and some multi-domain proteins containing at least one Trx module. With a few exceptions, most terrestrial plants contain the full Trx equipment, but the number of members in a given class for a given species varies essentially due to the occurrence of duplication events. Hence, the extrapolation of the roles of some Trxs from one organism to another is a complex task. Many of these Trxs are located in the chloroplast or at least predicted to be imported in this compartment (Table 1). Indeed, based on bioinformatics analyses and experimental data obtained in other species for orthologous proteins, and including the Trx domain of the NTRC protein (see below), out of the 46 Trxs found in the *Populus trichocarpa* genome, 22 Trxs would be located in the chloroplast. This subset includes Trxs m, f, x, y, CDSP32, HCF164, CiTrx, NTRC, Trx-like 2, Trx-lilium 1, or 2 (Fig. 1). This diversity is obviously large and it is probably related to the numerous functions that Trxs have to play in this compartment. The specificity of these Trxs versus their target proteins is discussed in the following sections, but we have to keep in mind that, in general, no exhaustive biochemical characterization has been achieved due to the recent discovery of new plastidial Trx members.

In most photosynthetic organisms, the reduction of Trxs in the chloroplast is achieved by a ferredoxin:thioredoxin reductase (FTR). FTR is an iron–sulfur protein, specific to photosynthetic eukaryotes and cyanobacteria, which uses Fdx as an electron donor source (Dai et al. 2004). Higher plant FTRs are nuclear-encoded $\alpha\beta$-heterodimers composed of a conserved large catalytic subunit of 13 kDa (FTRc or ß-chain) containing both a [4Fe–4S] cluster and a proximal redox-active disulfide, and a variable subunit of 8–12 kDa (FTRv; Schürmann and Jacquot 2000; Schürmann and Buchanan 2008). All sequenced photosynthetic organisms, including poplar, contain only one gene coding for the ß-chain, except *Physcomitrella patens* which possesses two genes very similar, most likely resulting from a duplication event (Chibani et al. 2009). Plants also contain one or two FTRv subunits in their genomes. It is important to mention that some archaea and proteobacteria contain genes coding for proteins very similar to the catalytic subunit of FTR and which are sometimes fused to a rubredoxin module (Jacquot et al. 2009). FTR enables oxygenic photosynthetic cells to switch between light and dark metabolisms and to adapt to changes in light intensity (Schürmann and Buchanan 2008). Concerning Fdxs, plants have generally multiple genes coding for proteins which have a single [2Fe–2S] cluster usually with a low redox potential, around −400 mV and ligated by four cysteine residues contained in the following sequence motif $CX_4CX_2CX_{22-33}C$ (Dai et al. 2004). FTR is not the single partner for Fdxs as the latter proteins transfer electrons to several other proteins, including ferredoxin:NADP+ reductase (FNR), ferredoxin:nitrite reductase, sulfite reductase, glutamate synthase (Knaff 1996). This might explain why several Fdx isoforms with different redox potentials exist (see below).

Besides the light- and Fdx-dependent electron pathway, there is a NADPH-dependent thioredoxin reductase (NTR) in the chloroplasts called NTRC. This particular fusion protein is composed of a NTR module in the N-terminal part and a Trx module in the C-terminus (Pérez-Ruiz et al. 2006; Serrato et al. 2004). As the two other isoforms of NTR, NTRA, and NTRB, which are localized both in the cytosol and in mitochondria, NTRC contains a FAD cofactor that receives electrons from NADPH and reduces an internal disulfide bond (Jacquot et al. 2009; Reichheld et al. 2005). Once reduced, the cysteines serve for the reduction of the Trx active site disulfide. Although NTRs exist in all sequenced organisms, genomic analyses have highlighted the presence of several types of proteins, the plant type NTR is present in fungi and most prokaryotes, whereas a larger or elongated form is found in animals, insects, and some algae (Jacquot et al. 2009). This can be either selonocysteine-containing NTR as in mammals and algae or cysteine-containing NTR as in insects (Jacquot et al. 2009). Green algae are unique as they contain small and large NTRs. Although the size of the subunits differs, NTRs are homodimeric flavoenzymes with two subunits of about 35 kDa for plant type NTR and of about 55 kDa for animal type NTR. This is probably also true for chloroplastic NTRC, the electrons being likely transferred from the NTR domain of one subunit to the Trx domain of the

Table 1 The poplar chloroplastic equipment for proteins of the redoxin families (Grx, Trx, and Fdx) of their reductases (GR and TR) and of the two thiol-antioxidant enzyme families, peroxiredoxins and methionine sulfoxide reductases

Gene name[a]	Gene model[b]	Protein ID[c]	Length[d]	Redox Center[e]	Exon[f]	EST[g]
Grx						
PtGrxS12	fgenesh4_pg.C_LG_II002543	756363	184	CSYS	4	Yes
PtGrxS14	gw1.XIV.2949.1	246206	170	CGFS	3	Yes
PtGrxS16	estExt_fgenesh4_pg.C_LG_XVI1087	825356	296	CGFS	2	Yes
Pt4	estExt_Genewise1_v1.C_LG_XIV2676	731916	103	CCMS	1	Yes
Pt24	eugene3.01870005	586055	152	CCMC	1	Yes
Trx						
PtTrxm1	eugene3.01420010	582703	196	WCGPC	2	Yes
PtTrxm2	estExt_Genewise1_v1.C_LG_XIX2392	738945	195	WCGPC	2	Yes
PtTrxm3	estExt_Genewise1_v1.C_LG_IX2199	722208	171	WCGPC	2	Yes
PtTrxm4.1	gw1.107.137.1	263504	190	WCGPC	2	Yes
PtTrxm4.2	estExt_Genewise1_v1.C_LG_XI3916	728401	190	WCGPC	2	Yes
PtTrxm5.1	estExt_fgenesh4_pg.C_LG_II0671	816237	179	WCGPC	2	Yes
PtTrxm5.2	estExt_fgenesh4_pg.C_LG_V1048	818567	180	WCGPC	2	Yes
PtTrxm6	eugene3.00700019	595378	181	WCGPC	2	Yes
PtTrxx	gw1.VII.2415.1	218110	185	WCGPC	2	Yes
PtTrxf	estExt_fgenesh4_pg.C_LG_XIX0571	826191	188	WCGPC	3	Yes
PtTrxy1	estExt_fgenesh4_pg.C_LG_V1100	818592	170	WCGPC	4	Yes
PtTrxy2	fgenesh4_pg.C_LG_II000621	754441	170	WCGPC	4	No
PtTrxlike2.2	gw1.X.2770.1	228073	197	WCRKC	5	No
PtTrxlike2.3	gw1.VII.1056.1	419628	197	WCRKC	5	No
PtTrxlilium1.1	estExt_Genewise1_v1.C_LG_XIX0973	738413	295	GCGGC	4	Yes
PtTrxlilium1.2	estExt_Genewise1_v1.C_LG_XIII2097	730026	304	GCGGC	4	Yes
PtTrxlilium2.1	gw1.VI.1032.1	416659	220	WCASC	4	Yes
PtTrxlilium2.2	estExt_fgenesh4_pg.C_1450020	828208	233	WCASC	4	Yes
PtCDSP32	gw1.V.1928.1	206527	298	HCGPC	2	Yes
PtHCF164	estExt_fgenesh4_pm.C_LG_VII0364	832358	260	WCEVC	4	Yes
PtCiTrx	gw1.I.7034.1	178434	185	WCGPC	4	Yes
GR/TR						
PtNTRC	gw1.VI.2404.1	418031	510	CAVC/HCGPC	11	Yes
PtFTRc	gw1.I.2355.1	173755	150	$CPCX_{16}CPCX_8CHC$	5	Yes
PtFTRv1	gw1.VIII.1629.1	420201	168	None	1	Yes
PtFTRv2	gw1.X.3020.1	228323	182	None	1	Yes
PtGR1	eugene3.00150408	575013	561	CVLRGC	10	Yes
Fdx						
PtFdx1.1	grail3.0067001301	645629	149	$CX_4CSSCX_{29}C$	1	Yes
PtFdx1.2	estExt_fgenesh4_kg.C_1630003	814694	147	$CX_4CSSCX_{29}C$	1	Yes
PtFdx2	fgenesh4_pg.C_LG_I003390	753787	148	$CX_4CSSCX_{29}C$	1	Yes
PtFdx3.1	estExt_fgenesh4_pm.C_LG_VIII0072	832476	155	$CX_4CSTCX_{29}C$	1	Yes
PtFdx3.2	grail3.0106013302	660159	155	$CX_4CSTCX_{29}C$	1	Yes
PtFdx4	eugene3.00660166	594972	150	$CX_4CCTCX_{29}C$	1	Yes
PtFdx5.1	grail3.0006000801	658518	144	$CX_4CMTCX_{28}C$	1	Yes
PtFdx5.2	eugene3.00081440	564845	144	$CX_4CMTCX_{28}C$	1	Yes
PtFdx6	estExt_Genewise1_v1.C_1180060	743149	190	$CX_4CTSCX_{25}C$	6	Yes
PtFdx7	grail3.0013034101	654077	178	$CX_5CGTCX_{32}C$	6	Yes
PtFdx8	gw1.I.313.1	171713	195	$CX_5CATCX_{32}C$	6	Yes

Table 1 continued

Gene name[a]	Gene model[b]	Protein ID[c]	Length[d]	Redox Center[e]	Exon[f]	EST[g]
Tpx						
PtPrx-2cys A	eugene3.00160660	576525	269	$CX_{121}C$	7	Yes
PtPrx-2cys B	estExt_fgenesh4_pm.C_LG_VI0567	832036	263	$CX_{121}C$	7	Yes
PtPrx Q1	eugene3.00280069	589333	214	CX_4C	4	Yes
PtPrx Q2	estExt_Genewise1_v1.C_LG_XVIII0612	736741	214	CX_4C	4	Yes
PtPrx IIE	gw1.41.572.1	288087	218	TCS	1	Yes
PtGpx1	grail3.0013048601	654252	232	$CX_{47}C$	6	Yes
PtGpx3.2	fgenesh4_KG.C_LG_III000037	749200	238	$CX_{47}C$	6	Yes
Msr						
PtMsrA4.1	estExt_fgenesh4_pg.C_LG_XV0857	824833	264	$CX_{149}CX_5C$	2	Yes
PtMsrA4.2	estExt_Genewise1_v1.C_2320013	746976	262	$CX_{149}CX_5C$	2	Yes
PtMsrB1	eugene3.00110858	568844	198	YCI	3	Yes
PtMsrB3.1	estExt_Genewise1_v1.C_LG_I4275	707507	214	$CX_{52}C$	3	Yes
PtMsrB3.2	fgenesh4_pg.C_LG_IX000814	767763	217	$CX_{52}C$	3	Yes

These are the proteins experimentally established in the chloroplast or predicted using several prediction programs such as Predotar (http://urgi.versailles.inra.fr/predotar/frenP.html), TargetP (http://www.cbs.dtu.dk/services/TargetP/), and Wolfpsort (http://wolfpsort.seq.cbrc.jp/). We cannot exclude that a few of them can be targeted only to mitochondria or targeted in both compartments as for Gpx3.2, for example, (Navrot et al. 2006) or even targeted elsewhere

[a] Pt stands for *Populus trichocarpa*. When possible, the nomenclature used is related to the one of *A. thaliana*

[b] The gene models come from the version 1.1 of *Populus trichocarpa* genome available at the JGI website (http://genome.jgi-psf.org/Poptr1_1/Poptr1_1.home.html)

[c] Protein ID is available at the *P. trichocarpa* JGI website and should be kept through the different annotated versions of the genome

[d] Length of the proteins in amino acids, including their targeting sequences

[e] The sequences surrounding the catalytic cysteines and their position are generally well conserved

[f] The exon/intron structure of each gene was found the *P. trichocarpa* JGI website or completed from our analysis

[g] tblastn searches against all *Populus* EST, regardless the species, have been performed to analyze the expression of those genes. Only three genes do not have representative ESTs, but we have been able to amplify the coding sequences from cDNA

other subunit (Pérez-Ruiz and Cejudo 2009). The poplar genome contains one gene coding for NTRC that has not been duplicated (Table 1).

In chloroplasts, NTRC was initially thought to play a very specific role in stress response as it seemed to specifically reduce some classes of thiol-dependent peroxidases or peroxiredoxins (Prxs), called 2-Cys Prx and to a lesser extent Prx Q (Fig. 1; Moon et al. 2006; Pérez-Ruiz et al. 2006). However, this view has been modified by the analysis of an Arabidopsis knock-out (KO) mutant for NTRC which presented several developmental and metabolic defects (Lepistö et al. 2009; Pérez-Ruiz et al. 2006; Serrato et al. 2004; Stenbaek et al. 2008). Under some conditions, especially short 8-h light photoperiod, the mutant shows abnormal chloroplast structure, accumulates precursors of protochlorophyllide and, thus, has reduced chlorophyll but also anthocyanin contents. Hence, it has been suggested that the couple NTRC/2-Cys Prx protects the diiron-containing cyclase responsible of protochlorophyllide formation, as this oxygen-dependent step is associated with the production of reactive oxygen species (ROS; Stenbaek et al. 2008). This mutant also displays modified levels of amino acids and auxin suggesting that it is affected in the shikimate pathway (Lepistö et al. 2009). In addition, it is hypersensitive to abiotic stress (methyl viologen, drought, and salt stress; Pérez-Ruiz et al. 2006; Serrato et al. 2004). Last but not least, NTRC is regulating starch synthesis in response to light or sucrose by activating the ADP-glucose pyrophosphorylase (AGPase) both in photosynthetic (leaves) and non-photosynthetic tissues (roots; Michalska et al. 2009). This regulation is linked to the reduction of an intermolecular disulfide bridge formed between two small subunits of this heterotetrameric enzyme. As the activity in the presence of light is only partially decreased by 40–60% in NTRC mutant, it is believed that the Fdx/FTR pathway also contributes to AGPase redox regulation according to the previous report that the potato tuber or pea leaf isoforms were activated in vitro both by Trxs f and m (Ballicora et al. 2000).

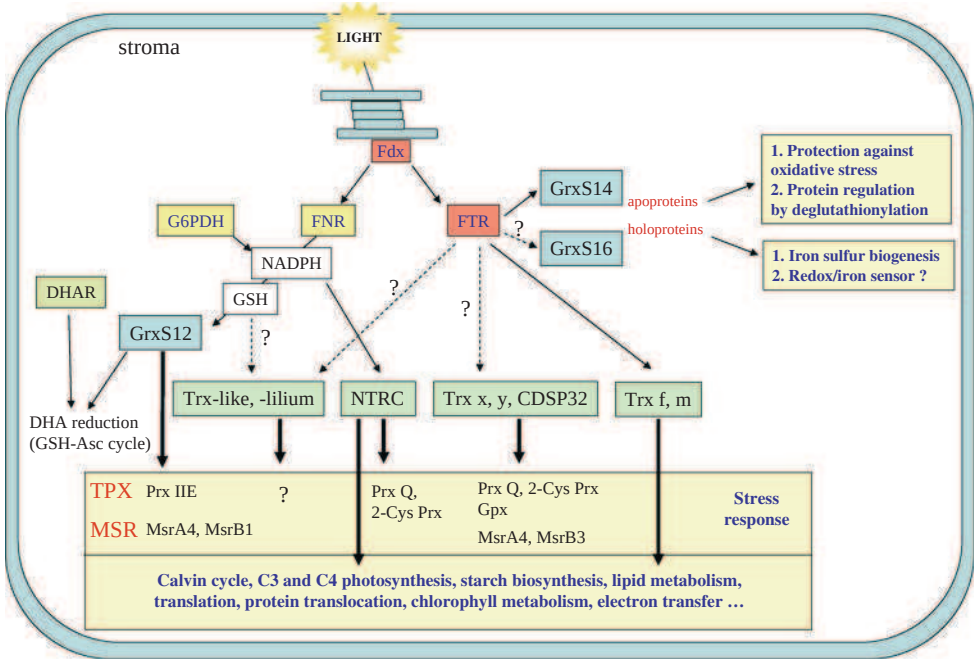

Fig. 1 The multiple roles of the poplar chloroplastic reducing systems. The sequencing of many plant genomes together with the biochemical characterization of new Trxs and Grxs expanded the roles of these oxidoreductases in plastids. The present view is as follows. Fdxs are central proteins as they transfer electrons from PSI for the reduction of both Trxs and some Grxs via FTR (ferredoxin thioredoxin reductase) or of $NADP^+$ via FNR (ferredoxin NADP reductase). NADPH, H^+ is used for the regeneration of NTRC and Grxs accepting GSH as electron donor. On the other hand, FTR is reducing most classical Trxs (Trx m, f, x, and y), and it is hypothesized here that it can support the activity of CDSP32 and CGFS Grxs (GrxS14 and S16; Zaffagnini et al. 2008). GrxS14 and S16 might play a dual function: in their apoform, they can probably participate in protein deglutathionylation, whereas in their holoform, they could participate in iron-sulfur cluster biogenesis or iron sensing. Among the target proteins, we highlighted the specificities between Trx, Grx and antioxidant enzymes, Tpx and Msr, which constitute probably the most complete picture. It seems that Trx f and m are essentially dedicated to the regulation of metabolic enzymes, while Trx x, y, and CDSP32 are more devoted to specific enzymes related to the stress response. NTRC has probably the possibility to regulate both categories. It is also very important to note that, among antioxidant enzymes, Grxs do not regenerate the same Tpx and Msr isoforms as Trxs

The chloroplastic glutaredoxin system: glutaredoxin isoforms and reduction pathways

Glutaredoxins are almost ubiquitous small oxidoreductases constituting an alternative reducing system to Trxs (Couturier et al. 2009a). Although they share a conserved 3D structure with other members of the Trx superfamily, their biochemical characterization indicates that they would rather function in the reduction of glutathionylated proteins than in the reduction of intra- or intermolecular disulfide bonds, as Trxs do. Glutathionylation is a reversible modification consisting in the formation of a mixed disulfide bond between a cysteine residue and glutathione. Protein glutathionylation is considered as a mechanism of protection of protein cysteine residues, but it could also constitute an important mechanism of redox signaling in plants by reversibly modulating protein activities (Rouhier et al. 2008a). Latest genomic and phylogenetic analysis on Grxs from photosynthetic organisms (including cyanobacteria), based on both the active site sequence and on amino acids potentially involved in glutathione binding, indicated that Grx isoforms can be classified into six classes (Couturier et al. 2009a). Although expanded, it is overlapping with previous classifications that described three distinct classes (Lemaire 2004, Rouhier et al. 2004a, 2006a). Classes I and II include Grxs conserved in all organisms. Classes III and IV are restricted, respectively, to land plants and eukaryote photosynthetic organisms (including many algae). Finally, classes V and VI are specific to cyanobacteria and will not be discussed further.

As for Trxs, several Grxs are located in the chloroplast or at least predicted to be imported in this compartment. In poplar, out of the 38 Grx isoforms, 5 Grxs which belong to class I (GrxS12), class II (GrxS14 and GrxS16), and class III (Pt4 and Pt24), but not to class IV, are predicted or confirmed to be localized in chloroplasts (Table 1). This localization has been experimentally confirmed only for poplar GrxS12, S14, and S16 (Fig. 1; Bandyopadhyay et al. 2008, Couturier et al. 2009b). Interestingly, some species such as *A. thaliana* possess at least two other putative chloroplastic Grxs, GrxC5 (class I) which is strongly related to GrxS12 and GrxS13 (class III) which seems

specific to Brassicaceae (Rouhier et al. 2004a). As for Trxs, it is important to stress that the large number of chloroplastic members is in favor of multiple roles for Grxs in this compartment.

Depending on their catalytic mechanisms and redox potentials, Grxs can be recycled either by reduced glutathione (GSH) via a NADPH-dependent glutathione reductase (GR), forming a NADPH/GR/GSH/Grx reducing system or by FTR forming in this case a Fdx/FTR/Grx reducing system (Couturier et al. 2009b; Rouhier et al. 2008a; Zaffagnini et al. 2008). Moreover, this property seems exclusive as poplar GrxS12 is only reduced by GSH, most likely because it does not form any intramolecular disulfide bridge which could be reduced by FTR, while poplar GrxS14 isoforms and presumably most if not all class II Grxs are reduced by FTR but not by GSH (Couturier et al. 2009b; Zaffagnini et al. 2008; Zaffagnini, Lemaire and Rouhier unpublished results). Indeed, the ortholog of GrxS14 in *Chlamydomonas reinhardtii*, CrGrx3, forms an intramolecular disulfide bridge with a quite low redox potential during its catalytic cycle, which allows its reduction by FTR but prevents GSH-dependent regeneration (Zaffagnini et al. 2008).

The chloroplastic ferredoxin equipment

To date, contrary to the well-described Trx and Grx families, there is no large scale genomic study concerning Fdxs from higher plants. From the 3D structure of a chloroplastic Fdx from spinach (pdb accession number 1A70), demonstrating that the [2Fe–2S] cluster is ligated by the sulfur atoms of four cysteines in position 38, 42, 44, and 76, we have used the following $CX_{4\text{-}5}CX_2CX_{22\text{–}33}C$ motif (where X represents the number of residues spacing these amino acids) as a basis for Fdx recognition (Binda et al., 1998). We first focused our attention on *P. trichocarpa* genome and we have found 11 Fdxs with a putative chloroplastic targeting sequence (Table 1). The mitochondrial Fdxs are, in general, sufficiently different from the chloroplastic ones in terms of sequence identity and they are not listed here. Compared to six other photosynthetic terrestrial plants (the bryophyte *P. patens* subsp. *patens*, the lycophyte *Selaginella moellendorfii*, the two monocots *Sorghum bicolor* and *Oryza sativa* and the dicot species *A. thaliana* and *Vitis vinifera*), it appears that *P. trichocarpa* and *S. bicolor* have an expanded Fdx family (11 members) compared to the other species (from 6 to 9 members; Fig. 2a). Overall, in these seven plants, we have successfully identified and reconstituted 58 Fdx sequences and all of them contain the four cysteines required for iron–sulfur cluster binding. The phylogenetic analysis achieved with these sequences indicates that they are distributed into five distinct phylogenetic clads, i.e., Fdx1/2, Fdx3/4, Fdx5, Fdx6, and Fdx7/8. Except for the absence of a Fdx3/4 ortholog in *P. patens*, each clad/branch contains sequences from each species, but the number of representatives for each organism is varying (Fig. 2b). In such a phylogenetic tree, mitochondrial Fdxs would constitute an additional group of [2Fe–2S] Fdxs (data not shown). As there is no classification for Fdxs and as *P. trichocarpa* possesses the highest number of members, it was chosen as a reference for the numbering. Nevertheless, we have kept the numbering for *A. thaliana* Fdxs 1–4, which have been characterized previously (Hanke et al. 2004).

The first group includes sequences named Fdx1 or Fdx2. All organisms possess one (*O. sativa* and *V. vinifera*), two (*A. thaliana* and *S. moellendorffii*), three (*P. trichocarpa* and *S. bicolor*), or five (*P. patens*) members. The identity between these members ranges from 32 to 87%, but if we exclude the two more distant organisms (*P. patens* and *S. moellendorffii*), the lowest identity gets to 53%. The second phylogenetic group includes isoforms (Fdx3 or 4) from each organism except *P. patens*. There is one member in *V. vinifera* and *S. moellendorffii*, two in *A. thaliana*, three in *P. trichocarpa*, and four in *O. sativa* and *S. bicolor* (Fig. 2a). The identity ranges from 37 to 92%.

Fig. 2 The plastidial ferredoxins from higher plants. **a** The gene content for each ferredoxin group is indicated from the genome analysis of *Arabidopsis thaliana* (At), *Oryza sativa* (Os), *Physcomitrella patens* subsp. *patens* (Pp), *Populus trichocarpa* (Pt), *Sorghum bicolor* (Sb), *Selaginella moellendorffii* (Sm) and *Vitis vinifera* (Vv). **b** Neighbor-joining phylogenetic tree. Accession numbers or gene models are: AtFdx1, At1g10960; AtFdx2, At1g60950; AtFdx3, At2g27510; AtFdx4, At5g10000; AtFdx5, At4g14890; AtFdx6, At1g32550; AtFdx7, At4g32590; OsFdx1, 13108.m00056; OsFdx3; 3103.m12896; OsFdx4.1, 13101.m06896; OsFdx4.2, 13104.m03256; OsFdx4.3, 13105.m03861; OsFdx6, 13103.m05184; OsFdx5, 13103.m04914; OsFdx7, 13105.m05112; OsFdx8, 13107.m03091; PpFdx1, estExt_Genewise1.C_3810035; PpFdx1.2, estExt_gwp_gw1.C_1430095; PpFdx2.1, e_gw1.47.219.1; PpFdx2.2, e_gw1.65.137.1; PpFdx2.3, estExt_gwp_gw1.C_1450044; PpFdx5, e_gw1.341.47.1; PpFdx6, e_gw1.98.84.1; PpFdx7, estExt_fgenesh1_pg.C_360001; PtFdx1.1, grail3.0067001301; PtFdx1.2, estExt_fgenesh4_kg.C_1630003; PtFdx2, fgenesh4_pg.C_LG_I003390; PtFdx3.1, estExt_fgenesh4_pm.C_LG_VIII0072; PtFdx3.2, grail3.0106013302; PtFdx4, eugene3.00660166; PtFdx5.1, grail3.0006000801; PtFdx5.2, eugene 3.00081440; PtFdx6, eugene3.00031457; PtFdx7, grail3.0013034101; PtFdx8, gw1.I.313.1; SbFdx1.1, estExt_fgenesh1_kg.C_chr_70006; SbFdx1.2, gw1.7.713.1; SbFdx2, estExt_fgenesh1_kg.Cchr_70007; SbFdx3, estExt_fgenesh1_pm.C_chr_10070; SbFdx4.1, gw1.3.19552; SbFdx4.2, estExt_Genewise1Plus.C_chr_64759; SbFdx4.3, Sb09g021810; SbFdx5, e_gw1.1.3722.1; SbFdx6, Sb01g011770; SbFdx7, Sb09g027890; SbFdx8, estExt_fgenesh1_pg.C_chr_23061; SmFdx1, fgenesh1_pm.C_scaffold_7000170; SmFdx2, fgenesh1_pm.C_scaffold_140000003; SmFdx4, gw1.6.757; SmFdx6, gw1.19.905; SmFdx5, gw1.10.1120; SmFdx7, gw1.21.671; VvFdx1, GSVIVP00035477001; VvFdx3, GSVIVP00007022001; VvFdx5, GSVIVP00019994001; VvFdx6, GSVIVP00015796001; VvFdx7, XP_002281853; VvFdx8, XP_002284206. **c** Amino acid comparison of the 11 putative plastidial Fdxs from *P. trichocarpa*

a

Organisms	Fdx1/Fdx2	Fdx3/Fdx4	Fdx5	Fdx6	Fdx7/Fdx8	Total
Arabidopsis thaliana	2	2	1	1	1	7
Populus trichocarpa	3	3	2	1	2	11
Sorghum bicolor	3	4	1	1	2	11
Oryza sativa	1	4	1	1	2	9
Vitis vinifera	1	1	1	1	2	6
Physcomitrella patens subsp. patens	5	0	1	1	1	8
Selaginella moellendorffii	2	1	1	1	1	6

b

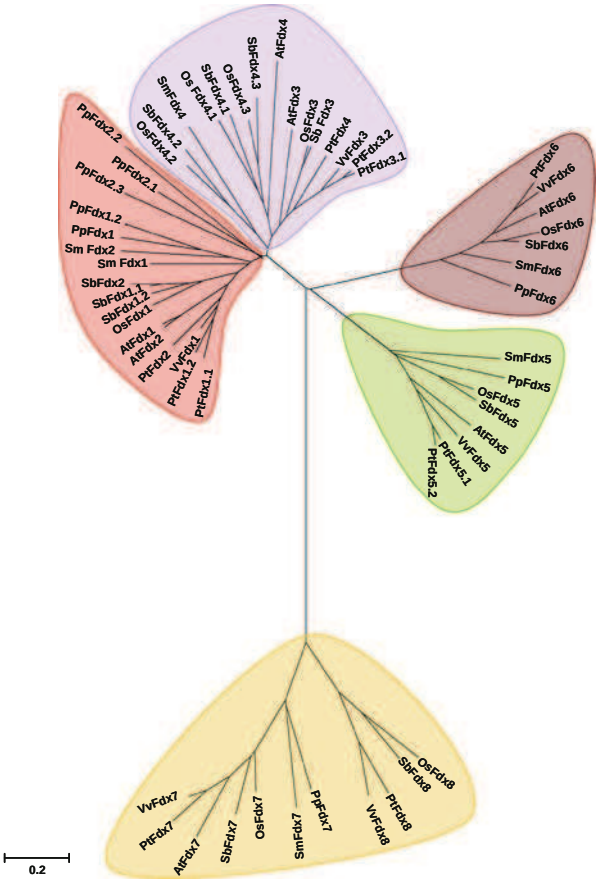

c

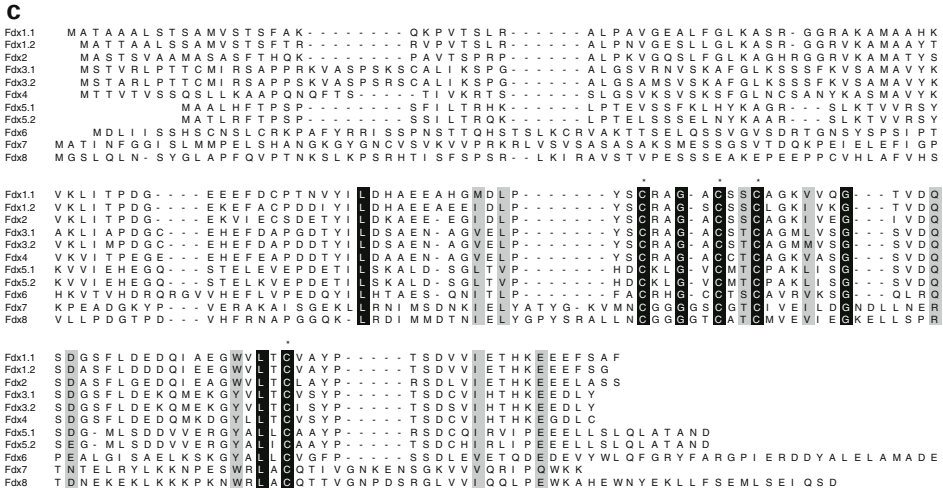

These two groups are close to each other (at least 30% identity between all members), whereas the identity of these two groups versus members of the three other groups is generally around 10–15%. Looking carefully at the amino acid sequence comparisons and with a few exceptions, each group exhibits a specific CxxC motif that can be used as a signature. For the Fdx1/2 group, the sequence is CSSC, while it is CSTC for the Fdx3/4 group. Overall, the large disparity in the number of Fdx genes between species for these two groups suggests that duplication events occurred specifically in some species. The third group (Fdx5) contains one representative from each organism analyzed except poplar, which has two members (Fdx5.1 and Fdx5.2; Fig. 2a, b). This difference most likely arises from a recent duplication event in poplar species or in a recent ancestor. In group 3, the identity between all these sequences oscillates between 48 and 89%. All members of group 3 possess a strictly conserved CMTC motif, not found in other groups. The fourth group contains one Fdx6 member from each organism, exhibiting 60–84% identity. Except for the two more primitive species, *P. patens* and *S. moellendorfii*, which have a CTAC motif, higher plant members exhibit a CTSC motif. The fifth group includes isoforms called Fdx7 and 8. All organisms possess only one Fdx7 isoform, with identity ranging from 47 to 80%. In addition, *P. trichocarpa*, *O. sativa*, *V. vinifera*, and *S. bicolor*, but not *A. thaliana*, *S. moellendorffii*, and *P. patens*, contain Fdx8 isoforms with identity ranging from 40 to 69% (Fig. 2a, b). With the exception of PtFdx8 which has a CATC motif, all other members possess a CGTC motif.

Besides this phylogenetic analysis, Fdxs can also be differentiated by their gene structure and sequence length. Indeed, genes encoding Fdxs 1–5 are constituted by a single exon, whereas, with only a few exceptions, genes coding for Fdxs 6–8 are composed by several exons, very often 6. Regarding the size of the proteins and including their targeting sequences, Fdxs 1–5 are generally constituted by 135–165 amino acids, whereas Fdxs 6–8 are composed of 170–190 amino acids. Compared to other Fdxs, Fdxs 6 have a C-terminal extension of about 25 amino acids, whereas Fdxs 7 and 8 have several small amino acid insertions (Fig. 2c, data not shown). Another striking feature of the Fdx7/8 group is the specific and different spacing (CGGGG[S/T]C, comprising 5 amino acids instead of four) between the first two ligand cysteines (Fig. 2c). Finally, the amino acid comparison of all *P. trichocarpa* Fdxs indicates that, in addition to the four cysteine residues, only four other amino acids, two leucine and two glycine residues, are strictly conserved. Surprisingly, Glu91 shown to be crucial in *Chlamydomonas* Fdx (Glu92 in spinach) for its interaction with FTR is replaced by a Gln in Fdx7 and 8, both in poplar and in other species (Jacquot et al. 1997c). This may indicate that they have acquired specific functions. In particular, the C-terminal part of Fdxs 7 is not acidic anymore but it is, on the contrary, very basic with the presence of 5–6 Lys or Arg residues and only 0–1 Glu in the last 17 residues.

Proteomic revolution and the identification of the Trx and Grx targets

Initially, the case-by-case biochemical characterization of chloroplastic enzymes has elucidated that redox regulation through the FTR/Trx pathway is able to regulate metabolic processes such as carbon, nitrogen and sulfur metabolisms, lipid or amino acid syntheses (Jacquot and Schürmann 2000; Schürmann and Buchanan 2008). Many studies have then been focused on target enzymes, in particular, those related to carbon fixation, to elucidate the molecular mechanisms and the structure–function relationships allowing their regulation by Trxs. This is well exemplified with Trxs m and f, which have been initially designated as such in relation with their respective capacity to activate the target enzymes, NADP-malate dehydrogenase (NADP-MDH), and fructose 1,6-bisphosphatase (FBPase; Jacquot et al. 1978; Schürmann and Buchanan 2008). Nevertheless, it has been shown later that, whereas FBPase is only efficiently reduced by Trx f, Trx f can also activate other enzymes such as the NADP-MDH (Schürmann and Jacquot 2000). Other examples concern the titration of the protein redox potential or the resolution of three-dimensional structures of individual proteins and FTR/Trx f and FTR/Trx m and Fdx/FTR/Trx f complexes, which helps understand the interactions at the molecular and structural levels (Dai et al. 2007; Hirasawa et al. 1999). The progress in genome sequencing and analysis enabled first to identify new chloroplastic Trxs and Grxs, which has made the situation more complex. For example, there are four Trx m isoforms in *A. thaliana* and eight in *P. trichocarpa*, raising the question of the function of these additional isoforms.

On the other hand, regarding the Trx and Grx target proteins, several groups developed proteomic approaches to identify new partners, resulting in a rapid increase of the number of enzymes and processes putatively regulated by these oxidoreductases. The ability of monocysteinic Trx and Grx mutated proteins to form a stable mixed disulfide with target oxidized proteins was one of the most used and powerful strategies developed during the last years. It was first used in vivo by trapping yeast candidate proteins using a strain where a monocysteinic *A. thaliana* Trx h (AtTrx3) was expressed (Verdoucq et al. 1999). Later, affinity columns where mutated disulfide reductases were immobilized have been developed for in vitro isolation of targets. Once trapped onto the columns, the soluble targets are eluted by a

reducing agent and identified by 2D-electrophoresis coupled to mass spectrometry or uniquely by LC/MSMS analyses (Balmer et al. 2003, 2004a, 2004b; Motohashi et al. 2001; Rouhier et al. 2005). More recently, membrane proteins have been identified by introducing some detergents to increase membrane protein solubility before or after incubation with mutated Trxs (Mata-Cabana et al. 2007; Bartsch et al. 2008).

Alternatively, the fluorescent dye mBBr (monobromobimane), which covalently binds to free thiols, has been a useful tool to detect potential Trx target proteins from peanut (Yano et al. 2001), wheat (Wong et al. 2004), medicago (Alkhalfioui et al. 2007) and barley (Marx et al. 2003) seeds and from chloroplast thylakoids (Balmer et al. 2006a; Motohashi et al. 2001). After protein separation, the fluorescent Trx targets can be visualized by their UV fluorescence. Although very useful, this technique showed some background signals due to exposed cysteine thiols of the non-reduced samples and exhibited some limits in sensitivity explaining that only the most abundant Trx targets were detected (Lindahl and Kieselbach 2009). This problem has been circumvented in many studies by using alkylating reagents such as NEM (*N*-ethylmaleimide), IAM (iodoacetamide) to block exposed thiol groups, or non-redox regulated disulfides. Similar strategies were adopted to study Trx targets from barley seeds or from Arabidopsis leaf extracts, but the proteins have been labeled with other specific thiol probes, a Cy5 maleimide dye, a compound comprising a biotin moiety (PEO-iodoacetylbiotin) or a radioactive IAM (Maeda et al. 2004; Marchand et al. 2004, 2006). As mentioned before, we have considered that all target proteins identified in other photosynthetic organisms than poplar are also putatively regulated in this organism if a close ortholog is found and if it contains the cysteine residues known to be subjected to redox regulation at conserved positions. As a consequence, we have listed as putative poplar Trx or Grx chloroplastic target proteins, all proteins, identified in photosynthetic organisms by biochemical or proteomic studies, susceptible to be redox-regulated, either via deglutathionylation or disulfide bond reduction (Table 2). It should be mentioned that the number of Trx targets is much larger than Grx targets, in particular, because only few proteomic studies have been devoted to the identification of glutathionylated proteins and Grx targets. Two major studies have been performed with Grxs either from higher plants (poplar, *A. thaliana* and *Pisum sativum*) or from the cyanobacterium *Synechocystis* sp. PCC6803 (Rouhier et al. 2005; Li et al. 2007). Additional large scale studies were also aimed at identifying glutathionylated proteins, essentially in *A. thaliana* and *C. reinhardtii* (Ito et al. 2003; Dixon et al. 2005; Michelet et al. 2008). Several reviews have already described Trx and/or Grx partners in detail or glutathionylated proteins leading to the view that in addition to the carbohydrate metabolism, a lot of other essential chloroplastic processes such as ATP synthesis, lipid, sulfur, nitrogen, hormone and vitamin metabolisms, protein translation, degradation, folding or translocation are at least partly regulated by dithiol–disulfide exchanges (Gao et al. 2009; Lemaire et al. 2007; Michelet et al. 2008; Montrichard et al. 2009; Schürmann and Buchanan 2008). We will thus essentially focus our attention on a few particular chloroplastic processes, i.e., stress response, carbohydrate metabolism, and chlorophyll/heme biosynthesis.

Some chloroplastic antioxidant proteins are regenerated by the Trx and Grx reducing systems

The presence of oxygen around living organisms generates suitable conditions for ROS production, essentially at the level of electron transport chains. Furthermore, environmental constraints, either biotic or abiotic, also contribute to an increase in cellular ROS concentrations. Hence, plants have developed numerous systems to tightly control ROS concentrations. In particular, superoxide ions are reduced by superoxide dismutases into hydrogen peroxide, which is then reduced by several classes of peroxidases, e.g., catalases, ascorbate peroxidases (Apx), glutathione peroxidases (Gpx), and peroxiredoxins (Prx). The latter two enzymes constitute the family of thiol-peroxidases (Tpx). All these peroxidases are able to decompose hydrogen peroxide within different cell compartments and with different efficiencies. For example, catalases are found almost exclusively in peroxisomes, whereas Apxs are preferentially found in the cytosol and in plastids (either in the stroma or attached to the thylakoids), but some isoforms are located in peroxisomes and mitochondria (Teixeira et al. 2006). Both enzymes are heme-containing enzymes that reduce hydrogen peroxide with a high efficiency but apparently not more complex peroxides. On the contrary, Gpxs and Prxs are non-heme peroxidases that can reduce, in addition to hydrogen peroxide, more complex substrates such as phospholipid and alkyl hydroperoxides or peroxynitrites, using critical cysteine residues (Dietz 2003; Rouhier and Jacquot 2002). Although their catalytic efficiencies seem lower when activities are measured in the presence of the reducing systems under steady-state conditions, they are present in most sub-cellular compartments and for some of them at high concentrations.

The requirement for Trx and/or Grx in stress response is very well documented in vitro, in particular for the regeneration of these thiol peroxidases and of another family of antioxidant enzymes called methionine sulfoxide reductases (Msr), enzymes that reduce methionine

Table 2 Putative or confirmed chloroplastic redox-regulated proteins

Protein name and processes regulated	Trx target	Grx target	P-SG
Calvin cycle and associated reactions			
Fructose 1,6-bisphosphatase[a,b,c,d,e,f]	14, 20	30	
Fructose-bisphosphate aldolase[a,b,c,d,e]	14, 20, 28	30	13
NADP-glyceraldehyde-3-phosphate dehydrogenase A_4[b]			35
NADP-glyceraldehyde-3-phosphate dehydrogenase A_2B_2[a,b,e]	3, 25, 28	30	
NADP-Malate dehydrogenase[b,d,k]	20		
Phosphoglycerate kinase[a,b,d,e,f,i]	4, 14, 20, 28	30	23
Phosphoribulokinase[a,b,c,d,f,g]	3, 14, 20	30	
Ribose 5-phosphate isomerase[b,d]	14, 20		23
Ribulose 5-phosphate epimerase[b,f]	20		
Ribulose phosphate 3 epimerase[f]	3		
Rubisco activase[c,b,f]	3, 20, 25	30	
Rubisco small chain[a,b,c,f,i,d]	3, 14, 20, 25	30	
Rubisco large chain[a,b,c,d,e,f,h,i]	1, 4, 14, 17, 21	30	
Sedoheptulose 1,7-bisphosphatase[b,d,f,g]	14, 20, 25		
Transketolase[a,b,c,e,f,i]	3, 20, 28	30	
Triose phosphate isomerase[a,b,f,h]	1, 3, 20	30	13
Chloroplastic protein CP12[b]	19, 20		
Carbonic anhydrase β[a,b,c,f]	3, 4, 20	30	
ATP Metabolism			
ATP synthase α subunit d[e,f]	4, 14, 21		
ATP synthase β subunit[d,f]			23
ATP synthase γ subunit[f]			
Inorganic pyrophosphatase[a,b,d]	14	30	23
Amino acid metabolism			
Ketol acid reductoisomerase[d]	14		
Threonine synthase[d]	14		
3-isopropylmalate dehydrogenase[b]	14		
3-isopropylmalate dehydratase[b]			9
Aspartate amino transferase[d]			23
Dihydroxy-acid-dehydratase[b,f]	14, 19, 20		
Nitrogen metabolism			
Glutamine synthetase[a,b,c,f,h]	1, 3, 14, 20, 25	30	
Nitrite reductase[b]	20		
Phosphoglycerate dehydrogenase[f,h]	1, 3		
Argininosuccinate synthase[b,d,e,f]	3, 14, 17	15	9
Ferredoxin-dependent glutamate synthase[a,e]	17	30	
Sulfur metabolism			
ATP sulfurylase[b]	20		9
Sulfite reductase[e]	17		
Cysteine synthase[a,f]	3	30	
Glycolysis			
Enolase[f]	3, 14		
Pentose phosphate cycle			
Glucose-6-phosphate dehydrogenase[j]	33		
6-Phosphogluconate dehydrogenase[f]	3		
Photosynthesis/electron transfer/respiration			
Ferredoxin [2Fe–2S][b,c,d]	14, 20	30	

Table 2 continued

Protein name and processes regulated	Trx target	Grx target	P-SG
Photosystem II oxygen evolving enhancer[b] OEE1-1	20		
Photosystem II oxygen evolving enhancer[b] OEE1-2	20		
Photosystem II oxygen evolving enhancer[b,f] OEE2-1	20		
Plastocyanin[b,f]	20		
Oxygen evolving complex (PsbO)[a]			23
16-kDa polypeptide oxygen evolving complex (PsbQ)[a,d]	14	30	
PSI reaction center, PsaK subunit[f]	5		
PSI reaction center, N subunit[f]	5		
Rieske FeS protein[f]	5		
Ferredoxin NADP reductase[a]		30	
Protein degradation			
ATP-dependent Clp protease[a,f,i]	3, 4	30	
Deg1[b]	31		
FTSH2 (Var2)[b]	26		
FTSH8[b]	26		
Subtilase[b]		30	
Protein folding			
Chaperonin HSP60α[a,b,c,d,h]	1, 3, 14	30	23
Chaperonin HSP60β[a,c,h]	1	30	
Cpn20[d]	14		23
Cyclophilin[b, f]	20, 25		
FKBP peptidylprolyl cis–trans isomerase[b]	11, 16, 20		23
HCF136[b]	31		
HSP70 kDa[a,b,d, f, h,i]	1, 3, 14, 20	30	23
3-Phosphoshikimate 1-carboxyvinyltransferase[e]		15	
Translation			
Elongation factor Tu[a,d,c,f]	3, 14	30	23
Elongation factor G[f]	3		
RNA-binding protein RB38[d]			23
RNA-binding protein RB60[d]	14		23
Nucleoside diphoshate kinase[a]		30	23
Ribosomal protein L4[f]	4	15	
Ribosomal protein L21[f]	4		
Ribosomal protein S1[f]	3		
Ribosomal protein S5[f]	4		
Ribosomal protein S6[f]	3		
Ribosomal protein S30[f]	4		
Isoprenoid biosynthesis			
DXP reductoisomerase[f]	3		
GcpE protein[f]	3		
LytB[d]	14		
Vitamin biosynthesis			
Thiamin biosynthesis protein[f]	3		
Thiazole biosynthetic enzyme[d,f]	3, 14		
Shikimate pathway			
DAHP synthase[b]	10		
Stress response			
Ascorbate peroxidase (APX1)[f]	6		

Table 2 continued

Protein name and processes regulated	Trx target	Grx target	P-SG
GlutaredoxinS12[a,b]		30	9
Glutathione peroxidase[a]	27		
Glutathione reductase[a]		30	
Glutathion-S-transferase[b]	20		
Methionine sulfoxide reductase A[b]	19		
Methionine sulfoxide reductase B1[b]	29, 32	32	32
Peroxiredoxin Q[a,b, f]	20, 25, 29	30	
Peroxiredoxin IIE[a,b,h]	1, 14, 17	30	
2-Cys peroxiredoxin[a,b,c,d,g,h,i,j,l]	1, 3, 14, 18, 25	30	9, 23
Cu/Zn Superoxide dismutase[g]	18		
Thioredoxin f[b]			13
Starch metabolism			
ADP-glucose pyrophosphorylase[b,c,e,f,i,j]	14, 17	30	
ß-Amylase[f]	4		
Alpha glycan water dikinase [j]	24		
Chlorophyll metabolism			
Chlorophyll *a/b* binding protein (LHCIIb)[f]	6		
Uroporphyrinogen decarboxylase[b]	20		
Mg-chelatase Chl-1[d]	12		23
Pheophorbide *a* oxygenase[b]	8		
Red chlorophyll catabolite reductase[a]		30	
NADPH:protochlorophyllide oxidoreductase translocon protein PTC52[b]	8		
GSA aminomutase[f]	3		
Fatty acid/lipid biosynthesis			
Acetyl-CoA carboxylase (CAC2)[b]	2		9
Acetyl-CoA carboxylase (BCC1)[d]			23
Malonyl CoA ACP transacylase[d]	14		
MGDG synthase[l]	34		
Acetyl-CoA biotin carboxyl carrier[d]			23
Jasmonic acid biosynthesis			
Allene oxide cyclase[a,b]		30	
DNA metabolism			
Nucleoid DNA binding protein[b]	20		
AIR synthase[d]	14		
ATP-dependent DNA helicase[f]	3		
Plastid division			
FtsZ protein[f]	3		
Transport-translocation			
Probable anion transporting ATPase[e]		15	
TIC110[b]	7		
TIC55[b]	8		
Other functions			
Glycerol-3-phosphate dehydrogenase[b]		30	
17.4 kDa lumenal protein[b]	19		
Plastid development protein[b]		30	
Plastid lipid-associated protein 10[d]			23

Table 2 continued

Protein name and processes regulated	Trx target	Grx target	P-SG
Ferritin[h]	1		
Apospory-associated protein c-like[b]	19, 20		

Most of these proteins have been identified via proteomic studies aimed at identifying Trx or Grx targets or glutathionylated proteins (P-SG) and using different model organisms: [a]*Populus trichocarpa*, [b]*Arabidopsis thaliana*, [c]*Pisum sativum*, [d]*Chlamydomonas reinhardtii*, [e]*Synechocystis* sp., [f]*Spinacia oleracea*, [g]*Hordeum vulgare*, [h]*Medicago truncatula*, [i]*Triticum* spp., [j]*Solanum tuberosum*, [k]*Sorghum bicolor*, [l]*Cucumis sativus*

References are as follows: (1) Alkhalfioui et al. 2007, (2) Ballicora et al. 2000, (3) Balmer et al. 2003, (4) Balmer et al. 2004b, (5) Balmer et al. 2006a, (6) Balmer et al. 2006b, (7) Balsera et al. 2009, (8) Bartsch et al. 2008, (9) Dixon et al. 2005, (10) Entus et al. 2002, (11) Gopalan et al. 2004, (12) Ikegami et al. 2007, (13) Ito et al. 2003, (14) Lemaire et al. 2004, (15) Li et al. 2007, (16) Lima et al. 2006, (17) Lindahl and Florencio, 2003, (18) Maeda et al. 2004, (19) Marchand et al. 2004, (20) Marchand et al. 2006, (21) Mata-Cabana et al. 2007, (22) Michelet et al. 2005, (23) Michelet et al. 2008, (24) Mikkelsen et al. 2005, (25) Motohashi et al. 2001, (26) Motohashi and Hisabori 2006, (27) Navrot et al. 2006, (28) Pérez-Pérez et al. 2006, (29) Rey et al. 2005, (30) Rouhier et al. 2005, (31) Ströher and Dietz 2008, (32) Tarrago et al. 2009b, (33) Wenderoth et al. 1997, (34) Yamaryo et al. 2006, (35) Zaffagnini et al. 2007

sulfoxide (MetSO) residues back to methionine (Vieira Dos Santos and Rey 2006; Rouhier et al. 2006b, 2008a). Methionine oxidation can indeed result in the formation of two different S- and R-enantiomers which are reduced specifically by two different groups of Msrs, named MsrA and MsrB, respectively. Both enzymes are required since methionine oxidation leads to a racemic mixture of both isomers. It has been proposed that Msrs participate in the antioxidant network both by repairing methionine residues critical for the functioning of some proteins but also by serving as a H_2O_2 scavenging system through the random and cyclic reduction of MetSO, some of the oxidized methionines being not essential for either the function or structure in some proteins (Levine et al. 1996). The genomic and phylogenetic analyses as well as the structural and catalytic aspects of plant Tpxs and Msrs have been detailed already (Rouhier and Jacquot 2005; Rouhier et al. 2006b; Gama et al. 2007; Rouhier et al. 2008b; Tarrago et al. 2009a). Briefly, the catalytic and regeneration mechanisms for Tpxs and Msrs are similar. The enzymes are grouped in different classes essentially based on the number of cysteine residues involved in these steps. Following substrate reduction, the first step of the catalytic mechanism is the formation of a sulfenic acid on the catalytic cysteine and the release of the product of the reaction. This sulfenic acid is either directly attacked by the reductant (Trx, Grx, or glutathione) or alternatively one or two cysteines acting as resolving cysteines can form intra- or intermolecular disulfides. These disulfides are then reduced by Trxs or Grxs. Hence, we will focus here on the specificities of the chloroplastic enzymes, many of them from poplar, with respect to their substrates and reductants.

Protein repair by MetSO reduction

Several studies achieved both with poplar and *A. thaliana* enzymes have led to the elucidation of the catalytic mechanism, substrate and reductant specificities of MsrA and MsrB. Poplar possesses nine Msr isoforms: five MsrA and four MsrB, with MsrA4.1, MsrA4.2, MsrB1, MsrB3.1, and MsrB3.2 being predicted as localized in chloroplasts (Table 1; Rouhier et al. 2006b). The difference with *Arabidopsis* is important as the latter species contains 14 Msrs (5 MsrA and 9 MsrB) but only 3 plastidial Msrs (MsrA4, MsrB1, and MsrB2; Tarrago et al. 2009a). The two MsrBs differ by the regeneration system used. Among chloroplastic Trxs, Trxs m, f and y may constitute preferential electron donors for MSRB2, but not for MsrB1, which is reduced by CDSP32 and GrxS12 (Vieira Dos Santos et al. 2007). The fact that chloroplastic poplar GrxS12 efficiently reduces *A. thaliana* MsrB1 in vitro suggests that the orthologous proteins can also interact in both organisms as there is one MsrB1 ortholog in poplar (Table 1). In *A. thaliana*, only one Grx, named GrxC5, is susceptible to replace GrxS12. This protein is apparently only present in Brassicaceae suggesting that the preferred physiological reductant in poplar is most likely GrxS12. The specificity of MsrB1 and MsrB2 toward their reductants is linked to the presence of a resolving cysteine in MsrB2, in addition to the catalytic cysteine, while MsrB1 has only one redox-active cysteine (Vieira Dos Santos et al. 2005). Indeed, an intramolecular disulfide bond, specifically formed in MsrB2, is only reduced by Trxs, whereas for MsrB1, the sulfenic acid is first glutathionylated after reaction with a GSH molecule and this adduct is specifically reduced by Grx (Tarrago et al. 2009b). The CDSP32-mediated regeneration mechanism is not elucidated yet.

The biochemical and enzymatic analyses of poplar MsrA2.1 (cytosol) and MsrA4.1 (plastidial) support a catalytic mechanism involving three cysteines, Cys46 is the catalytic cysteine, and the two C-terminal cysteines 196 and 202 (poplar MsrA4.1 numbering) are implicated in the Trx-dependent recycling mechanism (Rouhier et al. 2007a). In addition, although the catalytic mechanism is not yet elucidated, poplar MsrA4.1 can also be regenerated

by the GSH/Grx system (Rouhier and Couturier, unpublished data).

Although MsrA and B were not very often identified as Trx targets using proteomic approaches, the biochemical characterization of various Msr isoforms clearly showed that they are regenerated both by Trxs and/or Grxs. Nevertheless, cytosolic and plastidial MsrAs have been identified, respectively, in *C. reinhardtii* and *A. thaliana* extracts, and *A. thaliana* MsrB1 was retained on a CDSP32 (an elongated Trx overexpressed in drought conditions) affinity column (Lemaire et al. 2004; Marchand et al. 2004; Rey et al. 2005).

Numerous studies in plants and algae have indicated that Msrs are involved in the tolerance to oxidative stress conditions. Indeed, both biotic and abiotic stress conditions modify the Msr gene expression and protein abundance. Regarding plastidial Msrs, Arabidopsis MsrA4 expression is enhanced by oxidative treatments, high light and salt treatment (Romero et al. 2004; Vieira Dos Santos et al. 2005). The abundance of the plastidic poplar MsrA is increased during an incompatible reaction with the rust fungus *Melampsora larici populina* (Vieira Dos Santos et al. 2005). The levels of AtMsrB1 and AtMsrB2 proteins are slightly increased in Arabidopsis plants subjected to photooxidative stress (Vieira Dos Santos et al. 2005). The study of plants under- or overexpressing *msr* genes has also been investigated under various stress conditions. Compared to WT plants, plants overexpressing AtMsrA4 are more tolerant to photooxidative treatments (high light and methyl viologen) known to generate damages to photosynthetic membranes, whereas Arabidopsis plants underexpressing AtMsrA4 are more sensitive (Romero et al. 2004). From this study, it has been proposed that plastidial MsrA protects photosynthetic structures, most likely by repairing oxidatively damaged proteins (Romero et al. 2004). Only few proteins are known Msr substrates in photosynthetic or even non-photosynthetic organisms. In the chloroplast, MsrA is required to maintain the chaperone activity of the Hsp21 heat shock protein by reducing its oxidized methionines (Gustavsson et al. 2002; Sundby et al. 2005).

ROS degradation in the chloroplast: thiol dependency of antioxidant enzymes

The major chloroplastic enzymes (SOD, Apx, and Tpx) involved in the detoxification of superoxide ions and H_2O_2 might be dependent on the Trx or Grx reducing systems, SOD and Apx for the regulation of their activity and Tpx for their regeneration.

A plastidial Cu/Zn SOD has been identified as a putative Trx partner both in barley seeds and amyloplasts (Balmer et al. 2006b; Maeda et al. 2004). Cytosolic Cu/Zn SOD have also been identified in such proteomic studies (Wong et al. 2004). It is known that these dimeric proteins contain a structural disulfide bond, essential for the stability and thus for the activity of the protein. Grxs can reduce this disulfide in some mutated human SOD forms and to a lesser extent in human WT forms (Carroll et al. 2006). In addition, it has been demonstrated that glutathionylation of Cys111 in human SOD1 promotes the monomer formation, considered as a first step leading to protein aggregation (Wilcox et al. 2009). Nevertheless, this cysteine is not conserved in plant Cu/Zn SOD raising the question of their redox regulation in plastids and more generally in plants.

Ascorbate peroxidases, mostly cytosolic, have been identified as putative Grx or Trx partners but a plastidial Apx has also been isolated from an amyloplast extract (Balmer et al. 2006a, b; Marchand et al. 2004, 2006; Rouhier et al. 2005; Wong et al. 2004; Yamazaki et al. 2004). Pea cytosolic Apx contains one conserved cysteine residue located close to the ascorbate binding site and treatment with the NADPH-dependent Trx system leads to the quick inactivation of this enzyme (Gelhaye et al. 2006).

Phylogenetic analyses indicate that thiol-peroxidases can be subdivided into five classes, the so-called glutathione peroxidases, and four types of peroxiredoxins, 1-Cys, 2-Cys, type II, and type Q peroxiredoxins (Rouhier and Jacquot 2005). As Msr, the different Prx classes obviously differ by their primary structure, but also by their 3D structure and their catalytic mechanism which is dependent on the number and the position of cysteines involved in catalysis (Rouhier and Jacquot 2002). There are 15 genes in poplar (6 Gpx and 9 Prx), 17 in *A. thaliana* (8 Gpx and 9 Prx) and 12 in *C. reinhardtii* (7 Gpx and 5 Prx; Dayer et al. 2008; Dietz 2003; Gama et al. 2007; Navrot et al. 2006; Rouhier and Jacquot 2005). The comparative genomic analysis of these photosynthetic organisms associated to localization predictions or to experimental data indicates that the chloroplastic compartment contains one or two members of each following classes, 2-Cys Prx, Prx II, and Prx Q and Gpx (Dayer et al. 2008; Dietz et al. 2006; Rouhier and Jacquot 2005). Nevertheless, there are important differences between organisms. In *A. thaliana*, four Prxs are targeted to the chloroplast, 2-Cys Prx A and B, Prx Q and Prx IIE. In *P. trichocarpa* and *O. sativa*, five Prxs might be present in plastids, again with a small difference, 2-Cys Prx, Prx Q1, Prx Q2, Prx IIE1 and Prx IIE2 for *O. sativa* and 2-CysPrx A and B, Prx Q1, Prx Q2 and Prx IIE for *P. trichocarpa* (Dietz et al. 2006; Gama et al. 2007; Rouhier et al. 2004b). In *C. reinhardtii*, only three Prxs might be targeted to the chloroplasts, a 2-Cys Prx, a Prx Q, and a Prx II (Dayer et al. 2008). Concerning Gpxs, there are no experimental data concerning their localization in *A. thaliana* and *C. reinhardtii*, but one to three Gpxs

might possibly enter this organelle. In *P. trichocarpa*, the situation is much clearer as two Gpxs (Gpx1 and Gpx3.2) are targeted to the chloroplast, with Gpx1 being also targeted to mitochondria (Navrot et al. 2006).

Electron donor specificities of chloroplastic Gpxs and Prxs

Most Gpxs from photosynthetic organisms possess three strictly conserved Cys at the same relative position in their amino acid sequences (Rouhier and Jacquot 2005), and two of these cysteines are involved in catalysis and Trx-mediated regeneration mechanisms in most organisms outside the animal kingdom, including poplar (Herbette et al. 2002; Jung et al. 2002; Navrot et al. 2006). As these two cysteines are conserved in all Gpxs identified so far in higher plants, it is believed that this mechanism is common to all these Gpxs and these proteins are in fact thioredoxin peroxidases and not glutathione peroxidases as GSH is unable to regenerate them. There are some exceptions in *C. reinhardtii* with two members (CrGpx1 and 2) out of the five, related to the mammalian-type Gpx, that exhibit a selenocysteine instead of the N-terminal peroxidatic cysteine (Dayer et al. 2008). These proteins most likely use GSH for their regeneration but this possibility is clearly restricted to green algae. In addition, one of the three cysteine-containing Gpxs of Chlamydomonas (CrGpx3) does not contain the resolving cysteine essential for Trx regeneration.

Among the panel of plastidial Trxs tested (Trxs f, m, x, and y), poplar chloroplastic Gpxs display a marked selectivity in vitro toward their electron donors, being most efficiently reduced by Trx y (Navrot et al. 2006). This will have to be tested further as other Trxs, such as CDSP32, CiTrx or Trx-like or -lilium, have not been tested so far as possible reductants. Similarly, there is no complete investigation achieved with Gpxs from other sources. Interestingly, some cytosolic Gpxs have been retained on Trx affinity columns (Alkhalfioui et al. 2007; Wong et al. 2004). In addition, from immunoprecipitation experiments achieved with Gpx3 from *Saccharomyces cerevisiae*, a protein very similar to plant enzymes, yeast Grx2, was identified as a putative partner (Lee et al. 2008). Although Gpxs are apparently not regenerated by Grxs, their identification as Grx partner is puzzling and might be related to a regulation linked to glutathionylation (Navrot et al. 2006).

In addition to Gpxs, three different Prx classes are present in chloroplasts, i.e., 2-Cys Prx, Prx Q and Prx IIE. Interestingly, they were identified in many proteomic studies as both putative Trx and Grx partners. Nevertheless, in vitro activity measurements indicated that 2-Cys Prx and Prx Q are reduced via the Trx system, whereas PrxIIE, at least the one from poplar, is preferentially regenerated by Grxs (including the chloroplastic GrxS12), but it can also use Trx, as demonstrated previously for the cytosolic Prx IIB (Gama et al. 2008; König et al. 2002; Rouhier et al. 2001, 2004b). Considering the redox potential of the disulfide of 2-Cys Prx and Prx Q (around −315 mV and −325 mV, respectively) it was not expected that Grxs (redox potential around −170 mV) can efficiently reduce these two Prxs even with the help of GSH (König et al. 2003; Rouhier et al. 2004b, 2007b). Although it has been confirmed that poplar 2-Cys Prx cannot use Grxs in vitro for their regeneration, the glutathionylation of a 2-Cys Prx from *C. reinhardtii* promotes a switch from a dimeric to a monomeric state, suggesting that Grxs can at least in some organisms regulate the activity and/or oligomerization state of these proteins (Michelet et al. 2008; Rouhier et al. 2005).

A number of Trxs proved to be efficient for the reduction of 2-Cys Prx, and Trx x, CDSP32, and NTRC have thus far been shown to be the most efficient (Broin et al. 2002; Collin et al. 2003; König et al. 2002; Pérez-Ruiz et al. 2006). Unexpectedly, considering their redox potential (around −250 mV), the plastidial Trx-lilium (called AtACHT1, AtACHT2a, and AtACHT4a) were also recently shown to regenerate 2-Cys PrxA (Dangoor et al. 2009). As Trxs x are reduced through the Fdx/FTR pathway and NTRC using NADPH as a source of reducing power, it has been suggested that 2 Cys-Prxs might be reduced *in planta* both by the Fdx/FTR/Trx x and NTRC pathways during light periods and by NTRC during darkness (Collin et al. 2003; Pérez-Ruiz et al. 2006). As all these proteins are present in eukaryotic photosynthetic organisms, including poplar, we anticipate that all these pathways are viable in poplar (Chibani et al. 2009). Actually, it is not yet known how CDSP32 is reduced in the cells, but this pathway could be specifically activated during stress conditions (Broin et al. 2002).

In plants, Prx Q is a strict Trx-dependent peroxidase which is able to reduce in vitro, a broad variety of peroxides including phospholipid hydroperoxides (Lamkemeyer et al. 2006; Rouhier et al. 2004b). Regarding its regeneration, the Grxs tested so far are not able to provide electrons, whereas Trx y, CDSP32, and NTRC do (Collin et al. 2004; Moon et al. 2006; Rey et al. 2005; Rouhier et al. 2004b).

Prx IIE, which is addressed to the chloroplast, can reduce in vitro, both hydrogen peroxide and more complex peroxides (Bréhélin et al. 2003; Gama et al. 2008). As cytosolic poplar Prx IIB, poplar Prx IIE accepts both the Trx and the GSH/Grx system as electron donors but not GSH alone, unlike mitochondrial Prx IIF (Finkemeier et al. 2005; Gama et al. 2007; Gama et al. 2008). The electron donor specificity is directly linked to the unique catalytic mechanism used by these enzymes. Indeed, although

generally possessing two cysteines (a peroxidatic and a potential resolving cysteine), these Prx IIE most likely use a single cysteine as 1-Cys Prxs. Indeed, in the Grx-mediated regeneration, the sulfenic acid formed on the peroxidatic cysteine of Prx II is most likely attacked by a glutathione molecule forming a glutathione adduct, which is subsequently reduced by Grxs. For the cytosolic Prx IIB, this glutathionylation step leads to the switch from a dimeric to a monomeric state (Noguera-Mazon et al. 2006). In general, Prxs II are either poorly, or not, reduced by Trxs, further indicating that Trxs are poor reductants for sulfenic acid moieties (Bréhélin et al. 2003).

Physiological roles for Gpxs and Prxs inside the chloroplast

As for Msrs, the study of Prx gene and protein expression and of plants under- or overexpressing *prx* genes is crucial for understanding their function. Owing to their peroxidase activities, chloroplastic Tpxs are thought to participate in the protection against oxidative stress conditions. Different studies in *A. thaliana* and potato have shown that 2-Cys Prx could act as a constitutive protector of photosynthetic apparatus and membranes (Baier and Dietz 1999; Broin et al. 2002, Broin and Rey 2003; Dietz et al. 2006). From the numerous studies devoted to the analysis of 2-Cys Prx gene and protein expression under environmental constraints, it appears that 2-Cys Prxs are not strongly regulated (Gama et al. 2007). As a homodimer, this abundant enzyme is an efficient stromal peroxidase, but it has the possibility to form decamers attached to the thylakoids (König et al. 2002). By analogy to yeast Prxs, the decameric form could function as a chaperone (Jang et al. 2004).

Prx Q is also partly anchored to the thylakoid membrane and possibly facing the lumen (Lamkemeyer et al. 2006; Petersson et al. 2006; Rouhier et al. 2004b). Plants with decreased levels of Prx Q did not have an obvious different phenotype from the WT, but more precise analyses indicate that this Prx could nevertheless have a specific but distinct from 2-Cys Prx function in protecting photosynthesis (Lamkemeyer et al. 2006; Petersson et al. 2006). The Prx Q abundance is increased very early during incompatible interaction of poplar with *Melampsora larici populina*, whereas it is decreased during a compatible interaction (Rouhier et al. 2004b). Similarly, the protein from *Gentiana triflora* is also regulated during a pathogen infection (Kiba et al. 2005). The level of Prx Q protein in *A. thaliana* increases in response to photooxidative treatment and water deficit (Gama et al. 2008).

In *A. thaliana*, Prx IIE is constitutively expressed in all tissues analyzed and does not generally respond to oxidative stress conditions such as photooxidative treatment and water deficit, peroxide and diamide treatments or heavy metal exposure (Bréhélin et al. 2003, Collin et al. 2007; Gama et al. 2008; Horling et al. 2003). Nevertheless, application of ascorbate and salt stress affects its transcript levels (Horling et al. 2002). On the one hand, Prx IIE can reduce peroxynitrite, but on the other hand S-nitrosylation of the peroxidatic cysteine inhibits its peroxidase activity (Romero-Puertas et al. 2007). Plants under- or over-expressing *prxIIE* genes have no apparent phenotype under control conditions. Nevertheless, challenged with the avirulent bacteria *Pseudomonas syringae* pv *tomato*, KO plants display increased lipid peroxidation and tyrosine nitration compared to the WT, whereas overexpression lines present reduced levels of both (Romero-Puertas et al. 2007). This is consistent with a role linked to chloroplast NO- and ROS-signaling pathways.

The transcriptional expression analysis of *gpx* genes in several photosynthetic organisms provided some clues about the roles of Gpxs. In *C. reinhardtii*, most Gpxs are regulated by stress conditions. Concerning the putative chloroplastic *CrGpx5*, its transcription is induced in response to many ROS such as singlet oxygen or organic hydroperoxides (reviewed in Dayer et al. 2008). In higher plants, the expression of most *A. thaliana* Gpxs was investigated in several organs and under stress conditions (Rodriguez Milla et al. 2003). The two putative chloroplastic Gpxs (AtGpx1 and AtGpx7) have opposite transcriptional expression patterns. From EST analysis, AtGpx1 is one of the most expressed Gpx, while there is no EST for AtGpx7. Nevertheless, although slightly expressed, it is present in all *A. thaliana* tissues tested, but it was not further tested for stress response. The AtGpx1 transcript levels increase in response to many treatments such as heat shock, ABA, IAA and in response to salt and iron stresses. In *A. thaliana* plants exposed to metal (either copper or cadmium), the abundance of one Gpx, most likely Gpx1, is increased (Navrot et al. 2006). An *A. thaliana* transgenic line depleted for both chloroplastic Gpx genes is strongly affected for leaf development as it exhibits altered leaf cells and chloroplast morphology (Chang et al. 2009). In particular, these two Gpxs are regulating photooxidative tolerance and immune responses. The studies in poplar also confirmed that Gpx abundance is modified under stress conditions, in particular in response to a pathogen infection (Navrot et al. 2006). Nevertheless, owing to the lack of specificity of the antibody used, and although a leaf protein extract has been used, it was not possible to determine which isoform (plastidial or not) was regulated.

Finally, we have to keep in mind that Prx function will be affected by their oxidation state and by the one of their reductants. Depending on the peroxide concentration, the activity of most Tpxs is likely to be modulated by

inactivation through cysteine overoxidation or nitrosylation as observed, respectively, for 2-Cys Prxs and Prxs IIE. For instance, it is now recognized that overoxidation of 2-Cys Prxs is part of the peroxide signaling pathways. The presence in the chloroplast of a sulfiredoxin, an enzyme converting overoxidized 2-Cys Prxs back to their active form, is crucial for such regulation (Rey et al. 2007). It was proposed that a cytosolic *A. thaliana* Gpx isoform could serve as an oxidative signal transducer in ABA and drought stress signaling through its interaction with the 2C-type protein phosphatase Abi2 (Miao et al. 2006). All these examples illustrate how chloroplastic Tpxs might modulate oxidative stress signaling pathways.

Overall, the situation concerning Tpxs in the chloroplast is quite complex as there are three major reducing pathways, i.e., light/Fdx/FTR/Trx, NADPH/NTRC, and NADPH/GR/GSH/Grx. Assuming that CDSP32 is reduced by FTR, we propose the following scheme: (i) Gpxs would be exclusively reduced in the presence of light, (ii) 2-Cys Prxs, Prxs Q are reduced both by the light/Fdx/FTR/Trx and NADPH/NTRC systems, and (iii) Prx IIE is preferentially reduced by the NADPH/GR/GSH/Grx and to a lesser extent by the light/Fdx/FTR/Trx system (Fig. 1). Hence, depending on the redox state of each component of these systems and of the whole chloroplast, peroxides can be reduced by several Tpxs. The intra-organellar distribution and substrate specificity are also important. Some Tpxs attached to the envelope and/or thylakoid membranes (2-Cys Prx, Prx Q) might be important to prevent or repair lipid peroxidation and to protect the photosynthetic structures. With respect to their activities and specificities, it is worth mentioning that all Prxs do not reduce the same substrates, for example, 2-Cys Prx can reduce peroxynitrites and Gpxs might be more dedicated to the reduction of lipid hydroperoxides (Sakamoto et al. 2003). Looking at the expression pattern of all chloroplastic Tpxs, it seems that 2-Cys Prx and Prx IIE are not strongly responsive to biotic and abiotic stresses, whereas Prx Q and Gpxs are very often found to be regulated in response to such constraints.

Redox regulation of enzymes involved carbohydrate assimilation: a few case studies

Many proteins involved in processes related to carbon assimilation, i.e., electron transport, ATP formation, carbon fixation and assimilation, starch and sucrose synthesis have been demonstrated or proposed to be regulated by redox changes (Table 2; Ruelland and Miginiac-Maslow 1999). In particular, many Calvin cycle enzymes are known to be regulated by Trxs, and most if not all have been retained on Trx or Grx affinity columns or identified as glutathionylated proteins (Ito et al. 2003; Michelet et al. 2008; Rouhier et al. 2005; Zaffagnini et al. 2007). All these data suggest that glutathionylation of Calvin cycle enzymes could also constitute a regulation mechanism of photosynthetic metabolism and that plastidial Grxs might play an important role in this phenomenon by regulating either the Calvin cycle enzymes or their reductant as exemplified by the inactivation of Trx f after glutathionylation (Lemaire et al. 2007; Michelet et al. 2005).

We will focus our attention on a few enzymes belonging (i) to the reductive pentose phosphate cycle (Calvin cycle) such as FBPase, NADP-glyceraldehyde-3-phosphate dehydrogenase (GAPDH), and phosphoribulokinase (PRK) or (ii) to other steps of the carbohydrate metabolism such as NADP-MDH and glucose-6-phosphate dehydrogenase (G6PDH; Buchanan et al. 2002; Schürmann and Buchanan 2008). Basically nothing is known concerning the biochemical properties of these enzymes in poplar, but genomic analyses suggest that the corresponding enzymes should behave as their plant counterparts as the cysteines involved in the redox regulation are conserved.

Fructose 1,6-biphosphatase

FBPase is a key enzyme of the Calvin cycle, catalyzing the conversion of fructose-1,6-bisphosphate into fructose-6-phosphate and inorganic phosphate. FBPases are homotetrameric enzymes of about 160 kDa regulated by light through the the Fdx/Trx system as well as by effectors (Ca^{2+}, Mg^{2+}, substrate, and pH; Jacquot et al. 1997a). In general, redox-regulated FBPases contain an amino acid insertion varying from 14 to 19 residues between species and containing three cysteines at position 153, 173, and 178 in the pea enzyme. The 3D structure of oxidized pea FBPase has revealed the presence of a single disulfide between Cys153 and Cys 173 (Chiadmi et al. 1999). The mutation C153S in pea FBPase produces a constitutively active protein, while the C173S or C178S FBPase mutants are still partially redox regulated. This suggests that the formation of a disulfide bridge, between C153 and C173, preferentially inactivates the FBPase (Jacquot et al. 1997a). Similar mutagenesis results have been reported with the spinach enzyme, validating the pea model (Balmer et al. 2001). The 3D structure of the reduced spinach enzyme solved by X-ray crystallography has revealed that the three regulatory Cys are on a loop extending out of the core structure of the enzyme (Villeret et al. 1995). Comparing the two structures from pea and spinach has revealed that large rearrangements are required to transform the oxidized inactive form into the reduced active form. Pea FBPase can be reactived efficiently by Trx f and to a lesser extent by pea Trx m and the double hybride Trx f/m, but not or very poorly by Trx x and y (Collin et al. 2003, 2004; Geck et al.

1996, López-Jaramillo et al. 1998). Unexpectedly, the activity of the chloroplastic fructose-1,6-bisphosphatase was also shown to be modulated in vitro by 2-Cys peroxiredoxin by an unknown process which does not seem to be related to the cysteines involved in the redox regulation (Caporaletti et al. 2007). Interestingly, a chloroplastic FBPase from *Fragaria x ananassa*, which lacks the regulatory cysteines and which is conserved in higher plants, is not redox-regulated indicating that fructose-6-phosphate might be produced independently of the presence of light in this species (Serrato et al. 2009).

The NADP-dependent glyceraldehyde 3-phosphate dehydrogenase (NADP-GAPDH) and phosphoribulokinase (PRK) complex

NADP-GAPDH catalyzes the reduction of 1,3-bisphosphoglycerate to glyceraldehyde-3-phosphate. There are several chloroplast isoforms which contain two types of GAPDH subunits, GapA and GapB. The heterotetrameric A_2B_2 isoform constitutes the major GAPDH isoform in higher plant chloroplasts but it coexists with the homotetrameric A4 isoform (Sparla et al. 2002). A and B subunits resemble each other except that B has a C-terminal extension of 31 amino acids containing two cysteine residues required for Trx f regulation (Fermani et al. 2007; Marri et al. 2009). Regarding A_4-GAPDH, its activity is not dependent on Trx but is reversibly inhibited by glutathionylation (Zaffagnini et al. 2007). It is efficiently reactivated in vitro by Grxs such as CrGrx3 and poplar GrxS12, suggesting that Grxs may reactivate the A_4-GAPDH isoform via a deglutathionylation reaction and hence participate to the regulation of the Calvin cycle in vivo (Couturier et al. 2009b; Zaffagnini et al. 2008). In addition, as chloroplastic Trx f can undergo glutathionylation in vitro and as this modification strongly decreases its ability to activate the Calvin cycle A_2B_2-GADPH, it is hypothesized that glutathionylation might be an alternative way to control Calvin cycle enzymes in some conditions (Michelet et al. 2005).

PRK catalyzes the regeneration of ribulose-1,5- bisphosphate, using ribulose-5-phosphate and ATP as substrates. In photosynthetic eukaryotes, PRK is present as a 80-kDa homodimer but, in cyanobacteria, it is a homotetramer. Each subunit contains four cysteine residues at conserved positions. In the spinach enzyme, Cys16 and Cys55 are the regulatory cysteines which form an intramolecular disulfide bond in the oxidized inactive enzyme. Moreover, during catalysis, Cys55 plays a role in facilitating the binding of the sugar phosphate substrate and it forms a transient heterodisulfide with Cys46 of Trx f during reductive activation (Brandes et al. 1996). Besides, it has been demonstrated that Trx m is more efficient than Trx f to reduce PRK, but other Trxs have not been tested so far (Geck and Hartman, 2000). PRK has also been retained on Grx affinity columns raising the question of their regulation by glutathionylation (Table 2).

In the chloroplast stroma, GAPDH can form a complex with PRK through the action of a small redox protein called CP12. The formation and dissociation of the complex correlate with the quantity of light. As PRK and GAPDH are complexed in their reduced form in leaves in the dark, but are inactive, it has been proposed that light regulation of these two enzymes not only occurs via the direct Trx-mediated activation but also by the reversible dissociation of the PRK/CP12/GAPDH complex, mediated by Trx *f* (Howard et al. 2008). Besides its redox function, *C. reinhardtii* CP12 can act as a redox-independent specific chaperone for GADPH (Erales et al. 2009). In this case, the interaction between CP12 and GAPDH is necessary to prevent the aggregation and inactivation of the latter enzyme.

NADP-dependent malate dehydrogenase

The chloroplastic NADP-MDH converts oxaloacetate into malate with the concomitant oxidation of NADPH. Most of the NADH-dependent MDHs are constitutively active, and not regulated by metabolites, except for the mitochondrial isoform, allosterically regulated by citrate (Miginiac-Maslow et al. 1997). NADP-MDH is involved in the C_4 dicarboxylic acid cycle, responsible for the primary fixation and transfer of CO_2 in C_4 plants. It is also present in C_3 plants where it is implicated in chloroplast shuttle mechanisms which might help export reducing power. The enzyme has been isolated from a variety of plant sources including C_4 plants (sorghum, corn) and C_3 plants (pea, spinach). It is light-dependent and regulated via the reduction of specific disulfides by thiol–disulfide interchange with Trxs reduced by the photosynthetic electron transfer chain. NADP-MDH contains two different disulfides per subunit located, respectively, in N-terminal and C-terminal sequence extensions (Jacquot et al. 1997b; Miginiac-Maslow and Lancelin, 2002). Several single and multiple cysteine mutants of sorghum leaf NADP-MDH have been constructed by site-directed mutagenesis to investigate the Trx-mediated activation mechanism of this enzyme (Goyer et al. 2001; Ruelland et al. 1997). In the oxidized enzyme, the C-terminal extension is obstructing the active site and prevents the access of the substrate, oxaloacetate, whereas the N-terminal disulfide is contributing to the protein dimerization (Johansson et al. 1999). The reduction of these disulfides promotes a conformational change which

enables oxaloacetate to enter the active site (Miginiac-Maslow and Lancelin, 2002). In algae, the position of the Cys differs from that of land plant enzymes. For example, in the unicellular eukaryotic green alga *C. reinhardtii*, the two typical sequence extensions at the N- and C-terminus are present but the N-terminus lacks the regulatory Cys (Lemaire et al. 2005). The NADP-MDH from *S. bicolor* has been reported to be reduced by Trx m and even more efficiently by Trx f, but not by Trx x and y and Trx-lilium (Collin et al. 2003, 2004; Dangoor et al. 2009; Geck et al. 1996; Hodges et al. 1994). A study concerning the cytosolic poplar GrxC4 has also indicated that this Grx can activate the NADP-MDH although its efficiency is reduced compared to plant Trxs (Rouhier et al. 2002). Chloroplastic Grxs have not yet been tested with this target enzyme.

Glucose-6-phosphate dehydrogenase

G6PDH catalyzes the rate-limiting step of the oxidative pentose phosphate pathway. In higher plants, at least three G6PDH enzymes exist in two different cellular compartments, i.e., in the cytosol and in plastids (P1, P2 isoforms; Wendt et al. 2000). The two different plastidic G6PDH classes (P1 and P2) probably evolved from a common ancestral gene. Both the plastidic and cytosolic isoforms are regulated by a feedback inhibition by NADPH, whereas only the plastidial isoforms are inactivated by the Trx-mediated reduction of an intramolecular disulfide bond (Wakao and Benning 2005; Wendt et al. 2000). This property is linked to the presence of two cysteines (Cys149 and Cys157 in the potato enzyme) only conserved in the plastidial isoforms which form a disulfide bond targeted by reduced Trx, in particular Trx m (Wenderoth et al. 1997). Nevertheless, the P1 and P2 isoforms are not equally sensitive to inactivation by reduction, P2 isoforms being less sensitive to a reducing treatment (Wendt et al. 2000). A recent study exploring the in vitro reductant specificity of AtG6PDH1 demonstrated that this major Arabidopsis chloroplastic isoform is very efficiently deactivated by reduced Trx f and not only by Trx m (Née et al. 2009). On the other hand, activation kinetics indicated that oxidized Trxs m, f, and y can activate in vitro this G6PDH (Née et al. 2009).

The biogenesis of metalloproteins (heme and iron–sulfur containing proteins) and chlorophyll metabolism are also redox-regulated plastidial processes

In plants, iron–sulfur cluster biogenesis and siroheme and heme biosynthesis take place in organelles and, especially, in chloroplasts. Heme and chlorophyll biosynthesis pathways are intimately related since they are coupled to tetrapyrrole biosynthesis and their first steps are common until the formation of protoporphyrin IX (Fig. 3). A few enzymes also possess sirohemes which are synthesized in the chloroplasts. Sulfite reductases and nitrite reductases, two enzymes crucial for sulfur and nitrogen assimilation, possess both a siroheme and a [4Fe–4S] cluster. These are the only known class of enzymes that couple a metalloporphyrin to an iron–sulfur cluster in the construction of a catalytically active redox center. These centers function cooperatively to carry out the six-electron reduction of sulfite to sulfide and nitrite to ammonia, respectively. With the identification of some chloroplastic Grxs able to incorporate and then transfer iron–sulfur clusters to acceptor proteins and more generally probably involved in iron–sulfur cluster biogenesis, we have pictured how heme, siroheme, and chlorophyll synthesis, but also sulfate assimilation, could be regulated by Trxs or Grxs. This can happen through disulfide bond reduction or deglutathionylation and by regulation at the level of iron–sulfur cluster biosynthesis or incorporation.

As only two enzymes involved in the initial steps of protoporphyrin IX synthesis might be under redox control, we have schematized the heme and chlorophyll biosynthetic pathways starting at glutamate semialdehyde (GSA). This compound is transformed into aminolevulinic acid by a GSA mutase which has been retained from a stromal spinach extract on a Trx affinity column (Balmer et al. 2003). All subsequent steps for siroheme, heme, and chlorophyll biosynthesis are starting at the central uroporphyrinogen III molecule which is synthesized in two steps from aminolevulinic acid. For sirohemes, the terminal enzyme of the pathway, the sirohydrochlorin ferrochelatase (SirB) is localized in chloroplasts and contains a [2Fe–2S] cluster (Raux-Deery et al. 2005). Alternatively, uroporphyrinogen III can be transformed in three steps into protoporphyrin IX. The first step is mediated by uroporphyrinogen III decarboxylase, an enzyme identified among the putative Trx targets. After this point, the insertion of magnesium or iron into the center of the porphyrin conducts to chlorophyll and heme synthesis, respectively (Fig. 3). The Mg chelatase, which constitutes a subunit of the Mg protoporphyrin IX chelatase catalyzing the insertion of magnesium into tetrapyrroles, is activated by Trx f (Ikegami et al. 2007) and, in addition, it has been identified as a glutathionylated protein (Michelet et al. 2008). Three proteins belonging to chlorophyll metabolism may constitute Trx or Grx partners. Chlorophyllide *a* oxygenase (CAO) is a key enzyme for chlorophyll *b* biosynthesis containing a Rieske-type [2Fe–2S] cluster (Oster et al. 2000). A related protein, the pheophorbide *a* oxygenase (PAO) also possesses a Rieske-type [2Fe–2S] cluster but is involved in chlorophyll *a* breakdown (Pruzinská et al.

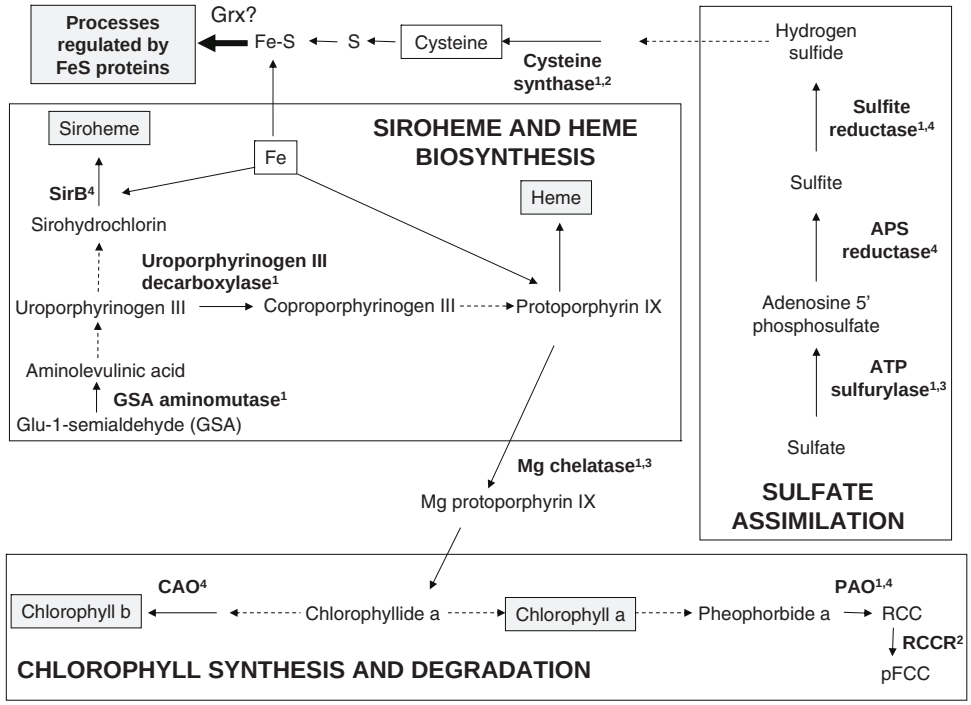

Fig. 3 Redox regulation of metalloprotein biogenesis and chlorophyll metabolic pathways. Enzymes are labeled according to their identification as putative or confirmed (1) Trx target, (2) Grx target, (3) glutathionylated protein, or (4) iron-sulfur cluster containing protein. *Broken lines* indicate that there are several intermediate enzymes. *RCC* red chlorophyll catabolite, *RCCR* red chlorophyll catabolite reductase, *pFCC* primary fluorescent chlorophyll catabolite, *PAO* pheophorbide *a* oxygenase, *CAO* chlorophyll *a* oxygenase, *SirB* sirohydrochlorin ferrochelatase B; APS reductase: Adenosine 5′-phosphosulfate reductase

2003). Moreover, this protein has recently been identified as a putative Trx target from the inner envelope membrane of the chloroplast, together with two proteins involved in protein translocation (TIC55 and PTC52, a NADPH:protochlorophyllide oxidoreductase translocon protein; Bartsch et al. 2008). The presence of a C-terminal CxxC motif in these proteins, but not present in CAO, could explain their identification as Trx target. Interestingly, the next enzyme involved in chlorophyll *a* degradation, the red chlorophyll catabolite reductase (RCCR) has been identified as a Grx target suggesting that this pathway could be regulated both by Trxs and Grxs (Rouhier et al. 2005).

The biogenesis of iron–sulfur clusters is directly linked to sulfate assimilation since the sulfide required for the formation of these clusters originates from cysteine. Many enzymes involved in sulfate assimilation, which seems to take place essentially in plastids, constitute putative Trx or Grx targets. The ATP sulfurylase has been identified both as glutathionylated protein in *Arabidopsis* and as a Trx target (Dixon et al. 2005; Marchand et al. 2006). Adenosine 5′-phosphosulfate (APS) reductase and sulfite reductase possess [4Fe–4S] clusters, and the incorporation of this center putatively requires Grxs (Kopriva et al. 2001). In addition, APS reductases contain a C-terminal Grx domain which makes these enzymes glutathione dependent (Bick et al. 1998). Finally, the last enzyme required for cysteine formation, cysteine synthase, has been identified both as putative Trx and Grx target from Arabidopsis and poplar extracts, respectively (Balmer et al. 2003; Rouhier et al. 2005).

Concluding remarks

With the identification of many new Trx and Grx isoforms, and of more than 400 Trx targets, 150 Grxs targets and 100 glutathionylated proteins in photosynthetic organisms, some of them being identified in the three pools, the field of protein redox regulation by dithiol–disulfide exchanges is getting more and more complex. It will require in the future a detailed analysis of all these putative interactions and these studies will have to be as exhaustive as possible especially in terms of reductants tested. In addition, the demonstration that poplar GrxS14, a Grx with a CGFS active site, can incorporate a labile [2Fe–2S] cluster and transfer it in vitro to an acceptor protein, apoferredoxin, led to the conclusion that some Grxs could also either act as scaffold proteins or as carrier proteins involved in the transfer of pre-formed Fe–S clusters from scaffold to acceptor proteins (Bandyopadhyay et al. 2008). This

suggests that Grxs can participate directly or indirectly to the assembly of iron–sulfur containing plastidial proteins and it might further increase the number of proteins and processes regulated by Grxs.

Acknowledgments This research was supported by grants from the ANR programs (GNP05010G and JC07_204825) to J.C., N.R., and J.P.J, and from the INRA-FORMAS cooperation program to K.C.

References

Alkhalfioui F, Renard M, Vensel WH, Wong J, Tanaka CK, Hurkman WJ, Buchanan BB, Montrichard F (2007) Thioredoxin-linked proteins are reduced during germination of *Medicago truncatula* seeds. Plant Physiol 144:1559–1579

Alkhalfioui F, Renard M, Frendo P, Keichinger C, Meyer Y, Gelhaye E, Hirasawa M, Knaff DB, Ritzenthaler C, Montrichard F (2008) A novel type of thioredoxin dedicated to symbiosis in legumes. Plant Physiol 148:424–435

Baier M, Dietz KJ (1999) Alkyl hydroperoxide reductases: the way out of the oxidative breakdown of lipids in chloroplasts. Trends Plant Sci 4:166–168

Ballicora MA, Frueauf JB, Fu Y, Schürmann P, Preiss J (2000) Activation of the potato tuber ADP-glucose pyrophosphorylase by thioredoxin. J Biol Chem 275:1315–1320

Balmer Y, Stritt-Etter AL, Hirasawa M, Jacquot JP, Keryer E, Knaff DB, Schürmann P (2001) Oxidation-reduction and activation properties of chloroplast fructose 1,6-bisphosphatase with mutated regulatory site. Biochemistry 40:15444–15450

Balmer Y, Koller A, del Val G, Manieri W, Schürmann P, Buchanan BB (2003) Proteomics gives insight into the regulatory function of chloroplast thioredoxins. Proc Natl Acad Sci USA 100:370–375

Balmer Y, Vensel WH, Tanaka CK, Hurkman WJ, Gelhaye E, Rouhier N, Jacquot JP, Manieri W, Schürmann P, Droux M, Buchanan BB (2004a) Thioredoxin links redox to the regulation of fundamental processes of plant mitochondria. Proc Natl Acad Sci USA 101:2642–2647

Balmer Y, Koller A, Val GD, Schürmann P, Buchanan BB (2004b) Proteomics uncovers proteins interacting electrostatically with thioredoxin in chloroplasts. Photosynth Res 79:275–280

Balmer Y, Vensel WH, Hurkman WJ, Buchanan BB (2006a) Thioredoxin target proteins in chloroplast thylakoid membranes. Antioxid Redox Signal 8:1829–1834

Balmer Y, Vensel WH, DuPont FM, Buchanan BB, Hurkman WJ (2006b) Proteome of amyloplasts isolated from developing wheat endosperm presents evidence of broad metabolic capability. J Exp Bot 57:1591–1602

Balsera M, Goetze TA, Kovács-Bogdán E, Schürmann P, Wagner R, Buchanan BB, Soll J, Bölter B (2009) Characterization of Tic110, a channel-forming protein at the inner envelope membrane of chloroplasts, unveils a response to Ca(2+) and a stromal regulatory disulfide bridge. J Biol Chem 284:2603–2616

Bandyopadhyay S, Gama F, Molina-Navarro MM, Gualberto JM, Claxton R, Naik SG, Huynh BH, Herrero E, Jacquot JP, Johnson MK, Rouhier N (2008) Chloroplast monothiol glutaredoxins as scaffold proteins for the assembly and delivery of [2Fe–2S] clusters. EMBO J 27:1122–1133

Bartsch S, Monnet J, Selbach K, Quigley F, Gray J, von Wettstein D, Reinbothe S, Reinbothe C (2008) Three thioredoxin targets in the inner envelope membrane of chloroplasts function in protein import and chlorophyll metabolism. Proc Natl Acad Sci USA 105:4933–4938

Bick JA, Aslund F, Chen Y, Leustek T (1998) Glutaredoxin function for the carboxyl-terminal domain of the plant-type 5′-adenylylsulfate reductase. Proc Natl Acad Sci USA 95:8404–8409

Binda C, Coda A, Aliverti A, Zanetti G, Mattevi A (1998) Structure of the mutant E92K of [2Fe–2S] ferredoxin I from *Spinacia oleracea* at 1.7 A resolution. Acta Crystallographica D 54:1353–1358

Brandes HK, Larimer FW, Hartman FC (1996) The molecular pathway for the regulation of phosphoribulokinase by thioredoxin f. J Biol Chem 271:3333–3335

Bréhélin C, Meyer EH, de Souris JP, Bonnard G, Meyer Y (2003) Resemblance and dissemblance of Arabidopsis type II peroxiredoxins: similar sequences for divergent gene expression, protein localization, and activity. Plant Physiol 132:2045–2057

Broin M, Rey P (2003) Potato plants lacking the CDSP32 plastidic thioredoxin exhibit overoxidation of the BAS1 2-cysteine peroxiredoxin and increased lipid Peroxidation in thylakoids under photooxidative stress. Plant Physiol 132:1335–1343

Broin M, Cuine S, Eymery F, Rey P (2002) The plastidic 2-cysteine peroxiredoxin is a target for a thioredoxin involved in the protection of the photosynthetic apparatus against oxidative damage. Plant Cell 14:1417–1432

Buchanan BB, Schürmann P, Wolosiuk RA, Jacquot JP (2002) The ferredoxin/thioredoxin system: from discovery to molecular structures and beyond. Photosynth Res 73:215–222

Caporaletti D, D'Alessio AC, Rodriguez-Suarez RJ, Senn AM, Duek PD, Wolosiuk RA (2007) Non-reductive modulation of chloroplast fructose-1,6-bisphosphatase by 2-Cys peroxiredoxin. Biochem Biophys Res Commun 355:722–727

Carroll MC, Outten CE, Proescher JB, Rosenfeld L, Watson WH, Whitson LJ, Hart PJ, Jensen LT, Cizewski Culotta V (2006) The effects of glutaredoxin and copper activation pathways on the disulfide and stability of Cu, Zn superoxide dismutase. J Biol Chem 281:28648–28656

Chang CC, Slesak I, Jordá L, Sotnikov A, Melzer M, Miszalski Z, Mullineaux PM, Parker JE, Karpinska B, Karpinski S (2009) Arabidopsis chloroplastic glutathione peroxidases play a role in cross talk between photooxidative stress and immune responses. Plant Physiol 150:670–683

Chiadmi M, Navaza A, Miginiac-Maslow M, Jacquot JP, Cherfils J (1999) Redox signaling in the chloroplast: structure of the oxidized pea fructose 1,6 biphosphatase. EMBO J 18:6809–6815

Chibani K, Wingsle G, Jacquot JP, Gelhaye E, Rouhier N (2009) Comparative genomic study of the thioredoxin family in photosynthetic organisms with emphasis on *Populus trichocarpa*. Mol Plant 2:308–322

Collin V, Issakidis-Bourguet E, Marchand C, Hirasawa M, Lancelin JM, Knaff DB, Miginiac-Maslow M (2003) The Arabidopsis plastidial thioredoxins: new functions and new insights into specificity. J Biol Chem 278:23747–23752

Collin V, Lamkemeyer P, Miginiac-Maslow M, Hirasawa M, Knaff DB, Dietz KJ, Issakidis-Bourguet E (2004) Characterization of plastidial thioredoxins from Arabidopsis belonging to the new y-type. Plant Physiol 136:4088–4095

Collin VC, Eymery F, Genty B, Rey P, Havaux M (2007) Vitamin E is essential for the tolerance of *Arabidopsis thaliana* to metal-induced oxidative stress. Plant Cell Environ 31:244–257

Couturier J, Jacquot JP, Rouhier N (2009a) Evolution and diversity of glutaredoxins in photosynthetic organisms. Cell Mol Life Sci 66:2539–2557

Couturier J, Koh CS, Zaffagnini M, Winger A, Gualberto JM, Corbier C, Decottignies P, Jacquot JP, Lemaire SD, Didierjean C, Rouhier N (2009b) Structure-function relationship of the chloroplastic GrxS12 with an atypical WCSYS active site. J Biol Chem 284:9299–9310

Dai S, Johansson K, Miginiac-Maslow M, Schürmann P, Eklund H (2004) Structural basis of redox signaling in photosynthesis: structure and function of ferredoxin: thioredoxin reductase and target enzymes. Photosynth Res 79:233–248

Dai S, Friemann R, Glauser DA, Bourquin F, Manieri W, Schürmann P, Eklund H (2007) Structural snapshots along the reaction pathway of ferredoxin-thioredoxin reductase. Nature 448:92–96

Dangoor I, Peled-Zehavi H, Levitan A, Pasand O, Danon A (2009) A small family of chloroplast atypical thioredoxins. Plant Physiol 149:1240–1250

Dayer R, Fischer BB, Eggen RI, Lemaire SD (2008) The peroxiredoxin and glutathione peroxidase families in *Chlamydomonas reinhardtii*. Genetics 179:41–57

Dietz KJ (2003) Plant peroxiredoxins. Annu Rev Plant Biol 54:93–107

Dietz KJ, Jacob S, Oelze ML, Laxa M, Tognetti V, de Miranda SM, Baier M, Finkemeier I (2006) The function of peroxiredoxins in plant organelle redox metabolism. J Exp Bot 57:1697–1709

Dixon DP, Skipsey M, Grundy NM, Edwards R (2005) Stress-induced protein S-glutathionylation in Arabidopsis. Plant Physiol 138:2233–2244

Entus R, Poling M, Herrmann KM (2002) Redox regulation of Arabidopsis 3-deoxy-D-arabino-heptulosonate 7-phosphate synthase. Plant Physiol 129:1866–1871

Erales J, Lignon S, Gontero B (2009) CP12 from *Chlamydomonas reinhardtii*, a permanent specific "chaperone-like" protein of glyceraldehyde-3-phosphate dehydrogenase. J Biol Chem 284:12735–12744

Fermani S, Sparla F, Falini G, Martelli PL, Casadio R, Pupillo P, Ripamonti A, Trost P (2007) Molecular mechanism of thioredoxin regulation in photosynthetic A2B2-glyceraldehyde-3-phosphate dehydrogenase. Proc Natl Acad Sci USA 104: 11109–11114

Finkemeier I, Goodman M, Lamkemeyer P, Kandlbinder A, Sweetlove LJ, Dietz KJ (2005) The mitochondrial type II peroxiredoxin F is essential for redox homeostasis and rootgrowth of *Arabidopsis thaliana* under stress. J Biol Chem 280:12168–12180

Gama F, Keech O, Eymery F, Finkemeier I, Gelhaye E, Gardeström P, Dietz KJ, Rey P, Jacquot JP, Rouhier N (2007) The mitochondrial type II peroxiredoxin from poplar. Physiol Plant 129:196–206

Gama F, Bréhélin C, Gelhaye E, Meyer Y, Jacquot JP, Rey P, Rouhier N (2008) Functional analysis and expression characteristics of chloroplastic Prx IIE. Physiol Plant 133:599–610

Gao X-H, Bedhomme M, Veyel D, Zaffagnini M, Lemaire SD (2009) Methods for analysis of protein glutathionylation and their application to photosynthetic organisms. Mol Plant 2:218–235

Geck MK, Hartman FC (2000) Kinetic and mutational analyses of the regulation of phosphoribulokinase by thioredoxins. J Biol Chem 275:18034–18039

Geck MK, Larimer FW, Hartman FC (1996) Identification of residues of spinach thioredoxin *f* that influence interactions with target enzymes. J Biol Chem 279:24736–24740

Gelhaye E, Rouhier N, Navrot N, Jacquot JP (2005) The plant thioredoxin system. Cell Mol Life Sci 62:24–35

Gelhaye E, Navrot N, Macdonald IK, Rouhier N, Raven EL, Jacquot JP (2006) Ascorbate peroxidase-thioredoxin interaction. Photosynth Res 89:193–200

Gopalan G, He Z, Balmer Y, Romano P, Gupta R, Héroux A, Buchanan BB, Swaminathan K, Luan S (2004) Structural analysis uncovers a role for redox in regulating FKBP13, an immunophilin of the chloroplast thylakoid lumen. Proc Natl Acad Sci USA 101:13945–13950

Goyer A, Decottignies P, Issakidis-Bourguet E, Miginiac-Maslow M (2001) Sites of interaction of thioredoxin with sorghum NADP-malate dehydrogenase. FEBS Lett 505:405–408

Gustavsson N, Kokke BP, Härndahl U, Silow M, Bechtold U, Poghosyan Z, Murphy D, Boelens WC, Sundby C (2002) A peptide methionine sulfoxide reductase highly expressed in photosynthetic tissue in *Arabidopsis thaliana* can protect the chaperone-like activity of a chloroplast-localized small heat shock protein. Plant J 29:545–553

Hanke GT, Kimata-Ariga Y, Taniguchi I, Hase T (2004) A post genomic characterization of Arabidopsis ferredoxins. Plant Physiol 134:255–264

Herbette S, Lenne C, Leblanc N, Julien JL, Drevet JR, Roeckel-Drevet P (2002) Two GPX-like proteins from *Lycopersicon esculentum* and *Helianthus annuus* are antioxidant enzymes with phospholipid hydroperoxide glutathione peroxidase and thioredoxin peroxidase activities. Eur J Biochem 269:2414–2420

Hirasawa M, Schürmann P, Jacquot JP, Manieri W, Jacquot P, Keryer E, Hartman FC, Knaff DB (1999) Oxidation-reduction properties of chloroplast thioredoxins, ferredoxin:thioredoxin reductase, and thioredoxin f-regulated enzymes. Biochemistry 38: 5200–5205

Hodges M, Miginiac-Maslow M, Decottignies P, Jacquot JP, Stein M, Lepiniec L, Crétin C, Gadal P (1994) Purification and characterization of pea thioredoxin f expressed in *Escherichia coli*. Plant Mol Biol 26:225–234

Horling F, König J, Dietz KJ (2002) Type II peroxiredoxin C, a member of the peroxiredoxin family of *Arabidopsis thaliana*: its expression and activity in comparison with other peroxiredoxins. Plant Physiol Biochem 40:491–499

Horling F, Lamkemeyer P, König J, Finkemeier I, Kandlbinder A, Baier M, Dietz KJ (2003) Divergent light-, ascorbate-, and oxidative stress-dependent regulation of expression of the peroxiredoxin gene family in Arabidopsis. Plant Physiol 131:317–325

Howard TP, Metodiev M, Lloyd JC, Raines CA (2008) Thioredoxin-mediated reversible dissociation of a stromal multiprotein complex in response to changes in light availability. Proc Natl Acad Sci USA 105:4056–4061

Ikegami A, Yoshimura N, Motohashi K, Takahashi S, Romano PG, Hisabori T, Takamiya K, Masuda T (2007) The CHLI1 subunit of *Arabidopsis thaliana* magnesium chelatase is a target protein of the chloroplast thioredoxin. J Biol Chem 282:19282–19291

Ito H, Iwabuchi M, Ogawa K (2003) The sugar-metabolic enzymes aldolase and triose-phosphate isomerase are targets of glutathionylation in *Arabidopsis thaliana*: detection using biotinylated glutathione. Plant Cell Physiol 44:655–660

Jacquot JP, Vidal J, Gadal P, Schürmann P (1978) Evidence for the existence of several enzyme specific thioredoxins in plants. FEBS Lett 96:243–246

Jacquot JP, Lopez-Jaramillo J, Miginiac-Maslow M, Lemaire S, Cherfils J, Chueca A, Lopez-Gorge J (1997a) Cysteine 153 is required for redox regulation of pea chloroplast fructose-1,6-bisphosphatase. FEBS Lett 401:143–147

Jacquot JP, Lancelin JM, Meyer Y (1997b) Thioredoxins: structure and function in plant cells. New Phytol 136:543–570

Jacquot JP, Stein M, Suzuki A, Liottet S, Sandoz G, Miginiac-Maslow M (1997c) Residue Glu-91 of *Chlamydomonas reinhardtii* ferredoxin is essential for electron transfer to ferredoxin-thioredoxin reductase. FEBS Lett 400:293–296

Jacquot JP, Eklund H, Rouhier N, Schürmann P (2009) Structural and evolutionary aspects of thioredoxin reductases in photosynthetic organisms. Trends Plant Sci 14:336–343

Jang HH, Lee KO, Chi YH, Jung BG, Park SK, Park JH, Lee JR, Lee SS, Moon JC, Yun JW, Choi YO, Kim WY, Kang JS, Cheong GW, Yun DJ, Rhee SG, Cho MJ, Lee SY (2004) Two enzymes in one; two yeast peroxiredoxins display oxidative stress-dependent switching from a peroxidase to a molecular chaperone function. Cell 117:625–635

Jansson S, Douglas CJ (2007) Populus: a model system for plant biology. Annu Rev Plant Biol 58:435–458

Johansson K, Ramaswamy S, Saarinen M, Lemaire-Chamley M, Issakidis-Bourguet E, Miginiac-Maslow M, Eklund H (1999) Structural basis for light activation of a chloroplast enzyme: the structure of sorghum NADP-malate dehydrogenase in its oxidized form. Biochemistry 38:4319–4326

Jung BG, Lee KO, Lee SS, Chi YH, Jang HH, Kang SS, Lee K, Lim D, Yoon SC, Yun DJ, Inoue Y, Cho MJ, Lee SY (2002) A Chinese cabbage cDNA with high sequence identity to phospholipid hydroperoxide glutathione peroxidases encodes a novel isoform of thioredoxin-dependent peroxidase. J Biol Chem 277:12572–12578

Kiba A, Nishihara M, Tsukatani N, Nakatsuka T, Kato Y, Yamamura S (2005) A peroxiredoxin Q homolog from gentians is involved in both resistance against fungal disease and oxidative stress. Plant Cell Physiol 46:1007–1015

Knaff DB (1996) Ferredoxin and ferredoxin-dependent enzymes. In: Yocum CF, Ort DR (eds) Advances in photosynthesis. Kluwer Academic Publishers, Dordrecht, The Netherlands, pp 333–361

König J, Baier M, Horling F, Kahmann U, Harris G, Schürmann P, Dietz KJ (2002) The plant-specific function of 2-Cys peroxiredoxin-mediated detoxification of peroxides in the redox-hierarchy of photosynthetic electron flux. Proc Natl Acad Sci USA 99:5738–5743

König J, Lotte K, Plessow R, Brockhinke A, Baier M, Dietz KJ (2003) Reaction mechanism of plant 2-Cys peroxiredoxin. Role of the C terminus and the quaternary structure. J Biol Chem 278:24409–24420

Kopriva S, Büchert T, Fritz G, Suter M, Weber M, Benda R, Schaller J, Feller U, Schürmann P, Schünemann V, Trautwein AX, Kroneck PM, Brunold C (2001) Plant adenosine 5′-phosphosulfate reductase is a novel iron-sulfur protein. J Biol Chem 276:42881–42886

Lamkemeyer P, Laxa M, Collin V, Li W, Finkemeier I, Schöttler MA, Holtkamp V, Tognetti VB, Issakidis-Bourguet E, Kandlbinder A, Weis E, Miginiac-Maslow M, Dietz KJ (2006) Peroxiredoxin Q of *Arabidopsis thaliana* is attached to the thylakoids and functions in context of photosynthesis. Plant J 45:968–981

Lee PY, Bae KH, Kho CW, Kang S, Lee do H, Cho S, Kang S, Lee SC, Park BC, Park SG (2008) Interactome analysis of yeast glutathione peroxidase 3. J Microbiol Biotechnol 18:1364–1367

Lemaire SD (2004) The glutaredoxin family in oxygenic photosynthetic organisms. Photosynth Res 79:305–318

Lemaire SD, Guillon B, Le Maréchal P, Keryer E, Miginiac-Maslow M, Decottignies P (2004) New thioredoxin targets in the unicellular photosynthetic eukaryote *Chlamydomonas reinhardtii*. Proc Natl Acad Sci USA 101:7475–7480

Lemaire SD, Quesada A, Merchan F, Corral JM, Igeno MI, Keryer E, Issakidis-Bourguet E, Hirasawa M, Knaff DB, Miginiac-Maslow M (2005) NADP-malate dehydrogenase from unicellular green alga *Chlamydomonas reinhardtii*. A first step toward redox regulation? Plant Physiol 137:514–521

Lemaire SD, Michelet L, Zaffagnini M, Massot V, Issakidis-Bourguet E (2007) Thioredoxins in chloroplasts. Curr Genet 51:343–365

Lepistö A, Kangasjärvi S, Luomala EM, Brader G, Sipari N, Keränen M, Keinänen M, Rintamäki E (2009) Chloroplast NADPH-thioredoxin reductase interacts with photoperiodic development in Arabidopsis. Plant Physiol 149:1261–1276

Levine RL, Mosoni L, Berlett BS, Stadtman ER (1996) Methionine residues as endogenous antioxidants in proteins. Proc Natl Acad Sci USA 93:15036–15040

Li M, Yang Q, Zhang L, Li H, Cui Y, Wu Q (2007) Identification of novel targets of cyanobacterial glutaredoxin. Arch Biochem Biophys 458:220–228

Lima A, Lima S, Wong JH, Phillips RS, Buchanan BB, Luan S (2006) A redox-active FKBP-type immunophilin functions in accumulation of the photosystem II supercomplex in *Arabidopsis thaliana*. Proc Natl Acad Sci USA 103:12631–12636

Lindahl M, Florencio FJ (2003) Thioredoxin-linked processes in cyanobacteria are as numerous as in chloroplasts, but targets are different. Proc Natl Acad Sci USA 100:16107–16112

Lindahl M, Kieselbach T (2009) Disulphide proteomes and interactions with thioredoxin on the track towards understanding redox regulation in chloroplasts and cyanobacteria. J Proteomics 72:416–438

López-Jaramillo J, Chueca A, Sahrawy M, Gorge JL (1998) Hybrids from pea chloroplast thioredoxins f and m: physicochemical and kinetic characteristics. Plant J 15:155–163

Maeda K, Finnie C, Svensson B (2004) Cy5 maleimide labelling for sensitive detection of free thiols in native protein extracts: identification of seed proteins targeted by barley thioredoxin h isoforms. Biochem J 378:497–507

Marchand C, Le Maréchal P, Meyer Y, Miginiac-Maslow M, Issakidis-Bourguet E, Decottignies P (2004) New targets of Arabidopsis thioredoxins revealed by proteomics analysis. Proteomics 4:2696–2706

Marchand C, Le Maréchal P, Meyer Y, Decottignies P (2006) Comparative proteomic approaches for the isolation of proteins interacting with thioredoxin. Proteomics 24:6528–6537

Marri L, Zaffagnini M, Collin V, Issakidis-Bourguet E, Lemaire SD, Pupillo P, Sparla F, Miginiac-Maslow M, Trost P (2009) Prompt and easy activation by specific thioredoxins of calvin cycle enzymes of *Arabidopsis thaliana* associated in the GAPDH/CP12/PRK supramolecular complex. Mol Plant 2:259–269

Marx C, Wong JH, Buchanan BB (2003) Thioredoxin and germinating barley: targets and protein redox changes. Planta 21:454–460

Mata-Cabana A, Florencio FJ, Lindahl M (2007) Membrane proteins from the cyanobacterium *Synechocystis* sp. PCC 6803 interacting with thioredoxin. Proteomics 7:3953–3963

Meyer Y, Reichheld JP, Vignols F (2005) Thioredoxins in Arabidopsis and other plants. Photosynth Res 86:419–433

Meyer Y, Siala W, Bashandy T, Riondet C, Vignols F, Reichheld JP (2008) Glutaredoxins and thioredoxins in plants. Biochim Biophys Acta 1783:589–600

Miao Y, Lv D, Wang P, Wang XC, Chen J, Miao C, Song CP (2006) An Arabidopsis glutathione peroxidase functions as both a redox transducer and a scavenger in abscisic acid and drought stress responses. Plant Cell 18:2749–2766

Michalska J, Zaubera H, Buchanana BB, Cejudoc FJ, Geigenberger P (2009) NTRC links built-in thioredoxin to light and sucrose in regulating starch synthesis in chloroplasts and amyloplasts. Proc Natl Acad Sci USA 106:9908–9913

Michelet L, Zaffagnini M, Marchand C, Collin V, Decottignies P, Tsan P, Lancelin JM, Trost P, Miginiac-Maslow M, Noctor G, Lemaire SD (2005) Glutathionylation of chloroplast thioredoxin f is a redox signaling mechanism in plants. Proc Natl Acad Sci USA 102:16478–16483

Michelet L, Zaffagnini M, Vanacker H, Le Maréchal P, Marchand C, Schroda M, Lemaire SD, Decottignies P (2008) In vivo targets of S-thiolation in *Chlamydomonas reinhardtii*. J Biol Chem 283:21571–21578

Miginiac-Maslow M, Lancelin JM (2002) Intrasteric inhibition in redox signaling: light activation of NADP-malate dehydrogenase. Photosyn Res 72:1–12

Miginiac-Maslow M, Issakidis E, Lemaire M, Ruelland E, Jacquot JP, Decottignies P (1997) Light-dependent activation of NADP-malate dehydrogenase: a complex process. Aust J Plant Physiol 24:529–542

Mikkelsen R, Mutenda KE, Mant A, Schürmann P, Blennow A (2005) Alpha-glucan, water dikinase (GWD): a plastidic enzyme with

redox-regulated and coordinated catalytic activity and binding affinity. Proc Natl Acad Sci USA 102:1785–1790

Montrichard F, Alkhalfioui F, Yano H, Vensel WH, Hurkman WJ, Buchanan BB (2009) Thioredoxin targets in plants: the first 30 years. J Proteomics 72:452–474

Moon JC, Jang HH, Chae HB, Lee JR, Lee SY, Jung YJ, Shin MR, Lim HS, Chung WS, Yun DJ, Lee KO, Lee SY (2006) The C-type Arabidopsis thioredoxin reductase ANTR-C acts as an electron donor to 2-Cys peroxiredoxins in chloroplasts. Biochem Biophys Res Commun 348:478–484

Motohashi K, Hisabori T (2006) HCF164 receives reducing equivalents from stromal thioredoxin across the thylakoid membrane and mediates reduction of target proteins in the thylakoid lumen. J Biol Chem 281:35039–35047

Motohashi K, Kondoh A, Stumpp MT, Hisabori T (2001) Comprehensive survey of proteins targeted by chloroplast thioredoxin. Proc Natl Acad Sci USA 98:11224–11229

Navrot N, Collin V, Gualberto J, Gelhaye E, Hirasawa M, Rey P, Knaff DB, Issakidis E, Jacquot JP, Rouhier N (2006) Plant glutathione peroxidases are functional peroxiredoxins distributed in several subcellular compartments and regulated during biotic and abiotic stresses. Plant Physiol 142:1364–1379

Née G, Zaffagnini M, Trost P, Issakidis-Bourguet E (2009) Redox regulation of chloroplastic glucose-6-phosphate dehydrogenase: a new role for f-type thioredoxin. FEBS Lett 583:2827–2832

Noguera-Mazon V, Lemoine J, Walker O, Rouhier N, Salvador A, Jacquot JP, Lancelin JM, Krimm I (2006) Glutathionylation induces the dissociation of 1-Cys D-peroxiredoxin non-covalent homodimer. J Biol Chem 281:31736–31742

Oster U, Tanaka R, Tanaka A, Rüdiger W (2000) Cloning and functional expression of the gene encoding the key enzyme for chlorophyll b biosynthesis (CAO) from *Arabidopsis thaliana*. Plant J 21:305–310

Pérez-Pérez ME, Florencio FJ, Lindahl M (2006) Selecting thioredoxins for disulphide proteomics: target proteomes of three thioredoxins from the cyanobacterium *Synechocystis* sp. PCC 6803. Proteomics 6:186–195

Pérez-Ruiz JM, Cejudo FJ (2009) A proposed reaction mechanism for rice NADPH thioredoxin reductase C, an enzyme with protein disulfide reductase activity. FEBS Lett 583:1399–1402

Pérez-Ruiz JM, Spinola MC, Kirchsteiger K, Moreno J, Sahrawy M, Cejudo FJ (2006) Rice NTRC is a high-efficiency redox system for chloroplast protection against oxidative damage. Plant Cell 18:2356–2368

Petersson UA, Kieselbach T, García-Cerdán JG, Schröder WP (2006) The Prx Q protein of *Arabidopsis thaliana* is a member of the luminal chloroplast proteome. FEBS Lett 580:6055–6061

Pruzinská A, Tanner G, Anders I, Roca M, Hörtensteiner S (2003) Chlorophyll breakdown: pheophorbide a oxygenase is a Rieske-type iron-sulfur protein, encoded by the accelerated cell death 1 gene. Proc Natl Acad Sci USA 100:15259–15264

Raux-Deery E, Leech HK, Nakrieko KA, McLean KJ, Munro AW, Heathcote P, Rigby SE, Smith AG, Warren MJ (2005) Identification and characterization of the terminal enzyme of siroheme biosynthesis from *Arabidopsis thaliana*: a plastid-located sirohydrochlorin ferrochelatase containing a 2Fe-2S center. J Biol Chem 280:4713–4721

Reichheld JP, Meyer E, Khafif M, Bonnard G, Meyer Y (2005) AtNTRB is the major mitochondrial thioredoxin reductase in *Arabidopsis thaliana*. FEBS Lett 17:337–342

Rey P, Cuiné S, Eymery F, Garin J, Court M, Jacquot JP, Rouhier N, Broin M (2005) Analysis of the proteins targeted by CDSP32, a plastidic thioredoxin participating in oxidative stress responses. Plant J 41:31–42

Rey P, Bécuwe N, Barrault MB, Rumeau D, Havaux M, Biteau B, Toledano MB (2007) The *Arabidopsis thaliana* sulfiredoxin is a plastidic cysteine-sulfinic acid reductase involved in the photooxidative stress response. Plant J 49:505–514

Rodriguez Milla MA, Maurer A, Rodriguez Huete A, Gustafson JP (2003) Glutathione peroxidase genes in Arabidopsis are ubiquitous and regulated by abiotic stresses through diverse signaling pathways. Plant J 36:602–615

Romero HM, Berlett BS, Jensen PJ, Pell EJ, Tien M (2004) Investigations into the role of the plastidial peptide methionine sulfoxide reductase in response to oxidative stress in Arabidopsis. Plant Physiol 136:3784–3794

Romero-Puertas MC, Laxa M, Mattè A, Zaninotto F, Finkemeier I, Jones AM, Perazzolli M, Vandelle E, Dietz KJ, Delledonne M (2007) S-nitrosylation of peroxiredoxin II E promotes peroxynitrite-mediated tyrosine nitration. Plant Cell 19:4120–4130

Rouhier N, Jacquot JP (2002) Plant peroxiredoxins: alternative hydroperoxide scavenging enzymes. Photosynth Res 74:93–107

Rouhier N, Jacquot JP (2005) The plant multigenic family of thiol peroxidases. Free Radic Biol Med 38:1413–1421

Rouhier N, Gelhaye E, Sautiere PE, Brun A, Laurent P, Tagu D, Gerard J, de Faÿ E, Meyer Y, Jacquot JP (2001) Isolation and characterization of a new peroxiredoxin from poplar sieve tubes that uses either glutaredoxin or thioredoxin as a proton donor. Plant Physiol 127:1299–1309

Rouhier N, Gelhaye E, Jacquot JP (2002) Exploring the active site of plant glutaredoxin by site-directed mutagenesis. FEBS Lett 511:145–149

Rouhier N, Gelhaye E, Jacquot JP (2004a) Plant glutaredoxins: still mysterious reducing systems. Cell Mol Life Sci 61:1266–1277

Rouhier N, Gelhaye E, Gualberto JM, Jordy MN, De Fay E, Hirasawa M, Duplessis S, Lemaire SD, Frey P, Martin F, Manieri W, Knaff DB, Jacquot JP (2004b) Poplar peroxiredoxin Q. A thioredoxin-linked chloroplast antioxidant functional in pathogen defense. Plant Physiol 134:1027–1038

Rouhier N, Villarejo A, Srivastava M, Gelhaye E, Keech O, Droux M, Finkemeier I, Samuelsson G, Dietz KJ, Jacquot JP, Wingsle G (2005) Identification of plant glutaredoxin targets. Antioxid Redox Signal 7:919–929

Rouhier N, Couturier J, Jacquot JP (2006a) Genome-wide analysis of plant glutaredoxin systems. J Exp Bot 57:1685–1696

Rouhier N, Vieira Dos Santos C, Tarrago L, Rey P (2006b) Plant methionine sulfoxide reductase A and B multigenic families. Photosynth Res 89:247–262

Rouhier N, Kauffmann B, Tete-Favier F, Palladino P, Gans P, Branlant G, Jacquot JP, Boschi-Muller S (2007a) Functional and structural aspects of poplar cytosolic and plastidial type a methionine sulfoxide reductases. J Biol Chem 282:3367–3378

Rouhier N, Unno H, Bandyopadhyay S, Masip L, Kim SK, Hirasawa M, Gualberto JM, Lattard V, Kusunoki M, Knaff DB, Georgiou G, Hase T, Johnson MK, Jacquot JP (2007b) Functional, structural, and spectroscopic characterization of a glutathione-ligated [2Fe–2S] cluster in poplar glutaredoxin C1. Proc Natl Acad Sci USA 104:7379–7384

Rouhier N, Lemaire SD, Jacquot JP (2008a) The role of glutathione in photosynthetic organisms: emerging functions for glutaredoxins and glutathionylation. Annu Rev Plant Biol 59:143–166

Rouhier N, Koh CS, Gelhaye E, Corbier C, Favier F, Didierjean C, Jacquot JP (2008b) Redox based anti-oxidant systems in plants: biochemical and structural analyses. Biochim Biophys Acta 1780:1249–1260

Ruelland E, Miginiac-Maslow M (1999) Regulation of chloroplast enzyme activities by thioredoxins: activation or relief from inhibition. Trends Plant Sci 4:136–141

Ruelland E, Lemaire-Chamley M, Le Maréchal P, Issakidis-Bourguet E, Djukic N, Miginiac-Maslow M (1997) An internal cysteine is involved in the thioredoxin-dependent activation of sorghum leaf NADP-malate dehydrogenase. J Biol Chem 272:19851–19857

Sakamoto A, Tsukamoto S, Yamamoto H, Ueda-Hashimoto M, Takahashi M, Suzuki H, Morikawa H (2003) Functional complementation in yeast reveals a protective role of chloroplast 2-Cys peroxiredoxin against reactive nitrogen species. Plant J 33:841–851

Schürmann P, Buchanan BB (2008) The ferredoxin/thioredoxin system of oxygenic photosynthesis. Antioxid Redox Signaling 10:1235–1274

Schürmann P, Jacquot JP (2000) Plant thioredoxin system revisited. Annu Rev Plant Physiol Plant Mol Biol 51:371–400

Serrato AJ, Pérez-Ruiz JM, Spínola MC, Cejudo FJ (2004) A novel NADPH thioredoxin reductase, localized in the chloroplast, which deficiency causes hypersensitivity to abiotic stress in *Arabidopsis thaliana*. J Biol Chem 279:43821–43827

Serrato AJ, Yubero-Serrano EM, Sandalio LM, Muñoz-Blanco J, Chueca A, Caballero JL, Sahrawy M (2009) cpFBPaseII, a novel redox-independent chloroplastic isoform of fructose-1,6-bisphosphatase. Plant Cell Environ 32:811–827

Sparla F, Pupillo P, Trost P (2002) The C-terminal extension of glyceraldehyde-3-phosphate dehydrogenase subunit B acts as an autoinhibitory domain regulated by thioredoxins and nicotinamide adenine dinucleotide. J Biol Chem 277:44946–44952

Stenbaek A, Hansson A, Wulff RP, Hansson M, Dietz KJ, Jensen PE (2008) NADPH-dependent thioredoxin reductase and 2-Cys peroxiredoxins are needed for the protection of Mg-protoporphyrin monomethyl ester cyclase. FEBS Lett 582:2773–2778

Ströher E, Dietz KJ (2008) The dynamic thiol-disulphide redox proteome of the *Arabidopsis thaliana* chloroplast as revealed by differential electrophoretic mobility. Physiol Plant 133:566–583

Sundby C, Härndahl U, Gustavsson N, Ahrman E, Murphy DJ (2005) Conserved methionines in chloroplasts. Biochim Biophys Acta 1703:191–202

Tarrago L, Laugier E, Rey P (2009a) Protein-repairing methionine sulfoxide reductases in photosynthetic organisms: gene organization, reduction mechanisms, and physiological roles. Mol Plant 2:202–217

Tarrago L, Laugier E, Zaffagnini M, Marchand C, Le Maréchal P, Rouhier N, Lemaire SD, Rey P (2009b) Regeneration mechanisms of *Arabidopsis thaliana* methionine sulfoxide reductases B by glutaredoxins and thioredoxins. J Biol Chem 284:18963–18971

Teixeira FK, Menezes-Benavente L, Galvão VC, Margis R, Margis-Pinheiro M (2006) Rice ascorbate peroxidase gene family encodes functionally diverse isoforms localized in different subcellular compartments. Planta 224:300–314

Verdoucq L, Vignols F, Jacquot JP, Chartier Y, Meyer Y (1999) In vivo characterization of a thioredoxin h target protein defines a new peroxiredoxin family. J Biol Chem 274:19714–19722

Vieira Dos Santos C, Rey P (2006) Plant thioredoxins are key actors in the oxidative stress response. Trends Plant Sci 11:329–334

Vieira Dos Santos C, Cuiné S, Rouhier N, Rey P (2005) The Arabidopsis plastidic methionine sulfoxide reductase B proteins. Sequence and activity characteristics, comparison of the expression with plastidic methionine sulfoxide reductase A, and induction by photooxidative stress. Plant Physiol 138:909–922

Vieira Dos Santos C, Laugier E, Tarrago L, Massot V, Issakidis-Bourguet E, Rouhier N, Rey P (2007) Specificity of thioredoxins and glutaredoxins as electron donors to two distinct classes of *Arabidopsis* plastidial methionine sulfoxide reductases B. FEBS Lett 581:4371–4376

Villeret V, Huang S, Zhang Y, Xue Y, Lipscomb WN (1995) Crystal structure of spinach chloroplast fructose 1, 6 biphosphatase At 2.8 Å resolution. Biochemistry 34:4299–4306

Wakao S, Benning C (2005) Genome-wide analysis of glucose-6-phosphate dehydrogenases in Arabidopsis. Plant J 41:243–256

Wenderoth I, Scheibe R, von Schaewen A (1997) Identification of the cysteine residues involved in redox modification of plant plastidic glucose-6-phosphate dehydrogenase. J Biol Chem 272:26985–26990

Wendt UK, Wenderoth I, Tegeler A, von Schaewen A (2000) Molecular characterization of a novel glucose-6-phosphate dehydrogenase from potato (*Solanum tuberosum* L.). Plant J 23:723–733

Wilcox KC, Zhou L, Jordon JK, Huang Y, Yu Y, Redler RL, Chen X, Caplow M, Dokholyan NV (2009) Modifications of superoxide dismutase (SOD1) in human erythrocytes: a possible role in amyotrophic lateral sclerosis. J Biol Chem 284:13940–13947

Wong JH, Cai N, Balmer Y, Tanaka CK, Vensel WH, Hurkman WJ, Buchanan BB (2004) Thioredoxin targets of developing wheat seeds identified by complementary proteomic approaches. Photochemistry 65:1629–1640

Yamaryo Y, Motohashi K, Takamiya K, Hisabori T, Ohta H (2006) In vitro reconstitution of monogalactosyldiacylglycerol (MGDG) synthase regulation by thioredoxin. FEBS Lett 580:4086–4090

Yamazaki D, Motohashi K, Kasama T, Hara Y, Hisabori T (2004) Target proteins of the cytosolic thioredoxins in *Arabidopsis thaliana*. Plant Cell Physiol 45:18–27

Yano H, Wong JH, Lee YM, Cho MJ, Buchanan BB (2001) A strategy for the identification of proteins targeted by thioredoxin. Proc Natl Acad Sci USA 98:4794–4799

Zaffagnini M, Michelet L, Marchand C, Sparla F, Decottignies P, Le Maréchal P, Miginiac-Maslow M, Noctor G, Trost P, Lemaire SD (2007) The thioredoxin-independent isoform of chloroplastic glyceraldehyde-3-phosphate dehydrogenase is selectively regulated by glutathionylation. FEBS J 274:212–226

Zaffagnini M, Michelet L, Massot V, Trost P, Lemaire SD (2008) Biochemical characterization of glutaredoxins from *Chlamydomonas reinhardtii* reveals the unique properties of a chloroplastic CGFS-type glutaredoxin. J Biol Chem 283:8868–8876

Références

Alamillo, J. M., et García-Olmedo, F. (2001). Effects of urate, a natural inhibitor of peroxynitrite-mediated toxicity, in the response of Arabidopsis thaliana to the bacterial pathogen Pseudomonas syringae. Plant J *25*, 529-540.

Alejandro, S., Rodríguez, P. L., Bellés, J. M., Yenush, L., García-Sanchez, M. J., Fernández, J. A., et Serrano, R. (2007). An Arabidopsis quiescin-sulfhydryl oxidase regulates cation homeostasis at the root symplast-xylem interface. EMBO J *26*, 3203-3215.

Alon, A., Heckler, E. J., Thorpe, C., et Fass, D. (2010). QSOX contains a pseudo-dimer of functional and degenerate sulfhydryl oxidase domains. FEBS Lett *584*, 1521-1525.

Alphey, M. S., König, J., et Fairlamb, A. H. (2008). Structural and mechanistic insights into type II trypanosomatid tryparedoxin-dependent peroxidases. Biochem J *414*, 375-381.

Anfinsen, C. B., Haber, E., Sela, M., et White, F. H. (1961). THE KINETICS OF FORMATION OF NATIVE RIBONUCLEASE DURING OXIDATION OF THE REDUCED POLYPEPTIDE CHAIN. Proc Natl Acad Sci U S A *47*, 1309-1314.

Antonenkov, V. D., Grunau, S., Ohlmeier, S., et Hiltunen, J. K. (2010). Peroxisomes are oxidative organelles. Antioxid. Redox Signal *13*, 525-537.

Aono, M., Kubo, A., Saji, H., Tanaka, K., et Kondo, N. (1993). Enhanced Tolerance to Photooxidative Stress of Transgenic Nicotiana tabacum with High Chloroplastic Glutathione Reductase Activity. Plant Cell Physiol *34*, 129-135.

Appenzeller-Herzog, C., Riemer, J., Christensen, B., Sørensen, E. S., et Ellgaard, L. (2008a). A novel disulphide switch mechanism in Ero1alpha balances ER oxidation in human cells. EMBO J *27*, 2977-2987.

Appenzeller-Herzog, C., et Ellgaard, L. (2008b). The human PDI family: versatility packed into a single fold. Biochim Biophys Acta *1783*, 535-48.

Appenzeller-Herzog, C., et Ellgaard, L. (2008c). In vivo reduction-oxidation state of protein disulfide isomerase: the two active sites independently occur in the reduced and oxidized forms. Antioxid. Redox Signal *10*, 55-64.

Appenzeller-Herzog, C., et Hauri, H. P. (2006). The ER-Golgi intermediate compartment (ERGIC): in search of its identity and function. J Cell Sci *119*, 2173-83.

Arasimowicz-Jelonek, M., et Floryszak-Wieczorek, J. (2011). Understanding the fate of peroxynitrite in plant cells - From physiology to pathophysiology. Phytochemistry. PMID:2142953 [PubMed - in process].

Arnér, E. S., et Holmgren, A. (2000). Physiological functions of thioredoxin and thioredoxin reductase. Eur. J. Biochem *267*, 6102-6109.

Arscott, L. D., Gromer, S., Schirmer, R. H., Becker, K., et Williams, C. H. (1997). The mechanism of thioredoxin reductase from human placenta is similar to the mechanisms of lipoamide dehydrogenase and glutathione reductase and is distinct from the mechanism of thioredoxin reductase from Escherichia coli. Proc. Natl. Acad. Sci. U.S.A *94*, 3621-3626.

Baier, M., et Dietz, K. J. (1999). Protective function of chloroplast 2-cysteine peroxiredoxin in photosynthesis. Evidence from transgenic Arabidopsis. Plant physiology *119*, 1407-14.

Baker, K. M., Chakravarthi, S., Langton, K. P., Sheppard, A. M., Lu, H., et Bulleid, N. J. (2008). Low reduction potential of Ero1alpha regulatory disulphides ensures tight control of substrate oxidation. EMBO J *27*, 2988-2997.

Balmer, Y., Vensel, W. H., Tanaka, C. K., Hurkman, W. J., Gelhaye, E., Rouhier, N., Jacquot, J.-P., Manieri, W., Schürmann, P., Droux, M., et al. (2004). Thioredoxin links redox to the regulation of fundamental processes of plant mitochondria. Proc. Natl. Acad. Sci. U.S.A *101*, 2642-2647.

Bardwell, J. C., McGovern, K., et Beckwith, J. (1991). Identification of a protein required for disulfide bond formation in vivo. Cell *67*, 581-589.

Bayer, E. M., Bottrill, A. R., Walshaw, J., Vigouroux, M., Naldrett, M. J., Thomas, C. L., et Maule, A. J. (2006). Arabidopsis cell wall proteome defined using multidimensional protein identification technology. Proteomics *6*, 301-311.

Bessette, P. H., Cotto, J. J., Gilbert, H. F., et Georgiou, G. (1999). In vivo and in vitro function of the Escherichia coli periplasmic cysteine oxidoreductase DsbG. J. Biol. Chem *274*, 7784-7792.

Bihlmaier, K., Mesecke, N., Kloeppel, C., et Herrmann, J. M. (2008). The disulfide relay of the intermembrane space of mitochondria: an oxygen-sensing system? Ann. N. Y. Acad. Sci *1147*, 293-302.

Biteau, B., Labarre, J., et Toledano, M. B. (2003). ATP-dependent reduction of cysteine-sulphinic acid by S. cerevisiae sulphiredoxin. Nature *425*, 980-4.

Björnberg, O., Ostergaard, H., et Winther, J. R. (2006). Measuring intracellular redox conditions using GFP-based sensors. Antioxid. Redox Signal *8*, 354-361.

Boschi-Muller, S., Gand, A., et Branlant, G. (2008). The methionine sulfoxide reductases: Catalysis and substrate specificities. Archives of biochemistry and biophysics *474*, 266-73.

Bozonet, S. M., Findlay, V. J., Day, A. M., Cameron, J., Veal, E. A., et Morgan, B. A. (2005). Oxidation of a eukaryotic 2-Cys peroxiredoxin is a molecular switch controlling the transcriptional response to increasing levels of hydrogen peroxide. The Journal of biological chemistry *280*, 23319-27.

Brandes, H. K., Larimer, F. W., Geck, M. K., Stringer, C. D., Schurmann, P., et Hartman, F. C. (1993). Direct identification of the primary nucleophile of thioredoxin f. J Biol Chem *268*, 18411-18414.

Breuza, L., Halbeisen, R., Jeno, P., Otte, S., Barlowe, C., Hong, W., et Hauri, H. P. (2004). Proteomics of endoplasmic reticulum-Golgi intermediate compartment (ERGIC) membranes from brefeldin A-treated HepG2 cells identifies ERGIC-32, a new cycling protein that interacts with human Erv46. J Biol Chem *279*, 47242-53.

Broin, M., et Rey, P. (2003). Potato plants lacking the CDSP32 plastidic thioredoxin exhibit over-

oxidation of the BAS1 2-cysteine peroxiredoxin and increased lipid Peroxidation in thylakoids under photooxidative stress. Plant physiology *132*, 1335-43.

Bryk, R., Griffin, P., et Nathan, C. (2000). Peroxynitrite reductase activity of bacterial peroxiredoxins. Nature *407*, 211-215.

Buchanan, B. B., Schürmann, P., Wolosiuk, R. A., et Jacquot, J.-P. (2002). The ferredoxin/thioredoxin system: from discovery to molecular structures and beyond. Photosyn. Res *73*, 215-222.

Busse, E., Zimmer, G., Schopohl, B., et Kornhuber, B. (1992). Influence of alpha-lipoic acid on intracellular glutathione in vitro and in vivo. Arzneimittelforschung *42*, 829-831.

Byrne, L. J., Sidhu, A., Wallis, A. K., Ruddock, L. W., Freedman, R. B., Howard, M. J., et Williamson, R. A. (2009). Mapping of the ligand-binding site on the b' domain of human PDI: interaction with peptide ligands and the x-linker region. Biochem. J *423*, 209-217.

Cabibbo, A., Pagani, M., Fabbri, M., Rocchi, M., Farmery, M. R., Bulleid, N. J., et Sitia, R. (2000). ERO1-L, a human protein that favors disulfide bond formation in the endoplasmic reticulum. J. Biol. Chem *275*, 4827-4833.

Cantrell, A., McGarvey, D. J., Truscott, T. G., Rancan, F., et Böhm, F. (2003). Singlet oxygen quenching by dietary carotenoids in a model membrane environment. Arch. Biochem. Biophys *412*, 47-54.

Capitani, G., Markovic-Housley, Z., DelVal, G., Morris, M., Jansonius, J. N., et Schurmann, P. (2000). Crystal structures of two functionally different thioredoxins in spinach chloroplasts. Journal of molecular biology *302*, 135-54.

Carrie, C., Giraud, E., Duncan, O., Xu, L., Wang, Y., Huang, S., Clifton, R., Murcha, M., Filipovska, A., Rackham, O., et al. (2010). Conserved and novel functions for Arabidopsis thaliana MIA40 in assembly of proteins in mitochondria and peroxisomes. J. Biol. Chem *285*, 36138-36148.

Carvalho, A. P., Fernandes, P. A., et Ramos, M. J. (2006). Similarities and differences in the thioredoxin superfamily. Prog. Biophys. Mol. Biol *91*, 229-248.

Chacinska, A., Pfannschmidt, S., Wiedemann, N., Kozjak, V., Sanjuán Szklarz, L. K., Schulze-Specking, A., Truscott, K. N., Guiard, B., Meisinger, C., et Pfanner, N. (2004). Essential role of Mia40 in import and assembly of mitochondrial intermembrane space proteins. EMBO J *23*, 3735-3746.

Chakravarthi, S., Jessop, C. E., et Bulleid, N. J. (2006). The role of glutathione in disulphide bond formation and endoplasmic-reticulum-generated oxidative stress. EMBO Rep *7*, 271-275.

Chang, C. C. C., Slesak, I., Jordá, L., Sotnikov, A., Melzer, M., Miszalski, Z., Mullineaux, P. M., Parker, J. E., Karpinska, B., et Karpinski, S. (2009). Arabidopsis chloroplastic glutathione peroxidases play a role in cross talk between photooxidative stress and immune responses. Plant Physiol *150*, 670-683.

Charbonnier, J. B., Belin, P., Moutiez, M., Stura, E. A., et Quéméneur, E. (1999). On the role of the

cis-proline residue in the active site of DsbA. Protein Sci *8*, 96-105.

Chibani, K., Couturier, J., Selles, B., Jacquot, J.-P., et Rouhier, N. (2010). The chloroplastic thiol reducing systems: dual functions in the regulation of carbohydrate metabolism and regeneration of antioxidant enzymes, emphasis on the poplar redoxin equipment. Photosyn. Res *104*, 75-99.

Chibani, K., Tarrago, L., Schürmann, P., Jacquot, J.-P., et Rouhier, N. (2011). Biochemical properties of poplar thioredoxin z. FEBS Lett *585*, 1077-1081.

Chibani, K., Wingsle, G., Jacquot, J.-P., Gelhaye, E., et Rouhier, N. (2009). Comparative genomic study of the thioredoxin family in photosynthetic organisms with emphasis on Populus trichocarpa. Mol Plant *2*, 308-322.

Chivers, P. T., Laboissière, M. C., et Raines, R. T. (1996). The CXXC motif: imperatives for the formation of native disulfide bonds in the cell. EMBO J *15*, 2659-2667.

Chivers, P. T., Prehoda, K. E., et Raines, R. T. (1997a). The CXXC motif: a rheostat in the active site. Biochemistry *36*, 4061-4066.

Chivers, P. T., Prehoda, K. E., Volkman, B. F., Kim, B. M., Markley, J. L., et Raines, R. T. (1997b). Microscopic pKa values of Escherichia coli thioredoxin. Biochemistry *36*, 14985-14991.

Christis, C., Lubsen, N. H., et Braakman, I. (2008). Protein folding includes oligomerization - examples from the endoplasmic reticulum and cytosol. FEBS J *275*, 4700-4727.

Coe, H., et Michalak, M. (2010). ERp57, a multifunctional endoplasmic reticulum resident oxidoreductase. Int. J. Biochem. Cell Biol *42*, 796-799.

Collet, J.-F., et Bardwell, J. C. A. (2002). Oxidative protein folding in bacteria. Mol. Microbiol *44*, 1-8.

Collet, J.-F., et Messens, J. (2010). Structure, function, and mechanism of thioredoxin proteins. Antioxid. Redox Signal *13*, 1205-1216.

Collin, V., Issakidis-Bourguet, E., Marchand, C., Hirasawa, M., Lancelin, J.-M., Knaff, D. B., et Miginiac-Maslow, M. (2003). The Arabidopsis plastidial thioredoxins: new functions and new insights into specificity. J. Biol. Chem *278*, 23747-23752.

Coppock, D. L., Cina-Poppe, D., et Gilleran, S. (1998). The quiescin Q6 gene (QSCN6) is a fusion of two ancient gene families: thioredoxin and ERV1. Genomics *54*, 460-468.

Coppock, D. L., Kopman, C., Scandalis, S., et Gilleran, S. (1993). Preferential gene expression in quiescent human lung fibroblasts. Cell Growth Differ *4*, 483-493.

Coppock, D., Kopman, C., Gudas, J., et Cina-Poppe, D. A. (2000). Regulation of the quiescence-induced genes: quiescin Q6, decorin, and ribosomal protein S29. Biochem. Biophys. Res. Commun *269*, 604-610.

Coppock, D. L., et Thorpe, C. (2006). Multidomain flavin-dependent sulfhydryl oxidases. Antioxid. Redox Signal *8*, 300-311.

Cosma, M. P., Pepe, S., Annunziata, I., Newbold, R. F., Grompe, M., Parenti, G., et Ballabio, A. (2003). The multiple sulfatase deficiency gene encodes an essential and limiting factor for the activity of sulfatases. Cell *113*, 445-456.

Crawford, N. A., Yee, B. C., Hutcheson, S. W., Wolosiuk, R. A., et Buchanan, B. B. (1986). Enzyme regulation in C4 photosynthesis: purification, properties, and activities of thioredoxins from C4 and C3 plants. Arch. Biochem. Biophys *244*, 1-15.

d'Aloisio, E., Paolacci, A. R., Dhanapal, A. P., Tanzarella, O. A., Porceddu, E., et Ciaffi, M. (2010). The Protein Disulfide Isomerase gene family in bread wheat (T. aestivum L.). BMC Plant Biol *10*, 101.

Dai, S., Schwendtmayer, C., Schürmann, P., Ramaswamy, S., et Eklund, H. (2000). Redox signaling in chloroplasts: cleavage of disulfides by an iron-sulfur cluster. Science *287*, 655-658.

Dai, S., Johansson, K., Miginiac-Maslow, M., Schürmann, P., et Eklund, H. (2004). Structural Basis of Redox Signaling in Photosynthesis: Structure and Function of Ferredoxin:thioredoxin Reductase and Target Enzymes. Photosyn. Res *79*, 233-248.

Dailey, F. E., et Berg, H. C. (1993). Mutants in disulfide bond formation that disrupt flagellar assembly in Escherichia coli. Proc. Natl. Acad. Sci. U.S.A *90*, 1043-1047.

Daithankar, V. N., Schaefer, S. A., Dong, M., Bahnson, B. J., et Thorpe, C. (2010). Structure of the human sulfhydryl oxidase augmenter of liver regeneration and characterization of a human mutation causing an autosomal recessive myopathy. Biochemistry *49*, 6737-6745.

Darby, N. J., Penka, E., et Vincentelli, R. (1998). The multi-domain structure of protein disulfide isomerase is essential for high catalytic efficiency. J. Mol. Biol *276*, 239-247.

Debarbieux, L., et Beckwith, J. (2000). On the functional interchangeability, oxidant versus reductant, of members of the thioredoxin superfamily. J. Bacteriol *182*, 723-727.

Debarbieux, L., et Beckwith, J. (2000). On the functional interchangeability, oxidant versus reductant, of members of the thioredoxin superfamily. J. Bacteriol *182*, 723-727.

Debarbieux, L., et Beckwith, J. (1998). The reductive enzyme thioredoxin 1 acts as an oxidant when it is exported to the Escherichia coli periplasm. Proceedings of the National Academy of Sciences of the United States of America *95*, 10751-10756.

Delaunay, A., Isnard, A. D., et Toledano, M. B. (2000). H2O2 sensing through oxidation of the Yap1 transcription factor. The EMBO journal *19*, 5157-66.

Delaunay, A., Pflieger, D., Barrault, M. B., Vinh, J., et Toledano, M. B. (2002). A thiol peroxidase is an H2O2 receptor and redox-transducer in gene activation. Cell *111*, 471-81.

Denisov, A. Y., Määttänen, P., Dabrowski, C., Kozlov, G., Thomas, D. Y., et Gehring, K. (2009). Solution structure of the bb' domains of human protein disulfide isomerase. FEBS J *276*, 1440-1449.

Deponte, M., et Hell, K. (2009). Disulphide bond formation in the intermembrane space of mitochondria. J. Biochem *146*, 599-608.

Depuydt, M., Leonard, S. E., Vertommen, D., Denoncin, K., Morsomme, P., Wahni, K., Messens, J., Carroll, K. S., et Collet, J. F. (2009). A periplasmic reducing system protects single cysteine residues from oxidation. Science *326*, 1109-11.

Depuydt, M., Messens, J., et Collet, J.-F. (2011). How Proteins Form Disulfide Bonds. Antioxid Redox Signal. PMID:20849374 [PubMed - as supplied by publisher].

Di Matteo, A., Calosci, N., Gianni, S., Jemth, P., Brunori, M., et Travaglini-Allocatelli, C. (2010). Structural and functional characterization of CcmG from Pseudomonas aeruginosa, a key component of the bacterial cytochrome c maturation apparatus. Proteins *78*, 2213-2221.

Dietz, K.-J. (2011). Peroxiredoxins in Plants and Cyanobacteria. Antioxid Redox Signal. PMID: 21194355 [PubMed - as supplied by publisher].

Dietz, K.-J., Jacob, S., Oelze, M.-L., Laxa, M., Tognetti, V., de Miranda, S. M. N., Baier, M., et Finkemeier, I. (2006). The function of peroxiredoxins in plant organelle redox metabolism. J. Exp. Bot *57*, 1697-1709.

Dixon, D. P., Van Lith, M., Edwards, R., et Benham, A. (2003). Cloning and initial characterization of the Arabidopsis thaliana endoplasmic reticulum oxidoreductins. Antioxid. Redox Signal *5*, 389-396.

Droux, M., Miginiac-Maslow, M., Jacquot, J. P., Gadal, P., Crawford, N. A., Kosower, N. S., et Buchanan, B. B. (1987). Ferredoxin-thioredoxin reductase: a catalytically active dithiol group links photoreduced ferredoxin to thioredoxin functional in photosynthetic enzyme regulation. Arch. Biochem. Biophys *256*, 372-380.

Dubuisson, M., Vander Stricht, D., Clippe, A., Etienne, F., Nauser, T., Kissner, R., Koppenol, W. H., Rees, J.-F., et Knoops, B. (2004). Human peroxiredoxin 5 is a peroxynitrite reductase. FEBS Lett *571*, 161-165.

Duplessis, S., Cuomo, C. A., Lin, Y.-C., Aerts, A., Tisserant, E., Veneault-Fourrey, C., Joly, D. L., Hacquard, S., Amselem, J., Cantarel, B. L., et al. (2011). Obligate biotrophy features unraveled by the genomic analysis of rust fungi. Proc Natl Acad Sci U S A. PMID: 21536894 [PubMed - as supplied by publisher].

Echalier, A., Trivelli, X., Corbier, C., Rouhier, N., Walker, O., Tsan, P., Jacquot, J.-P., Aubry, A., Krimm, I., et Lancelin, J.-M. (2005). Crystal structure and solution NMR dynamics of a D (type II) peroxiredoxin glutaredoxin and thioredoxin dependent: a new insight into the peroxiredoxin oligomerism. Biochemistry *44*, 1755-1767.

Endo, T., Yamano, K., et Kawano, S. (2010). Structural basis for the disulfide relay system in the mitochondrial intermembrane space. Antioxid. Redox Signal *13*, 1359-1373.

Enyedi, B., Várnai, P., et Geiszt, M. (2010). Redox state of the endoplasmic reticulum is controlled by Ero1L-alpha and intraluminal calcium. Antioxid. Redox Signal *13*, 721-729.

Ferrer-Sueta, G., Manta, B., Botti, H., Radi, R., Trujillo, M., et Denicola, A. (2011). Factors affecting protein thiol reactivity and specificity in peroxide reduction. Chem. Res. Toxicol *24*, 434-450.

Fischer, B. B., Dayer, R., Schwarzenbach, Y., Lemaire, S. D., Behra, R., Liedtke, A., et Eggen, R. I. L. (2009). Function and regulation of the glutathione peroxidase homologous gene GPXH/GPX5 in Chlamydomonas reinhardtii. Plant Mol. Biol *71*, 569-583.

Fischer, B., Eggen, R., Trebst, A., et Krieger-Liszkay, A. (2006). The glutathione peroxidase homologous gene Gpxh in Chlamydomonas reinhardtii is upregulated by singlet oxygen produced in photosystem II. Planta *223*, 583-590.

Flohé, L., Toppo, S., Cozza, G., et Ursini, F. (2010). A Comparison of Thiol Peroxidase Mechanisms. Antioxid. Redox Signal. PMID: 20649470 [PubMed - as supplied by publisher].

Foyer, C. H., et Noctor, G. (2005). Oxidant and antioxidant signalling in plants: a re-evaluation of the concept of oxidative stress in a physiological context. Plant Cell Env *28*, 1056-1071.

Foyer, C. H., Souriau, N., Perret, S., Lelandais, M., Kunert, K. J., Pruvost, C., et Jouanin, L. (1995). Overexpression of glutathione reductase but not glutathione synthetase leads to increases in antioxidant capacity and resistance to photoinhibition in poplar trees. Plant physiology *109*, 1047-57.

Fraldi, A., Zito, E., Annunziata, F., Lombardi, A., Cozzolino, M., Monti, M., Spampanato, C., Ballabio, A., Pucci, P., Sitia, R., et al. (2008). Multistep, sequential control of the trafficking and function of the multiple sulfatase deficiency gene product, SUMF1 by PDI, ERGIC-53 and ERp44. Hum Mol Genet *17*, 2610-21.

Francavilla, A., Hagiya, M., Porter, K. A., Polimeno, L., Ihara, I., et Starzl, T. E. (1994). Augmenter of liver regeneration: its place in the universe of hepatic growth factors. Hepatology *20*, 747-757.

Frand, A. R., Cuozzo, J. W., et Kaiser, C. A. (2000). Pathways for protein disulphide bond formation. Trends Cell Biol *10*, 203-210.

Frand, A. R., et Kaiser, C. A. (2000). Two pairs of conserved cysteines are required for the oxidative activity of Ero1p in protein disulfide bond formation in the endoplasmic reticulum. Mol. Biol. Cell *11*, 2833-2843.

Frand, A. R., et Kaiser, C. A. (1999). Ero1p oxidizes protein disulfide isomerase in a pathway for disulfide bond formation in the endoplasmic reticulum. Mol Cell *4*, 469-77.

Frand, A. R., et Kaiser, C. A. (1998). The ERO1 gene of yeast is required for oxidation of protein dithiols in the endoplasmic reticulum. Mol Cell *1*, 161-70.

Freedman, R. B., Hirst, T. R., et Tuite, M. F. (1994). Protein disulphide isomerase: building bridges in protein folding. Trends Biochem Sci *19*, 331-6.

Frickel, E.-M., Frei, P., Bouvier, M., Stafford, W. F., Helenius, A., Glockshuber, R., et Ellgaard, L. (2004). ERp57 is a multifunctional thiol-disulfide oxidoreductase. J. Biol. Chem *279*, 18277-18287.

Frickel, E.-M., Riek, R., Jelesarov, I., Helenius, A., Wuthrich, K., et Ellgaard, L. (2002). TROSY-NMR reveals interaction between ERp57 and the tip of the calreticulin P-domain. Proc. Natl. Acad. Sci. U.S.A *99*, 1954-1959.

Friso, G., Giacomelli, L., Ytterberg, A. J., Peltier, J.-B., Rudella, A., Sun, Q., et Wijk, K. J. van (2004). In-depth analysis of the thylakoid membrane proteome of Arabidopsis thaliana chloroplasts: new proteins, new functions, and a plastid proteome database. Plant Cell *16*, 478-499.

Fromm, H., Devic, M., Fluhr, R., et Edelman, M. (1985). Control of psbA gene expression: in mature Spirodela chloroplasts light regulation of 32-kd protein synthesis is independent of transcript level. EMBO J *4*, 291-295.

Gabriel, K., Milenkovic, D., Chacinska, A., Müller, J., Guiard, B., Pfanner, N., et Meisinger, C. (2007). Novel mitochondrial intermembrane space proteins as substrates of the MIA import pathway. J. Mol. Biol *365*, 612-620.

Gama, F., Brehelin, C., Gelhaye, E., Meyer, Y., Jacquot, J. P., Rey, P., et Rouhier, N. (2008). Functional analysis and expression characteristics of chloroplastic Prx IIE. Physiologia plantarum *133*, 599-610.

Gaymard, F., Pilot, G., Lacombe, B., Bouchez, D., Bruneau, D., Boucherez, J., Michaux-Ferrière, N., Thibaud, J. B., et Sentenac, H. (1998). Identification and disruption of a plant shaker-like outward channel involved in K+ release into the xylem sap. Cell *94*, 647-655.

Gebert, N., Chacinska, A., Wagner, K., Guiard, B., Koehler, C. M., Rehling, P., Pfanner, N., et Wiedemann, N. (2008). Assembly of the three small Tim proteins precedes docking to the mitochondrial carrier translocase. EMBO Rep *9*, 548-554.

Gelhaye, E., Rouhier, N., et Jacquot, J. P. (2003). Evidence for a subgroup of thioredoxin h that requires GSH/Grx for its reduction. FEBS Lett *555*, 443-8.

Gelhaye, E., Rouhier, N., Navrot, N., et Jacquot, J. P. (2005). The plant thioredoxin system. Cell Mol Life Sci *62*, 24-35.

Gelhaye, E., Rouhier, N., Gérard, J., Jolivet, Y., Gualberto, J., Navrot, N., Ohlsson, P.-I., Wingsle, G., Hirasawa, M., Knaff, D. B., et al. (2004). A specific form of thioredoxin h occurs in plant mitochondria and regulates the alternative oxidase. Proc Natl Acad Sci U S A *101*, 14545-14550.

Georgescu, R. E., Li, J. H., Goldberg, M. E., Tasayco, M. L., et Chaffotte, A. F. (1998). Proline isomerization-independent accumulation of an early intermediate and heterogeneity of the folding pathways of a mixed alpha/beta protein, Escherichia coli thioredoxin. Biochemistry *37*, 10286-10297.

Givol, D., Goldberg, R. F., et Anfinsen, C. B. (1964). OXIDATION AND DISULFIDE INTERCHANGE IN THE REACTIVATION OF REDUCED RIBONUCLEASE. J. Biol. Chem *239*, PC3114-3116.

Goldberger, R. F., EPSTEIN, C. J., et ANFINSEN, C. B. (1963). Acceleration of reactivation of reduced bovine pancreatic ribonuclease by a microsomal system from rat liver. J. Biol. Chem *238*, 628-635.

Gordon, E. H. J., Page, M. D., Willis, A. C., et Ferguson, S. J. (2000). Escherichia coli DipZ: anatomy of a transmembrane protein disulphide reductase in which three pairs of cysteine residues, one in each of three domains, contribute differentially to function. Mol Microbiol

35, 1360-1374.

Gross, E., Kastner, D. B., Kaiser, C. A., et Fass, D. (2004). Structure of Ero1p, source of disulfide bonds for oxidative protein folding in the cell. Cell *117*, 601-610.

Gross, E., Sevier, C. S., Vala, A., Kaiser, C. A., et Fass, D. (2002). A new FAD-binding fold and intersubunit disulfide shuttle in the thiol oxidase Erv2p. Nat. Struct. Biol *9*, 61-67.

Gruber, C. W., Cemazar, M., Heras, B., Martin, J. L., et Craik, D. J. (2006). Protein disulfide isomerase: the structure of oxidative folding. Trends Biochem. Sci *31*, 455-464.

Hall, A., Nelson, K., Poole, L. B., et Karplus, P. A. (2011). Structure-based Insights into the Catalytic Power and Conformational Dexterity of Peroxiredoxins. Antioxid Redox Signal. PMID: 20969484 [PubMed - as supplied by publisher].

Hall, A., Parsonage, D., Poole, L. B., et Karplus, P. A. (2010). Structural Evidence that Peroxiredoxin Catalytic Power Is Based on Transition-State Stabilization. Journal of Molecular Biology *402*, 194-209.

Hall, A., Sankaran, B., Poole, L. B., et Karplus, P. A. (2009). Structural changes common to catalysis in the Tpx peroxiredoxin subfamily. J. Mol. Biol *393*, 867-881.

Halliwell, B., et Gutteridge, J. M. C. (2007). Free Radicals in Biology And Medicine. Oxford University Press, 4th Revised edition (8 mars 2007).

Hanton, S. L., Bortolotti, L. E., Renna, L., Stefano, G., et Brandizzi, F. (2005). Crossing the divide--transport between the endoplasmic reticulum and Golgi apparatus in plants. Traffic *6*, 267-277.

Hatahet, F., Ruddock, L. W., Ahn, K., Benham, A., Craik, D., Ellgaard, L., Ferrari, D., et Ventura, S. (2009). Protein disulfide isomerase: a critical evaluation of its function in disulfide bond formation. Antioxid. Redox Signal *11*, 2807-2850.

Hayashi, S., Abe, M., Kimoto, M., Furukawa, S., et Nakazawa, T. (2000). The dsbA-dsbB disulfide bond formation system of Burkholderia cepacia is involved in the production of protease and alkaline phosphatase, motility, metal resistance, and multi-drug resistance. Microbiol. Immunol *44*, 41-50.

Heazlewood, J. L., Tonti-Filippini, J. S., Gout, A. M., Day, D. A., Whelan, J., et Millar, A. H. (2004). Experimental analysis of the Arabidopsis mitochondrial proteome highlights signaling and regulatory components, provides assessment of targeting prediction programs, and indicates plant-specific mitochondrial proteins. Plant Cell *16*, 241-256.

Heckler, E. J., Alon, A., Fass, D., et Thorpe, C. (2008a). Human quiescin-sulfhydryl oxidase, QSOX1: probing internal redox steps by mutagenesis. Biochemistry *47*, 4955-4963.

Heckler, E. J., Rancy, P. C., Kodali, V. K., et Thorpe, C. (2008b). Generating disulfides with the Quiescin-sulfhydryl oxidases. Biochim. Biophys. Acta *1783*, 567-577.

Hegde, R. S., et Ploegh, H. L. (2010). Quality and quantity control at the endoplasmic reticulum. Curr. Opin. Cell Biol *22*, 437-446.

Heras, B., Shouldice, S. R., Totsika, M., Scanlon, M. J., Schembri, M. A., et Martin, J. L. (2009). DSB proteins and bacterial pathogenicity. Nat. Rev. Microbiol *7*, 215-225.

Herbette, S., Menn, A. L., Rousselle, P., Ameglio, T., Faltin, Z., Branlard, G., Eshdat, Y., Julien, J.-L., Drevet, J. R., et Roeckel-Drevet, P. (2005). Modification of photosynthetic regulation in tomato overexpressing glutathione peroxidase. Biochim. Biophys. Acta *1724*, 108-118.

Herrera, E., et Barbas, C. (2001). Vitamin E: action, metabolism and perspectives. Journal of physiology and biochemistry *57*, 43-56.

Herrmann, J. M., et Hell, K. (2005). Chopped, trapped or tacked--protein translocation into the IMS of mitochondria. Trends Biochem. Sci *30*, 205-211.

Herrmann, J. M., et Köhl, R. (2007). Catch me if you can! Oxidative protein trapping in the intermembrane space of mitochondria. J. Cell Biol *176*, 559-563.

Hofhaus, G., Lee, J.-E., Tews, I., Rosenberg, B., et Lisowsky, T. (2003). The N-terminal cysteine pair of yeast sulfhydryl oxidase Erv1p is essential for in vivo activity and interacts with the primary redox centre. Eur. J. Biochem *270*, 1528-1535.

Hofmann, B., Hecht, H.-J., et Flohé, L. (2002). Peroxiredoxins. Biol. Chem *383*, 347-364.

Holmgren, A. (1976). Hydrogen donor system for Escherichia coli ribonucleoside-diphosphate reductase dependent upon glutathione. Proc. Natl. Acad. Sci. U.S.A *73*, 2275-2279.

Holmgren, A., et Björnstedt, M. (1995). Thioredoxin and thioredoxin reductase. Meth. Enzymol *252*, 199-208.

Holmgren, A., Söderberg, B. O., Eklund, H., et Brändén, C. I. (1975). Three-dimensional structure of Escherichia coli thioredoxin-S2 to 2.8 A resolution. Proc. Natl. Acad. Sci. U.S.A *72*, 2305-2309.

Holmgren, A. (1968). Thioredoxin. 6. The amino acid sequence of the protein from escherichia coli B. European journal of biochemistry / FEBS *6*, 475-84.

Hoober, K. L., Glynn, N. M., Burnside, J., Coppock, D. L., et Thorpe, C. (1999). Homology between egg white sulfhydryl oxidase and quiescin Q6 defines a new class of flavin-linked sulfhydryl oxidases. J. Biol. Chem *274*, 31759-31762.

Horta, B. B., de Oliveira, M. A., Discola, K. F., Cussiol, J. R. R., et Netto, L. E. S. (2010). Structural and biochemical characterization of peroxiredoxin Qbeta from Xylella fastidiosa: catalytic mechanism and high reactivity. J. Biol. Chem *285*, 16051-16065.

Houston, N. L., Fan, C., Xiang, J. Q., Schulze, J. M., Jung, R., et Boston, R. S. (2005). Phylogenetic analyses identify 10 classes of the protein disulfide isomerase family in plants, including single-domain protein disulfide isomerase-related proteins. Plant Physiol *137*, 762-78.

Hwang, C., Sinskey, A. J., et Lodish, H. F. (1992). Oxidized redox state of glutathione in the endoplasmic reticulum. Science *257*, 1496-502.

Inaba, K. (2009). Disulfide bond formation system in Escherichia coli. J. Biochem *146*, 591-597.

Inaba, K., et Ito, K. (2002). Paradoxical redox properties of DsbB and DsbA in the protein disulfide-introducing reaction cascade. EMBO J *21*, 2646-2654.

Inaba, K., Masui, S., Iida, H., Vavassori, S., Sitia, R., et Suzuki, M. (2010). Crystal structures of human Ero1α reveal the mechanisms of regulated and targeted oxidation of PDI. EMBO J *29*, 3330-3343.

Ito, K., et Inaba, K. (2008). The disulfide bond formation (Dsb) system. Curr. Opin. Struct. Biol *18*, 450-458.

Iwai, K., Naganuma, A., et Kuge, S. (2010). Peroxiredoxin Ahp1 acts as a receptor for alkylhydroperoxides to induce disulfide bond formation in the Cad1 transcription factor. J. Biol. Chem *285*, 10597-10604.

Iwasaki, K., Kamauchi, S., Wadahama, H., Ishimoto, M., Kawada, T., et Urade, R. (2009). Molecular cloning and characterization of soybean protein disulfide isomerase family proteins with nonclassic active center motifs. FEBS J *276*, 4130-41.

Jacob-Dubuisson, F., Pinkner, J., Xu, Z., Striker, R., Padmanhaban, A., et Hultgren, S. J. (1994). PapD chaperone function in pilus biogenesis depends on oxidant and chaperone-like activities of DsbA. Proc. Natl. Acad. Sci. U.S.A *91*, 11552-11556.

Jacquot, J. P., Gadal, P., Nishizawa, A. N., Yee, B. C., Crawford, N. A., et Buchanan, B. B. (1984). Enzyme regulation in C4 photosynthesis: mechanism of activation of NADP-malate dehydrogenase by reduced thioredoxin. Arch. Biochem. Biophys *228*, 170-178.

Jacquot, J. P., de Lamotte, F., Fontecave, M., Schürmann, P., Decottignies, P., Miginiac-Maslow, M., et Wollman, E. (1990). Human thioredoxin reactivity-structure/function relationship. Biochem. Biophys. Res. Commun *173*, 1375-1381.

Jaje, J., Wolcott, H. N., Fadugba, O., Cripps, D., Yang, A. J., Mather, I. H., et Thorpe, C. (2007). A Flavin-dependent Sulfhydryl Oxidase in Bovine Milk. Biochemistry *46*, 13031-13040.

Jakob, U., Muse, W., Eser, M., et Bardwell, J. C. (1999). Chaperone activity with a redox switch. Cell *96*, 341-352.

Janolino, V. G., et Swaisgood, H. E. (1975). Isolation and characterization of sulfhydryl oxidase from bovine milk. J. Biol. Chem *250*, 2532-2538.

Jaquinod, M., Villiers, F., Kieffer-Jaquinod, S., Hugouvieux, V., Bruley, C., Garin, J., et Bourguignon, J. (2007). A proteomics dissection of Arabidopsis thaliana vacuoles isolated from cell culture. Mol Cell Proteomics *6*, 394-412.

Jeng, M. F., Reymond, M. T., Tennant, L. L., Holmgren, A., et Dyson, H. J. (1998). NMR characterization of a single-cysteine mutant of Escherichia coli thioredoxin and a covalent thioredoxin-peptide complex. Eur. J. Biochem *257*, 299-308.

Jessop, C. E., Watkins, R. H., Simmons, J. J., Tasab, M., et Bulleid, N. J. (2009a). Protein disulphide isomerase family members show distinct substrate specificity: P5 is targeted to BiP client proteins. J Cell Sci *122*, 4287-95.

Jessop, C. E., Tavender, T. J., Watkins, R. H., Chambers, J. E., et Bulleid, N. J. (2009b). Substrate specificity of the oxidoreductase ERp57 is determined primarily by its interaction with calnexin and calreticulin. J. Biol. Chem *284*, 2194-2202.

Johnson, T. C., Cao, R. Q., Kung, J. E., et Buchanan, B. B. (1987). Thioredoxin and NADP-thioredoxin reductase from cultured carrot cells. Planta *171*, 321-331.

Jonda, S., Huber-Wunderlich, M., Glockshuber, R., et Mössner, E. (1999). Complementation of DsbA deficiency with secreted thioredoxin variants reveals the crucial role of an efficient dithiol oxidant for catalyzed protein folding in the bacterial periplasm. EMBO J *18*, 3271-3281.

Kadokura, H., et Beckwith, J. (2001). The expanding world of oxidative protein folding. Nat. Cell Biol *3*, E247-249.

Kadokura, H., Katzen, F., et Beckwith, J. (2003). Protein disulfide bond formation in prokaryotes. Annu. Rev. Biochem *72*, 111-135.

Kamauchi, S., Wadahama, H., Iwasaki, K., Nakamoto, Y., Nishizawa, K., Ishimoto, M., Kawada, T., et Urade, R. (2008). Molecular cloning and characterization of two soybean protein disulfide isomerases as molecular chaperones for seed storage proteins. FEBS J *275*, 2644-58.

Kamitani, S., Akiyama, Y., et Ito, K. (1992). Identification and characterization of an Escherichia coli gene required for the formation of correctly folded alkaline phosphatase, a periplasmic enzyme. EMBO J *11*, 57-62.

Kang, S. W., Baines, I. C., et Rhee, S. G. (1998). Characterization of a mammalian peroxiredoxin that contains one conserved cysteine. The Journal of biological chemistry *273*, 6303-11.

Karala, A.-R., Lappi, A.-K., et Ruddock, L. W. (2010). Modulation of an active-site cysteine pKa allows PDI to act as a catalyst of both disulfide bond formation and isomerization. J. Mol. Biol *396*, 883-892.

Kelley, R. F., et Richards, F. M. (1987). Replacement of proline-76 with alanine eliminates the slowest kinetic phase in thioredoxin folding. Biochemistry *26*, 6765-6774.

Keryer, E., Collin, V., Lavergne, D., Lemaire, S., et Issakidis-Bourguet, E. (2004). Characterization of Arabidopsis Mutants for the Variable Subunit of Ferredoxin:thioredoxin Reductase. Photosyn. Res *79*, 265-274.

Kho, C. W., Lee, P. Y., Bae, K. H., Cho, S., Lee, Z. W., Park, B. C., Kang, S., Lee do, H., et Park, S. G. (2006). Glutathione peroxidase 3 of Saccharomyces cerevisiae regulates the activity of methionine sulfoxide reductase in a redox state-dependent way. Biochem Biophys Res Commun *348*, 25-35.

Kikuchi, M., Doi, E., Tsujimoto, I., Horibe, T., et Tsujimoto, Y. (2002). Functional analysis of human P5, a protein disulfide isomerase homologue. J. Biochem *132*, 451-455.

Kleffmann, T., Russenberger, D., von Zychlinski, A., Christopher, W., Sjölander, K., Gruissem, W., et Baginsky, S. (2004). The Arabidopsis thaliana chloroplast proteome reveals pathway abundance and novel protein functions. Curr. Biol *14*, 354-362.

Kodali, V. K., et Thorpe, C. (2010a). Oxidative Protein Folding and the Quiescin-Sulfhydryl Oxidase Family of Flavoproteins. Antioxid Redox Signal. PMID:20136510 [PubMed - indexed for MEDLINE].

Kodali, V. K., et Thorpe, C. (2010b). Quiescin sulfhydryl oxidase from Trypanosoma brucei: catalytic activity and mechanism of a QSOX family member with a single thioredoxin domain. Biochemistry *49*, 2075-2085.

Koehler, C. M. (2004). New developments in mitochondrial assembly. Annu. Rev. Cell Dev. Biol *20*, 309-335.

Koh, C. S., Didierjean, C., Navrot, N., Panjikar, S., Mulliert, G., Rouhier, N., Jacquot, J.-P., Aubry, A., Shawkataly, O., et Corbier, C. (2007). Crystal structures of a poplar thioredoxin peroxidase that exhibits the structure of glutathione peroxidases: insights into redox-driven conformational changes. J. Mol. Biol *370*, 512-529.

König, J., Baier, M., Horling, F., Kahmann, U., Harris, G., Schürmann, P., et Dietz, K.-J. (2002). The plant-specific function of 2-Cys peroxiredoxin-mediated detoxification of peroxides in the redox-hierarchy of photosynthetic electron flux. Proc Natl Acad Sci U S A *99*, 5738-5743.

König, J., Lotte, K., Plessow, R., Brockhinke, A., Baier, M., et Dietz, K.-J. (2003). Reaction mechanism of plant 2-Cys peroxiredoxin. Role of the C terminus and the quaternary structure. J. Biol. Chem *278*, 24409-24420.

Kontush, A., Finckh, B., Karten, B., Kohlschütter, A., et Beisiegel, U. (1996). Antioxidant and prooxidant activity of alpha-tocopherol in human plasma and low density lipoprotein. J. Lipid Res *37*, 1436-1448.

Kozlov, G., Azeroual, S., Rosenauer, A., Määttänen, P., Denisov, A. Y., Thomas, D. Y., et Gehring, K. (2010a). Structure of the catalytic a(0)a fragment of the protein disulfide isomerase ERp72. J. Mol. Biol *401*, 618-625.

Kozlov, G., Määttänen, P., Schrag, J. D., Pollock, S., Cygler, M., Nagar, B., Thomas, D. Y., et Gehring, K. (2006). Crystal structure of the bb' domains of the protein disulfide isomerase ERp57. Structure *14*, 1331-1339.

Kozlov, G., Määttänen, P., Thomas, D. Y., et Gehring, K. (2010b). A structural overview of the PDI family of proteins. FEBS J *277*, 3924-3936.

Kramer, B., Ferrari, D. M., Klappa, P., Pöhlmann, N., et Söling, H. D. (2001). Functional roles and efficiencies of the thioredoxin boxes of calcium-binding proteins 1 and 2 in protein folding. Biochem. J *357*, 83-95.

Kranz, R., Lill, R., Goldman, B., Bonnard, G., et Merchant, S. (1998). Molecular mechanisms of cytochrome c biogenesis: three distinct systems. Mol. Microbiol *29*, 383-396.

Krause, G., et Holmgren, A. (1991). Substitution of the conserved tryptophan 31 in Escherichia coli thioredoxin by site-directed mutagenesis and structure-function analysis. J Biol Chem *266*, 4056-66.

Lafaye, C., Iwema, T., Carpentier, P., Jullian-Binard, C., Kroll, J. S., Collet, J.-F., et Serre, L. (2009).

Biochemical and structural study of the homologues of the thiol-disulfide oxidoreductase DsbA in Neisseria meningitidis. J. Mol. Biol *392*, 952-966.

Lambert, N., et Freedman, R. B. (1983). Kinetics and specificity of homogeneous protein disulphide-isomerase in protein disulphide isomerization and in thiol-protein-disulphide oxidoreduction. Biochem. J *213*, 235-243.

Lambeth, J. D. (2004). NOX enzymes and the biology of reactive oxygen. Nat. Rev. Immunol *4*, 181 -189.

Lange, H., Lisowsky, T., Gerber, J., Mühlenhoff, U., Kispal, G., et Lill, R. (2001). An essential function of the mitochondrial sulfhydryl oxidase Erv1p/ALR in the maturation of cytosolic Fe/S proteins. EMBO Rep *2*, 715-720.

Lash, L. H., et Jones, D. P. (1983). Characterization of the membrane-associated thiol oxidase activity of rat small-intestinal epithelium. Arch. Biochem. Biophys *225*, 344-352.

Laurent, T. C., Moore, E. C., et Reichard, P. (1964). Enzymatic Synthesis of Deoxyribonucleotides. Iv. Isolation and Characterization of Thioredoxin, the Hydrogen Donor from Escherichia Coli B. The Journal of biological chemistry *239*, 3436-44.

Lee, P. Y., Bae, K.-H., Kho, C. W., Kang, S., Lee, D. H., Cho, S., Kang, S., Lee, S. C., Park, B. C., et Park, S. G. (2008). Interactome analysis of yeast glutathione peroxidase 3. J. Microbiol. Biotechnol *18*, 1364-1367.

Lee, S. P., Hwang, Y. S., Kim, Y. J., Kwon, K. S., Kim, H. J., Kim, K., et Chae, H. Z. (2001). Cyclophilin a binds to peroxiredoxins and activates its peroxidase activity. The Journal of biological chemistry *276*, 29826-32.

Lemaire, S. D., Michelet, L., Zaffagnini, M., Massot, V., et Issakidis-Bourguet, E. (2007). Thioredoxins in chloroplasts. Current genetics *51*, 343-65.

Lemaire, S. D., et Miginiac-Maslow, M. (2004). The thioredoxin superfamily in Chlamydomonas reinhardtii. Photosyn. Res *82*, 203-220.

Lennon, B. W., Williams, C. H., et Ludwig, M. L. (2000). Twists in catalysis: alternating conformations of Escherichia coli thioredoxin reductase. Science *289*, 1190-1194.

Levitan, A., Danon, A., et Lisowsky, T. (2004). Unique features of plant mitochondrial sulfhydryl oxidase. J. Biol. Chem *279*, 20002-20008.

Li, Y., Liu, W., Xing, G., Tian, C., Zhu, Y., et He, F. (2005). Direct association of hepatopoietin with thioredoxin constitutes a redox signal transduction in activation of AP-1/NF-kappaB. Cell. Signal *17*, 985-996.

Lisowsky, T. (1992). Dual function of a new nuclear gene for oxidative phosphorylation and vegetative growth in yeast. Mol. Gen. Genet *232*, 58-64.

Longen, S., Bien, M., Bihlmaier, K., Kloeppel, C., Kauff, F., Hammermeister, M., Westermann, B., Herrmann, J. M., et Riemer, J. (2009). Systematic analysis of the twin cx(9)c protein family. J. Mol. Biol *393*, 356-368.

Lu, D., et Christopher, D. A. (2008). Endoplasmic reticulum stress activates the expression of a sub -group of protein disulfide isomerase genes and AtbZIP60 modulates the response in Arabidopsis thaliana. Mol Genet Genomics *280*, 199-210.

Lu, D., et Christopher, D. A. (2006). Immunolocalization of a Protein Disulfide Isomerase to Arabidopsis thaliana Chloroplasts and Its Association with Starch Biogenesis. International Journal of Plant Sciences *167*, 1-9.

Lundström, J., et Holmgren, A. (1990). Protein disulfide-isomerase is a substrate for thioredoxin reductase and has thioredoxin-like activity. J. Biol. Chem *265*, 9114-9120.

Ma, L.-H., Takanishi, C. L., et Wood, M. J. (2007). Molecular mechanism of oxidative stress perception by the Orp1 protein. J. Biol. Chem *282*, 31429-31436.

Maattanen, P., Kozlov, G., Gehring, K., et Thomas, D. Y. (2006). ERp57 and PDI: multifunctional protein disulfide isomerases with similar domain architectures but differing substrate-partner associations. Biochem. Cell Biol *84*, 881-889.

Maeda, K., Hägglund, P., Finnie, C., Svensson, B., et Henriksen, A. (2006). Structural basis for target protein recognition by the protein disulfide reductase thioredoxin. Structure *14*, 1701-1710.

Maiorino, M., Aumann, K. D., Brigelius-Flohé, R., Doria, D., van den Heuvel, J., McCarthy, J., Roveri, A., Ursini, F., et Flohé, L. (1998). Probing the presumed catalytic triad of a selenium-containing peroxidase by mutational analysis. Z Ernahrungswiss *37 Suppl 1*, 118-121.

Maiorino, M., Aumann, K. D., Brigelius-Flohé, R., Doria, D., van den Heuvel, J., McCarthy, J., Roveri, A., Ursini, F., et Flohé, L. (1995). Probing the presumed catalytic triad of selenium-containing peroxidases by mutational analysis of phospholipid hydroperoxide glutathione peroxidase (PHGPx). Biol. Chem. Hoppe-Seyler *376*, 651-660.

Maiorino, M., Ursini, F., Bosello, V., Toppo, S., Tosatto, S. C., Mauri, P., Becker, K., Roveri, A., Bulato, C., Benazzi, L., et al. (2007). The thioredoxin specificity of Drosophila GPx: a paradigm for a peroxiredoxin-like mechanism of many glutathione peroxidases. Journal of molecular biology *365*, 1033-46.

Mairet-Coello, G., Tury, A., Esnard-Feve, A., Fellmann, D., Risold, P.-Y., et Griffond, B. (2004). FAD-linked sulfhydryl oxidase QSOX: topographic, cellular, and subcellular immunolocalization in adult rat central nervous system. J. Comp. Neurol *473*, 334-363.

Mamathambika, B. S., et Bardwell, J. C. (2008). Disulfide-linked protein folding pathways. Annu. Rev. Cell Dev. Biol *24*, 211-235.

Marchand, C. H., Vanacker, H., Collin, V., Issakidis-Bourguet, E., Maréchal, P. L., et Decottignies, P. (2010). Thioredoxin targets in Arabidopsis roots. Proteomics *10*, 2418-2428.

Margis, R., Dunand, C., Teixeira, F. K., et Margis-Pinheiro, M. (2008). Glutathione peroxidase family - an evolutionary overview. FEBS J *275*, 3959-3970.

Melchers, J., Diechtierow, M., Fehér, K., Sinning, I., Tews, I., Krauth-Siegel, R. L., et Muhle-Goll, C. (2008). Structural basis for a distinct catalytic mechanism in Trypanosoma brucei tryparedoxin peroxidase. J. Biol. Chem *283*, 30401-30411.

Mesecke, N., Terziyska, N., Kozany, C., Baumann, F., Neupert, W., Hell, K., et Herrmann, J. M. (2005). A disulfide relay system in the intermembrane space of mitochondria that mediates protein import. Cell *121*, 1059-1069.

Meyer, A. J., Brach, T., Marty, L., Kreye, S., Rouhier, N., Jacquot, J. P., et Hell, R. (2007). Redox-sensitive GFP in Arabidopsis thaliana is a quantitative biosensor for the redox potential of the cellular glutathione redox buffer. Plant J *52*, 973-86.

Meyer, A. J., et Dick, T. P. (2010). Fluorescent protein-based redox probes. Antioxid. Redox Signal *13*, 621-650.

Meyer, Y., Buchanan, B. B., Vignols, F., et Reichheld, J. P. (2009). Thioredoxins and glutaredoxins: unifying elements in redox biology. Annu Rev Genet *43*, 335-67.

Miao, Y., Lv, D., Wang, P., Wang, X.-C., Chen, J., Miao, C., et Song, C.-P. (2006). An Arabidopsis glutathione peroxidase functions as both a redox transducer and a scavenger in abscisic acid and drought stress responses. Plant Cell *18*, 2749-2766.

Michelet, L., Zaffagnini, M., Marchand, C., Collin, V., Decottignies, P., Tsan, P., Lancelin, J.-M., Trost, P., Miginiac-Maslow, M., Noctor, G., et al. (2005). Glutathionylation of chloroplast thioredoxin f is a redox signaling mechanism in plants. Proc. Natl. Acad. Sci. U.S.A *102*, 16478-16483.

Mills, G. C. (1957). Hemoglobin catabolism. I. Glutathione peroxidase, an erythrocyte enzyme which protects hemoglobin from oxidative breakdown. The Journal of biological chemistry *229*, 189-97.

Mitra, S. K., Walters, B. T., Clouse, S. D., et Goshe, M. B. (2009). An efficient organic solvent based extraction method for the proteomic analysis of Arabidopsis plasma membranes. J. Proteome Res *8*, 2752-2767.

Moini, H., Packer, L., et Saris, N.-E. L. (2002). Antioxidant and prooxidant activities of alpha-lipoic acid and dihydrolipoic acid. Toxicol. Appl. Pharmacol *182*, 84-90.

Moller, I. M., Jensen, P. E., et Hansson, A. (2007). Oxidative modifications to cellular components in plants. Annual review of plant biology *58*, 459-81.

Monteiro, G., Horta, B. B., Pimenta, D. C., Augusto, O., et Netto, L. E. (2007). Reduction of 1-Cys peroxiredoxins by ascorbate changes the thiol-specific antioxidant paradigm, revealing another function of vitamin C. Proceedings of the National Academy of Sciences of the United States of America *104*, 4886-91.

Montemartini, M., Kalisz, H. M., Kiess, M., Nogoceke, E., Singh, M., Steinert, P., et Flohe, L. (1998). Sequence, heterologous expression and functional characterization of a novel tryparedoxin from Crithidia fasciculata. Biological chemistry *379*, 1137-42.

Montrichard, F., Alkhalfioui, F., Yano, H., Vensel, W. H., Hurkman, W. J., et Buchanan, B. B. (2009).

Thioredoxin targets in plants: the first 30 years. Journal of proteomics *72*, 452-74.

Moon, J. C., Jang, H. H., Chae, H. B., Lee, J. R., Lee, S. Y., Jung, Y. J., Shin, M. R., Lim, H. S., Chung, W. S., Yun, D.-J., et al. (2006). The C-type Arabidopsis thioredoxin reductase ANTR-C acts as an electron donor to 2-Cys peroxiredoxins in chloroplasts. Biochem. Biophys. Res. Commun *348*, 478-484.

Moore, A. L., Umbach, A. L., et Siedow, J. N. (1995). Structure-function relationships of the alternative oxidase of plant mitochondria: a model of the active site. J. Bioenerg. Biomembr *27*, 367-377.

Morel, C., Adami, P., Musard, J.-F., Duval, D., Radom, J., et Jouvenot, M. (2007). Involvement of sulfhydryl oxidase QSOX1 in the protection of cells against oxidative stress-induced apoptosis. Exp. Cell Res *313*, 3971-3982.

Morgan, B. A., et Veal, E. A. (2007). Functions of typical 2-Cys peroxiredoxins in yeast. Subcell. Biochem *44*, 253-265.

Mössner, E., Huber-Wunderlich, M., et Glockshuber, R. (1998). Characterization of Escherichia coli thioredoxin variants mimicking the active-sites of other thiol/disulfide oxidoreductases. Protein Sci *7*, 1233-1244.

Muhle-Goll, C., Füller, F., Ulrich, A. S., et Krauth-Siegel, R. L. (2010). The conserved Cys76 plays a crucial role for the conformation of reduced glutathione peroxidase-type tryparedoxin peroxidase. FEBS Lett *584*, 1027-1032.

Muthuramalingam, M., Seidel, T., Laxa, M., Nunes de Miranda, S. M., Gärtner, F., Ströher, E., Kandlbinder, A., et Dietz, K.-J. (2009). Multiple redox and non-redox interactions define 2-Cys peroxiredoxin as a regulatory hub in the chloroplast. Mol Plant *2*, 1273-1288.

Navrot, N., Collin, V., Gualberto, J., Gelhaye, E., Hirasawa, M., Rey, P., Knaff, D. B., Issakidis, E., Jacquot, J.-P., et Rouhier, N. (2006). Plant glutathione peroxidases are functional peroxiredoxins distributed in several subcellular compartments and regulated during biotic and abiotic stresses. Plant Physiol *142*, 1364-1379.

Nguyen, V. D., Saaranen, M. J., Karala, A.-R., Lappi, A.-K., Wang, L., Raykhel, I. B., Alanen, H. I., Salo, K. E. H., Wang, C.-C., et Ruddock, L. W. (2011). Two endoplasmic reticulum PDI peroxidases increase the efficiency of the use of peroxide during disulfide bond formation. J. Mol. Biol *406*, 503-515.

Nguyen, V. D., Wallis, K., Howard, M. J., Haapalainen, A. M., Salo, K. E. H., Saaranen, M. J., Sidhu, A., Wierenga, R. K., Freedman, R. B., Ruddock, L. W., et al. (2008). Alternative conformations of the x region of human protein disulphide-isomerase modulate exposure of the substrate binding b' domain. J. Mol. Biol *383*, 1144-1155.

Norgaard, P., Westphal, V., Tachibana, C., Alsoe, L., Holst, B., et Winther, J. R. (2001). Functional differences in yeast protein disulfide isomerases. J Cell Biol *152*, 553-62.

Ogusucu, R., Rettori, D., Munhoz, D. C., Soares Netto, L. E., et Augusto, O. (2007). Reactions of yeast thioredoxin peroxidases I and II with hydrogen peroxide and peroxynitrite: Rate constants by competitive kinetics. Free Radical Biology and Medicine *42*, 326-334.

Ortenberg, R., et Beckwith, J. (2003). Functions of thiol-disulfide oxidoreductases in E. coli: redox myths, realities, and practicalities. Antioxid. Redox Signal *5*, 403-411.

Packer, J. E., Slater, T. F., et Willson, R. L. (1979). Direct observation of a free radical interaction between vitamin E and vitamin C. Nature *278*, 737-738.

Pagani, M., Fabbri, M., Benedetti, C., Fassio, A., Pilati, S., Bulleid, N. J., Cabibbo, A., et Sitia, R. (2000). Endoplasmic reticulum oxidoreductin 1-lbeta (ERO1-Lbeta), a human gene induced in the course of the unfolded protein response. J. Biol. Chem *275*, 23685-23692.

Pan, J. L., et Bardwell, J. C. A. (2006). The origami of thioredoxin-like folds. Protein Sci *15*, 2217-2227.

Parker, M. S., Mock, T., et Armbrust, E. V. (2008). Genomic insights into marine microalgae. Annu. Rev. Genet *42*, 619-645.

Parsonage, D., Karplus, P. A., et Poole, L. B. (2008). Substrate specificity and redox potential of AhpC, a bacterial peroxiredoxin. Proc. Natl. Acad. Sci. U.S.A *105*, 8209-8214.

Parsonage, D., Youngblood, D. S., Sarma, G. N., Wood, Z. A., Karplus, P. A., et Poole, L. B. (2005). Analysis of the Link between Enzymatic Activity and Oligomeric State in AhpC, a Bacterial Peroxiredoxin†,‡. Biochemistry *44*, 10583-10592.

Pascual, M. B., Mata-Cabana, A., Florencio, F. J., Lindahl, M., et Cejudo, F. J. (2010). Overoxidation of 2-Cys peroxiredoxin in prokaryotes: cyanobacterial 2-Cys peroxiredoxins sensitive to oxidative stress. J. Biol. Chem *285*, 34485-34492.

Patel, S., Hussain, S., Harris, R., Sardiwal, S., Kelly, J. M., Wilkinson, S. R., Driscoll, P. C., et Djordjevic, S. (2010). Structural insights into the catalytic mechanism of Trypanosoma cruzi GPXI (glutathione peroxidase-like enzyme I). Biochem. J *425*, 513-522.

Pedrajas, J. R., Kosmidou, E., Miranda-Vizuete, A., Gustafsson, J. A., Wright, A. P., et Spyrou, G. (1999). Identification and functional characterization of a novel mitochondrial thioredoxin system in Saccharomyces cerevisiae. The Journal of biological chemistry *274*, 6366-73.

Perez-Ruiz, J. M., Spinola, M. C., Kirchsteiger, K., Moreno, J., Sahrawy, M., et Cejudo, F. J. (2006). Rice NTRC is a high-efficiency redox system for chloroplast protection against oxidative damage. The Plant cell *18*, 2356-68.

Peterson, F. C., Lytle, B. L., Sampath, S., Vinarov, D., Tyler, E., Shahan, M., Markley, J. L., et Volkman, B. F. (2005). Solution structure of thioredoxin h1 from Arabidopsis thaliana. Protein Sci *14*, 2195-2200.

Petersson, U. A., Kieselbach, T., García-Cerdán, J. G., et Schröder, W. P. (2006). The Prx Q protein of Arabidopsis thaliana is a member of the luminal chloroplast proteome. FEBS Lett *580*, 6055-6061.

Pollard, M. G., Travers, K. J., et Weissman, J. S. (1998). Ero1p: a novel and ubiquitous protein with an essential role in oxidative protein folding in the endoplasmic reticulum. Mol. Cell *1*, 171-182.

Poole, L. B. (1996). Flavin-dependent alkyl hydroperoxide reductase from Salmonella typhimurium. 2. Cystine disulfides involved in catalysis of peroxide reduction. Biochemistry *35*, 65-75.

Poole, L. B. (1996). Flavin-dependent alkyl hydroperoxide reductase from Salmonella typhimurium. 2. Cystine disulfides involved in catalysis of peroxide reduction. Biochemistry *35*, 65-75.

Poole, L. B., Karplus, P. A., et Claiborne, A. (2004). Protein sulfenic acids in redox signaling. Annu Rev Pharmacol Toxicol *44*, 325-47.

Poole, L. B., et Ellis, H. R. (1996). Flavin-Dependent Alkyl Hydroperoxide Reductase from Salmonella typhimurium. 1. Purification and Enzymatic Activities of Overexpressed AhpF and AhpC Proteins†. Biochemistry *35*, 56-64.

Poyton, R. O., Ball, K. A., et Castello, P. R. (2009). Mitochondrial generation of free radicals and hypoxic signaling. Trends Endocrinol. Metab *20*, 332-340.

Queval, G., Issakidis-Bourguet, E., Hoeberichts, F. A., Vandorpe, M., Gakière, B., Vanacker, H., Miginiac-Maslow, M., Van Breusegem, F., et Noctor, G. (2007). Conditional oxidative stress responses in the Arabidopsis photorespiratory mutant cat2 demonstrate that redox state is a key modulator of daylength-dependent gene expression, and define photoperiod as a crucial factor in the regulation of H2O2-induced cell death. Plant J *52*, 640-657.

Reddehase, S., Grumbt, B., Neupert, W., et Hell, K. (2009). The disulfide relay system of mitochondria is required for the biogenesis of mitochondrial Ccs1 and Sod1. J. Mol. Biol *385*, 331-338.

Redinbo, M. R., Yeates, T. O., et Merchant, S. (1994). Plastocyanin: structural and functional analysis. J. Bioenerg. Biomembr *26*, 49-66.

Regeimbal, J., et Bardwell, J. C. A. (2002). DsbB catalyzes disulfide bond formation de novo. J. Biol. Chem *277*, 32706-32713.

Reichheld, J. P., Khafif, M., Riondet, C., Droux, M., Bonnard, G., et Meyer, Y. (2007). Inactivation of thioredoxin reductases reveals a complex interplay between thioredoxin and glutathione pathways in Arabidopsis development. The Plant cell *19*, 1851-65.

Ren, B., Tibbelin, G., de Pascale, D., Rossi, M., Bartolucci, S., et Ladenstein, R. (1998). A protein disulfide oxidoreductase from the archaeon Pyrococcus furiosus contains two thioredoxin fold units. Nat. Struct. Biol *5*, 602-611.

Ren, G., Stephan, D., Xu, Z., Zheng, Y., Tang, D., Harrison, R. S., Kurz, M., Jarrott, R., Shouldice, S. R., Hiniker, A., et al. (2009). Properties of the thioredoxin fold superfamily are modulated by a single amino acid residue. J. Biol. Chem *284*, 10150-10159.

Rey, P., Cuine, S., Eymery, F., Garin, J., Court, M., Jacquot, J. P., Rouhier, N., et Broin, M. (2005). Analysis of the proteins targeted by CDSP32, a plastidic thioredoxin participating in oxidative stress responses. Plant J *41*, 31-42.

Reynolds, C. M., Meyer, J., et Poole, L. B. (2002). An NADH-dependent bacterial thioredoxin re-

ductase-like protein in conjunction with a glutaredoxin homologue form a unique peroxiredoxin (AhpC) reducing system in Clostridium pasteurianum. Biochemistry *41*, 1990-2001.

Rhee, S. G., Jeong, W., Chang, T.-S., et Woo, H. A. (2007). Sulfiredoxin, the cysteine sulfinic acid reductase specific to 2-Cys peroxiredoxin: its discovery, mechanism of action, and biological significance. Kidney Int. Suppl, S3-8.

Rhee, S. G., et Woo, H. A. (2011). Multiple Functions of Peroxiredoxins: Peroxidases, Sensors and Regulators of the Intracellular Messenger H(2)O(2), and Protein Chaperones. Antioxid Redox Signal. PMID: 20919930 [PubMed - as supplied by publisher].

Rice-Evans, C. A., et Miller, N. J. (1996). Antioxidant activities of flavonoids as bioactive components of food. Biochem. Soc. Trans *24*, 790-795.

Riemer, J., Fischer, M., et Herrmann, J. M. (2011). Oxidation-driven protein import into mitochondria: Insights and blind spots. Biochim. Biophys. Acta *1808*, 981-989.

Rietsch, A., Belin, D., Martin, N., et Beckwith, J. (1996). An in vivo pathway for disulfide bond isomerization in Escherichia coli. Proc. Natl. Acad. Sci. U.S.A *93*, 13048-13053.

Rissler, M., Wiedemann, N., Pfannschmidt, S., Gabriel, K., Guiard, B., Pfanner, N., et Chacinska, A. (2005). The essential mitochondrial protein Erv1 cooperates with Mia40 in biogenesis of intermembrane space proteins. J Mol Biol *353*, 485-92.

Ritz, D., et Beckwith, J. (2001). ROLES OF THIOL-REDOX PATHWAYS IN BACTERIA. Annu. Rev. Microbiol. *55*, 21-48.

Rodriguez Milla, M. A., Maurer, A., Rodriguez Huete, A., et Gustafson, J. P. (2003). Glutathione peroxidase genes in Arabidopsis are ubiquitous and regulated by abiotic stresses through diverse signaling pathways. Plant J *36*, 602-615.

Romero-Puertas, M. C., Laxa, M., Mattè, A., Zaninotto, F., Finkemeier, I., Jones, A. M. E., Perazzolli, M., Vandelle, E., Dietz, K.-J., et Delledonne, M. (2007). S-nitrosylation of peroxiredoxin II E promotes peroxynitrite-mediated tyrosine nitration. Plant Cell *19*, 4120-4130.

Rouhier, N., Gelhaye, E., Gualberto, J. M., Jordy, M. N., De Fay, E., Hirasawa, M., Duplessis, S., Lemaire, S. D., Frey, P., Martin, F., et al. (2004). Poplar peroxiredoxin Q. A thioredoxin-linked chloroplast antioxidant functional in pathogen defense. Plant physiology *134*, 1027-38.

Rouhier, N., Gelhaye, E., et Jacquot, J. P. (2002). Glutaredoxin-dependent peroxiredoxin from poplar: protein-protein interaction and catalytic mechanism. The Journal of biological chemistry *277*, 13609-14.

Rouhier, N., Gelhaye, E., Sautiere, P. E., Brun, A., Laurent, P., Tagu, D., Gerard, J., de Fay, E., Meyer, Y., et Jacquot, J. P. (2001). Isolation and characterization of a new peroxiredoxin from poplar sieve tubes that uses either glutaredoxin or thioredoxin as a proton donor. Plant Physiol *127*, 1299-309.

Rouhier, N., et Jacquot, J. P. (2005a). The plant multigenic family of thiol peroxidases. Free radical biology & medicine *38*, 1413-21.

Rouhier, N., et Jacquot, J.-P. (2002). Plant peroxiredoxins: alternative hydroperoxide scavenging enzymes. Photosyn. Res *74*, 259-268.

Rouhier, N., et Jacquot, J.-P. (2005b). The plant multigenic family of thiol peroxidases. Free Radic. Biol. Med *38*, 1413-1421.

Sanders, C., Turkarslan, S., Lee, D.-W., et Daldal, F. (2010). Cytochrome c biogenesis: the Ccm system. Trends Microbiol *18*, 266-274.

Scheerer, P., Borchert, A., Krauss, N., Wessner, H., Gerth, C., Höhne, W., et Kuhn, H. (2007). Structural basis for catalytic activity and enzyme polymerization of phospholipid hydroperoxide glutathione peroxidase-4 (GPx4). Biochemistry *46*, 9041-9049.

Schlecker, T., Comini, M. A., Melchers, J., Ruppert, T., et Krauth-Siegel, R. L. (2007). Catalytic mechanism of the glutathione peroxidase-type tryparedoxin peroxidase of Trypanosoma brucei. Biochem. J *405*, 445-454.

Schrader, M., et Fahimi, H. D. (2006). Peroxisomes and oxidative stress. Biochim. Biophys. Acta *1763*, 1755-1766.

Schurmann, P., et Buchanan, B. B. (2008). The ferredoxin/thioredoxin system of oxygenic photosynthesis. Antioxidants & redox signaling *10*, 1235-74.

Schurmann, P., et Jacquot, J.-P. (2000). PLANT THIOREDOXIN SYSTEMS REVISITED. Annu. Rev. Plant Physiol. Plant Mol. Biol *51*, 371-400.

Selles, B., Jacquot, J.-P., et Rouhier, N. (2011). Comparative genomic study of protein disulfide isomerases from photosynthetic organisms. Genomics *97*, 37-50.

Selles, B., Rouhier, N., Chibani, K., Couturier, J., Gama, F., et Jacquot, J.-P. (2009). Chapter 13 Glutaredoxin: The Missing Link Between Thiol-Disulfide Oxidoreductases and Iron Sulfur Enzymes. Dans (Academic Press), p. 405-436.

Senkevich, T. G., White, C. L., Koonin, E. V., et Moss, B. (2000). A viral member of the ERV1/ALR protein family participates in a cytoplasmic pathway of disulfide bond formation. Proc. Natl. Acad. Sci. U.S.A *97*, 12068-12073.

Serrato, A. J., Pérez-Ruiz, J. M., et Cejudo, F. J. (2002). Cloning of thioredoxin h reductase and characterization of the thioredoxin reductase-thioredoxin h system from wheat. Biochem. J *367*, 491-497.

Serve, O., Kamiya, Y., Maeno, A., Nakano, M., Murakami, C., Sasakawa, H., Yamaguchi, Y., Harada, T., Kurimoto, E., Yagi-Utsumi, M., et al. (2010). Redox-dependent domain rearrangement of protein disulfide isomerase coupled with exposure of its substrate-binding hydrophobic surface. J. Mol. Biol *396*, 361-374.

Sevier, C. S., Cuozzo, J. W., Vala, A., Aslund, F., et Kaiser, C. A. (2001). A flavoprotein oxidase defines a new endoplasmic reticulum pathway for biosynthetic disulphide bond formation. Nat. Cell Biol *3*, 874-882.

Sevier, C. S., et Kaiser, C. A. (2006). Conservation and diversity of the cellular disulfide bond for-

mation pathways. Antioxid. Redox Signal *8*, 797-811.

Sevier, C. S., et Kaiser, C. A. (2008). Ero1 and redox homeostasis in the endoplasmic reticulum. Biochim. Biophys. Acta *1783*, 549-556.

Sevier, C. S., Qu, H., Heldman, N., Gross, E., Fass, D., et Kaiser, C. A. (2007). Modulation of cellular disulfide-bond formation and the ER redox environment by feedback regulation of Ero1. Cell *129*, 333-344.

Shi, J., Vlamis-Gardikas, A., Aslund, F., Holmgren, A., et Rosen, B. P. (1999). Reactivity of glutaredoxins 1, 2, and 3 from Escherichia coli shows that glutaredoxin 2 is the primary hydrogen donor to ArsC-catalyzed arsenate reduction. J. Biol. Chem *274*, 36039-36042.

Staples, C. R., Ameyibor, E., Fu, W., Gardet-Salvi, L., Stritt-Etter, A. L., Schurmann, P., Knaff, D. B., et Johnson, M. K. (1996). The function and properties of the iron-sulfur center in spinach ferredoxin: thioredoxin reductase: a new biological role for iron-sulfur clusters. Biochemistry *35*, 11425-34.

Staples, C. R., Gaymard, E., Stritt-Etter, A. L., Telser, J., Hoffman, B. M., Schurmann, P., Knaff, D. B., et Johnson, M. K. (1998). Role of the [Fe4S4] cluster in mediating disulfide reduction in spinach ferredoxin:thioredoxin reductase. Biochemistry *37*, 4612-20.

Starzl, T. E., Terblanche, J., Porter, K. A., Jones, A. F., Usui, S., et Mazzoni, G. (1979). GROWTH-STIMULATING FACTOR IN REGENERATING CANINE LIVER. The Lancet *313*, 127-130.

Steiner, H., Kispal, G., Zollner, A., Haid, A., Neupert, W., et Lill, R. (1996). Heme binding to a conserved Cys-Pro-Val motif is crucial for the catalytic function of mitochondrial heme lyases. J. Biol. Chem *271*, 32605-32611.

Stenbaek, A., Hansson, A., Wulff, R. P., Hansson, M., Dietz, K.-J., et Jensen, P. E. (2008). NADPH-dependent thioredoxin reductase and 2-Cys peroxiredoxins are needed for the protection of Mg-protoporphyrin monomethyl ester cyclase. FEBS Lett *582*, 2773-2778.

Sweetlove, L. J., Heazlewood, J. L., Herald, V., Holtzapffel, R., Day, D. A., Leaver, C. J., et Millar, A. H. (2002). The impact of oxidative stress on Arabidopsis mitochondria. Plant J *32*, 891-904.

Sztajer, H., Gamain, B., Aumann, K. D., Slomianny, C., Becker, K., Brigelius-Flohé, R., et Flohé, L. (2001). The putative glutathione peroxidase gene of Plasmodium falciparum codes for a thioredoxin peroxidase. J. Biol. Chem *276*, 7397-7403.

Takanishi, C. L., Ma, L.-H., et Wood, M. J. (2010). The role of active site residues in the oxidant specificity of the Orp1 thiol peroxidase. Biochem. Biophys. Res. Commun *403*, 46-51.

Tarrago, L., Laugier, E., Zaffagnini, M., Marchand, C. H., Le Maréchal, P., Lemaire, S. D., et Rey, P. (2010). Plant thioredoxin CDSP32 regenerates 1-cys methionine sulfoxide reductase B activity through the direct reduction of sulfenic acid. J. Biol. Chem *285*, 14964-14972.

Tavender, T. J., et Bulleid, N. J. (2010). Molecular mechanisms regulating oxidative activity of the Ero1 family in the endoplasmic reticulum. Antioxid. Redox Signal *13*, 1177-1187.

Tavender, T. J., Sheppard, A. M., et Bulleid, N. J. (2008). Peroxiredoxin IV is an endoplasmic reticulum-localized enzyme forming oligomeric complexes in human cells. Biochem. J *411*, 191-199.

Tavender, T. J., Springate, J. J., et Bulleid, N. J. (2010). Recycling of peroxiredoxin IV provides a novel pathway for disulphide formation in the endoplasmic reticulum. EMBO J *29*, 4185-4197.

Terziyska, N., Lutz, T., Kozany, C., Mokranjac, D., Mesecke, N., Neupert, W., Herrmann, J. M., et Hell, K. (2005). Mia40, a novel factor for protein import into the intermembrane space of mitochondria is able to bind metal ions. FEBS Lett *579*, 179-184.

Tian, G., Xiang, S., Noiva, R., Lennarz, W. J., et Schindelin, H. (2006). The crystal structure of yeast protein disulfide isomerase suggests cooperativity between its active sites. Cell *124*, 61-73.

Tie, J.-K., et Stafford, D. W. (2008). Structure and function of vitamin K epoxide reductase. Vitam. Horm *78*, 103-130.

Toppo, S., Flohé, L., Ursini, F., Vanin, S., et Maiorino, M. (2009). Catalytic mechanisms and specificities of glutathione peroxidases: variations of a basic scheme. Biochim. Biophys. Acta *1790*, 1486-1500.

Toppo, S., Vanin, S., Bosello, V., et Tosatto, S. C. E. (2008). Evolutionary and structural insights into the multifaceted glutathione peroxidase (Gpx) superfamily. Antioxid. Redox Signal *10*, 1501-1514.

Torres, M. A. (2010). ROS in biotic interactions. Physiol Plant *138*, 414-429.

Tosatto, S. C. E., Bosello, V., Fogolari, F., Mauri, P., Roveri, A., Toppo, S., Flohé, L., Ursini, F., et Maiorino, M. (2008). The catalytic site of glutathione peroxidases. Antioxid. Redox Signal *10*, 1515-1526.

Trebitsh, T., Levitan, A., Sofer, A., et Danon, A. (2000). Translation of chloroplast psbA mRNA is modulated in the light by counteracting oxidizing and reducing activities. Mol. Cell. Biol *20*, 1116-1123.

Trombetta, E. S., et Parodi, A. J. (2003). Quality control and protein folding in the secretory pathway. Annu. Rev. Cell Dev. Biol *19*, 649-676.

Trujillo, M., Ferrer-Sueta, G., Thomson, L., Flohé, L., et Radi, R. (2007). Kinetics of peroxiredoxins and their role in the decomposition of peroxynitrite. Subcell. Biochem *44*, 83-113.

Tu, B. P., Ho-Schleyer, S. C., Travers, K. J., et Weissman, J. S. (2000). Biochemical basis of oxidative protein folding in the endoplasmic reticulum. Science *290*, 1571-1574.

Tury, A., Mairet-Coello, G., Poncet, F., Jacquemard, C., Risold, P. Y., Fellmann, D., et Griffond, B. (2004). QSOX sulfhydryl oxidase in rat adenohypophysis: localization and regulation by estrogens. J. Endocrinol *183*, 353-363.

Umbach, A. L., et Siedow, J. N. (1993). Covalent and Noncovalent Dimers of the Cyanide-Resistant

Alternative Oxidase Protein in Higher Plant Mitochondria and Their Relationship to Enzyme Activity. Plant Physiol *103*, 845-854.

Vala, A., Sevier, C. S., et Kaiser, C. A. (2005). Structural determinants of substrate access to the disulfide oxidase Erv2p. J. Mol. Biol *354*, 952-966.

Veal, E. A., Findlay, V. J., Day, A. M., Bozonet, S. M., Evans, J. M., Quinn, J., et Morgan, B. A. (2004). A 2-Cys peroxiredoxin regulates peroxide-induced oxidation and activation of a stress-activated MAP kinase. Mol. Cell *15*, 129-139.

Vitu, E., Bentzur, M., Lisowsky, T., Kaiser, C. A., et Fass, D. (2006). Gain of function in an ERV/ALR sulfhydryl oxidase by molecular engineering of the shuttle disulfide. J. Mol. Biol *362*, 89-101.

Vivancos, A. P., Castillo, E. A., Biteau, B., Nicot, C., Ayte, J., Toledano, M. B., et Hidalgo, E. (2005). A cysteine-sulfinic acid in peroxiredoxin regulates H2O2-sensing by the antioxidant Pap1 pathway. Proceedings of the National Academy of Sciences of the United States of America *102*, 8875-80.

Vlamis-Gardikas, A., Potamitou, A., Zarivach, R., Hochman, A., et Holmgren, A. (2002). Characterization of Escherichia coli null mutants for glutaredoxin 2. The Journal of biological chemistry *277*, 10861-8.

van Vliet, C., Thomas, E. C., Merino-Trigo, A., Teasdale, R. D., et Gleeson, P. A. (2003). Intracellular sorting and transport of proteins. Prog. Biophys. Mol. Biol *83*, 1-45.

Wadahama, H., Kamauchi, S., Ishimoto, M., Kawada, T., et Urade, R. (2007). Protein disulfide isomerase family proteins involved in soybean protein biogenesis. FEBS J *274*, 687-703.

Wadahama, H., Kamauchi, S., Nakamoto, Y., Nishizawa, K., Ishimoto, M., Kawada, T., et Urade, R. (2008). A novel plant protein disulfide isomerase family homologous to animal P5 - molecular cloning and characterization as a functional protein for folding of soybean seed-storage proteins. FEBS J *275*, 399-410.

Wajih, N., Hutson, S. M., et Wallin, R. (2007). Disulfide-dependent protein folding is linked to operation of the vitamin K cycle in the endoplasmic reticulum. A protein disulfide isomerase-VKORC1 redox enzyme complex appears to be responsible for vitamin K1 2,3-epoxide reduction. J. Biol. Chem *282*, 2626-2635.

Wang, W., Winther, J. R., et Thorpe, C. (2007). Erv2p: characterization of the redox behavior of a yeast sulfhydryl oxidase. Biochemistry *46*, 3246-3254.

Williams, C. H., Arscott, L. D., Müller, S., Lennon, B. W., Ludwig, M. L., Wang, P. F., Veine, D. M., Becker, K., et Schirmer, R. H. (2000). Thioredoxin reductase two modes of catalysis have evolved. Eur. J. Biochem *267*, 6110-6117.

Wittke, I., Wiedemeyer, R., Pillmann, A., Savelyeva, L., Westermann, F., et Schwab, M. (2003). Neuroblastoma-derived sulfhydryl oxidase, a new member of the sulfhydryl oxidase/Quiescin6 family, regulates sensitization to interferon gamma-induced cell death in human neuroblastoma cells. Cancer Res *63*, 7742-7752.

Wojtaszek, P. (1997). Oxidative burst: an early plant response to pathogen infection. Biochem. J *322 (Pt 3)*, 681-692.

Wood, Z. A., Schroder, E., Robin Harris, J., et Poole, L. B. (2003a). Structure, mechanism and regulation of peroxiredoxins. Trends in biochemical sciences *28*, 32-40.

Wood, Z. A., Poole, L. B., et Karplus, P. A. (2003b). Peroxiredoxin evolution and the regulation of hydrogen peroxide signaling. Science *300*, 650-653.

Wouters, M. A., Fan, S. W., et Haworth, N. L. (2010). Disulfides as redox switches: from molecular mechanisms to functional significance. Antioxid. Redox Signal *12*, 53-91.

Yang, K. S., Kang, S. W., Woo, H. A., Hwang, S. C., Chae, H. Z., Kim, K., et Rhee, S. G. (2002). Inactivation of human peroxiredoxin I during catalysis as the result of the oxidation of the catalytic site cysteine to cysteine-sulfinic acid. The Journal of biological chemistry *277*, 38029-36.

Yang, X.-D., Dong, C.-J., et Liu, J.-Y. (2006). A plant mitochondrial phospholipid hydroperoxide glutathione peroxidase: its precise localization and higher enzymatic activity. Plant Mol. Biol *62*, 951-962.

Zapun, A., Bardwell, J. C., et Creighton, T. E. (1993). The reactive and destabilizing disulfide bond of DsbA, a protein required for protein disulfide bond formation in vivo. Biochemistry *32*, 5083-5092.

Zapun, A., Missiakas, D., Raina, S., et Creighton, T. E. (1995). Structural and functional characterization of DsbC, a protein involved in disulfide bond formation in Escherichia coli. Biochemistry *34*, 5075-5089.

Zhang, Y., Marcillat, O., Giulivi, C., Ernster, L., et Davies, K. J. (1990). The oxidative inactivation of mitochondrial electron transport chain components and ATPase. J. Biol. Chem *265*, 16330 -16336.

Zito, E., Chin, K.-T., Blais, J., Harding, H. P., et Ron, D. (2010). ERO1-β, a pancreas-specific disulfide oxidase, promotes insulin biogenesis and glucose homeostasis. J Cell Biol *188*, 821-832.

Communications scientifiques & distinctions

Publications

1. Selles B, Jacquot JP, Rouhier N. (2011).

Comparative genomic study of protein disulfide isomerases from photosynthetic organisms. ***Genomics***. Jan;97(1):37-50.

2. **Selles B**, Hugo M, Trujillo M, Srivastava V, Wingsle G, Jacquot JP, Radi R, Rouhier N.

Catalytic mechanism and oxidative inactivation of the poplar thioredoxin-dependent glutathione peroxidase 5. ***En preparation.***

3. Selles B, Jacquot JP, Rouhier N.

Biochemical characterization of three poplar PDI isoforms with different domain organizations: emphasis on the oxidoreductase properties of PDI-M. ***En preparation.***

4. Duplessis S, Cuomo C, Lin Y-C, Aerts A, Tisserant E, Veneault-Fourrey C, Joly D, Hacquard S, Amselem J, Cantarel B, Readman C, Coutinho P, Feau N, Field M, Frey P, Gelhaye E, Goldberg J, Grabherr M, Kodira C, Kohler A, Kues U, Lindquist E, Lucas S, Mago R, Mauceli E, Morin E, Murat C, Pangilinan J, Park R, Pearson M, Quesneville H, Rouhier N, Sakthikumar S, Salamov A, Schmutz J, **Selles B**, Shapiro H, Tangay P, Tuskan G, Henrissat B, Van de Peer Y, Rouz P, Ellis J, Dodds P, Schein J, Zhong S, Hamelin R, Grigoriev I, Szabo L, Martin .F. (2011).

Obligate Biotrophy Features Unraveled by the Genomic Analysis of Rust Fungi. ***PNAS***, sous presse.

5. Selles B, Rouhier N**,** Chibani K**,** Couturier J**, Gama F,** Jacquot JP. (2009).

Chapter 13 Glutaredoxin: The Missing Link Between Thiol-Disulfide Oxidoreductases and Iron Sulfur Enzymes. ***Advances in Botanical Research***, Volume 52, Pages 405-436.

6. Chibani K, Couturier J, **Selles B**, Jacquot JP, Rouhier N. (2010).

The chloroplastic thiol reducing systems: dual functions in the regulation of carbohydrate metabolism and regeneration of antioxidant enzymes, emphasis on the poplar redoxin equipment. ***Photosynth Res***. Apr;104(1):75-99.

Communications orales et posters

Communication orales:

Reunion annuelle du "Groupement de Recherche (GDR) redoxin", 17-21 août 2009, Perpignan, France.

Communication orale, "Comparative genomic analysis of land plant Protein Disulfide Isomerases: isolation of promising poplar isoforms".

Poster:

The XIV Biennial Meeting of the Society for Free Radical Research International (14th SFRR), Octobre 18-22, 2008, Pekin, Chine.

Distinctions

Prix "Poster, *In recognition of extraordinary scientific achievements in the field of free radical research at the XIV biennial meeting of the Society for Free Radical Research International*" (14th SFRR).

The XIV Biennial Meeting of the Society for Free Radical Research International (14th SFRR), Octobre 18-22, 2008, Pekin, Chine.

Résumé

La formation de ponts disulfure constitue une modification post-traductionnelle des protéines importante pour de nombreux processus physiologiques, jouant un rôle particulier dans le repliement, la catalyse et la régulation de leur activité. Ce travail concerne l'étude des relations structure-fonction d'oxydoréductases de peuplier appartenant à deux familles de la superfamille des thiorédoxines, les glutathion peroxydases (Gpxs) et les protéine disulfure isomérases (PDIs).
L'étude biochimique fine de la Gpx5 a permis de montrer que cette peroxydase réduit le peroxynitrite, propriété inconnue pour ce type de Gpx et de détailler plusieurs étapes du mécanisme catalytique (formation de l'acide sulfénique, changement structural entre formes réduites et oxydées, régénération par les Trxs). La dimérisation de la Gpx5 n'est pas requise pour son activité mais pourrait jouer un rôle dans la reconnaissance de certains substrats. Enfin, l'inactivation de la cystéine peroxydatique par suroxydation suggère que les Gpxs pourraient également avoir une fonction dans la signalisation en réponse aux peroxydes.
Concernant les PDIs, suite à une analyse phylogénétique détaillée amenant à proposer une nouvelle classification en 9 classes chez les organismes photosynthétiques, la caractérisation biochimique de plusieurs isoformes présentant des organisations modulaires distinctes et appartenant à trois classes de PDIs a été entreprise. Aucune activité enzymatique typique n'a été identifiée pour la PDI-A, alors que les PDI-L1a et -M possèdent à la fois une activité oxydase et réductase. Les deux modules *a* de la PDI-M catalysent des réactions spécifiques, de réduction ou d'oxydation.

Mots clés: Protéine disulfure isomérase, glutathion peroxydase, thiorédoxine, stress oxydant, oxydation, réduction.

Abstract

Protein activity and folding can be regulated by post-translational modifications that can impact on their physiological functions. One of these is the formation/reduction of disulfide bridges. The aim of the present work is to study the structure-function relationship of protein members of the thioredoxin superfamily, the protein disulfide isomerases (PDI) and the glutathione peroxidases (Gpx).
A precise biochemical study has allowed us to demonstrate that this enzyme is an efficient peroxynitrite scavenger, a new finding for this type of protein and allowed investigating several steps of the Gpx5 catalytic mechanism (i.e. sulfenic acid formation, structural changes between reduce dand oxidized forms, Trx-mediated recycling). We also demonstrate that the dimer form of Gpx5 is not absolutely required for peroxide reduction but probably involved in peroxide specificity. Finally, the capability of the peroxidatic cysteine to be overoxidized brings some new clues in favor of an additional signaling function for Gpx5.
Concerning PDIs, a detailed phylogenetic analysis of photosynthetic organisms allowed us to identify 9 classes of PDIs and to propose a new nomenclature that fits all these organisms. The biochemical characterization of isoforms of interest has allowed us to highlight some specificity of PDI-L1a and PDI-M in terms of reduction or oxidation reactions catalyzed. A detailed analysis of PDI-M isoform also indicates that the two Trx modules of this protein show differential oxidation or reduction capacities. We could not detect any activity for PDI-A isoforms, leaving us to wonder whether this enzyme is simply active or possesses highly specific protein partners.

Key words: Protein disulfide isomerase, glutathione peroxidase, thioredoxin, oxidative stress, oxidation, reduction.